INTEGRATED DESIGN AND SIMULATION OF CHEMICAL PROCESSES

ALEXANDRE C. DIMIAN

COMPUTER-AIDED CHEMICAL ENGINEERING, 13

ELSEVIER

INTEGRATED DESIGN AND SIMULATION OF CHEMICAL PROCESSES

COMPUTER-AIDED CHEMICAL ENGINEERING

Advisory Editor: R. Gani

Volume 1:	Distillation Design in Practice (L.M. Rose)
Volume 2:	The Art of Chemical Process Design (G.L. Wells and L.M. Rose)
Volume 3:	Computer Programming Examples for Chemical Engineers (G. Ross)
Volume 4:	Analysis and Synthesis of Chemical Process Systems (K. Hartmann and K. Kaplick)
Volume 5:	Studies in Computer-Aided Modelling. Design and Operation Part A: Unite Operations (I. Pallai and Z. Fonyó, Editors) Part B: Systems (I. Pallai and G.E. Veress, Editors)
Volume 6:	Neural Networks for Chemical Engineers (A.B. Bulsari, Editor)
Volume 7:	Material and Energy Balancing in the Process Industries - From Microscopic Balances to Large Plants (V.V. Veverka and F. Madron)
Volume 8:	European Symposium on Computer Aided Process Engineering-10 (S. Pierucci, Editor)
Volume 9:	European Symposium on Computer Aided Process Engineering- 11 (R. Gani and S.B. Jørgensen, Editors)
Volume 10:	European Symposium on Computer Aided Process Engineering-12 (J. Grievink and J. van Schijndel, Editors)
Volume 11:	Software Architectures and Tools for Computer Aided Process Engineering (B. Braunschweig and R. Gani, Editors)
Volume 12:	Computer Aided Molecular Design: Theory and Practice (L.E.K. Achenie, R. Gani and V. Venkatasubramanian, Editors)
Volume 13:	Integrated Design and Simulation of Chemical Processes (A.C. Dimian)

COMPUTER-AIDED CHEMICAL ENGINEERING, 13

INTEGRATED DESIGN AND SIMULATION OF CHEMICAL PROCESSES

Alexandre C. Dimian
Department of Chemical Engineering
Faculty of Chemistry
University of Amsterdam
Nieuwe Achtergracht 166
1018 WV Amsterdam

2003
ELSEVIER
Amsterdam - Boston - London - New York - Oxford - Paris
San Diego - San Francisco - Singapore - Sydney - Tokyo

ELSEVIER SCIENCE B.V.
Sara Burgerhartstraat 25
P.O. Box 211, 1000 AE Amsterdam, The Netherlands

First edition 2003

Library of Congress Cataloging in Publication Data
A catalog record from the Library of Congress has been applied for.

British Library Cataloguing in Publication Data
A catalogue record from the British Library has been applied for.

ISBN: 0-444-82996-2
ISSN: 1570-7946 (Series)

♾ The paper used in this publication meets the requirements of ANSI/NISO Z39.48-1992 (Permanence of Paper).
Printed in The Netherlands.

PREFACE

In addition to high economic efficiency, Chemical Process Industries are confronted today with the challenge of sustainable development: the exploitation of the natural resources by the present society must not compromise the ability of future generations to meet their own needs. Sustainable development implies a profound change in developing and designing chemical processes, and implicitly in the education of designers. As an attempt to answer this challenge, the book deals with the design of innovative chemical processes by means of systematic methods and computer simulation techniques.

The current revolution in information technology, as well as the impressive progress in modelling and simulation has a significant impact on Process Design. Computer simulation is involved in all stages of a project, from feasibility studies, through conceptual design, to detailed engineering, and finally in plant operation.

In developing sustainable processes, the essential factor is the innovation capacity of chemical engineers to discover new processes and improve significantly the existing ones. The key to innovation is the integration of knowledge from different disciplines. It is also the distinctive feature of this work, in which the emphasis is set on the power of the conceptual methods incorporated in the new paradigm of *Process Integration*. Modern process design consists of developing not a unique flowsheet but alternatives, from which the best one is refined, integrated and optimised with respect to high efficiency of materials and energy, ecologic performance and operability properties.

This book aims is to treat the most important conceptual aspects of Process Design and Simulation in a unified frame of principles, techniques and tools. Accordingly, the material is organised in five sections, *Process Simulation*, *Thermodynamic Methods*, *Process Synthesis*, *Process Integration*, *Design Project*, and covered in 17 Chapters. Numerous examples illustrate both theoretical concepts and design issues. The work refers also to the newest scientific developments in the field of Computer Aided Process Engineering.

The book is primarily intended for undergraduate and postgraduate students in chemical engineering, as support material for various courses and projects dealing with Chemical Process Design and Simulation. The material can be customised to fulfil the needs of both general and technical universities. The work is intended also as a guide in advanced design techniques for practicing engineers involved in research, development and design of various chemical or related processes. The users of process simulators will find helpful guidelines and examples for an effective use of commercial systems.

This Page Intentionally Left Blank

ACKNOWLEDGMENTS

Writing this book has been a considerable challenge by the variety of topics and the amount of material. A large part of this book takes profit from the industrial experience acquired between 1982 and 1993 as consultant in process design and simulation for major French companies. In the last twenty years I had the privilege to work intensively with most of the simulation systems mentioned in this book, but also with other packages that unfortunately have not survived. Both the use of scientific principles in design and the systems approach in solving complex problems have deep roots in that industrial experience.

My first expression of gratitude is for my former teachers, as well as for my numerous colleagues from France, The Netherlands, Romania, Germany, England and USA, who helped me to progress along the years in this fascinating profession called Chemical Engineering.

I am grateful to the Department of Chemical Engineering at the University of Amsterdam, The Netherlands, for the excellent working conditions. I would like to express my gratitude to all my colleagues, particularly to Professors Alfred Bliek and Rajamani Krishna for their support and valuable advises.

The material of this book has been taught for about a decade at the University of Amsterdam. From a long list of former and actual PhD students who helped me with assistance during the course and design project I would mention only few names: Sander Groenendijk, Adrian Kodde, Sasha Kersten, Florin Omota. Susana Cruz was very obliging with the proofread of several chapters. In addition, Tony Kiss gave me a precious help to prepare simulation examples and to finish the document.

In particular I am pleased to acknowledge the important contribution of Dr. Sorin Bildea, now at the Technical University Delft, who is co-author of the chapters about Controllability Analysis and Integration of Design & Control.

Finally, I am indebted to my lovely family for the moral support and many-sided assistance during the hard work years needed to accomplish this book, most of all to my beloved wife and "editor-en-chief" Aglaia Dimian, as well as to my daughters Alexandra and Julia.

Alexandre C. Dimian

Department of Chemical Engineering
University of Amsterdam
The Netherlands

This Page Intentionally Left Blank

CONTENTS

Preface v

Acknowledgments vii

Nomenclature xv

1 INTEGRATED PROCESS DESIGN 1

1.1 Introduction 1
1.2 Sustainable Development 6
1.3 Process Design 7
1.4 Systems Engineering 11
1.5 Integrated Process Design 15
1.6 Production-Integrated Environmental Protection 22
1.7 Summary 29
1.8 References 30

PART I - PROCESS SIMULATION

2 INTRODUCTION IN PROCESS SIMULATION 33

2.1 Computer simulation in Process Engineering 33
2.2 Steps in a simulation approach 41
2.3 Architecture of flowsheeting software 46
2.4 Integration of simulation tools 50
2.5 Selection of simulation software 55
2.6 Summary 57
2.7 References 58

3 STEADY STATE FLOWSHEETING 59

3.1 Fundamentals of steady state flowsheeting 60
3.2 Degrees of freedom analysis 81
3.3 Methodology in sequential-modular flowsheeting 96
3.4 Results 105
3.5 Analysis tools 106
3.6 Optimisation 107
3.7 Summary 111
3.8 References 112

4 DYNAMIC SIMULATION 113

4.1 Transition from steady state to dynamic simulation 114
4.2 Dynamic flowsheeting 117
4.3 Numerical problems in dynamic simulation 119
4.4 Dynamic flash 121
4.5 Dynamic distillation column 125
4.6 Dynamic simulation of chemical reactors 129
4.7 Process Control tools 131
4.8 Further reading 133
4.9 References 134

PART II: THERMODYNAMIC METHODS

5 COMPUTATIONAL METHODS IN THERMODYNAMICS 137

5.1 PVT behaviour of fluids 138
5.2 Fundamentals of thermodynamics 142
5.3 Fugacity 155
5.4 Equations of state 163
5.5 Generalised computational methods using PVT relationship 171
5.6 Summary 179
5.7 References 180

6 PHASE EQUILIBRIA 181

6.1 Computation of vapour-liquid equilibrium 182
6.2 Models for liquid activity 192
6.3 The regression of parameters in thermodynamic models 202
6.4 Special topics in phase equilibrium 212
6.5 Further reading 224
6.6 References 225

PART III: PROCESS SYNTHESIS

7 PROCESS SYNTHESIS BY HIERARCHICAL APPROACH 229

7.1 Introduction 230
7.2 Outline of the Hierarchical Approach 233
7.3 Data and requirements 235
7.4 Input/Output analysis 238
7.5 Reactor design and recycle structure 247
7.6 General structure of the separation system 255
7.7 Vapour recovery and Gas separation systems 264
7.8 Liquid separation system 271
7.9 Separation of zeotropic mixtures by distillation 280
7.10 Enhanced distillation 288
7.11 Alternatives to distillation 291
7.12 Reactive distillation 292
7.13 Economic Potential after separations 294

7.14 Summary 296
7.15 References 297

8 SYNTHESIS OF REACTION SYSTEMS 299

8.1 Chemical reaction network 300
8.2 Chemical equilibrium 307
8.3 Reactors for homogeneous systems 310
8.4 Reactors for heterogeneous systems 318
8.5 Thermal design issues 322
8.6 Selection of chemical reactors 331
8.7 Synthesis of chemical reactor networks 340
8.8 Further reading 349
8.9 References 349

9 SYNTHESIS OF AZEOTROPIC SEPARATION SYSTEMS 351

9.1 Graphical representations for ternary mixtures 352
9.2 Homogeneous azeotropic distillation 362
9.3 Heterogeneous azeotropic distillation 376
9.4 Combined processes 382
9.5 Design issues 384
9.6 Further reading 388
9.7 Summary 389
9.8 References 390

PART IV: PROCESS INTEGRATION

10 PINCH POINT ANALYSIS 393

10.1 Introduction 394
10.2 Targets for energy recovery 399
10.3 Placement of utilities 411
10.4 Design of the Heat Exchanger Network 415
10.5 Mathematical programming 428
10.6 Design evolution 429
10.7 Extensions of the pinch principle 430
10.8 Summary of Pinch Point Analysis 432
10.9 References 433

11 PRACTICAL ENERGY INTEGRATION 435

11.1 Heat and Power Integration 436
11.2 Distillation systems 443
11.3 The integration of chemical reactors 459
11.4 Total Site integration 460
11.5 Summary 462
11.6 References 462

12 CONTROLLABILITY ANALYSIS **463**

12.1 Introduction 464
12.2 Modelling of dynamic systems 465
12.3 Controllability analysis of SISO systems 472
12.4 Controllability analysis of MIMO systems 483
12.5 Decentralized control 489
12.6 References 500

13 INTEGRATION OF DESIGN AND CONTROL **501**

13.1 Introduction 501
13.2 Steady state design and controllability 503
13.3 Dynamic effects in recycle systems 505
13.4 Control of component inventory 513
13.5 Steady state nonlinear effects of material recycle 522
13.6 Dynamic effects of energy recycle 533
13.7 Plantwide control procedure 537
13.8 Integrating plantwide control in Hierarchical Conceptual Design 543
13.9 Summary 552
13.10 References 554

PART V: DESIGN PROJECT

14 PROCESS DESIGN PROJECT **557**

14.1 Scope 558
14.2 Organisation 560
14.3 Process Integration courses 561
14.4 Process Integration project 563
14.5 Plant Design Project 564
14.6 References 570

15 ECONOMIC EVALUATION OF PROJECTS **571**

15.1 Introduction 572
15.2 Basic concepts 572
15.3 Time-value of money 578
15.4 Capital costs 583
15.5 Operating costs 591
15.6 Profitability Analysis 595
15.7 Further reading 604
15.8 References 604

16 EQUIPMENT SELECTION AND DESIGN **605**

16.1 Reactors 606
16.2 Separators 612
16.3 Heat exchangers design 625
16.4 Transport of fluids 636
16.5 References 638

17 CASE STUDIES **639**

17.1 Design and simulation of HDA plant 639
17.2 Dynamic Simulation of the HDA plant 651
17.3 Control of impurities in a complex plant 658
17.4 References 673

APPENDICES **675**

A. Estimation of basic equipment cost 677
B. Cost of utilities 683
C. Materials of construction 685
D. Saturated steam properties 688
E. Vapour pressures of some hydrocarbon 689
F. Vapour pressures of some organic components 690
G. Conversion factors 691

INDEX **693**

This Page Intentionally Left Blank

Nomenclature

The symbols given bellow are general. Supplementary notations are explained in context.

a	activity (kmol/m^3)
A	heat exchange area (m^2)
A_c	cross-sectional area
B	bottom product flow rate
c_i	molar concentration (kmol/m^3) of component I
C_i	dimensionless concentration
C_P	molar heat capacity at constant pressure (kJ/kmol/K)
C_V	molar heat capacity at constant pressure (kJ/kmol/K)
d	diameter (m^{-1})
d_p	particle diameter
D	distillate flow rate (kmol/s)
Da	Damköhler number $Da = kc_A^{n-1}\tau$
E	activation energy (kJ/kmol)
f_i	fugacity of component i (bar)
F	total molar feed flow rate (kmol/s)
F_i	partial molar flow rate of component i
F_T	temperature correction factor for shell & tubes heat exchangers
g	acceleration due to gravity (9.81 m/s)
G	mass feed flow rate (kg/s)
G	molar Gibbs free energy (kJ/kmol)
h	specific enthalpy (kJ/kg, kJ/kmol), heat transfer coefficient (W/m^{2}K)
H	molar or mass enthalpy (kJ/mol, kJ/kg)
H_i	Henry coefficient of component i
$\Delta H_{R,i}$	enthalpy of reaction with reference to component i
k	reaction constant [(kmol/m^3)$^{1-n}$s^{-1}]
k_0	pre-exponential Arrhenius factor [(kmol/m^3)$^{1-n}$s^{-1}]
K_a, K_c, K_f, K_x	reaction equilibrium constant (activity, concentration, fugacity, molar fractions)
K_i	K-factors or K-values
L	liquid flow rate (kmol/s or kg/s)
m	mass amount (kg)
M_i	molar weight of component i
n	molar amount (kmol)
N_c, N_{eq}, N_v	number of components, equations and variables
N_{min}	number minim of theoretical stages
P	pressure (bar)
$P_{v,i}$	vapour pressure of component i
P_c	critical pressure (bar)
t	time (s)
T	temperature (K or °C)
T_c	critical temperature (K or °C)
ΔT_{ad}	adiabatic temperature change (K or °C)
ΔT_{min}	minimum temperature approach (K or °C)
ΔT_{LM}	logarithmic mean temperature difference (K or °C)

Q	heat duty (kW)
Q_t	heat transferred (kW)
Q_v	volumetric flow rate (m^3/s)
r	radius
r_j	rate of reaction ($kmol/m^3/s$) of component j
R	universal gas constant, (R=8.31451 J/mol/K)
R_{min}	minimum reflux ratio
S	entropy (kJ/mol/K)
u	superficial fluid velocity (m^3/m^2s)
U	internal energy (kJ/kmol), overall heat transfer coefficient
v	velocity (m/s)
V	volume (m^3), vapour flow rate (kmol/s or kg/s)
V_c	critical volume (K)
V_R	reaction volume (m^3)
W	work (kJ), power (kW)
W_s	shaft work in compression, expansion
x	molar fractions of liquid phase
X_A	fractional conversion of the component A
y	molar fractions of vapour phase
z	molar fractions of feed stream, length co-ordinate (m)
Z	compressibility factor

Greek symbols

α	relative volatility
α, β	reaction orders
δ	width
∂	differential operator
Δ	finite difference operator
ε	error
γ	liquid activity coefficient
λ	thermal conductivity (W/mK)
μ_i	chemical potential of component i
ξ_j	molar extent of reaction j
η	fluid viscosity, efficiency in general
ω	accentric factor
ρ	density (kg/m^3)
σ	surface tension (N/m)
ν	stoichiometric coefficient
ϕ_i	fugacity coefficient of component i
τ	reaction time (s^{-1}), constant time (s^{-1})
θ	dimensionless time

Chapter 1

INTEGRATED PROCESS DESIGN

1.1 Introduction
1.1.1 Motivation
1.1.2 The road map of the book

1.2 Sustainable Development

1.3 Process Design
1.3.1 Creative aspects in Process Design
1.3.2 Trends in Process Design

1.4 Systems Engineering
1.4.1 Systems approach
1.4.2 Life cycle modelling

1.5 Integrated Process Design
1.5.1 Process Synthesis and Process Integration
1.5.2 Systematic methods
1.5.3 Trends in Integrated Process Design

1.6 Production-Integrated Environmental Protection
1.6.1 Concepts of environmental protection
1.6.2 Measures for environmental efficiency
1.6.3 Metrics for sustainability

1.7 Summary

1.8 References

1.1 INTRODUCTION

1.1.1 Motivation

The products manufactured by the Chemical Process Industries (CPIs) are of greatest importance for the modern society. Chemical processes are born from the imagination of researchers and engineers. The person in charge with transforming a valuable idea in laboratory or on paper into an industrial competitive process is the designer. Its first motivation is the creation of new processes, or improving significantly the existing ones. The creative effort must be rewarded by substantial economic advantages. Thus, innovation and efficiency are key motivations for designers.

However, in the today's business and social environment we may add another dimension to creativity. Much more than in the past, the designer should be concerned about the rational use of resources and the preservation of the natural environment. The process has to be novel, efficient, and competitive in a global business environment, but also sustainable. The immediate conclusion is that the job of a designer is becoming increasingly complex and challenging. The designer has to integrate in his project a large number of constraints, and to deal often with contradictory aspects. For example, the selection of the suitable chemistry should avoid hazards and unsafe reactions. The process should be compact and economical in energetic consumption, but offer flexibility and ready to accept other raw materials or other specifications of products. The optimal combination of so many aspects gives highly *integrated processes*. The design of complex processes implies the availability of adequate conceptual methods and of powerful computer-based tools, which form nowadays the core of Process Systems Engineering.

Hence, in the today's world the key issue for CPIs is the innovation. We believe that the creativity cannot be left as a skill of some gifted persons or some powerful organisations. Creativity should be accessible to anyone having the basic professional knowledge and motivation for discovery. Creativity can be enhanced by systematic learning and training, thus is a teachable matter. It not excludes but reinforces the skills and motivation of individuals. The intellectual support for enhancing creativity is the use of systematic design methods. A systematic approach has at least two merits: 1) Provide guidance in identifying what is and what is not feasible; 2) Not a single solution but several alternatives are generated, corresponding to the decisions that the designer has to take. After ranking, following some performance criteria, as for example the Total Annual Cost, the most convenient alternative is refined and optimised. A remarkable feature of the systematic methods available nowadays is that these can set quasi-optimal targets well ahead the detailed sizing of the equipment.

The assembly of the systematic methods applied to chemical processes forms the new design paradigm designated today by *Process Integration*. Its application relies on the intensive use of *Process Simulation*. Combining design and simulation allows the designer to understand the behaviour of complex systems, to explore several alternatives, and on this basis to propose effective innovative solutions.

1.1.2 The road map of the book

The book contains five sections, each of several chapters, in total seventeen. The road map depicted in Fig. 1.1 allows the reader an easy orientation in different topics. Because the emphasis is on the design process, a large avenue links the introductory chapter on *Integrated Process Design* with the section devoted to *Design Project*, the final goal. The activities on the right side deal with the logistic issues regarding computing tools and methods, grouped in two blocks devoted to *Process Simulation* and *Thermodynamic Methods,* respectively. The other two blocks on the left side handle conceptual activities, namely *Process Synthesis* dealing with the architectural design, as well as *Process Integration* handling the development of subsystems and the allocation of resources, and their optimisation in the frame of the whole process. A rapid tour along this roadmap will allow the user to be informed about the key issues in each chapter before she or he will take more time for a longer stay.

The tour begins with the chapter on *Integrated Process Design.* The key topic is the *Sustainable Development* and its implications on the design of chemical processes, as *Production-Integrated Environmental Protection.* Integrated Process Design is described as the marriage of two types of activities: Process Synthesis - architectural design, and Process Integration - development and optimisation of subsystems in a flowsheet. This distinction, although somewhat artificial, serves in fact to better structuring of the chapters devoted to learn the logical development of a design. This chapter describes also concepts from systems engineering useful in the managing engineering projects.

The first part of the book presents generic principles and techniques in *Process Simulation* that enable an innovative and efficient use of any commercial software. Chapter 2 serves as *Introduction in Process Simulation.* Particular attention is paid to the systems analysis of a design problem by means of simulation, commonly called *flowsheeting.* This chapter presents elements of the software architecture, as well as the main integrated commercial systems. Chapter 3 develops in larger extent the *Steady state Flowsheeting.* Major topics include the description of generic flowsheeting capabilities, as degrees of freedom analysis, treatment of recycles, and use of control structures. Mastering the flowsheeting techniques allows the user to get valuable insights into more subtle aspects, as plantwide control problems. Chapter 4 is devoted to *Dynamic Flowsheeting*, nowadays a major investigation tool in process operation and process control.

It is largely recognised that inappropriate thermodynamic modelling is the most important cause of failure in computer-aided design. That is why a section of the book - *Thermodynamic Methods* - reviews theoretical principles and practical aspects regarding the computer-based methods for physical properties and phase equilibria. Chapter 5 describes the *Generalised Computational Methods* for *PVTx* systems, largely based nowadays on the use of equations of state. Chapter 6 develops the computation of *Phase Equilibria* by various thermodynamic models, classified in equation of state and liquid activity models. Particular attention is paid to the regression of model parameters from experimental data.

After having solved the logistic elements, the third part of the book - *Process Synthesis* - enters in the core of the design. This part teaches how to invent process flowsheets by a generic approach based on systems analysis and systematic methods. Chapter 7 develops in detail the systematic development of flowsheets by applying the *Hierarchical Approach.* The emphasis is set on the material balance envelope formed by the sub-systems of reactions and separations connected by recycles. Reactor-Separator -Recycle structure is the basis for further integration of units with respect to low energetic consumption and good controllability properties. Additional chapters are devoted to deeper analysis of the sub-systems for reaction and separations. Chapter 8 dealing with the *Synthesis of Reaction Systems* is particularly important. The key issue is the reactor selection and its integration with the other units. Stoichiometry and thermodynamic calculations can supply valuable insights to designer, even when kinetic data are not available. Chapter 9 presents the *Synthesis of Distillation Systems*, particularly the treatment of the azeotropic mixtures. Particular attention is given to the new systematic technology based on Residue Curve Maps.

Process Integration part addresses the combination of units in an optimal system from the point of view of energetic consumption, controllability properties and environmental performance. The principles of achieving optimal energy consumption are addressed in the Chapter 10 devoted to *Pinch Point Analysis*. Chapter 11 deals with *Practical Energy Integration* by presenting specific techniques for saving energy. The next two chapters develop new challenging issues concerning the integration between design and control. This topic corresponds to the requirements set to modern plants with respect to high flexibility in manufacturing, but safe and robust controllability characteristics. Chapter 12 review basic concepts in process dynamics and control with emphasis on *Controllability Analysis*. Chapter 13 is devoted to *Plantwide Control*, a recent concept dealing with the strategy of controlling the whole plant and its relation with the design of units.

The last part, *Design Project*, addresses specific subjects for carrying out conceptual design projects. Chapter 14 discusses teaching aspects in *Process Integration*, as the organisation of courses and design projects, at both undergraduate and postgraduate levels. The *Economic Evaluation* of design projects is treated in Chapter 15 from the perspective of profitability analysis. Chapter 16 develops some guidelines for the *Selection and Sizing of Process Equipment,* namely reaction vessels, separation columns, heat exchangers, and devices for the transport of fluids. The last Chapter 17 presents two comprehensive *Case Studies* illustrating the design and simulation of complex plants, including full dynamic simulation with control implementation. Helpful information for design projects is given in Appendices.

This book can be used as support in teaching Process Design and Simulation. The chapters 1-3, 7, 10-11 and 14-17 are suitable for setting up an undergraduate course in Process Integration. Complementary courses or self-study could be necessary for upgrading the knowledge in thermodynamics (Chapter 5-6) and chemical reaction engineering (Chapter 8). Advanced material is more suited in postgraduate or continuous education courses, particularly the chapters 4, 9, 12-13, and 17. The best manner to consolidate the knowledge and skills in process engineering is working out a *Design Project* for a complete plant.

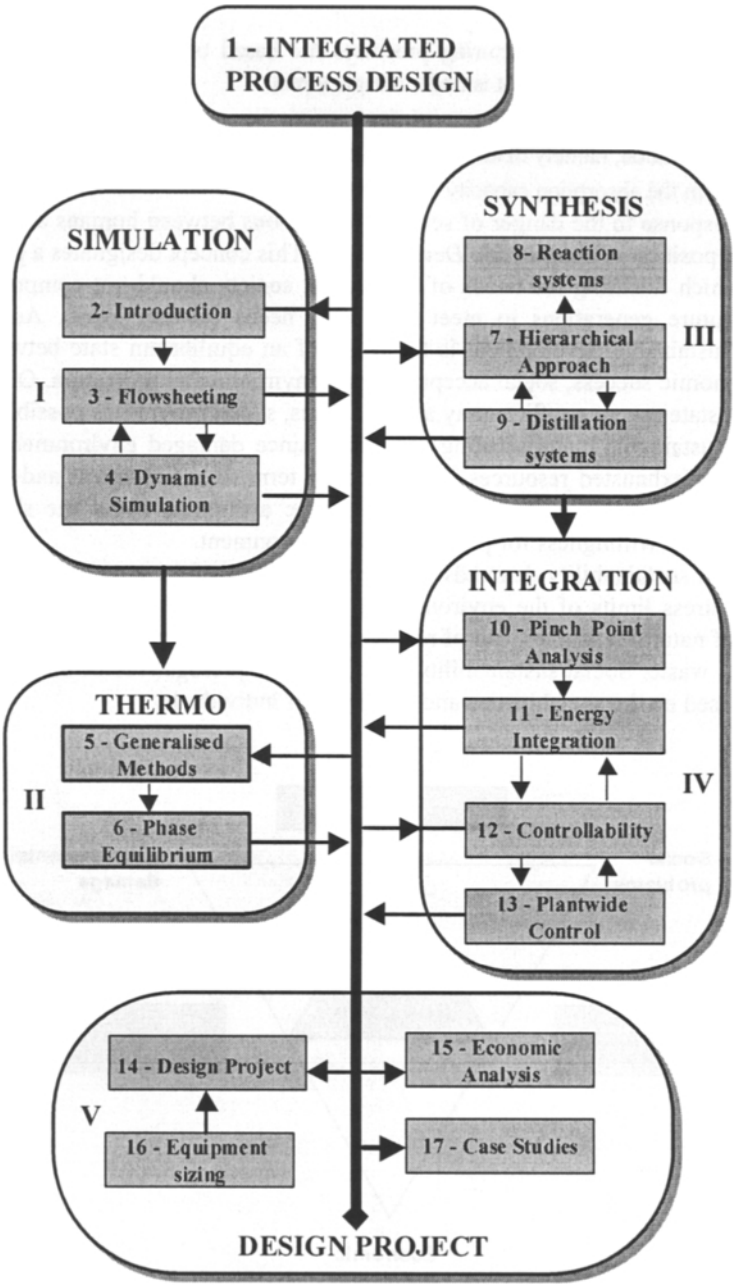

Figure 1.1 The road map of the book

1.2 SUSTAINABLE DEVELOPMENT

Nowadays, most of the manufacturing processes are based on the exploitation of fossil resources. The natural environment is under a triple threat:

- Exhaust of resources;
- Increased pollution, namely of air, water and soil;
- Reduction in the absorption capacity of the environment.

A rational response to the danger of severe dysfunctions between humans and nature is to adopt the position of *Sustainable Development*. This concept designates a production model in which fulfilling the needs of the present society should not compromise the ability of future generations to meet their own needs (Christ, 1999). As Fig. 1.1 illustrates, sustainable development is the result of an equilibrium state between three factors: economic success, social acceptance and environmental protection. Outside this equilibrium state severe conflicts may appear. Thus, social progress is possible only by employing sustainable manufacturing processes, since damaged environment and the perspective of exhausted resources lead at longer term to social unrest and economic decline. Therefore, it is imperative to develop the awareness about the shortage of resources and the willingness for preserving the environment.

Ecological sustainability demands to defend the bases of the natural life and not to exceed the stress limits of the environment. Economic sustainability means efficient utilisation of natural resources, use of renewable materials and alternative energies, and recycling of waste. Social sustainability recognises the prerogatives of the free market economy based on the social justice and the rights of individuals.

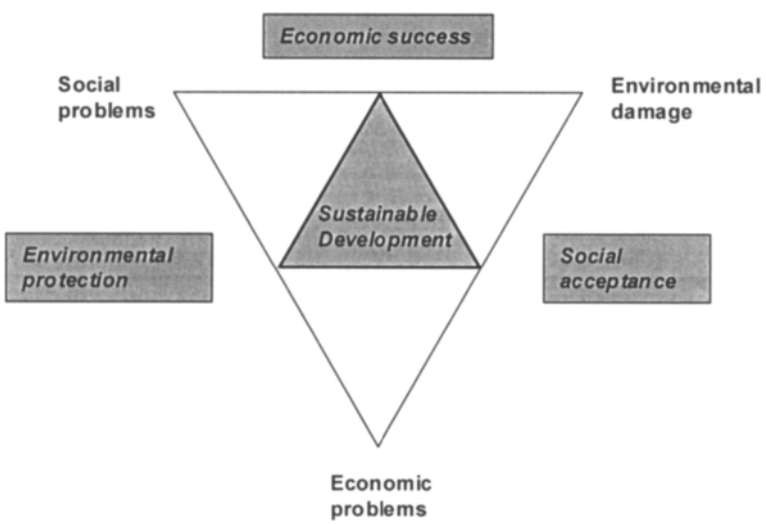

Figure 1.2 The concept of Sustainable Development (after Christ, 1999)

Chemical Process Industries are vital for the modern society. However, often these are perceived as major sources of risk and pollution. Modern technologies must face the challenge of changing this negative image into a safe and environmental friendly look. In addition, chemical processes must be more intensive. Modern plants should occupy a much modest place in the landscape compared with the old industrial giants, and offer absolute safety in operation.

An efficient use of scarce resources by non-polluting technologies is possible only by a large innovation effort in the research, development and design of processes. Sustainability must be integrated in the design practice, primarily by minimising and recycling the waste produced in the process, and not only by end-of-pipe corrections. In this respect, a systemic approach of the whole supply chain allows the designer to identify the stages of inefficient use of raw materials and energy, as well as the sources of toxic materials and pollution. Developing sustainable processes implies the availability of consistent sustainability measures.

1.3 PROCESS DESIGN

1.3.1 Creative aspects in Process Design

The following definition due to J. Douglas (1988) highlights the process design as an eminently creative activity:

Process Design is the creative activity whereby we generate ideas and then translate them into equipment and process for producing new materials or for significantly upgrading the value of existing materials.

Conceptual Design designates the part from the design project that deals with the basic elements defining a process: flowsheet, material and energy balances, specifications and equipment performance, utility consumption, safety and environmental issues, as well as economic efficiency. Therefore, in conceptual design the emphasis is on the behaviour of the process as a system rather than on the sizing of the equipment items.

It is important to note that conceptual design is responsible for the most part of the investment costs in a process plant, even if its fraction in the project's fees is very limited. An erroneous decision at the conceptual level will propagate throughout the whole chain of the detailed design and equipment procurement. Even much higher costs are necessary later in operation to correct misconceptions in the basic design.

Figure 1.2 illustrates the economic incentives of a plant project, from the conceptual phase down to construction and commissioning (Pingen, 2001). Conceptual phase takes only 2% of the total project cost, but it may contribute with more than 30% in cost-reduction opportunities. In the (detailed) design phase the cost of engineering rises sharply to 12%, but saving opportunities goes down to only 15 %. In contrast, the cost of procurement and construction are more than 80%, but the savings are below 10%. At the commissioning stage the total project cost is frozen.

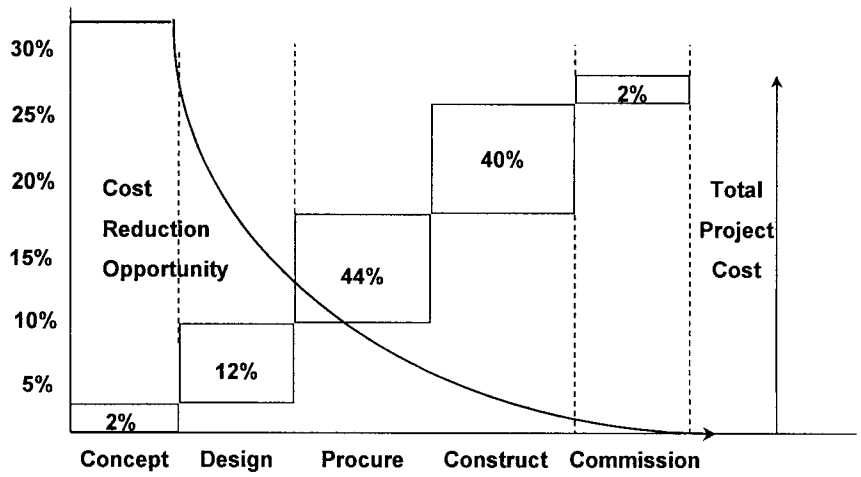

Figure 1.3 Economic incentives in a project

The long way from an idea to a real process can be managed nowadays by means of a systemic approach. This involves systematic methodologies for designing the whole process and its sub-systems, as reaction, separations, heat exchangers network and utilities.

A methodology consists of a combination of analysis and synthesis steps. In this context, we mean by *Analysis* activities devoted to the knowledge of the system's elements, as the investigation of physical properties of components and mixtures, performance characteristics of reactors and unit operations, or the evaluation of profitability. *Synthesis* deals with activities aiming to determine the architecture of the system, as well as the selection of the suitable components.

In the past, the development of a new process has been described often as a kind of 'art'. The strategy, called sometimes the *engineering method*, consisted of sketching a simple but inspired flowsheet, and improving it by successive layers of refinements, up to final optimisation. The experience of the designer, the expertise of the company, and the availability of pilot data were crucial.

Nowadays, the conceptual design of processes is becoming increasingly an applied chemical engineering science. Engineers having a solid scientific background and mastering computer design tools are capable of finding much quicker innovative ideas. Inspiration and expertise still play an important role, as well as the availability of practical data. Actually, the combination of science and engineering art makes the conceptual process design a fascinating challenge!

A design problem is always under-defined, either by the lack of data, or insufficient time and resources. Moreover, a design problem is always *open-ended*. There is never a single solution. The solution depends largely on *design decisions* that a designer has to take at different stages of project development to fulfil technical or economical constraints, or simply to avoid licence problems.

The systematic *generation of alternatives* is the most important feature of the modern conceptual design. The best solution is identified as the optimal one in the context of constraints by using consistent evaluation and ranking of alternatives.

1.3.2 Trends in Process Design

Process Intensification

Process Intensification designates the development of techniques and new equipment that can achieve significant improvement in productivity, as well as in the energetic efficiency and environmental friendliness of processes. The development in this field can be classified in two areas (Stankiewicz and Moulijn, 2000):

- *Process-intensifying equipment*, such as novel reactors, intensive mixing, heat-transfer and mass-transfer devices;
- *Process intensifying methods*, such as the integration of reaction and separation steps in multifunctional reactors (examples: reactive distillation, membrane reactors, fuel cells), hybrid separations (example membrane distillation), alternative energy sources, and new operation modes (example periodic operations).

Firstly, process intensification leads to a significant reduction in the equipment size and cost. Another benefit is the reduction of safety and ecological risks due to smaller inventories, particularly important in the case of hazardous materials. Mobile plants could bring the manufacture of dangerous chemicals closer to the end-user, eliminating costly storage and transport. Process intensification is also needed for developing equipment for emerging technologies, particularly in biochemical engineering.

In this perspective, the survival of the classical unit operations might be seen critical. It is reasonable to expect that unit operations, as distillation, absorption and extraction, will continue to be used, particularly in the field of large-scale commodities. Nevertheless, new designs will offer much higher productivity as today.

Process Engineering

Increasing globalisation, as well as tighter safety and environmental constraints will bring major changes in the methods and tools of process engineering. Because of the capital-intensive nature of process industries, the main equipment items having long lifetimes, there is an important resistance in implementing new technologies. However, on long-term the change is unavoidable. Figure 1.3 depicts some major directions of progress in Process Engineering (Keller and Bryan, 2000):

1. *Raw material-cost reduction.* High valorisation of raw materials is the factor with the strongest impact on process efficiency. In this respect, the breakthrough element is the chemistry. Here we mean also the development of more active and selective catalysts. Enhancing the selectivity of reactions can eliminate material and energy recycles and contributes significantly to massive cost reduction. The combination of reaction and separation steps in more compact devices eliminates intermediate costly separations, as in the case of novel processes based on reactive distillation or multifunctional reactors.

2. *Capital-investment reduction.* As mentioned, process intensification lead to significant reduction in the equipment size and capital costs. However, reducing the number of units by better flowsheet design can have a larger impact.
3. *Energy-use reduction.* Wide-range implementation of Pinch Point Analysis and Total Site integration are the most important factors in energy saving.
4. *Increased process flexibility and inventory reduction.* Computer Integrated Manufacturing systems designates the integration of plant operation with business activities. The integration has to consider not only planning and accounting tools, but also rigorous modelling technology. Process flexibility should be seen not only in term of variable production rate, but also in term of composition of the feedstock. Reduced inventory asks for the suppression of intermediate costly storage facilities.
5. *Emphasis on process safety.* Inherently safety can be achieved by incorporating more non-linear analysis in process dynamics and control.
6. *Increased attention to quality.* Reduction of impurities and by-products, and implementing advanced control systems can ensure constant product quality.
7. *Better environmental performance.* Modern process design should aim to zero-effluent plants by minimisation of gaseous emissions and of process waste, including wastewater.

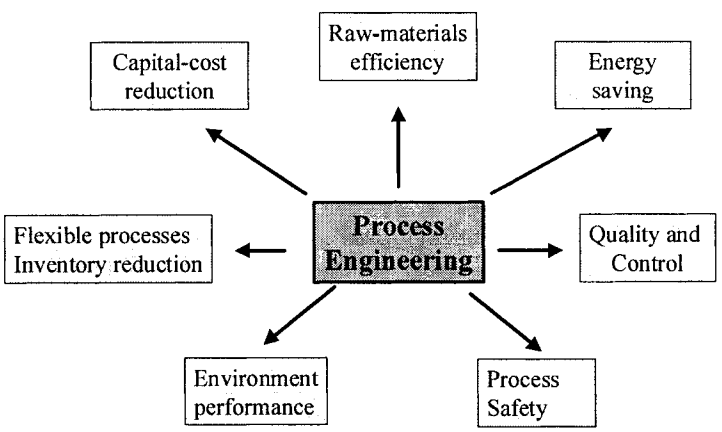

Figure 1.4 Main directions in Process Engineering

The challenges raised by the above themes prefigure the advent of a new paradigm in process engineering, the integration of Process Design with Research & Development. For example, the simulation of virtual alternative flowsheets should start at the discovery stage in laboratory. The simulation will highlight the key variables in design, and as a result, the experimental research will be performed on the interval of temperatures, pressures and concentrations really needed later in design. Some data needs only laboratory-bench experiments; some data make necessary the development of cold or hot pilots. Note that the running plants are valuable sources of experimental data. For example, VLE measurements on industrial distillation columns offer good opportunities for the calibration of thermodynamic models.

1.4 SYSTEMS ENGINEERING

1.4.1 Systems approach

McGraw-Hill Dictionary of Engineering (1997) gives the following definitions:
1. *System* is a combination of a several pieces of equipment integrated to perform a special function.
2. *Systems Analysis* is the investigation of an activity, procedure, method, technique, or business to determine what must be done and how the operation may be best accomplished. It consists of applying mathematical techniques to the study of systems.
3. *Systems Engineering* is the design of a complex interconnection system of many elements to maximise an agreed-upon measure of the system performance, taking into consideration all the elements related in any way to the system.

Systems Engineering applied to scientific and engineering activities regarding chemical-like processes is designated by *Process Systems Engineering*.

Properties belonging to the system, but not obvious from the properties of components, are called *emergent*. For instance, the taste of water or the flavour of a fragrance can be easily identified, and not only by experts, although these cannot be attributed to any single chemical component. Similarly, the 'operability' of a process is an emergent property of design, control and operation that the operators can acknowledge.

Systems approach consists of two steps:

- Modelling, in which each element of the systems is described and criteria for measuring performance are assigned;
- Optimisation, in which adjustable parameters are set in a manner that gives the best performance of the whole system.

Mathematical modelling makes use of computer simulation as the main tool of investigation. A systemic design deals mainly with the identification of parts (sub-systems, components) and their connection, as well as with optimal targets for parts.

1.4.2 Life cycle modelling

Life cycle is a concept of systems engineering based on the assumption that every product has a finite existence, sealed by three major events: initiation (conception), installation (birth) and termination. In between there are two main periods, called here 'initial development' and 'operation'. The last may be divided roughly in 'immaturity', 'maturity' and 'decay'. The life cycle of a product describes the evolution of its potential from conception to termination (Fig. 1.5). The potential grows continuously to a maximum, after which the decline is inevitable.

Life cycle forms are generic frameworks used in systems engineering to manage the development and maintenance of complex systems. These forms have been developed for the needs of software engineering, but can be applied to other complex activities, as for example car production or architectural works. The life cycle forms are also suitable to capture the formalism of organising a team work devoted to achieve an objective in short time with high degree of reliability.

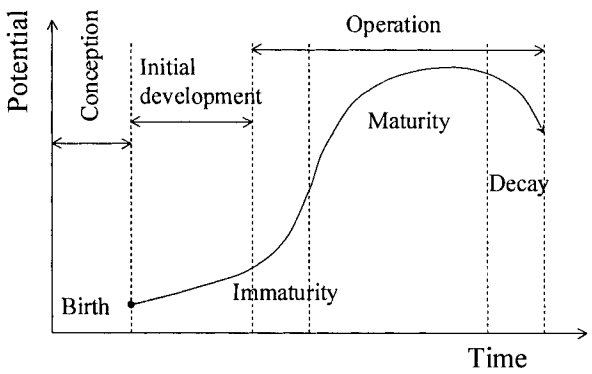

Figure 1.5 Life cycle evolution

We will describe here three basic life cycle forms: waterfall, V-model and spiral model. These forms are suited for the design of computer-based systems, but they may have larger applicability, particularly in the field of process engineering. The general theory is presented elsewhere (Thomé, 1993). Life cycle models can be used to manage the elaboration of a design project, or the development of a sophisticated simulation system for design, operation or computer integrated manufacturing.

Waterfall model

Waterfall model decomposes the development/production cycle of a complex project in four phases (Figure 1.6):

1. Requirements and system definition.
2. System design.
3. Implementation and test of units.
4. Systems test.

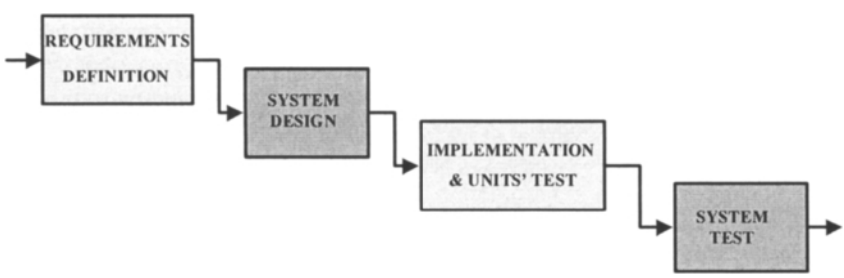

Figure 1.6 Life Cycle Waterfall Model

The above description of a waterfall model seems simplistic, but in fact expresses deliberately the key features of a systemic approach of a complex problem. The phases must be clearly defined such as the output of one falls cleanly into the input of the next.

Clear definition of *Requirements* comes first. The next phase is the *System (architectural) Design*. Systemic design precedes always the detailed design. The modelling of units should be at the level of detail capable to capture the behaviour of the system. After solving appropriately the conceptual phase, the project may proceed with the *Implementation and Units' Test*, and finally with the *System Test*.

Waterfall model indicates that the project sequencing should be organised such to avoid feedback between phases, particularly to review the architectural design. This important drawback regarding the flexibility and uncertainty the can be better treated by V-cycle or spiral models explained later.

The waterfall form can be related to the framework of an integrated design project following the Hierarchical Approach, as it will be explained in Chapter 7. As depicted in Fig. 1.7, the development of an (idealised) design project can be decomposed in four major phases: *Requirements*, *Conceptual Design*, *Basic Design*, and *Detailed Engineering*. Typical integration and simulation activities concerning each phase are displayed also. For example, the flowsheet developed during the *Conceptual Design* phase consists of the reactor and separation systems. Other systemic issues solved at this level are safety, hazards, environmental targets, plantwide control objectives and economic feasibility. By using Process Integration techniques targets for utilities, water and solvents may be assessed well ahead the design of units. Process Simulation consists mainly of material and energy balances. As mentioned, during the conceptual design several alternatives are developed, from which a base-case will be selected for further refinement and optimisation.

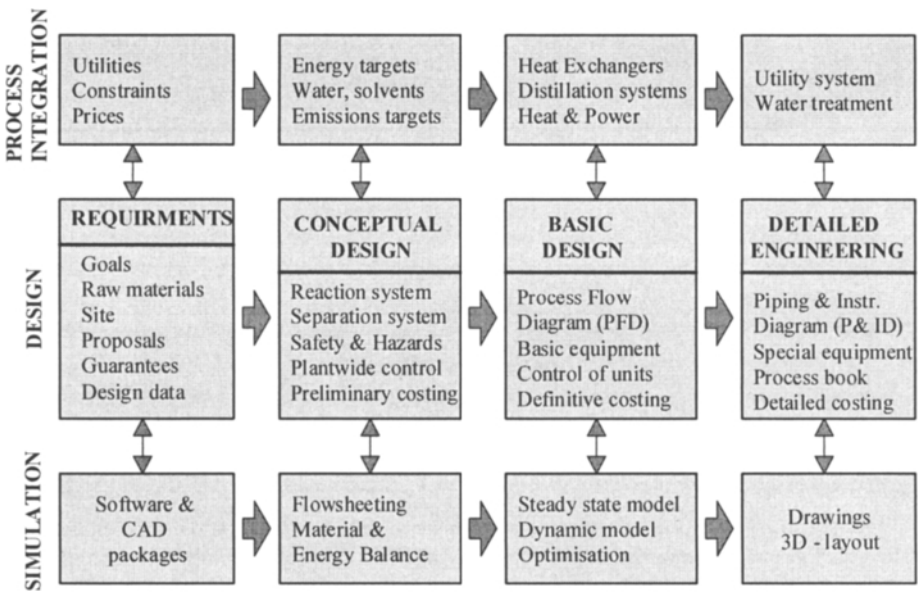

Figure 1.7 Life cycle of an integrated design project

The evolution of the selected alternative is continued in the *Basic Design* phase, by the integration of subsystems, which lead to final Process Flow Diagram (PFD). Specific integration activities regard the design of the heat exchanger network, the energetic integration of distillations, or combined Heat & Power generation. Completing the flowsheet, leads to the generation of a steady state plant model. This can be used later in plant operation. In parallel, a dynamic model can be developed for supporting the design of the process control system. *Detailed Engineering* is the downstream activity before commissioning, where the components of the project are assembled. In reality, some backflow exists between different phases, but this should be kept limited, and only between adjacent phases. For example, the modification of the conceptual design at the detailed engineering level is highly undesirable. Note that *parallel engineering* may be used to improve the overall efficiency of a design project.

V-cycle model

The **V**-cycle model (Fig. 1.8) is appropriate for managing complex systems when systematic validation is necessary. The two basic ideas are: 1) decompose the work in a number of tasks, and 2) separate 'specification & design' tasks from 'production' tasks.

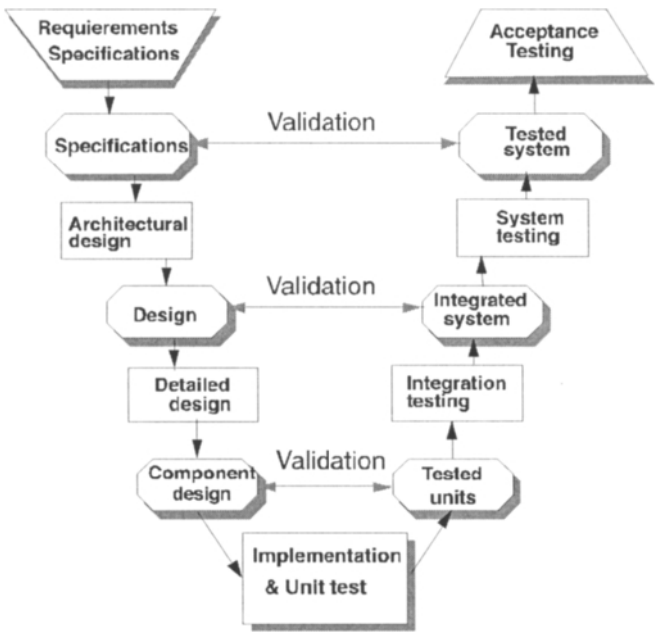

Figure 1.8 A generic V-cycle model

The left side of the cycle represents the *refinement of design,* while the right side describes the *assembly* tasks. The bottom of the **V** handles detailed design and test of units. Note that in a **V**-cycle the project management and quality assurance are carried out together. Each design step is verified before proceeding to the next one, and each production task is validated against the corresponding specification task. Here,

verification means that the product fulfils the quality characteristics, such as consistency, completeness and correctness, while *validation* means that the product satisfies the specifications. Unforeseen problems can be managed by cycling through specification-implementation-testing procedures.

The **V**-cycle model can be used as a generic framework for managing engineering projects. It is also a powerful concept in supervising the development of any complex system, as the development of a Plant Simulation Model (see Chapter 2). This is a software tool based on rigorous modelling that can be used firstly in diagnosis of operation problems and later, in revamping, debottlenecking and retrofitting projects.

Spiral model

The spiral life cycle model is a repeating waterfall form at successive levels of detail. In addition, it may accommodate unforeseen events by a *risk-driven approach.* Similar tasks but with different objectives are performed during each cycle iteration. The inner cycles carry out more evaluation and prototyping tasks, while the outer cycles deal with final design. The cumulative cost versus time is measured at each level. These characteristics make this life cycle a generic design frame, both in feasibility studies and technical proposals, as well as in contractor engineering projects.

In conclusion, the above life cycle forms are conceptual frameworks for organising a project, but not substitutes for planning tools. It is important to keep in mind that the architecture of the system is the goal, and must precede always the detailed design of components.

1.5 INTEGRATED PROCESS DESIGN

1.5.1 Process Synthesis and Process Integration

Process Integration (PI) emerged in the decade of 1980-90 as a new discipline in chemical engineering with emphasis on the efficient use of energy. PI revealed that significant energy saving can be achieved by analysing the problem only in the context of the whole process (system), and not from the viewpoint of the stand-alone units.

The traditional process design consists of a hierarchy of phases that can be depicted by an *Onion Diagram*, as illustrated in Fig. 1.9 (Linnhoff, 1994). Process design starts with the Reactor (R). Based on the mixture composition at the reactor outlet, the development continues with the Separation system (S). Then, the design addresses the Heat Recovery (H) and Utility (U) systems. It is clear that the complete separation of the above activities is not possible. For example, the plant energy management is intimately linked with the reactor design. Similarly, separation system, heat exchanger network and utility systems are interrelated. After a first trial, the designer should 'go back to the onion' and review the basic design.

It is clear that between different units and sub-systems there are large interactions. Actually, the complex plants are characterised by the existence of recycles of materials and energy, which make necessary their integration in a rational and systematic manner.

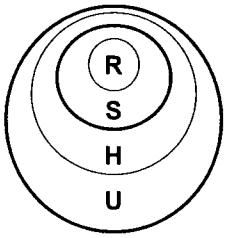

R – Reactor system
S – Separation system
H – Heat Recovery system
U – Utility system

Figure 1.9 Hierachical description of process design by the Onion diagram

It may be observed that the two inner layers, Reactor and Separations, define the *material balance envelope*. Moreover, these define the *basic structure* of the flowsheet also, which is the object of a design activity named *Process Synthesis*. The outer layers of Heat Recovery and Utility systems deal with the *heat balance envelope*. Both are objects of a design activity that was called *Process Integration*.

Up to 1990, Process Synthesis and Process Integration were considered largely as separate although complementary activities. A definition originated in 1995 from International Energy Agency (IEA) states Process Integration as "Systematic and general methods for designing integrated production systems, ranging from individual processes to total sites, with special emphasis on the efficient use of energy and reducing environmental effects" (Gundersen, 2002).

However, in the recent years the frontier between Process Synthesis and Process Integration has become vague and practically disappeared. A large number of activities, considered of synthesis-type, deals with integration problems too. For example, one cannot handle the optimal synthesis of distillation sequences without consider the minimisation of energy. Conversely, the best energy saving is achieved when the basic flowsheet structure is redesigned. Since the label of Process Integration appears more attractive, highlighting the scope of the modern process design - optimal integration of different units in a process system - many research groups around the world have adopted it.

In this book, we take the position that Process Synthesis and Process Integration are high complementary activities that form together the paradigm of the *Integrated Process Design* (IPD)[1]. Figure 1.10 depicts the concept by means of a representation similar with the Onion Diagram. Some differences are visible. Process Synthesis focus on the Reaction-Separation-Recycle structure that defines the material balance envelope and the flowsheet architecture. Process Integration deals mainly with energy recovery, but includes two supplementary layers: E - Environmental protection, and C - Controllability, safety and operability. In addition, the Utility layer (U) considers Site Integration. Synthesis and integration activities are interrelated. Some can be solved sequentially, some need simultaneous solution.

---

[1] In some engineering companies, IPD is understood as the integration of design and software tools in a coherent engineering framework. We prefer for it the label Integrated Process Engineering (IPE).

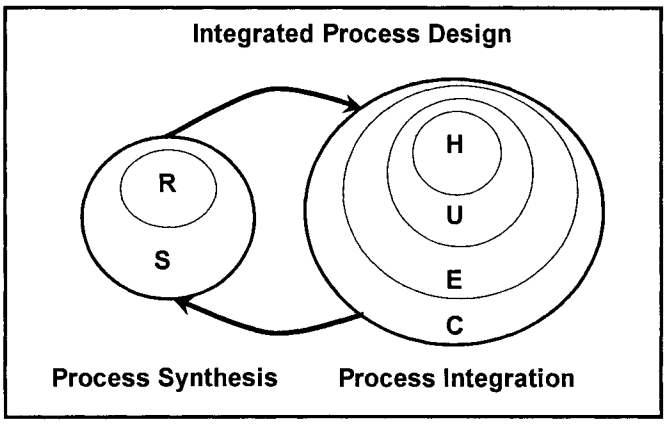

Figure 1.10 Integrated Process Design approach

Independent of the classification problem, it is clear that both Process Synthesis and Process Integration are systems-oriented activities and belong to the same conceptual purpose. Key features of an Integrated Process Design are listed below:

1. The main objective is the architecture of the process (flowsheet structure). Systemic design techniques are today available that are capable to determine optimal targets for sub-systems and components without detailed modelling of equipment. In this way, the detailed equipment sizing becomes a downstream activity.
2. IPD consists of developing alternatives rather than a unique flowsheet. The selected solution fulfils at best the optimisation criteria and the environment of constraints.
3. Computer simulation is the main tool for analysis and synthesis. However, the quality and efficiency of the final design depends on the capacity of the designer to integrate generic software capabilities with specialised engineering skills.
4. IPD addresses both new design, as well as debottlenecking and retrofit projects. The methods and tools of IPD can be applied to any type of process industries.

We stress again the importance of developing alternatives and of setting targets well ahead the sizing of equipment. The last feature indicates a qualitative change that take distance from the concept of unit operations in favour of a more generic approach based on generic *tasks*. Using tasks instead standard unit operations facilitates the invention of non-conventional equipment that can combine several functionalities, as reaction and separations. This approach is designated today by Process Intensification. Moreover, this is more suited for applying modern process synthesis techniques based on the optimisation of superstructures.

1.5.2 Systematic methods

In the last two decades, a number of powerful systematic techniques have emerged to support the Integrated Process Design activities. These can be classified roughly as:

- Heuristics-based methods
- Thermodynamic analysis methods
- Optimisation methods.

The principles of the systematic design of process plants have been organised for the first time by Jim Douglas (1988) in the frame of a methodology for conceptual process design. Other excellent books have been published since, as by Smith (1995), Biegler, Grossmann & Westerberg (1998), and Seider, Seader & Lewin (1999). Today the field of Integrated Process Design is an active area of scientific research with immediate impact on the engineering practice. Methods accepted by the process engineering community are described briefly below, but these will be developed in more detail in different chapters of the book.

Hierarchical Approach

Hierarchical Approach can be applied for the synthesis of the whole flowsheet. The methodology consists of decomposing a complex problem in simpler sub-problems. The approach is organised as 'levels' of design decisions and flowsheet refinement. Each level makes use of heuristics to generate alternatives. Consistent evaluation eliminates unfeasible alternatives, keeping only a limited number of schemes for further development. Finally, the methodology allows the designer to develop a good 'base-case', which further can be refined and optimised by applying integration techniques. Chapter 7 presents in detail this approach.

Pinch Point Analysis

Pinch Point Analysis deals in the first place with the optimal management of energy and the synthesis, as well as with the design of the corresponding heat exchanger network. The approach is based on the identification of the *Pinch Point* as the region where the heat exchange between the process streams is the most constraint. Chapter 10 will explain the theoretical principles, while Chapter 11 will develop in more detail the applications. The Pinch concept has been extended to other systemic issues, as process water saving and hydrogen management in refineries.

Residue Curves Map

The feasibility of separations of non-ideal mixtures, as well as the screening of mass separation agents for breaking azeotropes can be rationalised by means of thermodynamic methods based on Residue Curve Maps (Chapter 9).

Attainable Region

The synthesis of the chemical reaction systems can be placed in a generic conceptual approach based on the mathematical properties of the reaction rate vectors (Chapter 8).

Mathematical Programming

A process synthesis problem can be formulated as a combination of tasks whose goal is the optimisation of an economic objective function subject to constraints. Two types of mathematical techniques are the most used: Mixed Integer Linear Programming (MILP), and Mixed Integer Non-linear Programming (MINLP). Mathematical Programming is embedded today in some software for the optimal design of heat exchanger networks.

Superstructure optimisation

Process synthesis by superstructure optimisation consists of the identification of the best flowsheet from a superstructure that considers many possible alternatives, including the optimal one. Set in this term, the approach seems extremely complicated. An obvious theoretical advantage would be that allows the designer to consider simultaneously the synthesis and integration problems. Another practical advantage is the automation of the design process. However, there are two major difficulties:

- How to generate a comprehensive superstructure and what is the guarantee that the optimal one is embedded in the superstructure?
- How to manage the large size of the problem and its strong non-linear character?

The first issue could be addressed by considering a large redundancy of units and connections, but it is clear that this manner has little conceptual value. Incorporating alternatives discovered by applying other systematic techniques, for example thermodynamic or heuristic methods, seems more rational. Therefore, superstructure optimisation and synthesis techniques based on physical principles can be seen as complementary.

The second issue regards more the algorithmic approach. Because the efficiency of mathematical techniques in optimisation depends greatly on the nature of the problem, both conceptual and algorithmic aspects should be analysed simultaneously. For more details regarding mathematical programming and optimisation with application in integrated process design, see the book of Biegler, Grossmann and Westerberg (1998), the authors being recognised as scientific authorities in this field.

1.5.3 Trends in Integrated Process Design

Process Integration is a wide scope discipline of process engineering embracing all the activities dealing with optimal conceptual design and technology improvement. Process Integration goes far beyond energy saving. The major directions in research with applications in process design are presented below with indications to the chapters in this book where the topic is discussed in more detail. More references regarding the scientific publications can be found in the literature study due to Gundersen (2002) available on Internet.

Efficient use of raw materials

a. Novel reactor systems.

New design methodologies for chemical reaction systems try to go beyond the classical CSTR and PFR models. The systematic methods developed so far are based on the concept of Attainable Region and on Mathematical Programming (see Chapter 8).

b. Analysis of recycle systems.

Because of tight material and energetic integration, strong interactions between units can occur. Mastering the conceptual problems raised by the recycle systems enables a better design of complex plants. The research in this area is also at an incipient stage (see Chapter 13).

c. *Reactive separations.*

Housing the reaction and separation in the same unit could lead to significant savings in both capital and operation costs. Reactive (catalytic) distillation has received an increased interest in the recent years. Several industrial applications demonstrate its benefits, as shown in Chapter 7.

d. *Separation of non-ideal mixtures.*

The synthesis of separation sequences for non-ideal mixtures is handled nowadays by means of Residue Curve Maps. Major issues are feasibility and entrainer selection. However, there are still important unsolved problems (Chapter 9).

e. *Design of mass exchange networks.*

Similarly to energy integration, techniques have been developed for targeting and optimisation of operations based on the exchange of mass. Simple graphical representations are not available yet, but appropriate computer methods could facilitate the application of this concept in the design practice in the future.

f. *Hydrogen management.*

Hydrogen is today a major product because its large-scale application in refining and from the perspective of fuel cells for the automotive industry. 'Hydrogen Pinch' method has been developed to optimise the use and production of hydrogen in the context of integrated sites (Chapter 11).

Energy efficiency

a. *Complex columns.*

The complex columns can drastically reduce the costs of separations by performing several tasks in the same shell. Design methods based on mixed-integer linear programming (MILP) can avoid the combinatorial explosion, and can take into account other separations techniques besides distillation.

b. *Thermally coupled distillation systems.*

The coupling of distillation columns can offer substantial savings in energy. Chapter 11 shows some solutions, but industrial acceptance makes necessary more studies on design and control.

c. *Cogeneration and site utility systems.*

Cogeneration consists of simultaneous production of heat and electricity. This method is particularly attractive in the case of processes involving high exothermal reactions. Efficient solutions of cogeneration can be found by Total Site analysis (Chapter 11).

d. *Design of low-temperature systems.*

Refrigeration is a particularly expensive operation. Significant saving can be achieved by considering multilevel and cascaded systems, as well as by using mixed-refrigerants fluids. The design of refrigeration systems should follow the Pinch Point Analysis (Chapter 10), as well as Total Site analysis (Chapter 11).

e. *Automatic design of heat-exchanger network.*

Automatic design techniques of the heat exchanger network can increase dramatically the designer's productivity, making free more time to conceptual tasks. New techniques are available for retrofitting existing networks, as well as for guiding the implementation of heat intensification devices.

Emissions reduction

a. *Water system design.*

Similarly to heat saving, a 'water-pinch' method has been developed to rationalise the recycling of process water and optimise the load of wastewater treatment.

b. *Minimisation of flue-gas emissions.*

The minimisation of gas emissions as CO_2, SO_2, NO_x and other acid gases is a key topic in sustainable process design. This problem can be handled only by a systematic approach of all the pollution sources generated by energy integration, namely the utility system, heat recovery and cogeneration, as well as by process modifications.

c. *Ecologic characterisation of processes*

A systematic approach based on flowsheeting, steady state and dynamic, can be applied in view of eco-balances of impurities and hazards substances, both at the level of plants and industrial sites. Methods for assessing environmental performances of processes are desirable. Some new sustainability measures are discussed at the end of this chapter.

Controllability and Operability

a. *Integrated Design and Control*

The relation between design and controllability is a modern topic in Process Integration, and it is also a distinctive feature of this work. Chapter 12 describes the principles of controllability analysis oriented to design.

b. *Plantwide Control of integrated systems.*

Tight integration of units has as result stronger interactions through recycles of material and energy. The implementation of control structures for units should take into account not only their stand-alone performance, but also the interrelation with the other units. The interactions can have in some cases a negative effect on performances, but there are situations when the interactions are beneficial. Moreover, there are issues as production rate, quality of products, emissions control, etc., which regard the whole plant, not only some particular units.

Plantwide control has emerged in the last years as a design activity dealing with the best strategy of controlling the whole plant, and its relation with the design and control of units. The research in plantwide control area is supported today by the progress in software technology for dynamic simulation. Chapter 13 presents some recent developments in this area.

1.6 PRODUCTION-INTEGRATED ENVIRONMENTAL PROTECTION

1.6.1 Concepts of environmental protection

The manufacture of a desired product implies the use of raw materials and energy, as well as of auxiliary chemicals (solvent, catalyst, neutralisation agents, inert gas, etc.). The chemical route consists of main reactions and side-reactions. Thus, from ecological point of view the following generic relation can describe a manufacturing process:

$$(A+B+I) + (M+C+H) \xrightarrow{E} P + S + R + W + F$$

As inputs we have: main reactant A, co-reactant B, and impurities in the initial materials I, all forming the *raw materials*. Other *auxiliary materials* are: reaction medium M, catalyst C, and helping chemicals H. The process requires an amount of energy E, in most cases supplied from hydrocarbon sources. As outputs we have: main product P, secondary product S, residue R and waste W. The term *residue* signifies all by-products and impurities produced by reaction, including those generated from the impurities in raw materials, which have no selling value and are harmful for the environment. On the contrary, the secondary products may be sold. The term *waste* means materials that the cannot be recycled in the process. Waste can originate from undesired reactions involving the raw materials, as well as from the degradation of the reaction medium, of the catalyst, or of other helping chemicals. A separate term F accounts for emissions, as CO_2, SO_2 or NO_x, produced in the process or by the generation of steam and electricity.

Sustainable chemical production requires maximising the amount of the desired product P, while diminishing down to zero the amount of residues, waste and emissions. Minimum waste can be achieved in industry by the following approaches (Christ, 1999):

1. Production-integrated environmental protection.
2. End-of-pipe antipollution measures.

Production-integrated environmental protection implies that ecological issues take part from the conceptual design activities, starting with the earliest stages. Two directions can be envisaged:

- Development of intrinsically environmental friendly processes by avoiding the production of impurities in reactors,
- Recycling of waste in the manufacturing process.

End-of-pipe measures could be applied when the amount of waste is rather limited, or if there is no other possibility. As examples we may mention:

- Transformation of residues in environmental benign waste, as for example incineration of organic waste, or solidification followed by landfill,
- Gas cleaning of sour components by chemical adsorption,
- Removal of volatile organic components (VOC) from purges,
- Waste water treatment.

End-of-pipe measures can fix the pollution problem, but do not remove its cause. Sometimes the problem is solved only apparently. From a systemic viewpoint, the solution might be even a disadvantage. For instance, acid-gas scrubbing may cut air pollution, but creates liquid or solid chemical pollution, without regarding the pollution associated with the manufacture of supplementary chemicals.

End-of-pipe measures can be implement at short-term, need modest investment and do not imply process modifications. In contrast, production-integrated environmental protection necessitates longer-term policy and commitment towards sustainable development.

Figure 1.10 illustrates the difference between the two approaches. In the integrated approach, all residues and material waste are recycled, so that finally only saleable products leave the plants. The use of energy is optimal. On the contrary, the end-of-pipe measures handle the pollution problems at the end of the manufacturing process when residues and waste cannot be recycled.

Summing up, the following measures can be recommended for improving the environmental performances of a process:

- Change the chemical route. However, this measure is heavily constraint in practice by the available raw materials.
- Replace homogeneous catalyst by heterogeneous solid catalyst.
- Improve the selectivity of the reaction steps leading to the desired product by using more selective catalyst.
- Optimise the conversion that gives the best product distribution. Low conversion gives typically better selectivity, but implies higher recycling costs. Recycle costs can be reduced by energy integration and process intensification.
- Change the reaction medium that generates pollution problem. For example, replace water by organic solvents that can be recovered and recycled.
- Purify the feeds before the chemical reactors to prevent the formation of secondary impurities, more difficult to remove.
- Replace toxic or harmful solvents with inoffensive materials.

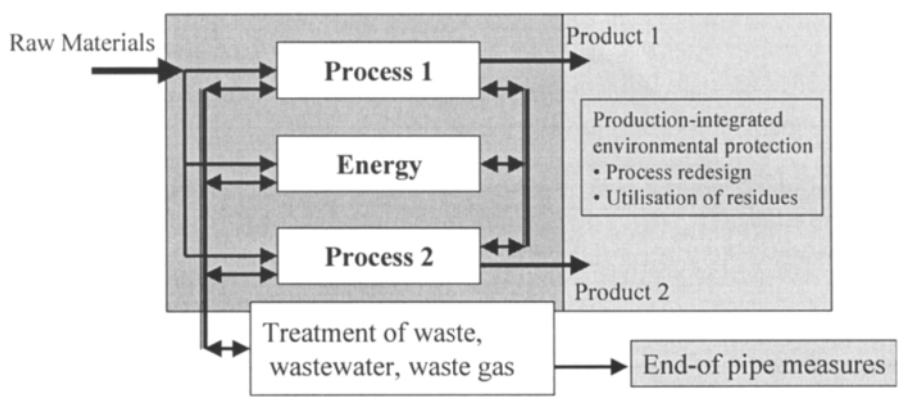

Figure 1.11 Approaches in environmental protection (after Christ, 1999)

1.6.2 Measures for environmental efficiency

The following measures can be used to evaluate the environmental efficiency of a process in term of material flow analysis (Christ, 1999).

Stoichiometric yield can be calculated as the ratio between the actual product to the theoretical amount to be obtained from the reference reactant:

$$RY = \frac{\nu_A}{\nu_p}\frac{M_A}{M_P}\frac{m_p}{m_A} \tag{1.1}$$

This measure is useful, but gives only a partial image on productivity, since it ignores the contribution of other reactants and auxiliary materials, as well as the formation of secondary products. From this point of view, the next indices are more suitable.

Theoretical balance yield BA_t is a measure of an ideal process. In contrast with the stoichiometric yield, the theoretical balance yield is calculated as the ratio between the moles of the target product and the total moles of the primary raw materials (*PRM*), including all reactants involved in the stoichiometry of the synthesis route:

$$BA_t = \frac{amount\ of\ \ target\ \ product}{amount\ \ of\ \ primary\ \ raw\ \ materials} = \frac{m_P}{\sum m_{PRM}} \tag{1.2}$$

Real balance yield BA is defined as the ratio between the amount of target product and the total amount of materials, including the secondary materials (*SRM*) as solvents and catalysts, and is given by:

$$BA = \frac{amount\ \ of\ \ target\ \ product}{amount\ \ of\ \ primary\ \ and\ \ secondary\ \ raw\ \ materials} = \frac{m_P}{\sum m_{PRM} + \sum m_{SRM}} \tag{1.3}$$

Specific balance yield represents the ratio of the above indices, and is a measure of the raw material efficiency:

$$sp_{BA} = \frac{BA}{BA_t} \tag{1.4}$$

The same index can be calculated by the following relation:

$$sp_{BA} = F \times RY \times EA_p \tag{1.5}$$

The factor EA_p characterises the efficiency of primary raw materials:

$$EA_p = \frac{amount\ of\ primary\ raw\ materials}{amount\ of\ primary\ and\ secondary\ raw\ materials} = \frac{m_{PRM}}{\sum m_{PRM} + \sum m_{SRM}} \tag{1.6}$$

The factor F expresses the excess of primary raw materials defined as:

$$F = \frac{stoichiometric\ raw\ materials}{excess\ of\ primary\ raw\ materials} \leq 1 \tag{1.7}$$

From (1.4) and (1.5) one gets:

$$BA = BA_t \times (F \times RY) \times EA_p \tag{1.8}$$

Therefore, BA can be seen as a productivity function that should be maximised by design. For example, the excess of reactant can give higher stoichiometric yield RY, but lower real balance yield BA. Increasing EA_p to the theoretical limit of one is an objective of process design. This can be achieved by replacing steps involving unrecoverable auxiliary chemicals with operations where the recycle of materials is possible.

EXAMPLE 1.1 Production of phenone by acetylation reaction

Phenone is produced by the acetylation of benzyl chloride with o-xylene via a Friedel-Crafts reaction. Calculate the environmental performance indices, knowing the material balance elements given in Table 1.1 (Christ, 1999).

Solution.

The stoichiometric equation is:

$$\underset{140.6}{C_6H_5\text{-}COCl} + \underset{106.2}{(C_6H_4)\text{-}(CH_3)_2} + \underset{133.4}{AlCl_3} + \underset{48}{3H_2O} =$$
$$\underset{210.2}{(C_6H_5)\text{-}CO\text{-}(C_6H_4)\text{-}(CH_3)_2} + \underset{78}{Al(OH)_3} + 4\ \underset{146}{HCl}$$

From the relations (1.1) to (1.8) we get:

$$RY = \frac{n_P}{n_A} = \frac{4.76}{4.98} = 0.956$$

$$BA_t = \left(\frac{m_p}{\sum m_{reactants}}\right)_{theoretical} = \frac{210.2}{(140.6+106.2+133.4+48)} = 0.484$$

$$BA = \left(\frac{m_p}{\sum m_{reactants}}\right)_{real} = \frac{1000}{3300} = 0.303 \qquad sp_{BA} = \frac{0.303}{0.484} = 0.626$$

$$EA_p = \frac{PRM}{\sum m_{reactants\ real}} = \frac{(700+550+700+258)}{3300} = 0.669$$

$$F = \frac{n_A \cdot \sum M_{w,reactants}}{PRM} = \frac{4.98 \ (140.6+106.2+133.4+48)}{(700+550+700+258)} = 0.979$$

Although the stoichiometric yield RY is acceptable, the theoretical balance yield BA_t is poor, because of the catalyst complex lost after reaction. A significant improvement would be the use of solid catalyst that will be preserved in reaction. In addition, regeneration of $AlCl_3$ complex is possible by recycling. The two solutions would lead to the same figures for the theoretical yield, but they will imply different costs. Therefore, a complete environmental investigation should consider also a cost flow analysis. More details can be found in Christ (1999).

Table 1.1 Material balance for the Example 1.1

Input				Output			
	Mw	**Mass**	**Moles**		**Mw**	**Mass**	**Moles**
PRM				**Target product**			
R-COCl	140.6	700	4.98	Phenone	210.2	1000	4.76
o-Xylene	106.2	550	5.18				
$AlCl_3$	133.4	700	5.25	**Waste water**			
H_2O	18	258	14.33	$Al(OH)_3$	78	410	5.26
				HCl	36.5	600	16.44
				Other		123	
SRM				**Waste**			
Toluene		900		Toluene		900	
H_2SO_4		192		Other		267	
Total		**3300**				**3300**	

PRM - primary raw materials; SRM - secondary raw materials

Industrial examples of integrated-environmental protection are described in the monograph of Christ (1999), with emphasis on German industries. One of this regards the VCM production, one of the largest chemical commodities. Here the environmental risk is apparently high, because of numerous hazardous materials, starting with raw materials (ethylene, chlorine, oxygen) and ending with the saleable product (vinyl chloride). A variety of chlorinated hydrocarbon impurities is formed in different reaction steps. However, modern VCM processes are environmental friendly, with emissions approaching zero, as well as with low consumption of energy. These performances have been obtained by means of extensive research and engineering work. Among the measures with the most impact we may cite:

- Minimisation of impurities by the improvement of selectivity in the all three reactors: chlorination, thermal cracking and oxy-chlorination.
- Recycle of chlorinated hydrocarbons in totally closed material balance loops.
- Advanced HCl recovery bringing the plant close to the stoichiometric balance.
- Reduction of waste-water and minimisation of emissions.
- Saving energy in distillations, as well as in vent-gas incineration units.

The handling of impurities in a VCM plant has been investigated by Dimian et al. (2001) by means of computer simulation. It has been demonstrated that selective chemical conversion of intermediate impurities can be used to prevent their accumulation and the occurrence of snowball effects in the separation units. The separation of impurities can be properly handled by exploiting the interaction effects through recycles. More details are given in the Chapter 17 (Case Study 3).

1.6.3 Metrics for sustainability

Promoting the sustainable development implies the availability of reliable measures. These measures should regard the complete manufacturing-supply chain over the predictable product life cycle. The metrics should be simple and understandable by the large public, useful for decision-making agents, consistent and reproducible. The sustainability measures proposed recently by Schwartz, Beloff & Beaver (2002) have these properties. They refer to the same unit of outputs, for example the to the *value-added dollar* $\$VA$, defined as ' Revenues minus Costs of raw materials and utilities '. The metrics that will be presented are consistent in the sense that 1) the lower the metric the more effective the process, and 2) all indicate the same direction.

The calculation of the proposed sustainability metrics is explained below:

1. *Material intensity* is expressed as the mass of waste (not converted material) per unit of output. Waste is calculated by subtracting the mass of products and saleable sub-products from the mass of raw materials. Water and air are not included unless these are incorporated in the product.
2. *Energy intensity* is the energy consumed per unit of output. It includes natural gas, fuel, steam and electricity, all converted in net-fuel or the same unit for energy. For consistent calculations 80% average efficiency is considered for steam generation and 31% for electricity generation, corresponding to 1350 BTU/lb steam and 11000 Btu/kWh electricity. This metric captures in a synthetic manner the energy saving not only by heat integration, reflected by diminished steam and fuel consumption, but also by more advanced techniques, as cogeneration of heat and power. Negative values would mean export of energy to other processes. This situation is likely for processes involving high exothermic reactions, where the heat developed by reaction should be added as negative term in the energy balance.
3. *Water consumption* gives the amount of fresh water (excluding rainwater) per unit of output, including losses by evaporation (7% from the recycled water) and by waste treatment.
4. *Toxic emissions* consider the mass of toxic materials released per unit of output. The list of toxic chemicals can be retrieved from the website of the Environmental Protection Agency (USA).
5. *Pollutant emissions* represent the mass of pollutants per unit of output. The nominator is calculated as equivalent pollutant rather than effective mass. This topic is more difficult to quantify, but the idea is to use a unified measure.
6. *Greenhouse gas emissions* are expressed in equivalent carbon dioxide emitted per unit of output. Besides the CO_2 from direct combustion, this metric includes other sources, as the generation of steam and electricity.

There are significant advantages of using these measures in design. The comparison of different alternatives allows the designer to identify the best chemistry and flowsheet design that leads to the lowest resources and environmental impact. Usually the objective function is profit maximisation. Including the above measures, at least as constraints, could contribute to conciliate the economic efficiency with the environmental care, a concept designated today by the label 'eco-efficiency'.

A distinctive feature of these metrics is that they can be stacked along the whole product supply chain. In this way, ecological bottlenecks can be identified readily. For example, a chemical product that might appear as benign for the environment, could involve in reality high toxic materials in some intermediate steps of manufacturing.

As illustration, Table 1.2 shows values for some representative chemical processes. The output units refer to the added-value dollar $VA explained before. It can be seen that phosphoric acid has very unfavourable indices on the whole line, being very intensive as material, energy and water consumption. Acrylonitrile produced by ammonoxidation has also poor environmental performance with respect to toxics and pollutants. Note also the large amount of CO_2 produced by methanol process. The best process in the list is the acetic acid made by the carbonylation of methanol.

Table 1.2 Sustainability metrics for some processes (after Schwartz et al., 2002)

Process	Material kg/$	Energy MJ/$	Water m^3/$	Toxics g/$	Pollutants g/$	CO_2 kg/$
Methanol (natural gas reforming)	0.2721	165.12	0.161	5.90	0	8.80
Acetic acid (MeOH carbonylation)	0.1769	16.76	0.029	0.313	0	1.10
Terephtalic acid (p-xylene oxidation)	0.4264	47.34	0.085	35.38	2.721	3.05
Acrylonitrile (Propylene ammonoxidation)	2.1228	62.74	0.121	63.50	99.789	6.22
Phosphoric acid (Wet process)	144.3	267.4	0.788	1909.62	0	17.10

Sustainability metrics can be used as decision-support instruments. Among the most important tools in *Life Cycle Analysis* of processes we mention:

- Practical minimum-energy requirements (PME) set reference values for the intensive-energy steps and suggests energy reduction strategies.
- Life cycle inventory (LCI) deals with the material inventories of each phase of a product life, namely by tracking the variation between input and output flows.
- Life cycle assessment (LCA) consists of determining the impact on the environment of each phase of a life cycle, as material and energy intensity, emissions and toxic releases, greenhouse gases, etc.
- Total cost assessment (TCA) provides a comparison of costs of sustainability, and by consequence, a consistent evaluation of alternative processes.

1.7 SUMMARY

In the today's economic and social environment, Chemical Process Industries are asked to discover innovative solutions that are not only economically efficient, but also sustainable. Production-integrated environmental protection implies that ecological issues are included in the conceptual design methodology. Besides economic efficiency, metrics for ecological and sustainability performance must be included in assessing the quality of a design solution.

The objective of this book is to develop a creative and integrated approach of a process design problem by means of a systemic viewpoint and of systematic techniques. In this context, systems approach means the design of a complex interconnected system of units to satisfy agreed-upon measures of performance, as high economic efficiency of raw materials and energy, down to zero waste and emissions, flexibility and controllability faced with variable production rate, etc.

Process Design should take into account the evolution of a process plant along its life cycle, from birth to death. Life cycle forms are generic concepts from systems engineering that can be used to manage the organisation of a process design project. Waterfall model consists of a sequential decomposition of the project assignment in tasks, ideally without backflow. V-cycle makes the distinction between conceptual and execution tasks, organising a systematic validation of performances against specifications.

In theory, the synthesis of the flowsheet structure should precede the integration of units. In practice solving the integration problem makes often necessary the revision of some structural elements, as for example the sequencing of separators. Therefore, a combined treatment of synthesis and integration is more appropriate. Nowadays the frontier between Process Synthesis and Process Integration is vague. In fact both are complementary and form the body of the Integrated Process Design. Extrapolating the label of Process Integration to the optimal design of the whole process is equally convenient. Because wide scope and multidisciplinary approach, Integrated Process Design is the today's paradigm for designing efficient and sustainable processes. Key features are:

- The main objective is the flowsheet architecture. Appropriate systemic techniques are capable to determine close-to-optimum targets for components without the need of their detailed design and sizing.
- Modern process design consists of developing several alternatives rather than a unique flowsheet. The reason is that every development step is controlled by design decisions. The selected solution among alternatives fulfils at best the optimisation criteria and the environment of constraints.
- Process Simulation is the main tool for analysis and synthesis. The power of modern simulation techniques makes possible the investigation of complex processes close to the real situation.
- The systematic methods and the analysis tools of Integrated Process Design can be applied to any type of chemical process industries, and addresses both new and retrofit projects.

1.8 REFERENCES

Biegler, L., I. Grossmann, A. Westerberg, 1998, Systematic Methods of Chemical Process Design, Prentice Hall

Christ, C. (editor), 1999, Production-Integrated Environmental Protection and Waste Management in the Chemical Industry, Wiley-VCH

Dimian, A. C., A. J. Groenendijk, P. D. Iedema, 2001, Handling of impurities in a complex plant, Ind. Eng. Chem. Res., 40, 5784-5794

Douglas, J. M., 1988, Conceptual Design of Chemical Processes, McGraw-Hill

Gundersen, T., 2002, A Process integration primer, SINTEF Energy Research, available on the website of the International Energy Agency

Linnhoff, B., 1993, Pinch Analysis. A-state-of-the-art overview, Trans. Inst. Chem. Eng., September, p. 501-522

Linnhoff, B., D. W. Townsend, D. Boland, G. F. Hewitt, B. Thomas, A. R. Guy, R. H. Marsland, 1994, User Guide on Process Integration for the Efficient Use of Energy, The Institution of Chemical Engineers

Keller, G. E., P. F. Bryan, 2000, Process Engineering: Moving in new direction, Chem. Eng. Progress, January, p. 41-49

McGraw-Hill Dictionary of Engineering, 1997

Pingen, J., 2001, A vision of future needs and capabilities in Process Modelling, Simulation & Control, ESAPE-11 Proceedings, Elsevier

Seider, W., D. J. D., Seader, D. R. Lewin, 1999, Design Process Principles, Wiley

Stankiewicz, A., J., A. Moulijn, 2000, Process intensification: transforming chemical engineering, Chem. Eng. Progress, January, p. 22-40

Smith, R., 1995, Chemical Process Design, McGraw-Hill

Thomé, B. (editor), 1993, Principles and Practice of Computer-based Systems Engineering, Wiley series in software based systems

PART I

PROCESS SIMULATION

This Page Intentionally Left Blank

Chapter 2

INTRODUCTION IN PROCESS SIMULATION

2.1 Computer simulation in Process Engineering
- 2.1.1 Flowsheeting
- 2.1.2 Applications of computer simulation
- 2.1.3 Simulation of complex plants
- 2.1.4 An historical view

2.2 Steps in a simulation approach

2.3 Architecture of flowsheeting software
- 2.3.1 Computation strategy
- 2.3.2 Sequential-Modular approach
- 2.3.3 Equation-Oriented approach

2.4 Integration of simulation tools
- 2.4.1 Integrated systems
- 2.4.2 Open software architecture
- 2.4.3 Internet simulation

2.5 Selection of a simulation software

2.6 Summary

2.7 References

2.1 COMPUTER SIMULATION IN PROCESS ENGINEERING

2.1.1 Flowsheeting

Simulation is a fundamental activity in Process Engineering. The following definition captures its essential features (Thomé, 1993):

> *Simulation is a process of designing an operational model of a system and conducting experiments with this model for the purpose either of understanding the behaviour of the system or of evaluating alternative strategies for the development or operation of the system. It has to be able to reproduce selected aspects of the behaviour of the system modelled to an accepted degree of accuracy.*

Simulation implies *modelling,* as well as *tuning* of models on experimental data. A simulation model serves to conduct 'virtual experiments'. Almost invisible in most cases, being incorporated in the software technology, modelling is the key feature in every simulation. It is important to keep in mind that the simulation is only an approximate representation of the reality, at a certain level of accuracy, and not the reality itself. That is why the user must always be able to evaluate the reliability of the results delivered by a simulator.

Simulation in Process Engineering requires specific scientific knowledge among we may cite accurate description of physical properties of pure components and complex mixtures, models for a large variety of reactors and unit operations, as well as numerical techniques for solving large systems of algebraic and differential equations.

The scientific and engineering activity that makes use of professional modelling and simulation for Chemical Process Industries (CPI) is designated by *Computed Aided Process Engineering* (CAPE). Since 1991 the European Federation of Chemical Engineering organises each year a scientific congress of the worldwide CAPE community under the label ESCAPE.

The main simulation activity in process engineering is *flowsheeting.* Following a previous definition (Westerberg et al., 1979) flowsheeting is *the use of computer aids to perform steady state heat and mass balancing, sizing and costing calculation for a chemical process.*

This interpretation reflects the fact that flowsheeting has deep roots in process design. The impressive progress in the last thirty years, both in modelling and in simulation technology, has enriched this definition. Nowadays flowsheeting is involved not only in the design of new processes, but also in the continuous improvement of existing technologies, by revamp and debottlenecking, in managing process operation and control, as well as in research and development (Dimian, 1994).

In a complex plant the units form a system that can be understood at best by simulation. Taking into account the evolution in the last decades, we may formulate a more extended definition as:

Flowsheeting is a systemic description of material and energy streams in a process plant by means of computer simulation with the scope of designing a new plant or improving the performance of an existing plant. Flowsheeting can be used as aid to implement a plantwide control strategy, as well as to manage the plant operation.

According to the above definition, in flowsheeting the behaviour of the system has the highest priority. The modelling of the individual units must be subordinated to the system's goals. Flowsheeting has different purposes in Design and Operation, but these converge when the knowledge acquired in the operation of an existing plant serves as basis for improving its design or for developing a new process.

In *Design* the first objective of flowsheeting is a systematic investigation of different alternatives that can be developed for a given design problem. Modern design relies upon systematic methods whose main merit is to be able to set optimal targets well ahead the detailed design of units. From several sub-optimal alternatives a base-case is selected, and further submitted to integration, sizing and optimisation. In addition, combined steady state and dynamic flowsheeting can help to understand the process dynamics, and on this basis support the implementation of a plantwide control strategy. Mastering the constraints of modelling in flowsheeting can help greatly the designer to deliver a reliable project despite the lack of data or of tight schedule.

In *Operation* the flowsheeting is more demanding, because it has to mirror the behaviour of an existing plant submitted to various disturbances. Plant data has to be reconciled against mathematical models embedded in simulator. Again, the modelling and accuracy must be subordinated to goals, as the monitoring of unit performance, maintenance, revamping, or support in process control activities.

It may be concluded that nowadays flowsheeting is heavily involved in both Design and Operation. Steady state flowsheeting is a daily activity in engineering companies and technical services of process plants. Dynamic flowsheeting is involved increasingly in advanced engineering activities, as for example in the design of process control systems, or in Real Time Optimisation and Computer Integrated Manufacturing.

Material and energy balances remain the most important results in flowsheeting. The stream report displays the way in which the raw materials are transformed in products for given performances of units. In addition, dynamic flowsheeting can mirror the time-variation of the component inventory in different locations, as well as the dynamics of energy streams.

The economic analysis, namely the profitability, is the moment of truth of every design. Flowsheeting is the only way to solve accurately this problem, because it can account accurately for the spread of all material and energetic costs in a flowsheet.

2.1.2 Applications of computer simulation

The current revolution in information technology, as well as the impressive progress in modelling and simulation technology has a significant impact on Process Engineering. A new paradigm is emerging, in which simulation is involved through all the stages of a process life cycle, from 'idea', through experiments in laboratory, during scale-up at different levels, to process design and plant operation (Edgar, 2000).

Figure 2.1 illustrates this new approach. Simulation is placed in the core of the three main engineering activities: Research & Development, Design and Operation. The unifying matter is the scientific knowledge embedded in universal models, as well as the generic character of computational methods. These activities, apparently disconnected, can share a large number of 'first-principle' models, as thermodynamics,

chemical kinetics, transport phenomena, etc.

Note that in a larger extent process simulation should include other computer-based activities, as Molecular Simulation and Computer Fluid Dynamics (CFD). However, in this book we will limit the presentation to the capabilities offered only by the flowsheeting software, commonly called *process simulators*.

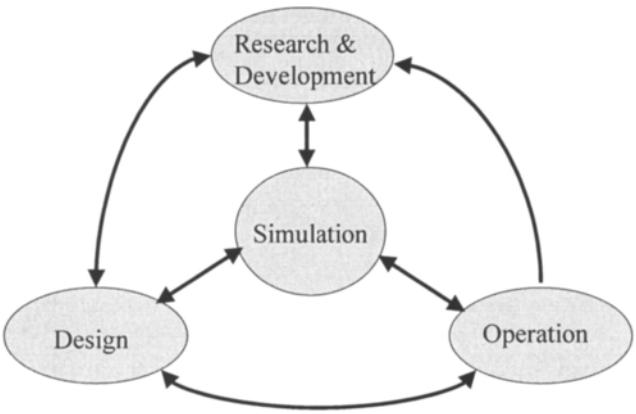

Figure 2.1 The new paradigm of Process Engineering: Simulation as core activity in Research & Development, Design and Operation

Research and Development

Process simulation can guide and minimise the experimental research, but not eliminate it. Actually, the calibration of models requires accurate experimental data. It is the experiment that proves the model, and not the opposite! Statistical planning of experiments is nowadays in a large extent obsolete. Instead, the experimental research should take profit from the power of rigorous models incorporated in simulation packages, particularly in the field of thermodynamics. For instance, simple vapour-liquid equilibrium (VLE) experiments in laboratory can be used to increase the reliability of a feasibility study in innovative processes. Conversely, industrial VLE measurements can be used to calibrate the thermodynamic models incorporated in a simulator when experimental information is not available.

The innovation of sustainable processes begins at the laboratory scale. The investigation of the feasible design space by simulation can reduce tremendously the experimental effort. We may speak about *computer-aided experimental research.*

Modelling and simulation can serve also as basis for *computer-aided scale-up*. Some models could pass unchanged from laboratory to the plant scale, while others should be modified to incorporate specific elements to each level.

Simulation can explore innovative solutions difficult to investigate experimentally. For example, the integration of process simulation with Computer Fluid Dynamics can replace costly prototypes. The flowsheeting of virtual plants involving rigorous hydraulic modelling of units is very likely in the next years.

Process Design

Globalisation and sustainable development set challenges for Process Design, as high efficiency of raw materials and energy, flexibility and responsiveness to market dynamics, safe and clean manufacturing. Clearly, these characteristics must be intrinsic in the conceptual design itself, and not added later by costly modifications. In this respect process simulation can bring significantly contributions, as:

- Development of novel sustainable technologies aiming to minimum energy and material requirements, as well as to zero waste and pollutants.
- Ensuring absolute safe operation and resiliency by integrating controllability in the conceptual design at early levels.
- Permanent improvement of existing technologies, by revamping, retrofitting, and debottlenecking.

Process Operation

The advent of Real Time Optimisation and of Computed Integrated Manufacturing in the decade 1990 opened large opportunities for applying simulation directly in the manufacturing process. In addition to model-based process control, we may mention preventive maintenance by systematic computer monitoring of equipment performance. The integration of manufacturing with the supplying chain can be realised only by setting up a complex computer-based system, in which simulation plays a central role.

Summing up, process simulation is a key factor in ensuring excellence in research, development, design and manufacturing. Table 2.1 illustrates the wide range of applications of modelling technology in Chemical Process Industries.

Table 2.1 Process Simulation applications in Chemical Process Industries

Chemical Process Industries	Applications
Oil & Gas	Offshore exploration, Surface treatment, Pipeline transport, Underground storage, Gas processing
Refining	Gasoline and fuels
Petrochemicals	Hydrocarbon based chemicals, Methanol, Monomers
Basic Organic Chemicals	Intermediates, Solvents, Detergents, Dyes
Inorganic Chemicals	Ammonia, Sulphuric Acid, Fertilisers
Fine Chemicals	Pharmaceuticals, Cosmetics
Biotechnology	Food and bio products
Metallurgy	Steel, Aluminium, Copper, etc.
Polymers	Polyethylene, PVC, Polystyrene, fibres, etc.
Paper & Wood	Paper pulp
Energy	Power plants, Coal gasification
Nuclear industry	Waste treatment, Safety
Environment	Water cleaning, Biomass valorisation

2.1.3 Simulation of complex plants

Nowadays, by means of commercial flowsheeting software, it is possible to produce a computerised tool for simulating complex process plants, called here *Plant Simulation Model* (*PSM*). Figure 2.2 illustrates the simplified generic structure of a complex plant, as often encountered in basic chemicals or petrochemical industry. Several large interconnected recycle loops exist, each of them containing quite a number of material, energy, or process control loops. To facilitate the investigation, the plant is split in sub-flowsheets, named here *A*, *B* and *C*, which could be analysed independently. Simulation models for sub-flowsheets are tuned and converged separately, and later, merged in a global model.

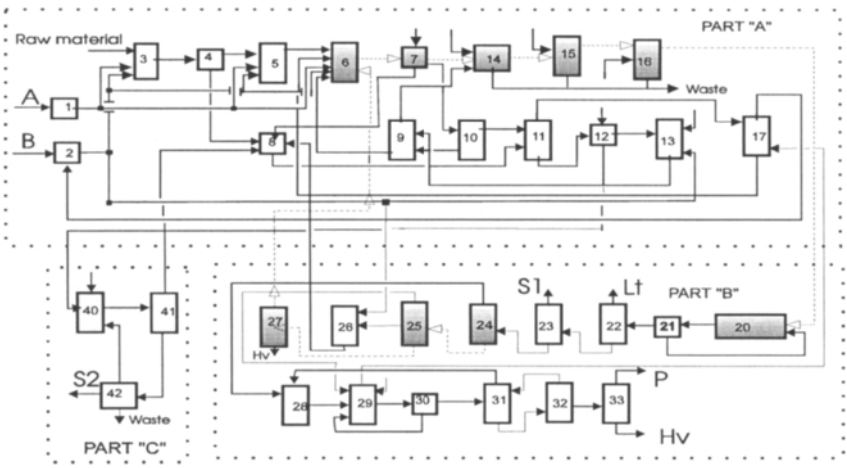

Figure 2.2 Abstraction of a complex plant

Steady state *PSM* serves to support both operation and design, including revamping and debottlenecking (Fig. 2.3). At higher level of complexity, a dynamic *PSM* can be developed to support the design of the process control system, but also for advanced applications, as operator training and real time optimisation.

The *PSM* should mirror the behaviour of the plant, such as the network of material and energy streams subject to variations in raw materials, energetic utilities and product specifications. Among its objectives we mention:

- Deliver a comprehensive report of material and energy streams.
- Determine the correlation between the reaction and separation systems.
- Investigate the formation and separation of by-products and impurities.
- Support preventive maintenance.
- Study how to eliminate wastes and prevent environment pollution.
- Evaluate the plant flexibility to changes in feedstock or products' policy.
- Validate the process instrumentation, and enhance process safety and control.
- Update the process documentation and prepare future investments.
- Optimise the economic performance of the plant.

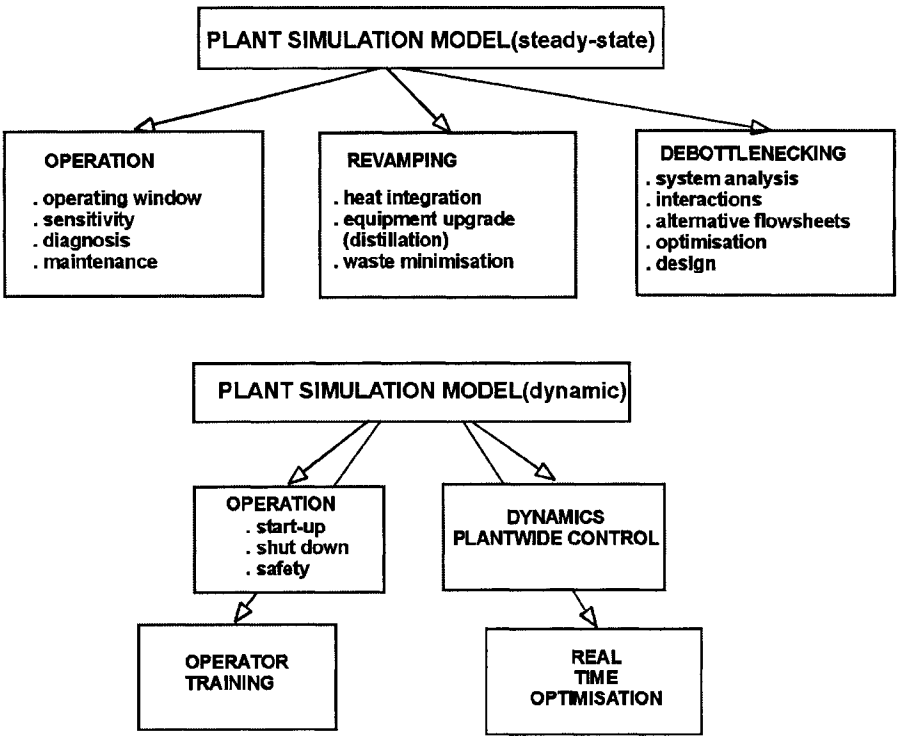

Figure 2.3 Applications of steady state and dynamic Plant Simulation Models

To achieve its goals, a *PSM* must be calibrated on plant data collected during special organised 'test-runs'. Additional *data reconciliation* programs may be used to increase the reliability of the plant data, by minimising the errors in measurements and supplying estimations for non-measured variables.

The basic document of a simulation is the *stream report*. This helps to understand the main problems in operation, but also offers a quantitative basis for communication between different members of the plant team, particularly between technical services and plant management. A remarkable feature of a *PSM* consists of its diagnosis value. For example, inconsistency in the material balance of some components can be explained by a malfunction of an equipment item, so that this can be traced by fault detection (Fig. 2.2 with shaded equipment); bad designed reboiler of the column 24 produces an impurity, which by propagation affects the selectivity of the reactor 20.

Hence, the development of a Plant Simulation Model is the proper approach to deal with industrial simulation problems. The progress in software technology makes possible today the development of integrated steady state and dynamic models. However, these require significant investment in qualified staff. Recently, generic simulation products have been proposed for applications in refining and petrochemical industries, which can be customised for specific processes.

2.1.4 An historical view

The story of process simulation began in 1966, when Simulation Science, a small company located in Los Angeles/USA, had the idea to commercialise a generic computer program for simulating distillation columns. This was the heart of a flowsheeting package, PROCESS[1], which might be considered the ancestor of process simulators. Three years later ChemShare (Houston/USA) released DESIGN[2], a capable flowsheeting program for gas & oil applications. At that time, the expansion of the refining and petrochemical industries motivated the advent of computer packages.

During the period 1970-80 the scientific computation has known its gold age. The algorithms used today have deep roots in the methods developed at that time. FORTRAN programming language became very popular among scientists and engineers. The simulations were executed on fast but expensive mainframe systems, to which the user was connected via a remote terminal. The *input file* was a bunch of cards, with instructions perforated on 80 columns format. Later the input of data became possible by editing a file on an electronic screen, the instructions for job execution being coded via a specific language based on 'key-words'.

In the period 1970-80's the major engineering bureaus, as well as some large manufacturing companies in refining and petrochemical industries developed in-house *flowsheeting programs*. Mostly adopted the *modular sequential* architecture. However, some were based on the *equations oriented* approach, as SPEEDUP at Imperial College in London (UK) and TISFLO at DSM in The Netherlands.

The first world oil crisis in 1973 has greatly stimulated the interest in simulating processes with alternative raw materials, as coal and biomass. In 1976, US Dept. of Energy and MIT launched jointly the ASPEN project[3]. The advent of high-speed computation systems boosted the business of small companies specialised in modelling and simulation. More generally, the scientific computation evolved from individual programs to large packages designed as industrial products. Beginning with 1980 several all-purpose steady state flowsheeting software were available on mainframes, and distributed in time-sharing on international networks. The worldwide time-sharing computer networks from 1980-90's were the precursors of the today's Internet.

Personal Computer arrived in 1982. Although the power of PC's was weak for flowsheeting, the idea of a 'personal' tool was strong enough to incite enthusiasts[4]. The challenge of leaving the elitist environment of mainframes was launched.

The arrival of workstations (1985) and of a new multi-tasking operating system, UNIX, is at the origin of a revolution in the scientific computation that continues today. Few scientific software companies survived these dramatic changes. The reusability of the old proven FORTRAN routines in a new 'object oriented programming' environment was critical.

At the beginning of 1990's the domination of PC products was a fact. The relative stabilisation in operating systems, dominated nowadays by UNIX and Windows,

---

1 precursor of PRO II (Simulation Science)
2 continued with DESIGN II and WINSIM
3 continued by ASPEN PLUS (ASPEN Tech)
4 development of ChemCAD (ChemStations) and Hysys (Hyprotech)

enabled the development of new generation of simulation software. The Graphical User Interface became a central part in the software development. The power of the former super-computers was available on desktops.

Nowadays process simulation is concentrated in a surprisingly low number of systems. On the other hand, the needs in modelling of industrial users are much larger than those supplied by generic software capabilities. The solution to this contradiction involves a large cooperation between specialised software firms and the community of CAPE users. This should exploit the Internet technology.

2.2 STEPS IN A SIMULATION APPROACH

The main steps of a simulation work will be introduced by means of an industrial example. The flowsheet is rather simple, but sufficient challenging for a new user. We adopt here the strategy of a sequential computation of units, which is the most used in steady state flowsheeting.

EXAMPLE 2.1 Approach of a simulation problem

Figure 2.4 displays the simplified flowsheet of a low-pressure methanol process[5] (Ullmann, 2001). The graphical user interface of a modern simulation packages could tempt a novice user to enter a simulation problem directly, without analysis. Examine the modelling issues that simulation of this process could arise.

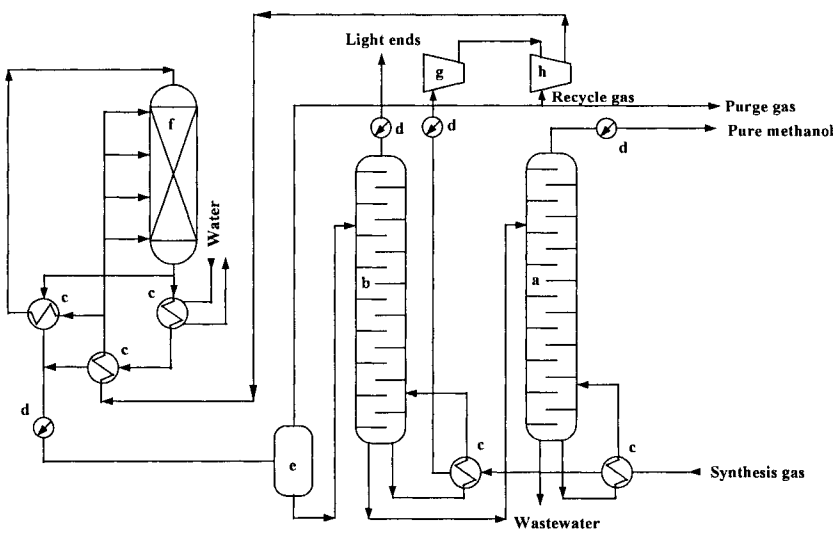

Figure 2.4 Flowsheet for the low pressure process for methanol (Ullmann, 2001)

---

[5] Low-pressure means here 10-100 bars relative to high-pressure of 100-500 bars.

Solution:

The process operates at pressures between 5-10 MPa and temperatures between 200-300 °C. A typical synthesis gas obtained by methane steam reforming has the composition 15 vol. % CO, 8 vol. % CO_2, 74 vol. % H_2, and 3 vol. % CH_4.
The formation of methanol is described by the equilibrium reaction:

$$CO + 2\,H_2 \rightleftharpoons CH_3OH \;\; ; \;\; \Delta H_{300\,K} = -\,90.77 \;\; kJ/kmol \qquad (I)$$

Because of CO_2 presence, there is a second independent equilibrium reaction:

$$CO_2 + H_2 \rightleftharpoons CO + H_2O \;\; ; \;\; \Delta H_{300\,K} = 41.21 \;\; kJ/kmol \qquad (II)$$

Typically the selectivity is above 99%. The following impurities may be found: higher alcohols, hydrocarbons and waxes, esters, di-methyl-ether, ketones. With these elements we may proceed with the flowsheet description.

The hot synthesis gas enters the process by two heat exchangers, in fact the reboilers of distillation columns for methanol recovery and purification. After cooling, the fresh gas is compressed, mixed with recycled gas, and preheated to the required inlet reactor temperature. To ensure an optimal temperature profile the cold gas is injected in several points. The reactor outlet is sent through a train of heat exchangers for heat recovery by feed preheating and steam generation. After cooling, the reaction mixture is submitted to phase split in a flash. Non-converted gas is recycled to the reactor, a small amount being purged to prevent inert build-up. Crude methanol containing light and heavy impurities is treated in a sequence of two distillation columns. The first removes light impurities, while pure methanol is obtained as overhead from the second column.

Now, let's see how to tackle the above process by simulation. Here we will illustrate the working procedure with ASPEN Plus release 10.2, but the approach is similar for other simulators. Figure 2.5 presents a first simulation diagram. Every simulation begins by entering the input streams, in this case designated by GAS. It is wise to enter all the components involved in simulation as earliest as possible.

Next, we may start to draw the flowsheet. A library of units is available, each characterised by input/output connections. We begin with the first two heat exchangers noted HX1 and HX2, which are coolers for the synthesis gas, but also reboilers for the distillation columns. These units can be coded as heat exchangers with duty available to exchange with other units. The next cooler HX3 is a simple utility heat exchanger. It follows the main compressor with the label COMP1. Here there are two choices, single-stage or multistage simulation model. We let the user decide and see later the consequences.

Now, some difficulties may appear around the reactor. The inspection of the heat recovery system reveals a rather complicated structure. To simplify this first analysis, the whole heat recovery system is lumped in a single unit, called FEHE, which is the abbreviation for Feed-Effluent-Heat-Exchanger. However, coding the reactor remains difficult. Selecting a Plug Flow Reactor (PFR) model, close to physical reality, requires kinetics. Again, we can simplify the analysis by assuming the main reactions close to equilibrium in a first unit R1 (REQUIL) followed by a second unit R2 (RSTOIC) that

describes the secondary reactions by a stoichiometric approach. In this way the reactor system supplies an outlet mixture with correct composition for separation.

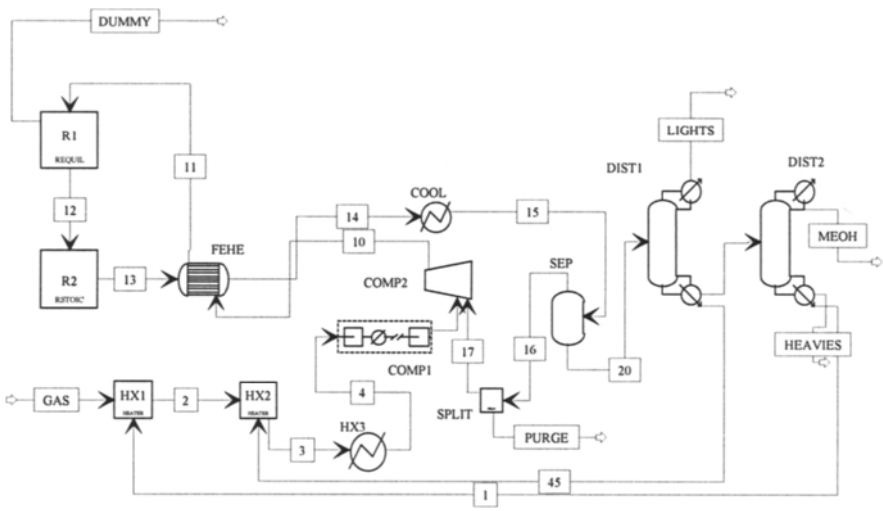

Figure 2.5 Process Simulation Diagram of the low-pressure methanol synthesis

After cooling, the separation of gas and liquid streams takes place in a simple flash unit SEP. The gas stream is sent back to reactor through the compressor COMP2. Purge is necessary to prevent the accumulation of inert, simulated by a splitter SPLIT.

We proceed with the liquid separation system. The insertion of a valve for pressure reduction is recommended. Then the problem is to simulate the two distillation columns. By browsing the user may find easily that the models for the separation units are in generally of two types: *design* or *rating mode*. In design mode the unit is defined by its performance, sizing characteristics being computed by shortcut methods. In rating mode the performance of the unit is computed for a given design. In a first attempt the design mode is more suitable: specify the desired separation and ask for the number of theoretical stages and the reflux ratio. In this way the desired outputs are always achieved. However, a rating model would be more convenient for coupling the reboilers with the blocks HX1 and HX2 by transmitting heat duty.

In this way, the layout of a complete flowsheet can be done. It may be observed that the flowsheet for simulation is somewhat different from Fig. 2.4! A first conclusion might be drawn: the technological flowsheet, commonly called *Process Flow Diagram*, must be translated in a diagram compatible with the capabilities of the simulator. This new flowsheet will be called here *Process Simulation Diagram*.

However, the work is not finished. It follows the 'specification phase'. Here the input procedure is guided usually by an intelligent navigation system. The specification of some units, as simple heat exchangers, compressors, flashes, mixers, valves, should not arise formal problems. However, they could arise infeasibility at the flowsheet level. For example, inlet reactor and flash temperatures are here key specifications for the

overall convergence. On the contrary, the specification of the distillation columns is formally more subtle, but with little effect on the whole flowsheet.

The next stage of the input consists of selecting thermodynamic models. Here the process has two distinct parts: (1) high-pressure reaction section (2) low-pressure distillation section. Consequently, two thermodynamic models should be considered: equation of state and liquid activity model, respectively.

Suppose that the specification phase is formally successful. Before to press the button 'run', the user might ask a simple last question. Where the simulation should start and what would be the order of computations units involved in the recycle loop around the reactor? Visibly, there is a need for a *topological analysis*. This will determine the *calculation sequence* by identifying the *tear streams* that must be initialised to allow a sequential computation of units. Normally, the simulator performs automatically a topological analysis, but this might be not always the best. In this case, there are three tear streams, 3, 13 and 16, which gives the following sequence:

SPLIT-HX3-COMP1-COMP2-FEHE-COOL-SEP-DIST1-DIST2-HX1-HX2-R1-R2

The initialisation of stream 3 is easy. Stream 13 should take into account a reasonable composition after reaction, which will help to initialise also the stream 16. Now the simulation is ready for 'run'. We may stop here the discussion and let the user finish the exercise. If the first attempt fails (very likely), there will be a good reason to read carefully the Chapter 3.

At this point we may remark that some differences do exist between different simulation systems, but these should not modify fundamentally the approach.

Approach of a simulation problem

Example 2.1 points out the methodological levels for setting-up a simulation problem (Fig. 2.6). These are briefly described.

1. Definition

A real *Process Flow Diagram* (PFD) must be translated in a scheme compatible with the software capabilities and with the simulation goals. The flowsheet scheme built up for simulation purposes will be called in this book *Process Simulation Diagram (*PSD). PSD is in general different from PFD. For example, some simple units, as for pressure or temperature change, may be lumped in more complex units (from simulation viewpoint). Contrary, complex units, as distillation columns or chemical reactors, may need to be simulated as small flowsheets. Hence, a preliminary problem analysis is necessary. The steps in defining a simulation problem are:

- Convert PFD in PSD. Split the flowsheet in several sub-flowsheets, if necessary.
- Analyse the simulation model for each flowsheeting unit.
- Define chemical components, including user-defined or petroleum fractions.
- Analyse the thermodynamic modelling issues regarding the global flowsheet, sub-flowsheets and key units.
- Analyse the specification mode (degrees or freedom) of complex units.

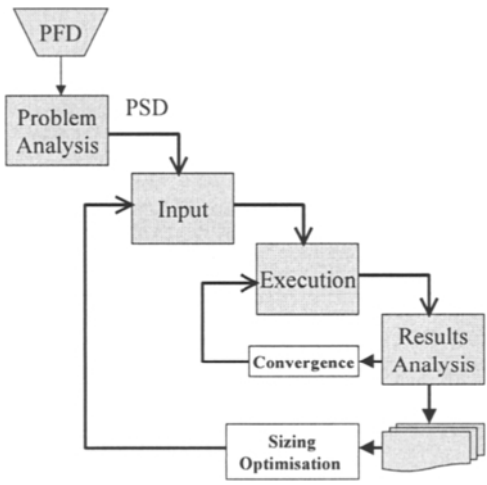

Figure 2.6 Methodological levels in steady-state simulation

2. Input

The input of a flowsheeting problem depends on the software technology. This activity is normally supported by a *Graphical User Interface* (GUI). The steps are:

- Draw the flowsheet.
- Select the components, from standard database or user defined.
- Specify the input streams.
- Specify the units (degrees of freedom analysis).
- Select the thermodynamic models. Check model parameters.
- Determine the computational sequence.
- Initialise tear streams and difficult units. Note that correct specifications do not always mean feasible specifications.

3. Execution

The simulation is successful when the convergence criteria are fulfilled both at the flowsheet and units' level. The user should pay particular attention to convergence history for troubles shootings. Here the steps involved are:

- Check the convergence algorithms and parameters, and change them if necessary.
- Check the convergence errors and the bounds of variables.
- Follow-up convergence history.

4. Results

A simulation delivers a large amount of results. The most important are:

- Stream report (material and heat balance), including flowsheet convergence report.
- Unit report, including material and heat balance, as well as unit convergence report.
- Rating performances of units.
- Tables and graphs of physical properties.

The graphical presentation of results may take various forms. Generally, advanced software provides their own analysis tools, but the exchange of data with all-purpose spreadsheets is usually available. Detailed results, as internal flows or tables of properties, may be exported to specialised design packages.

5. Analysis

Flowsheeting analysis tools enable to get more value from the simulation results. The most used is the *sensitivity analysis*. This consists usually of recording the variation of some 'sampled variables' as function of 'manipulated variables'. The interpretation of results can be exploited directly, as trends, correlation or pre-optimisation. *Case studies* can be employed to investigate combinations (scenarios) of several flowsheet variables. Finally, the simulation work may be refined by *multi-variable optimisation.*

A more advanced use of flowsheeting capabilities is the *controllability analysis* of standalone units, or the study of a *plantwide control* strategy. This issue will be developed in the Chapters 12 and 13.

2.3 ARCHITECTURE OF FLOWSHEETING SOFTWARE

2.3.1 Computation strategy

The architecture of a flowsheeting software is determined by the strategy of computation. Three basic approaches have been developed over the years:

- Sequential-Modular.
- Equation-Oriented.
- Simultaneous-Modular.

In *Sequential-Modular* (SM) architecture, the computation takes place unit-by-unit following a *calculation sequence*. A process with recycles must be decomposed in one or several calculation sequences. Each of these begins at a certain place, where the incoming streams have to be known either as inputs, or initialised as *tear streams*. The computation sequence of units involved in a recycle defines a *convergence loop*. When tear streams are present, the final steady state solution is obtained by iterative calculations. Tear streams are modified (accelerated) after successive iterations by applying an appropriate *convergence algorithm*. The computation stops when both the units and the tear streams satisfy some convergence criteria, usually the closure of the material and heat balance. The SM architecture was the first used in flowsheeting, but still dominates the technology of steady state simulation.

Among the advantages of the SM architecture we may cite:

- Modular development of capabilities.
- Easy programming and maintenance.
- Easy control of convergence, both at the units and flowsheet level.

There are also disadvantages, as for example:

- Need for topological analysis and systematic initialisation of tear streams.
- Difficulty to treat more complex computation sequences, as nested loops or simultaneous flowsheet and design specification loops.
- Difficulty to treat specifications regarding internal unit (block) variables.

- Rigid direction of computation, normally 'outputs from inputs'.
- Not well suited for dynamic simulation of systems with recycles.

Some modifications have been proposed to improve the flow of information and avoid redundant computations. Among these we may mention the *bi-directional transmission of information* implemented in Hysys™.

In *Equation-Oriented* (EO) approach all the modelling equations are assembled in a large sparse system producing Non-linear Algebraic Equations (NAE) in steady state simulation, and stiff Differential Algebraic Equations (DAE) in dynamic simulation. Thus, the solution is obtained by solving simultaneously all the modelling equations.

Among the advantages of the equation-solving architecture we may mention:

- Flexible environment for specifications, which may be inputs, outputs, or internal unit (block) variables.
- Better treatment of recycles, and no need for tear streams.
- Note that an object oriented modelling approach is well suited for the EO architecture.
- However, there are also substantial drawbacks, as:
- More programming effort.
- Need of substantial computing resources, but this is less and less a problem.
- Difficulties in handling large DAE systems.
- Difficult convergence follow-up and debugging.

In *Simultaneous-Modular* approach the solution strategy is a combination of Sequential-Modular and Equation-Oriented approaches. Rigorous models are used at units' level, which are solved sequentially, while linear models are used at flowsheet level, solved globally. The linear models are updated based on results obtained with rigorous models. This architecture has been experimented in some academic products.

It may be concluded that Sequential-Modular approach keeps a dominant position in steady state simulation. The Equation-Oriented approach has proved its potential in dynamic simulation, and real time optimisation. The solution for the future generations of flowsheeting software seems to be a fusion of these strategies. The release 11.1 of Aspen Plus (2002) incorporates for the first time EO features in the environment of a SM simulator.

2.3.2 Sequential-Modular approach

Sequential-Modular approach is mostly used in steady state flowsheeting, among we may cite as major products Aspen Plus, ChemCad, Hysys, ProII, Prosim, and Winsim (see Table 2.2 for information). However, there are some dynamic simulators built on this architecture, the most popular being Hysys.

The basic element in a modular simulator is the *unit operation model.* A simulation model is obtained by means of conservation equations for mass, energy and momentum. These lead finally to a system of non-linear algebraic equations as:

$$f(u, x, d, p) = 0 \tag{2.1}$$

Here the notations signify:

- u, connectivity variables formally classified in input and output variables;
- x, internal (state) variables, as temperatures, pressures, concentrations;
- d, variables defining the geometry, as volume, heat exchange area, etc;
- p, variables defining physical properties, as specific enthalpies, K-factors, etc.

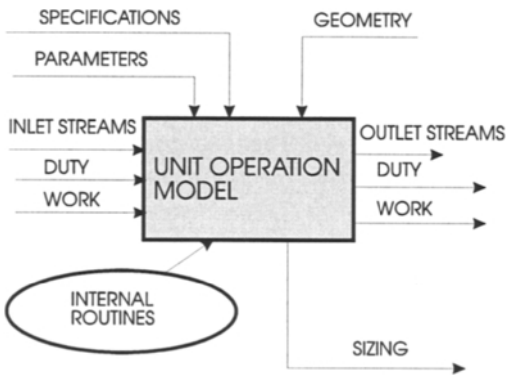

Figure 2.7 General layout of unit operation model

Note that the system (2.1) has a strong non-linear character, particularly due to the interdependence between physical properties and state variables. It is important to keep in mind that physical properties may consume up to 90% from the computation time. The above system should be seen as completed with equations for *constraints*.

The difference between the total number of non-redundant variables in the system (2.1) and the number of independent algebraic equations gives the *degrees of freedom*. These are usually *specifications* that a user must supply to run a simulation.

In SM approach each simulation unit (block) is treated by the rule:

output variables = function {input variables, unit variables, unit parameters} (2.2)

The functional relation is specific for each unit, as flash, pump, reactor, distillation column, etc. Because of a large variety of physical situations, it is rational to incorporate a part of the algorithm in the routine that solves the unit. From programming point of view it is said that the approach is *procedural*.

Note that the specification mode of a unit operation is important for convergence. This aspect, related to degree of freedom analysis, will be discussed in Chapter 3.

The architecture of software is a matter of computer science. However, as with every complex system, the user should be aware about the main elements. Figure 2.8 presents a generic architecture of a Sequential-Modular simulator. The heart of the system is the *Executive Program.* Its function is to manage both computation and data exchange tasks, as for example calculation sequence, retrieval of parameters for physical properties, routines for unit operations, convergence follow-up, and management of the data file system. Other essential components are:

- Databases with physical parameters for pure components and mixtures.
- Librarian for computing physical properties of components and mixtures.
- Librarian for physical and chemical equilibrium calculations.

- Librarian for unit operations and reactors.
- Librarian with mathematical solvers.
- Graphical User Interface (GUI).

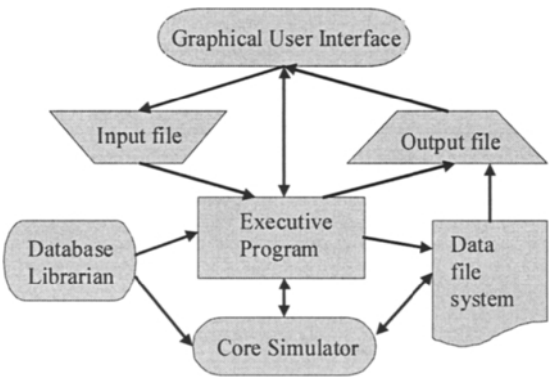

Figure 2.8 Software architecture of a Sequential-Modular simulator

From the above description, we may conclude that flowsheeting software is a very sophisticated computer-based system, and not a collection of algorithms for solving different unit operations. A process simulator must be designed with computer science development and management tools. It is interesting to note that in the total cost the software maintenance (typically more than 70 %) is by far more important than the cost of programming (typically under 10 %).

2.3.3 Equation-Oriented approach

In Equation-Oriented (EO) approach the software architecture is close to a solver of equations. EO is more suited for dynamic simulation since this can be modelled by a system of differential-algebraic equations (DAE) of the form:

$$\frac{dx}{dt} = f(u,x,d,p) \tag{2.3}$$

The steady state solution is obtained by setting the derivatives to zero. The overall DAE system (2.3) is sparse and stiff, its size varying between 10^3 and 10^5 equations.

Dynamic simulation is more demanding as its steady state counterpart. Firstly, it needs much more sizing elements. Then, the pressure variation cannot be neglected or lumped in the specification of simulation unit. However, in general the specification of variables is more flexible. Any flowsheet variable could be set as, irrespective if this regards input or output streams, or internal unit variables (see later in Chapter 3).
The software architecture built with an EO approach is presented in Fig. 2.9. The input of the simulation problem can be formulated by means of a meta-language, or be supported by an intelligent GUI. In Aspen Dynamics, the problem definition starts at

steady state in Aspen Plus in an SM environment. Adding accumulation terms to the equations of units generates the DAE system.

In an EO simulator the algorithmic treatment includes not only the mathematical solution, but also problem debugging, compilation/linking, as well as correction and addition of equations. An important feature is the post-processing of results, as time-recordings and plots of different variables.

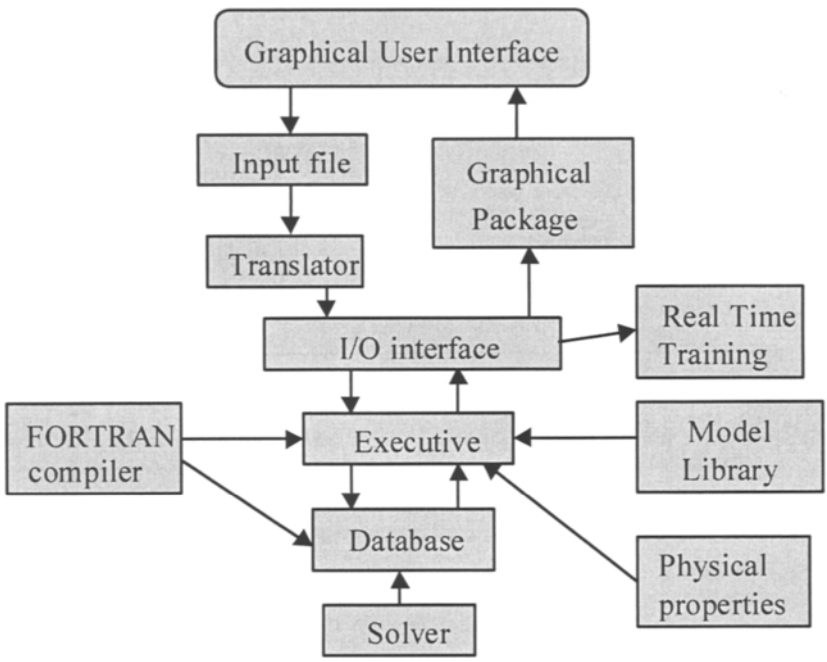

Figure 2.9 Software architecture of an Equation-Oriented simulator

2.4 INTEGRATION OF SIMULATION TOOLS

Computer simulation covers today practically all the activities devoted to process engineering. Flowsheeting is the key activity, but not the only one. Other computerised tools are necessary to take a true advantage from it. Some of more conceptual nature may be situated upstream, as thermodynamic analysis and process synthesis, other may be downstream, as detailed design of units and economic analysis, and some should be executed at the same level of design, as heat integration. Moreover, the simulation is involved more and more in sophisticated computer-based systems for Real Time Operation and operator training. Software for management and business planning can be also integrated with flowsheeting packages, taking into account that these tools need essential information about heat and material balance, best available via rigorous simulation. These components form the core of today's Computer Integrated Manufacturing systems.

Hence, the applications of process simulation are shared in two categories, design and operation. These are largely interdependent, but distinctive activities may be identified inside each one.

In *Computer Aided Design* the key activity is Conceptual Design that includes Process Synthesis (development of the process flowsheet diagram) and Process Integration (optimal valorisation of material and energetic resources). Other computer-supported activities deal with the detailed design of equipment, and the production of documents, as drawings and plans, including piping and instrumentation diagram, up to 2D and 3D plant layout. For batch processes the key activity is the planning in time of different manufacturing tasks called *Scheduling*.

In *Computer Aided Operation* we can mention the real time monitoring of material and energy balance, managed nowadays by means of *data reconciliation* programs. The plant operation can be adapted and optimised in real time by means of computerised tools based on dynamic flowsheeting. Other advanced applications are simulators for safety studies and operator training.

This variety of applications mentioned above is reflected by a large number of tools, of smaller or larger extent. However, the only way to ensure an efficient use is their integration in a coherent system. Three approaches may be imagined:

1. Integration of complementary products around a central flowsheeting system.
2. Interfacing of products supplied by different vendors by means of a dedicated file system (application program interface).
3. Clustering of several packages around a graphical environment and database environment, driven by general accepted standards.

The first approach dominates today, but only few integrated systems have survived in the rude competition of the 1990's. The second approach was considered occasionally as a partnership between generalist simulator suppliers and smaller developers specialised in niche applications. In practice, interfacing different systems, sometimes in direct competition, has proved to be unworkable. A reason might be the high cost of developing specialised interfaces that became rapidly obsolete because of fast changes in information technology. The third approach seems the most rational. Figure 2.10 describes the concept.

The core of an integrated system is the database system and the Graphical Use Interface (GUI). The assembly can be interfaced with simulation packages, primarily for physical property and thermodynamic computations, as well as for steady state flowsheeting. Packages devoted to conceptual activities, as process synthesis or heat integration, or to engineering tasks, as design of heat exchangers or piping, can be incorporated at a second level of complexity. Even more complex is the connection of a dynamic simulator. The integrated system should also be ready to accept user models.

Several projects for developing commercial process-engineering databases have been launched in the years 1980-1990, but none has survived. Rapid changes in technology made the development of such products very risky. Instead, each major supplier developed a proprietary database. However, the absence of standards affects both software producers and users. A collaborative approach based on *open software architecture* becomes necessary. An example is the CAPE-OPEN initiative that will be described later in this chapter.

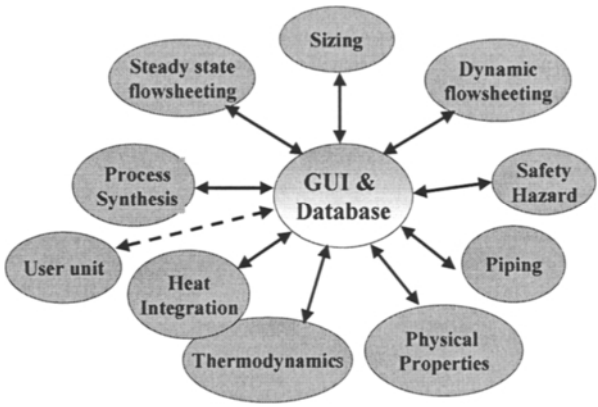

Figure 2.10 Integrated software system around a database environment

2.4.1 Integrated systems

Three major integrated simulation systems will be shortly presented. Update information may be found by consulting the respective web sites.

Aspen Technology

The integrated system includes both all-purpose flowsheeting system, and specialised packages. Different packages communicate via specific files, but share the same physical property methods and data. Here we mention only the major components. More complete and updated list can be found by consulting the website.

- **Aspen Plus**: steady state simulation environment with comprehensive database and thermodynamic modelling; feasibility studies of new designs, analysis of complex plants with recycles, optimisation.
- **Aspen Dynamics**: dynamic flowsheeting interfaced with Aspen Plus.
- **Aspen Custom Modeller:** modelling environment for user add-on units and programming in dynamic simulation.
- **Aspen Pinch**: Pinch analysis, optimal design of heat exchanger networks.
- **Aspen Split**: synthesis and design of non-ideal separation systems.
- **Polymer Plus**: simulation of polymerisation processes.
- **Aspen Properties**: physical property system including regression capabilities and estimation methods.
- **Aspen OLI**: simulation of aqueous electrolyte systems.
- **Batch Plus:** recipe-oriented batch process modeling.
- **Batchfrac**: batch reactions and separation processes.
- **RTO**: real time plant optimisation based on rigorous models.
- **Aspen Zyqad:** database environment for engineering projects.

Hyprotech

The special feature of the flowsheeting system proposed by Hyprotech is that steady state and dynamic simulation are available in the graphical environment. Other products have been developed as stand-alone applications for engineering or operation purposes. The system is designed for complete customisation. The main components are:

- **Hysys.Concept**: conceptual design package for design and retrofit applications, with two components:
  - DISTIL: distillation column sequences,
  - HX: heat integration projects by Pinch analysis.
- **Hysys.Process**: steady state flowsheeting for optimal new designs and modelling of existing plants, evaluate retrofits and improve the process.
- **Hysys.Plant**: steady state and dynamic simulation to evaluate designs of existing plants, and analyse safety and control problems.
- **Hysys.Operator Training**: start-up, shutdown or emergency conditions, consisting of an instructor station with DCS interface, and combined with Hysys.Plant as calculation engine.
- **Hysys.RTO+**: real-time multivariable optimisation; on-line models may be used off-line to aid maintenance, scheduling and operations decision-making.
- **Hysys.Refinery**: rigorously modelling of complete refining processes, integrating crude oil database and a set of rigorous refinery reactor models.
- **Hysys.Ammonia**: full plant modelling and optimisation of ammonia plants.

Simulation Sciences

The integrated system proposed by Simsci is built around a database environment (PROVISION), and can be in principle interfaced with third-party components. The system is oriented to applications in oil & gas industries, as described below.

Process Engineering: tools for process engineering design and operational analysis.

- **Pro/II**: general-purpose process flowsheeting and optimisation.
- **Hextran**: Pinch analysis and design of heat-transfer equipment.
- **Datacon**: plant gross error detection and data reconciliation.
- **Inplant**: multiphase, fluid flow simulation for plant piping networks.
- **Visual Flow**: design and modelling of safety systems and pressure relief networks.

Upstream Optimisation: decision-support tools designed for oil and gas production.

- **Pipephase**: multiphase fluid flow simulator for pipelines and networks.
- **Tacite**: multiphase simulator for complex transient flow phenomena.
- **Netopt**: optimisation of oil and gas production operations.

On-line Performance: Advanced Process Control (APC) and on-line optimisation.

- **ROMeo**: on-line plant modelling and optimisation, off-line analysis tool.
- **Connoisseur**: APC multivariable controls several via the plant's DCS.

2.4.2 Open software architecture

Despite the existence of powerful integrated software systems, there is a need for the integration of process modelling activity on a larger basis. This should take profit from Internet, as a worldwide network of knowledge and business. Following experts in information technology, two types of tools may be of interest for users: process modelling components (PMC) and process modelling environments (PME). The first category is very large, including not only the unit operation models of major software suppliers, but also specialised models of engineering and operating companies, as well as developments of consulting firms and academic research centres. The offer in PMC's in a sharing environment could be seen potentially huge compared with the options available today in commercial products. On the other hand, the offer in simulation environments is very limited.

One of the recent initiatives is the CAPE-OPEN consortium. This involves the collaboration of some major operating companies, software suppliers, and universities, with the support of the European Union (Braunschweig et al., 2000). The ultimate vision is to transform process modelling in a cooperative activity consisting of sharing a large number of components from a variety of sources. Moreover, the simulation might be conceived as an interactive process executed on different computers via Internet or Intranet facilities.

Figure 2.11 presents the concept of an open integrated system. The simulation environment could come from the Vendor A, to which in-house unit operations can be coupled. One of the user-model unit calls the library of the vendor B, which is linked to a thermo-server supplied by the vendor C, who in turn could consider an equation-of-state model from the supplier D. The vendor E might supply a special solver, while the database with information about physical properties could come from the vendor F, etc. It is clear that the PMC's should be provided with compatible plug-and–play interfaces. This can be done nowadays at best with an object-oriented technology.

Currently, the follow-up activity has the label of Global CAPE-OPEN (GCO) project. Another standardisation initiative is PDXI (Process Data Exchange Institute), which has been set-up already in the decade 1990 by AIChE. The mentioned initiatives claim looking for a close scientific and technical co-operation.

Opening the access to third parties ask for standards. More recently, the standard XML emerged, more convenient for transmitting structured information and queries. XML is a sort of meta-language that enables to built the structure of a personal document, but remaining compatible with the standard Web browsers, as Microsoft Explorer or Netscape. The adoption of XML can reconsider the idea of defining a standard process simulation database interface that failed in the past, but which is highly required for a truly open environment. The progress in communication can be spectacular, as for instance using the results of one simulator as starting data for another one. The interface of third-party design package or user programming with an all-purpose simulator could be tremendously simplified.

The probably adoption of CAPE-OPEN standards will federate the interests of both software producers and users. At the time where this book is written several projects are in development.

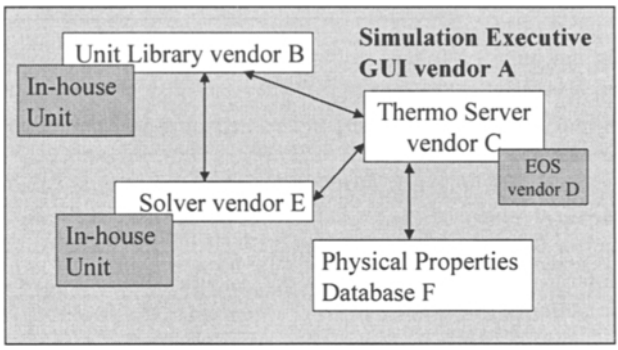

Figure 2.11 Vision of a typical CAPE-OPEN modelling tool (after Braunschweig et al., 2000)

2.4.3 Internet simulation

Nowadays most of the simulators are available via local networks. Typically each organisation has the licence of one simulator, but sometimes it may use a second or a third package. In a globalisation environment sharing the knowledge across remote offices demands a significant investment in communication facilities. In addition, a large category of potential users, small companies or consultants, are excluded because of licence procedures.

The advent of Internet as a worldwide network of transmitting and exchanging information will change profoundly the way of using process simulation. Remote access to a simulation system is possible from any point at any time. The availability on a global powerful server can relieve the users from the obsession of changing yearly the hardware and spending a fortune for maintenance. These are material advantages. But they are also even more important advantages in communication and productivity. The attraction of a much larger and motivated category of users will have significant positive effects on the chemical engineering profession.

At the time when these lines are written Internet simulation just begins. Some applications in operating and managing remotely process plants have been described (Zeng et al., 2001). There are also sites offering Internet access to remote use of simulation and design software.

2.5 SELECTION OF A SIMULATION SOFTWARE

The selection of a simulation system is a strategic decision for an organisation. It implies a medium/long term co-ordination policy, both in hardware platforms and in scientific software, as well as in the training of personnel, compatibility with third parties environment, etc. The procedure described below may be applied for a low-risk choice of any scientific software. The evaluation procedure takes the form of a questionnaire, as given hereafter.

1. Functional Analysis.
   - Typical applications.
   - Capabilities and options.
   - User interface.
   - Algorithms and numerical methods.
   - Complementary products.
   - Databases: size, applications, quality of data.
   - Post-treatment of results.
   - Typical benchmarks and library of examples.
   - User manual

2. Computer Science Analysis
   - Hardware: platforms and operating systems.
   - Resources: hard disk space, typical user space, memory.
   - Software analysis: architecture, file structure, programming languages.
   - Graphical User Interface: functions, portability.
   - Use of standards: graphics, communication, portability.
   - Software development tools and quality control.
   - Interface with known scientific or all-purpose software.
   - Customisation.

3. Commercial Analysis
   - Social reason, shareholders, financial report.
   - Commercial politics: market, clients, prices.
   - Training and user support.
   - Maintenance and updates.
   - Communication politics: users group meetings, newsletter
   - Academic and scientific contacts, publications.

Each question is quoted by a mark and weighted by a factor. Consequently, this procedure will produce a list of two or three good candidates. The final choice will imply a finer assessment of the above aspects. More information may be asked by experts, as benchmarks, customised demonstrations, programming samples, quality assurance documents, etc. In this respect it is important to test the product on problems close to the user application area.

Despite similar functionalities among generalist suppliers, every system has capabilities where it performs better than others. This could have historical reasons, or could come from the profile of clients. The reliability of physical properties and of parameters in thermodynamic models is an essential feature in design. That is why the quality of thermodynamics is a peculiar feature in selecting a simulation system for process design purposes. Other important features are customisation of units, programming capabilities, transmission of information and control structures, as well as debugging convergence problems with recycles. A system in which the user has the control on all the aspects of the modelling background should be preferred.

As mentioned, the process simulation market has known severe transformations in the 1985-1995 decade. Relatively few systems have survived. Table 2.2 presents a sample of the main commercial software at the end of 2001.

Table 2.2 Process Design & Simulation commercial software

	Supplier	Software	Applications
1	Aspen Tech Cambridge-MA/USA	Aspen Plus	Flowsheeting, sizing, costing
		Aspen Dynamics	Dynamic Simulation, Real time systems
		Advent	Energy Integration
		Split	Non-ideal Distillation Systems
		Bijac	Heat exchanger design
		Polymer Plus	Polymer processes
		Batchfrac	Batch and semi-continuous processes
2	Chemstations Houston-USA	ChemCad	Flowsheeting, sizing, costing
		CC-ReACS	Batch reactor simulator
3	Hyprotech Calgary-Canada	Hysys	Combined steady state and dynamic simulation
		Concept	Non-ideal Distillation Systems
		Hyprop	Thermodynamics
4	Prosim Toulouse-France	ProSim	Flowsheeting
5	Simulation Science Los Angeles-USA	Pro II	Flowsheeting, sizing
		Provision	Graphical environment
		Hextran	Energy Integration
		Datacon	Data reconciliation
		ROMeo	Rigorous on-line modelling
6	WinSim Houston –USA	Design II	Flowsheeting, sizing
7	Imperial College London-UK	g_PROMS	Dynamic Simulation
8	Bryan Research & Engineering	Prosim	Flowsheeting
		Tsweet	Gas purification
9	KBC/Linnhoff March	Supertarget	Energy integration
10	Intelligen, Scotch Plains, NJ-USA	BatchPro Designer	Scheduling and Design of batch processes

2.6 SUMMARY

Process Simulation is a key activity in Process Engineering covering the whole life cycle of a process, from Research & Development to Conceptual Design and Plant Operation. In this context, flowsheeting is a systemic description of material and energy streams in a process plant by means of computer simulation with the scope of designing the plant or understanding its operation.

Steady state flowsheeting is an everyday tool of the chemical engineer. The generalisation of the dynamic simulation in the design practice is the next challenge. By means of a capable commercial flowsheeting system, it is possible to produce a comprehensive computer image of a running process, a Plant Simulation Model, which can combine both steady state and dynamic simulation. This tool is particularly valuable in understanding the operation of a complex plant, and on this basis can serve for

continuous improving the process design, or for developing new processes.

Process simulation is based on models. A model should mirror the reality at the degree of accuracy required by application. Having a good knowledge of the modelling background is compulsory for getting reliable results and using the software effectively. The difference between successful and failed computer-aided project should be attributed more to an insufficient capacity of the user to take advantage from the modelling environment than to inadequate performance of the simulator. That is why a problem simulation must be carefully prepared.

Flowsheeting is still dominated by the Sequential-Modular architecture, but incorporates increasingly features of the Equation-Oriented solution mode. A limited number of systems can offer both steady state and dynamic flowsheeting simulators.

The integration of simulation tools is necessary to cope with the variety of needs in process engineering. It is desirable to open the access to simulation technology to a larger number of model suppliers. This can be realised by a cooperative approach between the community of users and of software producers. The availability of simulation systems on Internet can boost the use of simulation technology in a global environment.

2.7 REFERENCES

Braunschweig, B., C. Pantelides, I. B. Britt, S. Sama, 2000, Process modelling: the promise of open software architecture, Chem. Eng. Progress, September, p. 65-76.

Dimian, A. C., 1994, Use Process simulation to improve your operation, Chem. Eng. Progress, September, p. 54-63.

Edgar, F., 2000, Process information. Achieving a unified view, Chem. Eng. Progress, January, p. 51-59.

Thomé, B. (editor), 1993, Principles and Practice of Computer-based Systems Engineering, Wiley Series in Software Based Systems.

Ullmann's Encyclopedia of Industrial Chemistry, 2001, sixth Edition, Wiley-VCH

Westerberg, A. W., H. P. Hutchinson, R. L., Motard, P. Winter, 1979, Process Flowsheeting, Cambridge University Press.

Zeng, Y., S.M. Jang, C.C. Weng, 2000, Consider an Internet-based process simulation system, Chem. Eng. Progress, July, p. 53-60.

SOFTWARE

Aspen Plus, version 10.2, User Manual, 2001

Aspen Plus, version 11.1, User Manual, 2002

Aspen Dynamics, version 10.2, User manual, 2001

Hysys User Guide, release 2.4, HyproTech, 2001

Pro II Use Guide, release 5.4, Simulation Science, 2001

Chapter 3

STEADY STATE FLOWSHEETING

3.1 Fundamentals of steady state flowsheeting
- 3.1.1 General approach
- 3.1.2 Unit Operations
- 3.1.3 Thermodynamics
- 3.1.4 Control structures

3.2 Degrees of freedom analysis
- 3.2.1 Streams
- 3.2.2 Unit Operations
- 3.2.3 Flowsheet
- 3.2.4 Unfeasible specifications

3.3 Methodology in sequential-modular flowsheeting
- 3.3.1 Calculation sequence
- 3.3.2 Transmission of information
- 3.3.3 Design specifications
- 3.3.4 Treatment of convergence

3.4 Results

3.5 Analysis tools

3.6 Optimisation

3.7 Summary

3.8 References

3.1 FUNDAMENTALS OF STEADY STATE FLOWSHEETING

Example 2.1 emphasized some essential features in flowsheeting, particularly the necessity of analysing the simulation problem before entering it on computer. This chapter develops a general approach in steady state flowsheeting, in a manner that is independent of a commercial simulation package. The user should be able to use efficiently any simulator after becoming familiar with some specific technical elements.

The first topic is the approach in solving a flowsheeting problem explained by means of an example, the HDA plant. The next section describes the generic capabilities of the flowsheeting systems. Then a large subchapter deals with degrees of freedom analysis, an important topic in ensuring adequate specifications both for the simulation units and for the whole flowsheet. A section on methodology will describe how to solve convergence problems, and how to use control structures to bring the simulation closer to the industrial reality. A final subchapter deals with flowsheeting analysis tools, as sensitivity, case studies and optimisation.

3.1.1 General approach

Introductory example

The fundamental issues in flowsheeting will be illustrated by means of the HDA process. This abbreviation stands for the hydrodealkylation of alkyl-benzenes and alkyl-naphtalenes to their corresponding aromatic rings, as benzene or naphtalene. HDA process has been used intensively both in education and research to illustrate fundamental issues in Process System Engineering. We will use it also in several chapters of the book to examine different aspects in process synthesis and energy integration, as well as in integrating design and control.

Process description

The HDA process converts toluene to benzene in the presence of a large excess of hydrogen. A simplified approach considers two reactions:

- Main reaction: dealkylation of toluene to benzene and methane:

$$C_6H_5\text{-}CH_3 + H_2 \rightarrow C_6H_6 + CH_4 \qquad (1)$$

- Secondary reaction: formation of naphtalene as by-product:

$$2C_6H_6 \rightarrow C_{12}H_{10} + H_2 \qquad (2)$$

The reaction, globally exothermic, takes place in an adiabatic Plug Flow Reactor at pressures of 25 to 35 bars and temperatures between 620 and 720 °C. Large excess of hydrogen, typically 5:1 molar ratio, prevents the formation of coke. The reaction conversion is typically 60-80%, because at higher value the selectivity drops rapidly.

Figure 3.1 presents a simplified *Process Flow Diagram (PFD)* for the thermal hydrodealkylation of toluene (THDA) by UOP technology (Mowry, 1986). Fresh and recycled toluene is mixed with hydrogen at the reaction loop pressure. After

evaporation and preheating in a feed effluent heat exchanger **FEHE**, the mixture is heated-up in a **Furnace** at sufficient high temperature to initiate the reaction, and fed to the **Reactor**. The effluent is quenched with recycled liquid (not shown) to prevent thermal decomposition. Then the reaction mixture enters the heat recovery loop, which besides **FEHE** may include a **Steam Generator**. After passing through a **Cooler**, the reaction mixture is sent to separation in a **Flash** vessel.

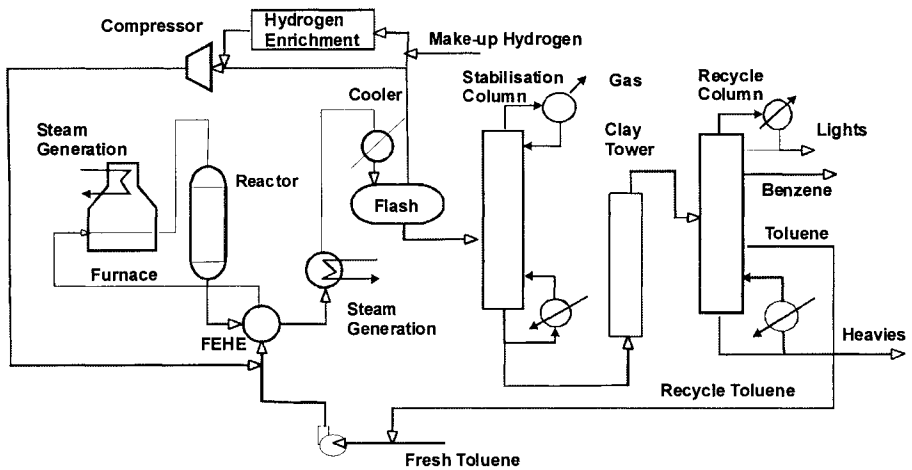

Figure 3.1 UOP HDA process for benzene production

The gas-phase consists of a hydrogen/methane mixture with small amounts of benzene and toluene. The liquid phase collects benzene and toluene, as well as heavy components and dissolved lights. The gas is recycled to the reactor via a **Compressor** and afterwards mixed with make-up hydrogen. Note that the make-up hydrogen may be recycled via a **Hydrogen Enrichment** section. The liquid phase enters the liquid separation section. After pressure reduction, the dissolved gases are removed in a **Stabilisation column**. Higher molecular components that might foul the internals of the distillation columns are removed in a **Clay Tower**. Finally, the complex distillation device named **Recycle column** performs the separation of light components in top as Lights, purified benzene and unconverted toluene as side-streams, and other heavy components in bottom as Heavies.

Problem Analysis

As shown in Chapter 2, the above Process Flow Diagram (PFD) has to be translated in a Process Simulation Diagram (PSD). This example has been worked out with ASPEN Plus™, but the approach is similar with other packages. The problem analysis takes into account the following aspects:

- Input/Output streams,
- Reactor system,
- Reactor-Separation-Recycle system,
- Separation system,

- Control of flowsheet specifications,
- Transformation of real units in simulation units,
- Degrees of freedom analysis,
- Thermodynamic issues,
- Tear streams and computational sequence.

These elements will be examined hereafter in detail.

1. Input/Output streams

The input streams are toluene of 100% purity and hydrogen with 5% CH_4. Input/Output analysis must ensure that the material balance is consistent. A golden rule in steady state flowsheeting says that any material entering or being created by chemical reactions must leave the process, such as no accumulation takes place. By the inspection of the Fig. 3.1 we find the following outputs: benzene product, lights gases from the stabilisation column, and heavies from the distillation column. The toluene side-stream is a recycle and not counted. However, something in the above picture is missing! A simple qualitative material balance detects that there is no exit place for the methane formed by reaction, but also entered as impurity with the hydrogen feed. Therefore, we must consider a gaseous purge stream. Finally, the input/output structure of the **HDA** process is presented in Fig. 3.2. Note that there are two inputs, Hydrogen and Toluene feeds, and four outputs, Purge, Benzene, Lights and Heavies.

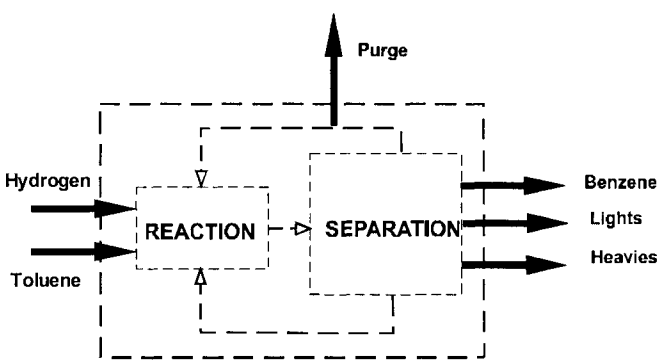

Figure 3.2 Input/Output streams for HDA process

2. Reactor Analysis

The reactor modelling in flowsheeting has to supply a reliable description of the transformation of reactants into products, by-products and impurities. The stoichiometric approach is simple but sufficient for material balance purposes. In this example, the stoichiometric modelling needs to know (1) the conversion of the main reaction and (2) the selectivity of the secondary reaction. Hence, in a first attempt we can model the **Reactor** by a *Stoichiometric Reactor* model.

If accurate kinetics data is available, and if there is a significant interaction between the reaction system and the rest of the flowsheet then a kinetic model may be considered. The type of reactor, as CSTR or PFR, need to be specified. However,

industrial reactors are much more complex as the ideal models. For this reason we do not advise the use of kinetic models in steady state flowsheeting, at least in early stages, except for more advanced purposes, as for operation or plantwide control. In these cases the combination of kinetic and stoichiometric models is appropriate. The kinetic model can account for the production determined by the main reaction rate, which depends on the reactor volume and the recycle flow rate and composition. The stoichiometric model can describe the formation of by-products and impurities necessary for the accurate simulation of separators.

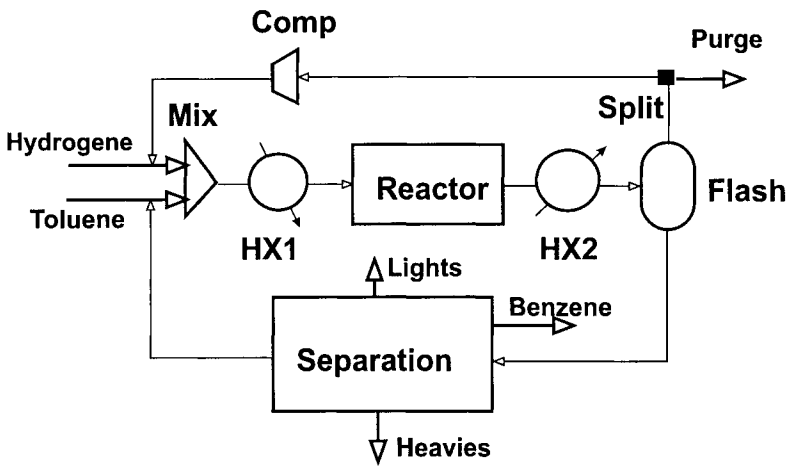

Figure 3.3 Reaction-Separation-Recycle structure for HDA process

3. Reactor-Separation-Recycle system

The simulation of a complex flowsheet should start by identifying the basic structures. Such structure is the Reactor-Separation-Recycle system, as illustrated in Fig. 3.3 for the HDA process. The fresh and recycled reactants enter a mixer unit **Mix**. Note that the cold side of the **Heat Exchanger** and the **Furnace** may be lumped in a single heat exchange unit named **HX1**. Similarly, the hot side of the **Heat Exchanger**, the **Steam Generator** and the **Cooler** can be lumped in a single unit heat exchange unit **HX2**. In this way, the effort can focus on the reactor behaviour, and not on the convergence of the heat integrated reaction loop.

The **Flash** is the place where gas and liquid phases separate. A vapour/liquid equilibrium model can simulate this operation. To simulate the purge we place the unit **Split** modelled by *Stream Splitter*. Then the gas is recycled via a compressor **Comp** simulated by a *Compressor* unit.

The simulation of the liquid separation system is more complicated. The simplest approach is to lump all the items in a *black-box unit* named **Separation**, simulated by a *Separator* module. This is specified in term of desired recoveries of components. In this way, we can concentrate the attention on the influence of the recycle on the reaction system rather than on the simulation of separators.

4. Separation system

The analysis of the separation system should determine the appropriate simulation models. The simulation of the train of distillation columns may be studied in a separate flowsheet (Fig. 3.4). After pressure reduction through the *valve* **V1,** the liquid mixture enters the stabiliser (**Stab**) where dissolved gases are removed. An appropriate model is *Rigorous Distillation* with vapour distillate. After a second pressure reduction through the *valve* **V2**, the separation of benzene, toluene and Heavies takes place in a second column (**Dist**), for which the same rigorous distillation model is used.

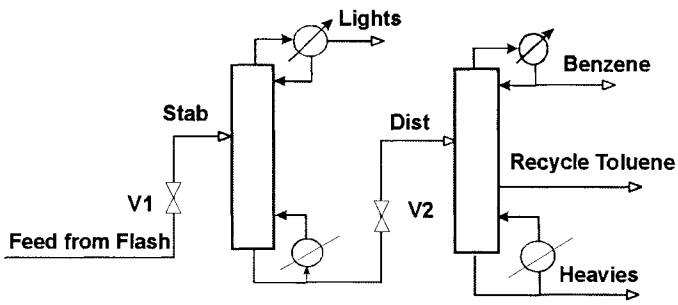

Figure 3.4 Liquid separation section of the HDA process

5. Control of flowsheet specifications

Some flowsheet variables may be 'controlled' by using other 'manipulated' variables. In our example, the molar ratio hydrogen/toluene at the reactor inlet should be kept strictly at 5:1. This can be realised by building-up a large gas recycle. For convergence reasons, developed later, we choose as manipulated variable the split-ratio of the purge. There are two possibilities: find the suitable split-ratio by means of case studies, or introduce explicitly a controller unit (see subchapter 3.1.4). Figure 3.5 illustrates the latest possibility. Firstly, we select the measured (sampled) variable(s), define the controlled variable, and specify the setpoint. There is also possible to formulate a controlled variable by a mathematical function of several sampled variables. Then, the manipulated variable is selected, and bounds of variations and tolerances are specified.

It can be seen that the above description simulates the steady state behaviour of a SISO (single input single output) feedback controller. Note that the use of controllers complicates the computational sequence, and could make arise convergence problems (see subchapter 3.3.3).

6. Transformation of real units in simulation units

Some real unit operations can find direct correspondence with the 'blocks' used in flowsheeting, as flashes, distillation columns, heat exchangers, etc. However, the equivalence could be difficult for many others. This is typical the case of the industrial chemical reactors and a number of separators. In some cases, a simple model may be satisfactory for a quite complex unit from mechanical point of view. Consequently, the modelling of real units can follow one of the following possibilities:

• Decomposition in elementary simulation blocks. Example: an azeotropic distillation column may be decomposed in reboiled stripping column, heat exchanger, three-phase flash separator and reflux splitter.

• Aggregation of units. Example: a heat exchanger and a flash vessel may be combined in a single flash block.

• Black box units. Examples: membranes, dryers, special separations, etc.

• Add-on user units. This possibility involves the existence of a programming environment, including the access to physical properties and other routines.

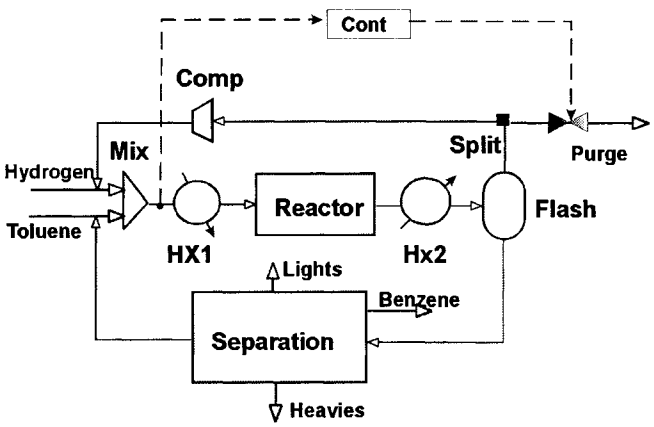

Figure 3.5 Flowsheet controller in the HDA process

For instance, the **Furnace,** which in practice is a sophisticated equipment item, can be modelled as simple *heater*. The cross **Heat Exchanger** may be described either as two-side heat exchanger, or as single-side heater and cooler coupled by common duty. The **Steam Generator**, the **Cooler** and the phase separator **Flash,** may be lumped in a single flash with duty. However, for the clarity of the flowsheet, as already shown in Fig. 3.3, we prefer to aggregate only the two heat exchangers in a single *cooler*, and to consider a distinct *adiabatic flash* for the separation vessel. Finally, the chemical reactor may be simulated by a kinetic PFR followed by a stoichiometric reactor.

7. Degrees of Freedom Analysis

The specification phase of the simulation units makes necessary the analysis of the degrees of freedom (see subchapter 3.2). This is the number of variables that must be set in order to solve the system of equations describing the model. Therefore, the user should have at least an idea about the type of equations and algorithms associated with different modelling units. Sometimes the user has to decide between alternative models, with quite different specification and convergence properties.

In the HDA process we might encounter some problems in simulating rigorously the distillation columns, because these are involved in a recycle loop. Imposing exact values for products could lead to failure of computations, because of inconsistency in

the material balance. Specification of component recovery, as the ratio between component flow rate in product and feed, gives always convergence.

8. Thermodynamic issues

The appropriate selection of thermodynamic models is probably the most important aspect of a simulation work. Sometimes preliminary work is necessary to estimate physical properties for non-library components, or to identify the parameters of thermodynamic models from experimental data. A thermodynamic model may be valid for the whole flowsheet, or only for some units. Specific thermodynamic options at unit level will increase the reliability of the results. For the **HDA** process we have the following possibilities:

- Equation of state model, as for example Peng-Robinson, for the whole flowsheet.
- Equation of state model only for the high-pressure section (gas loop), and specific model for aromatic hydrocarbons, as BK10, for low-pressure separations.

9. Computational sequence

The flowsheet must be decomposed in *computational sequences* if there are recycle loops and/or design specifications. The streams necessary to be initialised are called *tear streams*. Modern software can perform automatic topological analysis to determine the computational sequence and the corresponding tear streams.

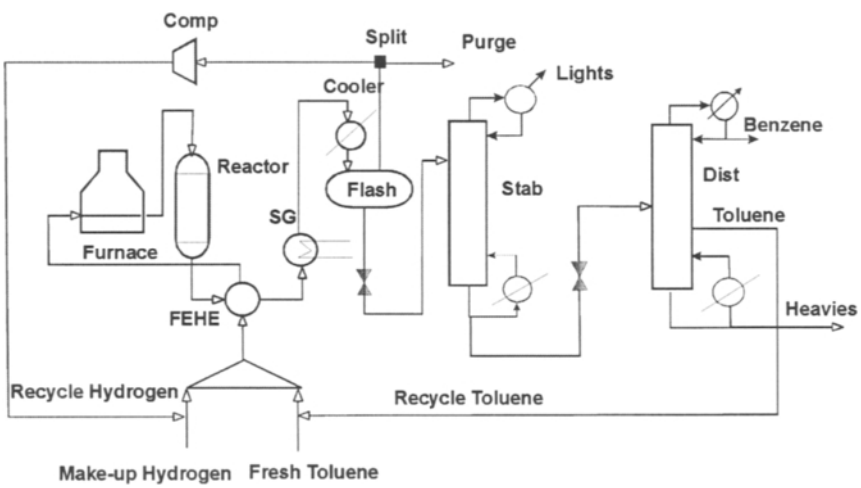

Figure 3.6 Process Simulation Diagram of the HDA process

Figure 3.6 presents the final Process Simulation Diagram of the **HDA** process. Disregarding the loop created by the flowsheet controller, three recycle loops may be identified: heat integration around the reactor, recycle of hydrogen and recycle of toluene. The last two loops have a common part from the mixer up to the flash. As a result, the two loops may be solved by only one tear stream. Hence, we have three loops but only two tear streams, as for example the exit streams from mixer and reactor. However, a further simplification is possible. We may break the loop around the heat

exchanger **FEHE** by splitting it in two one-side heat exchangers connected by a common duty. We have now only one tear stream for the whole flowsheet! This might be the exit of the mixer, whose initialisation is straightforward, or the flash inlet. The above example illustrates the technique of *transmission of information*, very useful in simplifying the computational sequence.

Simulation procedure

Once the PSD known, the following approach can be followed to run a simulation:

1. Draw the flowsheet.
2. Input the components.
3. Select the thermodynamic options.
4. Analyse the recycles and identify the tear streams.
5. Supply data for input and tear streams.
6. Supply specifications for the simulation units (blocks).
7. Run and make converge the simulation.
8. Analyse the results.

The *Graphical User Interface* (GUI) helps to draw the PSD, enter the specifications for units, run the simulation and analyse the results. On-line help and tutorial is provided. However, the user should follow professional training and become familiar with the advanced flowsheeting features before attempting more complex problems. This will avoid not only failures, but also an inefficient use of the software. The steps of the procedure mentioned above deserve short comments.

1. Drawing the flowsheet consists of defining input and output streams, selecting the unit operations from the software library, and placing all the information in a proper order on screen. Connecting the units by streams (material, energy or information) produces a graphical image of the simulation problem. Working with complicated PSD is cumbersome. Some software allows the decomposition in sub-flowsheets that can be converged separately and afterwards merged in a large model.
2. Component definition calls the database for physical properties. Three situations may appear: component available, component described as petroleum fraction or by characterisation methods, or user-defined component.
3. The choice of the thermodynamic options may be guided by an 'expert system'. However, the knowledge of the key features of thermodynamic methods is desirable.
4. The analysis of the computational sequence is recommended, even if this is found automatically. Selecting tear streams before key units, as reactors and separators, avoid severe failure and accelerate the flowsheet convergence.
5. Accurate initialisation of the tear streams is not normally needed, but it should give better chance for convergence. High sensitivity to tear stream initialisation might hide modelling problems, design problem, or inconsistent specifications.
6. Some software performs a degrees of freedom analysis and offers a selection of specifications from a menu. Note that the specification mode of individual units should be consistent with the overall flowsheet convergence, as it will be explained later.
7. Following the convergence history is important at both units and flowsheet level. The simulation of a complex flowsheet is usually difficult and requires a deeper knowledge of flowsheeting techniques.

8. The pivotal result in flowsheeting is the stream report. Follow-up the performance of individual units is also necessary, especially the composition of the reaction mixtures and the profiles of internal variables in the separation units.

A more advanced feature in flowsheeting is the use of analysis tools for design or operation. For example, a *sensitivity analysis* can capture interrelations between different variables in the simulation problem. A more elaborate research may involve *case studies.* The capacity of simulation to imagine virtual experiments is a real benefit from which the user should know to take full profit.

The HDA process example demonstrates that careful analysis of the simulation problem is necessary before rushing to the computer. Moreover, a converged run is not sufficient. Reliable results require a systematic validation work, as well as good knowledge of the modelling basis. These fundamental aspects will be developed in the following subchapters.

3.1.2 Unit Operations

A Process Simulation Diagram can be built-up by means of unit operations or simulation blocks. The list below cites the most frequent types, available in any all-purpose simulator:

1. Mixer, Splitter and (black box) Separators.
2. Flashes.
3. Heat exchangers.
4. Shortcut distillation.
5. Multistage separations.
6. Liquid-Liquid extraction.
7. Chemical reactors.
8. Pressure change: pump, compressor, valve.
9. Pipes and pressure drop units.
10. Special separation units: membrane unit, crystalliser, dryer, etc.
11. Controllers.
12. User added units.

We present hereafter a description of generic capabilities in commercial flowsheeting systems. More information may be found by consulting the user manual of different simulators. User programming is a powerful method to handle the limitations concerning the simulation of some industrial equipment items.

1. Mixers and splitters

Figure 3.7 Mixer and splitter units

Mixer is a unit that performs an adiabatic mixing of several inlet streams in a single outlet stream (Fig. 3.7). The streams are usually of material type. Heat or work may be considered, but not in combination with material streams. The outlet stream is flashed. Water deserves a special treatment: (1) included in the mixture, (2) decanted as immiscible phase, or (3) treated by VLL equilibrium. *Splitter* divides an inlet streams into more streams of the same composition and state.

In this category we may include the *black-box separation* (Fig. 3.8). This unit is very useful for the preliminary computation of material and energy balances. We mention only two types:

a. *General black-box separators*, with *m* inputs and *n* outputs. The separation is defined in term of component recovery, or/and mass or volume flow rates.
b. *Two-product separation column* is used to model simple distillation and absorption columns, but allows wider specifications, as for example purities.

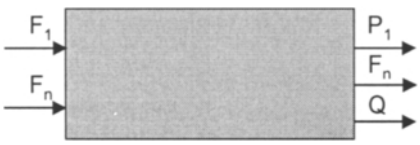

Figure 3.8 Black box separation unit

2. Flash units

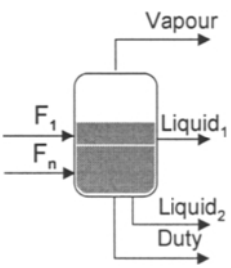

Figure 3.9 Flash separation unit

The flash unit (Fig. 3.9) is a key tool in flowsheeting, particularly for simulating operations based on phase equilibrium. The standard models are:

- Vapour/liquid flash, optional with free water decanting
- Three-phase flash vapour/liquid (1)/liquid (2).

The specification of a flash is given by the degrees of freedom analysis. Vessel sizing is optional in steady state, but becomes compulsory in dynamic simulation.

Note that simple flashes can simulate a number of simple equilibrium devices, as evaporators, decanters or crystallisers. The flash units can also be used to check thermodynamic options before more sophisticated separations, or to prepare tables and diagrams of properties, as temperature-enthalpy in heat integration.

3. Heat exchangers

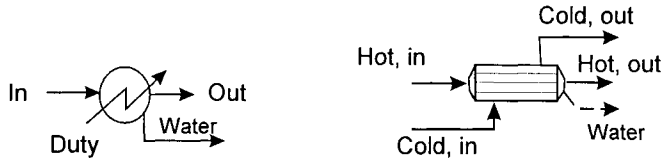

Figure 3.10 Simple heat exchangers Heater/cooler, and Shell-and-tubes exchanger.

Hereafter we describe the basic models. Detailed design and sizing are available via specialised packages that are normally interfaced with the flowsheeting simulator.

a. Energy modification

A simple heater/cooler unit is used to model operations where only the change of state variables of a stream is relevant (temperature, pressure), and not the thermal design of the heat exchanger (Fig. 3.10-left).

b. Shell-and-tubes heat exchangers.

This unit simulates a two-sides heat exchanger that may operate in counter current or co-current (Fig. 3.10-right). If computation is a simple thermal design limited to duty and exchange area calculation, then the overall heat transfer coefficient must be known. If the computation is of rating type, then the exchanger geometry must be supplied. Some simulators have as defaults the sizing characteristics of shell-and-tubes heat exchangers respecting the TEMA standards (see Chapter 16). Rigorous simulation (rating) may include pressure drop computation and zone analysis.

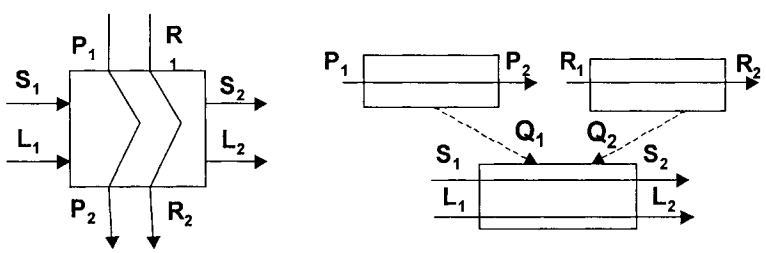

Figure 3.11 Multiple-streams heat exchanger

c. Multiple-stream heat exchanger.

The multiple-stream heat exchanger unit, often called LNG, is used to simulate heat transfer between multiple hot or cold streams (Fig. 3.11-left). Typical applications are the simulation of compact heat exchangers as the plate-type heat exchanger used extensively in gas processing. The simulation of this unit includes the automatic generation of multiple interconnected heaters, as illustrated in Fig. 3.11-right.

4. Shortcut Distillation

Shortcut distillation is used in preliminary design to determine the number of stages needed by a given separation (Fig. 3.12). The computation is based on the classical Fenske-Gilliland-Underwood procedure (see Chapter 9), adapted to handle total or partial condensers. Extensions have been developed in some simulators for the preliminary design of more complex column, as crude units and vacuum towers. We strongly recommend the use of shortcut models in early stages of flowsheeting for easier convergence of recycles, because the specifications will be always fulfilled, even if the column sizing might be questionable.

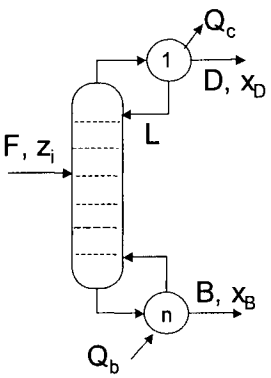

Figure 3.12 Shortcut distillation model

5. Rigorous distillation

Rigorous distillation is probably the most sophisticated unit in flowsheeting. The modelling may be classified in two categories: (a) Equilibrium stage based models, and (b) Rate-based models.

The equilibrium-stage models are still the most applied. They consist of rigorous solution of the MESH equations (Mass, Equilibrium, Summation, and Enthalpy balances) following different strategies (Haas, 1992). Real stages may be considered by means of stage efficiency (Murphree), although in the design practice it was found that this concept introduces more confusion that it solves (Kister, 1992). Stage and/or component efficiency can be used to monitor the column performance in operation.

Rate-based or *non-equilibrium models* can overcome the shortcomings of stage efficiency. A thorough description can be found in the book of Taylor and Krishna (1993). However, they require the knowledge of a large number of parameters, the most critical depending on the design of the contact device. When the emphasis is on process synthesis, the rate-based models are too demanding, and classical equilibrium stage models are more practical. However, the situation is different in operation or in final accurate design, where rate-based models are highly recommended. More experience with rate-based models and their availability as standard options in commercial packages could change this situation in the future.

Some basic simulation models for distillation-based operations column are described briefly below.

a. All-purpose separation column

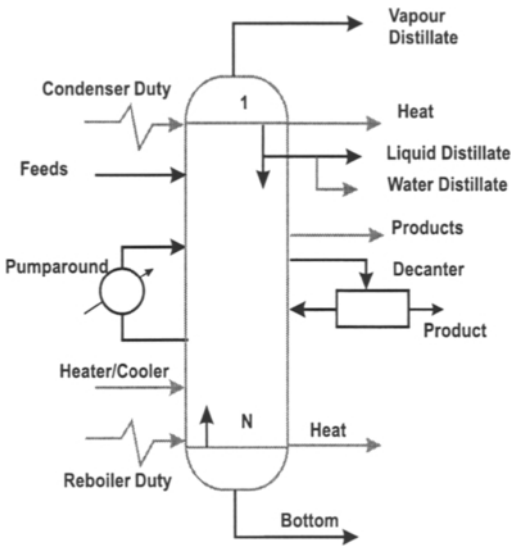

Figure 3.13 Single all-purpose separation column

This unit can simulate any type of separation processes, as distillation, absorption, stripping, or extraction columns, modelled as cascade of counter-current equilibrium stages. The model **Radfrac** in Aspen Plus is particular powerful. It is first built on the *inside-out algorithm* that increased dramatically the robustness in simulating distillation-based operations (Boston, 1980). Columns with multiple feeds, side streams products, stage heaters or coolers, can be treated, as illustrated in Fig. 3.13. The following capabilities are generally available:

- Treatment of various types of mixtures: ideal, non-ideal, azeotropes.
- Several algorithms tailored for a diversity of situations, among we mention:
  - Ideal and light non-ideal mixtures, with narrow and wide boiling points.
  - High non-ideal systems (extractive and azeotropic distillation).
  - Three-phase distillation.
  - Electrolytic distillation.
- Chemical reaction on plates either by assuming equilibrium or kinetic control.
- Wide choice of specifications on products (flow rates, recoveries, purities, ratio of components), but also on some internal variables (flows, temperature, physical properties of mixtures).
- Column sizing may include several types of trays, as sieves or valves, as well as several types of packing, dumped or structured.
- In-line programming used to customise the specifications.

b. Inter-linked columns

The block of inter-linked columns offers robust simulation of a combination of complex distillation columns, as heat-integrated columns, air separation system, absorber/stripper devices, extractive distillation with solvent recycle, fractionator/quench tower, etc. Because sequential solution of inter-linked columns could arise convergence problems, a more robust solution is obtained by the simultaneous solution of the assembly of modelling equations of different columns.

c. Petroleum refining columns

Specialised units are used to simulate complex fractionation processes in petroleum refining. Typical configuration consists of a main column with pump-around and side strippers (Fig. 3.14). Among applications, we may cite pre-flash tower, crude atmospheric distillation, or Fluid Catalytic Cracking (FCC) main fractionator.

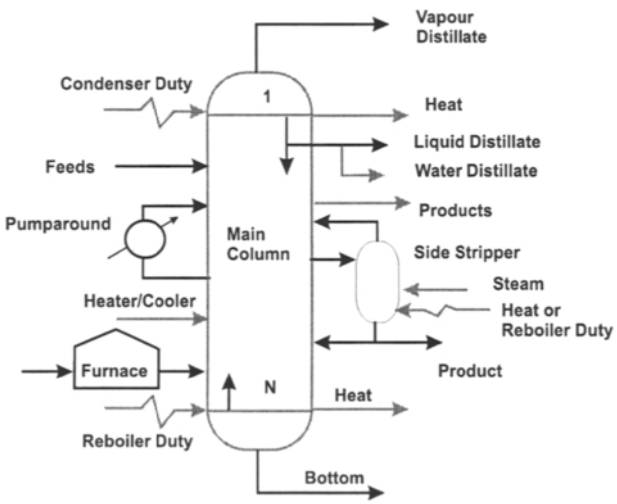

Figure 3.14 Petroleum refining model

Batch distillation

Batch distillation (Fig. 3.15) is a capability included in some flowsheeting software that can be used as stand-alone or in combination with a continuous process. The model solves the unsteady state MESH equations under the constraints of batch-wise operation, as variable reflux, variable column pressure, time-programmed collection of fractions, or controlled thermal policy. A powerful feature is the investigation of a distillation strategy that minimises the time of a batch.

Note that separate packages as Batchfrac of Aspen and CC-ReACS of ChemCad are more convenient for simulating discontinuous processes involving both reaction and separation, as encountered in speciality chemicals.

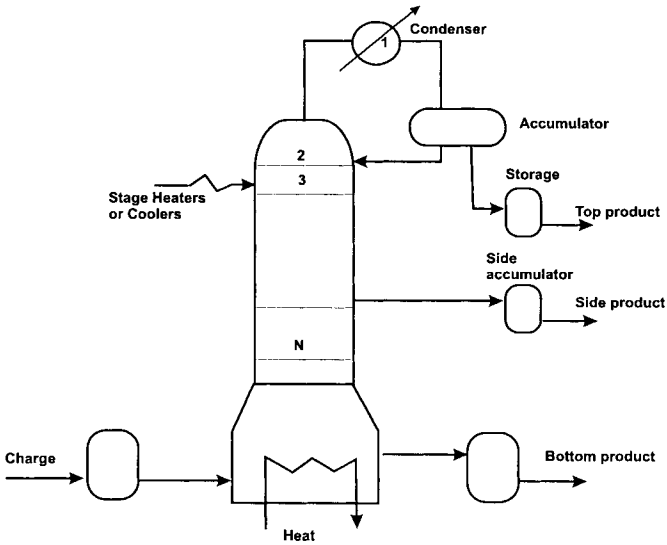

Figure 3.15 Batch distillation model

6. Extraction

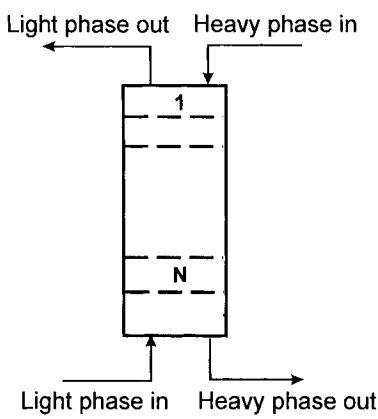

Figure 3.16 Liquid-liquid extraction model

Liquid-liquid extraction unit (Fig. 3.16) simulates a counter-current extraction device consisting of equilibrium stages. Multiple feeds, side products and heaters/coolers may be considered. Accurate modelling of liquid-liquid equilibrium is essential, particularly when the unit is involved in a recycle. If the thermodynamics is not reliable, a simple black box unit is recommended for closing the recycles. The analysis and design of a selected equipment type can be done as stand-alone unit by using rigorous models.

7. Reactors

As the main responsible for the changes in the material balance, the chemical reactor must be modelled accurately from this point of view. Basic flowsheeting reactors are the plug flow reactor (PFR) and continuous stirred tank reactor (CSTR), as shown in Fig. 3.17. The ideal models are not sufficient to describe the complexity of industrial reactors. A practical alternative is the combination of ideal flow models with stoichiometric reactors, or with some user programming. In this way the flow reactors can take into account the influence of recycles on conversion, while the stoichiometric types can serve to describe realistically selectivity effects, namely the formation of impurities, important for separations. Some standard models are described below.

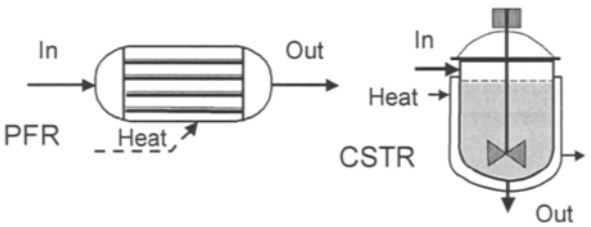

Figure 3.17 Models for chemical reactors

a. Stoichiometric reactor

The stoichiometric model describes the material balance of the reaction network by means of stoichiometric equations by using conversion or extent of reaction as reaction variable. In this approach the atomic balance is conserved. In the case of the model called *yield reactor* the distribution of products is given by algebraic correlations. This approach conserves the overall mass balance but it might not respect the atomic balance. In consequence, when using a yield reactor inconsistency in component material balance might occur, although the convergence of recycles could be achieved.

b. Equilibrium reactor

In the case of fast chemical reactions, as at high temperatures or accelerated by catalysts, the hypothesis of chemical equilibrium can give a realistic idea about the maximum achievable performance. Deviations in temperature or conversion with respect to the true equilibrium may be specified. Single-phase chemical equilibrium, or simultaneous chemical and multi-phase equilibrium may be treated. Great attention should be paid to the accuracy of computing Gibbs free energy functions and enthalpy. Two models are usually available:

- *Equilibrium reactions.* The chemical reactions are given explicitly. Input of expressions for equilibrium constants may be considered.
- *Gibbs free energy minimisation.* This model does not need the specification of stoichiometry, but only of the species taking part in reactions. Reliable algorithms are available due to the works of W. Seider and co-workers (1979-1981).

c. Kinetic models

Kinetic models can be used to link the reactor design with its performance. The reaction rate may be expressed by power law functions, by more complex expressions, as Langmuit-Hinselwood-Hougen-Watson (LHHW) correlations for catalytic processes, or by considering user kinetics. There are two ideal models, continuous stirred tank reactor (CSTR) or plug flow (PFR), available in rating mode (reaction volume fixed) or design mode (conversion specified).

d. Batch reactor

Batch or semi-batch reactors can be simulated as stand-alone or coupled with a continuous process. Specification may include cycle operation with buffer tanks, as well as reactions in single and multi-phases.

8. Change in pressure

Pressure models simulate the change in state variables and thermodynamic functions produced by a change in the pressure of fluid. Flash computation is systematically performed. The usual units are described below.

a. Pump

This unit simulates pumps for the transport of liquids, as well as hydraulic turbines. It may handle multiple phases and water decantation.

b. Compressor/Expander

The general multistage compressor model may have several functions: polytropic and isentropic compressor, positive displacement compressor, inter-cooler between stages, isentropic turbine. Single phase, as well as two- or three-phase calculations, is possible.

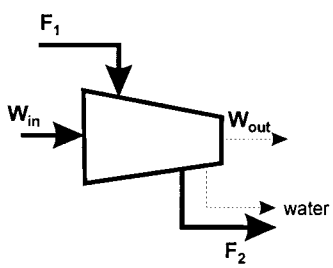

Figure 3.18 Compressor/expander model

c. Valve

Valve model simulates the change in the state of a fluid produced by a significant decrease in pressure, normally under adiabatic conditions. The modelling of a valve unit is similar to a flash. Note that some packages have the capability of a *safety relief valve*, which can be used to simulate the dynamics of an emergency situation, as the time needed for the depressurisation of a vessel.

9. Pressure drop module

Pressure drop unit are used to simulate hydraulic operations, as for example the pressure drop in a pipeline or in a distribution network. Adiabatic operation or heat transfer with the surroundings can be treated. In flowsheeting the module is generally tailored to simulate the transport of fluids in process plants. It can cover a large variety of physical conditions, as for example three-phase calculations in different flow regimes. However, special applications are better modelled by dedicated software, as the network of utilities (water and steam), or pipeline systems in oil & gas production.

3.1.3 Thermodynamics

Components

The main sources of information of thermo-physical properties are listed below:

- Design Institute of Physical Property Research (DIPPR)/AIChE-USA
- Physical Property Database System (PPDS2)/NEL-UK
- Thermodynamics Research Centre (TRC)/Houston-USA.

High quality data requires expensive checking, testing and maintenance. The user should not be surprised by some discrepancies between different systems. Checking the model parameters and validity range is recommended. When a property is not available, this is systematically estimated. A detailed description of the estimation methods can be found in the newest edition of the legendary book of Prausnitz et al. (2001). Most of the methods are implemented in simulators. The user should pay attention to the accuracy of each method, knowing that sometimes relatively small inaccuracies may have serious consequences, as in the case of Gibbs free energy on chemical equilibrium.

Thermodynamic options

The selection of appropriate thermodynamic models and the accuracy of parameters are crucial for the reliability of design studies aided by simulation. Chapters 5 and 6 are devoted to these issues. Table 3.1 presents a global view of the methods for separation processes. They are classified as matrix with mixture-type in rows against pressure range in columns. Low-pressure domain may be covered by traditional methods, as ideal vapour combined with liquid activity models. Vapour non-ideality must be considered already at medium pressures. The equations of state models have no alternatives at higher pressures.

Default thermodynamic options are usually based on cubic equations of state (EOS). The reason is that these can cover a large range of applications, particularly in processes involving hydrocarbons, offering consistent computations both for phase equilibrium and for energy & entropy based computations. Normally, every simulator has an internal database with interaction parameters for different models. When employed in a 'transparent manner' these parameters can produce good or bad results. When accuracy is important, the user has to check carefully the availability, the source of original data and the modelling errors. For example, in Aspen Plus the user must validate explicitly the interaction parameters proposed by the software.

Table 3.1 Classification of thermodynamic methods in separation

	Low Pressure 0.1 - 3 bar	Medium Pressure 3 - 20 bar	High Pressure > 20 bar
Ideal mixtures	Raoult-Dalton	EOS	EOS
Non-ideal mixtures	V - ideal/EOS L - LACT	1) V-EOS; L-LACT 2) Modified EOS	Modified EOS
Hydrocarbon+ supercritical	EOS	EOS	EOS
Non-ideal + supercritical	V - Henry coefficients L - LACT	Modified EOS	Modified EOS

EOS = equation of state model; LACT = liquid activity model

Table 3.2 presents a selection of the most used thermodynamic options for phase equilibrium with suitable enthalpy and entropy methods. The accuracy of both phase equilibrium and enthalpy/entropy computation must be examined when using EOS models. For example, often a cubic EOS underestimates the enthalpy of vaporisation. In this case other methods are more accurate, as those based on three-parameters corresponding states law (Lee-Kesler, Curl-Pitzer, etc.). Mixtures rich in components with particular behaviour, as H_2 or CH_4, need special methods for accurate simulation. When binary interaction parameters for liquid activity models are absent, the UNIFAC predictive method may be employed. It is worth to note that UNIFAC is suitable only for exploratory purposes, but not for final design. When high non-ideal mixtures are involved at higher pressure then the combination of EOS with liquid activity models is recommended (see Chapter 6).

Interaction parameters for mixtures

The thermodynamic models for handling mixtures contain a number of interaction parameters. They may be classified in the following categories:

1. Binary interaction coefficients for liquid activity models. Note that there are distinct values for VLE and LLE. Several sets of values may be available, depending on pressure and temperature range. The non-ideality of the vapour phase should be considered at higher pressure or vacuum applications. The possibility of molecular associations in vapour or liquid phase should be examined.
2. Interaction parameters for EOS models. The mixing rules for which the interaction parameters are valid must be checked for consistency with the physical situation (see Chapters 5 and 6).
3. Henry constants for binary gas/solvent (usually water) mixtures.
4. Solubility data for water/organic mixtures.
4. Electrolyte systems: ionic parameters for different species, equilibrium constants for different reactions, as well as interaction parameters in liquid activity models.
5. Interaction parameters for equations of state applied to polymer solutions.

If the accuracy is critical and experimental data are available, we recommend the regression of data on the range of variations needed in application. Chapter 6 describes the rules that should follow the regression procedure.

Table 3.2 K-factors, enthalpy and entropy methods in process simulation

K-factors method	T/P range	Mixture	Applications	Enthalpy/ entropy
Grayson-Streed	-20 to 450 °C	Hydrocarbon + H_2, CH_4	Refining Topping Heavy ends	Curl-Pitzer Lee-Kessler
Chao-Seader	20 to 250 °C 1 to 100 bar	Hydrocarbon + H_2 (max 20%)	Gas processing Depropaniser Debutaniser	Curl-Pitzer Lee-Kessler
BK10	0.1 to 7 bar 40 to 500 °C	Naphta C1 to C7 BTX	Vacuum distillation Atmospheric distillation BTX columns	Lee-Kessler Rice
SRK	$< T_c$ $< P_c$	Hydrocarbon LNG H_2S, $C0_2$, N_2	Oil & gas Cryogenics	SRK
PR	$<$ or $> T_c$ $<$ or $> P_c$	Hydrocarbon LNG H_2S, $C0_2$, N_2	Oil & gas Cryogenics	PR
Modified EOS	$<$ or $> T_c$ $<$ or $> P_c$	Hydrocarbon Polar Sub-critical Supercritical	Petrochemicals Basic organics Gas processing	Modified EOS PR, SRK
Wilson	20 to 200 °C < 5 bar	Non-ideal VLE	Organic Petrochemicals	Ideal + Latent heat
NRTL	20:200 °C < 5 bar	Non-ideal VLE, LLE	Organic Petrochemicals	Ideal + Latent heat
UNIQUAC	20 to 200 °C < 5 bar	Non-ideal VLE, LLE	Organic Petrochemicals	Ideal + Latent heat
UNIFAC	20 to 200 °C < 5 bar	Non-ideal VLE, LLE	Organic Petrochemicals	Ideal + Latent heat

3.1.4 Control structures

The use of control structures is an advanced flowsheeting feature. Flowsheet controllers are particularly useful in plant operation. An important application is the simulation of the steady state behaviour of SISO controllers. With respect to control action we can distinguish between two basic types, feedback and feedforward control.

A *feedback control loop* (Fig. 3.19) consists of varying the 'upstream' variable y in order to achieve the 'downstream' set point x in the limit of a specified tolerance.

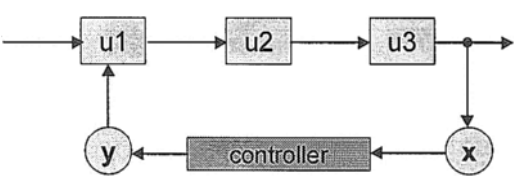

Figure 3.19 Feedback control structure

Feedback controller may be placed inside or outside of a flowsheet convergence loop. There are cases when the manual definition of the computation sequence is useful. As typical applications we cite:

- Keep constant some stream or unit variables by manipulating other variables. Example: vary a flash duty to reach a specified component recovery in a product.
- Manipulate make-up streams, as solvent, acid/base solutions or catalyst. Example: control the pH in a precipitation tank.
- Control emissions in gaseous purges or liquid bleeds. Example: control the concentration of an inert component in a recycle loop by manipulating the purge flow.

ASPEN Plus offers a powerful feedback controller known as *design specification* (Fig. 3.20). This capability can treat multi-variable specifications, accept programming, and mix design specification and tear streams in the same convergence loop.

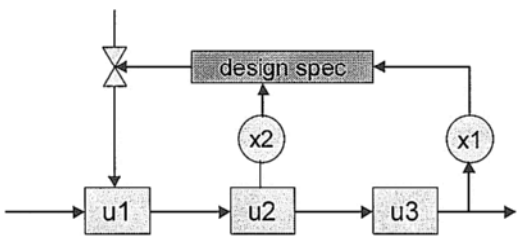

Figure 3.20 Design specification as feedback control structure

A *feedforward controller* can be used to transport information already available somewhere to other place in the flowsheet. Figure 3.21 displays a typical implementation. Here the controller sets a 'downstream' sampled variable at a given value based on an 'upstream' computed variable.

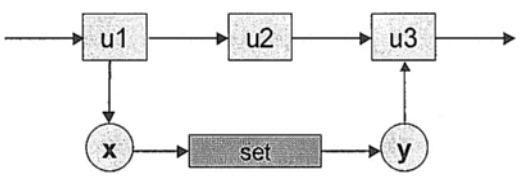

Figure 3.21 Feedforward control structure

Most of the software offers *in-line programming,* either by in FORTRAN, or Visual Basic. Programming is a powerful tool in flowsheeting that allows the user to customise the simulation, or introduce its knowledge. Among applications we may cite the formulation of complex specifications, the transmission of information between different units, to express complex reaction rate expressions, built user simulation units, or prepare data for presentation, interfacing or post-processing.

3.2 DEGREES OF FREEDOM ANALYSIS

The *degrees of freedom analysis* (*DOF*) allows the user to determine the variables needed to be specified to execute a simulation. In steady state simulation the degrees of freedom are the number of variables that must be assigned to solve the non-linear algebraic system describing the operational unit. Here we adopt the approach called *variable-minus-equations*, in which *DOF* is equal with the number of variables N_v minus the number of independent equations N_{eq}:

$$DOF = N_v - N_{eq} \tag{3.1}$$

Note that in the above formulation both extensive and intensive variables are included, in contrast with the phase rule, where only intensive variables are considered! Typical N_v variables are temperatures and pressures, partial flows, specific enthalpies, chemical potential or fugacities of components, heat duty and mechanical work, recycle ratios and split fractions. Be careful not to include in the list interdependent variables.

3.2.1 Streams

Let's consider a process stream containing N_c components, single-phase or multi-phase (Fig. 3.22). The question is how many independent variables must be known. Some situations are examined below.

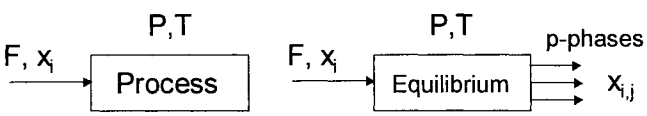

Figure 3.22 Degrees of freedom analysis of a stream

A single-phase stream without reaction is specified by (N_c+2) variables. These may be the partial mass flows (molar or weight units), or the composition for (N_c-1) components plus the total flow rate, as well as P and T. The phase condition can be determined by flash computation.

Table 3.3 illustrates the analysis for a multi-phase stream of flow rate F with N_c components split in F_j (j=1, ..., p) phases, each of composition x_{ij}. By counting the variables and the equations it is found that $DOF = N_c + 2$. The result is identical with the *DOF* for a mono-phase stream. The explanation is that the composition of each phase at equilibrium is 'implicitly' determined by means of the *K*-factors, although these are function of composition, pressure and temperature. This result may be generalised for a stream where equilibrium reactions occur. This time the composition of phases are fixed by knowing the chemical equilibrium constants, which are available via chemical potentials, function of temperature, pressure and composition.

Table 3.3 Degrees of freedom for a multiphase stream

	Equations	Variables	N_v	N_{eq}
Balance of phases	$F = \sum_{j=1}^{p} F_j$	F stream flow rate F_j phase flow rates	1 p-1	1
Component balance	$f_i = \sum_{j=1}^{p} x_{ij} F_j$	x_{ij} molar fractions	pN_c	N_c
Balance of components	$F = \sum_{i=1}^{c} f_i$	f_i component flow	0	1
Uniform T	$T_1 = T_2 = ...=T$	temperatures	p	p-1
Uniform P	$P_1 = P_2 = .. =P$	pressures	p	p-1
Phase equilibrium	$\mu_{i,1} = \mu_{i,2} = \cdots = \mu_{i,p}$	chemical potentials	N_c	$(p\text{-}1)N_c$
Mole fraction condition	$\sum_{j=1}^{p} x_{ij} = 1$		0	p
$DOF=N_c+2$			pN_c+3p+N_c	pN_c+3p-2

3.2.2 Unit Operations

1. Mixer/Splitter

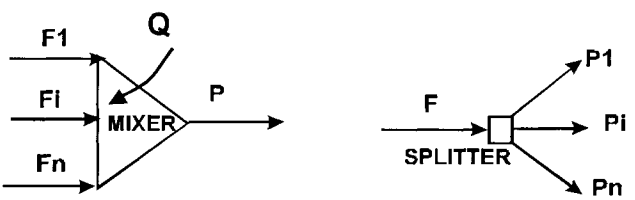

Figure 3.23 Specifications for Mixer and Splitter

The counting gives $(n+1)(N_c+2)+1$ variables (Fig. 3.23-left). It is not difficult to see that $DOF = n(N_c+2)+2$. Typical specifications are: n inlet streams plus two specifications, as for example (P, T) or (P, Q). The splitter divides an inlet stream in n outlet streams of identical state and composition (Fig. 3.23 -right). The split is usually defined by the feed fraction α_k passed in the outlet k. As result we have $DOF = (N_c+2)+(N_{outlets}-1)$.

2. Flash operations

Fig. 3.24 and Table 3.4 illustrate the analysis of a VLE flash. One gets $DOF = N_c+4$, from which N_c+2 may be attributed to the inlet stream. It remains two specifications that can be chosen among other variables. Table 3.5 presents typical specifications.

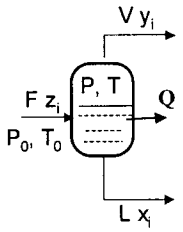

Figure 3.24 Specification of a vapour/liquid flash

Table 3.4 Degrees of freedom analysis of a vapour/liquid flash

	Equations	Variables	N_{eq}	N_v
Total balance	$F=L+V$	F, L, V	1	3
Component balance	$Fz_i = Lx_i + Vy_i$	z_i, x_i, y_i	N_c	$3N_c$
Equilibrium T	$T_L = T_V = T$	T, T_L, T_V	2	3
Equilibrium P	$P_L = P_V = P$	P, P_L, P_V	2	3
Phase equilibrium	$y_i = K_i x_i$	-	N_c	-
K-factors	$K_i = f_i(T,P,x_i,y_i)$	K_i	N_c	N_c
Bubble point	$\sum_{j=1}^{p} x_{ij} = 1$	-	1	-
Dew point	$\sum_{j=1}^{p} y_{ij} = 1$	-	1	-
Enthalpy balance	$Fh_F = Lh_L + Vh_V + Q$	h_F, h_L, h_V, Q	1	4
Feed enthalpy	$h_F = f(z_i,T_0,P_0)$	T_0, P_0	1	2
Liquid enthalpy	$h_L = f(x_i,T,P)$	-	1	-
Vapour enthalpy	$h_V = f(x_i,T,P)$	-	1	-
$DOF = N_c+4$			$3N_c+11$	$4N_c+15$

Table 3.5 Specification of a flash

Type of flash	Specifications			Computed variables
Isobaric/Isothermal	P, T			$Q, V; L, V, x_i, y_i$
Isobaric	P, Q	*or*	P, V	T, V *or* T, Q; L, V, x_i, y_i
Isothermal	T, Q	*or*	T, V	P, V *or* P, Q; L, V, x_i, y_i
Isenthalpic	Q, P	*or*	Q, T	T *or* P; L, V, x_i, y_i
Separation	$V(L), P$	*or*	$V(L), T$	Q, T *or* P; $L(V), x_i, y_i$
Purity	$P(T), x_j$	*or*	$P(T), y_j$	$Q, T(P)$; L, V, y_i *or* x_i

3. Heat exchangers

A shell-and-tube heat exchanger illustrates the approach (Table 3.6). It comes out that the degrees of freedom are ($N_{c,shell} + N_{c,tubes} + 7$). Typical specifications are:

- Stream flow rates on each side, in total ($N_{c,shell} + N_{c,tubes}$) variables,
- Inlet pressures and outlet pressures or pressure drop (four variables),
- Inlet/outlet temperatures of one side, plus a temperature on the other side, or duty and one temperature on each shell and tube sides (three variables).

Note that shell and tube sides are independent as material balance, but not as heat balance, being linked by the same duty.

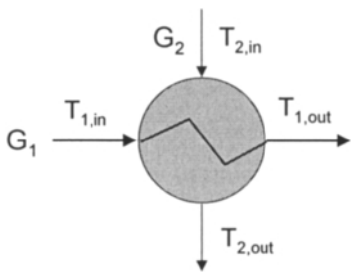

Figure 3.25 Specification of a tube and shell heat exchanger

Table 3.6 Degrees of freedom analysis of a shell-and-tube heat exchanger

Variables		Equations	
Stream flow rates	$2(N_{c,shell} + N_{c,tubes})$	Material balance	$N_{c,shell} + N_{c,tubes}$
Temperature	2 + 2	Energy balance	2
Pressure	2 + 2		
Duty	1		
$N_v = 2(N_{c,shell} + N_{c,tubes}) + 9$		$N_{eq} = N_{c,shell} + N_{c,tubes} + 2$	
$DOF = N_{c,shell} + N_{c,tubes} + 7$			

4. Reactors

a. Equilibrium reactor

Consider a stream containing N_c components where N_r equilibrium reactions occur. The generalised stoichiometric equation is given by

$$\sum_{j=1}^{N_c} \nu_{ij} A_j = 0 \quad \text{with} \quad i=1, 2, \ldots, N_r \tag{3.2}$$

where subscript i designates the component and subscript j designates the reaction. The equilibrium composition can be computed easier if the chemical transformation is

formulated in term of extent of reaction ξ_j. The number of moles of a component in a reacting mixture is given by the equation:

$$N_i = N_{i0} + \sum_{i=1}^{N_c} \nu_{ij} \xi_j \tag{3.3}$$

Chemical equilibrium may be calculated from the variation of chemical potentials:

$$\sum_{j=1}^{N_r} \nu_{ij} [\mu_{i0} + RT \ln f_i(T, P, x_i)] = 0 \qquad i=1, \ldots, N_c \tag{3.4}$$

The combination of equations (3.2) to (3.4) leads to a system of non-linear equations in ξ_j. The final result is that, besides the reaction stoichiometry, there are $(N_c + 2)$ specifications, usually the initial composition of the reacting mixture plus T and P.

b. Stoichiometric reactor

As before, an extent of reaction ξ_i can be defined for each *independent reaction* from a set of N_r reactions. Initial mixture composition and flow rate gives N_c specifications. It is assumed that the heat of reaction is known via the database. Because of enthalpy balance, four more specifications are required: initial temperature, initial pressure, final pressure or pressure drop, as well as the reactor duty.

Table 3.7 Degrees of freedom analysis of a kinetic reactor

	Equations	Variables	N_v	N_{eq}
Mass balance	$f_{0,i} - f_i + r_i V_R = 0$	$f_{0,i}$ - initial mixture	N_c	N_c
		f_i - final mixture	N_c	
		r_i - reaction rate	N_r	
		V_R - reaction volume	1	
Heat balance	$\sum f_{0,i} h_{0,i} = \sum f_i h_i +$	Q_t - heat transferred	1	1
	$+ \sum r_i \Delta H_{R,i} + Q_t$	$h_{0,i}$, h_i - inlet / outlet component enthalpy	N_c	
			N_c	
Component enthalpy	$h_i = h_i(T,P)$	$(T, P)_{\text{inlet}}$	2	N_c
		$(T, P)_{\text{outlet}}$	2	N_c
Reaction rate	$\nu_{R,i} = function_i(k_i, T, P, c_i)$	k_i - kinetic constants	N_r	N_r
	$c_i = function_i(f_i, T, P)$	C_i concentrations	N_c	N_c
$DOF = (N_c + 2) + N_r + 3$			$5N_c + 2N_r + 6$	$4N_c + N_r + 1$

c. Kinetic reactor.

Table 3.7 presents the analysis for a CSTR, where N_c components are involved in N_r independent reactions with known kinetics. Besides inlet stream $(N_c + 2)$ variables and N_r kinetic parameters, three other variables must be known: reactor pressure P or pressure drop ΔP, reaction volume V_R and the heat transferred.

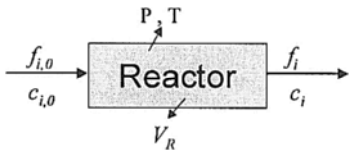

Figure 3.26 Specification of reactors

5. Equilibrium-stage separation

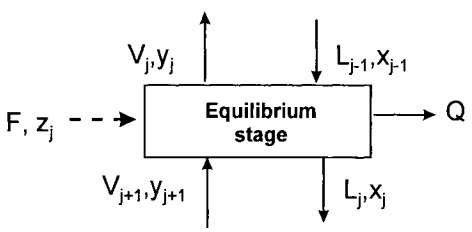

Figure 3.27 Specification of an equilibrium stage in distillation

a. Adiabatic equilibrium stage

There are two inlet and two outlet streams (Fig. 3.27). We assume adiabatic stage. The degrees of freedom can be found from the following analysis:

Number of variables (4 streams)	$4(N_c+2)$
Number of equations for stage	$2N_c+3$
-Pressure equality	1
-Temperature equality	1
-Phase equilibrium relationship	N_c
-Components material balance	N_c-1
-Total material balance	1
-Adiabatic enthalpy balance	1

Thus, for an adiabatic vapour-liquid equilibrium stage one gets $DOF = 2N_c + 5$. Typical specifications are the inlet liquid and vapour streams and the stage pressure.

b. Equilibrium stage with heater/cooler, feed and side stream.

It is easy to demonstrate that in this case the number of degrees of freedom is $DOF = 3N_c + 9$.

c. Condenser and reboiler.

As an exercise, the reader is invited to demonstrate that both for condenser and reboiler, the degrees of freedom are (N_c+4), identical with a flash. Typically, the specifications are: input stream ($N_c + 2$) variables plus two others. Outlet pressure is usually imposed. The remaining variable may be: liquid or vapour fraction, including bubble-point liquid (L=1), dew-point vapour (L=0), or sub-cooled liquid or superheated vapour (unusual). The above specifications enable to compute the duty Q, but this may be given also as specification. Note also that in steady state flowsheeting the reflux drum is included in the simulation of condenser. The type of condenser (partial, total, or sub-cooled liquid), as well as the type of reboiler (kettle or thermosyphon) does not change the analysis.

6. One feed, two products distillation column

Distillation is a complex unit. Both model formulation and counting variables are tedious. Here we adopt the strategy of assembling the device from simpler elements. This might be seen also as an introduction into degrees of freedom analysis of flowsheet. In this case the distillation column is assembled from components as trays, reboiler, condenser, reflux splitter and pump. Summing the *DOF* of elements and subtracting redundant values gives the total *DOF*.

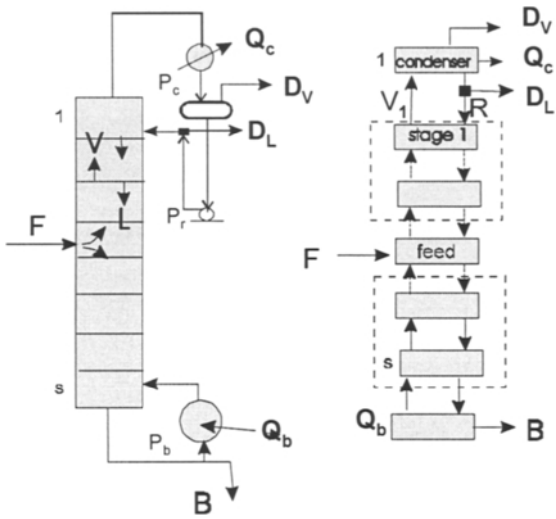

Figure 3.28 Degrees of freedom analysis of a distillation column

Fig. 3.28 presents a one-feed two-products column. This may be decomposed in feed tray, striping section, concentration section, condenser including the flash drum, reflux/distillate splitter, reflux pump and reboiler. We assume adiabatic equilibrium trays, with no heaters or coolers. The column has N_s theoretical trays, including the feed tray, but excluding condenser and reboiler. The count of the degrees of freedom looks as follows:

Feed tray considered as adiabatic stage	$(N_c+2)+(2N_c+5)=3N_c+7$
Striping and concentration sections (lumped)	$(N_s-1)(2N_c+5)$
Condenser (total or partial)	N_c+4
Reflux splitter with pump	N_c+4
Reboiler	N_c+4
Total DOF of units	$N_1=2N_sN_c+5N_s+4N_c+14$

Redundant variables are:

Liquid and vapour streams between stages	$(N_s-1)[2(N_c+2)]$
Stream from staged section to condenser	N_c+2
Stream from condenser to reflux divider	N_c+2
Stream from reflux divider to column	N_c+2
Stream from column to reboiler (liquid)	N_c+2
Connecting stream reboiler to column (vapour)	N_c+2
Total redundant variables	$N_2=2N_sN_c+4N_s+3N_c+6$

Hence, the total number of degrees of freedom of a simple distillation column is: $DOF = N_1 - N_2 = N_s + N_c + 8$. Note that liquid and vapour flow rates, as well as tray temperatures have been eliminated. The number of stages of each section does not appear explicitly. They are a result of counting some stage variables, in this case pressures or temperatures. Consequently, the feed location is a supplementary specification.

The following specifications are always needed:

1. Column feed	N_c+2
2. Stage pressures	N_s
3. Condenser pressure	1
4. Reboiler pressure	1
5. Reflux pump pressure	1
6. Condenser type (partial, total, sub-cooled liquid)	1

The reflux pump pressure should be higher than the pressure of the first tray. Hence, the pressure profile must always be specified. The rest of two variables may be:

6. Flow rate of one product, distillate (D) or bottoms (B), or as ratio by feed, D/F or B/F.
7. Reflux flow rate R or reflux ratio R/D.

The above specifications lead normally to rapid convergence. Alternative specifications may be used, but some are not always feasible. For example, specifying the recovery of a key component and product rate gives convergence if the column design is appropriate. The specification of product purity is difficult, sometimes impossible, because now recovery and distillate rate are interdependent. Similarly, the specification of a tray temperature is linked by composition and vapour/liquid flows. Generally, these specifications are 'indirect' and may be seen as of 'control' type. They require the manipulation of other variables. A controlled specification is feasible if the unit design is appropriate and if it shows continuous and sensitive variation with the manipulated variable.

Specifying reboiler and condenser duties is not recommended, unless they are accurately known. In addition, it is difficult to measure the reboiler and condenser duties for validation. Usually the enthalpy computation is not very accurate, particularly when using an equation of states model.

It is easy to demonstrate that the degrees of freedom for absorption, stripping and liquid-liquid extraction are zero, and therefore these units do not require specifications.

3.2.3 Flowsheet

Since the specification of interconnecting streams between units becomes redundant, the total degrees of freedom of a flowsheet may be computed with the formula:

$$DOF = \sum_{i=1}^{U} d_i - k(N_c + 2) \tag{3.5}$$

where d_i represents the degrees of freedom of units, while k is the number of interconnecting streams, each one with $(N_c + 2)$ specifications.

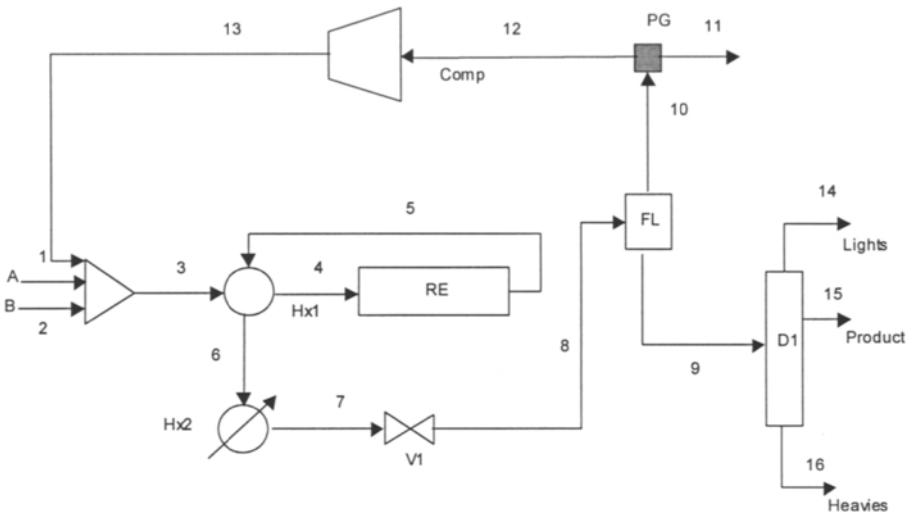

Figure 3.29 Flowsheet for degrees of freedom analysis

The procedure is illustrated by the flowsheet depicted in Fig. 3.29. Table 3.8 contains the details. The column named 'parameters' gives the variables to be specified for each unit, excluding the input streams. The degrees of freedom for the whole flowsheet are $12(N_c + 2) + N_s + 19$, from which we subtract $10(N_c + 2)$ values corresponding to connecting streams. This gives $2(N_c + 2) + N_s + 19$ variables, from which $2(N_c + 2)$ belong to input streams. It remains $(N_s + 19)$ degrees of freedom. This is exactly the value found by counting the variables in the column 'parameters'!

The above result leads to formulate the following rule: Flowsheet degrees of freedom may be obtained by counting the specifications of the input streams, including the tear streams, plus the minimum independent parameters for each unit operation.

Table 3.8 Degrees of freedom analysis of a flowsheet

	Unit		Degrees of freedom	Parameters
1	Mixer	Mix	$3(N_c+2)+1$	P_{out}
2	Heat Exch.	Hx1	$[(N_c+2)+2]\,\vert\,+[(N_c+2)+1]$	$(P, T)_{outlet1}$; $P_{outlet2}$
3	Reactor	RE	$(N_c+2)+1$	Conversion
4	Heat Exch.	Hx2	$(N_c+2)+2$	$(P, T)_{outlet}$
5	Valve	V1	$(N_c+2)+1$	P_{out}
6	Flash	FL	$(N_c+2)+2$	$Q=0$, P_{out}
7	Purge	PG	$(N_c+2)+1$	Purge ratio
8	Compressor	Comp	$(N_c+2)+1$	P_{out}
9	Distillation	D1	$(N_c+2)+N_s+7$ *	Number of trays, Feed location; N_s pressures; P_{cond}, P_{reb} Distillate (D_l, D_v); Reflux

* Stages and feed location is included; reflux pump pressure equals the top stage

3.2.4 Unfeasible specifications

Degrees of freedom analysis is necessary but insufficient in converging a simulation. It is obvious that the number of specifications must match the available DOF's. Normally DOF analysis is done automatically. However, the specifications must be feasible not only at the unit's level, but also for the flowsheet as a whole. From this point of view some common mistakes could be identified as, (1) inconsistent specifications, or (2) interdependent specifications.

Typical *inconsistent specifications* are those that violate the material balance. Figure 3.30 displays a very simple flowsheet that contains only mixer and splitter with recycle stream. This over-simplified scheme might be seen unrealistic but in fact can explain a basic source of non-convergence in more complex flowsheets, where the presence of large number of units and recycles could hide such simple situation. Several specifications of the splitter may be considered, as follows:

(1) s4 = 60 kmol/h: non-convergence, accumulation of material in the loop s5.

(2) s4 = 70 kmol/h: convergence, because the outlet flow match 'exactly' the input. However, with a complex flowsheet this mode of specification gives problems, because it is difficult if not impossible to give values that satisfy exactly the overall material balance.

(3) Specification of s5 at any value: convergence. Now the output can adapt itself to respect the material balance. Setting constant recycle rate, particularly as gas recycle, leads often to robust convergence.

(4) Specification of the split ratio (s4/s3 or s5/s3): convergence. This is a recommended practice: relative specifications as output flow/input flow can remove uncertainties due to the variation of the input flow during successive iterations.

Similarly, the simulation of some units cannot succeed because of inconsistency in material balance. For example, the simulation of a distillation column can fail if the specifications on products are not consistent with the feed. The specification in relative mode, as for example ratio distillate/feed, or component recoveries, is more convenient, particularly when the unit is incorporated in a recycle.

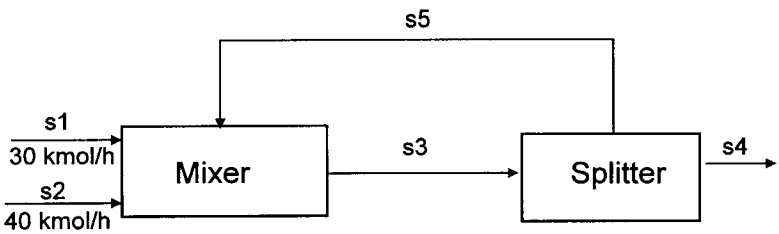

Figure 3.30 Consistent material balance

The convergence could fail because some specifications are interrelated. The distillation column is again a good example. The specification of both component recovery and purity is not recommended, because they are interrelated. Similarly, the possibility of interdependent or conflicting specifications should be examined in defining flowsheet controllers. The following two examples emphasise some problems raised by the specification of units involved in recycle loops containing reactors and separators, even if the stand-alone units are correctly specified.

EXAMPLE 3.1 Specification of a reactor/separator recycle loop

Figure 3.31 displays a generic reactor/separator flowsheet. The reaction is bimolecular of type A+B → P. Study the convergence properties of the flowsheet with respect to specifications for individual units.

Solution.

The specification of each unit is as follows:

- Feed stream: two components, A and B, with the partial flow rates F_{A0} and F_{B0}.
- Stoichiometric reactor: conversion X_A of the limiting reactant A.
- Separator: recovery (S_A, S_B, S_P).

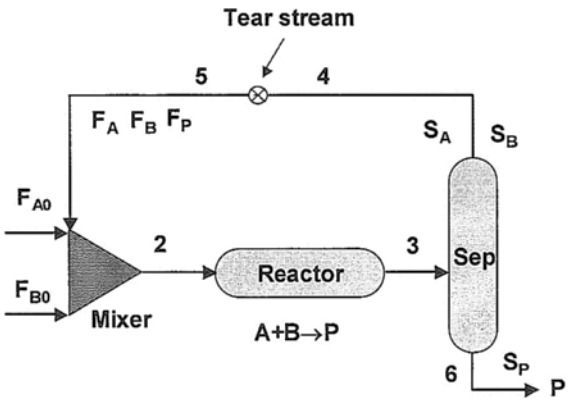

Figure 3.31 Correct but unfeasible specifications

We neglect the energy balance. We chose the recycle as tear stream, so that the computational sequence is: Mixer-Reactor-Separator. The tear stream has been cut explicitly in two parts, the streams 4 and 5. The convergence is obtained when the difference in component flow rates between the streams 4 and 5 is less than a prescribed tolerance. Let us denote the molar flow rates of the components A, B, C in the stream 5 by F_A, F_B, F_C. The convergence condition leads to the following algebraic equations:

$$F_A - [(F_A + F_{A0})(1 - X_A)]S_A = 0 \tag{i}$$

$$F_B - [(F_B + F_{B0}) - (F_A + F_{A0})X_A]S_B = 0 \tag{ii}$$

$$F_P - [F_P + (F_A + F_{A0})X_A]S_P = 0 \tag{iii}$$

After simplifications the system becomes:

$$\begin{cases} [1-(1-X_A)S_A]F_A & & & = F_{A0}(1-X_A)S_A \\ X_A S_B F_A & + (1-S_B)F_B & & = F_{Ao}(M - X_A)S_B \\ -X_A S_P F_A & & + (1-S_P)F_P & = F_{A0}X_A S_P \end{cases} \tag{iv}$$

where $M = F_{B,0} / F_{A,0}$ is the molar ratio of reactants. The Jacobian is obtained by the partial derivatives of each of the three equations with respect of F_A, F_B, F_C:

$$J = \begin{bmatrix} [1-S_A(1-X_A)] & 0 & 0 \\ X_A S_B & (1-S_B) & 0 \\ X_A S_P & 0 & (1-S_P) \end{bmatrix} \tag{v}$$

The matrix is lower diagonal, so the determinant is: $|J| = [1 - S_A(1 - X_A)](1 - S_B)(1 - S_P)$. This is singular only if $S_B = 1$ or $S_P = 1$. We can distinguish between the following situations:

1. Recycle of A. The full recovery of A in separator means $S_A = 1$ and it is feasible. From Eq. (i) the partial flow rate of the recycle stream is $F_A = F_{A0}(1 - X_A)/X_A$.

2. Recycle of B. If the reactants are not in a stoichiometric ratio, then the total recovery of B ($S_B = 1$) will give accumulation and non-convergence. $S_B = 1$ is not a feasible specification. On the other hand $S_B < 1$ is feasible, but implies both losses and impure product. It is obvious that the input definition has to be changed to avoid this situation. The reactants in feed must be in a stoichiometric ratio.

3. Recycle of P. The complete recycle ($S_P = 1$) is neither feasible nor desirable. Complete recovery of P in bottoms ($S_P = 0$) is feasible. Moreover, the recycle of a small amount P is allowed, this will simplify both the design and the control of the separation unit.

The case of the stoichiometric ratio deserves supplementary attention. If A is completely recovered, the recycle stream of B is $F_B = F_{A0}(M - 1)S_B/(1 - S_B)$. For M=1 we have $F_B = 0$, there is no recycle of B. The component B will be consumed entirely in reaction. However, there is possible to built-up a ratio of reactants at the reactor inlet more favourable for kinetics. We can develop the following expression:

$$\left(\frac{F_{A0}}{F_{B0}}\right)_{i,R} = \frac{F_A + F_{A0}}{F_B + F_{B0}} = \frac{F_{A0}/X_A}{F_{B0}} = \frac{1}{X_A}$$

Hence, the ratio of reactants before the reactor and the conversion achieved in reactor are not independent specifications.

The next example illustrates how a simple analysis of feasible specifications can help getting insights into plantwide control problems. This subject will be covered in more detail in Chapter 13.

EXAMPLE 3.2 Specification of the gas recycle loop in the HDA process

Figure 3.32 displays the simplified gas recycle loop of the **HDA** process, containing Mixer, Reactor, Flash, and Stream Splitter. Both energy balance and pressure variation is neglected. The reactants are hydrogen with 5% methane and pure toluene. We consider only the main reaction:

C_7H_8 (T) + H_2 (H) $\rightarrow$ C_6H_6 (B) + CH_4 (M)

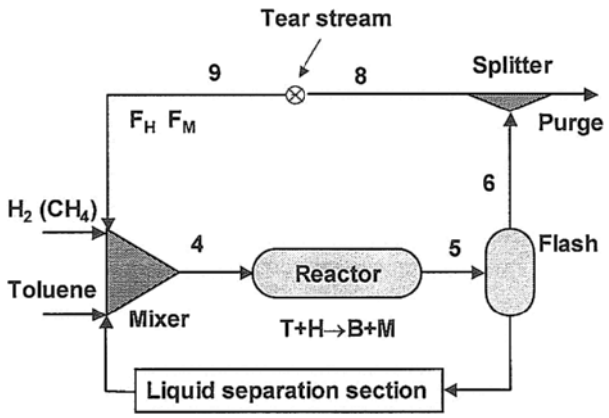

Figure 3.32 Specification of the gas recycle loop in HDA process

Again, we propose for each unit correct specifications, but we would like to know if these are feasible for the whole flowsheet. The recycle tear stream is cut in two parts, 8 and 9. The calculation sequence is: Mixer, Reactor, Flash, and Splitter. We denote with F_H and F_M the partial flow rates of hydrogen and methane in the stream 9. After one pass through the calculation sequence, the partial flow rates of the components in the stream 8 will change. The convergence is obtained when the difference in the component flow rates of the streams 8 and 9 becomes smaller than an error. Consider F_{H0}, F_{M0} and F_{T0} the molar fresh feed of hydrogen, methane and toluene. For reactor we specify the conversion of toluene. The component flow rates at the reactor outlet are:

Hydrogen: $F_H + F_{H0} - F_{T0}X_T$

Methane: $F_M + F_{M0} + F_{T0}X_T$

Toluene: $F_{T0} - F_{T0}X_T$

We assume that the recovery of hydrogen and methane in gas, and of toluene in liquid is 100%. The next step concerns the splitter. Although very simple, the specification of this unit can profoundly affect the convergence. Normally, a splitter is specified in two ways: absolute product flow rates, or relative fractions. Let us examine the two cases.

a. Purge flow rate specified. The convergence condition for the tear stream leads to the equations:

$$F_H - \{[(F_H + F_{H0}) - F_{T0}X_T] - F_P C_H\} = 0 \qquad \text{(i)}$$

$$F_M - \{[(F_M + F_{M0}) + F_{T0}X_T] - F_P C_M\} = 0 \qquad \text{(ii)}$$

where F_P is the purge rate, and C_H, C_M are the concentrations in hydrogen and methane. By substituting appropriate expression for C_H and C_M we obtain the system:

$$F_{H0} - F_{T0}X_T - F_P \frac{F_H + F_{H0} - F_{T0}X_T}{F_{H0} + F_{M0} + F_H + F_M} = 0 \quad \text{(i')}$$

$$F_{H0} + F_{T0}X_T - F_P \frac{F_M + F_{M0} + F_{T0}X_T}{F_{H0} + F_{M0} + F_H + F_M} = 0 \quad \text{(ii')}$$

After simplifications, one obtains a linear system. The determinant has the expression: $\Delta = F_P[F_P - (F_{H0} + F_{M0})]$. Thus, the Jacobian becomes singular for either $F_P = 0$ or $F_P = F_{H0} + F_{M0}$. The first solution, no purge, leads obviously to accumulation of material and non-convergence. The second means a purge equal with the inlet hydrogen plus methane. In other words, the gaseous input matches exactly the gaseous output. This can be explained by the fact that there is no variation in the number of moles due to reaction. However, we would expect a feasible solution! In fact, the specification is feasible, but we obtain for the recycle rate an infinite number of solutions! Any recycle flow rate is possible, with fixed C_H and C_M values. This is more visible by adding the equations (i') and (ii'), from which we get:

$$F_P = F_{H0} + F_{M0} \quad \text{(iii)}$$

This result confirms the previous statement that the purge cannot be set independently with respect to the input of hydrogen and methane. However, the recycle can take any value provide that the flow rates of hydrogen and methane are in the following ratio:

$$\frac{F_H}{F_M} = \frac{F_{H0} - F_{T0}X_T}{F_{M0} + F_{T0}X_T} \quad \text{(iv)}$$

b. Purge ratio specified. Let us designate by f the fraction of the inlet stream going to the purge. The convergence condition of the tear stream becomes:

$$F_H - [(F_H + F_{H0}) - F_{T0}X_T](1-f) = 0 \quad \text{(v)}$$

$$F_M - [(F_M + F_{M0}) + F_{T0}X_T](1-f) = 0 \quad \text{(vi)}$$

From these equations the flow rates of components in the recycle stream are:

$$F_H = (F_{H0} - F_{T0}X_T)(1-f)/f \quad \text{(vii)}$$

$$F_H = (F_{M0} + F_{T0}X_T)(1-f)/f \quad \text{(viii)}$$

The total recycle flow becomes:

$$F_H + F_M = (F_{H0} + F_{M0})(1-f)/f = F_0(1-f)/f \quad \text{(ix)}$$

Consequently, by specifying the purge ratio the solution is non-ambiguous. The purge composition is fixed by the feed and reactor conversion, and cannot be set.

Finally, we examine one more question. Could we set the ratio of reactants at the reactor inlet as specification? A simple algebraic manipulation gives:

$$M = \frac{F_H + F_{H0}}{F_{T0}} = \frac{F_{H0} - fF_{T0}X_T}{(1-f)F_{T0}} = \frac{K - fX_T}{1-f} \qquad (x)$$

where K is the ratio pure hydrogen to toluene in feed. It can be seen that M is dependent of both initial composition and purge fraction. Since both are interrelated, setting M implies to manipulate either the excess of hydrogen/toluene or the purge fraction, but not the absolute purge flow rate.

This example shows how plantwide control problems can be understood by the analysis of the flowsheet material balance. Chapter 13 will develop this subject.

3.3 METHODOLOGY IN SEQUENTIAL-MODULAR FLOWSHEETING

A flowsheet where the units are solved sequentially is ideal from computational view point. However, most of the process plants involve recycles, particularly those highly integrated. In Sequential-Modular mode, there are four methodological issues:

- Find a robust calculation sequence.
- Use transmission of information to simplify the calculation sequence.
- Use design specifications.
- Solve convergence problems.

These issues will be examined in more detail below.

3.3.1 Calculation sequence

We start the analysis by considering some simple flowsheet structures. Figure 3.33a presents a plant with a single recycle. Initially only the stream 1 is known. If the simulation starts with the unit *a*, the *tear stream 5* has to be initialised. Then the units *b*, *c*, *d* are calculated sequentially. At the end of the sequence *a-b-c-d* other values for the variables of the stream *5* are obtained. After passing through the sequence the calculated values are updated by means of a *convergence unit* (Fig. 3.33b). The computations continue iteratively until the difference between values obtained in two successive iterations becomes smaller than a prescribed tolerance. It is said that the calculation is converged. After completing the recycle loop, the simulation may continue with other downstream units, in this case the unit *e*.

Therefore, the calculation sequence in Fig. 3.33a may be formulated as follows: loop_1(convergence unit (tear stream *5-a-b-c-d*) - *e*. It is easy to observe that the choice of the tear streams is not unique. We would have as alternatives the streams *2*, *3* or *4*, which will produce just a simple permutation of units. However, this feature allows the selection of the most convenient tear streams, chiefly before units that need careful initialisation.

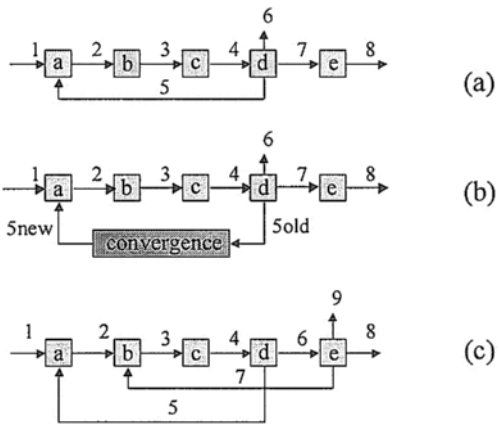

Figure 3.33 Calculation sequence and tear streams

We may proceed with a somewhat complicated flowsheet. Suppose that an exit stream of the unit *e* will be sent back to the unit *b* (Fig. 3.33c). A new loop is created, including the units *b*, *c*, *d*, *e*, nested with the previous loop *a*, *b*, *c*, *d*. If the stream *7* is selected as a new tear stream, the simulation of the flowsheet can be done in a single calculation sequence, as follows: *loop_1*(convergence unit (tear streams *5*, *7*)-*a*-*b*-*c*-*d*-*e*). Other tear stream combinations are possible, as (*2,6*) or (*2,7*). However, the convergence unit must converge two tear streams simultaneously.

We can continue a step further by observing that the number of tear streams can be reduced to one, if we select the streams *3* or *4*. In the last case both recycles may be broken to form a single calculation sequence, as follows: *loop_1*(convergence unit (tear stream *4*)-*d*-*e*-*a*-*b*-*c*). This situation is possible because the stream *4* is common to the both recycle loops.

In conclusion, a recycle structure can be transformed in a sequential calculation sequence by means of tear streams. The branches of the tear streams are input and output of a convergence unit. The convergence algorithm supplies updated values for the tear streams (see section 3.3.4). There is a minimum number of tear streams, but the tear streams set, as well as the sequence of units, is non-unique.

The extension of the above exercise at more complex flowsheets can be done by means of a *topological analysis*. The monograph of Mah (1990) is recommended for a detailed presentation of this topic. Nowadays most of the software performs an automatic identification of the computational sequence. However, the proposed sequence might be not always the most convenient for robust convergence. That is why it is still important to know how the topological analysis works.

A flowsheet can be represented by a directional graph (digraph), as illustrated in Fig. 3.34, which is equivalent with the Fig. 3.33b. The vertices represent the units, while the segments directed by arrows represent the connecting streams. Input and output stream may be attributed to the environment unit (E).

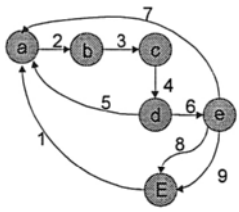

a	Mixer	1	-2		5				
b	Heater		2	-3					
c	Reactor			3	-4				
d	Separator				4	-5	-6		
e	Distillation						6	-7	-8	-9

Figure 3.34 Digraph and process matrix

Matrix representation of the digraph is more convenient for determining the computation sequence. Figure 3.34 presents also a form used frequently to represent a flowsheet known as *process matrix*. Note that the input streams are positive, while output streams are negative. The same information may be coded as *incidence matrix*, or *cycle (loop incidence) matrix,* and used in tearing algorithms. Here the most important step is to find the *partitions*. This consists of grouping units in sub-flowsheets that have independent input-output streams and cannot be reduced further. In this way, the simulation of the flowsheet is transformed in the solution of a number of sub-flowsheets sequenced by the *precedence ordering* (order of computation) of partitions.

Now we may formulate the general approach of finding the calculation sequence:

1. Decompose the flowsheet in partitions.
2. Determine the precedence ordering of partitions.
3. Find the tearing streams for each partition.
4. Determine the precedence ordering of the units in partitions.

Figure 3.35 illustrates the simplification of a flowsheeting problem by the effect of partitioning (Mah, 1990). The original problem involves *12* units and *5* recycle streams. The flowsheet may be decomposed in six partitions, the largest having only *4* units and *3* recycle streams. The tearing of each partition is now very easy. For the partition III we have to break only one loop. The partition II contains three loops, which may be broken by maximum three and minimum two tears. The reader can check himself that the finding the tear streams after partition is an easy task.

We have seen that inside a partition there are several possibilities for tearing. Consequently, the identification and the selection of tear streams may be subject of an optimisation procedure. Researches have identified four criteria:

1. Minimum number of iteration streams.
2. Minimum number of stream variables.
3. Minimum cost of streams by using weighting factors.
4. Minimum total number of loops torn.

They can be expressed by a unique mathematical formulation:

$$\min \sum_{j=1}^{n} w_j x_j \,, j=1,2,\ldots, n \text{ streams, subject to } \sum_{j=1}^{n} a_{ij} x_j \geq 1,\ i=1,2,..,m \text{ loops}$$

The weighting factors w_j may be allocated to express decision criteria or preferences, as the number of significant components, the difficulty to initialise values, the importance of incidence unit, etc. The factors a_{ij} are binary integer numbers (0,1) in the cycle matrix. As a result, the tearing procedure can be formulated as a linear programming problem. In most cases, the automatic algorithms minimise the maximum times a given loop is torn.

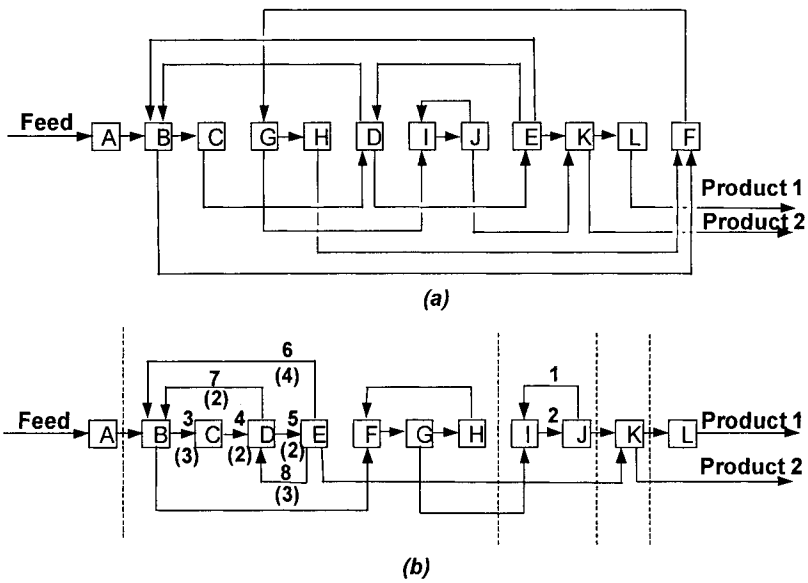

Figure 3.35 Effect of partitioning

EXAMPLE 3.3 Nested recycle loops

The flowsheet in Fig 3.37 consisting of three nested loops of mixers and flashes, is a standard problem in flowsheeting known as the *Cavett's problem* (Rosen, 1980). Table 3.9 gives the cycle matrix, where 1 marks each stream included in a recycle loop. For example, the stream Z_1 appears both in the loops 1 and 3, while the stream S_2 only in the loop 3. The last column shows the number of loops torn by each stream, and may be used to evaluate the tearing action. An obvious choice would be to consider three tear streams for three recycles, as for example R_1, R_2, R_3, which torn each loop only one. Another choice would be R_1, S_2, and R_3, where S_2 would replace R_2. However, it is possible to solve the flowsheet only with two tear streams, as Z_1 and Z_2, now each breaking two loops. Z_2 may be also replaced by R_3 or S_3. Hence, several tear sets are

feasible, but they behave differently in simulation. It may be demonstrated that when direct substitution method is used, the R_1, R_2, R_3 set (minimum loop tear) converge faster than the Z_1, Z_2 set (minimum tear streams).

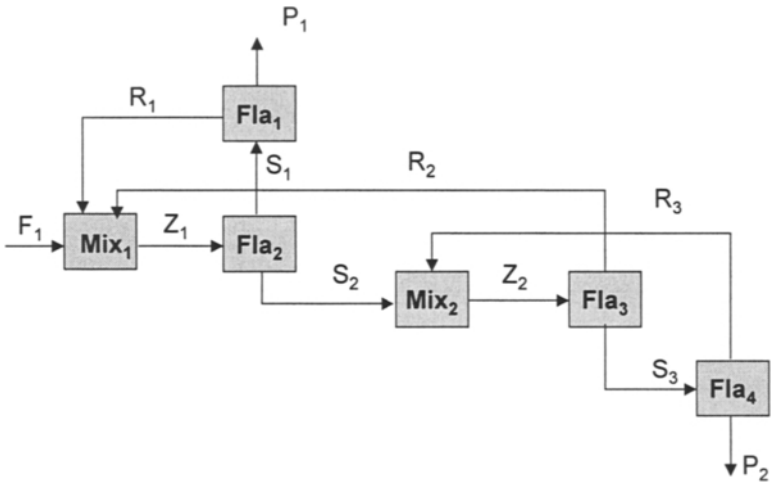

Figure 3.36 Nested recycle loops

Table 3.9 Cycle matrix for the Cavett's problem

Stream	Loops			Loop Sum
	1	2	3	
Z_1	1	0	1	2
S_2	0	0	1	1
S_1	1	0	0	1
Z_2	0	1	1	2
S_3	0	1	0	1
R_1	1	0	0	1
R_3	0	1	0	1
R_2	0	0	1	1

3.3.2 Transmission of information

The *transmission of information* is a powerful method to simplify the computational sequence. In principle, any type of information may be considered, but in practice this technique concerns mostly duty and work.

Heat duty

The transmission of a heat duty may take place inside the same unit or between different units. In Fig. 3.37, the cold and hot streams of a recycle cross in the same heat exchanger. The simulation implies tearing, in this case one tear stream, either 2 or 3. The unit HX can be replaced by a heater HX1 and a cooler HX2 linked by the same duty. In this way, the loop is broken and the simulation becomes purely sequential.

The second situation may be found in heat integrated flowsheets, when duty is exchanged between different units. An example is the simulation of heat integrated distillation systems (integration of condensers and reboilers of distillation columns, coupling with a refrigeration system, etc.). The transmission of information prevents the formation of internal recycle loops, occasionally quite large, whose iterative computation would penalise the overall solution (see the Example 3.4).

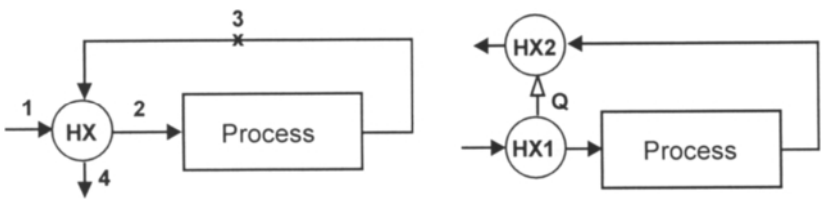

Figure 3.37 Breaking a recycle loop

Shaft work

The shaft work generated by a gas expander or a liquid turbine may be transmitted to a compressor or pump, as shown in Fig. 3.38. This technique is useful in gas processing.

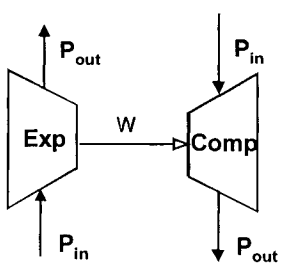

Figure 3.38 Transmission of shaft work

EXAMPLE 3.4 LNG/LPG Plant

This example illustrates the separation of LNG (liquid natural gas) and LPG (liquid propane gas) from a rich methane gas. The gas feed rate is 3000 m^3/h at 100 bars and 60 °C. A typical composition is C1 73%, C2 11%, C3 8%, C4+ 5% and N2 3%. Fig. 3.39 shows the flowsheet. Firstly, the temperature of the hydrocarbon feed GAS is

reduced by an air cooler HX1 to about 35 °C. Then the rich-gas goes through a 'cold box' (HLNG), where the temperature drops to a sufficient low value to allow a phase split CH4/C2+ in the flash FL1. An optimal value is ~5 °C. The cold streams have different origins. After flash separation, the gas stream 4 is sent to expansion at 30 bars, where the temperature drops to -63 °C. A second vapour-liquid separation takes place in the flash FL2. The stream 8 is now enriched to more than 86% methane, with about 8% C2, and less than 3% C3. The liquid stream 10 collecting C3 and C4+ plus the liquid from FL1 is sent to cryogenic distillation in the column DETH (25 bar). Note that the low temperature streams to the cold-box HLNG are produced by pressure reduction through valve and expander, as well as top vapour of the cryogenic distillation column. The bottom product of this column is a LPG type mixture, with 40% C3, 57% C4+, as well as 3% C2. The top is a mixture (stream 16) that can be sent to C2 separation, or mixed with methane rich gas 15 and compressed to the final user.

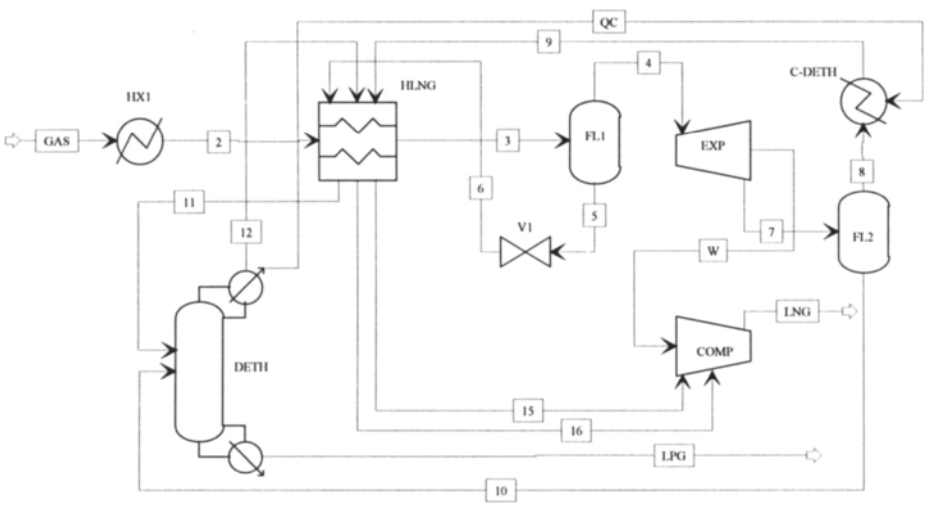

Figure 3.39 The simulation of a LNG/LPG plant

The final input/output stream report is as follows:

Streams (kmol/hr)	GAS	15	16	LNG	LPG
CH4	7400	6237	1163	7400	trace
C2	1100	579	499	1078	22
C3	800	160	30	190	610
C4+	400	18.5	0	18.5	381.5
C5+	100	1.5	0	1.5	98.5

Hence, the separation of LPG fraction by this process has a good yield, of (1090/1300)×100=83.8 %. It is worthy to observe that the energy of separation is due to

the initial high-pressure gas, and not to low temperature sources. Note the use of transmission of information for the shaft work of expander to methane gas compressor. The heat exchanger C-DETH is in fact the condenser of the column DETH.

3.3.3 Design specifications

We remember that a *design specification* is a feedback controller, where a value attributed to a unit or stream variable can be achieved by manipulating another unit or stream variable. A design specification creates a new convergence loop, between the unit whose specified variable is sampled and the unit whose variable is manipulated. This new loop will interact with the existing flowsheet recycle loops, with consequence on the strategy of computations. From this point of view, a design specification loop may be placed inside or outside of a flowsheet convergence loop, or converged simultaneously with the tear streams.

The user should pay attention to the convergence properties of the design specification loop. The variation should be sensitive, continuous, monotone and inside specified bounds of the manipulated variable. Each situation should be evaluated from physical and computational perspective.

3.3.4 Treatment of convergence

The simulation is converged if all units, tear streams and overall material balance have converged. The convergence of overall heat balance is optional. The computation of convergence can be expressed mathematically as the minimisation of the residuals between X, the estimated values at the beginning of an iteration, and X^*, the calculated values after a pass through the computational sequence:

$$R(X) = X - X^* \tag{3.6}$$

$X^* = \Phi(X)$ is the result of non-linear functions represented by operational units. Usually the convergence is treated by means of *convergence units*. These are mathematical units containing information about the tear streams, calculation sequence, convergence methods, tolerance, and convergence parameters.

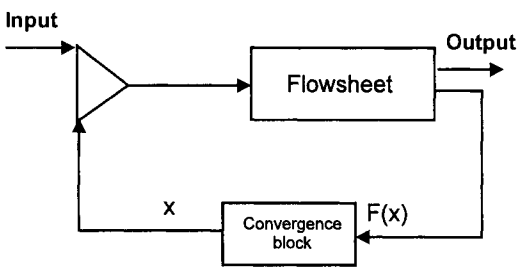

Figure 3.40 Treatment of convergence

Convergence Methods

1. *Direct substitution.* This method consists of a simple substitution of estimated values by calculated values as described by the relation:

$$X_{k+1} = F(X_k) \tag{3.7}$$

Theoretically the convergence is guaranteed only if the eigenvalues of the Jacobian of residual functions are in modulus less than one. In general this condition is not fulfilled, and therefore direct substitution is not recommended. However, it may be used to generate initial values for more powerful methods.

2. *Wegstein.* This method uses a parabolic extrapolation such that the updated values are computed from two previous iterations, with the formula:

$$X_{k+1} = qX_k + (1-q)F(X_k) \tag{3.8}$$

The acceleration parameter q is calculated as follows:

$$q = s/(s-1) \quad ; \quad s = \frac{F(X_k) - F(X_{k-1})}{X_k - X_{k-1}} \tag{3.9}$$

The parameter q may be bounded or modified for better convergence control. Wegstein is the default method in many simulators.

3. *Secant.* The method uses a linear approximation of the Jacobian. It may be implemented with some enhancements, as *half interval* option. It is recommended for single variable, discontinuous or flat convergence functions.

4. *Broyden.* This method solves directly the equation 3.6. It is worthy to note that the updating of the Jacobian takes place by algebraic computations on matrix elements and not by matrix inversion. It may be used for the convergence of multiple tear streams, design specifications, or mixed tear streams and design specifications.

5. *Newton.* This algorithm is an implementation of Newton-Raphson method for simultaneous solution of non-linear equations. It may be more robust than Broyden, but limited to small number of variables.

6. SQP method. This powerful optimisation method is used to converge simultaneously tear streams and design specifications. Two algorithms are possible:
- Feasible path: convergence of tear streams at each iteration on constraints.
- Infeasible path: tear streams and constraints are converged simultaneously.

Tips on convergence problems

Hereafter we put together some advises that could help the user avoiding the frustration of convergence failure:

1. Examine in the first place the Input-Output structure. Entering materials must also leave the process! Be sure that the material balance holds not only for the main components, but also for inert and trace components.
2. Examine carefully the computation of physical properties and the accuracy of the thermodynamic modelling. Use a model that is sufficiently accurate for your problem. Do not trust blindly default options. Change the model at the unit level, if

necessary. Verify the reliability of the model parameters (source, interval) and check their accuracy. Do not hesitate to perform identification of thermodynamic parameters from experimental data, if the accuracy is critical.

3. Check the reactor behaviour, as reactions, stoichiometry, conversion, etc. Do not forget that the most significant change in the material balance takes place here.
4. Decompose a large flowsheet in several sub-flowsheets. Avoid large recycles.
5. Check the automatic identification of the tear streams. Check the feasibility of the calculation sequence, the interaction between recycle loops, particularly between design-specifications and process recycles. If necessary, define your own sequence.
6. Minimise the number of recycle loops by using the transmission of information.
7. Start always with simple specifications, which may give a good starting point for the material balance. Avoid controllers (design-specifications) in an early stage.
8. Distillation is always a bottleneck! Start in material balance mode, typically specifying product(s) and reflux rates. Examine the internal profiles: temperature, compositions, and liquid/vapour traffic. Consider complex specifications later, after having converged the material balance with recycles.
9. Extract difficult units and make them converge separately. Generally, isolate convergence problems and treat it outside the flowsheet.
10. Follow the convergence of the key components in tear streams. Check if there is no systematic accumulation of some species. Study the mathematical behaviour of the convergence method. Do not increase the iterations before identifying the source of convergence troubles. Do not hesitate to run the flowsheet step-by-step.

3.4 RESULTS

Stream Report

The stream report is an image of the material and energy flows in the plant and the basic document in flowsheeting. The format of results depends on the type of process and on the level of details. This should contain state variables, as temperature, and pressure, vaporised fraction, total and partial flow rates, molar fractions, composition, on molar and mass basis, enthalpy, specific volume, etc. Normally the information can be exported to a spreadsheet.

The inspection of the stream report is also extremely useful for debugging convergence problems, as for example by identifying faults in the specification of units or inconsistencies in the material balance.

Unit operation report

The report around each unit includes material and energy balance, input and output streams, as well as some information about unit performance. Here we may include the *sizing report*. Some simulation systems may export the results of sizing in the form of *specification sheets*, which are basic documents in engineering. Here we may mention standardised documents for heat exchangers, distillation columns, vessels, pumps, filters, etc. Some simulators offer automatic interface of simulation data to engineering

packages, which can proceed with more detailed sizing computation or cost estimations. Advanced engineering post-treatment may incorporate elements from the stream report into engineering documents, as drawings of equipment items.

Internal Profiles

Visualisation of profiles inside complex equipment is a valuable instrument for understanding how the unit really works. A typical example is the plot of profiles insides a distillation column, in term of pressures, temperatures, and composition on stages, as well as of material and enthalpy flows. These profiles are highly recommended for debugging non-convergence problems. Even in the case of successful runs internal profiles allow the evaluation of design elements. For example, the inspection of temperatures and composition profiles can easily identify incorrect feed location or superfluous stages in a distillation column.

Table of properties

Tabulation of properties may be generated for different variables, mostly as function of temperature and composition. It may include physical properties, as vapour pressure, densities, viscosities, etc., as well as various thermodynamic functions. An example is the generation of *H-T* curves necessary in heat integration studies. Tabulation of properties is also highly recommended for checking the reliability of models for physical properties, as well as for phase and chemical equilibria.

3.5 ANALYSIS TOOLS

Sensitivity

A sensitivity study consists of plotting the variation of a single or several sampled variables against a manipulated variable. The list of accessed variables depends on each simulator, but in principle should be any calculated value of streams, as well as internal variables of units. The manipulated variables are usually specifications of streams, or of referenced unit. The results may be exported to a spreadsheet. An example of sensitivity analysis is given in the Case Study 1 (HDA process).

Computer programming, as FORTRAN or Visual Basic, may be used to formulate mathematical functions of any complexity. This is a powerful feature of simulators often underestimated. An example is the study of steady state controllability directly from non-linear plant models (see Chapter 12). Different controllability measures can be calculated directly by programming, or by exporting data to other packages.

Case Studies

When is aimed to investigate the influence of several variables, it is more efficient to use 'case study'. This is advantageous when using structural variables, as the numeber of stages in a distillation column. Case studies are useful as 'scenarios' for design or operation. The results may be tabulated and exported to spreadsheets. In addition, the case studies offers a better initialisation for convergence.

3.6 OPTIMISATION

Optimisation is an advanced feature in flowsheeting. The first step is the formulation of an *objective function*, which may be of technical or economic nature. In the first category we may cite the yield of transformation of raw materials in products, the energy consumed or saved in a process, the amount of emissions or impurities, etc. An economic function can be the total operation cost, the profit, or a measure of profitability, as the rate of return on investment (see Chapter 15).

Optimisation in flowsheeting implies by principle several variables, because a mono-variable optimisation can be solved easily by a sensitivity study. A flowsheeting optimisation problem is always constraint. Firstly, there are *equality constraints*, as for example the material and heat balances, but also phase equilibrium conditions, as the equality of component fugacities. Secondly, there are *inequality constraints*. Usually these consist of bounds on temperatures, pressures, flow rates, and concentrations, but they can express also performance limits, as minimum reflux ratio, temperature approach in heat exchangers, etc.

An optimisation in flowsheeting is a non-linear programming (NLP) problem when the flowsheet or unit operation structure remains unchanged. When structural variations are taken into account the optimisation problem can be formulated more generally as a Mixed Integer Non-linear Programming (MINLP). For example, the integer variables might describe the number of stages in a distillation column, the feed location, or the connection between units.

A NLP optimisation problem can be viewed as the minimisation of an objective function $F(\bar{d},\bar{x})$ in a design space $\bar{d}$ subject to equality $c(\bar{x})$ and inequality $g(\bar{x})$ constraints. Mathematically, the formulation is:

$$\text{Minimise } F(\bar{d},\bar{x}) \tag{3.10}$$

$$\text{Subject to } c(\bar{x}) = 0,\ g(\bar{x}) \le 0,$$

$$\text{with } \bar{x}_L \le \bar{x} \le \bar{x}_U$$

In the relation (3.10) the signification of notation is:

- $\bar{x}$ is the vector of process variable that may vary between lower bound $\bar{x}_L$ and upper bound $\bar{x}_U$,
- $\bar{d}$ is the vector of variables to be adjusted by optimisation, a subset of $\bar{x}$. Thus, $\bar{d}$ is given by the number of degrees of freedom that are not specified.

The algorithmic treatment depends on the architecture of the flowsheeting system. In Equation-Oriented mode, the approach consists of solving all the equations describing the problem simultaneously. In Sequential-Modular approach the mathematical solution must take into account the convergence of units and tear streams, as well as of all design specifications. Supplementary equations must be added, so that the general formulation of the optimisation problem (3.10) becomes:

Minimise $F(\bar{d},\bar{x})$ (3.11)

Subject to $h(\bar{d},\bar{t},\bar{x})=0$, $c(\bar{x})=0$, $g(\bar{x})\le 0$,
with $\bar{x}_L \le \bar{x} \le \bar{x}_U$

New equations $h(\bar{d},\bar{t},\bar{x})=\bar{t}-\varphi(\bar{d},\bar{t},\bar{x})=0$ have been added to the NLP problem (3.10) to account for the convergence of tear variables $\bar{t}$. The update function $\varphi(\bar{d},\bar{t},\bar{x})$ describes the action of simulation units on the tear variables.

Figure 3.41 illustrates the optimisation of a flowsheeting problem in a two dimensional space. Contours of the objective function F are plotted, where the two variables x_1 and x_2 are bounded by upper and lower values. The overall heat and material balance expressed by the function $h(\bar{d},\bar{t},\bar{x})=0$ set a supplementary constraint. The treatment of the flowsheet convergence and of the optimisation problem itself can be done in two manners. In an approach called *feasible path* the solution of the problem (3.11) satisfies the constraint of tear streams at each evaluation of the objective function. In *infeasible path* approach the constraints of the total material balance are satisfied only in the final run. Obviously, a combination of the two approaches may be used.

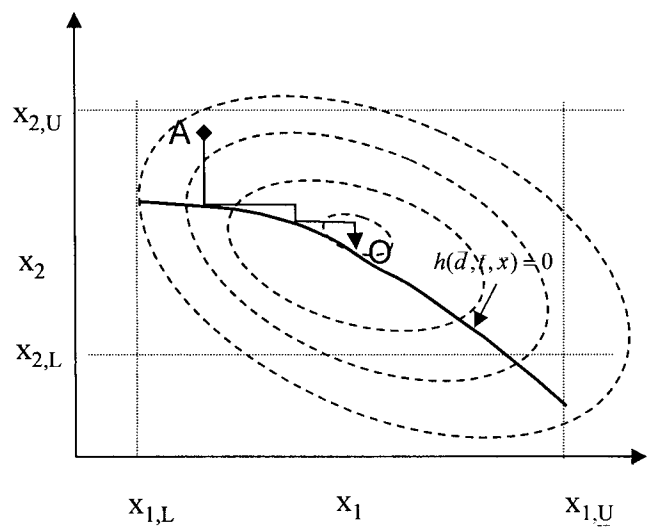

Figure 3.41 Optimisation approach in flowsheeting

The description of the optimisation techniques is outside the scope of this work. An excellent introductory tutorial can be found in the book of Biegler, Grossmann and Westerberg (1997). As a general reference we recommend the work of Himmelblau and Edgar (1988). Here we only mention that the most efficient algorithm in flowsheet optimisation is based on *Successive Quadratic Programming* (SQP).

An optimisation work must be carefully prepared. This starts by the judicious selection of the optimisation variables and by the definition of the objective function. It is important to ensure that the objective function is sensitive and continuous in the range of assumed variations.

A more fundamental problem is the treatment of control loops (design specifications) in an optimisation work. The convergence of a control loop may be solved outside, inside, or simultaneously with tear streams. Simultaneous solution of tear streams and specifications by using the Broyden's method works well in many cases. However, the insertion of control loops in the tearing algorithm is a burden for computation. An improvement in the mathematical solution can be obtained by transforming the control structures in equality constraints. This consists of reformulating the design specification as algebraic expression, and including the manipulated variable on the list of optimisation variables. As an illustration, we invite the reader to examine the Case Study 1 dealing with the optimisation of the HDA process.

We conclude this section with some remarks concerning the optimisation of a flowsheeting problem:

1. The optimisation variables are always bounded because of physical reasons. For example, the temperature in a reactor cannot exceed a safety limit for operation or catalyst integrity. Or, too low temperature may freeze a process mixture, etc.
2. There are always constraints in the performance of units, as achievable conversion, separation indices, etc.
3. The objective function shows in large number of cases an almost flat shape around the global optimum.

Consequently, most of the optimisation variables have the tendency to migrate to the bounds, and only a limited number of variables are free to move inside the space of variations. Often the constraints are expressed as optimum performance, so that the optimisation procedure will try to fulfil them as active (binding) constraints.

EXAMPLE 3.5 Optimisation of a gas plant

Figure 3.42 presents a simple gas plant processing of a natural gas. Initially, the gas has a pressure of 75 bars, the partial flow rates (kmol/h) being N2 150, C1 6000, C2 500, C3 300, C4+ 200. The optimisation problem consists of maximising the work produced by expansion, the optimisation variables being the cooling temperature in the flash unit and the final pressure after expansion. To this we may add as constraint the recovery of C2 in the bottom product of the column COL at least 70% from the initial amount in the plant feed. The temperature is bounded between 220 and 240 K, while the pressure is bounded between 25 and 40 bar.

Solution.

After cooling at an appropriate temperature, the mixture is separated in gas and liquid, both operations simulated by a single flash unit FLASH. The gas phase contains most of methane, with a significant amount of C2, and small C3+. The liquid phase collects most of ethane and C3+ components. The gas is submitted to expansion in the unit EXP, in order to get low temperature and eventually the condensation of C2 and C3+ components. The liquid from the flash is depressurised by means of a valve and sent to separation in a reboiled absorption unit COL, together with the stream issued from expander. The top product is a methane gas, while the bottom product collects ethane and heavier components. Note that the unit COL has 8 trays, with the feeds on top and above the third stage. The column pressure is 22.5 bar. Finally the top gas product is compressed by the unit COMP and sent to the consumer.

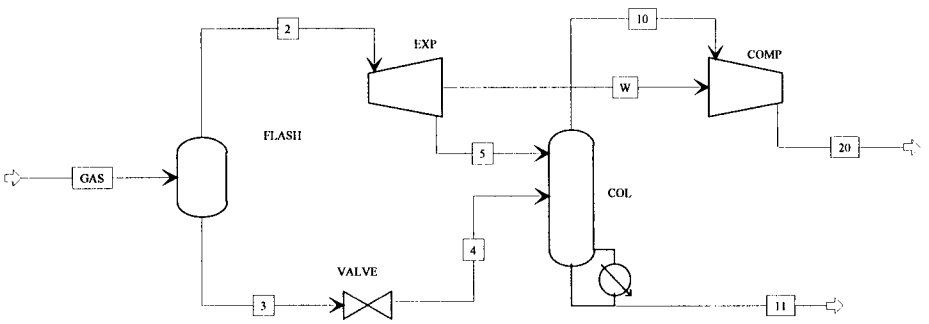

Figure 3.42 Optimisation of design parameters of a gas plant

The optimisation problem has been solved in Aspen Plus™ version 10.2. It can be seen that the expander drives the compressor COMP. The results of the optimisation found by an SQP algorithm are presented below:

- Flash temperature: 231.1 K
- Expander final pressure: 25 Bar (on lower bound),
- Objective function (isentropic work) 8.180 kW

Note that the optimal pressure is the on lower bound, because it increases monotonically the recovery of ethane from the gas stream. Contrary, a too low temperature in flash could give higher amount of methane in the liquid phase, which risks to violate the constraint of ethane recovery. Thus, we expect that this constraint should be fulfilled as equality, which is the case.

After this example, the reader is encouraged to revisit the Example 3.4 and reformulate it as an optimisation problem. We suggest as objective function the sale value of the total LNG and LPG produced. Optimisation variables could be the outlet hot gas temperature after the cold box, as well as the pressure after expander.

3.7 SUMMARY

When using a steady state simulator, the following aspects should be kept in mind:

1. A simulation problem must be carefully analysed before laying out the flowsheet. The problem analysis must take into account general modelling principles, but also the constraints set by the modelling environment of the simulator. Understanding the engine of the simulator is compulsory for getting reliable results.
2. The most critical aspect in simulation is the selection of appropriate thermodynamic models. Different models can be used on different parts of the flowsheet, or for some units. For example, equation of state model can be used for the whole flowsheet, but liquid activity models are more suitable for separations. The accuracy of model parameters should be checked systematically. Thermodynamic analysis tools should be used systematically to evaluate the accuracy of phase equilibria before detailed simulation of separations.
3. Entering feasible specifications both for unit operations and for flowsheet needs to understand the concept of degrees of freedom. For good selection of specifications the user should know, even loosely, the way in which the simulation algorithms work. Material balance specifications are the simplest and the most robust.
4. Some specifications perfectly feasible for stand-alone units might become infeasible when simulating the whole flowsheet. Most of the troubles in getting flowsheet convergence have as origin inconsistencies in the overall input/output material balance, as for example specifying all the outputs as absolute flow rates, or when no exit points are available for some components.
5. In Sequential-Modular approach, the calculation sequence plays an important role in obtaining overall convergence. Transmission of information techniques may be used to untie the nested loops and simplify the calculation sequence.
6. Flowsheet controllers are powerful tools in defining more complex specifications or in achieving desired performances of units. These tools can be also used for simulating the behaviour at steady state of process control structures.
7. Analysing the reasons of non-convergence is more efficient than increasing the number of iterations. In most cases the failures originates from incorrect problem statement, unreliable physical property methods, and conflicting specifications (see also convergence tips). A failure in steady state convergence might be an indication about possible troubles with dynamics and control.
8. The stream report is the most important document and a mirror of the plant behaviour. However, this is insufficient to evaluate the quality of the simulation run. Examining the performance of each unit is compulsory. Profiles of internal variables enable to understand how the unit really works.
9. Sensitivity Analysis and Case Studies are valuable tools for increasing the productivity of simulations, and for getting insights in design and operation problems.
10. Optimisation of the flowsheet is the ultimate goal. This task is difficult, and should be preceded by careful analysis regarding the definition of the objective function and its sensitivity to different variables.

3.8 REFERENCES

Biegler L. T., I. E. Grossmann, A. W. Westerberg, 1997, Systematic Methods of Chemical Process Design, Prentice Hall

Boston, J. F., 1980, ACS Symposium Series No. 124, p. 135

Edgar, T. F., D. M. Himmelblau, 1998, Optimisation of Chemical Processes, McGraw-Hill

Haas, J. R., 1992, Chapter 4 in Distillation (Design) by Kister H. Z., McGraw-Hill

Kister, H. Z., 1992, Distillation-Design, McGraw-Hill

Mowry, J. R., 1986, Thermal Hydrodealkylation (THDA) Process, in Handbook of Petroleum Refining Processes, editor R. A. Meyers, McGraw-Hill

Mah, R. S. H., 1990, Chemical Process Structures and Information Flows, Butterworths

Poling, B. E., J. M. Prausnitz, J. P. O'Connell, 2001, The Properties of Gases & Liquids, Fifth Edition, McGraw-Hill

Rosen, E. M., 1980, Steady State Chemical Process Simulation: A State-of-the-Art Review, Computer Applications to Chemical Engineering, ACS Symposium Series 124, p. 115-13

Seider, W. D., R. Gautam, C. W. White, 1980, Computation of Phase and Chemical Equilibrium. Computer Applications to Chemical Engineering, ACS Symposium Series 124, p. 115-13

Seider, W. D., J. D. Seader, D. R. Lewin, 1999, Process Design Principles. Synthesis, Analysis and Evaluation, Wiley

Taylor, R., Krishna, R., 1993, Multicomponent Mass Transfer, Wiley

Westerberg, A., H. P. Hutchinson, R. L. Motard, P. Winter, 1979, Process Flowsheeting, Cambridge University Press

SOFTWARE MANUALS

Aspen Plus, version 10.2, User Manual, 2001

ChemCad, User Guide, version 5.2, 2001

Hysys User Guide, release 2.4, Hyprotech, 2001

Pro II Use Guide, release 5.4, Simulation Science, 2001

Chapter 4

DYNAMIC SIMULATION

4.1 Transition from steady state to dynamic simulation

4.2 Dynamic flowsheeting

4.3 Numerical problems in dynamic simulation
4.3.1 Integration of DAE systems
4.3.2 Computation of physical properties (local models)

4.4 Dynamic flash

4.5 Dynamic distillation column

4.6 Dynamic simulation of chemical reactors
4.6.1 CSTR model
4.6.2 Tubular reactors

4.7 Process Control tools
4.7.1 Implementation of controllers
4.7.2 Tuning of PI controllers

4.8 Further reading

4.9 References

Dynamic simulation is an advanced process simulation activity, by integrating in the same simulation environment design, operation and control. Compared with steady state simulation, both modelling and software technology are much more demanding. This is valid also for users, because insufficient prepared simulations can easily fail or produce unreliable results. It is important to note that some optional elements in steady state are now required, as sizing characteristics and pressure/flow relation. For example, a simple flash cannot be seen only as a 'generic' multi-phase equilibrium vessel, but needs the specification of the vessel type and geometry, as well as the relation between flow and pressure drop for inlet and outlet lines. In addition, key operating variables, as levels, temperatures or pressures, should be kept at desired values by means of controllers. Therefore, dynamic simulation without process control implementation has little practical sense.

The chapter begins with the analysis of the transition from steady state to dynamic simulation, by emphasising the introduction of the accumulation terms in modelling equations. Then we will discuss the integration of differential-algebraic equation systems, which allows understanding the mathematical engine in dynamic simulation. Regarding the difficult topic of dynamic modelling, we will present only some basic unit operations, as flash vessels, distillation columns and chemical reactors. These units have important inventories that may affect the dynamics of the whole process. Finally, we will present the implementation of PID controllers, still the most encountered in process industries.

4.1 TRANSITION FROM STEADY STATE TO DYNAMIC SIMULATION

Dynamic flowsheeting is based on the unsteady state balance of mass and energy, and may be formulated in general terms by the following equation:

$$\left\{\begin{matrix}accumulation\\rate\end{matrix}\right\}=\left\{\begin{matrix}input\\flows\end{matrix}\right\}-\left\{\begin{matrix}output\\flows\end{matrix}\right\}+\left\{\begin{matrix}generation\\rate\end{matrix}\right\}-\left\{\begin{matrix}consumption\\rate\end{matrix}\right\} \tag{4.1}$$

The accumulation rate may be expressed in term of total mass M or energy E of the system, denoted as time-derivatives dM/dt and dE/dt. In systems with chemical reaction it is useful to consider the molar rate variation of individual components, dN_i/dt. The accumulation can be expressed by means of a *holdup* term as the product of an intensive property, as density, concentration, or volumetric enthalpy, by the control volume:

$$holdup = (intensive\ property) \times volume \tag{4.2}$$

The material holdup is designated often in process control studies by 'inventory'. Equation (4.2) indicates that, unlike in steady state simulation, in dynamic simulation the geometrical characteristics of the system are always required. Intensive variables entering in the accumulation term are designated by *state variables*, as for instance

concentrations implied in component material balance, but also pressure and temperature.

The unsteady state balance equations must be completed with *constitutive equations*, which are relations between some state variables, usually expressing natural laws or the kinetics of transport phenomena. Examples are *PVT* relations, as equations of state, or kinetics expressions, phase-equilibrium factors, etc. Specifying the initial and boundary conditions completes the problem formulation.

The mathematical complexity increases considerably from steady state to dynamic simulation, changing from algebraic to differential-algebraic equations. From mathematical viewpoint we may distinguish between two categories of models:

- *Lumped parameters*: uniform properties by perfect mixing, and therefore zero space-derivatives. The system is described by ordinary differential equations (ODE), in which only time derivatives appear.
- *Distributed parameters*: imperfect mixing, some spatial derivatives are nonzero. The system is described by unsteady state partial differential equations (PDE).

Writing rigorous dynamic models is difficult. This topic is not covered here, but recommendations are given at the end of this chapter. However, essential dynamic features of a process may be detected by examining simplified models, as illustrated by the next example.

EXAMPLE 4.1 Dynamic CSTR

Consider an isothermal continuous stirred tank reactor (CSTR). Analyse its dynamic behaviour in the case of a first-order irreversible reaction.

Solution.

The control volume V is the reacting liquid. Concentrations and temperature are uniform and equal with outlet values. Mass flow rates of input and output streams are G_{in} and G, respectively. The non-stationary overall material balance gives:

$$\frac{dm}{dt} = G_{in} - G \tag{4.3}$$

Mass holdup m is the product of liquid density ρ by volume V:

$$m = \rho V \tag{4.4}$$

The material balance of the component "i" has the form:

$$\frac{dm_i}{dt} = G_{in} g_{i,in} - G g_i - r_i V M_i \tag{4.5}$$

where m_i is the partial holdup, $g_{i,in}$ and g_i being the weight fractions in input and output streams, respectively. If the molar reaction rate is r_i the consumption/generation rate by chemical reactions is expressed by $r_i V M_i$.

The constitutive relations that complete the physical description are:

Kinetics. Assume first order irreversible reaction A → B. The reaction rate is:

$$r_A = kc_A = kg_A\rho \quad ; \quad r_B = -r_A \tag{4.6}$$

Mixture density. The density can be expressed as a function of temperature and composition:

$$\rho = \rho(\rho_i, T, g_i) \tag{4.7}$$

The initial conditions are:

$$t = 0, V = V_0, m_i = m_{i,0} \tag{4.8}$$

The integration of the equations (4.3) to (4.8) can be done with standard mathematical tools. Two routines should be programmed to calculate the density and the reaction rate.

In the above analysis the equations have been written in terms of weight and weight fractions. Alternatively, we may write the equation (4.5) as molar mass balance:

$$\frac{d(Vc_i)}{dt} = F_{i,in} - F_i - r_i V \tag{4.9}$$

$F_{i,in}$ and F_i are inlet and outlet molar flow rates of components, and c_i molar concentration inside the reactor.

To get more insight into process dynamics we assume constant density and consider that input and output volumetric flows are equal $Q_v = Q_{v,in} = Q_v$. As a result, the total holdup is constant, so that $dm/dt = 0$. The unsteady state material balance equation of the reactant A becomes:

$$V\frac{dc_A}{dt} = F_{A,in} - F_A - kc_A V \tag{4.10}$$

Input and output molar flows can be written as $F_{A,in} = Q_{v,in}c_{A,in}$ and $F_A = Q_v c_A$. Note that the ratio between volume and volumetric flow designates a dynamic characteristic of a CSTR, the reaction time τ:

$$\tau = V / Q_v \tag{4.11}$$

The equation (4.10) can be re-written in dimensionless form by introducing dimensionless concentration $C_A = c_A / c_{A,in}$, dimensionless time, $\theta = t/\tau$, and the Damköhler number $Da = k\tau$, as follows:

$$\frac{dC_A}{d\theta} + (Da + 1)C_A = 1 \tag{4.12}$$

At steady state $c_A = c_{A,s}$ and the dimensionless concentration is:

$$C_{A,s} = 1/(1 + Da) \tag{4.13}$$

The initial condition is:

$$t = 0,\ c_A = c_{A,0} \quad \text{or} \quad \theta = 0,\ C_A = C_{A,0} = c_{A,0} / c_{A,in} \tag{4.14}$$

The integration of Eq. 4.12 leads to the final relation:

$$C_A = C_{A,0} \exp[-(1 + Da)\theta] + [1 - \exp[-(1 + Da)\theta]/(1 + Da) \tag{4.15}$$

As numerical illustration Fig. 4.1 presents the transient of a CSTR for $c_{A,0} = 1$ with Da=1 and Da=3. Faster reaction gives higher conversion, but shorter transient.

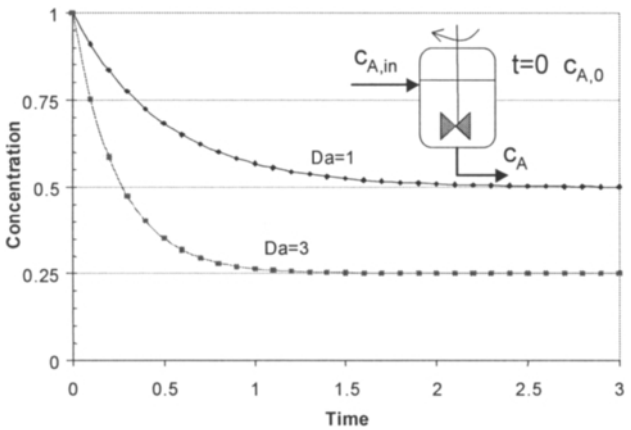

Figure 4.1 Variation of concentration in a transient CSTR reactor

4.2 DYNAMIC FLOWSHEETING

Dynamic flowsheeting consists of performing the dynamic simulation of the whole process plant rather than of a single unit. Commercial software for dynamic flowsheeting may be classified in two categories:

- Sequential-Modular (**SM**),
- Equation-Oriented (**EO**).

Advantages and disadvantages of each approach have been discussed in Chapter 2. For steady state flowsheeting most of the simulators have adopted the SM architecture. The situation is more complex in dynamic flowsheeting, mainly because of the way in which the time-derivatives are handled. Thus, the time may be seen locally, at unit level, or globally, at flowsheet level. In the case of flowsheets without recycles, the time is seen at the same horizon from every unit. The information is transmitted sequentially in a synchronised manner. In the case of flowsheet with recycles the count of time is less obvious. The integration should take place simultaneously in all units, with a time-

step sufficiently small to cope with the fastest unit. Hence, the **EO** is more suitable for dynamic simulation.

Initialisation is an important issue in dynamic simulation. This may follow different techniques, according to the software architecture. In **SM** mode the initialisation is done by a steady state run. Alternatively, the dynamic simulation could start from a state in which the units have some inventory, the steady state being achieved by numerical integration. In **EO** mode the steady state is found by setting all derivatives to zero and by solving the system of non-linear algebraic equations. The difference between the number of variables and the number of equations gives the variables to be supplied as *initial values*. Most of them are state variables, but there are also sizing parameters. This task is tedious if not done automatically. An efficient solution is to initialise a dynamic run from steady state simulation by taking care to bring the models compatible. This is the way of working of ASPEN Plus and ASPEN Dynamics.

Despite the progress in software technology in the last years, solving a dynamic simulation problem is not easy. A working procedure may be formalised as below.

1. Problem Analysis
   - Define the process dynamics problem including plantwide control (see Chapter 12).
   - Carry out a degree of freedom analysis, both for design and control.
   - Decide about slow and fast dynamic units. Slow units need dynamic models, while steady state models can be applied in the second case.
   - Analyse the modelling of units with significant inventory.
   - Analyse the modelling of the chemical reactor and of key separation units.
   - Examine plantwide control problems, as the input of reactants, the manipulation of the production rate, and the control of waste and impurities. Develop a plantwide control structure (see Chapter 13).
2. Steady state flowsheeting
   - Solve the steady state flowsheeting problem (see Chapter 3).
   - Size the units with whose dynamics is of significance.
   - Determine the effect of recycles by controllability measures (see Chapters 12).
   - Modify the design to ensure that the manipulated variables are effective for control.
   - Prepare the dynamic run.
3. Dynamic flowsheeting
   - Implement the basic control structures of units, primarily of levels and pressures.
   - Develop of a plantwide control structure (see Chapter 12).
   - Implement and tune the controllers of units, usually of PID type.
   - Execute closed loop simulation.
4. Analysis of results
   - Study the plant performance in closed loop faced to different disturbances.
   - Carry out dynamic controllability analysis if necessary (see Chapter 13).
   - Perform refinement of design and control, and finally optimisation.

An important issue in the above procedure is the degrees of freedom analysis (DOF) in dynamic simulation. We remember that design DOF is the number of variables that

must be specified to define the process. In principle, the *design degrees of freedom* can be determined by the rule "variables minus equations" by examining the steady state model, as discussed in Chapter 3. This procedure is practical for simple units, but less convenient for complex units. These can be solved, however, as assembly of simpler devices, or smaller flowsheets.

After steady state analysis, we have to examine the *control degrees of freedom.* This analysis corresponds actually to the selection of controlled and manipulated variables. Controlled variables are related to control objectives, usually levels, temperatures, pressures and compositions. Manipulations are variables that can be adjusted independently, have sufficient power on controlled variables, but do not affect the plant performance. As demonstrated by Luyben (1994), in a large number of cases control DOF and design DOF are equal, although with different parameters. For example, specifying the distillate rate and reflux ratio gives a number of stages in design. Conversely, at fixed number of trays the manipulation of reflux ratio and distillate can be used to adjust the separation. As a result, a practical method to determine the control DOF consists of "counting the valves" available on the process streams, plus the heat duties for heaters/coolers, as well as the mechanical power of compressors and pumps.

4.3 NUMERICAL PROBLEMS IN DYNAMIC SIMULATION

4.3.1 Integration of DAE systems

Models used in dynamic simulation lead typically to a differential-algebraic equation system (DAE), whose general form may be written as follows:

$$\frac{d\mathbf{x}}{dt} = \mathbf{f}(\mathbf{x}, \dot{\mathbf{x}}, \mathbf{y}, \mathbf{p}, \mathbf{d}, t) \tag{4.16}$$

$$\mathbf{g}(\mathbf{x}, \mathbf{y}, \mathbf{p}, \mathbf{d}, t) = 0 \tag{4.17}$$

Vector **x** contains state variables involved in the accumulation term. Vector **y** represents other state variables. The vector of parameters **p** contains constitutive relations between **x** and **y**. Finally, the vector **d** designates sizing parameters.

The integration of a DAE system can be performed by transformation in an ODE system. It is worthy to note that this operation might be confronted with the *index problem.* Index is the minimum number order of differentiation needed to transform a DAE system into a set of first-order ODEs. Problems of *index one* can be solved by means of standard differentiation methods. When the index is higher than one then the DAE system needs a special treatment. Modern codes have capabilities for automatic detection of index higher-than-one, diagnose the problem and suggest modifications.

To illustrate the index problem let's consider the following simple DAE system:

$$\dot{x}_1 = x_1 + 3y \tag{4.18}$$

$$\dot{x}_2 = x_2 - 2y \tag{4.19}$$

$$0 = x_1 + x_2 - y \tag{4.20}$$

By differentiating the last equation and replacing the derivatives $\dot{x}_1$ and $\dot{x}_2$ leads to:

$$\dot{y}_1 = x_1 + x_2 + y \tag{4.21}$$

The system of equations (4.18), (4.19) and (4.21) can be initialised consistently. Because only one differentiation was necessary the index is one.

Now consider that the equation (4.20) changed slightly in:

$$0 = x_1 + x_2 \tag{4.22}$$

Since any value might be assigned for y the initialisation becomes undetermined. Differentiating the relation (4.22) gives:

$$0 = \dot{x}_1 + \dot{x}_2 \tag{4.23}$$

Combining with (4.18) and (4.19) leads to:

$$0 = x_1 + x_2 + y \tag{4.24}$$

Differentiating a second time and replacing the derivatives for x_1 and x_2 gives a differential equation for y, as follows:

$$\dot{y}_1 = -x_1 - x_2 - y \tag{4.25}$$

Therefore, the index of the second problem is two. The initialisation becomes consistent by transforming the DAE system in ODEs.

However, in the context of a practical simulation with a large number of variables the mathematical diagnosis of an index problem is not trivial (Pantelides & Barton, 1992). The user might prevent such troubles by examining carefully the problem, particularly the definition of specifications, which can be different as those met in steady state simulation.

For example, in steady state simulation setting the purity of overhead product of a distillation column is usual, but in dynamic mode this specification may lead to higher-than-one index problem. The physical reason is that a conflict could occur in initialisation because of the input-output material balance. A better solution is to let free product purity, and set other variable that may have an influence on it, as for example the reflux. If a given purity must be achieved, then the best way is to implement a controller that can manipulate the reflux or the distillate rate.

4.3.2 Computation of physical properties (local models)

Most of the computing time in a simulation run is spent in evaluating physical properties. Very non-linear thermodynamic models need many iterative calculations at each step of the integration procedure. Therefore, the use of simpler non-iterative models can reduce appreciably the computing time and increase simultaneously the robustness of simulation. This is achieved by means of *local models* for physical

properties. For instance, the following linear relation may approximate the variation of K-factors in calculating phase equilibrium:

$$\ln K_i = A_i + B_i / T \tag{4.26}$$

The constants A and B can be determined from the full model by regression over a limited interval of temperature, pressure and composition, but used "locally" inside the iterative loops. Then the local model parameters are updated again at the outside level.

4.4 DYNAMIC FLASH

Dynamic flash is a simple but very useful unit in dynamic simulation. Fig. 4.2 depicts the layout of a vapour-liquid separation. A multi-component feed of molar flow rate F with the composition z_i is split in vapour V and liquid L, with the composition y_i and x_i, respectively. Optionally heat may be added or removed. Initially the flash operates at steady state. The problem is to study the dynamic response at various disturbances, as changes in throughput or composition. Modelling equations are presented below.

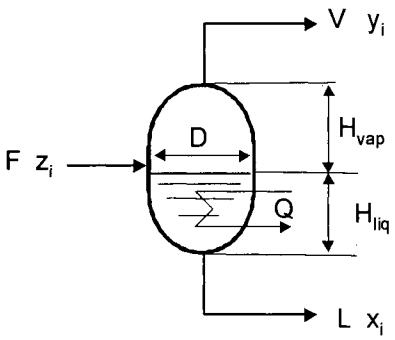

Figure 4.2 Dynamic Flash

Material Balance

- Component molar holdup m_i:

$$\frac{dm_i}{dt} = Fz_i - Vy_i - Lx_i \tag{4.27}$$

- Split the holdup between the two phases:

$$m_i = m_V y_i + m_L x_i \tag{4.28}$$

m_V and m_L being the total molar holdup of vapour and liquid phases, respectively.

- Total molar holdup of each phase as function of density and volume:

$$m_V = V_V \rho_V \ , \ m_L = V_L \rho_L \tag{4.29}$$

- Total volume and total mass:

$$V = V_V + V_L \tag{4.30}$$

$$m = \sum m_i \tag{4.31}$$

Energy Balance

- Differential enthalpy balance:

$$\frac{dH}{dt} = Fh_F - Vh_V + Lh_L + Q \tag{4.32}$$

h_F , h_V , h_L are specific molar enthalpies of feed, vapour and liquid. Q is the flash duty.

- Total enthalpy:

$$H = m_V h_V + m_L h_L \tag{4.33}$$

Phase equilibrium

- Vapour and liquid compositions at equilibrium:

$$y_i = K_i x_i \tag{4.34}$$

- Phase condition:

$$\text{Dew point } \sum_{i=1}^{n} x_i = 1 \text{; Bubble point } \sum_{i=1}^{n} y_i = 1 \tag{4.35}$$

- Pressure and temperature variations

$$P_V = P - \Delta P \ , \ P_L = P_V \ , \ T_L = T_V \tag{4.36}$$

Physical properties

- Vapour and liquid specific (per unit mass) enthalpy:

$$h_V = f(T_V, P_V, \mathbf{y}) \ ; \ h_L = f(T_L, P_L, \mathbf{x}) \tag{4.37}$$

- Vapour and liquid density:

$$\rho_V = f(T_V, P_V, \mathbf{y}) \ , \ \rho_L = f(T_L, P_L, \mathbf{x}) \tag{4.38}$$

- Phase-equilibrium constants:

$$\mathbf{K} = f(T_L, P_L, \mathbf{x}, \mathbf{y}) \tag{4.39}$$

The solution of the above system of equations can be done following different simulation strategies, as it will be shown in the next example.

EXAMPLE 4.2 Dynamic flash

Consider the separation of the reaction mixture in the HDA process by a simple flash. The total flow rate is 1670 kmol/hr from which hydrogen 680, methane 1020, and benzene 130. The feed is initially at 303 K and 40 bar. Built a dynamic model and examine the influence of some disturbances in open loop.

Solution.

We present results obtained with Aspen Dynamics. A dynamic simulation with this package can be conducted in two modes: flow or pressure driven.

In *flow-driven* simulation the flow rates and the pressure variations are decoupled. For example, the pressure and flow rate of an outlet stream are determined from the inlet conditions and block specifications. The pressure of the downstream block affects neither the outlet pressure nor the flow rate of the current unit. In other words, the flows are governed by the assumption of perfect control. This is often realistic, particularly for liquid flows. Therefore, in flow-driven mode the simulation of valves is not necessary. However, in some cases pressure and level controllers are added automatically with default tuning parameters.

In *pressure driven simulation* the flow rate is related with the pressure drop. Consequently, valves must be added for both inlet and outlet streams. For example, the inlet flow rate can be calculated from the pressure drop between feed supply and vessel. Similarly, the product flow rates can be calculated from the pressure drop between vessel and outlet lines. As before, controllers are added automatically for the *basic inventory* loops, as levels and pressures.

As illustration, we present the dynamic simulation of a flash in pressure driven mode. We consider a vertical cylindrical vessel of elliptical head shape with diameter of 1.5 m and height of 3 m. The liquid fraction is 0.5 and the residence time of 10 minutes.

Figure 4.3 illustrates the flowsheet with level and pressure controllers. Therefore, three valves V-1, V-2, and V-3 have been connected to the flash vessel. As specifications we select adiabatic operation and outlet pressure of 39.5 bar. In dynamic simulation the pressure and temperature inside the vessel cannot be set. These variables will change because disturbances, but we can use controllers to keep them between desired limits. Valve V-2 controls the temperature, and valve V-3 the pressure.

To investigate the open loop response we switch the controllers on manual. The total flow rate of the stream FEED is fixed, while the level is set free. The stream composition can be modified by changing the component flow rate in the script of the stream FEED.

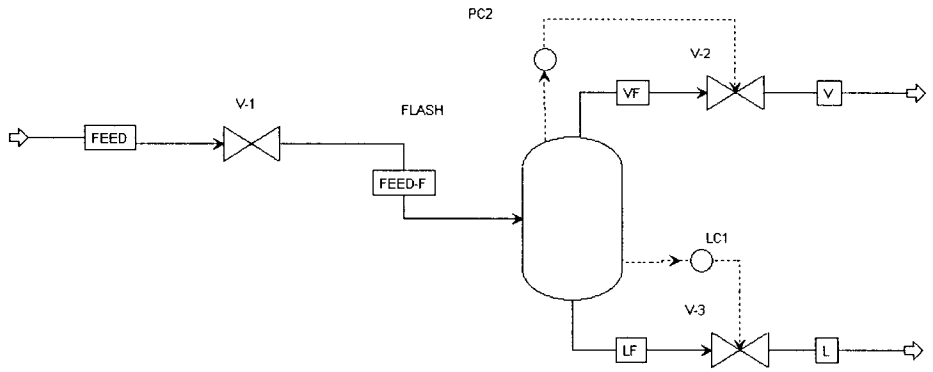

Figure 4.3 Dynamic flash in pressure driven mode

Figure 4.4 shows the open-loop response over three hours for the following scenario: after 0.5 h the feed temperature increases to 308.15 K for one hour, then for 0.5 h the total flow rises to 2000 kmol/h, followed by feed reset to 1870 kmol/hr, and finally feed temperature reset to 308.15 K. It can be observed that the flash temperature follows closely the disturbances with apparently first-order dynamics. The pressure is not affected by the disturbance in temperature, and only slightly by the feed flow.

It is interesting to note that the variation of level is sensitive. Thus, an increase in feed temperature makes decrease the level at longer time. The outlet liquid flow rises slightly, although a decrease was expected because of a vaporisation effect. By increasing the feed flow, the level decrease is stopped and the opposite effect takes place. The accumulation is reversed again when the feed flow rate is reduced. In conclusion, the influence of disturbances on the outlet streams is damped by the level variation. This effect is of great importance in practice, when the insertion of a tank is often used to cut disturbances both in flow and concentrations.

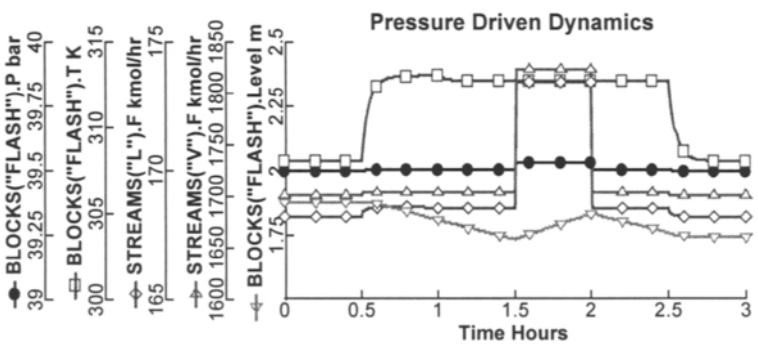

Figure 4.4 Dynamic response of HDA flash for different disturbances in open loop

4.5 DYNAMIC DISTILLATION COLUMN

A dynamic model of a distillation column can be assembled from simpler units, as trays, heat exchangers (condenser, reboiler), reflux drum, valves and pumps (Fig. 4.5). Tray modelling has to answer two issues: (1) accurate description of material and energy holdup, and (2) accurate pressure drop calculation.

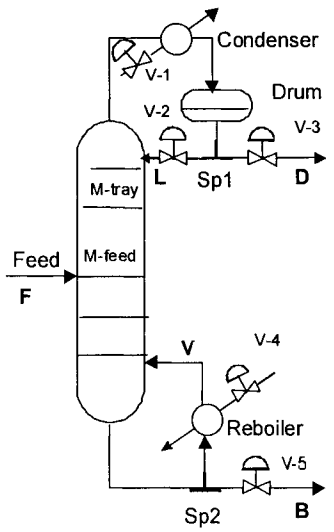

Figure 4.5 Dynamic model for a distillation column

Tray modelling

Modelling a single tray is similar with a dynamic flash discussed before. The solution of the assembly of trays, increased with condenser, flash drum and reboiler, is a much more difficult problem, however. The equations presented below (for notations see Fig. 4.6) are known as MESH equations for modelling distillation columns at steady state enlarged with left hand terms for accumulation.

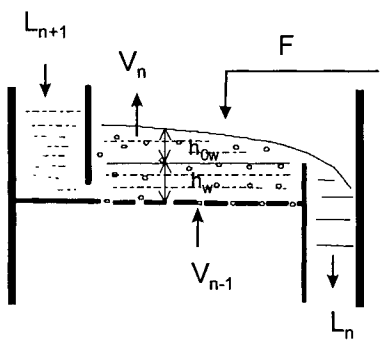

Figure 4.6 Tray modelling

- **M**aterial balance equations.

$$\text{Overall: } \frac{dm_n}{dt} = \frac{d}{dt}(m_{Ln} + m_{Vn}) = L_{n+1} + V_{n-1} - L_n - V_n \tag{4.40}$$

$$\text{Component: } \frac{d(m_n x_i)}{dt} = L_{n+1}x_{i,n+1} + V_{n-1}y_{i,n-1} - L_n x_{i,n} - V_n y_{i,n} \tag{4.41}$$

- Phase **E**quilibrium relations.

$$y_i = K_i x_i \tag{4.42}$$

- **S**ummation equations (phase conditions).

$$\text{Dew point } \sum_1^{N_c} x_i = 1; \qquad \text{Bubble point } \sum_1^{N_c} y_i = 1 \tag{4.43}$$

- Ent**H**alpy balance.

$$\frac{d}{dt}(m_n h_n) = \frac{d}{dt}(m_{Ln}h_{Ln} + m_{Vn}h_{Vn}) = L_{n+1}h_{n+1}^L + V_{n-1}h_{n-1}^V - L_n h_n^L - V_n h_n^V \tag{4.44}$$

The tray hydraulics supplies equations to calculate the liquid molar hold-up from geometry, as well as for coupling the pressure drop with vapour and liquid tray flows. The following relations hold for sieve trays. The liquid flow rate over a wire crest of length W and height h_w is given by the formula (Francis):

$$L_n = 1.839\rho_n^L W h_{ow}^{1.5} \tag{4.45}$$

where h_{0w} is the height over the crest given by:

$$h_{ow} = h_l - h_w \tag{4.46}$$

h_l is the liquid height, which in turn is related with the liquid hold-up m_{Ln} as:

$$h_l = m_{Ln}/(A_{tray}\rho_n^L) \tag{4.47}$$

The vapour flow can be related with the tray pressure drop, which in turn can be computed from the following contributions:

$$\Delta P_n = \Delta P_{dry} + \Delta P_{liq} + \Delta P_{res} \tag{4.48}$$

where

$$\Delta P_{dry} = C_0 V_n^{\ 2} \text{ is the dry plate pressure drop,} \tag{4.49}$$

$$\Delta P_{liq} = h_l \rho_L g \text{ is the static pressure drop,} \tag{4.50}$$

while ΔP_{res} accounts for superficial tension effects, froth, etc.

The temperature of stages and composition of vapour phase at equilibrium may be computed as follows:

- P, x flash: bubble point at given pressure and liquid composition. Specific liquid and vapour enthalpy are also determined.
- H, x flash at given saturated liquid enthalpy and liquid composition. It may be also used to compute plate pressure and temperature. However, the last method is less accurate, because of week sensitivity of liquid enthalpy with pressure.

The solution of the above set of implicit DAE system is highly non-linear and stiff. Different assumptions may facilitate the integration, depending on physical situation, modelling scope and numerical solver. The most common assumptions are:

- Negligible vapour hold-up (valid under 10 bar),
- Negligible variation of total liquid enthalpy,
- Constant molar vapour flows, but variable molar liquid flows!

If the computation of liquid flows is straightforward, the computation of vapour flows is more cumbersome, being linked with both energy balance and tray pressure drop. In this respect to three situations can be encountered:

1. *Energy balance accounted by the variation of tray liquid enthalpy*

By combining the equations (4.40) and (4.44) we get:

$$m_n \frac{dh_n^L}{dt} = L_{n+1}(h_{n+1}^L - h_n^L) + V_{n-1}(h_{n-1}^V - h_n^L) - V_n(h_n^V - h_n^L) \tag{4.51}$$

The column pressure drop may be handled in two ways:

a. Fixed plate pressure drop.

- V_{n-1} inlet vapour flow from the dry plate pressure drop,
- V_n outlet vapour flow from the algebraic energy balance (4.51), where dh_n^L/dt is taken as calculated in the previous time step.

b. Fixed top column pressure, but variable plate pressure drop. Note that vapour flow from reboiler, reflux flow and condenser pressure drop are set. The other values are:

- V_{n-1} from the dry plate pressure drop,
- V_n from the energy balance, as before,
- Height of liquid plate from the Francis formula.

The pressure drop profile is computed by an iterative procedure within a time interval, where pressure drop and L/V flows are updated with the above mentioned constraints.

2. *Negligible variation in liquid enthalpy on plate*

If $dh_L/dt = 0$ the equation (4.51) is purely algebraic. The approximation is acceptable if the molar heat capacity of the mixture depends only slightly on composition.

3. *Constant molar flows*

If the liquid enthalpy change is very small from plate to plate, and if the molar enthalpy of vaporisation of components is close, then we may safely assume that:

$V_n = V_{n-1}$ and $dm_n/dt = L_{n+1} - L_n$

In this case, the energy balance is not needed.

Taking into account the above elements we may formulate the following models, ordered by increasing complexity (Grassi, 1992):

- *Model 1a.* Assumptions: equimolar vapour flow, negligible vapour holdup, constant liquid holdup, constant pressure.
  Remark: Energy balance and overall mass balance are neglected. The only dynamic element is the tray composition. Consequently, this model might be useful for some dynamic studies, when the composition dynamics is relevant, but the process itself is rather slow. This model is not suitable for control, where an accurate description of the initial response is required.
- *Model 1b.* Assumptions: equimolar vapour flow, negligible vapour holdup, constant pressure.
  Remark: If the energy balance is disregarded, the dynamics is dominated by material balance and liquid flow rate.
- *Model 2a.* Assumptions: negligible specific liquid enthalpy change, negligible vapour hold-up, constant pressure or tray pressure drop.
- *Model 2b.* Assumptions: negligible change of specific liquid enthalpy, significant but constant vapour hold-up, constant tray pressure drop.
- *Model 3.* Assumptions: significant specific liquid enthalpy change, negligible vapour hold-up, variable tray pressure drop.
  Remark: Model 3 is suitable for most dynamic studies where the pressure variation is moderate.
- *Model 4.* Assumptions: significant specific liquid enthalpy change, significant vapour hold-up, variable tray pressure drop.
  Remark: Model 4 is suitable for high pressure, where the contribution of gas phase is significant. Downcomer modelling might be necessary.

EXAMPLE 4.3 Dynamic simulation of a distillation column

Consider the separation of a benzene/toluene mixture by distillation in a tray column. Study the building of a dynamic model and explore the behaviour of the separation without purity control.

Solution.

This time we will make use of a flow driven simulation. We consider 100 kmol/hr of equimolar mixture benzene/toluene. The distillate purity is moderate, of 98.5%. Steady state design gives 18 plates plus condenser and reboiler with the feed on the plate 10. The hydraulic sizing at 80% from flooding gives the following tray characteristics: diameter 1 m, tray spacing 0.6096 m, and weir height 0.05 m. The reflux drum is a

vertical cylindrical vessel with elliptical head and 2.3 m height by 1.14 m diameter. Similarly, the sump is 3 m height by 1.15 m diameter.

The flowsheet is completed with **P**-type controllers for level in the reflux drum and bottoms, and **PI** controller for pressure. These controllers ensure the basic inventory control, but are not sufficient for quality control. Therefore, we are interested by distillate flow rate and purity faced with disturbances in the feed. Fig. 4.7 presents the open loop response to feed variation of +/- 10%. Increasing the feed to 110 kmol/hr gives an increase in purity over 99%, but a decrease of the distillate rate to less than 47.5 kmol/hr. After reset to initial conditions, the feed is reduced to 90 kmol/h. This time the distillate rate increases at 52.5 kmol/hr, but the purity drops dramatically to 86%. This behaviour seems somewhat strange, so the reader is encouraged to find a physical explanation. The need for quality control in a distillation column is obvious. This issue will be treated in the Example12.2.

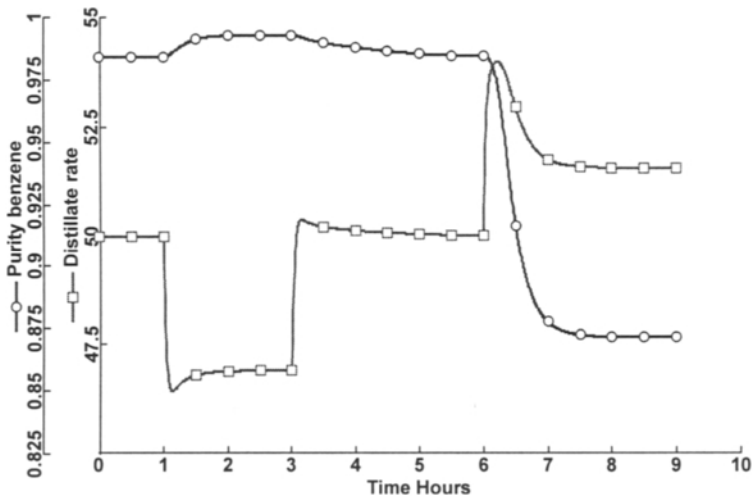

Figure 4.7 Dynamic response of a distillation column in open loop

4.6 DYNAMIC SIMULATION OF CHEMICAL REACTORS

4.6.1 CSTR model

The modelling of an isothermal CSTR have been presented in Example 4.1. Here we add the energy balance that may be formulated as following:

$$\frac{d(mh)}{dt} = G_0 h_0 - Gh - V\sum_{i=1}^{N_r} r_i(-\Delta H_{R,i}) + Q_t \tag{4.52}$$

The heat transfer term can be calculated by assuming that the thermal agent has a constant temperature T:

$$Q_t = UA(T - \overline{T}) \tag{4.53}$$

It can be observed that in this formulation the differential equation for energy balance does not contain explicitly the temperature, which is calculated implicitly from enthalpy. The same is valid for the volume, computed from mass and mixture density. Therefore, in dynamic simulation accurate values of physical properties are required at each integration step, as specific volume and specific enthalpy.

4.6.2 Tubular reactors

In a tubular reactor, the concentration and temperature may vary both in time and space. One speaks about a distributed system. The ideal plug flow reactor (PFR) model is the most used. Because of the flat velocity profile, the concentrations and temperature varies only along the length. Consider for simplification a homogeneous reaction. The unsteady state material balance of the reactive species leads to the following equation:

$$\frac{\partial c_i}{\partial t} + u_z \frac{\partial c_i}{\partial z} + r_i = 0 \tag{4.54}$$

The first term accounts for accumulation, the second for convective transport with the velocity u_z in the direction z, and the third for chemical reaction. The energy balance gives the following equation for the temperature profile:

$$\frac{\partial T}{\partial t} + u_z \frac{\partial T}{\partial x} + \frac{1}{\rho C_p} \sum_{i=1}^{N_r} r_i(-\Delta H_{R,i}) = 0 \tag{4.55}$$

The solution of the above equations requires both initial and boundary conditions. Usually the transient begins from the stationary state, so that at t=0 the profiles $c_{i,s}(0,z)$ and $T_s(0,z)$ are available. Inlet concentrations $c_{i,in}$ and temperature T_{in} coming from an upstream unit may be constant or fluctuate in time.

$$\begin{array}{lll} t = 0 & c_i(0,z) = c_{i,s}(z) & T(0,z) = T_s(z) \\ t > 0 & c_i(t,0) = c_{i,in} & T(t,0) = T_{in} \end{array} \tag{4.56}$$

The equations (4.54) and (4.55) contain partial derivatives with both time and length. Three approaches are usually employed:

1. Transformation of partial differential equations in algebraic equations by using finite differences. The most known approach is the 'method of lines'.
2. Use of special functions, as orthogonal polynomials in the class of methods based on 'collocation', to approximate concentration and temperature profiles.
3. Replacement of PFR by a series of CSTR's.

Finite difference methods are implemented in gPROMS (2001). Aspen Dynamics uses the third approach. Care should be paid to a convenient description of a PFR. A number of ten CSTR's is sufficient, but when the temperature variation is highly nonlinear, the use of several PFR reactors in series is recommended.

4.7 PROCESS CONTROL TOOLS

4.7.1 Implementation of controllers

The majority of controllers in industry are based on Single Input Single Output (SISO) loops. The implementation of such controllers consists of a succession of operations, as follows:

• Select the *process variable* (PV) that has to be controlled. This may be a stream or unit variable, usually pressure, temperature, concentration, mass or volumetric flow rates, as well as the liquid level. The variation can be expressed as a percentage from the range (PV_{max} - PV_{min}). *Setpoint SP* is the PV value that should be kept at a desired value. Usually the setpoint is positioned close to the midrange.

• Define the *controller output* (OP) as the manipulated variable. This is usually a stream flow rate or heat duty. The steady state design supplies the nominal value. The maximum output may be taken as twice the nominal value. The minimum output may be set to zero or to a non-zero safe value.

• Implement controller. The **PID** (proportional-integral-derivative) controllers are mostly used in practice. A **PID** controller modifies the manipulated variable following the algorithm:

$$OP = OP_{ss} + K_C[\varepsilon(t) + \frac{1}{\tau_I}\int_0^{\tau_i}\varepsilon(t)dt + \tau_D\frac{d\varepsilon(t)}{dt}] \tag{4.57}$$

In the above relation OP_{ss} is the steady state value, or the *bias* of the manipulated variable, and ε is the error defined as difference between PV and setpoint:

$$\varepsilon = SP(t) - PV(t) \tag{4.58}$$

A **PID** controller has three adjustable parameters K_C, τ_I, τ_D, which define proportional (P), integral (I) and derivative (D) actions. The most important is the *controller gain* K_C. Usually K_C is dimensionless, and is expressed as the ratio of scaled output to input, %OP/%PV. Higher gain gives faster response, but also more oscillatory behaviour. **P**-controller has always a steady state error. The error is reduced by integration over a time τ_I known as *reset time*. The derivative component may be considered for faster response, the parameter τ_D being known as *rate time*. Determining the above parameters implies a *tuning* procedure, as discussed later in this section.

• Define the mode of action. In *direct action*, when the process variable PV is above the setpoint (negative error) the manipulated variable (OP) is increased (negative gain), and vice versa. For instance, consider level control by outlet flow. When the level rises above the setpoint the outlet flow must increases too. In *reverse action*, when PV increases above SP (negative error), the manipulated variable decreases. Here we may give as example the control of purity by reflux. When the purity of the product increases above the setpoint, the reflux flow rate must diminish.

• Prepare the controller view and recorder settings.

4.7.2 Tuning of PI controllers

PI is the most used controller. The tuning consists of a **PI**-controller the finding the dynamic characteristics called 'ultimate gain' (K_U) and 'ultimate period' (P_U). A step disturbance is introduced, and the gain of controller in **P** mode is slowly increased. The value where sustained bounded oscillations appear designates the ultimate gain K_U. The ultimate period P_U can be measured directly.

In another method, called ATV (auto-tune variation), the controller is replaced by a relay of amplitude $\pm h\%$. The period is divided in each cycle by two up to the occurrence of oscillations. If a is the amplitude of oscillations, the ultimate gain can be calculated as:

$$K_U = 4h/\pi a \tag{4.59}$$

By knowing K_U and P_U, the parameters of a PI controller can be calculated with simple relations as given in the Table 4.1, according to Ziegler-Nichols (ZN) or Luyben-Tyreus (LT). It is considered that the ZN tuning is somewhat aggressive, while LT is rather soft. Note that the values of tuning parameters determined as above should be seen only as initial values. The tuning should continue up to the point where the performance of controller is satisfactory (see Chapter 12).

Another problem is the use of the tuning parameters for SISO loops in a multi-input multi-output (MIMO) environment. The influence of interactions between loops can be dumped in some cases only by 'detuning' the parameters, usually by diminishing the gains and increasing the reset times.

Table 4.1 Tuning rules for PI controllers

Tuning rule	K_C (%/%)	P_U (min)
Ziegler-Nichols (ZN)	K_U/2.2	P_U/1.2
Luyben-Tyreus (TL)	K_U/3.2	2.2 P_U

EXAMPLE 4.4 Closed loop dynamic simulation of a flash

Switch on automatic the controllers for level and pressure used for the flash discussed in the Example 4.2, and examine the closed-loop response.

Solution.

We use the default tuning parameters, as follows: LC1 with K_c=20 %/% and τ_I=10 min., and PC2 with K_C=20 %/%. Fig. 4.8 displays the closed loop response for the same scenario of disturbances as in Example 4.2. This time the liquid level is kept around the set point with small deviations. The response of the output streams is different from open loop dynamics: the outlet liquid flow rate decreases at increasing temperature, and vice versa. An inverse response is noted in both cases. Hence, keeping constant the liquid level will produce disturbances in the outlet flows, which might be undesirable

for the downstream unit. A looser level control would be more profitable. In fact, besides the separation in liquid and vapour, the role of a flash vessel is to dump disturbances in flows arriving from the upstream units. In conclusion, except chemical reactors, for the level control of units with liquid inventories, as reservoirs, flash drums and reboilers, a simple **P**-controller is convenient.

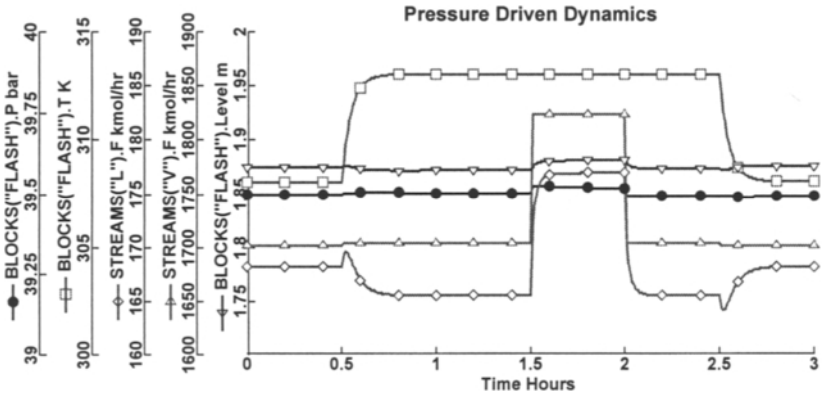

Figure 4.8 Dynamic response of a flash in closed loop

4.8 FURTHER READING

As general reference for mathematical modelling in chemical engineering we recommend the newest edition of the acclaimed textbook of Bird, Lightfoot & Stewart (2001). A classical guide for writing equations for deterministic systems is the book of Himmelblau & Bischoff (1968), probably now difficult to find. A refreshing retrospective of mathematical modelling has been revealed recently by Aris (2001).

Mathematical formulation of dynamic models and their linearisation is treated in books dealing with process dynamics and control. Here we mention the textbooks of Stephanopoulos (1984), Ogunnaike & Ray (1994), Luyben (1995), and Marlin (1995). Very useful theoretical and practical insights in dynamics and control of distillation processes, with so many implications in dynamic simulation, can be found in the monograph edited by Luyben (1992) with contribution of specialists in different areas. A useful presentation of process dynamics from a practical viewpoint can be found in the book of Ingham et al. (1994).

Nonlinear dynamics is becoming an important topic in design, since implied not only in safety aspects, but also in design for flexibility. Some applications will be presented in Chapter 13. An advanced treatment of nonlinear dynamics can be found in the book of Bequette (1998). More complex dynamic phenomena, as the occurrence of multiple steady states and chaotic behaviour, are presented in accessible but rigorous manner. Numerous examples built in Matlab illustrate the mathematical issues.

4.9 REFERENCES

Aris, R., 2001, Modelling principles, Academic Press

Bequette, R. W., 1998, Process Dynamics, Modelling, Analysis and Simulation, Prentice Hall, New Jersey

Bird, Lightfoot, Stewart, 2001, Transport Phenomena, Wiley, New York, 2nd Edition

Himmelblau, D., K. Bishoff, 1968, Process Analysis and Simulation. Deterministic Systems, Wiley, New York

Ingham, J., I. J. Dunn, E. Heinzle, J. E. Prenosil, 1994, Chemical Engineering Dynamics. Modelling with PC Simulation, VCH-Wiley, Weinheim

Luyben, W., 1989, Process Modelling, Simulation and Control, 2nd Edition, McGraw Hill, New York

Luyben, W. L., 1996, Design and control design of freedom, Ind. Eng. Chem. Res., 35, 2204-2214

Grassi, V. G., 1992, Rigorous modelling and conventional simulation, in Practical Distillation Control, Van Nostrand Reinhold, New York, p. 29-46

Marlin, T. E., 1995, Process Control, Mc Graw Hill, New York

Ogunnaike, B. A., W. H. Ray, 1994, Process Dynamics, Modelling and Control, Oxford University Press

Pantelides, C. C., P. I. Barton, 1992, Equation-Oriented dynamic simulation, Comp. & Chem. Eng., ESCAPE-2, S263-S285

Practical Distillation Control, 1992, edited by W. L. Luyben, Van Nostrand Reinhold

Stephanopoulos, G., 1984, Chemical Process Control, An Introduction to Theory and Practice, Prentice-Hall International

SOFTWARE MANUALS

Aspen Dynamics User Manual, version 10.2, Aspen Tech, 2001

g-Proms, User Manual, version 2.1, 2001

PART II

THERMODYNAMIC METHODS

This Page Intentionally Left Blank

Chapter 5

GENERALISED COMPUTATIONAL METHODS IN THERMODYNAMICS

5.1 PVT behaviour of fluids
- 5.1.1 Phase diagrams
- 5.1.2 Equations of state
- 5.1.3 Principle of corresponding state

5.2 Fundamentals of thermodynamics
- 5.2.1 Laws of thermodynamics
- 5.2.2 Free energy functions
- 5.2.3 Phase equilibrium condition
- 5.2.4 Gibbs-Duhem equation
- 5.2.5 The network of thermodynamic properties

5.3 Fugacity
- 5.3.1 Definition
- 5.3.2 Computation of fugacity

5.4 Equations of state
- 5.4.1 Virial family of equations of state
- 5.4.2 Cubic equations of state

5.5 Generalised computational methods using PVT relationship
- 5.5.1 Departure functions
- 5.5.2 Evaluation of the departure functions
- 5.5.3 Generation of thermodynamic property charts

5.6 Summary

5.7 References

This chapter deals with the fundamental concepts that allow a unified approach of the thermodynamic computations in process simulation, both in the field of physical properties and of phase equilibria. The last aspect is examined in more detail in the Chapter 6. The material is presented as a synthesis of a much more elaborated treatment that may be found in dedicated textbooks on Chemical Engineering Thermodynamics, as Smith and van Ness (1997), Kyle (2000), Sandler (2001). The description of the major methods for estimating fundamental properties, mostly being implemented in simulation packages, may be found in the thesaurus book of Reid and al. (1987) updated recently by Poling, Prausnitz and O'Connell (2001).

The chapter starts by examining the *PVT* behaviour of process fluids, as gases and liquids. We will introduce generic models, as the equations of state and the principle of corresponding states, which dominate nowadays the thermodynamic calculations by computer methods. Then we will review the laws of thermodynamics in order to ensure a coherent presentation of the fundamental equations. Particular attention will be given to the network of thermodynamic relations that makes possible to navigate between different properties, mostly not accessible by measurements, only on the base of very limited experimental information. We will formulate the general conditions of phase equilibrium. In this context, we will highlight the concept of fugacity and its calculation. A distinct section will be devoted to a more ample presentation of the equations of state, particularly of cubic type, which at presently are the default models in flowsheeting packages. We will end the chapter by describing the generalised computational methods for generating charts and tables for various properties.

5.1 PVT BEHAVIOUR OF FLUIDS

5.1.1 Phase diagrams

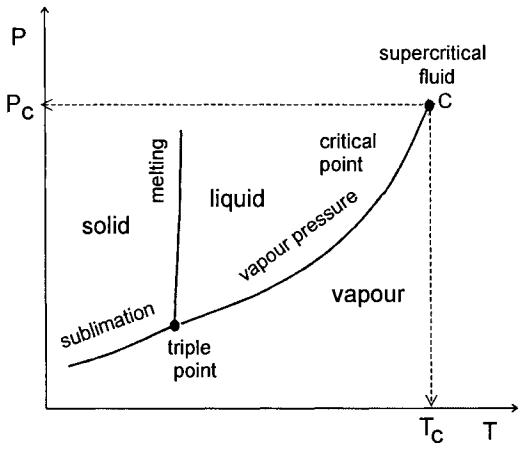

Figure 5.1 Generalised phase diagram

Figure 5.1 presents the behaviour of a pure species that can exist as solid, liquid or vapour in a pressure-temperature diagram. We may have three types of two-phase equilibrium: solid/liquid, vapour/liquid and solid/vapour. There is a point where all three phases coexist, designated by the *triple point*. Here the phase rule gives $F=C+2-P=1+2-3=0$ degrees of freedom. Neither pressure nor temperature can be used to modify the equilibrium. If only two phases can be found at equilibrium $F=1+2-2=1$, and either pressure or temperature can vary. The most important equilibrium in process engineering is *vapour-liquid equilibrium*, abbreviate as *VLE*. It may be observed that the two phases will coexist up to a point where it is difficult to make a distinction between vapour and liquid. This is the *critical point*, a fundamental physical property characterised by *critical parameters* P_c, T_c and V_c. Above the critical point the state of the fluid is *supercritical*. Actually, the properties of a supercritical fluid are quite different from a super-dense gas or a light liquid.

If the pressure P is represented as function of the molar specific volume V of a pure component at constant temperature, the isotherms have the aspect given in Fig. 5.2, where the state variables (reduced values) are scaled by reference to the critical point:

$$T_r = \frac{T}{T_c} \; ; \; P_r = \frac{P}{P_c} \; ; \; V = \frac{V}{V_c} \tag{5.1}$$

At the critical point the difference between liquid and vapour volumes approaches zero, suggesting that the energy needed for phase transition, in other words the enthalpy of vaporisation, should diminish to zero. The above observation illustrates in a simple manner the link between the *PVT* behaviour of a fluid and the energy implied in its physical changes.

Figure 5.3 presents the generic *PVT* relationship for a pure component in a **3D** diagram. This representation captures both the temperature evolution of the phase boundaries at equilibrium, as well as their volumetric behaviour. The **2D** representation for different cases is straightforward.

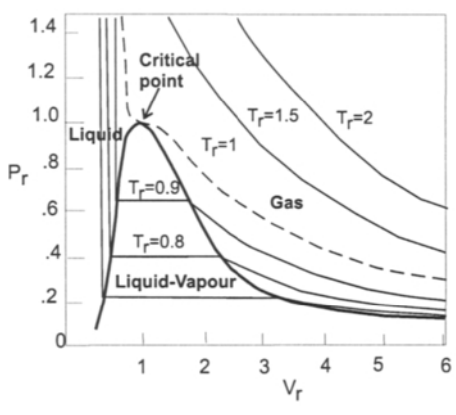

Figure 5.2 Pressure-Volume curves

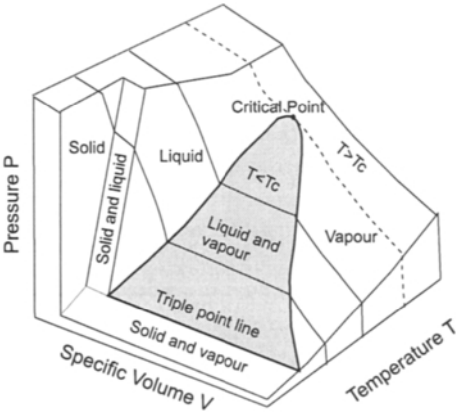

Figure 5.3 Generalised PVT diagram

5.1.2 Equations of state

An algebraic equation relating the fundamental state variables of a fluid P, V and T is known as an *equation of state*, abbreviated here by EOS. The simplest EOS is the ideal gas law $PV=RT$. The models based on equations of state are widespread in simulation because allow a comprehensive computation of both thermodynamic properties and phase equilibrium with a minimum of data. EOS models are applied not only to hydrocarbon mixtures, as traditionally, but also to mixtures containing species of the most various chemical structures, including water and polar components, or even to solutions of polymers. The most important equations of state are presented briefly below, but they will be examined in more detail in other sections.

a. Virial EOS

The non-ideality of a gas can be expressed by the compressibility factor Z, defined as:

$$Z = \frac{PV}{RT} \tag{5.2}$$

One of the simplest forms, called *Virial equation of state*, express the compressibility factor Z as a power series of molar volume or pressure:

$$Z = \frac{PV}{RT} = 1 + \frac{B}{V} + \frac{C}{V^2} + ... \tag{5.3}$$

$$Z = \frac{PV}{RT} = 1 + B'P + C'P^2 + ... \tag{5.4}$$

Note that the *Virial coefficients* B, C, or B', C', are function only of temperature. Virial EOS has a theoretical basis in statistical mechanics. For example, the B/V term accounts for interactions between pairs of molecules; C/V^2 describes three molecule interactions, etc. The form $Z=1+B/V$ called the *second virial coefficient* has found wide applications, but it is restricted to gas phase calculations at moderate pressures up to 20 bar.

Much more sophisticated is the form known as the BWR-EOS, proposed by Benedict, Webb and Rubin (1940)[1]. This model represents a more complex dependency of pressure as function of volume:

$$P = \frac{RT}{V} + \frac{B_0RT - A_0 - C_0/T^2}{V^2} + \frac{bRT - a}{V^3} + \frac{\alpha a}{V^6} + \frac{c}{V^3T^2}\left(1 + \frac{\gamma}{V^3}\right)exp\frac{-\gamma}{V^2} \tag{5.5}$$

The constants A, B, C, a, b, c, α and β are characteristic for a given fluid. BWR-EOS and its recent modifications permit accurate calculations of physical properties of light gases, non-polar or slightly polar components medium pressure. BWR-EOS can be used for both thermodynamic properties, as enthalpy and entropy, and phase equilibrium. It is also suited for light hydrocarbon processes, including rich methane and hydrogen mixtures, as well as in gas liquefaction.

---

[1] For complete references on EOS's see the book of Poling, Prausnitz and O'Connel (2001)

b. Cubic equation of state

The cubic EOS are based on the famous *van der Waals* equation (1873):

$$P = \frac{RT}{V-b} - \frac{a}{V^2} \tag{5.6}$$

The term a/V^2 accounts for increasing attractive forces between molecules at higher pressure, while b is a measure of the co-volume of molecules at infinite pressure. Note that both parameters a and b are functions only of critical pressure and temperature.

Long time the original van der Waals EOS did not found industrial applications. *Redlich and Kwong* (1949) discovered that a modified form was convenient for describing the hydrocarbon mixtures. The model, abbreviated here by RK-EOS, is represented by the relation:

$$P = \frac{RT}{V-b} - \frac{a}{T^{1/2}V(V+b)} \tag{5.7}$$

In fact, RK-EOS introduced an important modification in the formulation of van der Waals equation, the temperature dependency of the a parameter, such as:

$$a(T) = a_c(T_c, P_c)\alpha(T) \tag{5.8}$$

The correction factor of the parameter a is designated often by *alpha function.* For the RK-EOS this factor is $\alpha(T) = 1/\sqrt{T}$.

Much later *Soave* (1972) proposed a new modification, known as Soave-Redlich-Kwong EOS, abbreviated here SRK-EOS, in which the model incorporates another important molecular parameter, the *acentric factor* ω (see later the equation 5.12). The result was that the accuracy of VLE computations improved considerably. In the case of SRK-EOS the alpha function is:

$$\alpha^{0.5} = 1 + \kappa\left(1 - T_r^{0.5}\right) \tag{5.9}$$

The factor κ is a polynomial function of ω, $\kappa = f(\omega)$.

Another equation, due to *Peng* and *Robinson* (1976), denoted by PR-EOS, has proved similar accuracy, but more robustness near the critical point. The form is:

$$P = \frac{RT}{V-b} - \frac{a(T)}{V(V+b)+b(V-b)} \tag{5.10}$$

The function α is given by Eq. (5.9) but with different dependency $\kappa = f(\omega)$.

With the arrival of commercial simulators the cubic equations of state have become standard thermodynamic options. This fact may be attributed both to their simplicity and robustness in calculating thermodynamic properties and phase equilibrium. For example, a cubic EOS distinguishes without ambiguity between mono-phase and multi-phase systems. New modifications and mixing rules enlarged the field of applications from hydrocarbons to all (non-electrolytic) mixtures, including non-polar and polar components, over a large range of pressures and temperatures.

5.1.3 Principle of corresponding states

The *principle of corresponding states* was the first attempt toward a universal method for correlating thermodynamic properties. This is expressed as following: *The equilibrium properties that depend on intermolecular forces are related to critical properties in a universal way.* In *two parameters* formulation (van der Waals, 1873), the compressibility factor is a function only of the reduced temperature and pressure:

$$Z = f(T_r, P_r) \tag{5.11}$$

A major improvement in generalising the correlation of the compressibility factor was obtained with a *three-parameters* formulation. The third parameter is the acentric factor ω, which is a thermodynamic measure of the shape and size of a molecule. A mathematical definition is based on the slope of vapour pressure curve at T_r=0.7:

$$\omega = 1.0 - \log(P^{sat} / P_c)_{T_r=0.7} \tag{5.12}$$

Following Pitzer (1955)[2], the compressibility factor Z may be expressed by

$$Z = Z^0(T_r, P_r) + \omega Z^1(T_r, P_r) \tag{5.13}$$

Hence, the computation of Z is split in two parts: Z^0 - term for an ideal spherical molecule, and Z^1 - deviation function accounting for non-sphericity. A large number of generalised predictive methods for physical properties exploit this formulation, as for example the *Lee-Kesler*[3] method (see later the section 5.4).

5.2 FUNDAMENTALS OF THERMODYNAMICS

5.2.1 Laws of thermodynamics

Thermodynamics is the science that studies the changes in the state or condition of a system when changes in its internal energy are important. *Internal energy* designates all forms of energy associated with motions, interactions and bonding of molecules forming a material body. This is quite different from forms of *external energy*, as kinetic and potential energy, which are of primary interest in mechanics. In this book the sign conventions are:

- Energy: positive *in*, negative *out*.
- Work $dW = -pdV$: compression positive (dV<0), expansion negative (dV>0).
- Capital letters designates *molar values* of properties, as volume (V), internal energy (U), enthalpy (H), entropy (S) and free energy functions (A, G). Consequently, extensive values for a system containing n moles will be noted by (nV), (nU), etc.

---

[2] Pitzer, K.S., Curl, R. F., J. Am. Chem. Soc., **79**, 2369, 1957

[3] Lee, B.I., Kesler, M.G., AIChEJ, **21**, 510, 1975

First law of thermodynamics

The first law postulates the *conservation of energy*. The system is the part of the space where the process occurs. Everything not included in the system is considered *surroundings*. Let's consider a system, where work (W) and heat (Q) are the only forms of energy passed between system and surroundings. Moreover, the system is closed, such as no mass exchange takes place. The *first law of thermodynamics* is:

$$\Delta\,(\textit{energy of the surroundings}) + \Delta\,(\textit{energy of the system}) = 0 \tag{5.14}$$

The first term is given by the net amount of heat and work exchanged $Q+W$. The second term should take into account the change in energy of the system itself. This can be decomposed in several contributions. The most significant is the *internal energy U*, which includes all forms of energy associated with the activity of atoms and molecules forming a system, except those related to macroscopic movement (*kinetic energy*) or change in position (*potential energy*). Internal energy is a state function. Its absolute value cannot be known, but its variation ΔU between two states is always the same regardless the path followed.

In differential form, the first law postulates that in a closed system the *internal energy U* can be varied only by exchange of heat and/or of work:

$$dU = \delta Q + \delta W \tag{5.15}$$

The differential dU is 'exact', depending only on the initial and final states (pressure, volume, temperature, composition). Contrary, both δQ and δW are not exact differentials, depending on the path of transformation.

An important measurable physical property is the *constant-volume heat capacity* C_V, defined as:

$$\left(\frac{\partial U}{\partial T}\right)_V = \left(\frac{\partial Q}{\partial T}\right)_V = C_V \tag{5.16}$$

Because most of the industrial operations take place at fairly constant pressure, it is useful to associate U and PV in a new state function *enthalpy (H)*, whose definition is:

$$H = U + PV \tag{5.17}$$

By differentiation of (5.17) and combination with (5.15) leads to:

$$dH = \delta Q + VdP \tag{5.18}$$

Equation (5.18) is the first law expressed in differential form. From this we can define an important measurable physical property, the *constant-pressure heat capacity* C_P:

$$\left(\frac{\partial H}{\partial T}\right)_P = \frac{\partial Q_P}{\partial T} = C_P \tag{5.19}$$

C_V and C_P are functions of temperature. For an ideal gas $C_P^0 = C_V^0 + R$.

The energy balance in industry is usually formulated as an enthalpy balance. For open (flowing) systems, when thermal effects predominate, the first law becomes:

$$\Delta H = Q + W_s \tag{5.20}$$

The mechanical energy W_s is exchanged as *shaft work*. Note that the volumetric work is incorporated directly in the computation of enthalpy. If only change in temperature is involved, and no phase change occurs, the variation of the (sensible) enthalpy is:

$$\Delta H = H(T_2) - H(T_1) = \int_{T_1}^{T_2} C_P(T)dT \tag{5.21}$$

The above formula is acceptable for condensed phases, as solid or liquids, without phase transition, but not for real gases, where the influence of pressure has to be accounted for. Consequently, the formula (5.21), so much used in hand calculations, is of relatively minor importance in process simulation. Instead, computations of enthalpy based on equations of state or corresponding states principle are used.

An ideal gas is taken usually as reference for the thermodynamic properties of a real fluid. Because the enthalpy of an ideal gas does not depend on pressure, its variation between two states depends only on temperature. It is convenient to define an arbitrary *reference state*[4]. The enthalpy of an ideal gas H^0 can be set at zero for $T = T_0$. A convenient reference temperature is the absolute zero Kelvin. In this case the enthalpy of an ideal gas can be calculated simply as

$$H^0 = \int_0^T C_P^0(T)dT = aT + bT^2/2 + cT^3/3 + \ldots.. \tag{522}$$

As it will be demonstrated later in this chapter, the difference in enthalpy between a real fluid and an ideal gas, at the same T and a reference P_0, noted usually as *departure function* $(H - H^0)$, can be determined only from PVT information. Hence, the enthalpy of a real fluid, including contributions of both sensible heat and phase transition, may be found simply with the relation:

$$H = H^0 + (H - H^0) \tag{5.23}$$

This approach can be extended to other thermodynamic properties.

Second law the thermodynamics

The second law deals with the spontaneous evolution of a thermodynamic process and the efficiency of conversion between different forms of energy, particularly between work and heat. It is intimately linked with the notion of *entropy*. The work can be transformed spontaneously and integrally in heat, such that $W = JQ$. On the contrary, the conversion of heat in work is never spontaneous.

---

[4] A reference state may be different from a standard state, a concept used in equilibrium reactions.

The second law of thermodynamics postulates: *It is impossible for a device operating in a cyclic manner to completely convert heat into work.* If the heat flows spontaneously from higher to lower temperature, the opposite process requires a *heat engine*. Carnot demonstrated that the maximum work from a heat engine is given by a cycle formed by two adiabates and two isotherms whose efficiency is:

$$\eta = \frac{Q_1 - Q_2}{Q_1} = \frac{T_1 - T_2}{T_1} \tag{5.24}$$

T_1 is the absolute temperature at which the heat Q_1 is injected, and T_2 the temperature at which the heat Q_2 is rejected. It follows that we can write:

$$\frac{Q_1}{T_1} - \frac{Q_2}{T_2} = 0 \tag{5.25}$$

Equation (5.25) suggests that the ratio between the heat (received or rejected) and the temperature might be a system property that might characterise the *reversibility* [5]of the heat exchange in a cyclic process. By more rigorous reasoning, this observation leads to a new state function, *entropy*, defined as:

$$dS = \frac{\delta Q_{rev}}{T} \tag{5.26}$$

where δQ_{rev} is the infinitesimal amount of heat exchanged in a reversible process at the temperature T.

Entropy plays a central role in evaluating the reversibility of processes. For the transformation from the point A to the point B the following relation is valid:

$$S_B - S_A = \int \frac{dQ_{AB}}{T} \geq 0 \tag{5.27}$$

The equation (5.27) defines the following possibilities:
(1) $\Delta S = 0$, the process is reversible and adiabatic,
(2) $\Delta S > 0$, the process is irreversible, and
(3) $\Delta S < 0$ the process is impossible.

Third law of thermodynamics

The *third law* allows the calculation of an absolute value for entropy. By definition *the entropy of a perfect crystalline substance is zero at zero absolute temperature.* For a pure component ideal gas at the temperature T we may write:

$$S_T = \int_0^{T_f} \frac{C_{P,s}}{T} dT + \frac{\Delta H_{fusion}}{T_f} + \int_{T_f}^{T_v} \frac{C_{P,l}}{T} dT + \frac{\Delta H_{vap}}{T_v} + \int_{T_v}^{T} \frac{C_{P,v}}{T} dT \tag{5.28}$$

---

[5] A reversible process proceeds with infinitesimal gradients within the system. The direction can be reversed at any point by an infinitesimal change in external conditions.

T_f and T_v are the fusion and vaporisation temperatures, whereas ΔH_{fusion} and ΔH_{vap} are the enthalpies of the respective phase transitions.

5.2.2 Free energy functions

Free energy functions A and G are more appropriate for the computation of physical and chemical equilibrium than the primary functions U and S. The definitions are:

- *Helmholtz free energy* (A):

$$A = U - TS \tag{5.29}$$

- *Gibbs free energy* (G):

$$G = H - TS = U + PV - TS = A + PV \tag{5.30}$$

The functions A and G are called 'potentials' because allow the calculation of the maximum work W_{max} only from initial and final states. Consider a reversible process in a closed system. The maximum work can be produced only by a reversible transformation. Eqs (5.15) and (5.26), can be combined to give the following relation:

$$dU = TdS + \delta W_{max} \tag{5.31}$$

The *total work* W takes into account the *volumetric work* PV, as well as other forms of *useful work* (shaft, electrochemical), noted here by $W^{\#}$. The volumetric work is accounted as a change in volume at constant pressure. For an infinitesimal change the total work is $\delta W = -PdV + \delta W^{\#}$. Hence, the following relation can express the maximum useful work:

$$\delta W^{\#}_{\max} = dU - TdS + PdV \tag{5.32}$$

For a process at (T, V) constant we obtain:

$$\delta W^{\#}_{\max} = d(U - TS) \tag{5.33}$$

Hence, the quantity A=U-TS is a potential at (V, T) constant, because it gives the maximum work for finite variation:

$$W^{\#}_{\max} = \Delta A \tag{5.34}$$

Similarly G=H-TS is a potential at (P, T) constant, because:

$$W^{\#}_{\max} = \Delta G \tag{5.35}$$

The Gibbs free energy is preferred in technical calculations because most of industrial processes take place at fairly constant pressure.

Equation (5.31) can be extended to include irreversible processes being known as *Clausius inequality:*

$$\Delta U - T\Delta S + P\Delta V - W^{\#} \le 0 \tag{5.36}$$

The equality sign is valid for reversible processes, while the inequality applies for irreversible processes. Since the first three terms represents $\Delta G_{T,P}$ we can write:

$$\Delta G_{T,P} \leq W^{\#} \tag{5.37}$$

If there is only volumetric work then $W^{\#} = 0$, and consequently:

$$\Delta G_{T,P} \leq 0 \tag{5.38}$$

At equilibrium we have $\Delta G_{T,P} = 0$. On the other hand, a chemical process occurs spontaneously when $\Delta G_{T,P} < 0$.

The first and the second law of thermodynamics may be combined in the form of differential equations. Let's consider one mole of pure gaseous component in a closed system. The first law in a reversible process can be written as $dU = \delta Q_{rev} - \delta W_{rev}$. Replacing δQ_{rev} by the equation (5.26) and considering only volumetric work such as $\delta W_{rev} = PdV$ leads to:

$$dU = TdS - PdV \tag{5.39}$$

Similar expressions can be obtained by differentiating the other state functions:

$$dH = TdS + VdP \tag{5.40}$$

$$dA = -PdV - SdT \tag{5.41}$$

$$dG = VdP - SdT \tag{5.42}$$

The equations (5.39) to (5.42) are fundamental in thermodynamics, and the starting point to derive the network of thermodynamic properties.

Pressure and temperature dependency of Gibbs free energy

From the equation (5.42) at constant temperature we obtain:

$$dG = VdP \text{ or } \left(\frac{\partial G}{\partial P}\right)_T = V \tag{5.43}$$

Hence, G depends strongly on pressure for gases, but only slightly for liquids. Note that G can be obtained experimentally from volumetric measurements. In the case of an ideal gas the integration of (5.43) between P and P_0 at constant T leads to:

$$G = G^0 + RT\ln(P/1atm) \text{ (constant T)} \tag{5.44}$$

This relation can be generalised for real gases by means of the fugacity concept.
Similarly, at constant pressure but variable temperature we have:

$$dG = -SdT \quad or \quad \left(\frac{\partial G}{\partial T}\right)_P = -S \tag{5.45}$$

Therefore, phase transitions give important changes in the slope of Gibbs free energy versus temperature, because of the large entropy variation.

5.2.3 Phase equilibrium condition

Pure Components

Figure 5.4 shows the variation of the Gibbs free energy G for a pure species going from solid to liquid, and further to gas, at constant pressure but variable temperature. The reference is an ideal gas state. At phase transition the functions U, H, S change abruptly with the temperature, the slope becoming infinite. On the contrary, the Gibbs free energy has a remarkable mathematical property, being continuous everywhere. At phase transitions, the slope of the G-T curve changes significantly but remains finite.

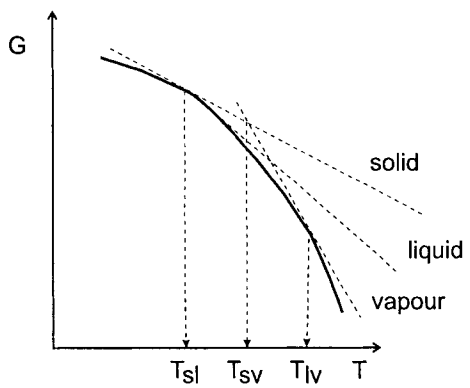

Figure 5.4 Gibbs free energy as function of temperature

The equilibrium condition for a pure species distributed between two phases α and β at the same and uniform P and T can be expressed as the equality of the Gibbs free energy in each phase:

$$[G^{\alpha} = G^{\beta}]_{P,T} \tag{5.46}$$

Equation (5.46) leads to an important thermodynamic relation that links the properties of phases at equilibrium. Assume an infinitesimal variation of temperature and pressure around the equilibrium, such as we can write $dG^{\alpha} = dG^{\beta}$. We may apply for each infinitesimal variation the equation (5.42) and obtain:

$$\frac{dP}{dT} = \frac{S^{\beta} - S^{\alpha}}{V^{\beta} - V^{\alpha}} \tag{5.47}$$

From the Gibbs free energy definition and the equilibrium condition (5.46) it is easy to found that $S^{\beta} - S^{\alpha} = (H^{\beta} - H^{\alpha})/T$. Replacing it in the relation (5.47) leads to the famous *Clapeyron equation*:

$$\frac{dP}{dT} = \frac{H^{\beta} - H^{\alpha}}{T(V^{\beta} - V^{\alpha})} \tag{5.48}$$

The relation (5.48) is valid for any phase transition. More specifically, at vapour-liquid phase transition it becomes:

$$\left(\frac{dP}{dT}\right)_{equil} = \frac{\Delta H_{vap}}{T\Delta V} \tag{5.49}$$

where $\Delta V = V^{v} - V^{l}$, V^{v} and V^{l} being the molar specific volumes of vapour and liquid. The relation (5.49) can be extended for other phase equilibria, as melting and sublimation. If the vapour is ideal $V^{v} - V^{l} \approx V^{v} = RT/P$, and the equation (5.49) leads to the *Clausius-Clapeyron equation*:

$$\frac{d\ln P}{d(1/T)} = -\frac{\Delta H_{vap}}{R} \quad \text{or} \quad \frac{d\ln P}{d(1/T)} = -\frac{\Delta H_{vap}}{R} \tag{5.50}$$

Hence, the enthalpy of vaporisation can be determined from vapour pressure data. Conversely, the vapour pressure may be estimated more accurately if the enthalpy of vaporisation is considered among experimental data. Details for estimating these two fundamental physical properties can be found in the monograph of Poling et al. (2001).

Mixtures

We can introduce a composition dependency in the analysis of any state function *U*, *H*, *A* or *G*. Thus for multi-component system the equation (5.42) may be formulated in extensive manner as:

$$d(nG) = (nV)dP - (nS)dT \tag{5.51}$$

For single-phase *closed* system without reaction we may write for an infinitesimal variation in *P* and *T*:

$$d(nG) = \left[\frac{\partial(nG)}{\partial P}\right]_{T,n} dP + \left[\frac{\partial(nG)}{\partial T}\right]_{P,n} dT \tag{5.52}$$

The comparison with the equation (5.52) leads to:

$$\left[\frac{\partial(nG)}{\partial P}\right]_{T,n} = (nV) \text{ and } \left[\frac{\partial(nG)}{\partial T}\right]_{P,n} = -(nS) \tag{5.53}$$

For single-phase *open system* the mixture composition may vary, and in consequence $nG = g(P, T, n_1, n_2, ..., n_i, ...)$. Thus, we may write the more general relation:

$$d(nG) = \left[\frac{\partial(nG)}{\partial P}\right]_{T,n} dP + \left[\frac{\partial(nG)}{\partial T}\right]_{P,n} dT + \sum_i \left[\frac{\partial(nG)}{\partial n_i}\right]_{P,T,n_j} dn_i \tag{5.54}$$

We introduce partial derivatives with the composition of the Gibbs free energy function for mixture (nG), which by definition are called *chemical potentials*:

$$\mu_i = \left[\frac{\partial(nG)}{\partial n_i}\right]_{P,T,n_j} \tag{5.55}$$

As a result, the generic relation (5.54) takes the more practical form:

$$d(nG) = (nV)dP - (nS)dT + \sum(\mu_i dn_i) \tag{5.56}$$

Equation (5.56) is fundamental for calculations regarding multi-component mixtures, which are designated in thermodynamics by *PVTx systems*. From this we can obtain the generalisation of the phase equilibrium condition as follows:

$$[\mu_i^{\alpha} = \mu_i^{\beta} = \mu_i^{\gamma} = ... = \mu_i^{\pi}]_{P,T} \tag{5.57}$$

To apply Eq. (5.57) we need *models* for chemical potentials, as function of temperature, pressure and composition. The next section presents a fundamental equation that defines a theoretical constraint for formulating such thermodynamic models.

5.2.4 Gibbs-Duhem equation

Chemical potential was introduced as a partial property of the Gibbs free energy to solve the phase equilibrium problem. Similar partial properties may be considered for other extensive properties, as volume, enthalpy, entropy, etc. It would be useful to generalise the approach. Let's consider again that M represents the mean molar value of a property. For the whole system we have $nM = f(T, P, n_1, n_2, n_3, ...)$. The derivation of the (nM) as function of T, P, and composition gives:

$$d(nM) = \left[\frac{\partial(nM)}{\partial T}\right]_{P,n} dT + \left[\frac{\partial(nM)}{\partial P}\right]_{T,n} dP + \sum \left[\frac{\partial(nM)}{\partial n_i}\right]_{P,T,n_j} dn_i \tag{5.58}$$

We may define as before a partial molar property:

$$\bar{M} = \left[\frac{\partial(nM)}{\partial n_i}\right]_{P,T,n_j} \tag{5.59}$$

The relation (5.58) can be re-written as:

$$d(nM) = n\left(\frac{\partial M}{\partial T}\right)_{P,x} dT + n\left(\frac{\partial M}{\partial P}\right)_{T,x} dP + \sum \bar{M}_i dn_i \tag{5.60}$$

Because $n_i = x_i n$, $dn_i = x_i dn + n dx_i$, and by replacing in the relations (5.60) gives:

$$ndM + Mdn = n\left(\frac{\partial M}{\partial T}\right)_{P,x} dT + n\left(\frac{\partial M}{\partial P}\right)_{T,x} dP + \sum \bar{M}_i (ndx_i + x_i dn) \tag{5.61}$$

Isolating the terms and multiplying by n and dn leads to:

$$[dM - \left(\frac{\partial M}{\partial T}\right)_{P,x} dT - \left(\frac{\partial M}{\partial P}\right)_{T,x} dP - \sum \bar{M}_i dx_i]n + [M - \sum x_i \bar{M}_i]dn = 0$$

The above equation is valid only when the both terms in brackets are zero. So we have:

$$dM - \left(\frac{\partial M}{\partial T}\right)_{P,x} dT - \left(\frac{\partial M}{\partial P}\right)_{T,x} dP - \sum \bar{M}_i dx_i = 0 \tag{5.62}$$

$$M = \sum x_i \bar{M}_i \tag{5.63}$$

The first condition is true because equivalent with (5.60). The second equation is important because states that a property of a mixture may be calculated from partial molar properties weighted by molar fractions. By differentiation we get:

$$dM = \sum x_i dM_i + \sum M_i dx_i \tag{5.64}$$

By replacing (5.64) into (5.62) leads to the relation:

$$\left(\frac{\partial M}{\partial T}\right)_{P,x} dT + \left(\frac{\partial M}{\partial P}\right)_{T,x} dP - \sum (x_i d\bar{M}_i) = 0 \tag{5.65}$$

The relation (5.65) known as *Gibbs-Duhem equation* is valid for any thermodynamic property in a homogeneous phase. At T, P constant it becomes:

$$\sum (x_i d\bar{M}_i) = 0 \tag{5.66}$$

This simplified Gibbs-Duhem equation is widely used, as for example in deriving models for liquid activity coefficients.

5.2.5 The network of thermodynamic properties

Thermodynamic state functions, as U, H, S, F, G, have the remarkable property that the variation between two states depends only on the *state-variables* (P, V, T) characterising the initial and the final state, but not on the path followed between these states, be *real* or *hypothetical*. It is said that the differential of a state functions is exact. Consider the function $z=f(x,y)$. We may write:

$$dz = \left(\frac{\partial z}{\partial x}\right)_y dx + \left(\frac{\partial z}{\partial y}\right)_x dy = Mdx + Ndy$$

The function z is an exact differential if the following relation holds:

$$\left(\frac{\partial M}{\partial y}\right)_x = \left(\frac{\partial N}{\partial x}\right)_y$$

Not only P, V, T, but also S may be considered as state variables. Useful relations between the state variables (P, V, T, S) and state functions (U, H, A, G) can be obtained from the fundamental equations (5.39) to (5.42). These are:

$$T = \left(\frac{\partial U}{\partial S}\right)_V = \left(\frac{\partial H}{\partial S}\right)_P \qquad (5.67) \qquad -P = \left(\frac{\partial U}{\partial V}\right)_S = \left(\frac{\partial H}{\partial V}\right)_T \qquad (5.68)$$

$$V = \left(\frac{\partial H}{\partial P}\right)_S = \left(\frac{\partial G}{\partial P}\right)_T \qquad (5.69) \qquad -S = \left(\frac{\partial A}{\partial T}\right)_S = \left(\frac{\partial G}{\partial T}\right)_P \qquad (5.70)$$

The derivatives of the state variables are interrelated by *Maxwell* equations as follows:

$$\left(\frac{\partial T}{\partial V}\right)_S = -\left(\frac{\partial P}{\partial S}\right)_V \qquad (5.71) \qquad \left(\frac{\partial T}{\partial P}\right)_S = -\left(\frac{\partial V}{\partial S}\right)_P \qquad (5.72)$$

$$\left(\frac{\partial P}{\partial T}\right)_V = \left(\frac{\partial S}{\partial V}\right)_T \qquad (5.73) \qquad \left(\frac{\partial V}{\partial T}\right)_P = -\left(\frac{\partial S}{\partial P}\right)_T \qquad (5.74)$$

The assembly of the fundamental equations (5.39) to (5.42) together with (5.67) to (5.70) and (5.71) to (5.74) defines the *thermodynamic network.* These relations are the starting point for finding generalised computational methods for non-measurable thermodynamic properties from other measurable properties.

For instance, let's see how to calculate the variation of enthalpy of a real fluid as function of pressure. From the fundamental equation (5.40) we have:

$$\left(\frac{\partial H}{\partial P}\right)_T = T\left(\frac{\partial S}{\partial P}\right)_T + V \qquad (5.75)$$

The derivative of entropy with pressure at constant temperature, $(\partial S / \partial P)_T$, is not available experimentally. We may replace it with $-(\partial V / \partial T)_P$, the derivative of volume with temperature at constant pressure, as justified by the equation (5.74). This may be available experimentally, or may be computed by an equation of state. Finally, the variation of enthalpy with pressure can be calculated by the relation[6]:

$$\left(\frac{\partial H}{\partial P}\right)_T = T\left(\frac{\partial S}{\partial P}\right)_T + V \qquad (5.76)$$

In this way, we can draw the isotherm curves in a property chart enthalpy-pressure.

---

[6] The reader may check that for an ideal gas the enthalpy does not depend on pressure

EXAMPLE 5.1 Enthalpy and entropy as functions of *T* and *P*

Develop a computational method for enthalpy and entropy using only PVT data and ideal gas heat capacity.

Solution. Both H and S are function of T and P as follows:

$$dH = \left(\frac{\partial H}{\partial T}\right)_P dT + \left(\frac{\partial H}{\partial P}\right)_T dP \tag{i}$$

$$dS = \left(\frac{\partial S}{\partial T}\right)_P dT + \left(\frac{\partial S}{\partial P}\right)_T dP \tag{ii}$$

The first term in equation (i) is the heat capacity at constant pressure. For the second term we may use the equation (5.76). The result is:

$$dH = C_P dT + \left[V - T\left(\frac{\partial V}{\partial T}\right)_P\right] dP \tag{iii}$$

In similar way we obtain for entropy:

$$dS = \frac{C_P}{T} dT - \left(\frac{\partial V}{\partial T}\right)_P dP \tag{iv}$$

How can we use these equations? Suppose that we want to compute the variation in enthalpy and entropy between the states (P_1, T_1) and (P_2, T_2). In both states the gas is not necessary ideal. Suppose that $P_2 >> P_1$. We may imagine two paths (Fig. 5.5):

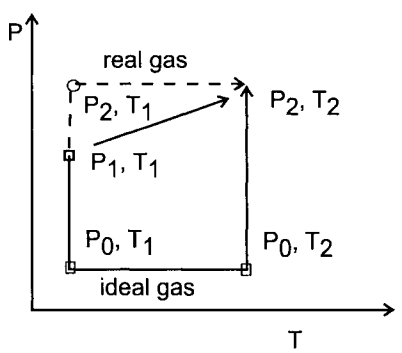

Figure 5.5 Computational paths for enthalpy and entropy

(A) Medium/high pressure $(P_1,T_1)\rightarrow(P_2,T_1)\rightarrow(P_2,T_2)$

(B) Low/high pressure $(P_1,T_1)\rightarrow(P_0,T_1)\rightarrow(P_0,T_2)\rightarrow(P_2,T_2)$

Clearly, the second path is more convenient, because the change in temperature takes place at low pressure, where the gas is ideal and accurate heat capacity is available. The computation follows the steps:

Step I: isothermal expansion to an ideal gas state, $(P_1,T_1)\rightarrow(P_0,T_1)$

$$\Delta H_1 = H_{P_0,T_1} - H_{P_1,T_1} = \int_{P_1}^{P_0} V_{T_1} dP - T_1 \int_{P_1}^{P_0} \left[\left(\frac{\partial V}{\partial T}\right)_P\right]_{T_1} dP \tag{v}$$

$$\Delta S_1 = S_{P_0,T_1} - S_{P_1,T_1} = -\int_{P_1}^{P_0} \left[\left(\frac{\partial V}{\partial T}\right)_P\right]_{T_1} dP \tag{vi}$$

Both enthalpy and entropy variations can be determined, since an equation of state can be used to describe the variation of volume with pressure at constant temperature, as well as the variation of volume with temperature at constant pressure.

Step II: isobaric heating, $(P_0,T_1)\rightarrow(P_0,T_2)$

$$\Delta H_2 = H_{P_0,T_2} - H_{P_0,T_1} = \int_{T_1}^{T_2} C_P^0(T)dT \tag{vii}$$

$$\Delta S_2 = S_{P_0,T_2} - S_{P_0,T_1} = \int_{T_1}^{T_2} \frac{C_P^0(T)}{T} dT \tag{viii}$$

Here, all we need is the ideal gas heat capacity.

Step III: isothermal compression $(P_0,T_2)\rightarrow(P_2,T_2)$. The relations are similar with step I:

$$\Delta H_3 = H_{P_2,T_2} - H_{P_0,T_2} = \int_{P_0}^{P_2} V_{T_2} dP - T_2 \int_{P_0}^{P_2} \left[\left(\frac{\partial V}{\partial T}\right)_P\right]_{T_2} dP \tag{ix}$$

$$\Delta S_3 = S_{P_2,T_2} - S_{P_0,T_2} = -\int_{P_0}^{P_2} \left[\left(\frac{\partial V}{\partial T}\right)_P\right]_{T_2} dP \tag{x}$$

This example demonstrates that reliable PVT correlation and constant-pressure heat capacity of an ideal gas are sufficient to determine a variety of thermodynamic properties, as enthalpy, entropy, Gibbs free energy, etc., and built comprehensive charts. This approach will be extended by means of departure functions.

5.3 FUGACITY

5.3.1 Definition

The fugacity concept was introduced initially to account for the non-ideal behaviour of real gases. Later the concept was generalised to phase equilibrium calculation. Let us go back to the equation describing the variation of Gibbs energy with the pressure at constant temperature $dG = VdP$. For an ideal gas we have $dG^{ig} = V^{ig}dP = \frac{RT}{P}dP$, from which it follows:

$$dG^{ig} = RTd\ln P \tag{5.77}$$

The equation (5.77) suggests similar relation for a real fluid, but where the pressure would be substituted by a more general property. Thus, by definition we may link the variation of Gibbs free energy with a thermodynamic property of a real fluid, called *fugacity* f, by the following differential equation:

$$dG = RTd\ln f \tag{5.78}$$

It may be observed that fugacity has the meaning of a real pressure that a fluid would have when obeying different thermodynamic changes. Fugacity is in general different from the external (measurable) pressure. The reference state is 1 atm, where Gibbs free energy is function only of temperature $G^0(T)$. The integration between the state of a real fluid and the reference state leads to the expression:

$$G(T,P) = G^0(T) + RT\ln(f/1\,atm) \tag{5.79}$$

Note that equation (5.79) applies equally to gases, liquids and solids.

A better perception of the fugacity concept can be obtained by relating it to pressure. Thus, by subtracting the equations (5.77) and (5.78) leads to the expression:

$$d(G - G^{ig}) = dG^R = RTd\ln(f/P) = RTd\ln\phi \tag{5.80}$$

At this point we may introduce an important class of thermodynamic functions called *residual* or *departure functions*. In this case, the *residual Gibbs free energy* may be defined as:

$$G^R(T,P) = G(T,P) - G^{ig}(T,P) \tag{5.81}$$

Further, we may introduce the *fugacity coefficient* ϕ, defined by:

$$\phi = \frac{f}{P} \tag{5.82}$$

Note that at low pressures $f = P$ or $\phi = 1$.

Another interpretation of fugacity may come by integrating the relation (5.80) between a state of an ideal gas, where G^R=0 and $\phi = 1$, and a real state. The result is:

$$\frac{G^R}{RT} = \ln \phi \tag{5.83}$$

Hence, the fugacity coefficient may be seen as a measure of the residual Gibbs free energy. It is also interesting to note that the equation (5.83) shows how to compute a non-measurable thermodynamic function, as Gibbs free energy, via an indirect measurable physical property, as fugacity. In fact, the opposite is used in practice. By appropriate modelling of G^R the fugacity may be calculated in various conditions of temperature and pressure, reducing considerably the experiments.

The above concepts can be applied to mixtures. Thus, we may define the fugacity $\hat{f}_i$ of a component in a mixture by the equation:

$$d\mu_i = d\overline{G}_i = RTd\ln \hat{f}_i \quad \text{(constant T)} \tag{5.84}$$

This time μ_i designates the chemical potential of the component *i*, identical with the partial Gibbs free energy $\overline{G}_i$. The circumflex sign emphasises that $\hat{f}_i$ is a property in a mixture, but not a partial property. The corresponding equation for an ideal gas is:

$$d\mu_i^{ig} = d\overline{G}_i^{ig} = RTd\ln(Py_i) \quad \text{(constant T)} \tag{5.85}$$

Hence, we may define a *fugacity coefficient in a mixture* as:

$$\hat{\phi}_i = \frac{\hat{f}_i}{y_i P} \tag{5.86}$$

The combination of the equations (5.84) and (5.86) gives the relation:

$$\ln \hat{\phi}_i = (\overline{G}_i - \overline{G}_i^{ig})/RT = \overline{G}_i^R / RT \tag{5.87}$$

It can be observed that now the quantity ($\ln \hat{\phi}_i$) is a partial property. Therefore, we may write the following relations:

$$\ln \hat{\phi}_i = \left[\frac{\partial(n \ln \phi)}{\partial n_i}\right]_{P,T} \tag{5.88}$$

$$\ln \phi = \sum x_i \ln \hat{\phi}_i \quad \text{(constant } P,T\text{)} \tag{5.89}$$

$$\sum x_i d\ln \hat{\phi}_i = 0 \quad \text{(constant } P,T\text{)} \tag{5.90}$$

The Eq. (5.90) is a form of the Gibbs-Duhem equation with $\ln \hat{\phi}_i$ as partial property.

Fugacity is a thermodynamic property intensively used in chemical engineering, the most important being chemical equilibrium of gases at high pressures, and vapour-liquid equilibrium. The first subject is not covered here, but second topic will be discussed in detail in Chapter 6. Therefore, the problem is how to calculate fugacities

from direct measurable quantities, as pressure, volume, temperature and composition. This problem is analysed in the next section.

5.3.2 Computation of fugacity

Pure components

Consider a process at a constant temperature. From the equations (5.78) and (5.43) we may formulate the following relation for Gibbs free energy:

$$dG = RTd\ln f = VdP \tag{5.91}$$

By adding and subtracting $RT\,d\ln P$ we get:

$$RTd\ln\frac{f}{P} = \left(V - \frac{RT}{P}\right)dP = d(G - G^{ig}) \tag{5.92}$$

The integration between zero pressure (ideal gas) and actual pressure leads to:

$$RT\ln\frac{f}{P} = \int_o^P \left(V - \frac{RT}{P}\right)dP = G - G^{ig} \tag{5.93}$$

An immediate result is that the fugacity can be computed with any PVT relationship. Replacing $Z=PV/RT$ in (5.93) leads to a formulation based on compressibility:

$$ln\phi = \int_o^P (Z-1)\frac{dP}{P} \tag{5.94}$$

Changing the integration variable in equation (5.93) from P to V gives another useful expression for practical calculations:

$$\ln\frac{f(T,P)}{P} = \ln\phi = \frac{1}{RT}\int_{V=\infty}^{V=ZRT/P}\left[\frac{RT}{V} - P\right]dV - \ln Z + (Z-1) \tag{5.95}$$

It is interesting to examine the fugacity dependency with pressure and temperature. From the definition, one gets:

$$RT\left(\frac{\partial \ln f}{\partial P}\right)_T = \left(\frac{\partial G}{\partial P}\right)_T = V \tag{5.96}$$

Consequently, the pressure dependency of fugacity is much higher for a gas than for a liquid, because the difference in phase volumes.

The variation of fugacity with the temperature can be found by examining the derivative of the equation (5.93):

$$\frac{\partial}{\partial T}(\ln\frac{f}{P})_P = \frac{\partial}{\partial T}\left[\frac{G - G^{ig}}{RT}\right] \tag{5.97}$$

Taking into account that $G = H - TS$ and $(\partial G / \partial T)_P = -S$ we obtain:

$$\frac{\partial}{\partial T}(\ln \frac{f}{P})_P = \left[\frac{H - H^{ig}}{RT^2} \right] \tag{5.98}$$

Note the similarity between the relation (5.98) and the Clausius-Clapeyron equation.

1. *Gases*

The basic relation is the equation (5.95), rewritten in this case as:

$$\ln \frac{f^V(T,P)}{P} = \ln \phi = \frac{1}{RT} \int_{V=\infty}^{V=Z^V RT/P} \left[\frac{RT}{V} - P \right] dV - \ln Z^V + (Z^V - 1)$$

For an *ideal gas* $Z^V = 1$ and $f^V(T,P) = P$. Hence, we find again that at low pressure the fugacity of a pure species is just the total pressure.

At moderate pressures we may consider the *Virial* EOS. Using the form with the second coefficient $Z = 1 + B(T)/V$, leads to the following simple expression:

$$\ln \phi = \frac{BP}{RT} \tag{5.99}$$

The computation of the second virial coefficient B can follow different ways. Here we illustrate the use of three-parameter corresponding states law. The following equations can be conveniently represent the behaviour of non-polar molecules:

$$\frac{BP_c}{RT_c} = B^{(0)} + \omega B^{(1)} \tag{5.100}$$

with

$$B^{(0)} = 0.063 - \frac{0.422}{T_r^{1.6}} \quad ; \quad B^{(1)} = 0.139 - \frac{0.172}{T_r^{1.2}} \tag{5.101}$$

Similar relations have been proposed for polar molecules (Poling et al., 2001). At higher pressure, the use of a cubic EOS is recommended. PR-EOS gives:

$$\begin{aligned} \ln \frac{f^V}{P} &= (Z^V - 1) - \ln(Z^V - \frac{bP}{RT}) - \frac{a}{2\sqrt{2}bRT} \ln \left[\frac{Z^V + (1+\sqrt{2})bP/RT}{Z^V + (1-\sqrt{2})bP/RT} \right] = \\ &= (Z^V - 1) - \ln(Z^V - B) - \frac{A}{2\sqrt{2}B} \ln \left[\frac{Z^V + (1+\sqrt{2})B}{Z^V + (1-\sqrt{2})B} \right] \end{aligned} \tag{5.102}$$

where the EOS parameters are $A = \frac{aP}{(RT)^2}; B = \frac{bP}{RT}$.

EXAMPLE 5.2 Fugacity of a pure gas

Calculate the fugacity of CO_2 at 37.7 °C and 13.8 bar with the following methods: (a) from experimental pressure-volume data (Kyle, 1999), (b) from a graphical correlation, (c) with a cubic EOS, and (d) with Virial EOS. The experimental data are:

P, (kPa)	689.5	68.95	137.9	275.8	551.6	827.4	1103.2	1379.0
V, (m^3/mol)	0.375181	0.037381	0.018616	0.009237	0.004551	0.002988	0.002206	0.001751

Solution.

a) The evaluation of the integral $\int_0^P (V - \frac{RT}{P})dP$ leads to the values $\ln(f/P) = -0.0692$, $f/P = 0.93314$ and $f = 12.85$ bar. Note that the deviation between the calculated fugacity and measured pressure is about 1 bar.

b) For CO_2 we know $T_c = 304.2$ K, $P_c = 72.9$ bar, $\omega = 0.239$. It follows $T_r = 1.023$ and $P_r = 0.1866$. From Fig. 3.1 from Reid et al. (1987) we find $f/P = 0.955$ and $f = 13.22$

c) Using our program (Dimian and Groenendijk, 1994) gives $f/P = 0.935$ and $f = 12.95$ bar with PR-EOS. The same result is obtained with SRK-EOS. The agreement of prediction by calculation with the experiment is excellent. Note that the solution of the equation (5.102) is possible with a spreadsheet.

d) With $T_r = 1.023$, $P_r = 0.1866$, $\omega = 0.239$ we obtain from (5.102) and (5.103):
$B^{(0)} = -0.34392$, $B^{(1)} = -0.02837$ and $BP_c/(RT_c) = \theta = -0.3507$
From $Z = 1 + BP/RT = 1 + \theta(P_r/T_r) = 0.936$ one gets $f = 12.86$ bar.

The results indicate close values between experimental data and different models based on equation of states. However, the pressure is moderate. At higher pressure the comparison could change, and probably the Virial EOS would show larger deviation.

2. *Liquids*

The fugacity of a pure liquid component is close, but not identical, to its vapour pressure. By assuming the liquid incompressible, by combining the equations (5.43) and (5.79), and by integrating at constant temperature between the saturation pressure P^{sat} and the system pressure P, gives the relation:

$$RT \ln \frac{f^L}{f^{L,sat}} = V^L (P - P^{sat}) \qquad (5.103)$$

V^L is the liquid molar volume that may be taken equal with the liquid volume in saturation conditions at P^{sat}. Replacing $f^{L,sat} = \phi^{sat} P^{sat}$ leads to following equation:

$$f^L = \phi^{sat} P^{sat} \exp \frac{V^L (P - P^{sat})}{RT} \tag{5.104}$$

The exponential term gives the influence of pressure on liquid fugacity being known as *Poynting correction*. At moderate pressures the Poynting correction is negligible. Therefore, the fugacity of a liquid is practically independent on pressure but strongly dependent on temperature.

At equilibrium the component fugacities in liquid and vapour phases must be equal:

$$f^L = f^V \tag{5.105}$$

It is important to note that in calculating fugacity coefficients with a cubic EOS the same expression holds for both vapour and condensed phase.

EXAMPLE 5.3 Phase equilibrium from fugacity computation

Find the equilibrium temperature for propane at 10 bar. Use PR-EOS.

Solution. Because we deal with a pure component the equilibrium is reached when the fugacity coefficients in each phase are equal $\phi^V = \phi^L$. The computation is presented graphically in Fig. 5.6. The equilibrium temperature is of 27.2 °C. The vapour fugacity shows little variation with the temperature. However, the fugacity coefficient is far from one; the non-ideality is obvious. On the contrary, the fugacity of the liquid varies strongly with the temperature, similarly with the vapour pressure.

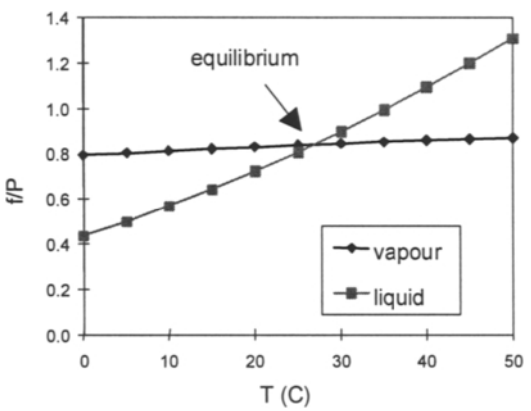

Figure 5.6 Liquid and vapour fugacity for propane

Mixtures

The computation of component fugacity in a mixture follows the same conceptual path as for pure species, but with a notable difference: there is necessary to account for the influence of composition. This aspect is taken into consideration by means of *mixing rules* for the parameters entering in the equation of state model. The approach will be illustrated in this section with Virial and cubic EOS. Chapter 6 contains more material about this topic, of greatest importance in phase equilibria.

If the equation of state is explicit in pressure, the computation of component fugacity coefficient in mixture is based on the expression:

$$RT \ln \hat{\phi}_i = -\int_{\infty}^{V^*} \left[\left(\frac{\partial P}{\partial n_i} \right)_{T,V^*,n_j} - \frac{RT}{V^*} \right] dV^* - RT \ln Z \tag{5.106}$$

where V^* denote the total mixture volume. If the equation of state is explicit in compressibility, then the following relation may be applied:

$$\ln \hat{\phi}_i = \int_0^P (\bar{Z}_i - 1) \frac{dP}{P} \tag{5.107}$$

As first example we will illustrate the application of mixing rules with the Virial EOS. If only the second term is kept, then we may write $Z = 1 + B_m(T)/V$, exactly as for a pure component. However, this time the coefficient B_m is function of temperature as well as of composition. It can be demonstrated by statistical mechanics that the following mixing rule applies:

$$B_m = \sum_i \sum_j y_i y_j B_{ij} \tag{5.108}$$

where y_i designate the molar composition. The computation of B_m implies virial coefficients B_{ij} characterising bimolecular interactions. It can be demonstrated that the fugacity coefficients of components can be related with the virial coefficients by the relation (Smith, van Ness, 1997):

$$\ln \hat{\phi}_i = \frac{P}{RT} \left[\frac{\partial (nB)}{\partial n_i} \right]_{T,n_j} \tag{5.109}$$

and finally computed with the equation:

$$\ln \hat{\phi}_i = \frac{P}{RT} \left[2 \sum_j y_j B_{ij} - B_m \right] \tag{5.110}$$

The equation (5.110) involves pure-species values B_{ii} and B_{jj}, as well as cross coefficients B_{ij}. These can be calculated from pure component data, but incorporates also binary interaction parameters k_{ij}. Details can be found in Poling et al. (2001).

The second application presents the common mixing rules used with a cubic EOS, called also *geometric* or *one-fluid van der Waals mixing rules*. The parameters a and b are averaged with the composition in the following manner:

$$a = \sum\sum x_i x_j a_{ij} \quad \text{with } a_{ij} = (1-k_{ij})\sqrt{a_{ii}a_{jj}} \tag{5.111}$$

$$b = \sum x_i b_i \tag{5.112}$$

It is important to note that the above formulas contain *interaction parameters* k_{ij} that account for the non-ideal behaviour of the mixture. The parameters k_{ij} can be determined by regression of experimental data, as shown in Chapter 6. As illustration, we present the result of integrating the equation (5.107) with PR-EOS model by using the geometric mixing rules (5.111). The component fugacity coefficient is:

$$\ln\frac{f_i^V}{y_i P} = \frac{B_i}{B}(Z^V - 1) - \ln(Z^V - \frac{bP}{RT}) - \frac{a}{2\sqrt{2}bRT}\left[\frac{2\sum_j y_j A_{ij}}{A} - \frac{B_i}{B}\right]\ln\left[\frac{Z^V + (1+\sqrt{2})bP/RT}{Z^V + (1-\sqrt{2})bP/RT}\right] \tag{5.113}$$

Note that the parameters a and b are dimensionless: $A = aP/(RT)^2$ and $B = bP/RT$. The same formula is valid for the fugacity in a liquid mixture, with the difference that fugacity coefficient is $\ln(f_i^L / x_i P)$ and compressibility factor is Z^L.

The above geometric mixing rules do not have a theoretical basis. However, they are suitable for applications involving hydrocarbons where the components are of comparable size, but not accurate enough for mixtures with strong non-ideal behaviour. More complex mixing rules, as well as predictive methods for non-ideality with EOS models will be presented in the Chapter 6.

EXAMPLE 5.4 Fugacity of components in a mixture

Consider an equimolar mixture of propane(1) / n-butane (2) at 10 bar. Find bubble-point and dew-point temperatures, and the corresponding phase compositions. Use PR-EOS neglecting the interaction parameters.

Solution. The equilibrium condition is the equality of the fugacity of each component in vapour and liquid phases. In addition, we consider the constraints of phase composition. The equations are:

$$y_1 P\hat{\phi}_1^v = x_1 P\hat{\phi}_1^l \tag{i}$$

$$y_2 P\hat{\phi}_2^v = x_2 P\hat{\phi}_2^l \tag{ii}$$

$$y_1 + y_2 = 1 \qquad \text{(iii)}$$

$$x_1 + x_2 = 1 \qquad \text{(iv)}$$

Bubble point condition is expressed by the constraint (iii), while dew point condition by the constraint (iv). By taking into account (i) and (ii) these can be written as:

$$\frac{\hat{\phi}_1^l}{\hat{\phi}_1^v} x_1 + \frac{\hat{\phi}_2^l}{\hat{\phi}_2^v} x_2 - 1 = 0 \qquad \text{(v)}$$

or

$$\frac{\hat{\phi}_1^v}{\hat{\phi}_1^l} y_1 + \frac{\hat{\phi}_2^v}{\hat{\phi}_2^l} y_2 - 1 = 0 \qquad \text{(vi)}$$

Note that the fugacity coefficient is a function of temperature, pressure and phase composition, $\hat{\phi}_i^* = (T, P, x_i \vee y_i)$. Consequently, the determination of the equilibrium temperature implies an iterative solution of the equations (v) or (vi). In this case the fugacity coefficients are computed with the relation (5.113). Results are given below. Note the differences in the variation of fugacities for vapour and liquid. As before, the temperature affects more the liquid than the vapour. The concentration has here only a slight influence, but for other systems it could be different.

	T, °C	$\hat{\phi}_1^v$	$\hat{\phi}_2^v$	$\hat{\phi}_1^l$	$\hat{\phi}_2^l$	x_1	y_1
Bubble point	47.2	0.873	0.784	1.274	0.427	0.500	0.736
Dew point	59.5	0.886	0.806	1.550	0.565	0.286	0.500

5.4 EQUATIONS OF STATE

5.4.1 Virial family of equations of state

The standard form of the Virial EOS formulates the compressibility as an infinite series of the inverse molar volume or pressure, as shown by the equations (5.3) and (5.4). In the low-pressure region, up to 15 bar, Virial EOS is the most accurate. The formulation known as 'second virial coefficient' is sufficient for technical computations. Virial EOS is able to handle a variety of chemical classes, including polar species. Hayden and O'Connell have proposed one of the best correlations for the second virial parameter[7]. The method is predictive, because considers only physical data, as dipole moment, critical temperature, critical pressure, and the degree of association between the interacting components. Usually Virial EOS it is an option to describe the vapour phase

[7] Hayden J. G., O'Connell, Ind. Eng. Chem. Proc. Des. Dev. **14**, 209, 1975

non-ideality with liquid activity coefficient models. It gives good results up to 20-30 bar.

The original Virial EOS was applicable only to the gas phase. This limitation incited the development of *extended forms*, as the *Benedict-Webb-Rubin* (BWR) correlation (equation 5.5). This equation may contain sophisticated terms with a large number of parameters, mostly between 10 and 20, and need substantial experimental data for tuning. The extended Virial-type EOS's have lost much of their interest after the arrival of various cubic EOS in the last decades. Some formulations are still used for special applications, notably in gas processing and liquefaction, as *BWR-Lee-Starling* (BWR-LS) equation[8], one of the most accurate for hydrogen rich hydrocarbon mixtures. Note that extended Virial EOS may calculate not only volumetric properties, but also VLE.

One of the most interesting applications in this class is the method of *Lee-Kesler* (LK). The compressibility factor is described by three-parameter corresponding states correlation of the form:

$$Z = Z^{(0)} + (Z^{(r)} - Z^{(0)})\frac{\omega}{\omega^{(r)}} \tag{5.114}$$

The contributions $Z^{(0)}$ and $Z^{(r)}$ are represented by generalised functions containing as parameters the reduced temperature and pressure. These have been obtained by using a special form of the BWR-EOS. Mixture critical parameters and acentric factor are calculated by means of mixing rules, which do not have interaction parameters. Tables of values for hand calculations may be found in Reid et al. (1987). Graphical representations of contributions are presented in Perry (1997). Note that this method can be used to compute phase properties (specific volume, enthalpy, entropy) for both vapour and liquid phase. It has been accepted as accurate option for enthalpy and entropy of hydrocarbons and slightly polar components.

Lee-Kesler method has been extended to oil and petrochemical type mixtures, as for example hydrocarbons and alcohols with CO_2, H_2, CH_4 and H_2S, and it is known as *Lee-Kesler-Ploecker* (LKP)[9]. Special mixing rules are designed to describe both symmetric (non-polar) and symmetric (polar) molecules. More details can be found in Poling et al. (2001).

5.4.2 Cubic equations of state

As mentioned, cubic EOS models are often default options in flowsheeting software. The reason is that these make possible to execute most of the basic engineering calculations involving thermodynamic properties and phase equilibria with the minimum amount of data. The intensive research in this domain enlarged considerably the area of applications. Among specialised works in this field we recommend the review of Sandler (1993), as well as the monograph on equations of state edited by IUPAC Commission on Thermodynamics (2000).

---

[8] Brulé, M.R., Lin, C.T., Lee, L.L., Starling, K.E., AIChEJ, 29, 616, 1982

[9] Ploecker, V., Knapp, H., Prausnitz, J. M., Ind. Eng. Chem. Proc. Des. Dev., 17, 324, 1978

a. Hydrocarbon mixtures

The origin of the cubic equations of states goes back in history to the famous van der Waals equation (VdW EOS), which corrects the ideal gas law by an *attraction term* on pressure and a *repulsion term* on volume. Van der Waals equation is explicit in pressure and implicit (cubic) in volume. It contains two parameters, a and b, which can be expressed as function of T_C and P_C. We write it here again as:

$$(p+\frac{a}{V^2})(V-b)=RT \tag{5.115}$$

The parameters a and b, can be found from the conditions set for the critical point, as
(1) maximum pressure, and
(2) inflection point of the isotherms.
Both are expressed mathematically by the conditions:

$$\left(\frac{\partial P}{\partial V}\right)_{T_c}=\left(\frac{\partial^2 P}{\partial V^2}\right)_{T_c}=0 \tag{5.116}$$

For der original Waals EOS the parameters are only function of critical properties, such as $a=27R^2T_c^2/64P_c$ and $b=RT_c/8P_c$.

A remarkable feature of van der Waals equation is its ability to calculate with reasonable accuracy the volumes of both liquid and vapour phases at equilibrium. This property made it attractive for some technical calculations, but a real breakthrough arrived only because of computer simulation. Slightly modifications have shown a surprising capacity to be adapted to various applications.

Modified van der Waals equations of state may be written in a general manner as:

$$P=\frac{RT}{V-b}+\Delta \quad \text{with } \Delta=\frac{\theta}{V^2+\delta V+\varepsilon} \tag{5.117}$$

Table 5.1 presents the most representative cubic EOS. It should also be remembered that an important feature is the temperature dependency of parameters. Thus, the parameter a can be expressed as a product of its value at the critical point a_c, and a dimensionless correction function $\alpha(T)$, such as expressed by the equation (5.8). Table 5.2 gives more details about the temperature dependency.

It is important to note that a cubic EOS can be written as third-degree polynomial of compressibility factor:

$$Z^3+\alpha Z^2+\beta Z+\gamma=0 \tag{5.118}$$

The coefficients α, β, γ can be expressed as functions of the dimensionless parameters A and B. They depend on the particular cubic EOS, as shown in the Table 5.2.

Table 5.1 General expression for some cubic equations of state

Author	Year	θ	δ	ε	Δ
van der Waals	1873	a	0	0	$\frac{a}{V^2}$
Redlich-Kwong	1949	$a/\sqrt{T}$	b	0	$\frac{a/\sqrt{T}}{V(V+b)}$
Soave	1972	$\theta_S(T)$	b	0	$\frac{\theta_s(T)}{V(V+b)}$
Peng-Robinson	1976	$\theta_{PR}(T)$	$2b$	$-b^2$	$\frac{\theta_{PR}(T)}{V(V+b)+b(V-b)}$
Patel-Teja	1981	$\theta_{PT}(T)$	$b+c$	$-cb$	$\frac{\theta_{PT}(T)}{V(V+b)+c(V-b)}$

Table 5.2 Parameters for SRK and PR equations of state

Parameter	Soave-Redlich-Kwong	Peng-Robinson
u	1	2
w	0	-1
α	-1	$-1+B$
β	$A-B-B^2$	$A-3B^2-2B$
γ	$-AB$	$-AB+B^2+B^3$
a	$\frac{0.42748R^2T_c^2}{P_cT^{0.5}}[1+\kappa(1-T_r^{0.5})^2]$ $\kappa=0.48+1.574\omega-0.176\omega^2$	$\frac{0.45724R^2T_c^2}{P_cT^{0.5}}[1+\kappa(1-T_r^{0.5})^2]$ $\kappa=0.37464+1.54226\omega-0.26992\omega^2$
b	$\frac{0.0866RT_c}{P_c}$	$\frac{0.07780RT_c}{P_c}$

$A=aP/(RT)^2$ and $B=bP/(RT)$.

Taking into account the general formulation (5.117) the fugacity coefficients for a pure species calculated by SRK or PR EOS may be expressed by a single relation:

$$\ln\phi=(Z-1)-\ln(Z-B)+\frac{A}{B\sqrt{u^2-4w}}\ln\frac{2Z+B(u+\sqrt{u^2-4w}}{2Z+B\sqrt{u^2-4w}} \tag{5.119}$$

Note that the same expression holds for vapour and liquid phase, but Z is different.

As mentioned, a weakness of a cubic EOS consists of an inaccurate computation of liquid density. A significant improvement has been obtained by the introduction of a

new parameter c_m on volume (Peneloux[10]). Thus, for SRK EOS the volume correction is: $V^L = V^L(SRK) - c_m$. The parameter c_m may be estimated with by:

$$c_m = 0.40768(0.29441 - Z_{RA})\frac{RT_c}{P_c} \tag{5.120}$$

Z_{RA} is the Rackett compressibility factor, computed with the equation:

$$Z_{RA} = 0.29056 - 0.08775\omega \tag{5.121}$$

It is notable that the Peneloux correction does not affect phase equilibrium.

At this level it is useful to mention the Rackett method itself that is one of the most accurate to calculate liquid densities. The following a equation recommended in Reid(1987):

$$V^{l,sat} = \frac{RT_c}{P_c} Z_{RA}^{[1+(1-T_r)^{2/7}]} \tag{5.122}$$

EXAMPLE 5.5 Volumetric properties by cubic EOS

Estimate the specific volume of iso-butane at equilibrium at 300 K, where the vapour pressure is 3.704 bar. Use SRK-EOS and PR-EOS, with the Penneloux correction. Compare the computed liquid density with the estimation given by Rackett equation. The experimental values are: V^L = 105.9 cm^3/mol, V^V = 6031 cm^3/mol.

Solution. From tables, Reid et al. (1987), we find T_c = 408.2, P_c = 36.5 bar, ω = 0.183, which gives Z_{RA} = 0.27569.

a) SRK-EOS

At fixed temperature we may use a trial-and-error procedure to find the equilibrium pressure. We start with a first guess P', then we solve the cubic EOS to find Z^V and Z^L, and finally we the fugacity coefficients ϕ^V and ϕ^L. The new trial will be at the pressure $P''=P'\ \phi^L/\phi^V$. The computation proceeds by successive iterations until the ratio ϕ^L/ϕ^V is less than an acceptable error. In this case we find an equilibrium pressure of 3.704 bar, which signifies that the pressure does not influence the fugacity. At this pressure and at the temperature of 300 K the SRK-EOS equation takes the form:

---

[10] Peneloux, A., Rauzy, E., Freeze, R., Fluid Phase Eq., **8**, 7-23, 1982

$Z^3 - Z^2 + 0.09668Z - 0.0011825 = 0$. The largest and the smallest roots correspond to Z^V =0.9057 and Z^L =0.01687. These values give:

V^V = (0.9057)(83.14·300/3.706) = 6096 cm^3/mol (1.1% error);

V^L = (0.01687)(83.14·300/3.706) = 113.5 cm^3/mol (7.2% error).

The estimation is good for vapour, but poor for liquid (it could be worse!).

b) Penneloux correction
From (5.130) c_m=(0.40768)(83.14/408.2/36.5)(0.29441-0.27569)=7.1 cm^3/mol. V^L= 113.5-7.1=106.4 cm^3/mol (error 0.5%). The improvement in the estimation of the liquid specific volume is spectacular.

c) PR EOS
Applying the same procedure leads to a saturation pressure of 3.683 bar. Now we have Z^3- 0.9893Z^2 + 0.08025Z - 0.0009738 = 0, which gives Z^V =0.9015 and Z^L =0.01479. One gets V^V = 6089 cm^3/mol (1.2% error); V^L= 100.2 cm^3/mol (5.4% error). There is an improvement in estimating liquid specific volume, but the error is still not negligible.

d) Rackett
By replacing the known values in the equation (5.122) one obtains:

$$V^L = \frac{RT_c}{P_c} Z_{RA}^{[1+(1-T_r)^{2/7}]} = \frac{83.14 \times 408.2}{36.5} 0.27569^{[1+(1-0.735)^{2/7}]} = 106.15\, cm^3/mol \text{ (error 0 .2\%)}$$

---

b. Polar fluids

The first modified EOS for polar fluids have been proposed by Soave[11] (1979). The modification called SRK2-EOS consists of two adjustable parameters in the alpha function:

$$\alpha(T) = 1 + m(1 - T_r) + n(1/T_r - 1) \qquad (5.123)$$

The parameters m and n, characteristic for each pure component, can be determined by regression of experimental vapour pressure data. SRK2 EOS is very convenient for the simulation of separation processes involving hydrocarbon and highly non-ideal mixtures, including azeotropes (Dimian & Crico, 1985). The program Thermowin (Dimian & Groenendijk, 1994) contains a database of 250 pure components and a database with interaction coefficients for geometric and Vidal-Huron mixing rules. The accuracy of SRK2 EOS is typically better as an order of magnitude than the classical SRK-EOS over a broad range of chemical classes. Table 5.3 illustrates this spectacular

---

[11] Soave, G., Ind. Chem. Eng. Symp. Series, 1979, No. 56; also in Chem. Eng. Sci., 1984, 39, 357

improvement in terms of vapour pressure for some relevant components. It is also interesting that the accuracy of liquid density prediction improves too.

Table 5.4 shows the capacity of SRK2 EOS to estimate accurately the density of vapour and liquid, as well as the enthalpy of vaporisation, for a strong non-ideal component as the freon 1,1-CCl_2F_2. The agreement between predictions and experimental data is excellent.

Table 5.3 Accuracy of SRK and SRK2 EOS models (% std. dev in P_v)

	SRK2	SRK
Methane	0.187	1.741
1-butyne	1.988	44.52
Methanol	0.245	6.00
Di-methyl-amine	0.692	7.53
1,1-difluoroethane	1.544	26.36
Bromo-ethane	1.754	32.9
Water	0.682	12.88
Hydrogen	3.080	9.79
Ammonia	1.909	5.72
HCN	0.244	9.16

Table 5.4 Estimation of properties with SRK2 EOS for 1,1-CCl_2F_2 (Freon 12)

T	Computed values				Experimental values			
	P	d liq.	d. vap	Hv	P	d liq.	d. vap	Hv
°C	bar	kg/m^3	kg/m^3	kJ/kg	bar	kg/m^3	kg/m3	kJ/kg
-20	1.555	1458.2	9.36	163.5	1.56	1460	9.84	163.8
-10	2.267	1426.3	13.33	158.8	2.27	1433	12.8	160.0
0	3.198	1397.7	18.46	153.9	3.19	1389	17.7	155.0
10	4.384	1361.0	24.98	148.7	4.38	1365	23.8	150.0
20	5.863	1327.3	33.12	143.1	5.86	1331	31.5	145.0

SRK2 EOS has incited the research of other modifications of vdW EOS accurate for polar components. Thus, Strijek and Vera (1986) proposed modified formulations based on PR EOS. In the simplest modification, called PRSV[12], the factor α is still given by the equation (5.8), but the temperature dependency is:

$$\alpha^{0.5} = k_o + k_1\left(1 - T_r^{0.5}\right)(0.7 - T_r) \tag{5.124}$$

The parameter k_0 is a general function of the acentric factor ω, while k_1 is a parameter to be found by regression. The evaluation of accuracy showed an error in correlating the vapour pressure under 1%, typically between 0.2 and 0.3%. The accuracy of PRSV is by an order of magnitude better as PR EOS and the same as Antoine equation. SRK2 and PRSV are of comparable accuracy.

[12] Strijek, R., Vera, J. H., Can. J. Chem. Eng., 1986, p. 64

Another form, called *PRSV2*[13], more accurate, has three adjustable parameters k_0, k_2, k_3. The improvement in accuracy over the classical PR is even more spectacular. High accuracy in predicting vapour pressure data is an advantage when treating phase equilibrium. PRSV and PRSV2 EOS are implemented in HYSYS.

Similarly, other EOS for polar components, this time implemented in Aspen Plus, makes use of variations in the alpha function. Among these we may cite:

- Mathias and Copeman[14]

$$\alpha(T) = [1 + \kappa(1 - T_r^{0.5}) + c_2(1 - T_r^{0.5}) + c_3(1 - T_r^{0.5})]^2 \tag{5.125}$$

- Schwartzentraub, Renon, Watanasiri[15] (SR POLAR)

$$\alpha(T) = [1 + \kappa(1 - T_r^{0.5}) - (1 - T_r^{0.5})(p_1 + p_2 T_r + p_3 T_r^2)]^2 \tag{5.126}$$

The parameter κ can be computed either with SRK or PR EOS. The parameters c_2 and c_3, and p_1, p_2, p_3, respectively, must be identified from experimental data.

As mentioned, the ability of a cubic equation of state to describe accurately the physical properties and behaviour of a fluid depends both on the alpha function and the mixing rules (see Chapter 6). A discussion about the last development in commercial simulators, namely in Aspen Plus and Hysys, can be found in a recent article written by Twu, Sim and Tassone (2002).

We may conclude that there are significant advantages in using cubic EOS is simulation:

- They enable a comprehensive simulation of a problem with a minimum of input data, for both phase equilibrium and energy balance purposes.
- They can handle mixtures of various chemical species, from non-polar to very polar molecules. The mixing rules should be carefully selected.
- Cubic EOS models make possible a unified treatment of both supercritical and sub-critical components, removing the inconvenience of using Henry constants and asymmetric convention in computing K-values.

There are also some disadvantages:

- A cubic equation of state model cannot predict all the properties with equal accuracy. Usually there is a non-negligible error in estimating liquid volume, which produces also errors in computing enthalpies, frequently underestimated. More accurate methods for enthalpy and entropy are based on corresponding states correlation (Lee-Kesler).
- VLE and LLE calculations at lower pressure are by far more accurate with a liquid activity approach.

---

[13] Strijek, R., Vera, H., Can. J. Chem. Eng. 1986, p. 323

[14] Mathias, P. M., Copeman, T. W., Fluid Phase Eq., 1983, p.91

[15] Scwartzentrauber, J., Renon, H., Watanasiri, S., Chem. Eng., 1990, (March), p. 118

5.5 GENERALISED COMPUTATIONAL METHODS USING PVT RELATIONSHIP

5.5.1 Departure functions

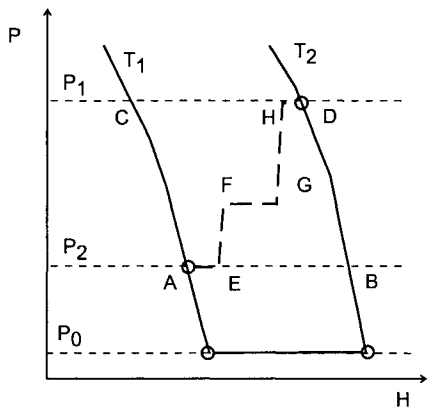

Figure 5.7 Paths for enthalpy computation

The computation of thermodynamic properties in computer simulation is based largely on generalised methods using *PVT* relationship. Let examine how we could calculate the variation of enthalpy of a fluid when going from (T_1, P_1) to (T_2, P_2). As with any thermodynamic function the variation is independent of path. There are several possibilities (Fig. 5.7). A first one could be an isothermal compression at T_1 followed by an isobaric heating at P_2 (ACD):

$$H_2 - H_1 = \int_{P_1}^{P_2} \left(\frac{\partial H}{\partial P}\right)_{T_1} dP + \int_{T_1}^{T_2} \left(\frac{\partial H}{\partial T}\right)_{P_2} dT \tag{5.127}$$

while the second could be an isobaric heating at P_1 followed by an isothermal compression at T_2 (ABD):

$$H_2 - H_1 = \int_{P_1}^{P_2} \left(\frac{\partial H}{\partial P}\right)_{T_2} dP + \int_{T_1}^{T_2} \left(\frac{\partial H}{\partial T}\right)_{P_1} dT \tag{5.128}$$

We may try another path, as AEFGHD, which includes now a phase transition. All these routes are feasible, but not practical: partial derivatives of enthalpy with pressure and temperature should be available at different isotherms or isobars. We can imagine another way by a sufficient low pressure P_0, where the gas is ideal. We may write:

$$H_2 - H_1 = \int_{P_1}^{P_0} \left(\frac{\partial H}{\partial P}\right)_{T_1} dP + \int_{T_1}^{T_2} C_p^0 dT + \int_{P_0}^{P_2} \left(\frac{\partial H}{\partial P}\right)_{T_2} dT \tag{5.129}$$

$$\Delta H = (H^0 - H_{p1})_{T_1} + \int_{T_1}^{T_2} C_p^0 dT - (H^0 - H_{p2})_{T_2} \tag{5.130}$$

The first and the third term consider the variation of enthalpy between a *real fluid*, at given P and T, and an *ideal gas state*, at the same T, but a reference pressure P_0. These may be designated by the function $(H - H^0)_{P,T}$, called the *departure enthalpy*. More generally, we may define the departure function for a property M as:

$$(M - M^0) = M(P,T) - M^{ig}(P_0,T) \tag{5.131}$$

Now we may write the equation (5.130) in a more convenient way:

$$\Delta H = \int_{T_1}^{T_2} C_p^0 dT + \{(H_{p2} - H^0)_{T_2} - (H_{p1} - H^0)_{T_1}\} \tag{5.132}$$

Hence, the enthalpy change between T_1, P_1 and T_2, P_2 may be computed from the variation for an ideal gas plus the variation of the departure function, which accounts for non-ideality. The big advantage of the departure functions is that they can be evaluated with a PVT relationship, including the corresponding states principle. Moreover, the use of departure functions leads to a unified framework of computational methods, both for thermodynamic properties and phase equilibrium.

A similar treatment may follow the concept of *residual property*. By definition, a residual property M^R is the difference between a molar value of any extensive thermodynamic property (V, U, H, S, G) of a real fluid, M, and its counterpart as an ideal fluid, M^{ig}, at the same P and T. Thus, in general we may consider:

$$M^R(P,T) = M(P,T) - M^{ig}(P,T) \tag{5.133}$$

Note that the difference between residual and departure functions comes only from the quantity $M^{ig}(P,T) - M^{ig}(P_0,T)$. Thus, residual and departure functions are identical for U and H, but slightly different for S and G. Hence, for the last function the difference is $G^R = (G - G^0) - R\ln(P/P_0)$, where P_0 is the reference pressure.

5.5.2 Evaluation of the departure functions

Consider the Helmholtz free energy. At constant temperature this can be calculated as:

$$A - A^0 = -\int_{V^0}^{V} P dV \tag{5.134}$$

Note that the reference ideal gas state is taken at the same temperature T, but at the pressure P_0, where the volume has value V^0. As previously, we may consider a path passing by a very low pressure (infinite volume):

$$A - A^0 = -\int_{\infty}^{V} P dV - \int_{V^0}^{\infty} P dV \tag{5.135}$$

Adding and subtracting $\int_{\infty}^{V}(RT/V)dV$, and replacing $P=RT/V$ in the second integral, leads to the expression:

$$A-A^0=-\int_{\infty}^{V}(P-\frac{RT}{V})dV-RT\ln\frac{V}{V^0} \tag{5.136}$$

Other departure functions come out in a straightforward manner:

$$S-S^0=-\frac{\partial}{\partial T}(A-A^0)_V=\int_{\infty}^{V}\left(\left(\frac{\partial P}{\partial T}\right)_V-\frac{R}{V}\right)dV+R\ln\frac{V}{V^0} \tag{5.137}$$

$$H-H^0=(A-A^0)+T(S-S^0)+RT(Z-1) \tag{5.138}$$

$$U-U^0=(A-A^0)+T(S-S^0) \tag{5.139}$$

$$\begin{aligned}&G-G^0=(A-A^0)+RT(Z-1)=\\&=-\int_{\infty}^{V}\left(P-\frac{RT}{V}\right)dV+RT(Z-1)-RT\ln\frac{V}{V_0}\end{aligned} \tag{5.140}$$

Note that the value of *(A-A⁰)*, *(G-G⁰)* and *(S-S⁰)* depend on the choice of the reference state V_0! Contrary, *(U-U⁰)* and *(H-H⁰)* are independent. The fugacity coefficient may be found by starting from the definition relation:

$$RTln(f/P)=G(T,P)-G^{ig}(T,P) \tag{5.141}$$

The right term is the residual Gibbs energy. Further we obtain:

$$\begin{aligned}&G(T,P)-G^{ig}(T,P)=G(T,P)-G^{ig}(T,P_0)-[G^{ig}(T,P)-G^{ig}(T,P_0)]=\\&=(G-G^0)-RT\ln\frac{p}{p^0}=\left(G-G^0\right)-RT\ln Z-RT\ln\frac{V_0}{V}\end{aligned} \tag{5.142}$$

The equations (5.131) to (5.133) and (5.127) leads to the following expression for the fugacity coefficient:

$$\ln\frac{f}{P}=-\frac{1}{RT}\int_{\infty}^{V}\left(P-\frac{RT}{V}\right)dV+(Z-1)-\ln Z \tag{5.143}$$

Equations of state

Any equation of state may be used to generate analytical expressions for residual or departure functions. In the case of PR-EOS the results for enthalpy and entropy are:

$$H(T,P)-H^0(T,P)=RT(Z-1)+\frac{T\left(\frac{da}{dT}\right)-a}{2\sqrt{2}b}\ln\left[\frac{Z+(1+\sqrt{2})B}{Z+(1-\sqrt{2})B}\right] \tag{5.144}$$

$$S(T,P)-S^0(T,P)=R\ln(Z-B)+\frac{\left(\frac{da}{dT}\right)}{2\sqrt{2}b}\ln\left[\frac{Z+(1+\sqrt{2})B}{Z+(1-\sqrt{2})B}\right] \tag{5.145}$$

$$\text{with } \frac{da}{dT}=-0.45724\frac{R^2T_c^2}{P_c}\kappa\left(\frac{\alpha}{TT_c}\right)^{1/2} \tag{5.146}$$

The equation (5.105) has already presented the result for fugacity.

Corresponding states law

Lee and *Kesler* (reference cited) found an accurate representation for compressibility of both gases and liquids by combining BWR-EOS with corresponding states law. They generated departure functions for enthalpy, entropy, fugacity coefficient and heat capacity. Tables are given in Reid et al. (1987), whereas illustrative graphs are presented in Perry (1997). The method is similar to that developed for compressibility. As an example, the enthalpy departure function may be calculated with the relation:

$$\left(\frac{H^0-H}{RT_c}\right)=\left(\frac{H^0-H}{RT_c}\right)^{(0)}+\omega\left(\frac{H^0-H}{RT_c}\right)^{(1)} \tag{5.147}$$

Lee-Kesler method is considered more accurate for enthalpy and entropy than those based on cubic EOS. It is preferred in cryogenics or gas processing.

EXAMPLE 5.6 Departure functions

Calculate values for enthalpy by departure functions for propylene at P=20 bar by means of several *PVT* methods. Compare with values available in Perry (1997).

Solution.

Table 5.5 presents values calculated with ASPEN Plus for the following quantities: vapour enthalpy H_v, liquid enthalpy H_l, enthalpy of vaporisation ΔH_{vap}, ideal gas enthalpy H^0, departure enthalpy vapour $(H\text{-}H^0)_v$, departure enthalpy liquid $(H\text{-}H^0)_l$, all in kJ/kg, as well as the boiling point T_b in °C. Several *PVT* methods have been tried: PR and SRK EOS, Virial BWR-LS, as well as Lee-Kesler (*LK*) and Lee-Kesler-Ploecker (*LKP*) method based on corresponding states principle.

In Perry (1997) both tabular and graphical values for enthalpy of propylene are available. The key property for comparison is the enthalpy of vaporisation. From tables one obtains $(\Delta H_{vap})^{tab} = 342.4$ kJ/kg. From a chart (different source) one gets a value of $(\Delta H_{vap})^{gr} \approx 357$ kJ/kg.

Table 5.5 Comparison in accuracy between different methods for enthalpy estimation*

	H_v	H_l	ΔH_{vap}	H^0	$(H-H^0)_v$	$(H-H^0)_l$	T_b, °C
PR EOS	431.9	84.1	359.7	459.8	-27.9	-375.6	19.3
SRK EOS	431.7	80.1	363.4	459.3	-27.6	-379.3	19.1
LK	436.2	123.3	323.7	461.2	-25.1	-337.9	20.3*
LKP	427.2	81.6	360.1	460.2	-33.9	-376.9	19.6
BWR-LS	428.1	85.2	357.9	459.3	-27.6	-379.2	20.9

* Phase equilibrium calculated with Grayson-Streed method

It can be seen that except *LK*, all the other methods give closed results, in good agreement with the graphical value, but not with the tabular value. The *LK* estimation seems inaccurate when compared with other estimation methods, but is more acceptable when compared with the tabular value. Two comments could be of interest:

- The computation of liquid departure enthalpy $(H-H^0)_l$ is determinant for the accuracy. Its value is typically an order of magnitude greater than the vapour departure enthalpy.
- Departure function methods are accurate to calculate thermodynamic properties.

5.5.3 Generation of thermodynamic property charts

Thermodynamic diagrams have been used for years in chemical engineering in design processes based on thermodynamic computations, as gas processing and refrigeration. These tools allow the designer to determine key properties, as enthalpy, entropy, and specific volume, and to execute by simple graphical representations some essential calculations, as adiabatic transformations. Large-scale charts are available for technical important substances as water, methane, oxygen, CO_2, NH_3, freons, etc. The most common property diagrams are:

- *T-S*: temperature/entropy
- *P-H*: pressure/enthalpy
- *H-S*: enthalpy/entropy or Mollier diagram.

Charts and tables may be found in handbooks (Perry, 1997), or in specialised publications. The tables are more accurate than small-scale diagrams[16]. All these representations have been obtained with great effort by combining experimental data and correlation methods. In the computer simulation era charts and tables might be seen as obsolete. To answer this issue we should take into account the followings:

- Thermodynamic diagrams and computer simulation have in common the same body of thermodynamic network. In other words, they are consistent at the methods' level. However, they might be different at the correlation level, namely with respect to the *PVT* representation and the available experimental data.

[16] Comprehensive tables have been published in International Tables of the Fluid State, Pergamon Press. See also the compilations of the U.S. Bureau of Standards.

- Specialised representations contain more experimental information as generic computer routines, and should be more accurate. For some technically important components, as water, the general accepted property tables are implemented as special options in process simulators[17].
- In general, the accuracy of results produced by generic computer method cannot be guaranteed. More important is the availability of accurate parameters. Over a limited range, the accuracy of computer methods can be greatly improved by tuning the parameters on experimental data. This is particularly necessary for mixtures.
- The possibility of data regression in simulation is a key feature. Consequently, the customisation of generic computer methods is a determinant advantage over traditional methods, which are fixed by the knowledge of the authors.

In conclusion, generic simulation methods can replace successfully the use of specialised charts and tables, if the accuracy is managed. By this we mean: 1) selection of the most appropriate method, 2) validation over the range of interest, and 3) calibration of parameters, if necessary. The following example illustrates the construction of property charts by means of generalised computational methods developed in this chapter.

EXAMPLE 5.7 Thermodynamic charts for R-123 with PR EOS

R-123 (2,2-dichloro-,1,1,1-trifluoroethane) is considered a more environmental friendly refrigerant. Generate property charts. Fundamental physical properties are available in Polling et al. (2001).

Solution. The data are: M_w=152.9; T_c=456.9 K; P_c=36.74 bar; V_c=278.05 m^3/kmol. Z_c=0.269, ω=0.282. The ideal gas heat capacity is:
$C_P/R = 2.996 + 39.49\times10^{-3}T - 2.743\times10^{-5}T^2$-0.122+$0.572\times10^{-11}T^4$ J/kmolK.

1) Phase equilibrium

First consider the vapour-liquid equilibrium below the critical point. The equilibrium condition is $f^v = f^l$. Temperature or pressure may be specified. Because the relation between fugacity and pressure is implicit, the solution is obtained as follows:

The compressibility Z is found by the solution of the following cubic equation:

$$Z^3 - (-1+B)Z^2 + (A - 3B^2 - 2B)Z + (-AB + B^2 + B^3) = 0 \qquad \text{(e1)}$$

with $B = \frac{bP}{RT}; A = \frac{aP}{(RT)^2}$ (e2) $a(T) = 0.45724\frac{R^2T_c^2}{P_c}\alpha(T)$; $b(T) = 0.07780\frac{RT_c}{P_c}$ (e3)

---

[17] NBS steam tables are usually available as a separate option for water.

$$[\alpha(T)]^{1/2} = 1 + \kappa(1 - \sqrt{T/T_c}) \quad \text{(e4)} \qquad \kappa = 0.37464 + 1.54226\omega - 0.26992\omega^2 \quad \text{(e5)}$$

Two real roots are obtained, the smallest for liquid, the highest for vapour. Then the fugacity coefficient (vapour or liquid) calculated by

$$\ln\frac{f^v}{P} = (Z^v - 1) - \ln(Z^v - B) - \frac{A}{2\sqrt{2}B}\ln\left[\frac{Z^v + (1+\sqrt{2})B}{Z^v + (1-\sqrt{2})B}\right] \qquad \text{(e6)}$$

2) P-V relation in the monophase region

In this region F=1+2-1=2, so T and P must be fixed. The equation (e1) has only one real root. In the ideal gas region the plot V-T is liniar.

3) Enthalpy and entropy

- Enthalpy $H = (H - H^0) + \int_{T=298.15}^{T} C_P^0 dT$
- Entropy $S = (S - S^0) + \int_{T=298.15}^{T} \frac{C_P^0}{T} dT - R\ln\frac{P}{1\,bar}$

The following diagrams have been calculated with EXCEL. The results are plotted in Fig. 5.8 to 5.10. Comparison with the data from Perry (1997) shows good agreement.

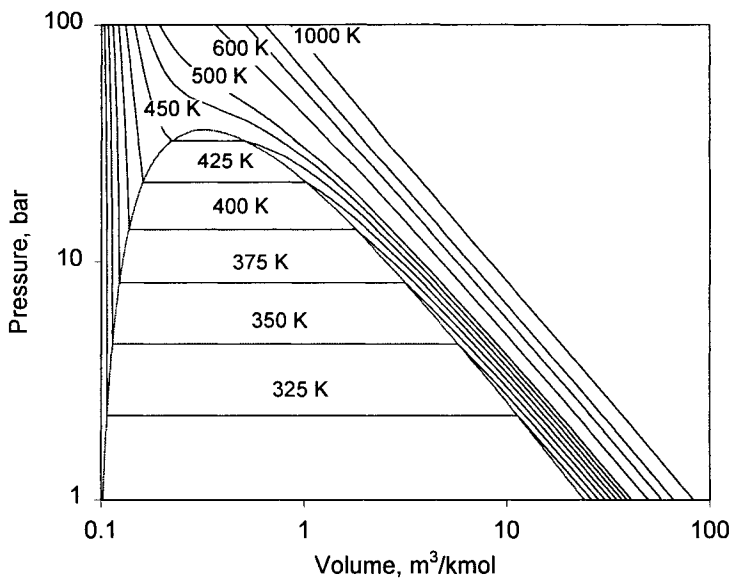

Figure 5.8 Pressure-volume chart for R-123 with PR EOS

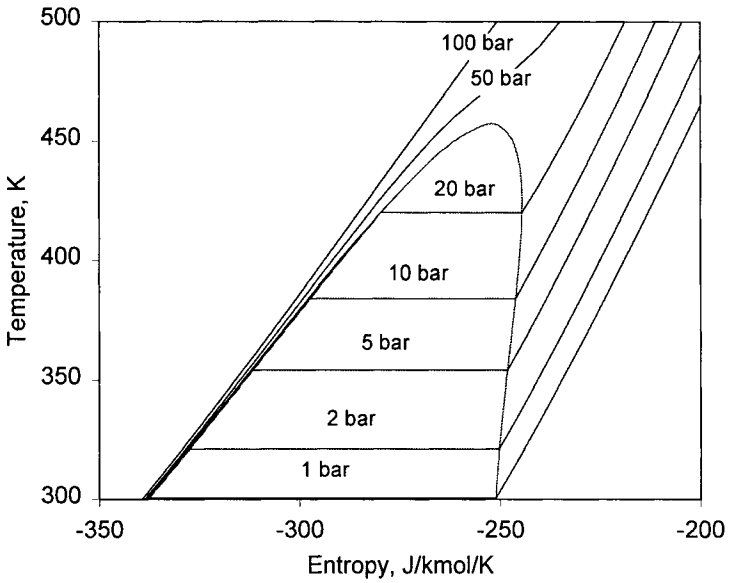

Figure 5.9 Pressure-entropy chart for R-123with PR EOS

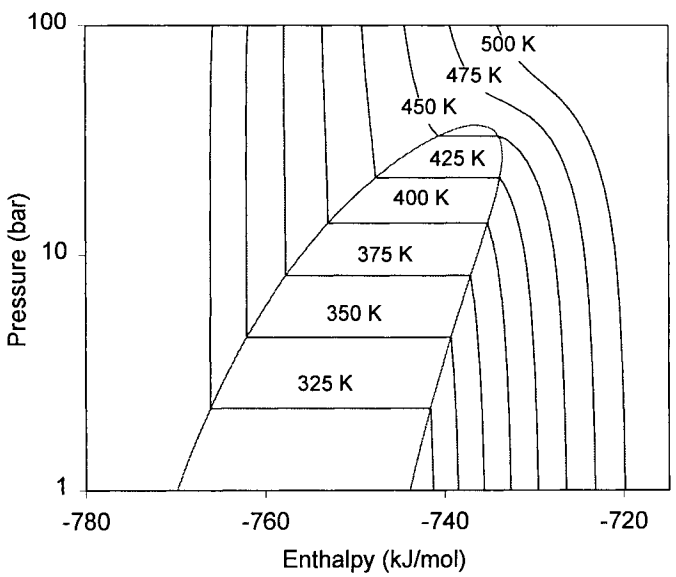

Figure 5.10 Pressure-enthalpy chart for R-123 with PR EOS

5.6 SUMMARY

This chapter reviews the fundamental concepts in thermodynamics that a user should master to obtain reliable results in simulation. The thermodynamic network (equations 5.39 to 5.42, and 5.68 to 5.74) links the fundamental thermodynamic properties of a fluid, as enthalpy, entropy, Gibbs free energy and fugacity, with the primary measurable state parameters, as temperature, pressure, volumes, concentrations. The key consequence of the thermodynamic network is that a comprehensive computation of properties is possible with a convenient *PVT* model and only a limited number of fundamental physical properties, as critical co-ordinates and ideal gas heat capacity.

Two types of *PVT* representation are used in simulation: equation of state and corresponding states principle. The equations of state are today the most applied. Particularly advantageous are the cubic equations of state, since they offer a consistent computation of both thermodynamic properties and phase equilibria. However, there is no single equation of state that could predict accurately the properties of all components, from hydrogen and methane up to polar species and polymers. That is why there are many models, each being accurate for a particular application.

Fugacity is a key concept in phase equilibria. The phase equilibrium condition consists of the equality of fugacities of a component among coexistent phases. The computation of fugacities implies two routes: equation of states, for both pure components and mixtures, and liquid activity coefficients for non-ideal liquid mixtures. The methods based on equations of state are more general.

Cubic EOS, as Soave-Redlich-Kwong and Peng-Robinson are today standard options in flowsheeting, but are suitable only for processes involving hydrocarbons. On the contrary, modified cubic EOS with several adjustable parameters can be used also for polar components. The improvement in accuracy is determined by the form of the 'alpha function that corrects the attraction term, namely by the number of parameters and their dependency on temperature. In addition, the capability of a particular EOS in calculations involving mixtures depends greatly on the 'mixing rules' applied to average the parameters by composition. Simple geometrical mixing rules can be used for hydrocarbon, but not for the treatment of non-ideal mixtures (see Chapter 6).

Generalised methods for calculating thermodynamic properties of fluids are based on the concept of 'departure functions'. A departure function designates the difference between the property of a real fluid and its counterpart as ideal fluid, at given pressure and temperature. On this basis a complete set of thermodynamic properties can be determined, as enthalpy, entropy, Gibbs free energy and fugacity. The integration of the closed-form equations for different functions makes necessary the availability of an accurate *PVT* relationship. Therefore, the generalised computer methods are competitive in accuracy with specialised tables and charts if the parameters of models have been carefully calibrated by regression.

Many thermodynamic options and routes of methods are possible when performing a simulation. Model compatibility with the physical situation, as well as the availability of parameters, should guide the user's choice.

5.7 REFERENCES

Aspen Plus, Physical Property Models and Methods, 2001, release 10.2

Dimian, A. C., A. Crico, 1985, Microcomputer software in chemical engineering, Information Chimie & Génie Chimique (F), No. 285, Novembre, p. 177-184

Dimian, A. C., A. J. Groenendijk, 1995, Thermowin - Thermodynamic Calculations Software, University of Amsterdam

Kyle, B. G., Chemical and Process Thermodynamics, 1999, McGraw-Hill, third edition

Perry, R. H., Green, D. W., Chemical Engineer's Handbook, 1997, 7th edition, McGraw-Hill

Reid, R. C., J. M. Prausnitz, B. E. Poling, 1987, 4th edition, The Properties of Gases and Liquids, McGraw-Hill

B. E. Poling, J. M. Prausnitz, J. O'Connell, 2001, 5th edition, The Properties of Gases and Liquids, McGraw-Hill

Sandler, S., 1993, Equations of State, in Models for Thermodynamics and Phase Equilibria Calculations, Marcel Dekker

Sandler, S., Chemical and Engineering Thermodynamics, 1999, third edition, Wiley

Smith, J. M., H. C. Van Ness, 1997, Introduction in Chemical Engineering Thermodynamics, 5th edition, McGraw-Hill

Twu, C. H., W. D. Sim, V. Tassone, 2002, Get handle on advanced cubic equations of state, Chem. Eng. Progress, November, p. 58-65

Chapter 6

PHASE EQUILIBRIA

6.1 Computation of vapour-liquid equilibrium
6.1.1 Ideal solution concept
6.1.2 Equation of state approach
6.1.3 Liquid activity coefficient approach

6.2 Models for liquid activity
6.2.1 Modelling excess Gibbs free energy
6.2.2 Correlation models for liquid activity
6.2.3 Predictive methods for liquid activity

6.3 Regression of parameters in thermodynamic models
6.3.1 Thermodynamic consistency
6.3.2 Methodology
6.3.3 Evaluation of models

6.4 Special topics in phase equilibrium
6.4.1 Gas-Liquid equilibrium
6.4.2 Partial miscible systems

6.5 Further reading

6.6 References

Selecting the appropriate thermodynamic model and supplying correct parameters is a key step in solving a simulation problem. The purpose of this chapter is to review the fundamentals of phase equilibria in process simulation. Modern thermodynamic methods make possible the treatment of very complex mixtures, including supercritical and subcritical components, hydrocarbons or polar species, water, etc. Such calculations are impossible by hand or even with spreadsheets. However, the user should be aware that only a good understanding of theoretical bases could ensure reliable results.

The material of this chapter is devoted mainly to vapour/liquid (VLE), vapour liquid/liquid (VLLE) and gas/liquid (GLE) equilibria of various mixtures including hydrocarbons, functional organic species, water and soluble gases. These equilibria cover the largest part of the industrial applications. Two basic approaches are presented based on liquid activity and equations of state models. Special attention is paid to the regression of interaction parameters. Phase equilibrium with electrolytes is not covered here. Similarly, we will not deal with specific methods for oil and gas processing, although some general models may be applied in these areas. Supplementary references are given at the end of the chapter.

6.1 COMPUTATION OF VAPOUR-LIQUID EQUILIBRIUM

6.1.1 Ideal solution concept

The concept of *ideal solution* signifies no interactions between molecules. The only information regards pure component properties and mixture composition. Following the *Lewis & Randall rule*, the component fugacity in an ideal solution is obtained by multiplying the pure species fugacity at given T and P by its molar fraction. Thus, for the vapour phase we may write:

$$\hat{f}_i^V = f_i^{0,V} y_i \tag{6.1}$$

Note that $\hat{f}_i^V$ and f_i^{0V} are the fugacities of the species i in mixture, and as pure component, respectively. Note the analogy with the Dalton law $p_i = P_i y_i$. Similarly, in an ideal liquid solution the component fugacity $\hat{f}_i^L$ can be found by multiplying the value as pure liquid $f_i^{0,L}$ by its molar fraction x_i:

$$\hat{f}_i^L = f_i^{0,L} x_i \tag{6.2}$$

At equilibrium the component fugacities in both phases are equal, so we may write:

$$\hat{f}_i^V = \hat{f}_i^L \tag{6.3}$$

Replacing (6.1) and (6.2) into (6.3) leads to the following expression for *ideal K-values*:

$$K_i^{id} = \frac{y_i}{x_i} = \frac{f_i^{0,L}}{f_i^{0,V}} \tag{6.4}$$

Hence, ideal K-values can be determined as the ratio of fugacity of the pure components in liquid and vapour phase, and these depend only on T and P. The result is similar with ideal mixtures defined by the Raoult-Dalton law, where $K_i = P_i / P$, P_i being the vapour pressure and P the total pressure. A notable difference is that equation (6.4) may be used at high pressures, where the fugacity concept is more suitable.

There is a substantial analogy between the concepts of ideal solutions and ideal gases. Table 6.1 presents formulas for averaging some properties. Some are additive, as volume and enthalpy, while others, as entropy and free Gibbs energy, need correction for composition. Let's examine the entropy of an ideal gas. Due to mixing the component pressure goes from the system pressure P to the partial pressure p_i. Since at constant temperature $dS_i^{ig} = -Rd\ln P$, the integration from P to p_i gives:

$S_i^{ig}(T,P) - S_i^{ig}(T,p_i) = -R\ln(P/p_i) = R\ln y_i$

As a result, for one mole of mixture the entropy is:

$$S^{ig} = \sum y_{ig} S_i^{ig}(T,p_i) = \sum y_i S_i^{ig}(T,P) - R\sum y_i \ln y_i$$

Table 6.1 Analogy between ideal gas and ideal solution

	Ideal gas	Ideal solution
Volume	$V^{ig} = \sum y_i V_i$	$V^{id} = \sum x_i V_i$
Enthalpy	$H^{ig} = \sum y_i H_i^{ig}$	$H^{id} = \sum x_i H_i^{id}$
Entropy	$S^{ig} = \sum y_i S_i^{ig} - R\sum y_i \ln y_i$	$S^{id} = \sum x_i S_i^{id} - R\sum x_i \ln x_i$
Gibbs free energy	$G^{ig} = \sum y_i G_i^{ig} + RT\sum y_i \ln y_i$	$G^{id} = \sum y_i G_i^{id} + RT\sum x_i \ln x_i$
Chemical potential	$\mu_i^{ig} = \mu_i^0 + RT\ln y_i$	$\mu_i^{id} = G_i^0 + RT\ln x_i$

6.1.2 Equation of state approach

A cubic equation of state model is capable to calculate the fugacity for both phases at equilibrium. We need a relation correlating fugacity and composition. The derivation starts by writing the variation of the chemical potential as:

$$d\hat{\mu}_i = \left(\frac{\partial V}{\partial n}\right)_{T,P,n_j} dP = RTd\ln\hat{f}_i \tag{6.5}$$

A term $RTd(\ln p_i)$ containing the partial pressure p_i may be subtracted from the both sides to account for a reference ideal state. This operation leads to the relation:

$$RTd\ln\frac{\hat{f}_i}{p_i}=\left(\frac{\partial V}{\partial n_i}\right)_{T,P,n_j}dP-RTd\ln p_i \tag{6.6}$$

We have $RTd\ln p_i = RTd\ln P + RTd\ln y_i = RTd\ln P$, because $d\ln y_i = 0$. It follows:

$$RTd\ln\frac{\hat{f}_i}{p_i}=\left[\left(\frac{\partial V}{\partial n}\right)_{T,P,n_j}-\frac{RT}{P}\right]dP \tag{6.7}$$

The inversion property of thermodynamic functions allows to change the volume variation by the pressure variation, such as:

$$\left(\frac{\partial V}{\partial n_i}\right)_{T,P,n_j}dP=-\left(\frac{\partial P}{\partial n_i}\right)_{T,V,n_j}dV \tag{6.8}$$

Further, we may introduce in analysis the fugacity coefficient. For vapour phase by definition we have $\hat{\phi}_i^V=\frac{f_i(T,P,y_i)}{Py_i}$. Combining (6.7) and (6.8) leads to the relation:

$$\ln\hat{\phi}_i^V=\frac{1}{RT}\int_V^\infty\left[\left(\frac{\partial P}{\partial N_i}\right)_{T,V,N_j}-\frac{RT}{V}\right]dV-\ln Z^V \tag{6.9}$$

Similarly, one gets for the liquid phase

$$\ln\hat{\phi}_i^L=\frac{1}{RT}\int_V^\infty\left[\left(\frac{\partial P}{\partial N_i}\right)_{T,V,N_j}-\frac{RT}{V}\right]dV-\ln Z^L \tag{6.10}$$

The above equations require the knowledge of pressure dependency on composition via mixing rules.

Replacing the fugacity coefficients in the condition (6.3) leads to the relation:

$$\hat{\phi}_i^V y_i P=\hat{\phi}_i^L x_i P \tag{6.11}$$

from which the calculation of real *K*-values is straightforward:

$$K_i=\frac{y_i}{x_i}=\frac{\hat{\phi}_i^L}{\hat{\phi}_i^V} \tag{6.12}$$

Hence calculating *K*-values with an EOS model consists of determining the ratio of the fugacity coefficients. The essential difference with the equation (6.4) is that besides *T* and P the fugacity coefficients incorporate the effect of composition.

The EOS method, particularly when using cubic EOS's, gives very good results for the most hydrocarbon systems, especially at medium and high pressures. It can be extended to polar components by using modified EOS's with appropriate mixing rules.

Mixing rules

Mixing rules are relations used to calculate mean values for the parameters of an equation of state from pure component values and mixture composition. Note that the accuracy of predictions for pure component properties is a necessary but not sufficient condition for the accuracy for mixture properties. Equally important is the type of mixing rules, as well as the quality of the *interaction parameters* used in these relations.

This section continues the discussion from Chapter 5. We presented simple geometric mixing rules for cubic EOS. With more than one adjustable parameter and temperature dependency, these mixing rules could handle also some non-ideal mixtures. As example, the following relations are implemented in ASPEN Plus with the option SR-POLAR (Schwartzentruber and Renon[1], 1989):

$$a_m = \sum_i \sum_j x_i x_j (a_i a_j)^{0.5} [1 - k_{aij} - l_{ij}(x_i - x_j)] \tag{6.13}$$

$$b_m = \sum_i \sum_j x_i x_j \frac{b_i + b_j}{2} (1 - k_{bij}) \tag{6.14}$$

However, modern mixing rules for high non-ideal mixtures are founded on a more rigorous approach. Huron and Vidal[2] (1979) obtained the first significant advance by making use of excess Gibbs free energy. The starting point is the following equality:

Excess Gibbs free energy of mixing calculated with EOS approach =
Excess Gibbs free energy of mixing from activity coefficient model

High-dense phase should be considered to make compatible the two models, in other words infinite pressure. The above condition becomes:

$$G^{ex}_{EOS}(T, P = \infty, x_i) = G^{ex}(T, P = \infty, x_i) \tag{6.15}$$

The basic assumption is that G^{ex} may be replaced by the Helmholtz free energy A^{ex}, such that we may write:

$$G^{ex} = A^{ex} + PV^{ex} \cong A^{ex} \tag{6.16}$$

where V^{ex} is the excess volume. Since for a liquid phase A^{ex} is practically independent of pressure it follows that V^{ex}=0, and further:

$$V^{ex} = V - \sum x_i V_i = b - \sum x_i b_i = 0 \tag{6.17}$$

---

[1] Schwartzentruber, J., H. Renon, Fluid Phase Eq., 52,127-134, 1989

[2] Huron, M.J., J. Vidal, Fluid Phase Equil., 3,255-271, 1979

From (6.17) we can obtain a mixing rule for the parameter b_m as:

$$b_m = \sum x_i b_i \tag{6.18}$$

Note that equation (6.18) is identical with one-fluid van der Waals mixing rule presented in Chapter 5. Further, a mixing rule for the parameter a_m is obtained by solving the equation (6.15), leading finally to the following relation:

$$\frac{a_m}{RTb_m} = \sum x_i \frac{a_i}{RTb_i} - \frac{G^{ex}}{CRT} \tag{6.19}$$

It is important to note that in the equation (6.19) G^{ex} is excess Gibbs free energy. This function can be calculated accurately by means of liquid activity models. C is a constant depending on the particular type of EOS. Note also that in the mixing rules of Huron & Vidal the parameters in the liquid activity model are not equal with those found at other pressures, and must be regressed again from experimental data.

Wong & Sandler (1992) reviewed the approach, and proposed more thermodynamic consistent mixing rules. Thus, the first mixing rule sets a constraint on both a and b as follows:

$$b_m - \frac{a_m}{RT} = \sum\sum x_i x_j \left(b_{ij} - \frac{a_{ij}}{RT}\right) \tag{6.20}$$

where

$$b_{ij} - \frac{a_{ij}}{RT} = \frac{1}{2}\left[\left(b_{ii} - \frac{a_{ii}}{RT}\right) + \left(b_{jj} - \frac{a_{jj}}{RT}\right)\right] \tag{6.21}$$

The second mixing rule remains unchanged, as given the equation (6.19). By combining (6.19) with (6.20) the following mixing rules are obtained:

$$\frac{a_m}{RT} = Q\frac{D}{1-D} \quad ; \quad b_m = \frac{Q}{1-D} \tag{6.22}$$

with

$$Q = \sum\sum x_i x_j \left(b_{ij} - \frac{a_{ij}}{RT}\right) \quad ; \quad D = \sum x_i \frac{a_i}{b_i RT} + \frac{G^{ex}(x_i)}{CRT} \tag{6.23}$$

This time the mixing rules proposed by Wong & Sandler can make use of the interaction parameters already identified for liquid activity models, such as no supplementary regression is needed. In this way, a huge existing experimental information can be re-used. Moreover, if UNIFAC is used to express G^{ex}, then the mixing rules of Wang & Sandler become purely predictive.

EXAMPLE 6.1 Interaction parameters for cubic equations of state

Bubble pressure found experimentally for a mixture of 50.2% CO_2 and 49.8 % n-butane at 344.2 K is 64.8 bar. Specific volume of saturated liquid is 99.13 cm^3/mol. The interaction coefficients are: O_2 (1)/n-butane (2): $k_{12} = 0.143$ for SRK and $k_{12} = 0.133$ for PR EOS. Compare bubble point pressure values estimated by the two equations of state, as well as the prediction of the liquid volume, and compare it with the value calculated by Rackett equation. The critical data are:

	T_c, K	P_c, bar	V_c	ω
CO_2	304.15	73.8	93.9	0.2373
n-butane	425.18	38.0	255	0.2008

Solution. We use our program (Dimian and Groenendijk, 1994). Bubble point pressures, equilibrium K-factors and densities are presented in Table 6.2. Values calculated using interaction coefficients are marked by star. The differences between properties with and without binary interaction parameters are considerable.

Table 6.2 Equilibrium computations with EOS model

Method	Bubble pressure bar	K_{CO_2}	K_{but}	V^V cm^3/mol	V^L cm^3/mol	% Error in V^L
SRK	64.8 *	1.552	0.443	276.9	116.9	16.9
	51.0	1.589	0.406	380.0	108.6	10.5
PR	66.13*	1.539	0.456	257.8	104.1	6.01
	52.14	1.581	0.414	361.1	97.1	-2.0

This example highlights some important aspects related to the use of EOS models.

1. Interaction parameters are essential for accurate prediction of phase equilibrium. Here SRK gives exactly the experimental bubble pressure, but PR is also accurate.

2. The improvement in K-values does not automatically ensure accuracy of other properties. In this example the estimation of liquid volume is poor for SRK, but acceptable for PR. Without interaction coefficients the prediction of the liquid volume is even better! Note that when the volumetric properties are important, as in reservoir engineering, special equation of state or mixing rules should be applied, as Teja-Sandler EOS given in Chapter 5. The same observation holds for the enthalpy of vaporisation, which could be in serious error. Another method for enthalpy/entropy computation should be used, as for example based on the principle of corresponding states.

The next example deals with an important application of EOS modelling, the calculation of a phase envelope of a natural gas mixture. Phase envelope is a thermodynamic tool intensively used in the exploration of oil and gas fields, as well as in designing pipelines for natural gas transportation.

EXAMPLE 6.1 Phase envelope of a natural gas

Construct a phase envelope for a hydrocarbon mixture with the molar composition: CH_4 - 90%; ethane - 2%; propane - 3%; n-butane - 4% , C5+ 1%. Use PR EOS.

Solution.
A phase envelope maps the equilibrium behaviour of a complex mixture in a *P-T* space at constant composition. Figure 6.1 displays the plot obtained with ASPEN Plus with curves of constant vapour fraction, from bubble (V=0) to dew points (V=1).

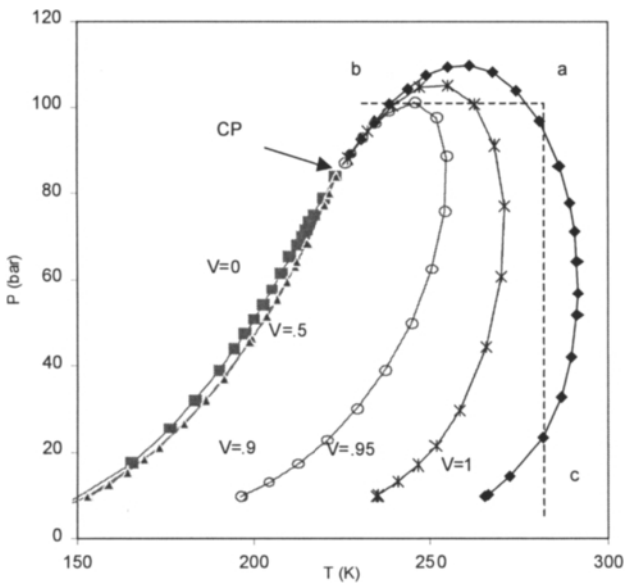

Figure 6.1 Phase envelope of a rich natural gas

The examination of the above phase envelope allows some remarks:

1. The critical point (CP) of the mixture is located at *P=83* bar and *T=220* K, much lower than the maximum pressure (cricodenbar) that is at 115 bar. There is also a maximum temperature (cricodenterm) at about 290 K.

2. The curves of constant vaporisation show large asymmetry. In the boiling region (*V*=0 to 0.5) they are practically indistinguishable. Contrary, in the condensation region (*V*=0.5 to 1) the curves span a considerable area, where large variation in temperature or pressure occurs for small amount of condensed phase.

3. Multiple states may occur. Let's consider an initial state represented by the point *a*. By lowering the temperature the dew point curve is intersected at two different pressures (segment *ab*). Firstly the gas condenses, producing a small amount of liquid, but vaporises again by lowering the temperature. A similar behaviour may be noted by

dropping the pressure (segment *ac*). On the same isotherm we may have two condensation pressures. This phenomenon, called *retrograde condensation*, is fundamental in the exploration of gas and oil.

6.1.3 Liquid activity coefficient approach

The application of the Raoult-Dalton law fails for non-ideal mixtures. An efficient method to cope with this problem is to use a correction method based on the *liquid activity coefficient*. The starting point in analysis is the equality of component fugacity in each phase, $\hat{f}_i^V = \hat{f}_i^L$. The computation of the vapour phase fugacity can follow a method based on fugacity coefficient, so we may write:

$$\hat{f}_i^V = y_i P \hat{\phi}_i^V \tag{6.24}$$

For the computation of $\hat{\phi}_i^V$ we may chose any appropriate *PVT* relationship. Beside an equation of state, as SRK or PR, the method of Hayden and O'Connell[3] (1975) based on virial EOS can be applied, which in addition could consider the association of molecules. More material about the chemical theory of VLE may be found in the book of Prausnitz et al. (1980).

For the liquid phase the computation of fugacity we can follow another route based on the concept of *liquid activity coefficient*. This is theoretically founded by the concept *of excess Gibbs energy*. G^{ex} is the difference between the actual Gibbs free energy and the value corresponding to an ideal solution, in the same conditions. Thus, by definition we have:

$$G^{ex}(T,P,x_i) = G(T,P,x_i) - G^{id}(T,P,x_i) \tag{6.25}$$

The above relation is valid for one mole of mixture. After multiplication by n (moles of mixture) and differentiation with respect to n_i, we obtain:

$$\left[\frac{\partial(nG^{ex})}{\partial n}\right]_{P,T,n_j} = \left[\frac{\partial(nG\ )}{\partial n}\right]_{P,T,n_j} - \left[\frac{\partial(nG^{id})}{\partial n}\right]_{P,T,n_j} \tag{6.26}$$

or

$$\overline{G}_i^{ex} = \overline{G}_i - \overline{G}_i^{id} \tag{6.27}$$

---

[3] Hayden, J. G., J. P. O'Connell, A Generalised Method for Predicting Second Virial Coefficients, Ind. Eng. Chem. Proc. Des., 14, 209, 1975

Here the notation $\overline{G}_i$ designates the partial Gibbs energy of the component *i* in the mixture. By definition we have $d\overline{G}_i = d\mu_i = RTd\ln\hat{f}_i$. The state of a *pure liquid* can be chosen as reference, for which $\overline{G}_i = G_i(T,P)$ and $\hat{f}_i = f_i^{0,L}$. By integrating at constant *T* and *P* between the reference state and the actual state we obtain:

$$\overline{G}_i - G_i = RT\ln\frac{\hat{f}_i}{f_i^{0,L}} \tag{6.28}$$

For an ideal solution we may apply the Lewis-Randall rule and write the fugacity as $\hat{f}_i = f_i^{0L}x_i$. It follows that:

$$\overline{G}_i^{id} - G_i = RT\ln x_i \tag{6.29}$$

By combining the equations (6.27) to (6.29) leads to the following expression for the excess Gibbs energy of a component in a mixture:

$$\overline{G}_i^{ex} = \overline{G}_i - \overline{G}_i^{id} = RT\ln\frac{\hat{f}_i}{x_i f_i^{0L}} \tag{6.30}$$

By definition, the *activity coefficient* a_i indicates the deviation of the activity of a species from its measured concentration. If molar fraction is chosen as composition variable, we may write:

$$\gamma_i = \frac{a_i}{x_i} \tag{6.31}$$

On the other hand activity may be defined by the ratio of component fugacity in the mixture to its standard-state value as pure liquid at system's *T* and *P*:

$$a_i = \frac{f_i}{f_i^{0,L}} \tag{6.32}$$

By combining (6.31) and (6.32) we obtain:

$$\gamma_i = \frac{\hat{f}_i}{x_i f_i^{0,L}} \tag{6.33}$$

Consequently, the fugacity of a component in the liquid phase may be formulated as:

$$\hat{f}_i^L = \gamma_i x_i f_i^{0,L} \tag{6.34}$$

Finally, combining the equations (6.24) and (6.34) leads to the fundamental relation:

$$y_i P\phi_i^V = \gamma_i x_i f_i^{0,L} \tag{6.35}$$

It follows that real *K*-values can be obtained by:

$$K_i = \frac{\gamma_i f_i^{0,L}}{P\phi_i^V} \tag{6.36}$$

The equation (6.36) combines the fugacity description for the vapour phase with liquid activity modelling, but needs the pure liquid fugacity f_i^{0L} as function of more accessible properties. In Chapter 5 the following relation was demonstrated:

$$f_i^{0L} = P_{s,i}\phi_{s,i}^V \int_{P_{s,i}}^{P} \frac{\overline{V}_i}{RT} dP \tag{6.37}$$

$P_{s,i}$ represents the vapour pressure at the saturation temperature T, while $\phi_{s,i}^V$ is the fugacity of the saturated vapour. For an ideal vapour $\phi_{s,i}^V = 1$. The last term is known as the *Poynting correction*. Its computation makes use of the variation of the partial molar liquid volume of the component. In many situations the Poynting correction is negligible. Therefore, at low pressures the fugacity of the pure liquid is practically the vapour pressure, $f_i^{0,L} \approx P_i$, and in consequence the equation (6.35) becomes:

$$y_i P\phi_i^V = \gamma_i x_i P_i \tag{6.38}$$

Equation (6.38) finds large applications in the simulation of separations.

The above relation show also that the accuracy of the vapour pressure is determinant in VLE calculations. A more general Antoine-type correlation can be written as:

$$\ln P_s = C_1 + \frac{C_2}{C_3 + T} + C_4 T + C_5 \ln T + C_6 T^{C_7} \tag{6.39}$$

For accurate results at least the constants C_1, C_2 and C_3 should be available.

In the case of hydrocarbon mixtures the *Chao-Seader*[4] (1961) method is often used. The fugacity coefficients may be calculated by a corresponding states formulation, as the sum of two contributions, for spherical molecule and deviation from sphericity:

$$\ln \frac{f_i^{0,L}}{P} = \ln \upsilon_i^{(0)} + \omega_i \ln \upsilon_i^{(1)} \tag{6.40}$$

$\upsilon_i^{(0)}$ and $\upsilon_i^{(1)}$ are semi-empirical functions of reduced temperature and pressure.

Excess Gibbs free energy and activity coefficients

Excess Gibbs energy and activity coefficients are linked. From the equations (6.30) and (6.33) the following fundamental relation is obtained:

$$\overline{G}_i^{ex} = RT \ln \gamma_i \tag{6.41}$$

---

[4] Chao, K,C., J. D. Seader, AIChEJ, 7, 598, 1961

Since $\overline{G}_i^{ex}$ is a partial property of G^{ex}, it follows that $\ln\gamma_i$ is also a partial property. The total excess Gibbs free energy becomes:

$$G^{ex}/RT = \sum_i x_i \ln\gamma_i \tag{6.42}$$

Hence, the total excess Gibbs energy can be easily determined from experimental values of activity coefficients, as it will be shown in the next section. Because $\ln\gamma_i$ is a partial property, the following relation may be written:

$$(\sum_i x_i d\ln\gamma_i = 0)_{P,T} \tag{6.43}$$

The relation (6.43) is a form of the Gibbs-Duhem equation. Let's examine the case of a binary mixture, for which we have:

$$x_1 d\ln\gamma_1 + x_2 d\ln\gamma_2 = 0 \tag{6.44}$$

For an infinitesimal variation dx_1 it follows:

$$x_1 \frac{d\ln\gamma_1}{dx_1} + x_2 \frac{d\ln\gamma_2}{dx_1} = 0 \tag{6.45}$$

Because $dx_1 = -dx_2$ we obtain further:

$$x_1 \frac{\partial\ln\gamma_1}{\partial x_1} = -x_2 \frac{\partial\ln\gamma_2}{\partial x_1} = x_2 \frac{\partial\ln\gamma_2}{\partial x_2} \tag{6.46}$$

Hence, the liquid activity coefficients in a binary mixture are interdependent. $\ln\gamma_1$ and $\ln\gamma_2$ have opposite slopes approaching pure component corner with zero slope.

6.2 MODELS FOR LIQUID ACTIVITY

6.2.1 Modelling excess Gibbs free energy

Let's consider some experimental data, as those presented in the Table 6.3 for the binary methyl-ethyl-ketone (1) / toluene (2) at 50°C (Smith and Van Ness, 1987). Activity coefficients may be computed with (6.38), then $\ln\gamma_1$ and $\ln\gamma_2$, and finally excess Gibbs free energy by the relation (6.42). Figure 6.4 presents the plot. A quasi-parabolic shape is obtained with maximum deviation of $0.075RT$ at $x_1 \approx 0.5$.

In a second step, we attempt to linearise the model. A suitable function is G^{ex}/RTx_1x_2. By least square fitting the following equation is obtained:

$$\frac{G^{ex}}{RT} = x_1 x_2 (0.198 x_1 + 0.372 x_2) \tag{6.47}$$

Therefore, we may assume that the following correlation model is appropriate:

$$\frac{G^{ex}}{x_1 x_2 RT} = A_{21} x_1 + A_{12} x_2 \tag{6.48}$$

Relation (6.48) is consistent because satisfies Gibbs-Duhem equation.

Table 6.3 VLE for the system MEK(1)/Toluene (2) at 50 °C

P/kPa		y_1	$\ln\gamma_1$	$\ln\gamma_2$	*Gex/RT*	*Gex/RTx₁x₂*
12.3	0	0		0	0	
15.51	0.0895	0.2716	0.266	0.009	0.032	0.389
18.61	0.1981	0.4565	0.172	0.025	0.054	0.342
21.63	0.3193	0.5934	0.108	0.049	0.068	0.312
24.01	0.4232	0.6815	0.069	0.075	0.072	0.297
25.92	0.5119	0.744	0.043	0.1	0.071	0.283
29.96	0.6996	0.805	0.023	0.127	0.063	0.265
30.12	0.7135	0.8639	0.01	0.151	0.051	0.248
31.75	0.7934	0.9048	0.003	0.173	0.038	0.234
34.15	0.9102	0.999	-0.003	0.237	0.019	0.227
36.09	1	1	0	....	0	

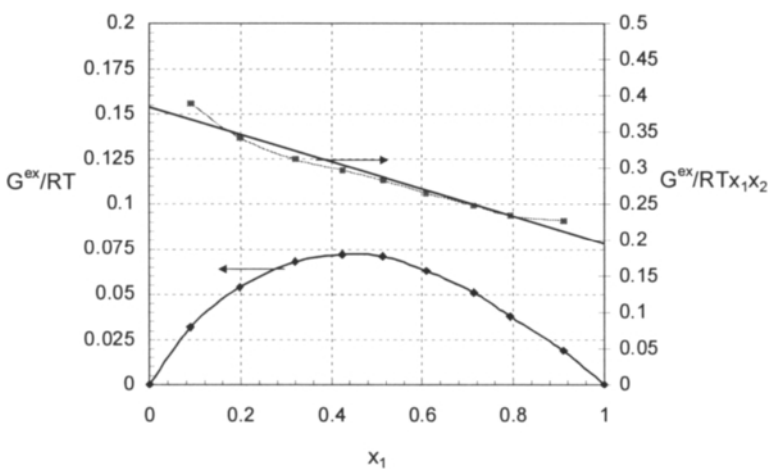

Figure 6.2 Variation of excess Gibbs free energy with composition

We may generalise the above treatment: we can use any form of functional dependency for excess Gibbs energy, if it respects de Gibbs-Duhem equation. Two

types of series expansion have proved to be the most suitable: power series and Legendre functions.

The power expansion consists of the following expression:

$$\frac{G^{ex}}{RT} = x_1 x_2 (a + bx_1 + cx_1^2 + ...) \tag{6.49}$$

An alternative form is known as Redlich-Kister expansion:

$$\frac{G^{ex}}{RT} = x_1 x_2 [A + B(x_1 - x_2) + C(x_1 - x_2)^2 + ...] \tag{6.50}$$

A direct application of the power series is the development of Margules equations. If B=C=0 then one gets a *two-suffix equation*, because G^{ex} is a second degree function:

$$\frac{G^{ex}}{RT} = Ax_1 x_2 \tag{6.51}$$

The equation (6.51) has only one constant, but it may be used for qualitative computations. If both A and B are non-zero, then one gets a *three-suffix equation*:

$$\frac{G^{ex}}{RT} = x_1 x_2 (A_{21} x_1 + A_{12} x_2) \tag{6.52}$$

There is also an accurate four-suffix formula that may be employed to test the thermodynamic consistency of VLE data.

Another expansion accurate for data correlation is:

$$\frac{G^{ex}}{RT} = x_1 x_2 [p_0 + p_1 (2x_1 - 1) + p_2 (6x_1^2 - 6x_1 + 1) + ...] \tag{6.53}$$

The terms in parenthesis are *Legendre polynomials*. Their advantage over the ordinary polynomial expansion is that the coefficients p_k are orthogonal. This means that the values of p_k found by regressing experimental data are independent of each other, and in consequence the accuracy can be adapted to the number of data points.

At this point is worthy to mention DECHEMA database (Nagata, Gmehling and Onken, 1977), as a thesaurus of interaction parameters with various liquid activity models. This database has been updated several times, and may be accessed from some software systems, as Aspen Plus.

6.2.2 Correlation models for liquid activity

Firstly we present classical models, as Margules and van Laar, traditionally used in hand-calculations. These are still applicable when the accuracy is not crucial, or for local models in dynamic simulation. Then we will discuss in more detail accurate models suited for computer simulation, as Wilson, NRTL and UNIQUAC. Here we present only formulas for binary mixtures. Extension to multi-component mixtures is given in textbooks on thermodynamics (Smith et al., 1997)

1. Margules

Margules-type correlation has been already derived before. The most used form is:

$$\ln\gamma_1 = x_2^2[A_{12} + 2(A_{21} - A_{12})x_1] \qquad \ln\gamma_2 = x_1^2[A_{21} + 2(A_{12} - A_{21})x_2] \tag{6.54}$$

Margules model can be used for both VLE and VLLE computations.

2. Van Laar

Van Laar model is simple, gives good results, and can be used for both VLE and VLLE. The model has two adjustable parameters:

$$\ln\gamma_1 = \frac{B_{12}}{[1 + (B_{12}x_1 / B_{21}x_2)]^2} \qquad \ln\gamma_2 = \frac{B_{21}}{[1 + (B_{21}x_2 / B_{12}x_1)]^2} \tag{6.55}$$

Note that van Laar allows direct calculation of binary interaction parameters from a single data, as for example the azeotropic point, where we have simply $\gamma_1 = P / P_1(T_{az})$ and $\gamma_2 = P / P_2(T_{az})$. Binary parameters can be calculated with the following equations:

$$B_{12} = \ln\gamma_1\left[1 + \frac{x_2 \ln\gamma_2}{x_1 \ln\gamma_1}\right]^2 \qquad B_{21} = \ln\gamma_2\left[1 + \frac{x_1 \ln\gamma_1}{x_2 \ln\gamma_2}\right]^2 \tag{6.56}$$

3. Wilson

Wilson[5] (1964) brought the first major contribution in the field of modern liquid activity models by developing the *local composition* concept. This is related to the segregation caused by different interaction energies between pairs of molecules. Thus, the probability of finding a species 1 surrounded by molecules of species 2, relative to the probability of being surrounded by the same species 1, is given by the expression:

$$\frac{x_{12}}{x_{11}} = \frac{x_2 \exp(-\lambda_{12} / RT)}{x_1 \exp(-\lambda_{11} / RT)} \tag{6.57}$$

The quantities λ_{12} and λ_{11} signify interaction energies between molecules. The quantity x_{12} has the meaning of a local composition. Furthermore, a local volume fraction of the component 1 can be formulated as:

$$\zeta_1 = \frac{v_{1L}x_{11}}{v_{1L}x_{11} + v_{2L}x_{12}} \tag{6.58}$$

The quantities v_{1L} and v_{2L} are the molar liquid volumes of the two components. The following relation can describe the excess Gibbs free energy:

---

[5] Wilson, G. M., Vapour-Liquid Equilibrium. XI. A new expression for the Excess Free Energy of Mixing, J. Amer. Chem. Soc. 86, 127, 1964

$$\frac{G^{ex}}{RT} = x_1 \ln\frac{\zeta_1}{x_1} + x_2 \ln\frac{\zeta_2}{x_2} \tag{6.59}$$

Binary interaction constants may be defined as:

$$\Lambda_{12} = \frac{v_{2L}}{v_{1L}} \exp\left[-\frac{(\lambda_{12}-\lambda_{11})}{RT}\right] \tag{6.60}$$

$$\Lambda_{21} = \frac{v_{1L}}{v_{2L}} \exp\left[-\frac{(\lambda_{21}-\lambda_{22})}{RT}\right] \tag{6.61}$$

The energies of interaction are $\lambda_{12} = \lambda_{21}$ but $\lambda_{11} \neq \lambda_{22}$. After substitution of (6.60-61) in (6.62) the excess Gibbs energy becomes:

$$\frac{G^{ex}}{RT} = -x_1 \ln(x_1 + \Lambda_{12}x_2) - x_2 \ln(x_2 + \Lambda_{21}x_1) \tag{6.62}$$

Finally, the following equations for the activity coefficients are obtained:

$$\ln\gamma_1 = -\ln(x_1 + x_2\Lambda_{12}) + x_2\left(\frac{\Lambda_{12}}{x_1 + x_2\Lambda_{12}} - \frac{\Lambda_{21}}{x_2 + x_1\Lambda_{21}}\right) \tag{6.63}$$

$$\ln\gamma_2 = -\ln(x_2 + x_1\Lambda_{21}) - x_1\left(\frac{\Lambda_{12}}{x_1 + x_2\Lambda_{12}} - \frac{\Lambda_{21}}{x_2 + x_1\Lambda_{21}}\right) \tag{6.64}$$

Wilson model describes very accurately the VLE of strong non-ideal mixtures, but unfortunately is not convenient for liquid/liquid equilibrium.

If infinite-dilution γ_i^{∞} data are available from chromatographic measurements, the interaction parameters can be found readily by solving the following algebraic system:

$$\ln\gamma_1^{\infty} = 1 - \ln\Lambda_{12} - \Lambda_{21} \tag{6.65}$$

$$\ln\gamma_2^{\infty} = 1 - \ln\Lambda_{21} - \Lambda_{12} \tag{6.66}$$

The interaction parameters from γ_i^{∞} may be used over the whole concentration range.

4. NRTL

NRTL (non-random two-liquids) model developed by Renon and Prausnitz[6] (1968) is an extension of the local composition concept that accounts for the non-randomness of interactions. The following expression for G^{ex} is obtained:

$$\frac{G^{ex}}{RT} = x_1x_2\left(\frac{\tau_{21}G_{21}}{x_1 + x_2G_{21}} + \frac{\tau_{12}G_{12}}{x_2 + x_1G_{12}}\right) \tag{6.67}$$

---

[6] Renon, H., Prausnitz, J. M., Local Compositions in Thermodynamic Excess Functions for Liquid Mixtures, AIChEJ, 14, 135, 1968

Quantities τ_{ij} express differences in interaction energies, $\tau_{ji} = (g_{ji} - g_{ii})/RT$. The parameters G_{ij} take into account the non-randomness of interactions such as $G_{ij} = \exp(-\alpha\tau_{ij})$. The parameter α can be treated as adjustable, although better it should be fixed. Some recommendations are:

- α=0.20 for saturated hydrocarbon with polar non-associated species;
- α =0.30 for non-polar compounds, but also for water and non-associated species;
- α =0.40 for saturated hydrocarbon and homologue per-fluorocarbons;
- α =0.47 for alcohol and other self-associated non-polar species.

Binary activity coefficients are given by the following equations:

$$\ln\gamma_1 = x_2^2\left[\frac{\tau_{21}G_{21}^2}{(x_1 + x_2G_{21})^2} + \frac{\tau_{12}G_{12}}{(x_2 + x_1G_{12})^2}\right] \tag{6.68}$$

$$\ln\gamma_2 = x_1^2\left[\frac{\tau_{12}G_{12}^2}{(x_2 + x_1G_{21})^2} + \frac{\tau_{21}G_{21}}{(x_1 + x_2G_{12})^2}\right] \tag{6.69}$$

In three parameter formulation we have to regress τ_{12}, τ_{21} and α. Even if τ_{12} and τ_{21} account implicitly for the effect of temperature, it is possible to introduce temperature dependency explicitly, as for example $\tau_{ij} = a_{ij} + b_{ij}/T$. NRTL model is somewhat sensitive in computation, but it can be used to describe very accurately both VLE and VLLE of high non-ideal mixtures.

5. UNIQUAC

UNIQUAC stands for UNIversal QUAsi-Chemical model, and has been developed by Abrams and Prausnitz (1978). Unlike Wilson and NRTL, where local volume fraction is used, in UNIQUAC the primary variable is the local surface area fraction θ_{ij}. Each molecule is characterised by two structural parameters: r, the relative number of segments of the molecule (volume parameter) and q, the relative surface area (surface parameter). Values of these parameters have been obtained in some cases by statistical mechanics. There is also a special form of UNIQUAC for systems containing alcohols, where a third surface parameter q' can increase significantly the accuracy (Prausnitz et al., 1980).

In UNIQUAC the excess Gibbs free energy is computed from two contributions. The first called *combinatorial part* represents the influence of the structural parameters, as size (parameter r) and shape (area parameter q). The second called the *residual part* account for the energy of interactions between segments. In the case of a binary mixture the expression for the excess Gibbs free energy is:

- Combinatorial part:

$$\frac{G_C^{ex}}{RT} = x_1 \ln\frac{\phi_1}{x_1} + x_2 \ln\frac{\phi_2}{x_2} + \frac{z}{2}\left(q_1x_1 \ln\frac{\theta_1}{\phi_1} + q_2x_2 \ln\frac{\theta_2}{\phi_2}\right) \tag{6.70}$$

- Residual part:

$$\frac{G_R^{ex}}{RT} = -q_1 x_1 \ln(\theta_1 + \theta_2 \tau_{21}) - q_2 x_2 \ln(\theta_2 + \theta_1 \tau_{12}) \tag{6.71}$$

The parameters in the above equations have the following significance:

- ϕ_1 - average segment fraction, $\phi_1 = \dfrac{x_1 r_1}{x_1 r_1 + x_2 r_2}$
- θ_1 - average surface area fraction, $\theta_1 = \dfrac{x_1 q_1}{x_1 q_1 + x_2 q_2}$
- τ_{ij} - binary interaction energy $\tau_{ji} = \exp\left(-\dfrac{u_{ji} - u_{ii}}{RT}\right)$
- z - lattice co-ordination number, set equal to 10.

Size and area parameters can be computed from other two quantities, van der Waals area A_W and volume V_W. This information is usually stored in the database for pure component properties. Finally, UNIQUAC has only two adjustable parameters, τ_{12} and τ_{21}, but these rise to four if temperature dependency is considered.

UNIQUAC is as accurate as Wilson's model, but it may be applied to liquid/liquid equilibrium. Despite its apparent complexity the UNIQUAC model is robust in computations.

As conclusion to this section, it is useful to mention two observations regarding the multi-component mixtures:

- Only binary interaction parameters are sufficient for accurate simulation of VLE based operations, as distillation. However, accurate simulation of LLE based operations, as liquid-liquid extraction, might need ternary data.
- The quality of the binary interaction parameters is crucial for the reliability of results. By consequence, special attention must be given to parameter regression. This aspect will be discussed in detail in a separate section.

6.2.3 Predictive methods for liquid activity

Predictive methods make possible to treat the non-ideality of a liquid mixture without the knowledge of binary interaction parameters fitted from experimental data. Obviously, the predictive should be used only for exploratory purposes. Here we present two approaches. The first one, called the *regular solution* theory, requires information only about pure components. The second one, UNIFAC, is based on group contributions, and makes use indirectly of experimental data.

1. Regular solution theory

The *regular solution* concept is based on two assumptions: molecules of equal size and no heat of mixing. Scatchard and Hildebrand (for more details see Sandler, 1999) arrived at the following simple relation for the activity coefficient:

$$\ln \gamma_{i,L} = \frac{\upsilon_{i,L}(\delta_i - \sum \Phi_i \delta_i)^2}{RT} \tag{6.72}$$

Φ_i is the volume fraction of the component *i*, which can be found from the component molar liquid volumes υ_{iL} by

$$\Phi_i = \frac{x_i \upsilon_{i,L}}{\sum x_i \upsilon_{i,L}} = \frac{x_i \upsilon_{i,L}}{V_L} \tag{6.73}$$

δ_i is called *solubility parameter* can be determined by the relation:

$$\delta_i = \left[\frac{\Delta H_i^{vap} - RT}{\upsilon_{i,L}} \right]^{1/2} \tag{6.74}$$

Hence, the key information in calculating the liquid activity is the partial volume and enthalpy of vaporisation of components ΔH_i^{vap}.

2. UNIFAC

UNIFAC is an extension of UNIQUAC, in which the interaction parameters are estimated by means of contributions of groups. Firstly, the molecules are decomposed in characteristic structures, as functional groups and subgroups. Some small molecules are considered separately for more accuracy. Then the parameters involved in UNIQUAC-type equations are determined, as follows:

- Molecular volume and area parameters in the combinatorial part are replaced by:

$$r_i = \sum_k v_k^{(i)} R_k \; ; q_i = \sum_k v_k^{(i)} Q_k \tag{6.75}$$

$v_k^{(i)}$ is the number of functional group of type *k* in the molecule *i*, while R_k, Q_k are *volume* and *area parameter*s of the functional group.

- Residual term is replaced by:

$$\ln \gamma_i^R = \sum_k v_k^{(i)} (\ln \Gamma_k - \ln \Gamma_k^{(i)}) \tag{6.76}$$

Γ_k is the residual activity coefficient of the functional group *k* in the actual mixture. $\Gamma_k^{(i)}$ is the residual activity coefficient of the functional group *k* in a reference mixture which contains only *i* molecules. The activity coefficient for the group *k* in molecule *i* depends on the molecule *i* in which the *k* group is situated. The following relation gives the activity coefficient of each group:

$$\ln \Gamma_k = Q_k \left[1 - \ln\left(\sum_m \theta_m T_{mk} \right) - \sum_m \frac{\theta_m T_{km}}{\sum_n \theta_n T_{nm}} \right] \tag{6.77}$$

θ_m is the area fraction of group m, given by the equation: $\theta_m = \dfrac{X_m Q_m}{\sum_n X_m Q_m}$

X_m is the mole fraction of group m in the solution: $X_m = \sum_i v_m^{(i)} x_j / \sum_j \sum_n (v_n^{(j)} x_j)$

There are also group interaction parameters T_{mk} expressed by the equation $T_{mk} = \exp(-\dfrac{a_{mk}}{T})$, where is $a_{mk} \neq a_{km}$ but $a_{mk} = 0$ when $m=k$.

Table 6.4 illustrates some UNIFAC groups. For example, for the *group* 1 (alcane) there are four subgroups: CH_3, CH_2, CH, C, each characterised by R_k and Q_k values. A number of polar molecules are counted as groups, as H_2O, CH_3OH, CS_2, furfural, DMF, acrylonitrile, etc.

Table 6.4 Example of UNIFAC decomposition

No. group	Group name	Sub-group	Formula	R_k	Q_k
1	CH_2 alcane	1	CH_3	.....	.....
		2	CH_2		
		3	CH		
		4	C		
2	C=C alcene	5	CH_2=CH		
5	Alcohol	15	OH		
7		17	Water		
8		18	AcOH		
	.....		.....		
47		88	$CON(Me)_2$		

For instance, ethanol CH_3-CH_2-OH can be considered as 1×sgrp_1+ 1×sgrp_2+1×sgrp_15. But if we consider the binary acetone/n-hexane, the system would behave as a mixture from the groups CH_3, CH_2 and CH_3-C=O. For an equimolar mixture acetone/n-hexane we have: 3 groups CH_3, 4 groups CH_2 and 1 group CH_3CO. It should be kept in mind that the precision of UNIFAC depends on the available experimental information used for the subsequent groups. Some remarks:

- UNIFAC is recommended only for exploratory purposes. A true liquid activity model should replace it when experimental data becomes available. Sometimes the predictions by UNIFAC are surprisingly good, when sufficient experimental data was available.
- UNIFAC is not reliable for LLE, which is more difficult for modelling than VLE. Note that VLE and LLE make use of different UNIFAC parameters.

- Modern software has built-in UNIFAC automatic decomposition algorithms. Check the availability of the UNIFAC parameters when the molecule decomposition is not obvious, or it contains less common atoms. Note also that there are several updates of UNIFAC parameters.

EXAMPLE 6.2 Prediction of phase equilibrium by UNIFAC

Examine the accuracy of estimation for VLE by UNIFAC and by other LACT methods for the following non-ideal binaries: water/1-propanol and water/acid acetic. Compare with experimental data from Perry (1997).

Solution.
Here we present results obtained with ASPEN Plus. Let's examine first the behaviour of the binary water/1-propanol at normal pressure. We select among options the model UNIFAC with ideal vapour phase. 1-propanol can be decomposed in the following subgroups: $1 \cdot CH_3 + 2 \cdot CH_2 + 1 \cdot OH$. Water is stand-alone component.
Figure 6.3a presents the result of a *Txy* analysis at constant pressure. It may be observed that UNIFAC predicts an azeotrope with the water mol fraction of 0.525 at 81.15 °C. Now, the computation is repeated by using NRTL with ideal vapour phase, drawn as full line. Note that this time the calculation makes use of binary interaction parameters stored in the internal database. The results are similar, although shifted slightly to lower temperatures. For comparison experimental values are plotted, and these are reproduced with high accuracy by NRTL. However, UNIFAC gives also good results, being able to predict correctly the azeotrope.

For the second mixture, water/acetic acid, UNIFAC predicts an azeotrope, but the comparison with experimental data reveals that the prediction is completely wrong! There is no azeotrope, although the binary shows a high non-ideal behaviour toward diluted acid solutions. We may try with Wilson, changing the option for the vapour phase to Hayden-O'Connell method. Now the estimation is very accurate (not shown). We may retry to use UNIFAC with Hayden-O'Connell. In fact, the azeotrope disappears, but the accuracy is rather modest.

This example demonstrates that UNIFAC is useful but not always accurate for design. Even with more accurate models the reliability of predictions has to be carefully examined. For instance, the analysis of the binary water/1-propanol with another set of NRTL or UNIQUAC parameters could predict immiscibility, which in fact is a false indication.

We will end this example with a recommendation: when checking high non-ideality specify two liquid phases. If the software does not find two phases the immiscibility is highly improbable, so the system is homogeneous.

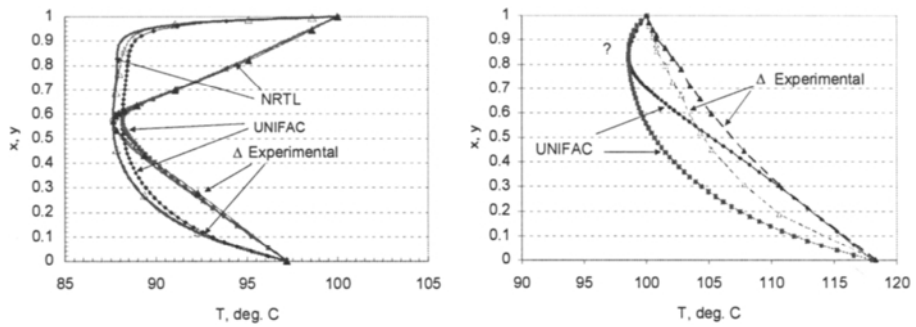

Figure 6.3 Prediction of phase equilibrium by UNIFAC

6.3 THE REGRESSION OF PARAMETERS IN THERMODYNAMIC MODELS

The most accurate thermodynamic model could fail without good parameters. That is why the validation of parameters in thermodynamic models should be a systematic activity in process design.

Binary interaction parameters involved in liquid activity (LACT) models are described by the following general relation:

$$\gamma_i^* = f_i(x_i, T; \theta_{ij}) \tag{6.78}$$

The function f_i depends on the type of model, and incorporates a number of parameters, here designated by θ_{ij}, which should be found by regression.

Similarly, in the equation of state (EOS) approach the problem consists of fitting parameters involved in the mixing rules, following the generic relation:

$$\phi_i^* = g(y_i, T, P; \theta_{ij}) \tag{6.79}$$

The quality of the experimental data is essential. It is desirable to cover the experimental space with a large number of data, but experiments are expensive. The simulation may help a lot to guide and reduce the experimental effort. It is worthy to mention that industrial data may be used for the calibration of thermodynamic models for design purposes.

The following type of equilibrium data can be considered:

1. *PTxy data* contain the maximum of information. Isobaric data are preferable in design because incorporate the temperature effect. Indeed, the activity coefficients are much more dependent on temperature than pressure. Isothermal data are preferred in scientific studies. Vapour composition data are less accurate than liquid composition.

2. *Bubble pressure (P-x) or temperature (T-x)* is the easiest information to obtain. In this category we may include industrial data consisting of sampling temperature and tray liquid composition of running distillation columns.

3. *Azeotropic points* are available for a great number of binary mixtures. The information can be extrapolated via a liquid activity model over the whole concentration range, but the accuracy is not guaranteed.

4. *Infinite dilution activity coefficients* can be measured accurately by chromatographic methods. There are studies claiming that the extrapolation of data is reliable for homogeneous mixtures over the whole range of composition.

5. *Reciprocal solubility.* This information is necessary for treating liquid/liquid systems. The knowledge of the azeotropic point and of reciprocal solubility may be considered sufficient for design purposes.

6. *Solubility of gases in liquids.* The thermodynamic treatment is subtler in the region of concentrated solutions. This aspect will be analysed in the section 6.4.

6.3.1 Thermodynamic consistency

The quality of experimental data can be assessed before regression by a test for *thermodynamic consistency.* The treatment is based on the Gibbs-Duhem equation written here as:

$$\frac{\Delta H_m}{RT^2}dT + \frac{\Delta V_m}{RT}dP + x_1 d\ln\gamma_1 + x_2 d\ln\gamma_2 = 0 \tag{6.80}$$

ΔH_m and ΔV_m are molar enthalpy and molar volume of mixing, respectively. The heat of mixing is negligible in most cases. In an isobaric system the second term vanishes, and the Gibbs-Duhem equation takes the form:

$$x_1 d\ln\gamma_1 + x_2 d\ln\gamma_2 = 0 \tag{6.81}$$

The following relation is obtained for the thermodynamic consistency test:

$$\int_{x_i}^{x_f} \ln\frac{\gamma_1}{\gamma_2}dx_1 = 0 \tag{6.82}$$

Thus, the test consists of plotting the logarithm of the activity coefficients ratio versus molar fraction of one component. The integral should be close to zero.

However, the above test is necessary but not sufficient, since the ratio of activity coefficients eliminates the effect of pressure, which should be checked for correctness. The calculated value of the pressure can be obtained from the relation:

$$P^* = \frac{x_1\gamma_1^* f_1^{0,L}}{\phi_1} + \frac{x_2\gamma_2^* f_2^{0,L}}{\phi_2} \tag{6.83}$$

where the asterisk marks the estimated (computed) values. Consequently, there is necessary a pre-correlation of the activity coefficients γ_i^*, for instance by Legendre polynomials or four-suffix Margules type model. Note that the correction for vapour

non-ideality ϕ_i should be included. Equally important is the accuracy of liquid fugacities $f_i^{0,L}$.

The parameters entering in the pre-correlating of γ_i^* can be obtained by minimising the following objective function:

$$Q = \sum_{i=1}^{n} \left(P - P^*\right)_i^2 \tag{6.84}$$

The next step is to compute values for the vapour phase molar fractions y_i^* from the previous estimated quantities, as:

$$y_1^* = \frac{x_1 \gamma_1^* f_1^{0,L}}{P^* \phi_1} \tag{6.85}$$

Accurate consistency test is passed if two conditions are satisfied (Gess et al., 1991):

- Average deviation $\Delta y = \frac{1}{n} \sum_{i=1}^{n} |(y - y^*)_i|$ below 0.01.
- Deviation $\Delta y = y_i - y_i^*$ evenly distributed, as measured by the bias $\frac{1}{n} \sum_{i=1}^{n} \Delta y$.

6.3.2 Methodology

The regression of parameters from experimental data can follow two statistical techniques: least square (LSQ) and maximum likelihood (ML).

Least square regression

LSQ method consists in finding the set of model parameters that minimise the square error between measured and experimental values. As mentioned, two type of regression may be encountered: LACT and EOS models.

In the LACT approach the equilibrium equations for a binary system are:

$$y_1 P \phi_1 = x_1 \gamma_1 f_1^{0,L}, \quad y_2 P \phi_2 = x_2 \gamma_2 f_2^{0,L} \tag{6.86}$$

Direct measured variables are x, y, P, and T, while γ may be seen as an indirect measurable quantity. Different formulations of the objective function have been studied. The following two alternatives are recommended:

- Bubble pressure[7]:

$$Q = \sum_{i=1}^{n} (P_i - P_i^*)^2 \tag{6.87}$$

---

[7] Often referred as Baker's (BM) method

- Vapour composition and bubble pressure:

$$Q = \sum_{i=1}^{n} \left\{ (y_1 - y_1^*)^2 + (y_2 - y_2^*)^2 + \left(\frac{P - P^*}{P}\right)^2 \right\} \tag{6.88}$$

An objective function formulated in terms of K-values has proved good results for fitting interaction parameters from EOS models:

$$Q = \sum_{i=1}^{n} \left\{ \left[\frac{K_1 - K_1^*}{K_1} \right] + \left[\frac{K_2 - K_2^*}{K_2} \right] \right\} \tag{6.89}$$

Note that the experimental and calculated values are $K_i = y_i / x_i$ and $K_i^* = \phi_i^V / \phi_i^L$.

Maximum likelihood approach

The basic assumption in the ML approach is that all measured and calculated variables are subject to random errors. Moreover, the errors are normally distributed and independent. Data errors may be characterised by a variance σ^2, either globally or individually. The numerical method consists of finding a suitable set of parameters that maximise the *likelihood* between true values and measured data.

Several types of objective function may be considered. One of the most efficient that has a least-square formulation consists of minimising the deviations in T, P, x, y weighted by the variance of errors.

$$S = \sum_{i=1}^{n} \left\{ \frac{(P_i^o - P_i^e)^2}{\sigma_{P,i}^2} + \frac{(T_i^o - T_i^e)^2}{\sigma_{T,i}^2} + \frac{(x_i^o - x_i^e)^2}{\sigma_{x,i}^2} + \frac{(y_i^o - y_i^e)^2}{\sigma_{y,i}^2} \right\} \tag{6.90}$$

The superscripts m and c designate measured and calculated values, respectively. The notation $\sigma_{X,i}^2$ represents the standard deviation of measurements in pressure, temperature and compositions.

A problem in ML approach is the estimation of experimental errors, seldom reported in original articles. Recommended values are ΔT= 1 K, ΔP= 133 Pa (1mmHg), Δx=0.005, Δy=0.015.Note that in the ML approach the equilibrium equations are considered as constraints of the optimisation algorithm.

It is interesting to compare the two approaches. ML method should produce better estimates than LSQ, if the errors are random and not systematic. When the errors are systematic, the graphical representation is the simplest way for detection. With good quality data the two approaches give similar results. If the data are inaccurate, the regression procedure plays an important role.

The quality of data regression should be checked systematically by inspecting the deviation of individual points with respect to model prediction, as the statistical significance of parameters. As Prausnitz noted (1980), 'the choice of a model is not as important as the procedure used to obtain the parameters from limited and inaccurate experimental data'.

EXAMPLE 6.3 Thermodynamic consistency of experimental data

VLE data for the binary methanol (1)/water (2) mixture at 760 mmHg are given below:

T, °C	96.4	93.5	91.2	89.3	87.7	84.4	81.7	78	75.3	73.1	71.2	69.3	67.5	66	65
x_1	0.02	0.04	0.06	0.08	0.1	0.15	0.2	0.3	0.4	0.5	0.6	0.7	0.8	0.9	0.95
y_1	0.134	0.23	0.304	0.365	0.418	0.517	0.579	0.665	0.729	0.779	0.825	0.87	0.915	0.958	0.979

Antoine equation's constants $lgP = A\text{-}B/(T+C)$, with T in °C and P in mmHg, are:

	A	B	C
Methanol	8.07131	1730.63	233.426
Water	8.08097	1582.271	239.726

Examine the thermodynamic consistency of the experimental data. Evaluate the capacity of van Laar model to correlate the data by means of LSQ and ML techniques.

Solution.
Figure 6.4 displays the VLE experimental data. Asymmetric lens shape suggests non-ideal behaviour, confirmed by the comparison with a virtual ideal system. Experimental liquid activity coefficients are shown by marked values in Fig. 6.5.

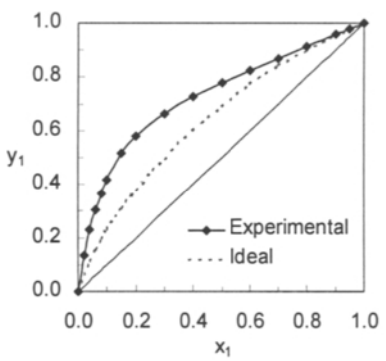

Figure 6.4 Experimental values

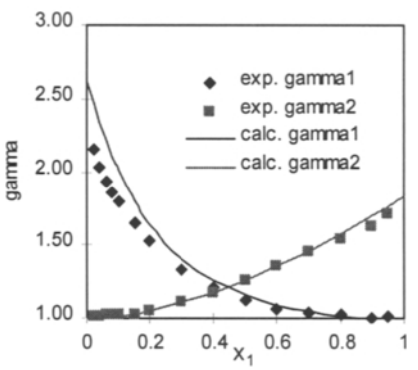

Figure 6.5 Activity coefficients

As discussed, some liquid activity models can be put in a linear form by means of the function $Q = x_1 \ln\gamma_1 + x_2 \ln\gamma_2$, in fact the excess Gibbs free energy. The linearisation of the van Laar model may be formulated as follows:

$$\frac{x_1 x_2}{Q} = \frac{1}{B_{12}} + \frac{B_{12} - B_{21}}{B_{12} B_{21}} x_1 \qquad \text{(i)}$$

The regression of parameters by least-squares regression can be done with EXCEL™. The values obtained by LSQ are: B_{12}=0.9646 and B_{21}=0.6058 (fig. 6.6).

The quality of regression seems to be modest. Note the scatter of data at low methanol concentration. Figure 6.5 presents calculated against experimental values for liquid activity coefficients. The fit is good at high methanol concentration, but gives systematically higher values at low methanol concentration.

The comparison of vapour composition is a better measure for accuracy, and is given in Fig. 6.7. The correlation seems satisfactory, although not very accurate. Indeed, the mean deviation of vapour molar fraction is 0.025, greater than the default error in regressions of 0.015.

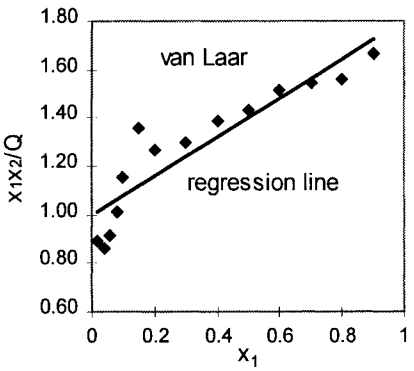

Figure 6.6 Least- square regression

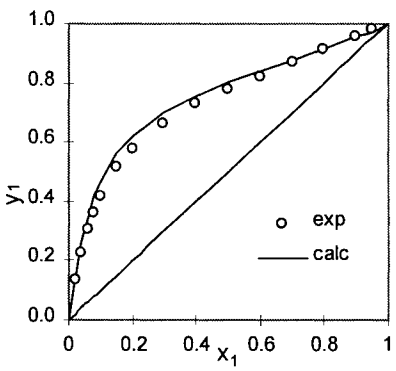

Figure 6.7 Accuracy of regression

The analysis presented so far shows that the least-squares procedure cannot distinguish between the inaccuracy of data and the model capacity to describe a particular system. We need a deeper insight. Firstly, we apply the test of activity coefficients found from experimental data by means of the equation (6.82). Figure 6.8 presents the plot of $\ln(\gamma_2 / \gamma_1)$ against x_1. Two areas are formed around x-axis. Data are consistent if the following condition is satisfied (Sandler, 1999):

$$-0.02 \le \frac{|Area\,I| - |Are\,II|}{|Area\,I| + |Area\,II|} \le 0.02 \qquad \text{(ii)}$$

Evaluation of the integral gives: *AreaI*=-0.15332 and *AreaII*=0.18708. The area test is:

$$\frac{0.18708 - 0.15332}{0.1878 + 0.15332} = 0.099 > 0.02$$

Hence, the consistency test suggests that the data are not accurate.

In a second attempt, we treat the same problem by the maximum likelihood method by using the Data Regression System available in Aspen Plus. The results are: B_{12}=0.8449 and B_{21}=0.5274.

Figure 6.9 shows a comparison between the two methods as the deviation in vapour phase composition between experimental and computed values. The distribution of is odd, almost all negative, indicating possible systematic errors. However, the difference in accuracy by the two regression techniques is significant. LSQ gives poor results, the deviation being particularly large at small concentration of methanol, or large concentration of water. ML gives much better results. The deviations are now below 0.01 and uniform distributed. Even if the original data might contain errors, the model can spread them out over the interval of concentrations.

Thus, this example illustrates that in parameter regression the most important features are the quality of data and the regression procedure. The model should be accurate, but it cannot alone determine the quality of regression.

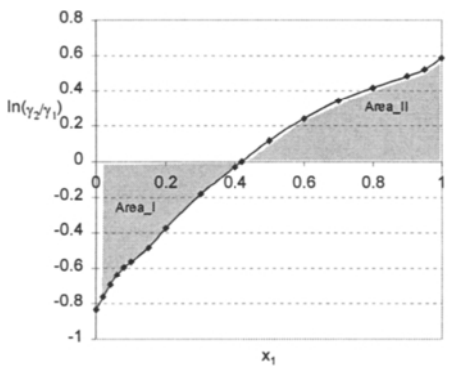

Figure 6.8 Thermodynamic consistency

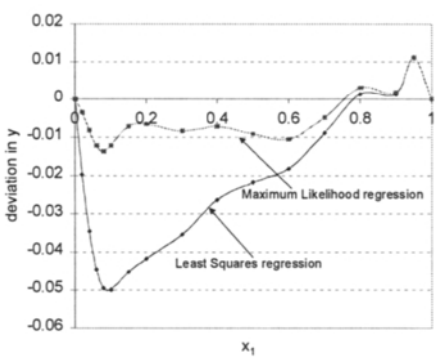

Figure 6.9 Accuracy of data reduction

6.3.3 Evaluation of models

The monograph of Gess, Danner and Nagvekar (1991) contains a comprehensive evaluation of the adequacy of different thermodynamic models. A number of 104 binaries covering a large variety of chemical classes have been selected. The components were assigned to the following categories: non-polar (NP), weakly polar (WP), strongly polar (SP), aqueous. Typical systems have been formed by combining components with different polarity from different chemical classes, as described in the Table 6.5. They have been completed with mixtures containing carboxylic acids and immiscible systems. A special attention was paid to the quality of the VLE data.

The authors propose a simple method to distinguish between ideal and non-ideal systems. This consists in correlating excess Gibbs free energy with a simple one-suffix Margules equation of the form $G^{ex}/RT=Ax_1x_2$. Theoretically A=0 for non-ideal mixtures, but practically this limit may be set to A=0.6. Note that ideal systems may be

formed not only from non-polar components, but also from the combination of some polar components, as alcohols.

The conclusions of the above study are:

- For slightly non-ideal systems there is little difference between models. Simpler models, as van Laar or Margules, may be used.
- UNIQUAC is the best for NP/WP, WP/WP, WP/SP combinations, although the other models are very close.
- Wilson seems the best for NP/SP mixtures, but UNIQUAC and Margules are the most accurate in some cases. Note that in one case UNIQUAC was the worst!
- In the case of SP/SP systems the above research did not draw a conclusion. Sometimes simple models, as van Laar and Margules, behave much better than local composition models. UNIQUAC and Margules may be here recommended.
- For aqueous miscible systems UNIQUAC and Wilson behave the best.
- EOS models are in general of lower accuracy than LACT models, particularly for systems containing SP components. However, for NP/WP combinations the EOS models were in some cases among the best. Huron-Vidal mixing rules produce better results than conventional geometrical mixing rules. For NP/NP systems there is no difference. Note that modified EOS for polar species and mixing rules of Wong-Sandler type have not been used.
- At higher pressure EOS models should be always considered. On the contrary, at lower pressure LACT models are superior over EOS models.
- Immiscible systems can be handled only by NRTL, UNIQUAC, van Laar, and Margules. The first two models are the best.

Table 6.5 summarises the recommendations regarding liquid activity models. UNIQUAC gives good results in most cases. For mixtures of strong polar molecules all LACT models should be checked. Wilson is a good choice for homogeneous organic mixtures. NRTL and UNIQUAC are recommended for immiscible systems.

Table 6.5 Recommendations on liquid activity models

	Non-polar (NP)	Weakly polar (WP)	Strong polar (SP)
Non-polar (NP)	All models	-	-
Weakly polar (WP)	UNIQUAC	UNIQUAC	-
Strong polar (SP)	Wilson	UNIQUAC	None
Aqueous miscible	-	-	UNIQUAC
Aqueous immiscible	NRTL	or UNIQUAC	

EXAMPLE 6.4 Comparison of liquid activity and equation of state models

Study the ability of different thermodynamic models to describe the VLE for the binary mixture 1-propanol/water. Experimental data are from Perry (1977). Check the accuracy of the following models: (1) liquid activity: Wilson, Uniquac, NRTL, UNIFAC, and (2) equations-of-state: SRK, SR-Polar.

Solution.

The ideality of vapour phase is taken as a working hypothesis. Experimental data together with calculated γ_i and *K*-values are presented in Table 6.6. The regression of the interaction parameter has been done with Aspen Plus. Note that the program performs automatically a thermodynamic consistency test.

Table 6.6 Experimental data, activity coefficients and K-values

T	P	x	y	P	P	γ_{12}	γ_{21}	K_1	K_2
		1-prop	1-prop	1-prop	water	1-prop	water	1-prop	water
°C	bar	-	-	bar	bar	-	-	-	-
98.59	1.013	0.0030	0.0544	1.066	0.963	17.23	1.00	18.13	0.95
95.09	1.013	0.0123	0.1790	0.934	0.848	15.78	0.99	14.55	0.83
91.05	1.013	0.0322	0.3040	0.798	0.729	11.98	1.00	9.44	0.72
88.96	1.013	0.0697	0.3650	0.734	0.674	7.22	1.03	5.24	0.68
88.26	1.013	0.1390	0.3840	0.714	0.656	3.92	1.10	2.76	0.72
87.96	1.013	0.2310	0.3970	0.705	0.648	2.47	1.23	1.72	0.78
87.79	1.013	0.3110	0.4060	0.701	0.644	1.89	1.36	1.31	0.86
87.66	1.013	0.4120	0.4280	0.697	0.641	1.51	1.54	1.04	0.97
87.83	1.013	0.5450	0.4650	0.702	0.645	1.23	1.85	0.85	1.18
89.34	1.013	0.7300	0.5670	0.746	0.684	1.06	2.38	0.78	1.60
92.3	1.013	0.8780	0.7210	0.838	0.764	0.99	3.03	0.82	2.29

Liquid activity models.

The computation takes into account the following assumptions:

- Wilson and UNIQUAC models have an explicit temperature dependency of the form $\ln(A_{ij}) = a_{ij} + b_{ij}/T + c_{ij}\ln T + d_{ij}T$. By default the regression considers the terms b_{ij}. Here we select a four parameter formulation with both a_{ij} and b_{ij}.
- Five parameters for NRTL model with the formulation: $G_{ij} = exp(-\alpha_{ij}\tau_{ij})$ with $\tau_{ij} = a_{ij} + b_{ij}/T + e_{ij}\ln T + f_{ij}T$, where $\alpha_{ij} = c_{ij} + d_{ij}(T - 273.15)$. Beside the pairs a_{ij} and b_{ij}, the fifth parameter $\alpha = \alpha_{ij} = \alpha_{ji}$ is fixed at 0.3.

Table 6.7presents the values of binary interaction parameters obtained by regression, and used in the back calculation of liquid activity coefficients.

Table 6.7 Parameters of liquid activity models issued from regression

	Comp. 1	Comp. 2	Wilson	UNIQUAC	NRTL
a_{12}	1-prop	water	12.8268	-11.1626	13.19915
a_{21}	water	1-prop	4.454137	6.193759	-4.33146
b_{12}	1-prop	water	-5772.21	3990.636	-4805.76
b_{21}	water	1-prop	-1754.01	-2436.78	2603.956
α	-	-	-	-	0.3

Table 6.8 presents the comparison of experimental versus calculated data with four liquid activity models. The results given by Wilson, NRTL and UNIQUAC activity seem good, although some errors can be detected with UNIFAC. Figure 6.10-left presents a graphical comparison between experimental and calculated values for liquid activity coefficients. No clear advantage of a particular model can be seen in this type of representation. However, the difference becomes visible in a plot of vapour phase errors against liquid composition (Fig. 6.10-right). Clearly the Wilson model is the most accurate. Errors are larger in the dilute region, but after x_1=0.2 they become very small. UNIQUAC and NRTL are less accurate, but still good. Also UNIFAC gives satisfactory results, except in the dilute region where the error climbs to 15%.

Table 6.8 Experimental and calculated liquid activity coefficients

Experimental values		Calculated γ_1			
x	γ_1	Wilson	NRTL	UNIQUAC	UNIFAC
0.0000	-	17.460	18.875	18.426	16.131
0.0030	17.225	17.362	17.909	17.671	15.423
0.0123	15.785	15.980	15.322	15.359	13.461
0.0322	11.984	11.553	11.422	11.475	10.273
0.0697	7.223	6.838	7.366	7.343	6.695
0.1390	3.919	3.824	4.138	4.108	3.781
0.2310	2.468	2.462	2.493	2.482	2.330
0.3110	1.887	1.920	1.853	1.852	1.793
0.4120	1.510	1.540	1.442	1.446	1.439
0.5450	1.231	1.267	1.188	1.193	1.209
0.7300	1.055	1.078	1.049	1.051	1.065
0.8780	0.992	1.014	1.009	1.009	1.0141

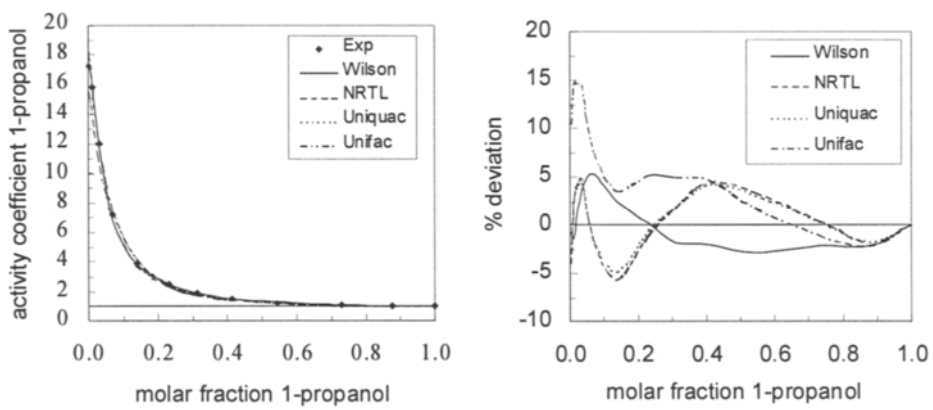

Figure 6.10 Liquid activity models

EOS models

The following cubic equation of state are tested:

- SRK equation, with geometrical mixing rules, with one interaction parameter, k_{ij} .
- SR-Polar, with mixing rules given by equation (6.13) and (6.14).

We have chosen to identify only the two parameters regarding the attraction term, k_{aij} and l_{ij}, neglecting the correction on the b parameter. The results are:

SRK: k_{ij} =-0.118156; SR-Polar k_{aij}= -0.082925 and l_{ij} = 0.0384094

Figure 6.11 shows the comparison between experimental and calculated K-values. As expected, the SRK EOS is not accurate. On the contrary, SR-Polar gives excellent results, as good as the more capable Wilson model.

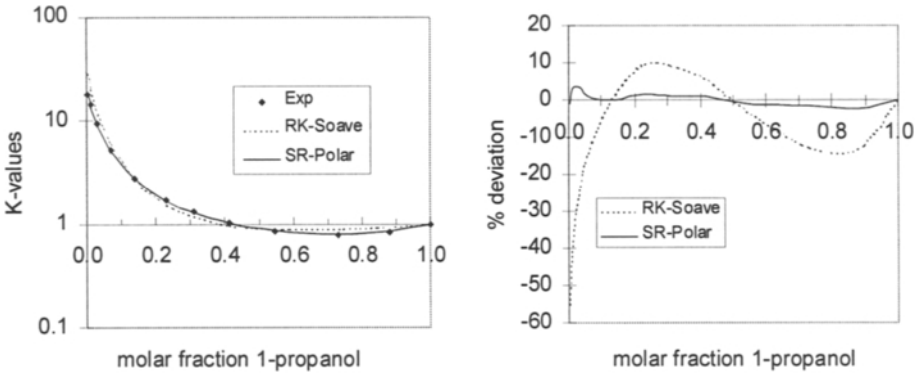

Figure 6.11 Equation of state models

6.4 SPECIAL TOPICS IN PHASE EQUILIBRIUM

6.4.1 Gas-liquid equilibrium

Gas-liquid and vapour-liquid equilibria display similarities, but also significant differences. Let's consider a component i in a gaseous mixture dissolved in a solvent, at equilibrium at constant temperature. If the solution is very diluted and there is no chemical reaction, then the *Henry law* expresses a simple proportionality between the solute partial pressure p_i and its molar fraction in liquid x_i:

$$H_{iA} = p_i / x_i \tag{6.91}$$

Henry constant H_{iA} is characteristic for a pair component-solvent, depends strongly on temperature, and has the dimension of a pressure. Similarly with VLE the gas-liquid equilibrium may be described by an equilibrium constant K_i, as:

$$K_i = \frac{y_i}{x_i} = \frac{H_{iA}}{P} \tag{6.92}$$

However, the Henry law is not valid at higher solute concentration. Since important gas absorption processes take place at higher pressure, the influence of the pressure should be accounted for. Here we present two approaches. The first one is based on the *asymmetric definition* of the *K*-values. The second one takes profit from the ability of cubic equations of state to handle simultaneously sub-critical and supercritical components. They are examined in more detail below.

Asymmetric definition of equilibrium constants

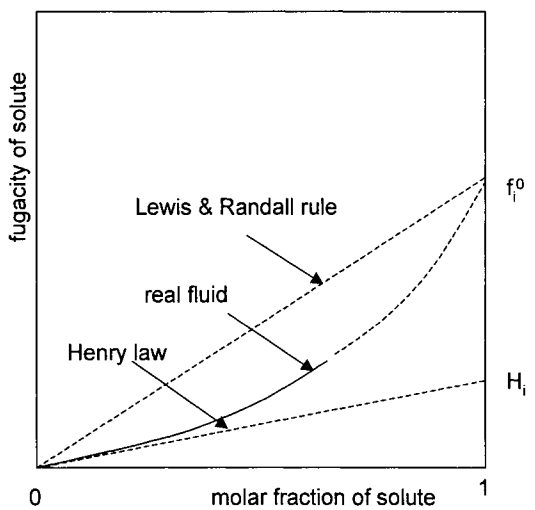

Figure 6.12 Asymmetric definition of the reference states

The approach is illustrated in Figure 6.12, where the fugacity of a solute in liquid $\hat{f}_i^l$ is displayed as function of its molar fraction x_i. A Henry constant H_i may be defined as the limit of component fugacity $\hat{f}_i^l$ at infinite dilution (left corner of the diagram):

$$H_i(T,P) = \lim_{x_i \to 0} \frac{\hat{f}_i^l(T,P,x_i)}{x_i} \tag{6.93}$$

Henry constant H_i depends on the pair solute-solvent, but the last will be omitted from notations for clarity reasons. The temperature dependency of H_i may be expressed similarly with the vapour pressure as:

$$\ln H_i = A + B/T + C\ln T + DT^2 \tag{6.94}$$

A relation similar with liquid fugacity can describe the pressure dependency of H_i:

$$H_i(T,P) = H_i(T,P_{ref}) \exp\left[\int_{P_{ref}}^{P} \frac{V_i^l}{RT} dP \right] \tag{6.95}$$

The reference pressure P_{ref} is usually 1.013 bar. In the correction term, analogue with the Poynting factor, V_i^l is the solute liquid molar volume, found in tables or estimated by different methods (Reid et al., 1987). The Poynting correction is small at low pressures, but necessary at higher pressures.

Another reference-state for the solute *i* may be its pure liquid fugacity, f_i^0. This state is a virtual one, because in practice $x_i << 1$. If the actual liquid mixture has as reference an ideal solution obeying the Lewis-Randall rule, we may define the reference-state f_i^0 as the limit of component fugacity at $x_i \to 1$:

$$\lim_{x_i \to 1} \frac{\hat{f}_i(T,P,x_i)}{x_i} = f_i^0(T,P) \tag{6.96}$$

Obviously, the values of the two standard states are different, so that $H_i \neq f_i^0$.

Ideal solution is often chosen as reference in analysis. In this case we may write for the fugacity of a component the relations $\hat{f}_i^{id}(HL) = x_i H_i$ and $\hat{f}_i^{id}(LR) = x_i f_i^0$, where HL stands for Henry law and L-R for Lewis-Randall assumption. The problem is now how to express the phase equilibrium? A possible approach would be to use Henry law for solute, and Lewis-Randall rule for solvent. For this reason such definition of *K*-values is considered *asymmetric*.

The examination of a binary system involving a solute (1) and solvent (2) allows more insight into the problem (Figure 6.13). For the solvent the reference-state f_2^0 may be seen as real, because this is always a liquid with negligible vapour pressure at the working temperature. The fugacity of the component 2 can be approximated by an ideal solution obeying the Lewis-Randall rule, as $\hat{f}_2^{l,id} = x_2 f_2^0$. For a non-ideal liquid behaviour, we may consider an activity coefficient model, such as $\gamma_2 = \hat{f}_2^l / \hat{f}_2^{l,id}$. Therefore, the fugacity of the solvent component may be written as $\hat{f}_2^l = \gamma_2 x_2 f_2^0$.

As discussed, for the solute 1 it is rational to take as reference state an ideal solution obeying the Henry law. Therefore, we may define a 'virtual' activity coefficient γ_1^* having as reference the infinite diluted solution, as expressed by the equation:

$$\gamma_1^* = \frac{\hat{f}_1^l}{x_1 H_i} \tag{6.97}$$

Note the boundary condition $\gamma_1^*(x_i \to 0) = 1$. On the other hand a 'normal' activity coefficient γ_1 may be defined with reference to an ideal solution obeying the Lewis-Randall rule (see also equation 6.33):

$$\gamma_1 = \frac{\hat{f}_1^l}{x_1 f_1^0} \tag{6.98}$$

At infinite dilution γ_1 would take the value γ_1^∞. It is easy to find that the following relation links the two fictitious reference states for the solute:

$$H_1 = \gamma_1^\infty f_1^0 \tag{6.99}$$

It follows that the two type of the activity coefficient are linked by the relation:

$$\gamma_1^* = \frac{\gamma_1}{\gamma_1^\infty} \tag{6.100}$$

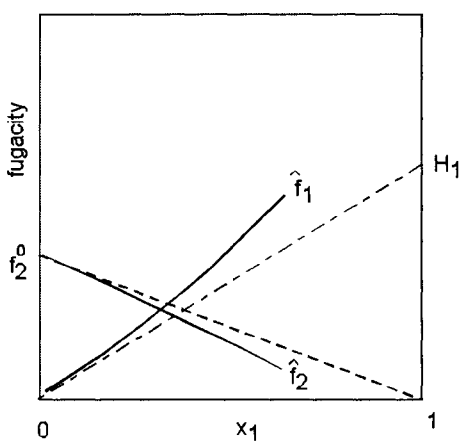

Figure 6.13 Asymmetric definition of the gas-liquid equilibrium

Taking into account the above reasoning, we may write the following relations for the phase equilibrium of solute and solvent, respectively:

$$y_1 P \phi_1^V = x_1 H_1 \gamma_1^* \quad \text{and} \quad y_2 P \phi_2^V = x_2 f_2^0 \gamma_2 \tag{6.101}$$

Because for low pressure $\phi_i^V = 1$, the solvent fugacity is usually equal with its vapour pressure, $f_2^0 = P_2$. The *K*-values become:

$$K_1 = \gamma_1^* H_1 / P, \; K_2 = \gamma_2 P_2 / P \tag{6.102}$$

Hence, following the *asymmetric convention* the *K*-values are defined by two references:

- Solute, by a Henry constant ($x_1 \to 0$).
- Solvent, by a liquid fugacity ($x_2 \to 1$).

The important fact is that we may use a standard liquid activity model, as van Laar or NRTL, to describe the non-ideality of the interaction solute-solvent. Example 6.6 will illustrate this topic.

Summing up, the *asymmetric* convention for *K*-values is a powerful approach useful in solving difficult industrial problems, among which we may cite:

1. Absorption in various solvents of gases containing both sub-critical and supercritical components. For instance, by the absorption in water of a gas containing CO_2, H_2, CH_4 and CH_3OH, the first three species may be treated as Henry components, while for CH_3OH is subcritical. By asymmetric convention applied to all components the thermodynamic treatment is consistent and accurate.
2. Absorption of sour gases (NH_3, SO_2, CO_2) in water at low pressures. Here gas/liquid equilibrium should be described correctly over a large concentration interval. Use of Henry constants without correction for concentration effects gives large errors.
3. Describing gas-liquid processes with very concentrated solutions, as the concentration of ammonia-water solutions, and more generally, processes with strong interactions solute-solvent.
4. Design of stripping columns of volatile organic components (VOC). This is a counter-illustration of the above examples. Here a VLE model has difficulty to describe accurately the process, while the description of light species in the dilute region by Henry law is easier and more reliable.

EXAMPLE 6.5 Gas-liquid equilibrium by asymmetric convention

Ammonia is considered a gas at normal pressure and ambient temperature, although is not supercritical (T_c=405.5 K, P_c=11.3 atm). Traditionally, the design of an absorption column for ammonia in water makes use of the Henry law, but this approach may be justified only when the solution is very diluted. Investigate the possibility to handle more concentrated NH_3 solutions by using symmetric and asymmetric convention.

Solution.

Experimental data found in Perry are solubility *S* (g NH_3/100g H_2O) function of ammonia partial pressure p_{NH_3} at different temperatures. Equilibrium data are:

$$x_{NH_3} = S/17/(S/17+100/18) \tag{i}$$

$$P = p_{NH_3} + p_{H_2O} = p_{NH_3} + P^0_{H_2O}(1-x_{NH_3})\gamma_{H_2O} \tag{ii}$$

$$y_{NH_3} = p_{NH_3}/P \tag{iii}$$

As a good approximation $\gamma_{H_2O} \approx 1$. Figure 6.14 shows experimental curves p_{NH_3} vs. x_{NH_3} for 20 °C and 40 °C. Note that the solutions are relatively concentrated.

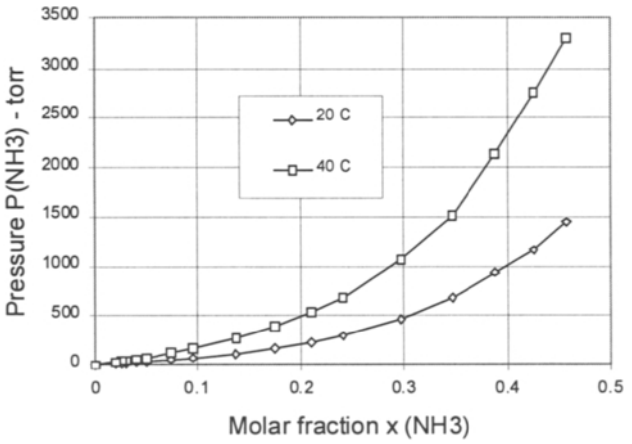

Figure 6.14 Partial pressure of ammonia versus molar fraction

The plots indicate that the non-ideality is significant at higher concentrations. Consequently, liquid activity coefficients should be used. Because NH_3 is subcritical, there is a choice between symmetric and asymmetric conventions. In the first case, Antoine equation is necessary for both components. In the second case, Henry constant for ammonia-water pair is required, but this may be obtained from the slope of the experimental curves plotted in Fig. 6.14. Vapour pressures and Henry constants are:

T (°C)	$P^0_{NH_3}$ (torr)	H_{NH_3} (torr)
20	6409.6	566.6
40	11623.7	1405.5

The following relations give the experimental liquid activity coefficients for ammonia:

- Symmetric convention $\gamma_{NH_3} = p_{NH_3} / (P^0_{NH_3} x_{NH_3})$
- Asymmetric convention $\gamma^*_{NH_3} = \gamma_{NH_3} / \gamma^\infty_{NH_3}$

where $\gamma^\infty_{NH_3}$ is the infinite dilution activity coefficient by symmetric convention at zero molar fraction. In this case $\gamma^\infty_{NH_3}$ can be determined by extrapolating γ_{NH_3} values.

Figure 6.15 displays the experimental values for liquid activity coefficients defined above. The non-ideality is significant. Note also that the shape of curves seems to indicate some errors in the high concentration domain.

The next step is the regression of experimental data with a liquid activity model. As illustration we select van Laar, with temperature dependency, $\alpha_{ij} = a_{ij} + b_{ij} / T$.

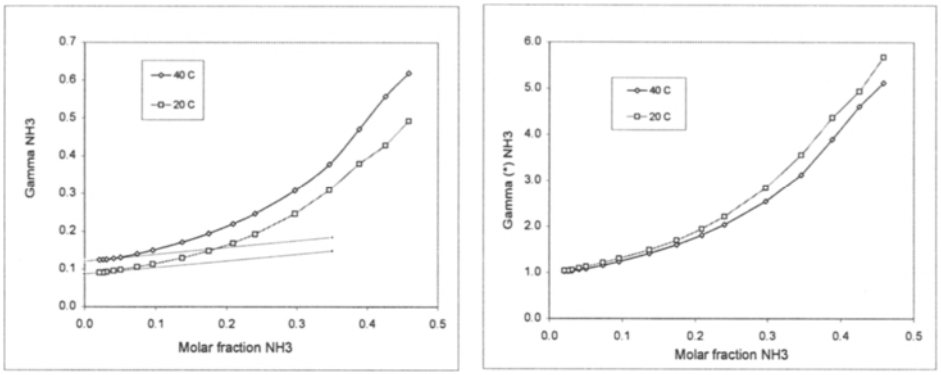

Figure 6.15 Liquid activity coefficients for ammonia in water. Left - symmetric convention; Right - asymmetric convention

Symmetric convention

Figure 6.16 shows a comparison between calculated and experimental data, with Antoine parameters from the database, and Maximum Likelihood objective function. The accuracy is sufficient for technical computations, but it could be better when Antoine parameters are simultaneously regressed.

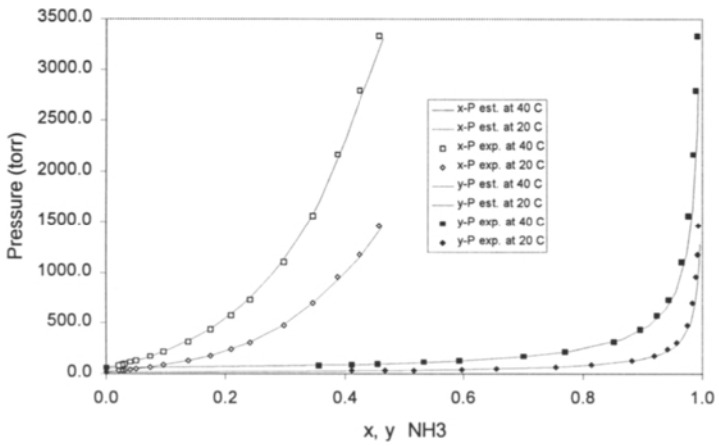

Figure 6.16 Data regression with symmetric convention

Asymmetric convention

The procedure follows the same route, with the difference that NH_3 is defined as a Henry component. The Henry-constant can be obtained from the slope at zero concentration. The back computation of data gives very closed results with the symmetric convention; therefore they are not given again. Note that the Henry coefficients can be simultaneously regressed. A temperature dependency may be

considered as $\ln H_i = A + B/T$. Figure 6.17 presents the relative deviation on the variables T, P, x and y. The accuracy is remarkable. Hence, simultaneous regression of Henry-constant and interaction parameters of liquid activity can lead to high accuracy in gas-liquid equilibrium over the large range of concentration and temperature.

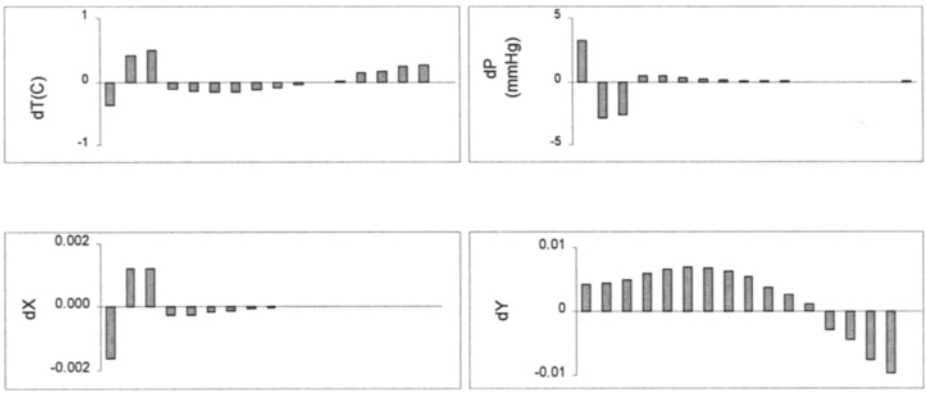

Figure 6.17 Simultaneous regression of interaction parameters and Henry constant. Absolute deviations in T (°C), P (mmHg), X (molar fraction), and Y (molar fraction)

The values of the regressed parameters are presented in the following table (SI units):

	a_{12} ammonia water	a_{21} water ammonia	b_{12} ammonia water	b_{21} water ammonia	A ammonia water	B ammonia water
Symmetric convention	1.7855	11.3862	-1271.37	-4114.03	-	-
Asymmetric convention	-7.1831	-46.3283	818.76	1000	26.2744	-4134.26

Cubic equations of state approach

Cubic equations of state, particularly modified van der Waals equations for polar species, are also suitable for computing the phase equilibrium of gas-liquid systems. The EOS approach enables elegant and efficient simulation of processes at higher pressures. The remarkable advantage is that all components, supercritical or sub-critical, are treated by the same equation of state. Here the key problem is the selection of appropriate mixing rules, as well as the regression of binary interaction parameters. Sufficient data should be available. After the conversion of solubility data in PTxy data, the regression of binary interaction parameters can follow the usual way. The method gives good results if the variation of solubility with the concentration is moderately non-linear.

6.4.2 Partial miscible systems

The occurrence of immiscibility may be explained by means of Gibbs free energy of mixing ΔG_{mix}. This quantity can be expressed by the relation:

$$\Delta G_{mix} / RT = (x_1 \ln x_1 + x_2 \ln x_2) + (x_1 \ln \gamma_1 + x_2 \ln \gamma_2) \tag{6.103}$$

The first term describes the contribution of the ideal mixing itself, while the second one describes the excess energy due to interactions The variation can exhibit a particular shape, as illustrated by a numerical example in the Figure 6.18, where the activity coefficients have been calculated by Margules model with A_{12}=2 and A_{21}=1.5. It may be observed that in the immiscibility region *a-b* the value ΔG_{mix}, resulting by combining the distinct phases *a* and *b*, is lower than the value which would be obtained by extrapolating the curve's shape from the homogeneous region. In other words, phase splitting contributes to minimise the Gibbs free energy of mixing.

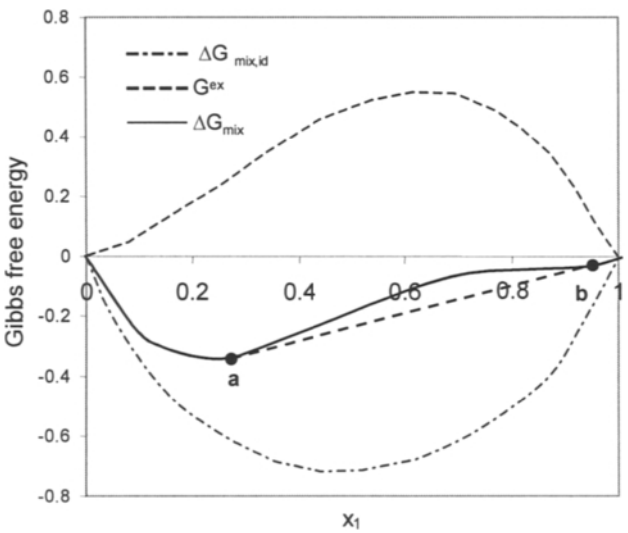

Figure 6.18 Mixing Gibbs energy and immiscibility

The computation of phase immiscibility involves two steps, (1) estimating the occurrence of immiscibility, and (2) determining the solubility limits. The first aspect may be solved by observing that the curve ΔG_{mix} is concave in the two liquid phases region. This may be expressed mathematically as:

$$\left(\frac{\partial^2 \Delta G_{mix}}{\partial x_1^2} \right)_{T,P} < 0 \tag{6.104}$$

By consequence, the test of phase splitting consists of checking if the excess Gibbs energy model satisfies somewhere the condition (6.104). Then, the immiscibility range

can be determined from the observation that at the limit solubility points both slopes of ΔG_{mix} against x_1 are identical, such as:

$$\left(\frac{\partial \Delta G_{mix}}{\partial x_1}\right)_{T,P} = m \quad \text{at both} \quad x_1 = x_{1,a} \text{ and } x_1 = x_{1,b} \tag{6.105}$$

From the above explanation we can conclude that the simulation of separations with two liquid phases depends heavily both on the ability of the thermodynamic model and on the regression procedure. The next examples illustrate this problem.

EXAMPLE 6.6 Data regression with immiscible systems

Water (1) and 1-butanol (2) form a typical immiscible system. The normal boiling points of pure components are 100 °C and 117.5 °C, respectively. The heterogeneous azeotrope has the co-ordinates x_{az}=y_{az}=0.654 and T_{az}=92.7 °C. The following experimental data are known at a pressure of 1.043 at:

T (°C)	110.95	106.4	100.85	96.65	94	93	92.8	95.4	95.8
x_1	0.05	0.097	0.181	0.291	0.417	0.55	0.98	0.991	0.992
y_1	0.253	0.402	0.556	0.66	0.724	0.753	0.76	0.839	0.85

Limiting solubilities of 1-butanol in water at 92.7 °C are $x_{1,\min} = 0.565$ and $x_{1,\max} = 0.975$. Study the correlation of both VLE and LLE data.

Solution.

We select NRTL model with 5 parameters. Note that the regression in Aspen Plus can handle simultaneously VLE and LLE data. The table below presents results obtained with ML function, and a weighting factor of 1:1 for each data set.

Parameter	Comp. 1	Comp. 2	Value	Std. Dev.
a_{12}	WATER	N-BUT-01	94.88852	123.1874
a_{21}	N-BUT-01	WATER	209.0816	19.24899
b_{12}	WATER	N-BUT-01	-7425.68	45078.14
b_{21}	N-BUT-01	WATER	-10148.8	7101.122
α	N-BUT-01	WATER	0.452372	0.058497

Standard deviations show the range of values that would not affect the accuracy of computation. Thus, b_{12} and b_{21} have large standard deviation, and by consequence little importance in fitting. Contrary, random parameter α is of significance.

Figure 6.19 shows that the accuracy of regression is excellent, both for vapour-liquid and liquid-liquid equilibria. This is reflected in very small errors in estimating the solubility and the azeotropic point, as it may be seen from the following table.

	$x_{1,min}$	$x_{1,max}$	y_{az}	T_{az}
Experimental	0.5850	0.9750	0.7540	92.70
Estimated	0.5833	0.9765	0.7536	92.70
Errors (%)	-0.283	0.154	-0.052	0.

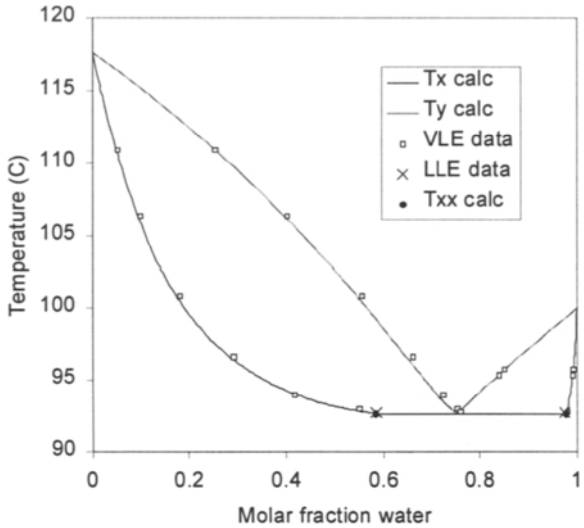

Figure 6.19 Boiling diagram for water /1-butanol

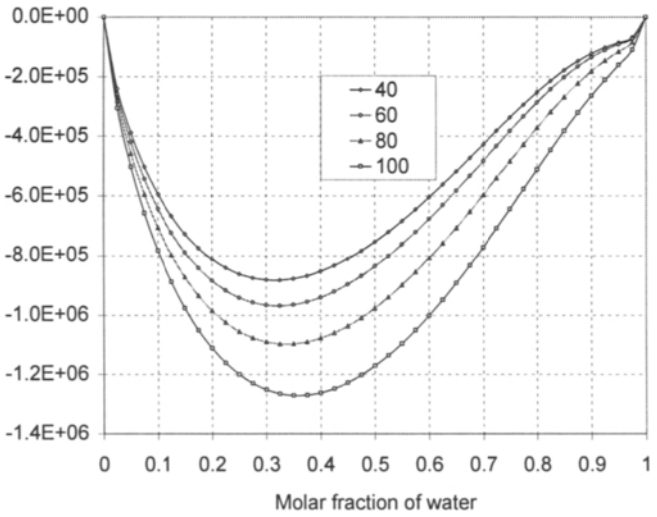

Figure 6.20 Gibbs energy of mixing versus molar fraction of water

Figure 6.20 displays curves ΔG_{mix} versus x_1 at normal pressure and several temperatures. The concave shape allows the detection of an immiscibility region located roughly between 0.55 and 0.975, diminishing with increasing temperature. The right limit, rich water solution with small amount of alcohol is accurately described. The left limit, 1-butanol-rich solution with significant amount of water, is more difficult to locate. This fact might be explained by less sharp slope *dy/dx*.

The next example presents an even more difficult problem when handling simultaneously immiscibility and azeotropy. Both the model selection and the regression procedure play a significant role.

EXAMPLE 6.7 Immiscibility and azeotropy

The binary mixture water (1) / butanone (2) exhibits an interesting phase behaviour: the azeotrope lies outside the immiscibility region. Study the ability of a liquid activity model to describe accurately both VLE and LLE.

Solution. We present results of regression obtained in ASPEN Plus with NRTL model. Experimental data comes from Landolt-Börnstein. Fig. 6.21 displays the comparison of data at 1.033 at when both VLE and LLE data have been combined. The accuracy is excellent. Both immiscible region and position of the azeotrope are correctly described. Fig. 6.22 displays ΔG_{mix} at the split temperature of 73.2 °C. The characteristic concave shape is reproduced. As before, the variation is sharper at the water-rich zone limit.

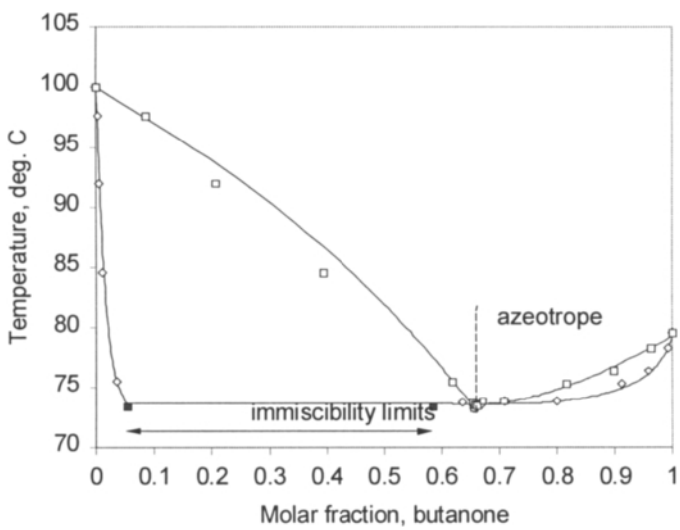

Figure 6.21 Mixture water/butanone-2: correlation of VLLE by NRTL

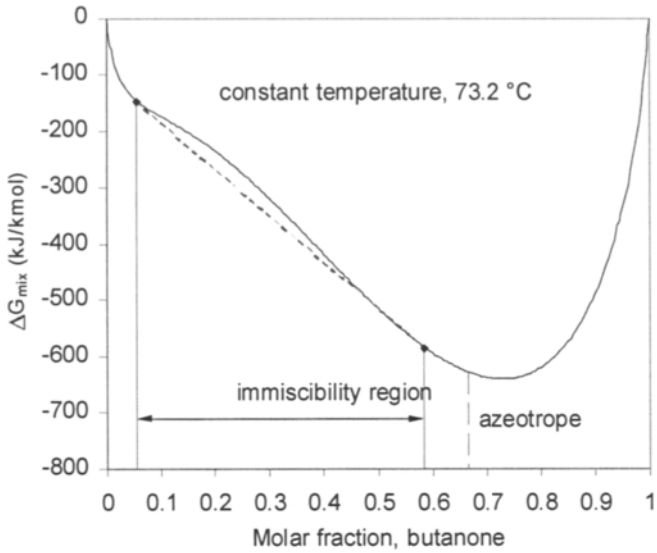

Figure 6.22 Phase splitting

It is interesting to see how this approach may be extrapolated. With interaction parameters from only LLE both immiscibility range and azeotropy are correctly predicted (comparison not shown). The correlation becomes excellent when azeotropic points are added (Fig. 6.23 left). If only VLE data were used then the prediction of LLE would have been possible, but with very poor results (Fig. 6.23 right).

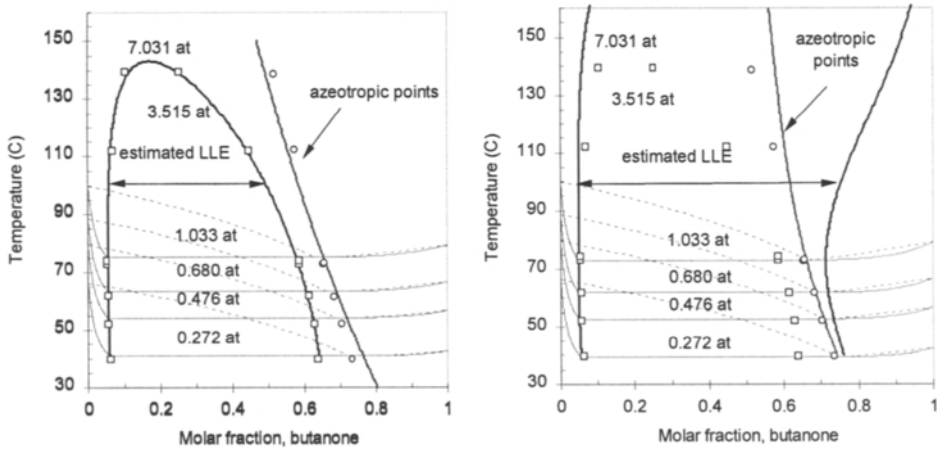

Figure 6.23 Immiscibility and azeotropy

6.5 FURTHER READING

For a deeper understanding of various topics presented here some excellent books may be consulted. The main concepts in phase equilibria are clearly and rigorously explained in one of the most acclaimed books in chemical engineering thermodynamics written by Smith and Van Ness (1995), the 5th edition being re-published in 1997. Other popular textbooks in thermodynamics have been republished in new editions, as by Kyle (1999) and Sandler (1999). These new editions make use of helping programs on CD-ROM. In this respect we could mention a good introductory textbook published by Elliott and Lira (1999) that employ spreadsheets.

However, more advanced material is necessary for subtle differentiations between models that could make the difference in an industrial application. The excellent book about phase equilibria edited by Sandler (1994) contains chapters written by experts, representing the main directions in the thermodynamic modelling for chemical process design, namely modelling excess Gibbs free energy, equations of state, thermodynamics of polymer solutions, group contribution estimation methods, molecular simulation methods, and models for electrolyte solutions. The last topic is quite specific and difficult, but increasingly important because environmental applications. The book of Zemaitis and al. (1986) remains the most comprehensive so far.

The field of equations of state remains one of the most active in phase equilibria. We should mention the two-volume treatise published recently (2000) under the auspices of the International Union of Pure and Applied Chemistry. Here the reader may found very advanced topics, as associating fluids, ionic fluids, polydisperse systems, or polymers.

6.6 REFERENCES

Abbott, M. M., J. M. Prausnitz, 1994, Modelling the Excess Gibbs Energy, in Models for Thermodynamic and Phase Equilibria, edited by S. Sandler, Marcel Dekker

Abrams, D. S., J. M. Prausnitz, 1978, Statistical thermodynamics of liquid mixtures. A new expression for Excess Gibbs Energy, AIChEJ, 20, p. 24

American Petroleum Institute, 1976, Technical Data Book, Petroleum Refining, 3rd ed, API, Division of Refining, Washington

Elliot, J. R., C. T. Lira, 1999, Introductory Chemical Engineering Thermodynamics, Prentice Hall

Fredenslund, A., R.L. Jones, J. M. Prausnitz, 1975, AIChEJ, 21, 1086

Fredenslund, A., J. Gmehling, P. Rasmussen, Vapour-Liquid Equilibria Using UNIFAC, Elsevier (Amsterdam), 1977

Gess, M.A., P.R. Danner, M. Nagvekar, 1991, Thermodynamic Analysis of Vapour-Liquid Equilibria: Models and a Standard Database, DIPPR, AIChE

Gmehling, J., J. Menke, J. Krafczyk, K. Fischer, 1994, Azeotropic Data, Part I and Part II, VCH, Weinheim

Landolt-Boernstein, 1980, Zahlenwerte und Funktionen, Springer Verlag

Kyle, B.G., 1999, Chemical and Process Thermodynamics, third edition, Prentice-Hall

Nagata, I., 1977, in J. Ghmeling, U. Onken, W. Arlt, Vapour-Liquid Equilibrium Data Collection, DECHEMA, Frankfurt,

Perry's Chemical Engineers Handbook, 1997, 7th edition

Prausnitz, J. M., T. F. Anderson, E. A. Grens, C. A. Eckert, R. Hsieh, J. P. O'Connell, 1980, Computer Calculations for Multicomponent Vapour-Liquid and Liquid-Liquid Equilibria, Prentice-Hall

Rafal, M., J.W. Berthold, N.C. Scrivner, 1994, Models for Electrolyte Solutions, in Models for Thermodynamic and Phase Equilibria Calculations, edited by S. Sandler, Marcel Dekker

Reid, R. C., Prausnitz, J. M., Poling, B. E., 1987, The Properties of Gases and Liquids, Mc Graw-Hill, 4th edition

Sandler, S., 1999, Chemical and Engineering Thermodynamics, third edition, Wiley

Sandler, S. J., H. Orbey, B. Lee, 1994, Equation of States, in Models for Thermodynamic and Phase Equilibria Calculations, edited by S. Sandler, Marcel Dekker

Smith, J. C., H. C. Van Ness, Abott, M., 1997, Introduction to Chemical Engineering Thermodynamics, McGraw-Hill, 5th edition, McGraw-Hill

Wong, H., Sandler, S., 1992, AIChEJ, 38, p. 671-680

Swan Arons, J., T. W. de Loos, 1994, Phase Behaviour: Phenomena, Significance and Models, in Models for Thermodynamic and Phase Equilibria Calculations, edited by S. Sandler, Marcel Dekker

Zemaitis, J.F., D.M. Clark, M. Rafal, N. C. Scrivner, 1986, Handbook of Aqueous Electrolyte Thermodynamics, AIChE Publ.

PART III

PROCESS SYNTHESIS

This Page Intentionally Left Blank

Chapter 7

PROCESS SYNTHESIS BY HIERARCHICAL APPROACH

7.1 Introduction
7.2 Outline of the Hierarchical Approach
7.3 Data and requirements
7.4 Input/Output analysis
- 7.4.1 Number of simple plants
- 7.4.2 Input/Output structure
- 7.4.3 Economic Potential

7.5 Reactor design and recycle structure
- 7.5.1 Number of recycle streams
- 7.5.2 Material balance with recycles
- 7.5.3 Reactor design issues
- 7.5.4 Economic Potential with recycles

7.6 General structure of the separation system
- 7.6.1 Phase condition of the reactor effluent
- 7.6.2 First phase split
- 7.6.3 Superstructure of the separation system
- 7.6.4 Knowledge-based synthesis approach

7.7 Vapour recovery and Gas separation systems
- 7.7.1 Selectors and separation methods
- 7.7.2 Sector analysis and split sequencing

7.8 Liquid separation system
- 7.8.1 Application issues
- 7.8.2 Liquid split manager
- 7.8.3 Separation methods
- 7.8.4 Selector analysis
- 7.8.5 Split sequencing

7.9 Separation of zeotropic mixtures by distillation
- 7.9.1 Alternative separation sequences
- 7.9.2 Heuristics for sequencing
- 7.9.3 Complex columns
- 7.9.4 Sequence optimisation

7.10 Enhanced distillation
7.11 Alternatives to distillation
7.12 Reactive Distillation
7.13 Economic Potential after separations
7.14 Summary
7.15 References

The goal of this chapter is to present a systematic approach in developing flowsheets for chemical processes. The methodology designated by *Hierarchical Approach* has been developed by Douglas in the decade of 1980, and presented in his now classical book on Conceptual Design of Chemical Processes (Douglas, 1988). The methodology was intended initially for petrochemical type processes. The engineering experience has revealed a much broader interest, most of all as a strategy for solving a process synthesis problem. Combined with intelligent programming the methodology can be used as working frame for the automatic generation of flowsheets (Han et al., 1994).

Hierarchical Approach is based on physical reasoning. Some steps might be perceived as 'obvious'. This is rather a merit than a weakness, because once understood the methodology can be easily applied into a variety of situations, independently of a computing tool. Actually, the construction of the whole methodology, as a coherent paradigm of structured levels and design decisions represents a contribution of high conceptual value in chemical engineering.

In the subsequent sections, we will explain the approach in detail illustrated by examples. To learn it properly, it is important that the reader goes through all the steps. Because of the complexity of the overall synthesis problem, some issues regarding the synthesis of subsystems, as chemical reactors, azeotropic distillations, or heat exchangers networks, will be presented in separate chapters.

7.1 INTRODUCTION

The development of a flowsheet following the Hierarchical Approach is essentially a *top-down analysis* organised as clearly defined sequence of tasks grouped in *levels*. Each level contains a decision-making mechanism based on the identification of dominant *design decisions* that will generate *flowsheet alternatives*. An evaluation procedure eliminates unfeasible alternatives. By keeping only the best alternative at each level, the solution proceeds through a *depth-first approach*. Finally, the procedure leads to a *base-case* flowsheet, which will serve for more detailed analysis and refinement. The above presentation may be completed by two comments:

1. The hierarchical evolution of the design is a necessary condition for getting a *computational tractable* problem.
2. The procedure can guarantee the identification of the optimal design space. This is possible for the following reasons:
   - Design decisions set bounds in searching the optimal solution at each level.
   - The design space is progressive reduced, by retaining only feasible solutions that include always the optimal one.
   - Few alternatives are selected for optimisation.
   - Systematic techniques can perform structural refinement of subsystems, as well as the pre-optimisation of operational parameters and equipment sizing.

We adopt here the principle of 'learning by example'. The methodology will be illustrated by developing flowsheet alternatives for the process known as the *Hydrodealkylation of Toluene*, commonly abbreviated as HDA. This example, already

introduced in Chapter 3, has been selected by Douglas to support his methodology. HDA process has been used also extensively in the scientific literature to illustrate different topics in process synthesis and plantwide control.

EXAMPLE 7.1 HDA process

HDA process converts alkylbenzenes and alkylnaphtalenes to their aromatic rings. As typical example, toluene is transformed to benzene in the presence of hydrogen, following the reaction:

$$\text{Toluene} + H_2 \rightarrow \text{Benzene} + CH_4 \quad (1)$$

In the case of a thermal process, the conditions are: temperature 620-700 °C, pressure 25-35 bar. Here we consider as raw materials toluene and H_2 with 5 % CH_4. A ratio H_2/Toluene approximately 5/1 must be ensured at the reactor entry to prevent coke formation. By-products are diphenyl, naphtalene and other heavy hydrocarbons. Here we consider only the formation of diphenyl, following the reversible reaction:

$$2\ \text{Benzene} \leftrightarrow \text{Diphenyl} + H_2 \quad (2)$$

Figure 7.1 presents an intuitive flowsheet. After the dissolution of hydrogen in toluene at high pressure, the mixture is evaporated and heated to the reaction temperature. The reactor outlet stream is cooled and separated in gas and liquid streams by simple flash. The gas stream containing excess hydrogen and methane is recycled, a purge preventing the accumulation of methane. The liquid stream is sent to the separation system. In the first column, the liquid mixture is 'stabilised' by removing dissolved gases. The second column delivers benzene in top, while the third column recovers toluene from diphenyl and other heavies.

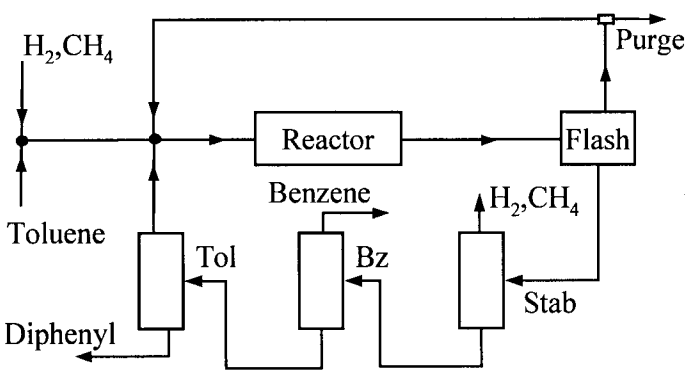

Figure 7.1 HDA process: non-integrated plant

The above flowsheet has a major drawback: inefficient use of energy. Indeed, the heating and cooling make use exclusively of external utilities. It is obvious that energy can be saved by appropriate combination of hot and cold streams. This could be found by using intuition or previous experience, and then checking the solution by simulation. However, this approach requires extensive work and can never guarantee that the solution is the best.

Figure 7.2 presents the optimal solution found by Douglas (1988) by applying Hierarchical Approach for flowsheet synthesis and Pinch Point Analysis for energy saving. The flowsheet requires some explanations. Reactants are pre-heated through successive heat exchangers, in counter current with the reactor-exit. Then the reaction mixture is passed through a furnace and heated-up to the required reaction temperature. Note that the enthalpy of the outlet mixture is used not only for preheating reactants, but also to drive the reboilers of the distillation columns. By recovering energy, no external steam is necessary for the distillation section. Only cold utilities are required for condensers. Note also that the distillation columns for benzene production and toluene recycle are thermally integrated. However, some questions may arise:

1. Is this flowsheet really 'the best' solution?
2. Why do we need a furnace, when the reaction is exothermic?
3. What about the control and operation of this high-integrated plant?
4. Could the plant handle a mixture of toluene with other alkylbenzenes?

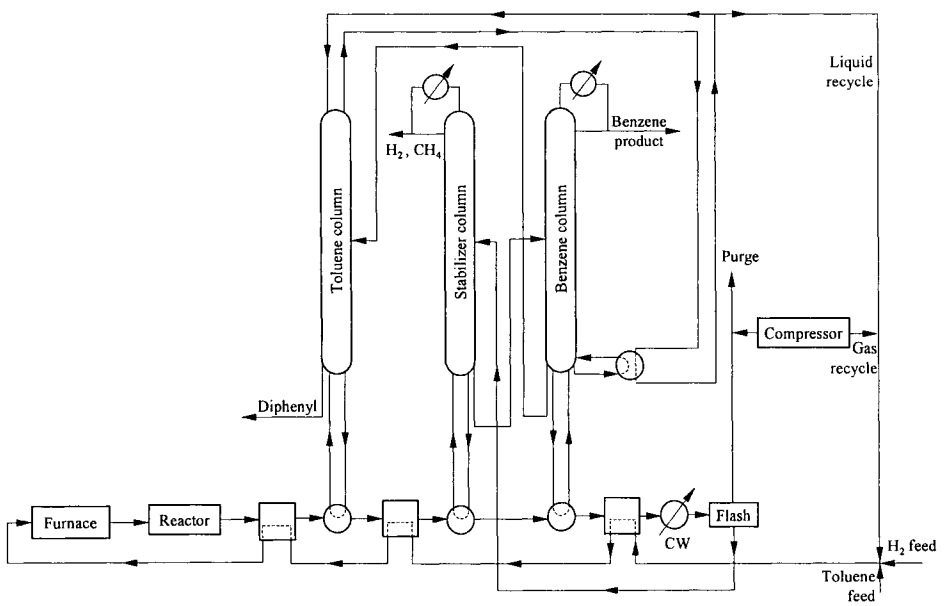

Figure 7.2 HDA plant, maximum energy recovery (after J. Douglas, 1988)

Another solution is given in Fig. 7.3 (Dimian, 1996). This time the heat integration considers a more global viewpoint based on 'site integration'. Excess heat available at high temperature is exported to the utility system. The heat needed to drive the distillation columns is imported from the steam network, at a temperature level compatible with the site policy. Exported energy as high-pressure steam is more valuable, and can be used to produce electricity in a combined heat and power cycle. Therefore, heat recovery is more efficient if treated as a plantwide problem.

The controllability properties of the two flowsheets are also different. In a very tight integrated plant, as in Fig. 7.2, disturbances in the reactor system will strongly affect other parts, namely the separation system. On the contrary, for the plant in the Fig. 7.3 the disturbances will be quickly compensated by the buffering effect of the utility system. A finer analysis will reveal that despite the exothermal heat effect, the presence of a heater before the reactor is necessary to prevent unstable reactor operation.

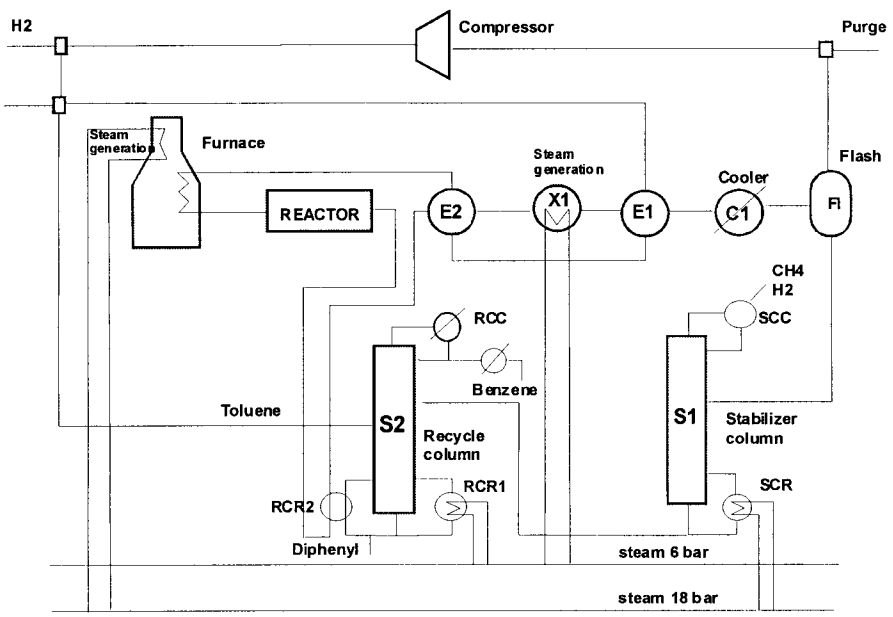

Figure 7.3 Energy Integrated HDA plant (site integration)

Summing up, a conceptual design problem is always open-ended. The result is never unique. The optimality of a flowsheet depends not only on the definition of the objective function and constraints, but also on numerous design decisions that the designer must consider. Moreover, only static evaluation of the design performances (steady-state behaviour) is not sufficient. Dynamic characteristics and flexibility in manufacturing should be also considered in assessing the optimality.

7.2 OUTLINE OF THE HIERARCHICAL APPROACH

Hierarchical Approach is a methodological frame for the conceptual synthesis of process systems. The overall strategy is organised in a number of *levels*, each level being decomposed in a number of *tasks*. The approach presented below is organised in eight levels as follows (Douglas and Stephanopoulos, 1995):

Level 0 - Input information

Collect data on chemistry, raw materials, product specifications, economic constraints and legal regulations.

Level 1 - Number of Plants

Determine the number of plants for multi-step reactions.

Level 2 - Input-Output Structure and Plant Connections

Specify feed, exit and recycle streams for each plant. Specify interconnections between plants. Estimate minimum capital and operation costs.

Level 3 - Recycle structure of the simple plants

For each plant specify reactor type, recycle streams and flows. Set upper and lower limits for conversion by taking into account the cost of recycles.

Level 4 - Separation systems of the simple plants

For each plant specify the separation system and estimate its annualised cost. Additional hierarchical refinement reveals seven sub-levels.

4a. General separation structure: identify specific separation subsystems.
4b. Vapour separation and recovery system: separate gaseous products and recover valuable liquid components.
4c. Solid recovery system: recover valuable solids from solutions.
4d. Liquid separation system(s); separate products from liquid mixtures.
4e. Solid separation system: separate solid products.
4f. Combine separation systems in the whole flowsheet, and study interactions.

Level 5. Process Integration

5a. Pinch Point Analysis: Heat Exchanger Network (HEN) design for optimal heat and power saving.
5b. Water Minimisation: design an efficient system for the recycling of water.
5c. Solvent Minimisation: design an efficient system for the recycling of solvents.

Level 6. Evaluate Alternatives

6a. Examine alternative design decisions.
6b. Examine alternatives for the reactor design.
6c. Consider more efficient separation systems.

Level 7. Hazop analysis

7a. Identify sources of hazards and risks.
7b. Perform hazard and operability study.

Level 8. Control system synthesis

8a. Plantwide Control: develop the control strategy of the whole plant.
8b. Control structure for units: design control structures for individual units.

Consistency of the Hierarchical Approach

The activities involved at each level may be grouped in the following categories:

1. Synthesis tasks: generate structural alternatives by using heuristic reasoning, systematic methods or numerical procedures.

2. Analysis tasks: solve material and energy balances, design equipment by short-cut methods or by computer simulation, and generate cost estimates.

3. Evaluation Tasks: evaluate flowsheet alternatives by means of performance indices of economic nature or technical significance. An alternative is rejected as unfeasible when one of several indices violates predefined bounds. On the contrary, an alternative is retained for further evolution and refinement if satisfies the constraints and shows potential for optimality.

Because the Hierarchical Approach keeps only the best design or a short list of the most promising candidates, it is considered a *depth-first search.*

4. Constraint Propagation Tasks. Setting constraints ensures proper bounding of the feasible design region. The propagation of constraints can take place by the following mechanism:

- *Propagation of constraint values*. For instance, Input/Output material balance must be consistent at each level, within percentage of errors for impurities and losses. Here we may add design variables that propagate as set values, as conversion, reactants' ratio, reaction temperatures, product purity, etc.
- *Induction of new constraints*. Some constraints may change if new information becomes available. This is the case of the Economic Potential.
- *Generation of context-dependent constraints*. Design decisions at one level may generate a context of constraints for subsequent levels. For example, a non-condensable reactant identified at the Level 0 (input information) will determine the use of a gas recycle and a purge at the Level 2 (Input/Output structure), of a plug flow reactor at the Level 3 (recycle structure), and of a flash drum at the Level 4 (separation system).

The following subchapters will present the methodology in more detail. However, some more complex subjects will be developed in separate chapters, particularly the energy integration and the synthesis of distillation sequences for non-ideal mixtures.

7.3 DATA AND REQUIREMENTS

The reliability of a project depends greatly on the amount and quality of the available design information. Usually the project schedule is tight and the time insufficient for an extensive research. The input data required by a design project may be collected in a systematic manner, following the checklist presented below.

Product rate

Product rate should be expressed in both mass and molar units. Consider an annual working time of 8000 hours. Decide if the process will be continuous or batch. Continuous processes are suitable for commodities, while batch processes are more advantageous for specialities, the boundary being around 10000 tones/year.

Chemical Reaction Engineering

The most important aspects in this category are:

a. Stoichiometry
- Express the stoichiometric equations for the main components that can be associated with reaction steps in the manufacture of the desired product(s). Include intermediates that can be separated and recycled. At each step indicates the phase of reaction, and the range of feasible temperatures and pressures.
- List the thermal effect for each reaction. Identify high exothermal reactions, as well as temperature sensitive reactions with high activation energy.
- List technological constraints, as the reactants' ratio at the reactor inlet, maximum allowable concentrations, flammability and explosion limits.

b. Selectivity
- List secondary reactions leading to by-products, in the range of temperatures and pressures mentioned above.
- Find data about selectivity, and its variation with conversion. This information is essential in conceptual design. Data about product distribution in different conditions can be also of interest.
- Pay special attention to the formation of impurities in chemical reactors. Include reactions involving impurities entered with raw materials.

c. Chemical equilibrium
- Identify reversible reactions. When chemical equilibrium is important, a preliminary study is strongly recommended.

d. Catalyst
- List potential catalysts. Estimate their costs.
- Examine the effect of temperature and of impurities on catalyst activity.
- Examine the environmental problems raised by regeneration, as the need for solvents or special chemicals. Estimate the cost of regeneration and disposal.

e. Reactor Engineering
- Describe alternative reactor types. Collect information about the reactor design; minimum data are residence time, and operating temperature and pressure.

- List reaction constraints: minimum feed temperature, maximum temperature and pressure, as well as safety aspects.
- Search information about the kinetics of main reactions, as well as about selectivity. The last is crucial for developing a realistic process.

Economic data

a. Product price versus purity.
Identify impurities that affect the price of the product. Find information regarding the price variation with purity. Here you may list downstream applications and potential markets. Search also prices for valuable by-products and intermediates.

b. Raw materials prices
Get reliable information about the prices of raw materials as function of purity. Consider internal prices, if the process could be integrated on an existing platform. For remote sources include transport fees and storage costs.

c. Prices of utilities
List prices for utilities: fuel, steam (high, medium and low pressure), cooling water, chilled water, brines, electricity, and refrigeration. Specify limitations in supply.

d. Price of waste disposal
List the prices of by-products disposal, as well as the price to treat volatile organic components (VOCs), polychlorinated biphenyls (PCBs), and other impurities forbidden by the environmental regulations.

Plant and site data

The site selection has a strong impact on feasibility. Hereafter we list some key aspects:

a. *Location.*
Proximity to the source of raw materials is preferable. Consider as first choice the integration on an existing industrial platform, where other processes could supply reactants or intermediate at lower costs. Consider also a location favourable for shipping the products.

b. *Storage facilities.*
The costs for storage of raw materials, products and intermediates are significant in the case of large-scale commodities.

c. *Climate.*
Get data about minimum and maximum temperatures, humidity, wind and meteorological variability. These data are necessary in designing the insulation of equipment and in examining the possibility of using air-coolers.

d. *Utility system.*
Determine the type of utility available on the selected industrial site, particularly the levels of process steam (high, medium and low pressure), the temperature of the cooling water (recycled from cooling towers), inert gas, refrigeration facilities.

e. *Environmental legislation.*
List specific requirements that the process must fulfil with respect to the environmental legislation, as greenhouse gases, soil and water pollution.

Physical properties

Fundamental physical properties must be known at the beginning of a design, both for raw materials and for products and sub-products. Minimal data are: physical state at normal pressure and temperature, vapour pressure, and density in storage conditions.

Safety and Health Considerations

A list with safety and hazard problems must be supplied at the beginning of any design. These can be the reasons of important design decisions. The following elements deserve attention:

a. *Explosions risks.* List potential explosive mixtures involving the components in reactors and storage facilities. Specify concentration and temperature range, particularly for the gas-air mixtures.

b. *Fire risks.* Find information about the flash point, auto-ignition temperature and flammability limits.

c. *Toxicity.* Specify the toxic or non-toxic character of the main chemicals involved in the process. The indication of volatility of liquid toxic components is compulsory. Information over toxicity and hazard effects can be found on the websites of national agencies for public environment and health, as for example Environmental Protection Agency of US (EPA).

The engineering aspect regarding environmental protection and safety are specialised topics that cannot be treated properly here. As general introduction in environmental engineering we recommend the book of Allen and Rosselot (1996). In the field of process safety the book of Crowl and Louvar (1989) is very popular. The topics of hazard and operability (Hazop), as well as hazard analysis (Hazan) are covered in a book due to Kletz (1992). A concise presentation of these issues sufficient for a student project may be found in Coulson & Richardson vol. 6 (Sinnott, 1993).

7.4 INPUT/OUTPUT ANALYSIS

7.4.1 Number of simple plants

The main steps in the reaction network determine the number of reactors and the number of simple plants. The following approach may be used:

1. Consider a plant for each reactor system.
2. If the reaction network involves intermediate species produced in different reactor, consider the possibility of common separations for some components. The separations become simpler, but interactions between recycles may occur.
3. In a first attempt, do not consider large recycle loops due to the recovery of some helping materials, as water, solvents or hydrogen.

EXAMPLE 7.2 Number of simple plants in a VCM process

Vinyl Chloride (VCM) is produced by the thermal cracking of di-choroethane (DCE) following the reaction:

$$C_2H_4Cl_2 \text{ (DCE)} \rightarrow C_2H_3Cl \text{ (VCM)} + HCl \quad \text{(i)}$$

We have to consider a plant for manufacturing the intermediate DCE. This can be obtained directly from ethylene and chlorine, as described by the reaction:

$$C_2H_4 + Cl_2 \rightarrow C_2H_4Cl_2 \quad \text{(ii)}$$

Because selling HCl is not profitable, a third plant can reconverted it to DCE by oxidative reaction with ethylene:

$$C_2H_4 + 2HCl + 0.5O_2 \rightarrow C_2H_4Cl_2 + H_2O \quad \text{(iii)}$$

Alternatively, HCl can produce Cl_2 by direct oxidation:

$$2HCl + 0.5O_2 \rightarrow Cl_2 + H_2O \quad \text{(iv)}$$

Hence, a *balanced process* can be described by the overall stoichiometry:

$$2C_2H_4 + Cl_2 + 0.5O_2 \rightarrow 2C_2H_3Cl + H_2O \quad \text{(v)}$$

At this point, we have the choice between two alternatives:

1. Consider three separate plants, chlorination, cracking and oxy-chlorination, each with its separation section.
2. Combine two reaction steps, as direct chlorination and cracking, in a single plant (VCM), and treat separately the recovery of HCl. Thus, DCE coming from the oxy-chlorination, becomes an external feed for the VCM plant, which has two distinct reactors, but a common part for the separation system.

The conceptual design should consider not only the behaviour of individual plants, but also their interaction through recycles. This is the case in the VCM manufacturing. These aspects will be covered in Chapter 17 by the Case Study 3.

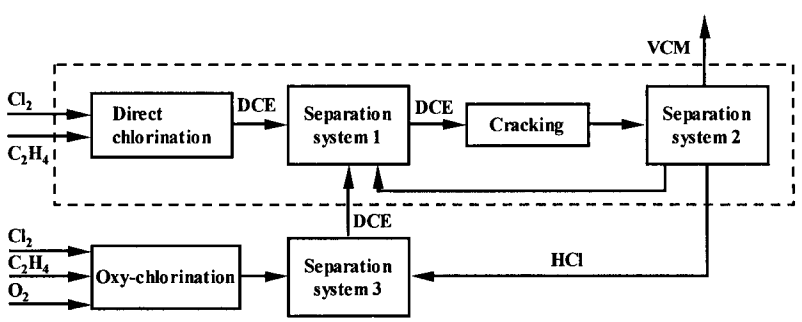

Figure 7.4 Number of plants in VCM manufacturing

7.4.2 Input/Output structure

Input/Output structure defines the *overall material balance boundary* of the flowsheet. A golden rule for any steady-state material balance requires that *the total mass flow of all components entering the process must be equal with the total mass flow of all components leaving it.* The recycles affect only internal process streams, but not the overall Input/Output material balance! It is recommended to start with a simplified approach, in which only feeds, products and sub-products are considered. As a rule of thumb, we may recover more than 99 % of all valuable materials. From this point of view, there could be at least two flowsheet alternatives (Fig. 7.5):

- Recovery of all reactants (process A).
- Loss of some reactants because of purge of gaseous streams (process B).

A typical example is the synthesis of ammonia. Here the reactants, N_2 and H_2, are relatively inexpensive. Purge is necessary to avoid the accumulation of inert gases. If a membrane technique is competitive, the reactants may be recovered almost completely from purge, reducing the overall material consumption.

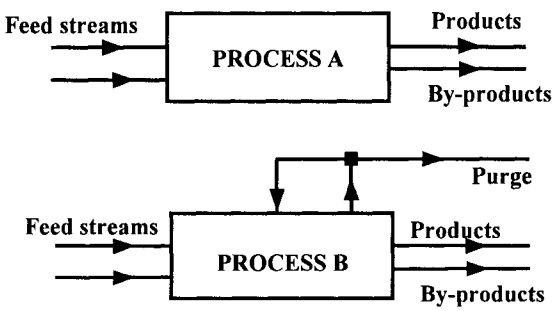

Figure 7.5 Input-Output structures of a flowsheet

Design decisions at the level of Input/Output structure are sources of flowsheet alternatives (Douglas, 1988). These decisions are briefly commented below.

a. Feed Purification

The following guidelines help to decide if a feed purification is necessary.

1. If an impurity is not an inert but in significant amount, remove it. Otherwise, the cost of separation may be higher.
2. If an impurity is present in a gas feed, as first choice let the impurity enter the process.
3. If an impurity in a liquid feed stream is also a by-product or a product component, usually is better to pass the feed through a separation system.
4. If an impurity is present as azeotrope with the reactant, often is better to process it.
5. If a feed impurity is an inert that can be separated easier from the product than from the feed, it is better to let it pass through the process.

6. Impurities affecting catalyst activity must be removed. Evaluate the cost of an extra purification system for feeds, as well as the cost of recycling some harmful impurities, including equipment fouling and maintenance.

b. Recycling of reversible by-products

The recycling of by-products in reversible reactions leads to over-sizing, but may also produce undesirable side reactions. In addition, the removal of by-products needs supplementary investment in separation equipment or special reactors. There are no heuristics for such issue, but a sensitivity analysis may help to take a decision.

For example, in the HDA process the by-product (diphenyl) can be removed in the separation system or recycled to the reactor. The first alternative requires a supplementary distillation column. The second option leads to an accumulation of diphenyl in the plant that could create troubles in long-time operation. Hence, a wise design decision is not to recycle a by-product that would create troubles in operation.

c. Purge and bleed streams

Gas-phase reactions may lead to gaseous by-products and impurities. Similarly, a gaseous reactant may contain light impurities that will pass through the reaction system or produce other impurities. As result, processes with gas recycles need the placement of one or several purges to prevent the accumulation of some gaseous components. The above observation may be extended to heavy components, for which exit points (bleeds) must be provided.

The above topic illustrates the fact that *environmental issues* should be examined at early design stages. The following preventive actions are recommended:

1. Minimise purge and bleeding streams by producing a material balance with raw materials consumption close to the stoichiometric requirements.
2. Examine the post-treatment of purges and other emissions, for example by physical operations (ex: adsorption) or by chemical conversion (ex: combustion).
3. Consider the transformations of light impurities by chemical conversion in more heavy components that can be easy eliminated as bleed streams.

Note that new separation techniques, as membranes, could recover efficiently valuable components from purges and bleeds. For non-valuable species these techniques are rather expensive.

d. Non-recycled components

Many industrial reactions make use of excess air, as for example in hydrocarbon oxidation. Moreover, combustion reactions can be used to supply 'in situ' the heat needed for endothermic reactions. Because of low cost, the air is not normally recycled. The exit point of gases is the flare.

Oxygen has replaced air in many processes. Besides a significant reduction in the volume of emissions, the reaction rate and selectivity may also greatly improve.

Unlike air, the recycling of water is imperative. Water can be used as reactant, as in hydrolysis reactions. Water can be also a direct heat transfer agent, as steam for supplying heat by some endothermic reactions (dehydrogenation of hydrocarbons), or to remove heat (polymerisation of styrene by suspension process).

Because water treatment implies substantial expenses, it must be considered as negative term in the Economic Potential at the Input/Output level. If the economic analysis is negative, then alternative reactors should be considered.

e. Number of outlet streams

An important aspect in the discussed methodology is the number of streams leaving the process. Some guidelines are given below:

1. Examine carefully the reactor outlet and list all the components.
2. Assign a destination code to each component. Table 7.1 gives more details.
3. Order the components by their normal boiling points.
4. Group neighbouring components with the same destination.

The number of all groups minus the recycle streams gives the number of the outlet streams. Be careful with azeotropes or solid components that may change the rule.

The correct assignment of the product streams ensures the consistency of the Input/Output material balance. At each stage of the flowsheet synthesis be certain that all products, by-products and impurities leave the process!

Table 7.1 Destination codes and component classification

	Component classification	Destination code
1	Reactant (liquid)	Recycle (exit)
2	Reactant (solid)	Recycle or Waste
3	Reactant (liquid)	Gas Recycle & Purge, Vent
4	By-product (gas)	Fuel or Flare
5	By-product (reversible reaction)	Recycle or Exit
6	Reaction intermediate	Recycle (exit)
7	Product	Product storage
8	Valuable by-product	By-product storage
8	Fuel by-product	Fuel supply
9	Waste by-products	Pay for disposal!
	• aqueous waste	Biological treatment
	• incineration waste	Incinerator
	• solid waste	Landfill
10	Feed impurity	Same as by-product
11	Homogeneous catalyst	Recycle
12	Homogeneous catalyst activator	Recycle
13	Reactor or Product solvent	Recycle (exit)

f. Design variables

Design variables arise from assumptions regarding the design decisions. These decisions are mostly of technological and economical nature, but also justified by the respect of environmental or legal constraints. At the Input/Output level, the design variables define also the degrees of freedom for the overall material balance. That is why it is impossible to develop a unique material balance for a process. Table 7.2 lists some possible choices.

Table 7.2 Design variables at the Input/Output level

Reaction system	• level of conversion and selectivity • molar ratio of reactants • reaction temperature and/or pressure
Reactants	• need for feed purification • reactants not recovered • use of gas recycle and purge
By-products	• separation or recycling • waste treatment

g. Overall Material Balance

The overall material balance gives the relation between the input streams (raw materials) and the output streams (products, by-products, purge) of the process. In the first attempt, a simplified approach is sufficient. Usually the assumptions are:

- Consider only product and by-products, but neglect sub-products and impurities.
- Consider 100% recovery of all recycled components.

Thus, in the first stage it is more important to find the variation range of the variables of significance in the overall material balance, than to include all losses. The result is a kind of ideal reference material balance. The procedure given below requires only a spreadsheet. The steps are:

1. Identify the inlet and outlet streams (Input/Output structure).
2. Express the production rate in convenient units.
3. Determine the flow rates for every component implied in the chemical reaction network.
4. Express the formation of by-products in terms of design variables (conversion, molar ratio, etc.). For complex reactions, consider correlations for product distribution.
5. Determine the flow rates for excess reactants that are not recycled, and include them in outlet streams.
6. Determine the inlet flow rates for impurities entered with some reactant streams.
7. Calculate outlet flow rates for impurities in purge or bleed streams.

EXAMPLE 7.3 Overall material balance of the HDA process

Figure 7.6 shows the Input/Output structure of the HDA process. Input streams are toluene and hydrogen. Outlet streams are benzene, diphenyl and purge. Toluene is pure, but hydrogen has 5% methane. The design decisions are: (1) not purify the feed, (2) recycle hydrogen, and (3) consider purge for methane.

a. Simplified material balance

In a first approximation, we may neglect the by-product formation and consider a stoichiometric reactant ratio. However, the impurities introduced with feeds are

accounted for. Table 7.3 presents the Input/Output material balance for a production of 100 kmol/h. Note that the internal recycles do not change the Input/Output material balance, as long as the reaction selectivity is not affected!

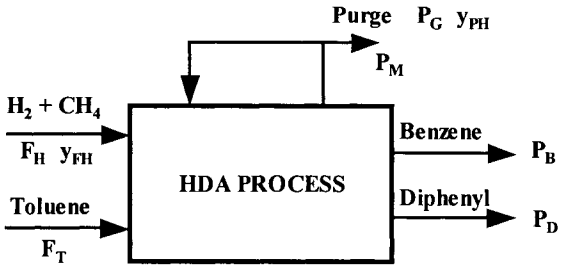

Figure 7.6 Input/Output structure of the HDA process

Note also that the per-pass conversion of toluene is not necessarily one, but it will not influence the Input/Output material balance in this case, because we neglected the by-product formation.

Table 7.3 Simplified Input/Output material balance for HDA process

Component	Input			Output			
	Hydrogen	Toluene	Total	Benzene	Diphenyl	Purge	Total
H_2	100	-		-	-	-	
CH_4	5.26	-		-	-	105.26	
Benzene	-	-		100	-	-	
Toluene	-	100		-	-	-	
Diphenyl	-	-		-	-	-	
Total kmol/h	105.26	100		100	0	105.26	
Mw	2.7	92		78	154	16	
Total kg/h	284.21	9200	9484.21	7800	0	1684.21	9484.21

b. Rigorous material balance

Now we consider the formation of by-products, as well as the possibility to feed some reactants in excess. The selectivity of the main reaction is given by the following relation (Douglas, 1988):

$$S = 1 - 0.0036 / (1 - x_T)^{1.55} \tag{7.1}$$

where x_T is the toluene conversion to benzene. Graphical representation (Fig. 7.7) shows that the selectivity is high up to a conversion of 0.5, but drops rapidly after. Clearly, the conversion is an important design variable at the Input/Output level.

The next step in procedure is to formulate the material balance as a function of dominant design variables, toluene conversion, and excess of hydrogen. In this case, it is possible to examine the problem analytically (for notations see Fig. 7.6).

- P_B, P_D, P_M, P_G : molar rate of benzene, diphenyl and methane, and purge flow.
- F_T, F_H : molar feed of toluene and hydrogen.

- y_{FH} , y_{PH} : hydrogen mole fraction in feed and purge.

The following equations describe the material balance for a given production rate.

$$F_T = \frac{P_B}{S} \quad \text{(i)} \qquad P_M = \frac{P_B}{S} \quad \text{(ii)} \qquad P_D = \frac{P_B}{S}\frac{1-S}{2} \quad \text{(iii)}$$

$$y_{FH}F_H = \frac{P_B}{S} - \frac{P_B}{2S}(1-S) + P_G y_{PH} \quad \text{(iv)}$$

$$(1-y_{FH})F_H + \frac{P_B}{S} = (1-y_{PH})P_G \quad \text{(v)}$$

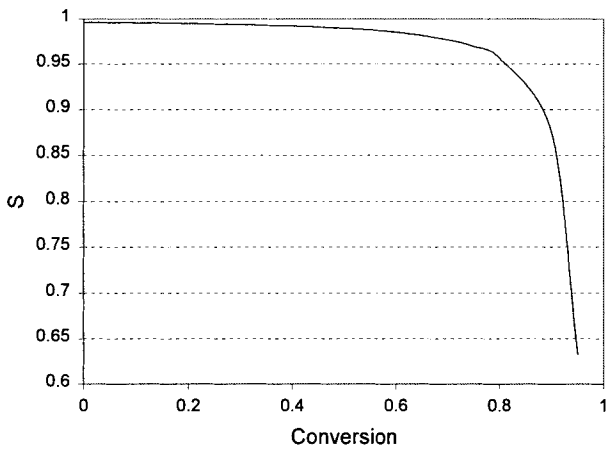

Figure 7.7 Selectivity of as function of conversion

The combination of equations (iv) and (v) gives the purge flow rate for given production, selectivity and input of hydrogen:

$$P_G = F_H + \frac{P_B}{S}\frac{1-S}{2} \quad \text{(vi)}$$

From (v) and (vi) the following relation for the make-up hydrogen can be found:

$$F_H = \frac{P_B[1-(1-y_{PH})\frac{1-S}{2}]}{S(y_{FH}-y_{PH})} \quad \text{(vii)}$$

Because hydrogen concentration in feed y_{FH} is fixed, it might be concluded that the purge concentration y_{PH} might be another design variable. However, equation (vii) indicates that y_{PH} cannot be set independently of the hydrogen feed. The result is

important for the process control strategy. Controlling both make-up hydrogen and hydrogen concentration in purge is not possible for the simple reason that the problem is over-specified at steady state.

Table 7.4 presents the material balance for the following design variables: conversion 0.75 giving selectivity 0.969, and hydrogen excess of 40%. Comparison with simplified analysis shows an increase of material consumption with 4.3%. This is due mainly to the formation of by-product, but the purge rate increases too.

The main conclusion from this simple example is that important design decisions can be taken at the Input/Output level. Material balance analysis must consider the reaction selectivity. Impurities present in raw materials or formed by reactions generate environmental problems that must be detected at very early stages.

Table 7.4 Rigorous Input/Output material balance for HDA process

Component	Input			Output			
	Hydrogen	Toluene	Total	Benzene	Diphenyl	Purge	Total
H2	140	0		0	0	38.40	
CH4	7.37	0		0	0	110.57	
Benzene	0	0		100	0	0	
Toluene	0	103.20		0	0	0	
Diphenyl	0	0		0	1.60	0	
Total kmol/h	147.37	103.20		100	1.60	148.97	
Mw	2.7	92		78	154	12.39	
Total kg/h	397.89	9494.70	9892.60	7800	246.65	1845.94	9892.60

7.4.3 Economic Potential

At each level of the Hierarchical Approach the feasibility of design alternatives are evaluated by means of an *Economic Potential (EP)*. This index is a measure of profitability representing the difference between earnings and expenses on yearly basis. *EP* must be high enough to accept further reduction at the other levels of flowsheet development. If *EP* is not positive and high enough, the analysis stops. It is worthy to note that the raw material costs dominate the operation costs in chemical process industries by more than 60%, particularly in commodities.

Uncertainties in costs can have a major impact in evaluating the feasibility of a process. Fluctuations of product prices are easier to manage, because they are regulated by the market. The prices of raw materials are more uncertain. These should consider the transportation costs, whose contribution is significant for remote sources. Internal prices of commodity chemicals are much more advantageous on an integrated platform.

An important observation is that in a highly uncertain environment the computation of an Economic Potential at I/O level can put minimum/maximum targets for selling and acquisition prices, respectively. As a rule of thumb, the ratio of product selling price to raw materials purchasing price should be greater than two (see an explanation in Chapter 15). If the economic environment is highly uncertain, the comparison of

alternatives could be done on the basis of only cumulative operating costs, excluding raw materials.

Sensitivity analysis can estimate the risks with respect to each cost element. Although the procedure varies for each organisation, the values in the Table 7.5 may be used as reasonable (Gary and Handwerk, 1994):

Table 7.5 Range of variables for a sensitivity analysis of the Economic Potential

	Decrease by %	Increase by %
Product prices	5	5
Raw materials costs	3	5
Investment costs	15	20
Operating volumes	5	2

In conclusion, at the *Input/Output* stage (Level 2) the computation of the Economic Potential considers only material costs, including the treatment of waste generated by by-products and impurities, following the relation:

$$EP_2 = \{\text{Product value}\} + \{\text{By-product value}\} - \{\text{Raw material costs}\} - \{\text{Waste treatment cost}\} \quad (7.2)$$

In the case of the HDA process we get:

$$EP_2 = \{\text{Benzene cost}\} + \{\text{Fuel value of di-phenyl}\} + \{\text{Fuel value of purge}\} - \{\text{Toluen cost}\} - \{\text{Make-up gas cost}\}$$

Table 7.6 Prices for HDA process

Materials		Cost	Utilities	Unit	Cost
Toluene	$/tone	170	Electricity	$/kWh	0.5
Hydrogen	$/tone	350	Fuel (methane)	$/GJ	2.5
Benzene	$/tone	570	Water (chilled 10 °C)	$/m^3	0.15 (0.30)
Diphenyl (fuel)	$/tone	100	Steam (boilers)	$/tone	15
Purge (fuel)	$/tone	50	Refrigeration	$/GJ	400

Plotting EP_2 as function of conversion can bound the domain of feasible designs. Fig. 7.8 presents curves for 10%, 30% and 70% excess of hydrogen. If $H_{2,ex}$ is the excess of hydrogen, the purge concentration should be $H_{2,ex}/(1+H_{2,ex})$, but it varies slightly with the conversion because of the secondary reaction. The examination of the results reveals that EP_2 is very sensitive with the excess of hydrogen. Optimal hydrogen/toluene should be close to the stoichiometric ratio, because the purge value is much lower than the hydrogen price. In this case, the maximum conversion is limited at approximately 0.8, but there is no indication about the lower bound. The lower bound will be set by evaluating the cost of recycles.

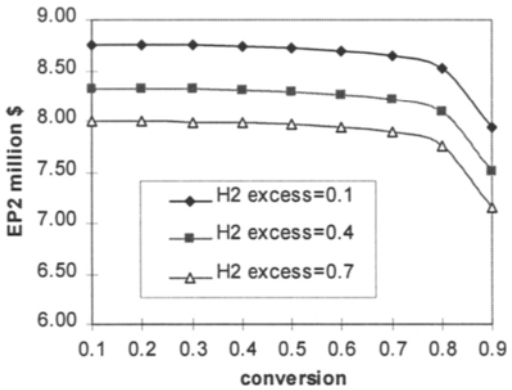

Figure 7.8 Economic Potential at the Input/Output level

7.5 REACTOR DESIGN AND RECYCLE STRUCTURE

The behaviour of the reactor determines the recycle structure of a flowsheet. In this respect, the following aspects have to be analysed (Douglas, 1988):

1. Number of recycle streams.
2. Excess of some reactants at the reactor inlet.
3. Chemical equilibrium.
4. Cost of the reactor system.
5. Cost of recycles, particularly of gas compression
6. Energy management around the reactor system.

The next sections will examine each aspect in more detail.

7.5.1 Number of recycle streams

Finding the recycle streams consists of the following steps:

- Firstly, associate reaction steps with reactor numbers.
- Then, associate feed streams and recycle streams with reactor numbers, taking into account the path of individual components. To do this, consider the list of all components leaving the reactor ranked by their normal boiling point.
- Group recycle components with neighbouring boiling points, if they have the same reactor destination. The number of recycle streams is merely the number of groups identified above.

The following heuristic should be obvious: Do not separate two components and then remix them at a reactor inlet. We must also have in mind the significant difference between the cost of recycling a gas or a liquid. Compressors are very expensive and the cost of compression is very high, whereas the cost of pumping is much lower, except in special applications (viscous liquids, slurries, aggressive solutions, etc).

As illustration, consider the definition of product and recycle streams in HDA process. The design decision is: not recycle diphenyl. Table 7.7 presents the analysis following the above procedure. The result is that there are two recycle streams, gas recycling hydrogen and methane, and liquid recycling toluene.

Table 7.7 Product and Recycle streams in HDA process

Component	Normal Boiling Point, °C	Destination Code
Hydrogen	-253	Gas Recycle
		Purge
Methane	-161	Gas Recycle
		Purge
Benzene	80	Primary product
Toluene	111	Recycle-liquid
Diphenyl	253	Fuel by-product

7.5.2 Material balance with recycles

The central issue in performing the material balance with recycles is the behaviour of the reaction system. Besides conversion, a design variable inherited from the previous level, the molar reactant ratio becomes now a design variable, which will affect the flow rate of the recycle streams. Note that the assumption of 100% overall recovery of unconverted reactants is maintained.

Excess reactant

Use of a reactant above the stoichiometric ratio can bring some advantages, as:

- Shift the maximum conversion for equilibrium controlled reactions.
- Shift the component distribution by kinetic effects.
- Help to convert completely an unrecoverable reactant.
- Increase the rate of heat and mass transfer.
- Prevent undesired secondary reactions.

As mentioned, the excess of a reactant at the reactor inlet should be realised by means of recycles, and not by feeding fresh reactant above the stoichiometric ratio! However, if this happens, because of technological reasons, as difficult recovery or low reactant price, the excess must be removed in purge or bleed stream. In this case, the excess of reactant becomes an optimisation variable.

Material balance

In general, the material balance problem can be solved simply by means of a flowsheeting simulator replacing the whole separation section by a single black-box. In some cases, the problem can be solved analytically, as for HDA process (Fig. 7.9). If F_T and F_R are fresh feed and recycled toluene then the reactor feed F_0 is:

$$F_0 = F_T + F_R \tag{7.3}$$

The recycle flow and the conversion of toluene are related by the relation:

$$F_R = F_T(1-x_T)/x_T \tag{7.4}$$

Note that when the conversion approaches zero the recycle flow becomes infinitely large, while at total conversion the recycle is zero.

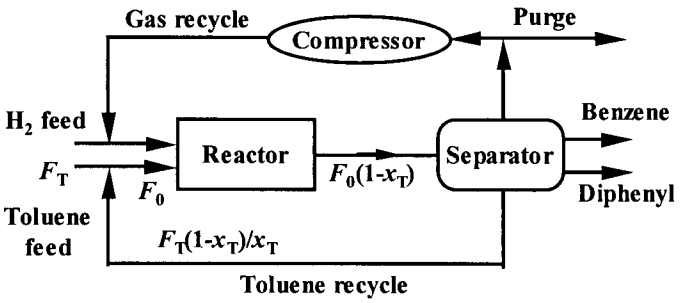

Figure 7.9 Recycle structure of the HDA plant

After estimating the recycle of the limiting reactant, we may use the specification for the molar ratio(s) of reactants to obtain the flows of the other component(s). We may write the following equation for hydrogen balance at the reactor inlet:

$$y_{FH}F_H + y_{PH}R_G = M_R(\frac{F_T}{x_T}) \tag{7.5}$$

R_G is the flow rate of the gas recycle and M_R the molar ratio hydrogen/toluene at the reactor inlet. Equation (7.5) gives the gas recycle if the input of hydrogen and toluene are specified. Further, we may work out the relation that links the feed of toluene F_T and of hydrogen F_H as function of production, selectivity and purge concentration in hydrogen (see Example 7.3). Finally, for the gas recycle we obtain the relation:

$$R_G = \frac{P_B}{Sy_{PH}}\left(\frac{M_R}{x_T} - \frac{y_{PH}}{y_{FH}-y_{PH}}\frac{1-S}{2}\right) \tag{7.6}$$

The Equation (7.6) indicates that as design variables we may choose x_T (conversion), y_{PH} (fraction of hydrogen in purge) and M_R (molar ratio). Unfortunately, there are no design heuristics to guide their selection. This issue is in fact a constraint optimisation problem, the objective function being the Economic Potential at the level of recycle stricture Level 3 (see later in this chapter).

It is worthy to note that we could be tempted to set these values as specifications when designing the plant control structure. However, some specifications might be in conflict. As it can be seen from the relation (7.5), it is not possible to control simultaneously gas recycle flow, ratio hydrogen/toluene and hydrogen concentration in purge. Normally, it is recommended to fix the recycle flow rate R_G at the maximum capacity of the compressor. If M_R is imposed since technological reasons, it comes out that y_{PH} must be let free. This is again an important plantwide control decision that can

be obtained by analysing only the input/output material balance! Chapter 13 will analyse this issue in more detail.

7.5.3 Reactor design issues

Stoichiometry and kinetics

The chemical reactor has a determinant role on both the material balance and the structure of the whole flowsheet. It is important to stress that the downstream levels in the Hierarchical Approach, as the separation system and heat integration, depend entirely on the composition of the reactor exit stream. However, a comprehensive kinetic model of the reaction network is hardly available at an early conceptual stage. To overcome this shortcoming, in a first attempt we may neglect the interaction between the reactor and the rest of the process, and use an analysis based on stoichiometry. A reliable quantitative relationship between the input and the output molar flow rates of components would be sufficient. This information is usually available from laboratory studies on chemistry. Kinetics requires much more effort, which may be justified only after proving that the process is feasible. Note that the detailed description of stoichiometry, taking into account the formation of sub-products and impurities is not a trivial task. The effort is necessary, because otherwise the separation system will be largely underestimated.

Heat effects

A good measure of the heat effects associated with a chemical reaction is the adiabatic temperature change, ΔT_{ad}. This can be computed from the relation:

$$\Delta T_{ad} = T_{R,out} - T_{R,in} = \frac{-\Delta H_R}{FC_p} \tag{7.7}$$

$T_{R,in}$ and $T_{R,out}$ are the input and output temperatures, ΔH_R being the heat of reaction, F the molar feed, and C_P the mixture heat capacity. The adiabatic change of temperature may serve to compare different alternatives regarding the reaction system, even if the reactor itself is not an adiabatic one. Some design guidelines are as follows:

1. Exothermic reactions. If $\Delta T_{ad} > 0$ is too high, then:
   - Increase the flow rate and/or lower the per-pass conversion.
   - Use a heat carrier to remove heat (example excess hydrogen).
   - Consider the heat transfer to a cold source.
2. Endothermic reactions. If $\Delta T_{ad} < 0$ is too high, then:
   - Preheat the reactants at sufficiently high temperature.
   - Consider the heat transfer from a hot source.
   - Use a direct heat carrier to supply heat (example steam).
   - Consider the possibility of internal heat generation by exothermic reactions (example in-situ combustion).

Equilibrium limitations

1. Reversible exothermic reactions
In this situation it is necessary to optimise the temperature profile. Higher temperature is advantageous for the reaction rate, but not for equilibrium conversion, while lower temperature has the opposite effect. For this reason, the reaction should start at a higher temperature and end at a lower one.
2. Reversible endothermic reactions
The reaction temperature should be set as high as the technological constraints allow. Use of heat carriers may be considered, as steam, hot gas or solid inert. If the number of moles increases by reaction, the dilution with inert shifts the equilibrium conversion to higher values. However, more energy is needed for inert recycling. Therefore, the molar ratio inert/hydrocarbon is an optimisation variable.
3. Equilibrium reaction with separation (distillation, extraction)
Removal of a by-product by means of a separative operation (distillation, stripping, extraction, membrane) can bring the conversion to completition. An important application is the *Reactive Distillation*, discussed later in this chapter.

Reactor selection, design and simulation

The selection and design of a chemical reactor is covered in Chapter 8. As mentioned, in an early stage of process development a detailed stoichiometric description is sufficient. Kinetics is necessary only when the recycles have significant influence on products' distribution and in consequence on separations. In this case, accurate modelling of the whole reaction system is required, which often is not a simple matter.

A practical way to overcome the above shortcoming is to combine a kinetic simulation mode for the main reaction(s) with a stoichiometric description of by-products and impurities. The recycle flow rates will reflect the performances of the reaction system for a given design, but the separation system will be not underestimated. This approach is very advantageous when assessing the plant flexibility to large variations in throughput or when studying the process dynamics.

7.5.4 Economic Potential with recycles

Level 3 includes the first elements of the flowsheet structure. The central issue is the cost of recycles. However, only some elements can be expressed quantitatively. The easiest is the cost for recycling fluids, as gases via compressors. Because the recycle flow rate varies inverse proportionally with the conversion, the cost of recycling fluids introduces the first element setting a lower bound for conversion. The next element is the cost of the reactor, including devices for feed conditioning. Because kinetic information is hardly available in an evaluation project, the reactor cost can be estimated only loosely. The cost of separations that deliver the recycle streams is yet not known. Hence, the formula for computing the Economic Potential at the Level 3 is:

$$EP_3 = \{\text{Product value}\}+\{\text{By-product value}\}-\{\text{Raw-mat. costs}\} - \\ -\{\text{Waste costs}\}-\{\text{Reaction system costs}\}-\{\text{Recycle costs}\} \quad (7.8)$$

The rationale of computing an economic potential at the *Level 3* is to consolidate the design of the reaction system. There are three aspects of interest :

a) Evaluate alternatives for the selection of the *reactor type*. For example, a gas-phase catalytic reactor can be compared against a slurry gas/liquid reactor.

b) Evaluate alternatives for the *reactor design*. For example, we may have interest to compare a heat carrier versus a heat transfer system.

c) Define the *optimality range* for design variables characterising the reactor system. These are usually temperature, pressure, conversion, and reactant ratio. The central issue is the optimal domain for conversion. Because the conversion determines both the nature and the flow rates of the chemical species, this variable affects decisively the separation system.

The cost of recycles

The cost of recycles considers only the transport and the conditioning of the fluid between the separation section and reactor. Gas recycling is expensive because needs a compressor. On the contrary, the cost of pumping liquids is in most cases negligible.

Usually the compressor is multi-staged with intermediate cooling. The number N of stages can be calculated with the formula:

$$N = \log(P_N / P_0) / \log K \tag{7.9}$$

P_0 and P_N are the initial and final pressures. K is the compression factor, typically between 3 to 4 for piston compressors, and 1.1 to 1.5 for turbo-compressors. The cost of the equipment can be estimated based on the power for adiabatic compression. For multistage stage compression with intermediate cooling at the inlet temperature T_0 the compression power W is given by the relation:

$$W = N \frac{\gamma}{\gamma - 1} \frac{GRT_0}{M_w} \left[K^{(\gamma-1)/\gamma} - 1 \right] \tag{7.10}$$

G is the mass flow rate, M_w the gas molecular weight, R universal gas constant, and γ the isentropic compression coefficient. The effective work can be obtained dividing W by the compressor efficiency, usually between 0.8 and 0.9.

The cost of gas recycle can be expressed as an operation cost, proportional with the compressor power, plus the installed cost IC expressed on an annualised basis. A reasonable payback time is three years. The annual cost of gas recycle is:

$$TAC_{gas} = 8150*W*e + IC/3 \tag{7.11}$$

In the relation (7.11) e is the cost of electricity and 8150 the annual hours of operation. Because the cost of the compression is high, the pressure drop in the gas recycle loop should be minimised. Another solution is exploring the possibility of producing power internally, as for example by gas or steam turbines.

Note that the cost of expensive equipment for thermal conditioning of reactants should be accounted for, as furnaces, as well as the cost of heat carriers, or devices needed for conditioning solid recycled reactants.

EXAMPLE 7.4 Economic Potential with recycles for HDA process

The Economic Potential at the Level 3 is:

$$EP_3 = \text{Benzenecost} + \text{Fuel value of diphenil+Fuel value of purge} \\ \text{-Toluen cost - Makeup gas cost-Compresor cost - Furnace cost- Reactor cost} \quad (7.12)$$

The design decision is to set the hydrogen/toluene molar ratio at the reactor inlet at 5:1. We fix also the purge concentration in hydrogen, y_{PH}. Consequently, the make-up hydrogen is left free.

Tables of material balance with recycles have been prepared for different conversions of toluene with y_{PH} as parameter. Fig. 7.10 displays gas-recycle flow rate against conversion for hydrogen purge concentration of 0.1, 0.4 and 0.7. The plot shows a large variation of the gas flow rate with conversion, over several orders of magnitude, for the concentration of H_2 in purge between 0.1 and 0.7. Therefore, it is rational to work at higher conversion, but also with substantial excess in hydrogen.

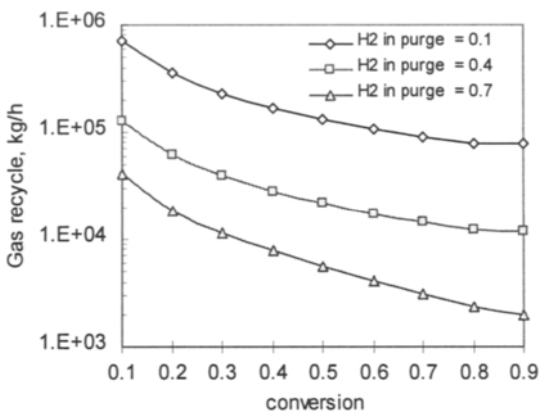

Figure 7.10 Gas recycle versus conversion with hydrogen in purge as parameter

The next step is to evaluate the cost of recycles. In a first attempt we consider only the gas recycle. The compressor power is computed with the equation 7.10, taking a pressure ratio in the gas loop of 1.15. The cost of the compressor can be estimated by the factorial method (see Chapter 15). Generally, the cost correlation has the form:

$$\text{Cost,\$} = (\text{M\&S}/280)\times(\text{constant})\times(\text{capacity})^{\alpha}\times(\text{correctionfactor})$$

M&S is an inflation factor for the chemical equipment. More information is given in the section 15.4.3. M&S was 1060 in mid 1998. Next, the cost of gas recycle is computed by lumping the contributions of capital and operating costs. We consider a payback

time of three years as generally acceptable. The total annual recycle cost becomes: Recycle Cost = 0.333×Installed Cost + *Operating Costs*.

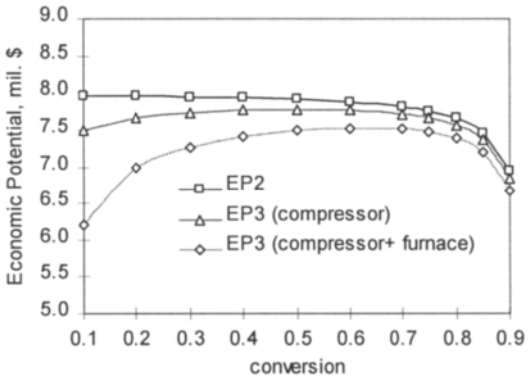

Figure 7.11 Economic Potential with recycle

We proceed with a first evaluation of EP_3 for the prices given in Table 7.8. Fig. 7.11 displays EP_3 against conversion for hydrogen concentration in purge of 0.4. The first plot shows only the influence of gas recycle. It may be observed that the conversion range has been reduced to 0.4-0.8. The Economic Potential is sufficiently high, so we may proceed with the *Level 4*. Nevertheless, it would be interesting to examine other elements that might modify this analysis.

Therefore, we consider the cost of the reaction system. We have seen that a furnace is necessary to preheat the reaction mixture. A more careful analysis will indicate that this equipment is also necessary to 'stabilise' the reactor operation against possible multiple steady states (Bildea and Dimian, 1998). We can again apply the factorial method, where the duty is the measure of the equipment capacity. The furnace duty can be determined by considering a temperature increase from 520 °C to 620 °C. As before, annual-basis investment and costs are calculated. Fig. 7.12 presents the result as a second EP_3 plot. It can be seen that the optimum conversion is around 0.7.

7.6 GENERAL STRUCTURE OF THE SEPARATION SYSTEM

Level 4 of the Hierarchical Approach deals with the synthesis of the Separation System. A separation problem can be formulated as follows:

For given data (flow rate, composition, product specifications, and potential separation methods) find at least a separation sequence that fulfils the product requirements with minimum costs.

The methodology that we develop in this section consists of decomposing the complex problem in sub-problems, for which partial solutions can be found easier. By analysing the generic problem of separations, Douglas (1988) found the following sub-levels:

Level 4a - General structure.
Level 4b - Vapour Recovery System and Gas Separations.
Level 4c - Solid Recovery System and Solid Separations.
Level 4d - Liquid Separation System.
Level 4e - Combine the separation systems for multiple plants.

The methodology for flowsheet synthesis presented in this book combines the Hierarchical Methodology of Douglas with a knowledge-based approach, proposed by Barnicki and Fair (1990, 1992). Since distillation is the main separation method, the reader should be familiar with modern design concepts described in specialised books as written by Kister (1992), and more recently by Stichlmair & Fair (1999) and Doherty & Malone (2001). For a more detailed treatment of separation techniques, we recommend the book of Seader and Henley (1998).

The structure of the separations is determined by the composition and the thermodynamic properties of the mixture leaving the reactor. The first phase-split is essential, because it enables the decomposition of the separation problem in sub-problems or subsystems, where specific systematic procedures can be applied. Therefore, we will start the flowsheet development by examining this key topic.

7.6.1 Phase condition of the reactor effluent

We will analyse some simple cases, after which their generalisation in the frame of a superstructure will be easier to understand.

1. Liquid reactor effluent

A liquid reactor effluent may be of the following types:
(1) Homogeneous organic or aqueous fluid.
(2) Homogeneous fluid that can split in two liquid phases by further cooling.
(3) Homogeneous fluid that can separate a second solid phase by crystallisation.
(4) Three phase liquid/liquid/solid mixture.
Fig. 7.12 displays the structure of the separation problem of type 1 with a single liquid separation system.

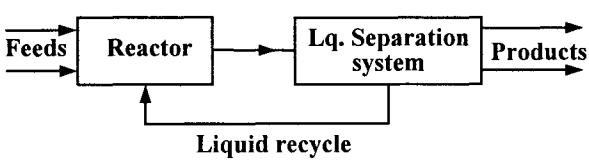

Figure 7.12 Recycle structure for liquid reactor effluent

2. Two-phase (vapour and liquid) reactor effluent

A heterogeneous gas/liquid reactor illustrates a two-phase effluent (Fig. 7.13). The two phases are already present inside the reaction space. Vapour phase may undergo a new phase-split after condensation. The secondary vapour enters the vapour separation system. Gaseous reactants are recycled to the reactor, but purge may be necessary to eliminate gaseous products or avoid the accumulation of inert. The liquid streams from phase split and vapour recovery are sent to the liquid separation system, from which the liquid reactant is recycled.

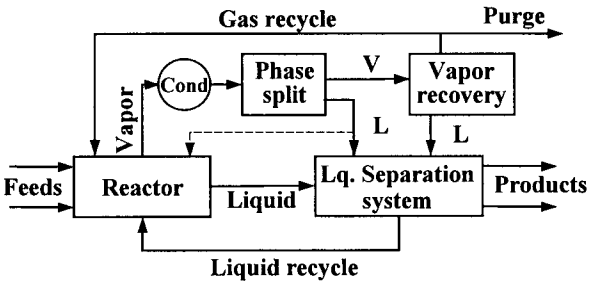

Figure 7.13 Recycle structure for two-phase reactor effluent

3. Vapour-phase reactor effluent

The effluent reactor mixture is normally submitted to condensation. Two situations will be examined following the thermodynamic behaviour of the components.

a. Condensable/non-condensable components

Firstly, the mixture must be condensed and split in gas and liquid phases in a flash vessel (Fig. 7.14). The condensable components are sent to the liquid separation system, while the non-condensable components are treated in the gas separation system. Another solution is applying a quench to the reactor outlet with recycled solvent.

The phase-split block can be a single flash, a series of flashes, or a combination of flash and absorption/stripping columns. Flash temperature and pressure are design variable that may be optimised to fulfil a separation objective, as sharp gas/liquid split or recovery of some components. For water-driven condensers the recommended condensation temperature is of about 35 °C. Vapour components can be condensed and sent to the liquid separation system. The supercritical components carried in the liquid phase can be recovered in a stabiliser column (see later in this section). Further, these can be sent to the gas separation system, used as fuel, or purged.

b. Non-condensable (supercritical) components

In this case, there is only a gas separation system. The separation of valuable product, from the reaction mixture can take place by appropriate methods, as selective adsorption/desorption with solvents, described later in this chapter. An example is the separation and purification of acetylene with various solvents, as NMP or DMF.

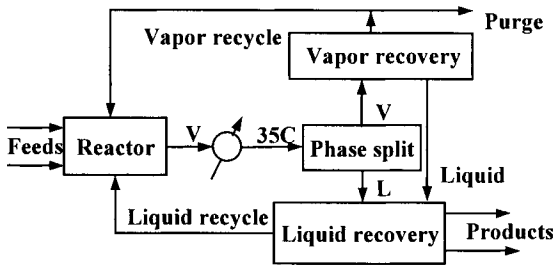

Figure 7.14 Recycle structure for a vapour phase reactor effluent

---

EXAMPLE 7.5 Separation subsystems in the HDA process

The reactor effluent in the HDA process contains both condensable components and non-condensable species. Examine the separation of these components by a first split.

Solution. Fig. 7.15 illustrates the structure of the separation system, where the first separation step is a simple gas-liquid flash. The gas outlet contains H_2 and CH_4 with traces of benzene and toluene, while the liquid outlet consists of benzene and toluene, with small amounts of H_2 and CH_4.

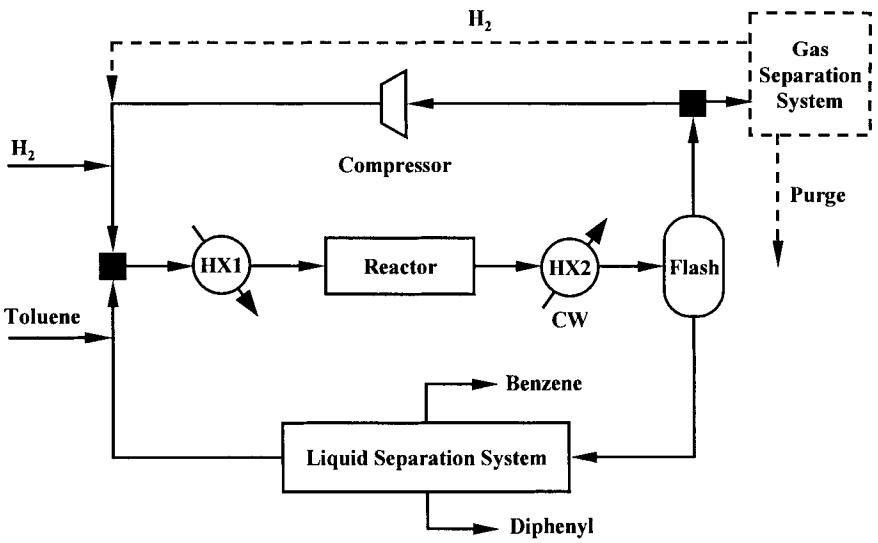

Figure 7.15 Separation subsystems of HDA process

Table 7.8 presents *K*-values and phase compositions computed by Aspen Plus with Peng-Robinson EOS. The following remarks are useful:

- Large differences in *K*-values between condensable and non-condensable components give sharp condensation temperature.
- *K*-values vary significantly with the pressure for supercritical components, but only slightly with the temperature. The trend is opposite for condensable components.
- Flash temperature and pressure are optimisation variables, which should ensure a compromise between the losses of benzene and hydrogen in the gas and liquid streams, respectively. The cost of recycling hydrogen sets a lower bound for pressure, while the temperature is constraint by the available cooling agent.
- After solving the first separation step the solution of the whole problem is greatly simplified. Hydrogen-rich gas is recycled, but alternatively it can be sent to the gas separation system for methane recovery. The synthesis of the liquid separation system can be also examined separately.

Table 7.8 Split of components in a flash (mole fraction/K-value)

Components	P (bar)	T=20 °C			T=40 °C		
		x	*y*	*K*	*x*	*y*	*K*
H_2	30	3.74E-03	0.400	106.9	4.07E-03	0.397	97.7
	40	5.06E-03	0.401	79.1	5.50E-03	0.398	72.5
CH_4	30	4.48E-02	0.596	13.3	4.13E-02	0.593	14.4
	40	5.83E-02	0.596	10.2	5.40E-02	0.594	11.0
C_6H_6	30	0.648	3.64E-03	5.62E-03	0.640	7.95E-03	1.24E-02
	40	0.639	3.12E-03	4.88E-03	0.634	6.69E-03	1.06E-02
C_7H_{10}	30	0.296	5.13E-04	1.73E-03	0.306	1.30E-03	4.23E-03
	40	0.290	4.51E-04	1.56E-03	0.298	1.10E-03	3.69E-03

7.6.2 First phase split

1. Gas/Liquid systems

A first evaluation of phase separation may be obtained by performing a flash at 35 °C. *K*-values larger than 10 are characteristic for gas-phase components, while *K*-values smaller than 0.1 indicate condensing components. Another method is ranking the components by normal boiling points. Table 7.9 shows the relation between the normal boiling point T_b and the pressure needed to separate the component by simple distillation (Barnicky & Fair, 1992). Gases are components with T_b < -20 °C, which would require a distillation pressure higher than 25 bars. In general, the condensable components have boiling points above 50 °C and can be separated by distillation at pressures below five bars. For the intermediate range, there is no obvious choice. The component will be shared between gas and liquid separations. Note that if complete condensation can be obtained by acceptable temperature and pressure combination, the distillation is in many cases the best separation method.

Table 7.9 Grouping of components by distillation separation

Component group	Boiling point range, °C	Distillation pressure range, bar	Condenser type
gas	$T_b < -20$	$P > 25$	refrigeration
gas-liquid	$-20 < T_b < 0$	$15 < P < 25$	partial
	$0 < T_b < 50$	$P < 15$	total
liquid	$T_b > 50$	$P < 15$	total

The following techniques can be used as the first separation step (Fig. 7.16):

- Simple V/L flash or sequence of flashes.
- Physical or chemical absorption.
- Reboiled stripping.

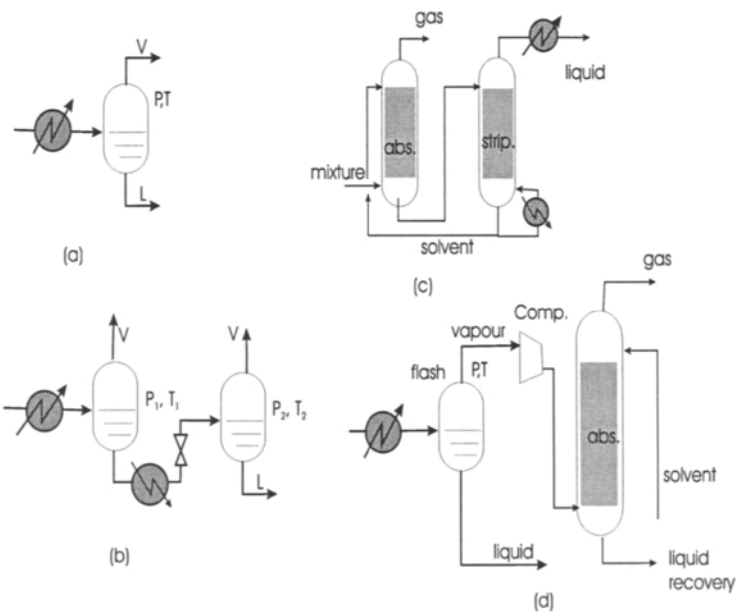

Figure 7.16 Techniques for the first separation step

Simple flash is suitable in a large number of cases, when the difference in K-values between light and heavies is quite large, over 10 (Fig. 7.16a). Pressure and temperature are optimisation variables against recovery specifications. Better separation can be obtained in more stages with intermediate heating/cooling, in which the temperatures and pressures are also subject to optimisation (Fig. 7.16b).

Advanced recovery can be realised by means of a gas-absorption device. The absorbent can be a process stream or a recycled solvent (Fig. 7.16c). When reactive components are present in the gas phase the separation can involve absorption with chemical reaction. If the pressure of the original stream is not sufficient, vapour recompression could be used to improve the separation after a first flash (Fig. 7.16d).

Reboiled stripping is an efficient first-step technique for mixtures containing an important amount of light and intermediate components. An example is the separation of C2/C3 components from a mixture issued from fluid catalytic cracking. The original stream serving is sent to the top of a distillation column that is provided only with reboiler. The top product contains gases and light components stripped-out by the vapour produced in the reboiler, while the bottoms collect the remaining heavy components. Note that the temperature of the inlet mixture stream should be low enough to prevent the entrainment of heavier components in the top product. A recycled heavy solvent may be used to increase the efficiency of the separation, in which case the mixture to be separated is fed in a lower position.

2. Gas/Liquid/Solid systems

Solid particles can be present in the reactor liquid effluent or generated by deeper cooling. Another method is precipitation of solids by means of a suitable Mass Separation Agent (MSA). This technique is more expensive than simple cooling, because it introduces a new recycle loop. Adding water might lead to waste treatment problem. After precipitation, the suspension is sent to filter or centrifuge. In general, two liquid recovery systems are generated, for reactant and solvent, respectively.

7.6.3 Superstructure of the separation system

The separation systems studied so far can be assembled in a 'superstructure', as presented in the Fig. 7.17 (Douglas, 1995). It may be observed that the subsystems are interconnected. Because recycling is not economical, a challenge for designer is to minimise the number and the flow rates of recycles. Special attention should be paid to accumulation of by-products and impurities, because of interactions through recycles. Some methods will be presented when discussing the gas recovery & separation system. Here we only mention that the chemical conversion of impurities accumulated in recycles is often a better solution than the physical treatment. As an example, we may cite the combustion of organic components or the selective hydrogenation of non-saturated hydrocarbons.

Regarding the strategy, in the first place should be considered the synthesis of the vapour recovery and gas separation systems, from which recovered condensable components are sent to the liquid separation system. For the same reason, the synthesis of the solid recovery and solid separation systems should be placed in the second place. The subsystems for gas and solid separations are largely uncoupled, and can be treated as stand-alone. Thus, the synthesis of liquid separation system is the last, but by far the most difficult. Its decomposition in subsystems is again the best approach.

The inspection of the superstructure illustrated by the Fig. 7.17 emphasises again the role of the first-separation step. Sharp recovery will minimise the interactions between subsystems. On the other hand, the selection of the separation techniques and the design of units should bring flexibility to prevent bottlenecks. For example, adsorption or membranes should not be used in the first split, but could be certainly considered in the synthesis of the subsystem for gas separations.

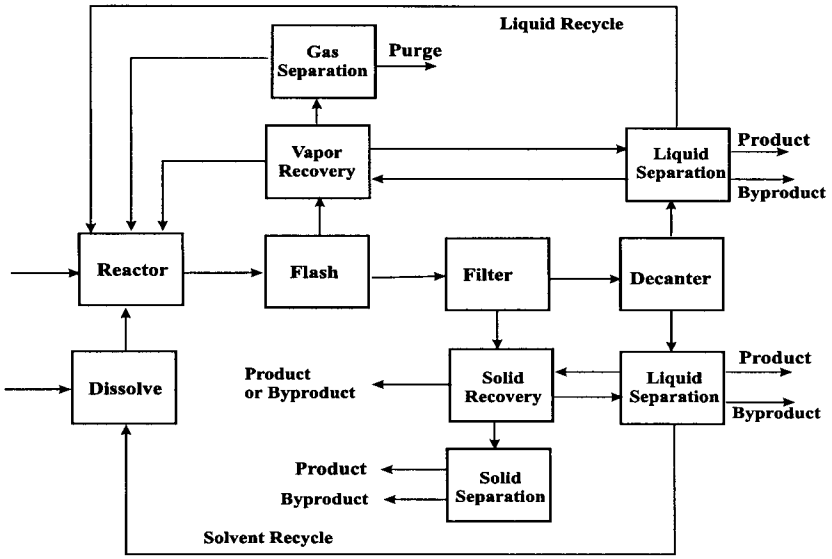

Figure 7.17 Superstructure of the separation system (after Douglas, 1995)

7.6.4 Knowledge-based synthesis approach

The principle of the knowledge-based approach for the synthesis of separation systems (Barnicki & Fair, 1990, 1992) is displayed in Fig. 7.18. On the top of we place the generation of the superstructure of separations depicted in Fig. 7.17, where three separation subsystems have been identified:

1) Vapour Recovery & Gas Separation.
2) Liquid separations.
3) Solid separations.

Thus, the overall problem can be decomposed in smaller problems, namely the synthesis of separation subsystems. This activity can be done by means of specialised 'managers', in this case designated by Gas Split Manager (GSM), Liquid Split Manager (LSM) and Solid Split Manager (SSM).

The next step is a secondary decomposition of the separation problem of each subsystem by means of so-called 'selectors'. These designate groups of separation methods capable of splitting the initial mixture in sub-mixtures by a procedure that generates a separation sequence. For example, LSM can operate on two selectors: *zeotropic* and *azeotropic* separations. GSM can operate on three selectors: *enrichment*, *purification*, and *sharp split*.

The decomposition in selectors has as effect a significant reduction in the searching space of all possible separations. The managers are supported by a number of specialised 'designers' bringing the expertise necessary to implement the required task. Roughly, the designers can be identified with standard unit operations.

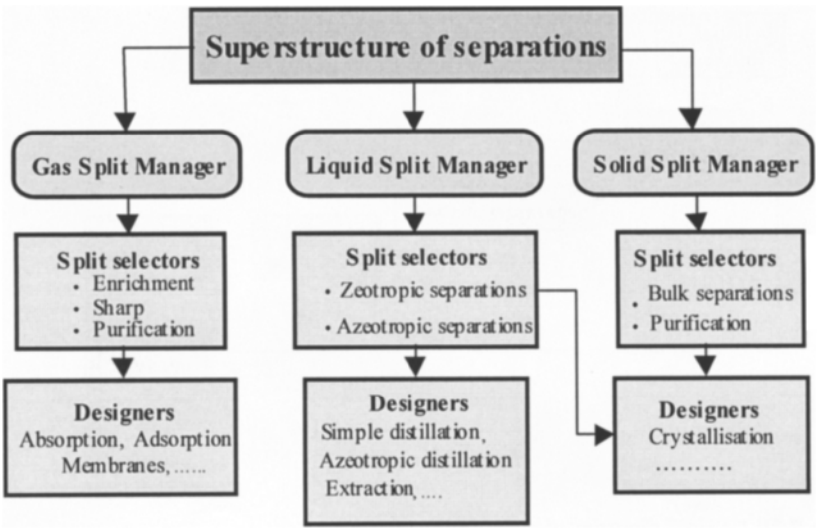

Figure 7.18 Separation synthesis hierarchy of a knowledge-based system

The synthesis of subsystems can be described by a logical diagram in Fig. 7.19. The steps are briefly explained below.

1. *Split generation.* Starting with the mixture composition and product specifications possible splits are proposed by making use of specific *heuristics*. Then the selected splits are placed in corresponding selectors.
2. *Selector analysis.* In each selector, a logical diagram will guide the identification of the suitable separation method. A split becomes 'potential' if it can be accomplished by at least one separation method. The selection of a separation method is supported by a *ranked list of characteristic properties*. For example, the relative volatility is a characteristic property for the separation of a mixture by simple distillation. However, it can be used only in for zeotropic mixtures, but not for azeotropic mixtures.
3. *Split sequencing.* The potential splits identified above are compared to decide the best to perform next. For instance, in the case of zeotropic mixtures the split sequencing may be assisted by heuristics, On the contrary, for azeotropic mixtures a more sophisticated approach is necessary, based on Residue Curve Maps.
4. *Separator design.* The goal of this activity is to determine the basic sizing elements of the unit operation performing the split, as well as the distribution of components in the resulting sub-mixtures. Each potential split selected at the step 3 is subject to a design procedure that may be of shortcut type or based on rigorous simulation.
5. *Sub-mixture analysis.* The composition of intermediate streams generated in each split is confronted against product specifications. The steps 1 to 4 are repeated for all the intermediate mixtures, until the generation of all products is accomplished.

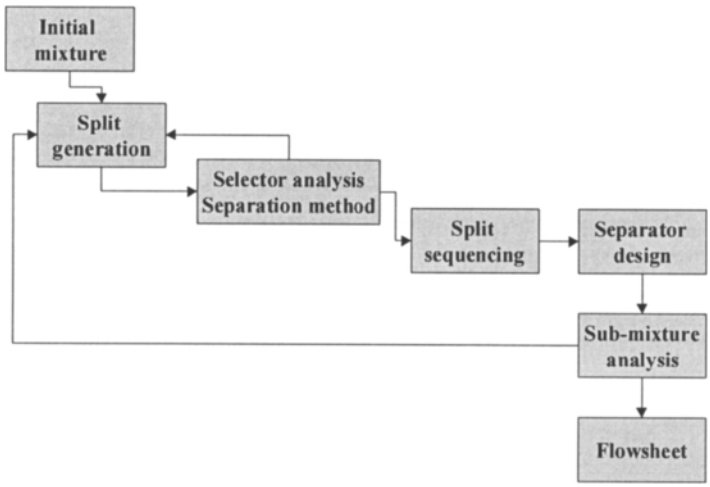

Figure 7.19 Logical diagram of a separation manager

Remarks:

1. The procedure does not necessarily lead to an unique solution, but rather to a number of alternatives, from which an optimal solution could be developed by more elaborated methods.
2. The synthesis of the liquid separation system is better founded by systematic methods as for vapour-phase or solid-phase separations. Computer simulation can be used to support the procedure, namely when distillation is the preferred method.

7.7 VAPOUR RECOVERY AND GAS SEPARATION SYSTEMS

Vapour Recovery system aims to recover valuable condensable components from a gas stream or to remove undesired components as corrosive, toxic, bad-odour, polymerisable, freezable, etc. The Gas Separation system has to separate recycled gaseous reactants, and to deliver purified products and by-products.

The location of the Vapour Recovery System is an important practical issue. Douglas (1988) recommends the following heuristics:

- On purge, if significant product amount is being lost.
- On the gas-recycle stream, if impurities could affect the reactor.
- On the vapour stream after flash, if both items 1 and 2 are valid.
- Do not use vapour recovery if neither item 1 nor 2 is important.

7.7.1 Selectors and separation methods

The Gas Separation Manager presented in this section includes both Vapour Recovery and Gas Separation systems. The flowsheet synthesis can be decomposed in subsystems following the following split selectors:

1) Enrichment separations.
2) Sharp separations.
3) Purifications.

Table 7.10 presents characteristic properties used for the sequencing of separations, as well as suitable separation methods.

Table 7.10 Methods used in vapour recovery and gas-phase separations

Method	Characteristic property	Condition	Observation
Condensation	Boiling points Relative volatility	Difference in boiling points > 40 C or $\alpha_{ij} > 7$	Optimise pressure and temperature
Cryogenic Distillation	Boiling points Relative volatility	$\alpha_{ij} > 2$	Large scale processes Remove first freezable components
Physical Absorption	Solubility	$S_{ij} > 4$	
Chemical Absorption	Reactive function as acid or base groups	Reversible process	Optimise the solvent ratio
Molecular Sieve Adsorption	Size / shape	Significant differences	Remove first fouling components
Equilibrium Limited Adsorption	Adsorption coefficient	Favourable adsorption	Remove first fouling components
Membranes	Perselectivity	Perselectivity greater than 15	Remove first fouling components
Catalytic oxidation	Chemical family	impurities below 10% of the flammability point	Do not destroy halogenated organics
Catalytic hydrogenation	Chemical family	Components containing double bound	Impurities more reactive with H2 than the bulk stream

The separation methods need some brief comments.

1. *Condensation.* This is the simplest separation, making use of higher pressure or lower temperature, or the combination of both. When the condensation temperature is bellow ambient, there is need for refrigerant. The temperature and pressure in a condensation operation are optimisation variables.

Heuristic: Separation by condensation may be considered when the relative volatility between the key components is greater than 7, or boiling point difference bigger as 40 °C.

2. *Desublimation.* Sometimes a solid phase can be obtained directly by desublimation, as for example the separation of phtalic anhydride by the oxidation of ortho-xylene.

3. *Physical Absorption.* The separation is based on differences in solubility of gases in a solvent. The selectivity index is defined as the ratio of liquid-phase mole fractions of two competing gaseous solutes, $S_{ij}^{abs} = x_i / x_j$. Normally, physical absorption is commonly combined with stripping. The common applications are in the area of enrichment and sharp separations.

Heuristic: If the selectivity is greater than 3 for enrichment, or than 4 for sharp separation, then the separation by physical absorption is feasible technique.

4. *Chemical Absorption.* In this operation, the separation involves a true chemical reaction between the gas solute and a solvent. Examples:
- Amine systems (MEA, DEA) for purification of gases CO2 and H2S,
- Sour gases absorption in alkaline water solutions,
- Special solvent formulation for gas purification (Solexol).

Chemical absorption is recommended for advanced purification of diluted gases, when ppm purity is required. Note that the use of a chemical solvent is costly.

Heuristic: If the species to be separated contain different acid-base functional groups (or if one contains neither), then chemical absorption, based on acid-base reaction, may be a feasible alternative.

5. *Adsorption.* Gaseous components (adsorbates) can be removed and recovered by selective adsorption/desorbtion by means of appropriate solid separation agents (adsorbents), as activated carbon, aluminium oxide, silica gel, synthetic zeolites (molecular sieves). Two types of adsorption may be distinguished: *Equilibrium Limited Adsorption, and Molecular Sieve Adsorption.*
Both adsorption and regeneration are operated periodically. The following methods can be considered for regeneration: Thermal Swing Adsorption (TSA), Pressure Swing Adsorption (PSA), inert gas stripping, and displacement desorption.

6. *Membrane separation.* Here the separation takes place by a selective diffusion of one or more gaseous components across a semi-permeable barrier. In most applications, the membrane is a micro-porous solid, but there are also liquid membranes. The feasibility may be evaluated by using an index of *perselectivity* α_{ij} defined by means of solubility (S_i) and diffusivity (D_i) ratios as follows:

$$\alpha_{ij} = \left[\frac{P_i}{P_j}\right] = \left[\frac{S_i}{S_j}\right]\left[\frac{D_i}{D_j}\right] \tag{7.13}$$

Heuristic: Membrane permeation can be feasible if α_{ij} is greater than 15.

7. *Cryogenic distillation.* Because of high pressures and low temperatures cryogenic distillation is feasible at higher throughput, usually more than 10-20 tons/day.

Heuristic: Consider cryogenic distillation only for bulk, sharp or enrichment separations involving high throughput, if the relative volatility of key components is greater than two.

8. *Catalytic conversion.* The most efficient way to prevent the accumulation of impurities that are difficult to remove is chemical conversion. Here we consider only two types of reactions: catalytic combustion and hydrogenation. By catalytic combustion, a gaseous impurity is destroyed to CO_2, SO_2, N_2 and H_2O. For safety reasons, the impurity concentration should be kept well below the lower explosion limit. By catalytic hydrogenation, unsaturated organic components are transformed in species easier to remove. High catalyst selectivity is required.

Here we mention as advanced technique the use of *supercritical water oxidation* (SCWO) for destroying organic impurities. Note that organic species become highly soluble in supercritical water. For example, highly harmful PCBs can be converted in benign small molecules, as CO_2, HCl and NH by oxidation is supercritical water. However, this is a typical end-of-pipe antipollution measure.

Heuristic: Consider catalytic oxidation to remove volatile organic impurities in concentration below 10% of the lower flammability point. Do not use it to destroy halogenated organics.

7.7.2 Sector analysis and split sequencing

Gas Separation Manager considers three selectors: enrichment separations, sharp separations and purifications. The selectors and suitable separation methods are described below. Table 7.11 presents a list of separation methods that may be used in each of the selectors.

1. *Enrichment separation* consists of increasing the concentration of one or several species in a desired stream. This operation does not mean high recovery or purity. The following separation techniques are convenient: condensation, physical absorption, membrane permeation, cryogenic distillation, and adsorption.

2. *Sharp separation* consists of obtaining two high-purity, high-recovery product streams from one input stream. The concentration of components in input is not restrictive. The split sharpness is defined as the ratio of key component concentrations in products:

$$S = c_1 / c_2 > 9 - 9.5 \text{ if } c_1 > c_2 \text{ or } S = c_1 / c_2 > 0.111 - 0.115 \text{ if } c_1 < c_2.$$

Potential techniques in sharp separations are: physical absorption, cryogenic distillation, molecular sieve adsorption, and equilibrium adsorption (when the molar fraction of adsorbate is less than 0.1). Chemical absorption may be also considered, but it is applicable when the component concentration is low.

3. *Purification separation* is meant here as the removal of one or more impurities from a stream to achieve very high concentration (purity) of the dominant component. The initial concentration of impurity in mixture should be lower than 2% or 2000 ppm. The final concentration of impurity in product should be less than 100 ppm. Separation methods suitable for purification are: equilibrium adsorption, molar sieve adsorption, chemical absorption and catalytic conversion.

Split generation and their sequencing can be managed by means of heuristics. General heuristics are presented in Table 7.12, which are inspired by the use of distillation. Firstly must be removed corrosive, hazardous, and any troublesome materials. This is particularly true for gas phase separations. For example, components that freeze, as water and CO_2, may foul the equipment in cryogenic distillation. Then, the next should be splits that separate directly a product. The same priority is valid for the removal of the most plentiful component, which reduces the cost of downstream operations. Finally, if possible, a 50/50 split is the best solution for further sequencing.

Table 7.11 Gas Separation Manager: separation methods used in selectors

Separation Method	Enrichment Separations	Sharp Separations	Purifications
Condensation	yes	no	no
Cryogenic Distillation	yes	yes	no
Physical Absorption	yes	yes	no
Chemical Absorption	no	yes	yes
Molecular Sieve Adsorption	yes	yes	yes
Equilibrium Limited Adsorption	yes	yes	yes
Membranes	yes	yes	no
Catalytic oxidation	no	no	yes
Catalytic hydrogenation	no	no	yes

Table 7.12 General sequencing heuristics for the Gas Split Manager

1. Remove corrosive and hazardous materials first.
2. Remove troublesome trace impurities first.
3. Favour separations that match the desired products. If the separation leads to a sub-stream that requires no further separation, and is a desired product, and if that product is the most plentiful in the mixture, remove it next.
4. Favour separations that give equimolar splits. When ease of separation and composition are similar, perform the separation that divides the feed as equally as possible.

Table 7.13 displays other heuristics, more specific for gas separations (Barnicki and Fair, 1992). Note those regarding the removal of small amounts of water, as well as the catalytic conversion of impurities. Removal of impurities that may accumulate or generate other troublesome impurities by interactions of recycles is an important issue in operation and control (see the Case Study 3 in Chapter 17).

Table 7.13 Special sequencing heuristics for Gas Split Manager

1. Favour condensation for removal of high boilers from non-condensable gases when cooling water can be used as the condensing medium.
2. Favour catalytic conversion when the impurities can be converted into a desired product or when they tend to accumulate in recycles or when they produce other impurities by side-reactions.
3. Favour adsorption for small-scale desiccation operations. This is the cheapest alternative for processing small amounts of gas.
4. Favour adsorption for processes that require essentially complete removal of water vapour. This is capable of achieving dew point depression of more than 44 C.
5. Favour glycol absorption for large-scale desiccation operations requiring dew point depression of 27 °C or less.

EXAMPLE 7.6 Synthesis of a gas separation system

This example adapted from Barnicki & Fair (1992) presents the separation and purification of a typical landfill gas produced by anaerobic decomposition of municipal waste. This contains approximately 200 kg organics/ton waste. The gas composition is 40-60 mol% CH_4, 40-50 mol% CO_2 and 5000 ppm various impurities. A medium-size plant can produce between 50000-60000 m^3/day methane. Table 7.14 shows the initial landfill gas composition, as well as product specifications.

Table 7.14 Gas composition and product specifications

Component	Gas mol%	Purity CO_2	Purity methane
Methane	47.5	-	99.98 mol%
Carbon dioxide	47.0	99.985 mol%	-
Nitrogen	3.70	-	-
Oxygene	0.99	-	-
Hydrogen sulfide	0.01	0.3 ppm max	1.25g/100SCF
Aromatics (benzene)	0.30	5 ppm max	-
Halohydrocarbons (chloroethane)	0.50	-	0.25g/100 SCF

The analysis starts by ordering the components by composition, as given in Table 7.14. The first split suggested is the removal of the last three trace components: hydrogen sulfide, benzene, and chloro-ethane. This split would correspond to the second heuristic in Table 7.12: remove troublesome trace impurities. The appropriate selector is of purification type. Four methods could be considered: chemical absorption, catalytic conversion, molecular sieve adsorption and physical adsorption.

Table 7.15 Ranked property list for purification separation

Chemical absorption		Molecular sieve adsorption		Equilibrium adsorption	
Component	Chemical family	Component	Kinetic diameter (Å)	Component	Loading (mol/g ads)
CO_2	acid gas	Oxygen	<3	Oxygen	0
H_2S	acid gas	Nitrogen	<3	Nitrogen	0
Nitrogen	inert gas	H_2S	<4	Methane	0.0005
Oxygen	inorg. gas	CO_2	<4	CO_2	0.0035
Chloroethane	chloride	Methane	<4	Benzene	0.0046
Benzene	aromatic	Chloroethane	<5	H_2S	0.0069
Methane	n-alkane	Benzene	<8	Chloroethane	0.0070

In order to select the separation method, Table 7.15 lists some characteristic properties of components. Chemical absorption is not feasible, because all the trace

components belong to different chemical families. For the same reason, we eliminate the catalytic conversion. To evaluate the molecular sieve adsorption, we compare the kinetic diameter of components. Since benzene has the largest size, this method would imply the absorption of other components. Finally, we examine the feasibility of equilibrium adsorption. The values regarding the loading capacity of adsorbent indicates that all the trace components can be conveniently removed, and therefore this method can be applied.

The remaining gas mixture has now the composition: oxygen 3.7 mol%, nitrogen 1.0 mol%, methane 47.9 mol%, CO_2 47.4 mol%. These values suggest sharp splits for the products, either CO_2 or methane, or the separation of nitrogen /oxygen from the rest. Consequently, the suitable selector will be of 'sharp separation' type. Potential methods are: absorption (physical or chemical), cryogenic distillation, molecular sieve adsorption and equilibrium-limited adsorption. The corresponding lists of ranked properties are presented in Table 7.16.

The first method, absorption, is feasible. It is known that CO_2 can be absorbed in water or solvents, as amines or Selexol. Because high purity is required, physical absorption should be followed by chemical absorption. Cryogenic distillation is not feasible because the condenser would freeze in the presence of CO_2. Molecular sieves of 3 Å allow the separation of the mixture oxygen/nitrogen from the bulk gas mixture, CO_2/methane. The equilibrium-limited adsorption on activated carbon would give poor separation. In conclusion, at this step there are two potential splits: physical/chemical absorption of CO_2 and molecular sieve adsorption of nitrogen/oxygen. Application of the third heuristics, 'favour separations which match the desired products', gives preference to the first split.

After CO_2 removal, the remaining mixture has the composition 91mol % CH_4, 7.1mol% oxygen and 1.9 % nitrogen. The examination of the Table 7.16 indicates that the separation of methane by cryogenic distillation might be considered in competition with molecular sieve adsorption. Cryogenic distillation is expensive and unsafe in this case. Molecular sieve adsorption remains the only possibility.

Table 7.16 Ranked lists of properties for sharp separations selector

Absorption		Cryogenic Distillation		Mol. Sieve Adsorption		Equil. Adsorption	
Comp.	Family	Comp.	Relative Volatility	Comp.	Kinetic diam. (Å)	Comp.	Loading (mol/g)
Oxygen	inorg gas	Nitrogen	1.13	Oxygen	<3	Nitrogen	≈ 0
Nitrogen	inorg gas	Oxygen	2.73	Nitrogen	<3	Oxygen	≈ 0
CO_2	acid gas	Methane	1	CO_2	<4	Methane	0.005
Methane	n-alkane	CO_2	freeze	Methane	<4	CO_2	0.0035

Fig. 7.20 presents the final flowsheet. Firstly, the landfill gas enters an equilibrium adsorption unit, where the trace impurities H_2S, aromatics and halo-hydrocarbons are removed. The next step is the separation of CO_2 by physical or chemical absorption.

The residual gas containing CH_4, N_2 and O_2 could be used as fuel, or be purified further by using molecular sieve adsorption.

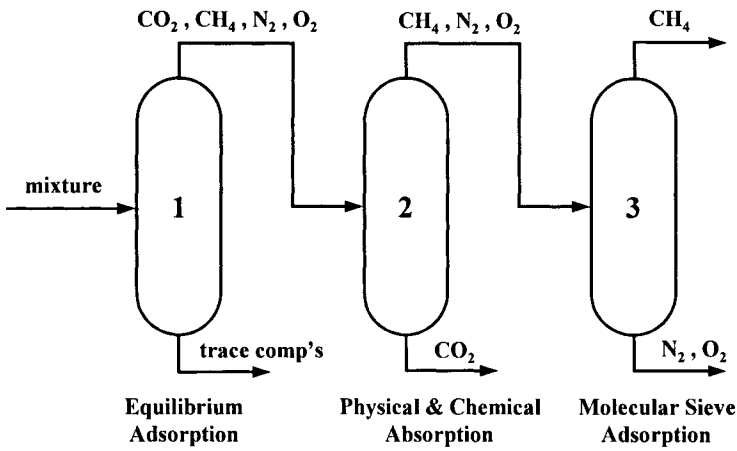

Figure 7.20 Example synthesis of a gas separation system

7.8 LIQUID SEPARATION SYSTEM

The synthesis of a flowsheet for the separation of a liquid mixture is a difficult activity, the main reason being the complexity of the thermodynamic behaviour. In the most cases, there is an interaction between the selection of the separation method and the processing conditions, as the concentration of components and the required recovery and purity. Except ideal or slight non-ideal mixtures, it is difficult to find the optimal sequencing of operations involving complex phase equilibria, as azeotropic distillation, liquid/liquid extraction, crystallisation or adsorption. In this subchapter we analyse only issues regarding the global strategy. More elaborated topics, as systematic methods for azeotropic mixtures, will be treated in the Chapter 9.

7.8.1 Application issues

The overall objective of the liquid separation system is to deliver purified products and by-products, and to recover recycled reactants and solvents. Questions regarding design decisions at this level are:

- How to remove the light ends (gaseous components dissolved in liquids)?
- How to recycle components that form azeotropes with the reactants?
- What separations can be made by distillation?
- What is the sequence of distillation columns?
- Alternatives if the distillation is not feasible?

The first question addresses more a technical detail than a separation principle. The other four questions are more fundamental, and will be handled in the frame of the synthesis strategy explained further on. Before entering the subject we must emphasise that distillation remains the most applied and reliable technique for the separation of liquid mixtures. When distillation is feasible, it should be immediately adopted. Other methods that may be applied should be rated against distillation.

Removal of light-ends

If the first split is a vapour/liquid flash at high pressure, some light components remain dissolved in the liquid phase. The removal of gases and lights is recommended before other separations. Several possibilities may be considered

1. Successive flashes, by dropping the pressure or/and increasing the temperature.
2. Vapour distillate. Several possibilities could exist (Figure 7.21). In a *partial condenser* column, both vapour and liquid distillate are overhead products. In a *stabiliser* column, only vapour distillate is taken-off, while the liquid is returned in the column as reflux. In a *pasteurisation* column, the gases are removed as top vapour distillate, while the purified product is obtained as liquid-side stream, few stages below the condenser. In all cases the top temperature depends on available cooling agent. Column pressure is optimised against losses in valuable components.
3. Reboiled stripping. The vapour needed to strip-out gaseous and light components is produced internally by the reboiler. The initial mixture is fed at sufficiently low temperature on the top stage.

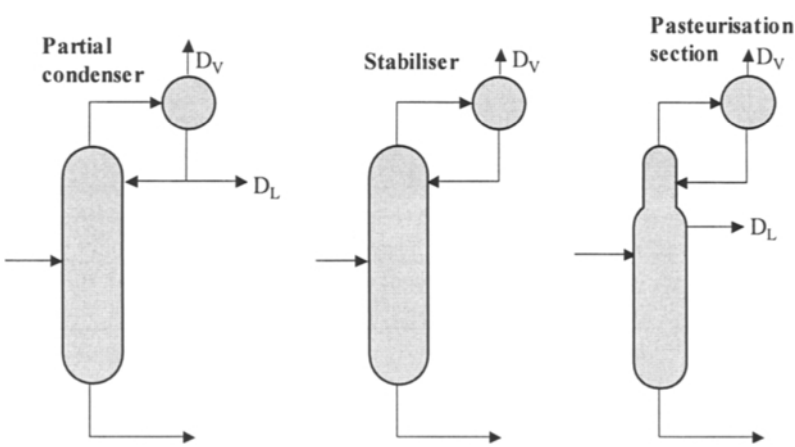

Figure 7.21 Alternatives for removing lights

Removal of heavy-ends

High molecular components may be found in the effluent of some reactors, as for cracking, oxidation, etc. Because there is a danger of fouling downstream units, these heavies should be removed before other separators. Fig. 7.22 presents some solutions. An adsorption device, as for example a clay tower, could solve partially the problem.

The inconvenient is that the retention capacity of the absorbent change with time, which must be cleaned or changed.

Another solution is the use of a flash as pre-separator of lights from heavies, while the purification of the bulk component takes place in a second side-stream column. This device offers the simultaneous removal of lights and heavies. A practical example is the purification of phtalic anhydride (Dimian, 1997).

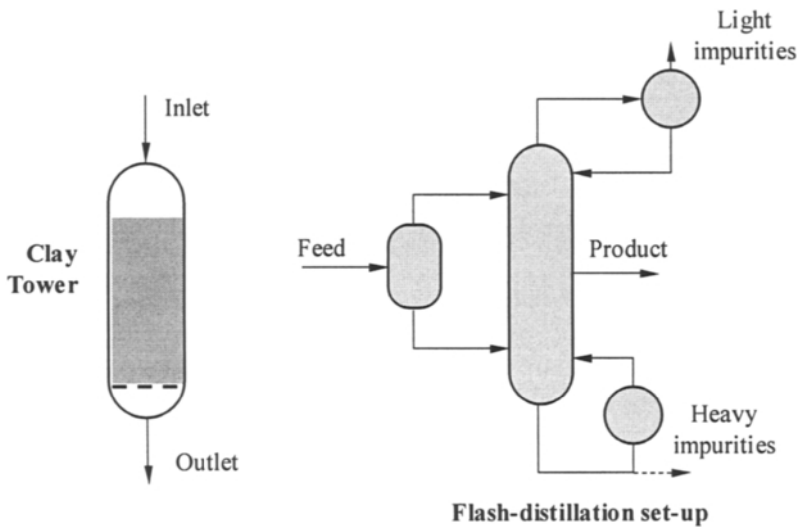

Figure 7.22 Alternatives for removing heavies

7.8.2 Liquid split manager

The logic diagram of the Liquid Split Manager follows the pattern from the Fig. 7.18:

(1) Study the mixture. Identify all known and potential azeotropes. Decide product streams and their specifications. Prepare ranked lists of characteristic properties.
(2) Identify possible splits in the ranked lists by using heuristics.
(3) Identify appropriate selector and separation methods.
(4) Examine the split sequencing. Decide the next split to be performed.
(5) Consult the designer and check the feasibility of the separation method by rigorous simulation. If the design is not feasible go back to the point (4) and select another split. If the split is acceptable, find the component distribution in the product streams. Do not optimise the design at this stage.
(6) Compare the composition of intermediate mixtures with the specifications of products. Restart the procedure from the point 2, until all the products are found.
(7) Assembly the final flowsheet from the partial separations. Optimise the design.

It is clear that the above procedure does not produce a unique design. In practice the number of alternatives is limited because of the heuristics and physical constraints.

Liquid separation methods and corresponding characteristic physical properties are presented in Table 7.17. Note that besides distillation, stripping and extraction, other unit operations, as melt crystallisation, adsorption and membranes can be used.

Table 7.17 Separation methods included in Liquid Separation Manager

Separation Method	Characteristic property	Observation
Simple distillation	Relative volatility α	Use heuristics for split sequencing. Not feasible if $\alpha < 1.1$.
Simple and azeotropic distillations	Vapour pressure	Check thermal stability of components.
Stripping, L-L extraction, extractive distillation	Boiling point	Use stripping for thermal sensitive components. Prefer L-L extraction.
Melt crystallisation	Freezing point	Differences in freezing points greater than 20 °C.
Adsorption	Polarity	Use molecular sieves.
Membrane permeation	Shape and size	Emerging technology.
Azeotropic distillation, Extractive distillation, L-L extraction	Chemical family	Solvent selection is the main issue. Recycling increases the costs.
L-L extraction, stripping, adsorption, crystallisation	Temperature sensitivity	

7.8.3 Separation methods

Here we discuss only basic features of separation techniques suitable for the synthesis of a liquid separation system. The nomenclature is compatible with the monograph of Seader and Henley (1998), recommended for deeper insight.

1. *Simple Distillation.* In this category, we include the separation of ideal or slightly non-ideal mixtures that do not form azeotropes, based on the differences in the relative volatilities of components. A simple column designates a device that separates one or several feeds in only two products: top distillate and bottoms. Complex columns are can deliver more than two products. In this category we include columns with side-streams, columns equipped with auxiliary devices, as prefractionators, side-strippers and side-rectifiers, as well as thermally integrated columns.

Two heuristics are worth to mention:

Heuristic 1 (Relative volatility α). For $\alpha > 1.5$ the simple distillation is the most economical separation. For $\alpha < 1.1$ distillation is not feasible. For $1.1 < \alpha < 1.5$ the column requires very large number of stages and/or very high reflux. Other separation methods could be more appropriate.

Heuristic 2 (Slope of the vapour pressure curves). The relative volatility may be improved by selecting an appropriate operating pressure. Low pressures enhance the relative volatility, but increases the energetic consumption.

2. *Stripping.* The separation by striping is still based on relative volatility, but the vapour/liquid flows are realised by means of an external separating agent. A *simple stripping* column uses the injection of gas or steam to remove the light components. This method is appropriate when the bottom product is thermally sensitive. In *reboiled stripping* the vapour flow is created by means of an external reboiler, as in a simple distillation, but the condenser for the top vapour is missing. There is also a *refluxed stripping*, used to separate light organics by direct steam injection (steam distillation). Then the top vapour is condensed and sent to phase separation by decanting.

3. *Azeotropic distillation.* Azeotropes could exist in the initial mixture or created by means of an entrainer. The synthesis of separation sequences involving azeotropes is a complicated matter, but systematic methods based on Residue Curve Maps are available. These methods will be developed in larger extent in Chapter 9.

4. *Extractive distillation.* In extractive distillation the solvent, usually a high boiler, is added near the top of the column to enhance selectively the volatility between the components to be separated. This method could be considered both in zeotropic and azeotropic selectors.

5. *Liquid-liquid extraction.* A mass separation agent MSA (solvent) is added to extract selectively the desired component (solute) in a phase (extract) from another phase (raffinate). Because the solvent selection is a central issue, a screening method is of great help. Table 7.18 presents a group interaction method for solvent selection proposed by Cusack et al (1991). UNIFAC method can be used to detect potential solvents, but should be used with caution for simulating extraction devices.

6. *Liquid Adsorption.* Adsorption takes place selectively because of (1) polarity differences between adsorbate and unadsorbed liquid, or (2) differences in size and structural characteristics of molecules. In the first category we may mention activated carbon, in the second one the *molecular sieves*. Liquid adsorption is suitable for both recovery of small amounts from dilute solutions, and for bulk separations. Purification is feasible with very selective adsorbent. Recovery of adsorbate and regeneration of the adsorbent may be performed by (1) Thermal Swing Adsorption, (2) Pressure Swing Adsorption, (3) inert-purge swing, or (4) displacement desorption.

7. *Melt crystallisation.* Differences of 20-30 °C are typically required between the freezing points of the components to be separated and the bulk of the solution. Note that low temperature requires expensive refrigeration system and operating costs.

8. *Membranes.* Despite intensive research, the use of membranes is viewed an emerging technology. Most of applications are small-scale oriented. The availability of suitable membranes are still problematic and can explain the reluctance of designers. The most interesting for large-scale separations are pervaporation and reverse osmosis. Pervaporation was successfully employed for the purification of organic solvents containing small amounts of water, for breaking the azeotrope ethanol-water, and to remove volatile organic components (VOC) from wastewater. The enrichment of gases by membrames is another successful application. More information about membranes can be found in specialised works, as Strathmann (1990) and Seader & Henley (1998).

Table 7.18 Solvent selection method for L-L extraction (after Cusak, 1991)

Group	Solute	Solvent								
		1	2	3	4	5	6	7	8	9
1	Acid, aromatic OH (phenol)	0	-	-		-	0	+	+	+
2	Paraffinic OH (alcohol), water, imide or amide with active H	-	0	+	+	+	+	+	+	+
3	Ketone, aromatic nitrate, tertiary amine, pyridine, sulfone, trialkyl phosphate or phosphine oxide	-	+	0	+	+	-	0	+	+
4	Ether, oxide, sulfide, sulfoxode, primary and secondary amine and imine	-	+	+	0	+	-	+	+	+
5	Ether, oxide, sulfide, sulfoxide, primary and secondary amine or imine	-	+	+	+	0	-	0	+	+
6	Multihaloparraffin with active H	0	+	-	-	-	0	0	+	0
7	Aromatic halogenated aromatic, olefin	+	+	0	+	0	0	0	0	0
8	Paraffin	+	+	+	+	+	+	0	0	0
9	Monohaloparaffin or olefin	+	+	+	+	+	0	0	0	0

Note: To use Table 7.18, place the solute in row and choose the solvent from the column groups that lowers the activity coefficient. Sign (+) means that the column group component tends to increase the activity coefficient, sign (-) means decrease, while sign (0) means no effect.

7.8.4 Selector analysis

Liquid Split Manager incorporates two split selectors: *zeotropic* (ideal or slightly non-ideal) mixtures, and *azeotropic* mixtures. Each selector is divided further as function of two criteria: mixture composition and sensitivity to the effect of temperature. The first generates other two categories: *dilute* and *bulk* separations. The second demarcates between *temperature sensitive* and *temperature insensitive* separations.

A separation is considered *dilute* when distillate (D) or bottom product (B) is less than 5% weight of the feed (F). The separation of a dilute mixture by distillation (simple, extractive or azeotropic) is not economical, and other methods, as liquid-liquid extraction, stripping, crystallisation, adsorption, or membrane permeation, should be applied (Barnicki and Fair, 1990). It is obvious that the decision depends on the mixture composition and the nature of components. However, even in the case of dilute mixtures, distillation may be interesting, for example as indirect sequence (see later in this section).

In a *bulk* separation, the products to be separated are in significant amounts in the initial mixture, more than 5%. Distillation is the most interesting separation method, but the vapour/liquid phase behaviour of the mixture is essential. The logic diagrams for the separation method selection can follow two patterns: zeotropic mixtures, and azeotropic mixtures. The first is relative easy to handle, the second is much more difficult. Chapter 9 will be entirely devoted to this topic.

When the components to be separated are *temperature sensitive*, the separation should occur at a sufficient low temperature to prevent thermal decomposition. In this

respect appropriate methods are stripping, liquid-liquid extraction, adsorption and crystallisation. Note that vacuum distillation may be also used, because it can supply high purity products. This is the case of monomers used in polymerisation processes.

The above classification is summarised in Table 7.19. Note that the synthesis procedure follows the logical diagram illustrated in Fig. 7.19

Table 7.19 Liquid Separation Manager: selectors and separation methods

Separation Method	Dilute Separations	Zeotropic mixtures	Azeotropic Mixtures	Temperature sensitive
Simple distillation	Yes	Yes	Yes	Yes*
Complex distillation	No	Yes	No	No
Stripping	Yes	Yes	No	Yes
Extractive distillation	No	Yes	Yes	No
Azeotropic distillation	No	No	Yes	No
L-L extraction	Yes	Yes	Yes	Yes
Adsorption	Yes	Yes	Yes	Yes
Molecular Sieves	Yes	Yes	Yes	Yes
Membrane permeation	Yes	No	Yes	Yes
Melt crystallisation	No	Yes	No	Yes

* Vacuum distillation

7.8.5 Split sequencing

Without a systematic approach, the number of separations to investigate could be enormous. It can be demonstrated that for N components mixture to be separated by M potential methods the number of separation sequences S can be determined by the following relation (Thompson & King, 1972):

$$S = \frac{[2(N-1)]!}{N!(N-1)!} M^{N-1} \tag{7.14}$$

Thus, for six components mixture with five separation methods there are 13125 possible sequences. If only two methods are applicable the choice reduces to 1344 alternatives. Even with only one method, the analysis of all sequences for more than five components would be still prohibitive, as indicated in Table 7.20.

Table 7.20 The number of separation sequences using simple distillation columns

Components	2	3	4	5	6
Sequences	1	2	5	14	42

Thus, a mixture of six components can be separated in 42 different sequences. If a first sharp split may isolate 2 mixtures each of 3 components, then the number of sequences diminish to 1+2×2=5. Note that the decision to remove only one component reduces considerably the number of alternatives. Consequently, we need

methodological tools for sequencing. There are two approaches: 1) the use of heuristics, and 2) algorithmic methods. The last requires programming tools that are not available for commercial use. That is why the heuristic methods are still the most practical and easy to combine with simulation tools.

Table 7.23 presents generic heuristics for sequencing the separation of liquid mixtures. More rules, specific for the separations of zeotropic mixtures by distillation, will be shown later. The separation for azeotropic mixtures is treated in Chapter 9, although the emphasis is on the solvent selection and not on the number of splits.

Table 7.21 General heuristics for separation sequencing

1	Remove first corrosive, hazardous, fouling, reactive and any troublesome components. Consider also in the first place the removal of light ends.
2	Deliver high-purity products as top distillate. The same is valid for reactants sent to reactors sensitive to impurities.
3	When distillation-like separation is feasible, prefer it in a first attempt.
4	Isolate zeotropic and azeotropic mixtures.
5	Perform difficult zeotropic separations later, but before azeotropic separations. Examine other options, as extractive distillation, L-L extraction, crystallisation, adsorption, or molecular sieves.
6	Examine the separation of azeotropic mixtures last.
7	Remove the components in order of decreasing percentage of the feed. This operation will reduce the cost of the next separation.
8	Favour 50/50 splits.

Some comments might be of interest:

1. The first heuristic eliminates troublesome problems early. Safety and environmental aspects have priority.
2. The second heuristic is a 'golden rule' in industry, but other end-purification methods could be competitive. The components to be recycled to reactors should be of good purity with respect to undesirable species.
3. Distillation remains the most reliable separation technique. If it is feasible, it is unlikely that other method could be competitive.
4. The isolation of zeotropic and azeotropic mixtures simplifies tremendously the analysis. If some components are distributed then the systems may be still treated separately, but they will be coupled by recycle and bridge separations.
5. Difficult zeotropic separations demand large number of stages and very high reflux ratio. Energy integration system should be investigated (see Chapter 10). Other methods, as crystallisation, could be competitive.
6. The separation of azeotropes requires special analysis (Chapter 9). The use of entrainers and combined separation methods are the best solutions.
7. The removal of the most plentiful component will reduce drastically the cost of separation for the next column.
8. When the components are evenly distributed, 50/50 split leads to a drastic reduction of the number of splits.

EXAMPLE 7.7 Selection of methods to separate a liquid mixture

Liquid-phase oxidation of n-butane to acetic acid gives formic acid as by-product and some impurities, as listed in Table 7.22 (Barnicky & Fair, 1990). Propose a separation sequence to recover the acetic and formic acids as pure products.

Solution.
We start by ranking the components function of composition and some characteristic properties. The most important is the normal boiling point (nbp). Thus, it can be seen that formaldehyde is a gas, and acetaldehyde vaporises at room temperature. The next four components with boiling points in the range 329-352 K are lights that can be lumped in a single fraction. The first six components are only 7.0 %mole. The separation may be considered as diluted. Potential azeotropes between these species are not of significance. On the other side, the formic acid gives maximum boiler azeotrope with water at 107.65 °C with 22.6% water.

Table 7.22 Composition and component properties of a liquid mixture

	Component	mol%	M_W	nbp, K	Freezing Point, K	Dipole moment	Kinetic diameter
1	Formaldehyde	0.5	30	254	-	-	-
2	Acetaldehyde	0.5	44	294	-	-	-
3	Acetone	1.0	58.8	329.2	178.2	1.71	5.2
4	Methanol	1.5	32.0	337.7	175.5	1.71	4.1
5	Ethanol	3.5	46.1	351.4	159.1	1.67	5.1
6	MEK	1.0	72.1	352.7	186.5	2.70	6.1
7	Water	50.0	18	373.2	273.2	1.83	3.0
8	Formic acid	11.5	46	373.8	281.5	1.52	5.5
9	Acetic acid	30.5	60	391.1	298.8	1.74	5.3

The application of the heuristics indicates that the gaseous components should be removed in the first split. This separation can be done by a simple flash, which will be the first step in the sequence. The second split should take as lights the four next components, up to water. This split corresponds also to the heuristics three and four. A suitable separation technique could be the reboiled stripping.

The next mixture contains formic acid (11.9 %), acetic acid (31.4%) and water (56.7%). The difference of freezing points of water and acids is too close (9 and 16 °C respectively), so that the separation by crystallisation is not feasible. If distillation is applied, one can separate two binary mixtures, formic acid/water and acetic acid/water. The separation of these mixtures is known, and it can be solved by standard techniques. Figure 7.23 shows the final sequencing that will consists from a flash, a distillation column, and a special device of extractive azeotropic distillation.

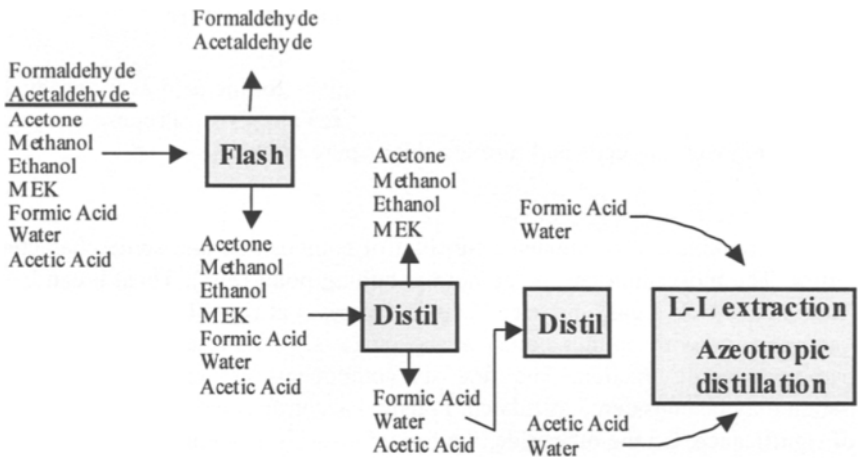

Figure 7.23 Synthesis of a Liquid Separation System

7.9 SEPARATION OF ZEOTROPIC MIXTURES BY DISTILLATION

7.9.1 Alternative separation sequences

A simple column performs the separation of a single feed into two products. The simplest case is the separation of a ternary mixture ABC, with components ordered by decreasing volatility. Figure 7.24 shows the alternatives. In the *direct sequence*, the components are separated in the order of volatilities, firstly A and then B as overhead products. In the *indirect sequence*, the first split delivers the heaviest component C as bottoms from the first column, followed by the A-B separation in the second column.

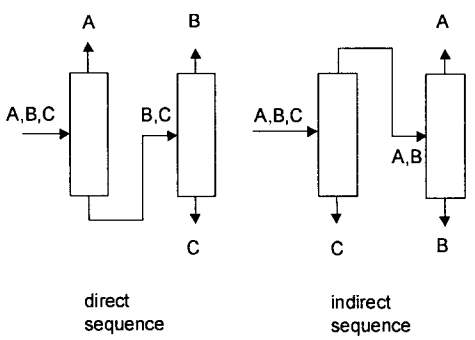

Figure 7.24 Direct and indirect sequences of simple distillation columns

In the case of a four-component mixture ABCD there are five possible sequences, each of three columns, as shown in Table 7.23. In 'direct' sequence all the components except the heaviest are taken as top products, while in 'indirect' sequence all the components are obtained as bottom products except the lightest component. In 'equal split' A and C are obtained as overhead products, while B and D as bottoms. There also two mixed sequences, 'direct/indirect' and 'indirect/direct' depending on the second split, while the third split is the same.

Table 7.23 Sequences for separating four-component mixture by simple columns

No.	Type	First split	Second split	Third split
1	Direct	**A**/BCD	**B**/CD	C/D
2	Equal split	AB/CD	A/B	C/D
3	Indirect	ABC/**D**	AB/**C**	A/B
4	Direct/indirect	**A**/BCD	BC/**D**	B/C
5	Indirect/direct	ABC/**D**	**A**/BC	B/C

A five-component mixture can be separated following 14 sequences, as shown in Table 7.24. The sequences are similar with those commented before, although with one more column.

Table 7.24 Sequences for separating five-component mixture by simple columns

First split	Second split	Third split	Fourth split	No
A/BCDE	**B**/CDE	**C**/DE	**D**/**E**	1
		CD/**E**	**C**/**D**	2
	BC/DE	**B**/**C**	**D**/**E**	3
	BCD/E	**B**/CD	**C**/**D**	4
		BC/**D**	**B**/**C**	5
AB/CDE	**A**/**B**	**C**/DE	**D**/**E**	6
		CD/**E**	**C**/**D**	7
ABC/DE	**D**/**E**	**A**/BC	**B**/**C**	8
		AB/**C**	**A**/**B**	9
ABCD/**E**	**A**/BCD	**B**/CD	**C**/**D**	10
		BC/**D**	**B**/**C**	11
	AB/CD	**A**/B	**C**/**D**	12
		A/BC	**B**/**C**	13
	ABC/**D**	AB/**C**	**A**/**B**	14

7.9.2 Heuristics for sequencing

The procedure explained bellow, known equally as the *list processing method,* allows the designer the identification of feasible sequences in separating ideal or slightly non-ideal zeotropic mixtures using simple distillation columns. Table 7.25 presents the list of more specific heuristics that can be used for sequencing, supplementary to those in Table 7.21. The first heuristic indicates that the most difficult problem should be isolated and pushed the last in the sequence. The second heuristic favours the separation

of the lightest components leading to the direct sequence. The third rule considers in the first place the separation of the majority component. When none of the before mentioned heuristics applies, dividing the mixture in nearly equal amounts leads to a more advantageous situation for the next split. The next example presents an application.

Table 7.25 Heuristics for separation sequencing of zeotropic mixture

1	Perform difficult separations in the last stage, but before azeotropic separations.
2	Remove firstly the lightest component one by one as overhead products.
3	Remove components in order of decreasing percentage of the feed. This operation will reduce the cost of the next separation.
4	Favour near 50/50 splits.

EXAMPLE 7.8 Separation of an aromatic mixture

Examine suitable separation sequences for the mixture of alkanes given in Table 7.26 (Smith, 1995).

Table 7.26 Data for sequencing a separation of alkanes

Component	Flowrate $kmol.h^{-1}$	Nbp, K	Relative volatility	Adjacent relative volatility
A. Propane	45.4	231	7.98	
B. i-Butane	136.1	261	3.99	2
C. n-Butane	226.8	273	3.0	1.33
D. i-Pentane	181.4	301	1.25	2.40
E. n-Pentane	317.5	309	1.0	1.25

Solution. Table 7.26 lists the normal boiling points and the relative volatilities of components. The sequence starts by examining potential splits for the first column C-1. The results are as follows:

Heuristic	C-1	Observation
1	?	D/E last but B/C is also difficult
2	A/BCD	Design for A/B keys
3	ABCD/E	Conflict with the heuristic 1
4	ABC/DE	Design for C/D keys

All four heuristics give contradictory results. For example, the most difficult split D/E that should be done last is recommended as first by the heuristic 3. Heuristics 2 and 4 would imply the design with the A/B or C/D keys, respectively. We take the decision to accept the heuristic recommending the split A/BCDE. We apply again the heuristics sequentially for the split C-2. The results are:

Heuristic	C-2	Observation
1	?	D/E last but B/C is also difficult
2	B/CD	Design for B/C keys
3	BCD/E	Conflict with the heuristic 1
4	BC/DE	Design for C/D keys

The results are again in conflict, but the heuristic 4 is acceptable, because the split B/C is more difficult. Thus, the full sequence is: A/BCDE, BC/DE, B/C, D/E. Similar reasoning would be valid with other heuristics in the first and the second split (given in parenthesis). In this way, few candidates are obtained, as given in Table 7.27.

Table 7.27 Candidate sequences for separating a mixture of alkanes

Sequence Table 7.24	C-1	C-2	C-3	C-4	Total feed vaporisation	Rank
3	(2) **A/B**CDE	(4) B**C/D**E	**B/C**	**D/E**	A+2B+C+D	1
8	(4) AB**C/D**E	(2) **A/B**C	**B/C**	**D/E**	2A+2B+C+D	2-3
9	(4) AB**C/D**E	(3 or 4) A**B/C**	**A/B**	**D/E**	2A+2B+C+D	2-3
11	(3) ABC**D/E**	(2) **A/B**CD	**BC/D**	**B/C**	2A+3B+2C+D	4
12	(3) ABC**D/E**	(4) A**B/C**D	**A/B**	**C/D**	3A+2B+2C+D	5

At this point a question arises: which sequence is the best? Intuitively, a ranking method could be the amount of feed vaporised in each split, which is a measure of the total energy consumption. From this viewpoint, the sequence (3) from Table 7.27 is the best. Later in this chapter, we will try to check this result by a more rigorous method.

7.9.3 Complex columns

By complex column, we mean a distillation set-up that can handle a mixture of at least three components, and deliver more than two products. The arrangement consists of a main distillation column surrounded by additional devices, as prefractionator, heaters, inter-coolers, side-strippers and side-rectifiers. Figure 7.25 presents seven design alternatives for separating a ternary mixture ABC. Note that direct and indirect two-column sequences are included in this list, since they may be seen as reference alternatives. The operation of different types may be summarised as follows:

1. Side-stream rectifier: take A and C from the main column, but B as top product of a side rectifier.
2. Side-stream stripper: A and C as before, but take off B as bottom product of a side stripper.
3. Prefractionator: pre-separate AB and BC mixture in a first column (sloppy separation), then take the pure components A, B, and C as products in a second column.
4. Side-stream low position: take off B as side stream below the feed.
5. Side-stream high position: take off B as side stream above the feed.

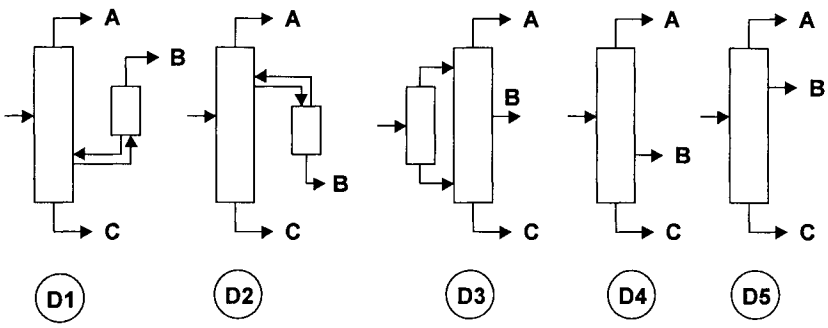

Figure 7.25 Types of complex columns

The key advantage of a complex column over a sequence of simple columns is more compact equipment and substantial reduction of costs, as investment, instrumentation, manpower and maintenance. A salient example is the topping column in oil refining. Another outstanding application is the production of oxygen, nitrogen and other inert gases by air distillation. However, complex columns have known relatively few applications in chemical process industries. This situation is changing rapidly because of recent advances in simulation, dynamics and control.

Heuristics for the selection of complex columns have been proposed by Tedder & Rudd (1978). The selection is based on the 'ease-of-separation' (ESI) index, defined as:

$$ESI = \frac{\alpha_{AB}}{\alpha_{BC}} = \frac{K_A / K_B}{K_B / K_C} \tag{7.15}$$

If $ESI > 1$ then splitting A/B split is easier than B/C, and conversely if ESI < 1 then splitting A/B is harder than B/C. The rules are:

- For ESI < 1.6 then:
  1. If 0.4 < B < 0.8 and A ~ B use prefractionator (D3).
  2. If B > 0.5 and C < 0.05 use side-stream low position (D4).
  3. If B > 0.5 and A < 0.05 use side-stream high position (D5).
  4. If B < 0.15 and A ~ B use side-stream rectifier (D1).
  5. Otherwise favour the sequence that removes the most plentiful first.
- For ESI > 1.6
  1. If C >0.6 then indirect sequence.
  2. If B > 0.5 and 0.05 < C < 0.20 then prefractionator D3.
  3. If B > 0.5 and C < 0.05 then side-stream low position (D4).
  4. If B > 0.5 and A < 0.05 then side-stream high position (D5).
  5. Otherwise favour side-stream stripper (D2).

  Other heuristics may be added as :

  1. Thermally coupled design 1 and 2 should be considered as alternatives to two-column design, if less than half of the feed is middle product.
  2. Designs 1, 2, 4 and 5 should be considered for separating all mixtures where a low middle purity is acceptable.

A rational strategy in applying complex columns is to reduce the separation of a mixture of n-components to a sequence of pseudo-ternary splits, where the most difficult separation will be the last. However, this heuristic does not guarantee structural optimality, neither explicitly consider all complex column alternatives.

EXAMPLE 7.9 Liquid separation system of the HDA process

Develop the liquid separation system for the HDA. Table 7.28 gives the composition of the stream that leaves the flash at 306 K and 35 bar.

Table 7.28 Mixture to be separated by HDA process

Components	nbp, K	Molar flow kmol/h	*K*-values 11 bar, 306 K	Relative volatility
Hydrogen	21	0.47	237	>>1
Methane	111.5	4.51	30	>>1
Toluene	110	23.65	0.022	1
Benzene	353	70.59	0.007	0.32
Diphenyl	528	0.77	1.0e-05	<<1

We start by ordering the components by increasing boiling points. The gaseous components, H_2 and CH_4, should be removed before any other separation. This corresponds also to the general first heuristic for separations (Table 7.21). The first separation is a stabilisation column. The pressure will be determined such as the condenser temperature not exceed 33 °C, simultaneously with minimal losses in benzene and toluene. In this case, a pressure of 10 to 11 bar is suitable.

Now, we have to separate the ternary mixture benzene, toluene and diphenyl. Application of the special heuristics from Table 7.25 gives the following sequencing:

Heuristic	C-1	C-2	Observation
1	Not applicable	Not applicable	No difficult split
2	A/BC	B/C	A the lightest
3	A/BC	B/C	A most plentiful
4	Not applicable	Not applicable	A~ 70%

The direct sequence is favoured. Moreover, high purity benzene is taken-off as distillate. Figure 7.26 presents the flowsheet.

In the second part of this problem, we will examine the possibility to separate the ternary mixture benzene/toluene/diphenyl in a complex column. The relative volatility of the components is approximately 2.5/1/0.3. For the composition from Table 7.28 we obtain $ESI<1.6$, and A<0.72, B <0.26, C~0.02. Consequently, a side-stream draw of toluene below the feed position is recommended. This design ensures high purity of benzene, but only moderate purity of the toluene to be recycled, which in addition may tolerate small amounts of diphenyl.

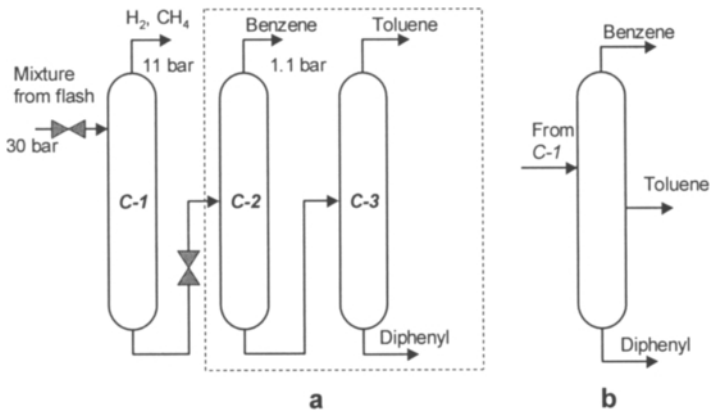

Figure 7.26 Liquid Separation System of HDA

7.9.4 Sequence optimisation

The above heuristics may produce a feasible but not always optimum sequence. In principle, the sequences can be compared by means of operation and capital costs. The first depends on the total utility consumption, proportional with the vapour rate. The second depends on the number of stages. Glinos & Malone (1988) demonstrated that optimal sequencing depends less on the total number of stages, but near-optimum sequences are those minimising the total vapour rate of key components. Therefore, when the relative volatility of keys differs considerably the estimation of total vapour flow based only on partial feeds is in large error. It is worth to mention that the method described before can be used for ranking of sequences, but not to determine the effective optimal vapour flow.

A true optimal sequencing can be found by a mathematical programming approach. A thorough treatment of this topic can be found in the book of Biegler, Grossmann & Westerberg (1998). Earlier attempts proposed the optimisation of a superstructure including all the possible sequences and using detailed modelling of columns. However, finding the solution is hindered by various non-linear and non-convex elements, making this method unpractical for process synthesis studies.

More efficient is a generic tree representation of the separations based on 'tasks'. The sequencing can be formulated as a structural optimisation problem where standard techniques based on Mixed Integer Linear Programming (MILP) apply. The tasks consist of simple distillation columns, as well as of hybrids for complex column arrangements, modelled by appropriate shortcut or semi-rigorous methods. Details can be found in Doherty and Malone (2001).

The progress in simulation allows, however, a rapid and accurate solution of the sequencing problem for zeotropic mixtures. We recommend the following procedure:

1. Generate a (large) list of candidates by using general and specific heuristics, as given in Table 7.21 and 7.25.
2. Produce a shortlist of few candidates by ranking the alternatives following the total vapour rate. The accuracy of minimum reflux calculation should be sufficiently good. Some approximations of the Underwood method based on key components are in large errors when applied to multicomponent mixtures. We recommend the use of the original Fenske-Underwood-Gilliland method, which is relatively easy to program in a spreadsheet.
3. Evaluate the best candidates by paying attention to heat integration problem and to other technological constraints.
4. Select the optimum sequence. Use rigorous simulation for the final assessment.

EXAMPLE 7.10 Sequence optimisation for alkane separation

Examine the optimisation of the separation of alkanes discussed in Example 7.8.

Solution.
The sequences identified by heuristics (Table 7.26) are evaluated by simulation with Aspen Plus using short cut model DSTWU, based on the Underwood method for minimum reflux. In all cases the initial mixture is at 6 bar and 300 K. The pressure in all columns is also at six bar. No intermediate heat exchangers are considered. The thermodynamic option is 'ideal', based only on vapour pressure data. The measure for total vapour is the reboiler duty.

Table 7.29 indicate that the results obtained by shortcut calculations are quite different with those predicted by heuristics (see Table 7.27). It can be seen the sequences can be classified in two groups: higher energetic consumption (3, 8, 9) and lower energetic consumption (11,12). The best is the sequence 12 where the first split is 'indirect' removing the most plentiful as bottoms. The second is the sequence 11 that has the same first split. Sequence 12 is only slightly better because 50/50 second split. Third is the sequence 9 based on 50/50 first split, but well behind the first two in term of total duty. The other two sequences gives very close results.

Table 7.29 Total vapour flow rate for alternative sequences

Seq.	C-1	Q1*	C-2	Q2*	C-3	Q3*	C-4	Q4*	Q total	Rank
3	A/BCDE	2.72	BC/DE	5.28	B/C	6.34	D/E	16.15	30.5	4
8	ABC/DE	6.92	A/BC	1.25	B/C	6.34	D/E	16.15	30.7	5
9	ABC/DE	6.92	AB/C	6.25	A/B	0.81	D/E	16.15	30.14	3
11	ABCD/E	16.76	A/BCD	1.44	B/CD	6.89	C/D	3.35	28.42	2
12	ABCD/E	16.76	AB/CD	6.81	A/B	0.81	C/D	3.35	27.72	1

* Duty in MW

To find an explanation Table 7.30 present comparative results regarding the sequences 9 and 12. It can be observed that the sequence 9 handles the most difficult separation D/E as the last, while sequence 12 treated it as the first. We would expect the first solution to be more advantageous. The results shows practically the same duty, 16.15 versus 16.76, although we would expect much more energetic consumption when the four components ABCD are taken as overhead distillate instead just D. Actually, the presence of the other components has as effect a considerable reduction of the minimum reflux, 3 instead 12! Thus, minimum reflux calculation based only on key components would give false predictions. This result reinforces the statement made before that the minimum vapour flow in sequencing should be determined by accurate methods.

Table 7.30 Comparision between two representative distillation sequences

	Sequence 9					Sequence 12				
Results	C-1	C-2	C-3	C-4		C-1	C-2	C-3	C-4	
	ABC/DE	AB/C	A/B	D/E	Total	ABCD/E	AB/CD	A/B	C/D	Total
R_{min}	0.99	5.02	2.32	12.33		3.02	5.45	2.32	1.43	
R	1.19	6.02	2.78	14.79		3.62	6.54	2.78	1.72	
N_{min}	17	43	14	69	143	69	43	14	17	143
N	36	81	27	126	270	130	80	28	34	272
Feed	18	40	14	63		65	40	14	17	
Q_{reb} *	**6.92**	**6.25**	**0.81**	**16.15**	**30.14**	**16.76**	**6.81**	**0.81**	**3.35**	**27.73**
Q_{cond}*	4.59	6.21	0.77	16.15	27.72	14.6	6.7	0.8	3.2	25.31
T_{dist}**	317.8	305.4	**281.6**	**365.3**		327.7	305.4	**281.6**	**331.1**	
T_{bot}**	370.9	**331.1**	**318.4**	**374.3**		**374.3**	343.1	**318.4**	**365.3**	
D/F	0.45	0.44	0.25	0.36		0.65	0.31	0.25	0.56	

* Duty in MW; ** Temperature in K

The above sequencing methods valid for zeotropic systems cannot be applied in the case of mixture with strong non-ideal character and displaying distillation boundaries, as those in the case of breaking azeotropes. Fortunately, the sequencing problem in this case has a different character. Most of the separations of multi-component non-ideal mixtures can be reduced by appropriate splits to the treatment of ternary mixtures, for which two or three columns are normally sufficient. The separation sequence follows direct or indirect sequence. The energetic consumption due to the recycle of entrainer dominates the economics. From this viewpoint preferred is that sequence in which the entrainer is recycled as bottoms. Hence, in azeotropic distillation the main problem is the solvent selection and not columns' sequencing.

7.10 ENHANCED DISTILLATION

This term designates a class of distillation techniques used to separate non-ideal azeotropic mixtures or zeotropic systems with very low relative volatility. In most cases the presence of a mass separation agent (MSA) is necessary.

Azeotropic distillation

In broader sense, the azeotropic distillation may handle the separation of azeotropic systems without and with a MSA. In the first situation, the entrainer originates from the process. In the second case the entrainer is recycled. In the past, this problem was solved by means of experience and intuition. Nowadays this it handled by means of systematic methods based on the representation in Residue Curve Maps (RCM). This topic will be developed in more extent in Chapter 9.

Extractive distillation

Extractive distillation is based on the ability of an entrainer to increase selectively the relative volatility of components. The choice of entrainer is based on its chemical affinity with one of the components to be separated. Extractive distillation can be used to separate both zeotropic and azeotropic mixtures. Table 7.31 presents a list of industrial applications.

Table 7.31 Industrial examples of extractive distillation

Mixture	Solvent
Butadiene/Butene from C4 fractions	Furfural, Acetonitrile, NMP, DMF
Butanes/Butenes	Acetone
Butene/Isoprene	DMF
Acetone/Methanol	Water, Aniline, Etylenglycol
Ethanol/Water	Ethylengycol, Glycerine
Benzene/Cyclohexane	Aniline
Toluene/Heptane	Aniline, Phenol
Propylene/Propane	Acrylonitrile
HCl/Water, Nitric acid/Water	Sulfuric acid
Tetrahydrofuran/Water	DMF, Propylene glycol
Cumene/Phenol	Phosphates

The entrainer (solvent) is fed near the top of the column when the mixture is zeotropic or forms a minimum-boiling azeotrope. In the case of a maximum-boiling azeotrope the solvent is introduced with the feed. The separation sequence has normally two columns. The first separates the non-extracted components in top, while the second column recovers the useful component. Normally the solvent is a heavy component that is recycled as bottoms. Chapter 9 gives more explanations about this technique.

Fig. 7.27 presents the separation of the ethanol-water mixture using ethylene glycol. Column *C-1* removes the excess of water and supplies a mixture with the composition close to azeotrope with 90% mol ethanol. The top distillate is sent to the second column

C-2 near the base, while the solvent enters near the top. The behaviour of this column seems more close to absorption than distillation (Stichlmair & Fair, 1999). Ethanol is recovered in the top of the column *C-2*, The third column *C-3* separates water in top and ethylene glycol in bottoms for recycling.

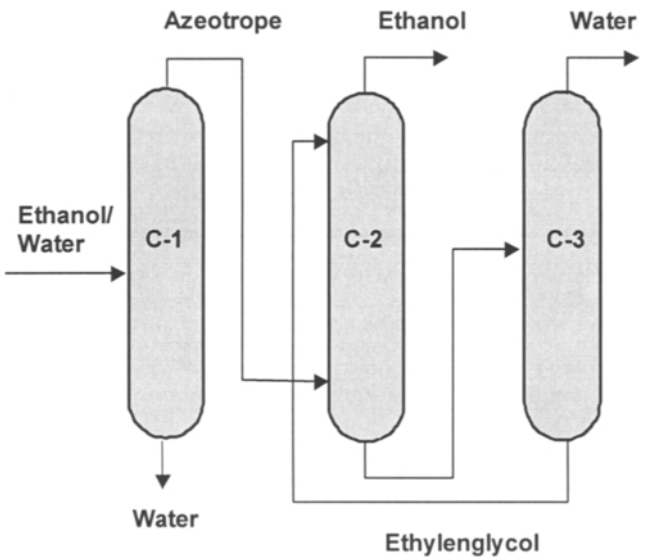

Figure 7.27 Separation of a binary mixtures by extractive distillation

Salt distillation

This technique is similar with extractive distillation, but the solvent is an ionic salt. For example, acetone distillates easier from a solution with methanol in the presence of a concentrated solution of calcium chloride. The salt can be also a complex organic molecule. An example is the use of sulfonates of alkyl-aromatics to separate more heavy organic molecules, as phenols.

Pressure-Swing Distillation

When the composition of an azeotrope is sensitive to moderate changes in pressure, then pressure-swing distillation may be used to separate almost pure components. The flowsheet displayed in the Fig. 7.28 consists of two columns operated at different pressures. The first column separates pure A in top or in bottom, if this is a minimum or maximum boiler, respectively. The second feed is placed on the other side of the azeotrope, which makes possible the separation of pure B. The other product is recycled to the first column. Some industrial separations may be cited as hydrochloric, hydrofluoric and formic from water solutions.

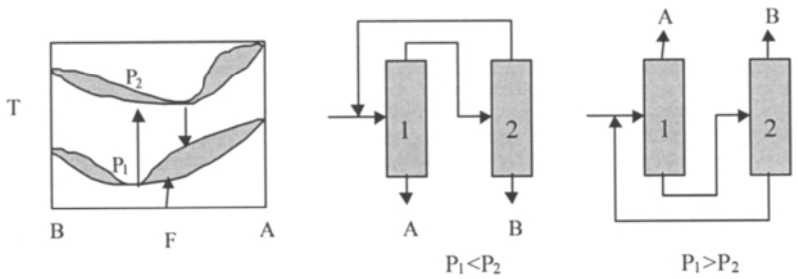

Figure 7.28 Pressure Swing Distillation

7.11 ALTERNATIVES TO DISTILLATION

Extraction

Usually extraction implies distillation, because of solvent recycling. Fig. 7.29 displays a typical application, the separation of acetic acid from an aqueous solution with isopropyl-ether. After extraction, the organic phase is sent to the column *C-1* where the acetic acid is recovered as bottoms. The distillate separates in two phases in decanter. The organic phase is sent back to *C-1* as reflux and as solvent to the extractor, while the water-rich phase goes to the second column *C-2*. The raffinate from the extraction column is sent to *C-2*, from which wastewater is recovered in bottom, while the solvent separating in top is sent to the decanter of *C-1* and recycled to the extraction unit.

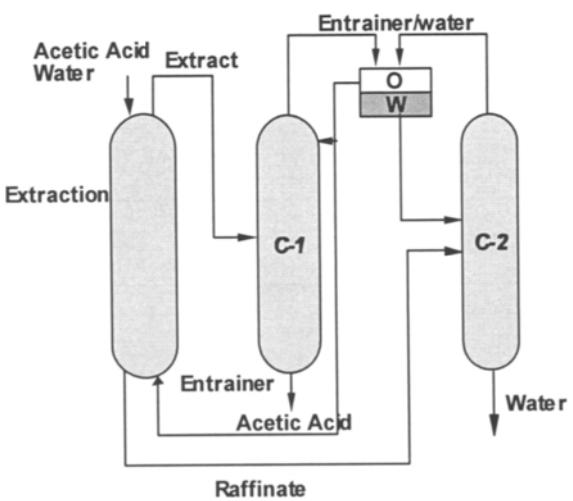

Figure 7.29 Combined extraction and distillation

Supercritical extraction

Supercritical extraction (SCE) is a modern separation technique that uses the dramatic increase in solubility of some solutes in supercritical fluids. Important applications have been found in food industry, as the extraction of caffeine from coffee, fats from butter, etc. Ethanol may be also recovered by extraction with CO_2. We should also mention the use of supercritical water to solve environmental problems, as the destruction of poly-chloro-benzenes (PCBs) by oxidation in supercritical water.

7.12 REACTIVE DISTILLATION

Combining reaction and separation in the same device leads in principle to the most compact and economic design. For this reason Reactive Distillation (RD) has raised a high interest, both from industrial and scientific point of view. A synonym term is Catalytic Distillation, because only a catalyst can enhance the reaction rate at values compatible with the separation requirements.

A salient application of RD is the manufacture of methyl-acetate. The conventional process consisted of a reactor and 10 separation units: eight distillation columns, one liquid extraction unit, and one decanter. An innovative process developed by Eastman Chemical Company (Agreda et al., 1990) and displayed in Fig. 7.30 replaces the whole flowsheet by a single RD unit. The economic advantage is impressive, five times reduction both in capital and operation costs (Siirola, 1996).

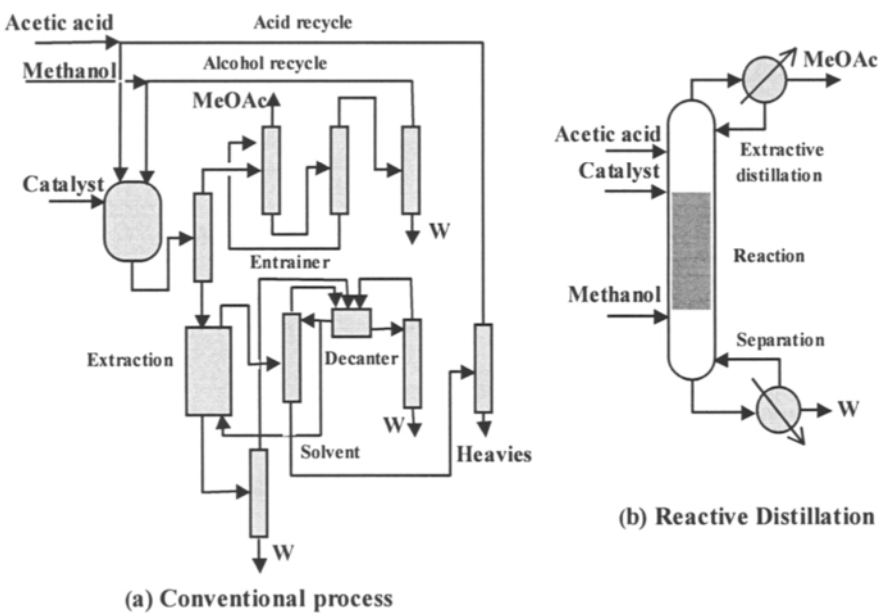

Figure 7.30 Reactive Distillation and conventional process for methyl acetate synthesis

Another important potential application is the class of benzene alkylation, as the manufacture of ethylbenzene or isopropyl-benzene (cumene). The synthesis is described by a set of parallel-consecutive equilibrium reactions, as for example:

$$C_6H_6 + C_2H_4 \rightleftharpoons C_6H_6\text{-}C_2H_5 \text{ 9 (a)}; \; C_6H_6\text{-}C_2H_5 + C_2H_4 \rightleftharpoons C_6H_4\text{-}(C_2H_5)_2 \text{ (b)}; \text{ etc.} \quad (7.16)$$

Modern alkylation processes make use of solid catalysts based on zeolites. According to different technologies, the reaction can be performed in vapour or liquid phase. The selection of a suitable chemical reactor for ethylbenzene is discussed in the Example 8.3. A conceptual flowsheet is depicted in Fig. 7.31 for a vapour-phase process (Mobil-Badger), one of the most widely used. The reactor works at 390-440 C and 0.6-3 MPa. Besides the main product ethylbenzene (EB), polyethylbenzenes (PEB) are formed, their amount depending on the reaction conditions. Large excess of benzene, over 6:1, is needed to shift the equilibrium to the desired product. The reaction mixture is sent to the separation section. Final yield can increase over 99% by converting PEB's to EB in a separate transalkylation reactor.

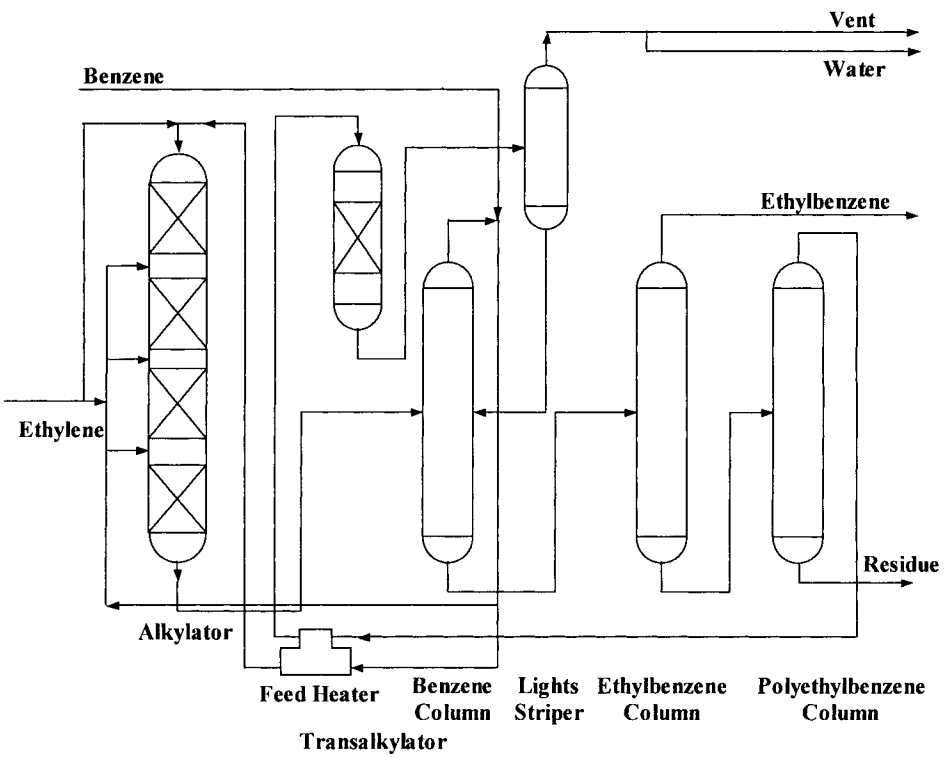

Figure 7.31 Vapour-phase Mobil-Badger ethylbenzene process

The above flowsheet can be simplified tremendously by catalytic distillation. Figure 7.32 depicts a conceptual configuration. The RD column consists of a reactive zone at the top, and a distillation section at the bottom. The reaction mixture is sent to a purification column, from which ethylbenzene is obtained as top distillate. A side-stream containing PEB is sent to transalkylation for EB recovery. Obviously, the feasibility of this process depends largely on the availability of an active and selective catalyst. For zeolites the optimal operating conditions are about pressure around 3 MPa, temperature less than 200 °C, and reaction rate capable to give a space-time of ~5 h^{-1} for almost complete ethylene conversion.

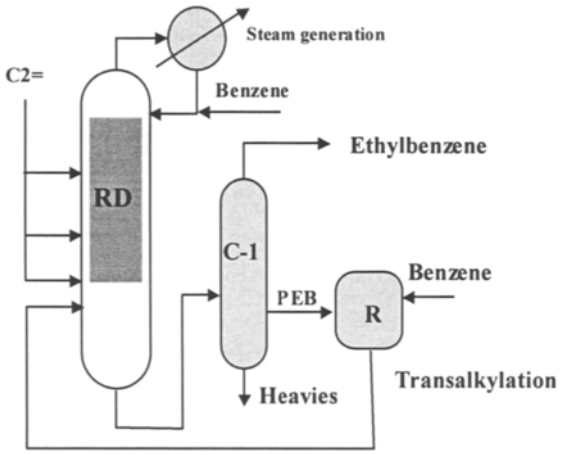

Figure 7.32 Reactive distillation column for ethylbenzene production.

The development of reactive separation processes is a complex activity that requires advanced knowledge in various domains, as catalysis, computer modelling, hydraulics of internals, etc. The state-of-the art in reactive distillation can be found in recent reviews (Taylor & Krishna, 2000), as well as in specialised books, as Doherty & Malone (2001), and Stichlmair & Fair (2000).

7.13 ECONOMIC POTENTIAL AFTER SEPARATIONS

After developing the separation system, the computation of the Economic Potential at the Level 4 becomes:

Economic Potential for Level 4

$$EP_4 = \{\text{Product value}\} + \{\text{By-product value}\} - \{\text{Raw-mat. costs}\} - \{\text{Reactor costs}\} - \{\text{Recycle costs}\} - \{\text{Separation costs}\} \quad (7.17)$$

The Economic Potential at Level 4 can be used to optimise the performances of the reaction and separation subsystems with respect to raw material consumption and the reactor conversion. Lower conversion gives in general better selectivity, but means higher recycle rates and higher cost of separations, as well as for the transport of fluids. Higher conversion gives lower costs for operations depending on throughput, as transportation and heating/cooling, but gives more sub-products and impurities. Therefore, at higher conversion the cost of separations increases sharply since more constraints on purity specifications, and more separation units necessary to remove impurities. The difficulty in optimisation consists of finding simple but reliable cost estimation of different units as function of throughput and separation performance. Case Study in Chapter 17 presents such calculation for the HDA process.

After completing the flowsheet, it is useful to reconsider the discussion about optimisation. In this respect, the key design variable is the conversion of the main reaction. Figure 7.33 illustrates the variation of the Economic Potential during the flowsheet synthesis at different stages. A minimum EP_{min} is necessary to continue the flowsheet development. At the Level 2 (input/output), an upper boundary on conversion can be set because sharp decrease in selectivity afterwards. At this point, it would be interesting to consider other reaction conditions, or other catalyst. At the Level 3 (reactor and recycles) a low bound of conversion can be set, because of the cost of recycles, particularly high when transporting gases. At Level 4, where the cost of separations is accounted for, the two bounds get closer to each other. A feasible domain can be defined, where the optimal conversion is located.

Typical for the chemical processes is that the region around optimum is rather flat. Thus, the effort to locate accurately this optimum is not essential at the process synthesis stage. Here we just state that steady state optimum is not always the most convenient from operability and controllability viewpoint. A certain back-off from optimum is necessary to ensure flexibility in production rate, as well as robust control faced to different disturbances. This issue will be handled in Chapter 13.

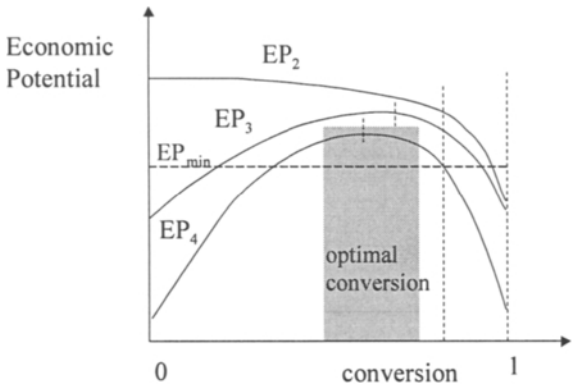

Figure 7.33 Optimal conversion at different levels of the process synthesis by the Hiearchical Approach

Hence, at the level Reactor-Separators-Recycles the material balance can be brought in a narrow optimal region. On this basis can be started the process integration steps regarding the optimal management of energy, mass separation agents, process water, waste minimisation, etc.

7.14 SUMMARY

Hierarchical Approach is a simple but powerful methodology for the synthesis of process flowsheets. It consists of a top-down analysis organised as a clearly defined sequence of tasks grouped in levels. Each level solves a fundamental problem as, number of plants, input/output structure, reactor design and recycle structure, separation system, energy integration, environmental analysis, safety and hazard analysis, and plantwide control. At each level, systematic methods can be applied for the synthesis of subsystems, as chemical reaction, separations, or heat exchangers network.

In applying the methodology, the designer has to identify dominant design variables and take design decisions. As a result, a number of alternatives are produced that are submitted to an evaluation procedure based on economical and technological criteria. In principle, at each level only one alternative could be retained for further development, so that the procedure leads finally to a good 'base-case'. This serves for improvement and optimisation, namely by applying Process Integration techniques.

Thus, the major merit of the Hierarchical Approach is that it offers a consistent frame for developing alternatives rather than a single design. The final solution is never unique, depending on a number of design decisions and constraints.

The key result of the Hierarchical Approach is the development of the *basic flowsheet structure*, formed by Reactor-Separations-Recycles. This structure defines the material balance envelope. In this respect of highest importance is the behaviour of the reaction system, which should deliver a realistic image of the reaction mixture. Other constraints regarding the reactor operation, as molar ratio of reactants, or safety requirements, are determinant for the structure of recycles. Optimal conversion represents a complex optimisation problem between the valorisation of raw materials and the cost of reactor, separators and recycles.

The Hierarchical Approach developed in this chapter incorporates a knowledge-based procedure for the synthesis of separations. This consists of dividing the separation section in three subsystems: gas & vapour, liquid and solid separations. Each subsystem is further managed by selectors, which makes use of unit operations. Split sequencing is based mainly on heuristics, although may include algorithmic or optimisation techniques. This chapter describe in more detail the synthesis of distillation trains for zeotropic distillations, the non-ideal case being left for the Chapter 9.

After solving the material balance problem, the next step is the energy integration. Here we can apply a powerful systematic methodology, Pinch Point Analysis, which will be the object of Chapters 10 and 11. Integration of controllability and operability will form the object of Chapters 12 and 13. Integrating other elements of design, may

require the revision of some elements of the material balance, namely the operation parameters, but, in principle, not the basic structure of the flowsheet.

Finally, the flowsheet structure and the performances of the integrated design have a determinant role on process profitability. The heat and material balance built upon supplies the key elements for investment and operation costs.

7.15 REFERENCES

Agreda, V.H., L. R. Partin, W.H. Heise, 1990, High-purity methyl acetate via Reactive Distillation, Chem. Eng. Progr., 86 , February, 40-46

Allen, D.T., K., S. Rosselot, 1996, Pollution Prevention for Chemical Processes, Willey

Bildea, C. S., A. C. Dimian, 1998, Stability and Multiplicity Approach to the Design of Heat-Integrated PFR, AIChE J, vol. 44, 2703-2712

Barnicki, S.D., J.R. Fair, 1990, Separation System Synthesis: A knowledge based approach: 1. Liquid Mixture Separations, Ind. Eng. Chem. Res., 29, 431-439

Barnicki, S.D., J.R. Fair, 1992, Separation System Synthesis: A knowledge based approach: 2. Gas/Vapour mixtures, Ind. Eng. Chem. Res., 31, 1679-1694

Barnicki S. D., J. J. Siirola, 1997, Separation system synthesis, in Kirk-Othmer Encyclopedia of Chemical Technology, 4th edition, vol. 21, 923-962

Crowl, D., J. F. Louvar, 1989, Chemical Process Safety: Fundamentals with Applications, Prentice Hall,

Cusack, R. W., 1991, Chem. Eng., 98(2), 66-71

Dimian, A. C., 1996, Process Integration course, University of Amsterdam,

Dimian, A. C., 1997, Compact distillation system, in Distillation & Absorption '97, IChemE, Symp. Ser. 142, 279-288

Douglas, J. M., 1988, Conceptual Design of Chemical Processes, McGraw-Hill Publ.

Douglas, J. M., 1995, Synthesis of separation system flowsheets, AIChEJ, 41, 252

Doherty, M.F., G.A. Caldarola, 1985, Design and synthesis of homogeneous azeotropic distillation, Ind. Eng. Chem. Fundam., 24, 474-485

Doherty, M., M. Malone, 2001, Synthesis of Distillation systems, McGraw-Hill

Douglas, J., G. Stephanopoulos, 1995, Hierarchical Approaches in Conceptual Design: framework and computer implementation, Foundations of Computer Applications in Process Design (FOCAPD), AIChE Publ.

Gary, J.H., G.E. Handwerk, 1994, Petroleum Refining, Marcel Dekker

Glinos, K., Malone, M., 1988, Optimality regions for complex column alternatives in distillation systems, Chem. Eng. Res. Des., 66, 229-240

Han, C., G. Stephanopoulos, J. M. Douglas, 1994, Automation in design: The conceptual synthesis of chemical processing schemes, in Paradigms of Intelligent Systems in Process Engineering, Advances in Chemical Engineering Series, Academic Press

Ho, W. S., K. K. Sirkar, 1990, Membrane Handbook, Van Nostrand-Reinhold

Kister, H. Z., 1992, Distillation Design, McGraw-Hill

Kletz, T., 1999, Hazop and Hazan: Identifying and Assessing Process Industry Hazards, Hemisphere Publ.

Malone, M. F., M. F. Dogerthy, 1996, Separation system synthesis for non-ideal liquid mixtures. Foundations of Computer Aided Process Design, p. 9-18

Perry's, 1997, Chemical Engineers Handbook, 7th edition

Schweitzer, P. A (editor), 1988, Handbook of Separation Techniques, Mc-Graw Hill

Seader, J. D., E. J. Henley, 1998, Separation Process Principles, John Wiley

Siirola, J.J., 1996, Industrial applications of chemical process synthesis, in Advances in Chemical Engineering, vol. 23, Process Synthesis, Academic Press

Sinnott, R. K., 1993, Coulson and Richardson's Chemical Engineering, vol. 6, Pergamon Press

Smith, R., 1995, Chemical Process Design, McGraw-Hill

Stichlmair, J., J.R. Fair, J. L. Bravo, 1989, Separation of azeotropic mixture via enhanced distillation, Chem. Eng. Progress, 85(1), 63-69

Stichlmair, J., J. R. Herguijuela, 1992, Separation regions and processes of zeotropic and azeotropic ternary distillation, AIChEJ, 38, p. 1523-1535

Stichlmair, J. G., J. R. Fair, 1999, Distillation, Principles and Practice, Willey-VCH

Strathmann, H., 1990, Membrane and Membrane Separation Processes, Ullmann's Encyclopaedia of Industrial Chemistry, vol. A16

Taylor, R., Krishna, R., 2000, Modelling reactive distillation, Chem. Eng. Sci., 52, 993-1005

Tedder, D. W., D. F Rudd, 1978, Parametric studies in industrial distillation, AIChEJ 24, 303-334

Thompson, R., W., C. J. King, 1972, Systematic synthesis of separation systems, AIChEJ, 18, 941

Westerberg, A.W., O. M. Wahnshaft, 1996, Synthesis of distillation based separation processes, in Advances in Chemical Engineering, vol. 23, Process Synthesis, Academic Press

Widago, S., W. D. Seider, 1996, Azeotropic distillation, AIChEJ, 42(1), 96-130

Chapter 8

SYNTHESIS OF REACTION SYSTEMS

8.1 Chemical reaction network
- 8.1.1 Stoichiometry
- 8.1.2 Reaction rate
- 8.1.3 Kinetics
- 8.1.4 Conversion and selectivity

8.2 Chemical equilibrium
- 8.2.1 Equilibrium constant
- 8.2.2 Equilibrium composition

8.3 Reactors for homogeneous systems
- 8.3.1 Reactor volume
- 8.3.2 Performance of ideal reactors in simple reactions
- 8.3.3 Performance of ideal reactors in complex reactions
- 8.3.4 Non-ideal reactor models

8.4 Reactors for heterogeneous systems
- 8.4.1 Solid catalysed reactions
- 8.4.2 Heterogeneous fluid/fluid reactors

8.5 Thermal design issues
- 8.5.1 Temperature profile
- 8.5.2 Stability of the thermal regime
- 8.5.3 Types of thermal design

8.6 Selection of chemical reactors
- 8.6.1 Reactors for homogeneous systems
- 8.6.2 Reactors for heterogeneous systems

8.7 Synthesis of chemical reactor networks
- 8.7.1 Attainable Region concept
- 8.7.2 Optimisation methods

8.8 Further reading

8.9 Summary

8.10 References

The reaction system is the core of a chemical process. It is also the starting point in process design. By proper selection and design of the chemical reaction system, the modern process plants must cope with large flexibility with respect to production rate and selectivity. A greater attention should be paid to the formation of by-products and impurities. The selection and the design of the reactor system must be done in the context of interactions with the whole process, particularly with the separation system.

The goal of this chapter is to analyse elements from chemical reaction engineering necessary to consider in the conceptual design of a process as a system. The chapter is organised as follows. Preliminary sections will review basic concepts with regard to stoichiometry and chemical equilibrium, as compulsory steps in evaluating the feasibility of a chemical process. Then, we will discuss design principles in the field of homogeneous reactions, with reference to the two ideal reactor models, mixed and plug flow reactors. These will be followed by heterogeneous reactors, where we will point-out the problems rather than to enter in detailed analysis. A larger attention will be paid to thermal design issues, related to safety and heat integration, both essential for flowsheet development. On this basis we will present some guidelines for the reactor selection. A final section is devoted to new systematic methods developed by the process systems community, in particular to the concept of Attainable Region.

8.1 CHEMICAL REACTION NETWORK

8.1.1 Stoichiometry

The chemical transformation between the components involved in a network of chemical reactions can be described quantitatively by means of stoichiometric relations. In the case of multiple reactions, the stoichiometric relations form a system of linear algebraic equations:

$$\sum_{i=1}^{S} \nu_{i,j} A_j = 0 \,,\; i=1,\ldots,\, R \tag{8.1}$$

$\nu_{i,j}$ is the stoichiometric coefficient in the reaction i of the species j, the network consisting of S components and R independent reactions. The relation (8.1) may be extended to the atomic balance. If the atomic species are E_k (k=1, ...,N) and the atomic coefficients ε_{jk}, the material balance is constrained by the atomic balance as follows:

$$A_j = \sum_{k=1}^{N} \varepsilon_{jk} E_k \,,\; j=1,\ldots,\, S \tag{8.2}$$

$$\sum_{j=1}^{S} \nu_j \varepsilon_{jk} = 0 \,,\; k=1,\, \ldots,\, N \tag{8.3}$$

It is worthy to note that only *independent reactions* must be employed to express the composition of a reaction mixture. This is usually the case of complex reactions, as the cracking of hydrocarbons, where much more stoichiometric equations may be written than strictly necessary. The number of independent reactions can be simply determined as the rank of the matrix of stoichiometric coefficients.

EXAMPLE 8.1 Stoichiometric independent reactions

The following reactions can be written for the catalytic reforming of methane with water, at high temperature:

$$CH_4 + H_2O \rightarrow CO + 3H_2 \quad \text{(i)}$$
$$CH_4 + 2H_2O \rightarrow CO_2 + 4H_2 \quad \text{(ii)}$$
$$CO + H_2O \rightarrow CO_2 + H_2 \quad \text{(iii)}$$
$$CH_4 \rightarrow C + 2H_2 \quad \text{(iv)}$$
$$CO_2 + C \rightarrow 2CO \quad \text{(v)}$$
$$C + H_2O \rightarrow CO + H_2 \quad \text{(vi)}$$

Find the number of stoichiometric independent reactions.

Solution.

The species are: CH_4, H_2O, H_2, CO, CO_2, and C. By convention, the stoichiometric coefficients for reactants are negative, and positive for products. The matrix of stoichiometric coefficients of the reactions (i) to (vi) is:

$$\mathbf{v} = \begin{array}{c} \begin{matrix} CH_4 & H_2O & H_2 & CO & CO_2 & C \end{matrix} \\ \begin{bmatrix} -1 & -1 & 3 & 1 & 0 & 0 \\ -1 & -2 & 4 & 0 & 1 & 0 \\ 0 & -1 & 1 & -1 & 1 & 0 \\ 0 & 0 & 0 & 2 & -1 & -1 \\ 0 & -1 & 1 & 1 & 0 & -1 \end{bmatrix} \end{array}$$

The rank of the above matrix may be found by standard methods, for example by triangulation. After algebraic manipulations of rows and columns the final matrix is:

$$\mathbf{v} = \begin{bmatrix} -1 & -1 & -3 & -1 & 0 & 0 \\ 0 & -1 & 1 & -1 & 1 & 0 \\ 0 & 0 & 0 & 0 & 0 & 0 \\ 0 & 0 & 0 & -2 & 0 & 0 \\ 0 & 0 & 0 & 0 & 0 & 0 \\ 0 & 0 & 0 & 0 & 0 & 0 \end{bmatrix}$$

There are three non-zero diagonal elements, so the rank of the matrix is three. As a result, there are three independent reactions, which might be for example the reactions (i), (ii) and (iv).

8.1.2 Reaction rate

In extensive manner the reaction rate can be defined as the rate of reactant consumption or product formation. Let's consider the singular reaction $A \rightarrow products$. By reference to the reactant A the reaction rate might be seen simply as $-dN_A/dt$, being expressed in (moles of A transformed/time). More useful for design is an intensive definition, in which we may introduce an element characterising the reaction device itself, as volume, mass or contact surface. Here we adopt the convention that the reaction rate is positive for products and negative for reactants. Selecting the product j as reference, the following definitions of the reaction rate may be written (Levenspiel, 1999):

$$r_j = \frac{1}{V}\frac{dN_j}{dt} = \frac{moles\ j\ formed}{(volum\ of\ fluid)(time)} \tag{8.4}$$

$$r_j = \frac{1}{W}\frac{dN_j}{dt} = \frac{moles\ j\ formed}{(mass\ of\ solid)(time)} \tag{8.5}$$

$$r_j = \frac{1}{S}\frac{dN_j}{dt} = \frac{moles\ j\ formed}{(surface\ of\ contact)(time)} \tag{8.6}$$

Equation (8.4) is suitable for homogeneous system, equation (8.5) is useful for fluid/solid catalyst reactors, while equation (8.6) is applicable for gas/liquid or liquid/liquid reactors.

We may express the variation of the number of moles in a reaction system in a generic manner by means of the *molar extent of reaction* ξ, as:

$$N_j = N_{jo} - \nu_j \xi \tag{8.7}$$

Note that ξ characterises the reaction itself and not a particular component. Thus, for the stoichiometric independent reaction i we may define an *equivalent reaction rate*, as:

$$r_i = \frac{1}{V}\frac{d\xi_i}{dt} \tag{8.8}$$

This time ξ_i defines the molar extent of the reaction i. If the component j is implied in several reactions, the net reaction rate is given by:

$$r_j = \sum_{i=1}^{R} \nu_{i,j} r_i \quad j=1,2,\ldots,S \tag{8.9}$$

or in matrix notation:

$$[r_j] = [\nu_{i,j}][r_i] \tag{8.10}$$

The relation (8.10) can be used also to analyse kinetic experimental data in the case of complex reactions. Usually the number of species is much larger than the number of independent reactions. Therefore, it is sufficient to choose a number of R key species among the components that can be measured with good accuracy. Let's denote by $\Re_j$ the known measured reaction rates. Then the system can be solved to find the rates of the individual reactions r_i as:

$$[r_i] = [\Re_j][\nu_{i,j}]^{-1} \tag{8.11}$$

The other species may be determined easily from the remaining set of equations (8.10).

As example, we consider the following consecutive-parallel reactions, often found in organic chemistry processes, as nitration, alkylation, chlorination, etc:

$$\begin{aligned} &A + B \rightarrow C + S \qquad r_1 \\ &C + B \rightarrow D + R \qquad r_2 \\ &D + B \rightarrow E + F \qquad r_3 \end{aligned} \tag{8.12}$$

There are six chemical species and three reactions. We select A, B and C as key components. The matrix of stoichiometric coefficients is:

$$[\nu_{ij}] = \begin{bmatrix} -1 & -1 & 1 \\ 0 & -1 & -1 \\ 0 & -1 & 0 \end{bmatrix} \qquad [\nu_{i,j}]^{-1} = \begin{bmatrix} -1 & -1 & 2 \\ 0 & 0 & -1 \\ 0 & -1 & 1 \end{bmatrix} \tag{8.13}$$

The equation (8.12) becomes:

$$\begin{bmatrix} r_1 & r_2 & r_3 \end{bmatrix} = \begin{bmatrix} r_A & r_B & r_C \end{bmatrix} \begin{bmatrix} -1 & -1 & 2 \\ 0 & 0 & -1 \\ 0 & -1 & 1 \end{bmatrix} \tag{8.14}$$

from which one gets:

$$r_1 = r_A;\ r_2 = -r_A - r_C;\ r_3 = 2r_A - r_B + r_C \tag{8.15}$$

The reaction rates of the other species can be obtained from the relation (8.10) as:

$$\begin{bmatrix} r_D & r_E & r_S \end{bmatrix} = \begin{bmatrix} r_1 & r_2 & r_3 \end{bmatrix} \begin{bmatrix} 0 & 0 & 1 \\ 1 & 0 & 1 \\ -1 & 1 & 1 \end{bmatrix} \tag{8.16}$$

$$r_D = r_2 - r_3\ ;\ r_E = r_3\ ;\ r_S = r_1 + r_2 + r_3$$

8.1.3 Kinetics

The reaction rate is a function of concentration, temperature and pressure. In a large number of practical cases, the reaction rate may be expressed as function of only temperature and concentration, as follows:

$$r_i = f_1(T) f_2(c_j) \tag{8.17}$$

The dependency on temperature is given by the Arrhenius law:

$$f_1(T) = k_0 \exp(-E/RT) \tag{8.18}$$

where k_0 is the pre-exponential factor and E the activation energy. The dependency on concentration can be formulated as a power-law function:

$$f_2(c_j) = c_A^{\alpha} c_B^{\beta} ..... \tag{8.19}$$

In the relation (8.19) α, β, ... are partial orders of reaction. Their sum gives the global order of reaction $n = \alpha + \beta + ...$ If the reference component is A then the reaction rate is expressed in general by the following relation:

$$r_A = k_o e^{-E/RT} c_A^{\alpha} c_B^{\beta} ... \tag{8.20}$$

Note that the partial orders of reaction α, β, ... correspond to the stoichiometric coefficients only for *elementary reactions*. In the case of *non-elementary reactions* the apparent orders of reactions are different from stoichiometric coefficients, and more than one reaction step must be considered to explain the reaction mechanism.

It is worthy to note that there is a thermodynamic constraint in formulating kinetic expressions for reversible reactions: the partial reaction orders must be consistent at equilibrium. Let's examine the reversible reaction $aA + bB \leftrightarrow pP + rR$, for which the following reaction rate expression is proposed:

$$r_A = k_1 c_A^{\alpha} c_B^{\beta} - k_2 c_P^{\pi} c_R^{\rho} \tag{8.21}$$

Since at equilibrium $c_P^p c_R^r = K_c c_A^a c_B^b$, reaction orders and stoichiometric coefficients should respect the condition:

$$\frac{\alpha}{a} = \frac{\beta}{b} = \frac{\pi}{p} = \frac{\rho}{r} \tag{8.22}$$

8.1.4 Conversion and selectivity

The molar extent of reaction ξ introduced previously has the disadvantage of an extensive variable, since depends on the amount of reactants. It is often more convenient to use *conversion* as an intensive measure of a chemical transformation. The use of a *reference reactant* is compulsory. If N_{A0} is the initial molar amount of the reactant A, and N_A the amount after reaction, the conversion X_A is by definition:

$$X_A = \frac{N_{A0} - N_A}{N_{A0}} \tag{8.23}$$

The number of moles of other species can be expressed as function of X_A, as follows:

$$N_j = N_{j0} + \frac{\nu_j}{a} N_{A0} X_A \tag{8.24}$$

The total number of moles in the system is:

$$N_t = N_0 + N_{A0} \frac{\Delta \nu}{a} X_A \tag{8.25}$$

From (8.7) and (8.24) it follows that the link between conversion and molar extent of reaction is simply:

$$X_A = \frac{a}{N_{A0}} \xi \tag{8.26}$$

The use of conversion is suited for simple reactions, while the molar extent of reaction is more convenient for multiple reactions. In this case a molar extent of reaction ξ_i can be attributed to each independent reaction. The number of moles of component j involved in R reactions is:

$$N_j = N_{j0} + \sum_{i=1}^{R} \nu_{i,j} \xi_i \tag{8.27}$$

The total number of moles becomes:

$$N_t = N_0 + \sum_{j=1}^{S} \sum_{i=1}^{R} \nu_{i,j} \xi_i = N_0 + \sum_{i=1}^{R} \Delta \nu_i \xi_i \tag{8.28}$$

where $\Delta \nu_i$ is the variation of the number of moles in the reaction i.

Selectivity and yield are important concepts when dealing with multiple reactions. Three types of components are of interest: reactants, including the reference, main product, and by-products. In this book we use the following definitions:

$$\text{Selectivity } (\sigma) = \frac{\text{Amount of useful product formed}}{\text{Amount of reference reactant transformed}} \tag{8.29}$$

$$\text{Yield } (\eta) = \frac{\text{Amount of useful product formed}}{\text{Initial amount of reference reactant}} \tag{8.30}$$

Let's consider the simple reaction $a\,A + b\,B \rightarrow p\,P + r\,R$, where A is the reference reactant and P the desired product. Note that the above relations must take into account the stoichiometric coefficients. The following relations define selectivity and yield:

$$\sigma_{P/A} = \frac{a}{p}\frac{N_P}{N_{A0} - N_A} \tag{8.31}$$

$$\eta_{P/A} = \frac{a}{p}\frac{N_P}{N_{A0}} \tag{8.32}$$

Yield, selectivity and conversion are linked by the relation:

$$\eta_{P/A} = \sigma_{P/A} X_A \tag{8.33}$$

EXAMPLE 8.2 Selectivity of complex reactions

The following reactions may be considered at the catalytic burning of ammonia:

$4NH_3 + 5O_2 \rightarrow 4NO + 6H_2O$ (i)

$2NO + O_2 \rightarrow 2NO_2$ (ii)

$2NO \rightarrow N_2 + O_2$ (iii)

$4NH_3 + 3O_2 \rightarrow 2N_2 + 6H_2O$ (iv)

$4NH_3 + 6NO \rightarrow 5N_2 + 6H_2O$ (v)

$N_2 + O_2 \rightarrow 4NO + 6H_2O$ (vi)

The feed reaction mixture has the following composition: NH_3 - 20%, NO_2 - 2%, NO - 3%, N_2 - 5%, O_2 - 35%, H_2O - 5%, the rest being other inert gases. The following molar fractions have been measured at the reactor exit: y_{NH3}=0.086, y_{NO2}= 0.1075, y_{N2}=0.064. Determine the conversion of ammonia. Calculate the amounts of NO and NO_2 for 2000 Nm^3/h initial mixture. Determine yield and selectivity in nitric oxides, the reference reactant being ammonia.

Solution.

Following the example 8.1 three reactions are stoichiometric independent. We select the reactions (i), (ii) and (iii) with the extent of reaction ξ_1, ξ_2, ξ_3, The numeber of moles of each component is:

NH_3: $N_1 = N_{10} - 4\xi_1$ NO_2: $N_2 = N_{20} + 2\xi_2$

N_2: $N_3 = N_{30} + \xi_3$ O_2: $N_4 = N_{40} - 5\xi_1 - \xi_2 + \xi_3$

H_2: $N_5 = N_{50} + 6\xi_1$ NO: $N_6 = N_{60} + 4\xi_1 - 2\xi_2 - 2\xi_3$

Inert: $N_7 = N_{70}$

Total flow: $N_t = N_{t0} + \xi_1 - \xi_2$

The molar fractions at the reactor exit are:

$$y_1 = \frac{N_{10} - 4\xi_1}{N_{t0} + \xi_1 - \xi_2} \quad y_2 = \frac{N_{20} + 2\xi_1}{N_{t0} + \xi_1 - \xi_2} \quad y_3 = \frac{N_{30} + \xi_3}{N_{t0} + \xi_1 - \xi_2}.$$

It is convenient to use as variable the extent of reaction referred to the initial number of moles $\xi_{ni} = \xi_i / N_{t0}$. The above equations becomes:

$$y_1 = \frac{0.20 - 4\xi_{n1}}{1 + \xi_{n1} - \xi_{n2}} = 0.086 \quad y_2 = \frac{0.02 + 2\xi_{n2}}{1 + \xi_{n1} - \xi_{n2}} = 0.1075 \quad y_3 = \frac{0.05 + \xi_{n1}}{1 + \xi_{n1} - \xi_{n2}} = 0.064$$

By solving the system it comes: ξ_{n1}=0.0288, ξ_{n2}=0.0428 and ξ_{n1}=0.0131. The other molar fractions are y_4=0.1788, y_5=0.226, y_6=0.0334, y_7=0.3043. The ammonia conversion is from definition: $X_{NH3} = 1\text{-}N_1/N_{10} = 1\text{-}(y_{10} - 4\xi_{n1})/y_{10} = 0.576$.

The molar flow rates are:

Input: $F_0 = 2000/22.4 = 89.285$ kmol/h.

Output: $F = F_0(1 + \xi_{n1} - \xi_{n2}) = 88.036$ kmol/h.

The flow rates of the main components are:

	Input	Output	Change
NH_3	17.857	7.571	-10.386
NO	2.678	2.940	0.262
NO_2	1.786	9.460	7.678

By definition the yield is obtained as the amount of product formed divided by the initial reference reactant: In molar units the yield for NO and NO_2 is respectively:

$$\eta_{NO/NH_3} = \frac{0.262}{17.857} 100 = 1,47\% \ , \ \eta_{NO_2/NH_3} = \frac{7.678}{17.857} 100 = 43\%$$

The selectivity in the two products is obtained dividing the amount of product formed by the amount of reference reactant transformed. One gets:

$$\sigma_{NO/NH_3} = \frac{0.262}{10.386} 100 = 2.522\% \ , \ \sigma_{NO_2/NH_3} = \frac{7.678}{10.386} 100 = 73.93\%$$

The above values verify the relation between conversion, yield and selectivity.

8.2 CHEMICAL EQUILIBRIUM

Chemical equilibrium is a key issue in process design. Chemical equilibrium might set in many cases an upper limit for the achievable conversion, if nothing is done to remove one of the products from the reaction space. Because the equilibrium conversion is independent of kinetics and reactor design, it is also convenient to use it as reference. Note that important industrial reactions take place close to equilibrium, as the synthesis of ammonia and methanol, esterification of acids with alcohols, dehydrogenations, etc, particularly when the reaction rate is fast. Therefore, the investigation of chemical equilibrium should be done systematically in a design project.

8.2.1 Equilibrium constant

The analysis of chemical equilibrium is based on the concept of chemical potential (Chapter 5). Consider a homogeneous gaseous system. The chemical potential $\hat{\mu}_j$ of a component j in a mixture is given by:

$$\hat{\mu}_j(P,T,y_j) = \mu_j^0(T) + RT\ln\hat{f}_j \tag{8.34}$$

μ_j^0 is the chemical potential of the pure component, function only of temperature. $\hat{f}_j$ is the fugacity of the component j in mixture, depending on pressure, temperature and composition. The over-hat designates a component property in a mixture. In the case of singular reaction involving S components the following relation describes the chemical equilibrium:

$$\Delta G^0 = \sum_{j=1}^{S} \nu_j \hat{\mu}_j = 0 \tag{8.35}$$

In the case of R multiple reactions a similar expression is:

$$\Delta G^0 = \sum_{i=1}^{R}\sum_{j=1}^{S} \nu_{i,j}\hat{\mu}_j = 0 \tag{8.36}$$

From (8.36) we find the following definition for the equilibrium constant:

$$\Delta\ G^0(T) = -RT\ln K_f \tag{8.37}$$

where ΔG^0 is the variation of Gibbs free energy of the system given by:

$$\Delta G^0(T) = \sum \nu_j \mu_j^0 = (\nu_j \mu_j^0)_{\text{products}} - (\nu_j \mu_j^0)_{\text{reactants}} \tag{8.38}$$

The equilibrium constant K_f based on fugacity is given by:

$$K_f = \prod_{j=1}^{S} \hat{f}_j^{\nu_j} \tag{8.39}$$

By convention the stoichiometric coefficients ν_j are positive for products and negative for reactants. Similarly with (8.37) for multiple reactions we obtain a system of equilibrium relations:

$$\Delta G_i^0(T) = -RT\ln K_{f,i} \qquad \text{i=1,2,...}R \tag{8.40}$$

Now, the problem is to express fugacity as function of P, T and composition, and on this basis to determine the equilibrium composition. Two possibilities exist: assume ideal or real solutions.

a. Ideal solutions.

In the case of ideal solutions the Lewis-Randall approximation can be used:

$$\hat{f}_j = f_j^0 y_j = P\phi_j^0 y_j \tag{8.41}$$

The equilibrium constant becomes:

$$K_f = K_y K_\phi^0 P^{\Delta\nu} \tag{8.42}$$

where $K_y = \prod_{j=1}^{S} y_j^{\nu_j}$, $K_\phi^0 = \prod_{j=1}^{S} (\phi_j^0)^{\nu_j}$ and $\Delta\nu = \sum \nu_{j,products} - \sum \nu_{j,\text{reactants}}$.

Note that the equilibrium constant of fugacity coefficients of pure components K_ϕ^0 is independent of composition, and can be calculated with a suitable equation of state, as Viral or cubic EOS. The pressure correction $P^{\Delta\nu}$ depends on the variation of the number of moles. It follows that the equilibrium composition may be calculated from K_y, by expressing the composition of each species as function of conversion or of the molar extent of reaction.

b. Real solutions

In this case the component fugacity is $\hat{f}_j = \hat{\phi}_j P y_j$, where $\hat{\phi}_j$ is the fugacity coefficient of the component that now considers the effect of composition. This can be accounted for by means of *mixing rules* (see Chapters 5 & 6). Equation (8.42) remains formally valid, but takes now into account the equilibrium constant of fugacity coefficients $K_{\hat{\phi}} = \prod_{j=1}^{S} (\hat{\phi}_j)^{\nu_j}$. For liquid phase reactions the treatment is similar, by replacing fugacity with activity. Because the relation $a_j = \gamma_j x_j$ links the activity with composition, we obtain:

$$K_a = K_\gamma K_x \tag{8.43}$$

The equilibrium constant of the activity coefficients $K_\gamma = \prod_{j=1}^{S} \gamma_j^{\nu_j}$ can be calculated by means of a *liquid activity model* (see Chapter 6).

The case of heterogeneous equilibrium is more difficult, but less frequent in practice. Supplementary material may be found in more specialised books on thermodynamics.

8.2.2 Equilibrium composition

In the case of simple reactions, the equilibrium composition can be calculated by solving the equation (8.39) with conversion as variable for chemical transformation. On the contrary, the extent of reaction is more suitable for multiple reactions. The solution may be obtained by solving a system of algebraic equations of type (8.40).

A second possibility to calculate the equilibrium composition is by *Gibbs free energy minimisation.* The starting point is the system of equations generated by the relation (8.36). Phase equilibrium may be included in analysis. This method is particularly powerful, because it does not imply necessarily the knowledge of the stoichiometry. However, the user should consider only species representative for equilibrium. As in any optimisation technique, this approach might find local optimum. Specifying explicitly the equilibrium reactions is safer.

The effect of temperature on equilibrium is given by *van't Hoff equation*:

$$\frac{d \ln K}{dT} = \frac{\Delta H_R}{RT^2} \tag{8.44}$$

K stands for either K_f or K_a, while ΔH_R is the heat of reaction. If the reaction is exothermic (negative heat effect) then both equilibrium constant and conversion decreases with increasing temperature. On the contrary, in endothermic reactions the equilibrium conversion increases with the temperature (Fig. 8.1).

The above discussion has important practical consequences. In endothermic reactions the operating temperature must be kept as high as possible, while in exothermic reactions the temperature should follow an optimal profile, which should start at higher temperature and ends-up at lower temperature.

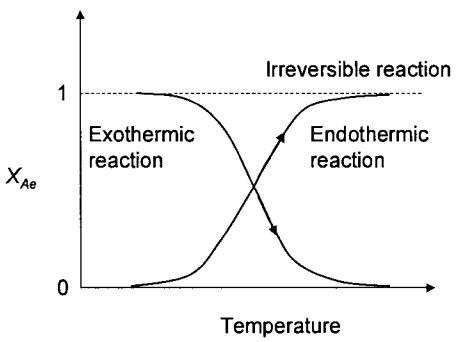

Figure 8.1 Effect of temperature on equilibrium conversion

8.3 REACTORS FOR HOMOGENEOUS SYSTEMS

In this section we will review basic equations for calculating the reaction volume necessary to achieve a given conversion for simple reactions.

8.3.1 Reactor volume

We may distinguish between two approaches in calculating the volume of a chemical reactor: *kinetic* and *shortcut* design. In kinetic design, at least the kinetics of the main reaction must be known. Perfect mixing and plug flow are known as 'ideal models', as CSTR and PFR, respectively. Real models, with intermediate degree of mixing, can be described as combinations of ideal models.

a. Continuous Stirred Tank Reactor (CSTR).

In a CSTR the reaction rate is uniform in space and constant in time, at the level of exit concentrations (Fig. 8.2). At constant volume V the material balance of the reactant A is:

$$V\frac{dc_A}{dt} = F_{A,0} - F_A - (-r_A)V \tag{8.45}$$

At steady state the following 'characteristic equation' is obtained:

$$\frac{V}{F_{A0}} = \frac{X_{Af}}{-r_{Af}} \quad \text{or} \quad \tau = \frac{V}{Q_{v0}} = \frac{c_{A0}X_{Af}}{-r_{Af}} \tag{8.46}$$

where the subscript f refers to the outlet conditions. The equation (8.46) can be used to calculate the reaction time τ and the reaction volume V for a given conversion.

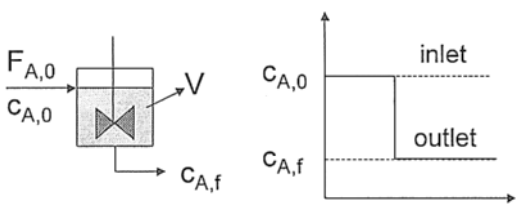

Figure 8.2 Illustration of a Continuous Stirred Tank Reactor

For multiple reactions, the solution of the characteristic equation involves a system of algebraic equations as follows:

$$\tau = \frac{V}{Q_{v0}} = \frac{c_j - c_{j0}}{r_j} = \frac{c_j - c_{j0}}{\sum_{i=1}^{R} \nu_{i,j} r_i} \tag{8.47}$$

We may write $c_j - c_{j0} = \sum_{i=1}^{R} \nu_{i,j}\xi_{vi}$, making use of the extent of reaction with reference to the reaction volume, $\xi_v = \xi_v / V$. The equation (8.47) becomes:

$$\tau \sum_{i=1}^{R} \nu_{i,j} r_i = \sum_{i=1}^{R} \nu_{i,j}\xi_{vi} \quad , \quad j=1,2, \ldots\ldots,S \tag{8.48}$$

The equation (8.48) is equivalent with the following system of algebraic equations:

$$\xi_{vi} = \tau\ r_i(\xi_{v1}, \xi_{v2}, ..., \xi_{vi})\ ,\quad i=1,2,....,R \tag{8.49}$$

The system (8.49) is non-linear but can be solved by means of standard techniques.

b. Plug Flow Reactor (PFR).

In a PFR the component concentrations and the reaction rate vary continuously along the reactor length (Fig. 8.3). A component balance on an infinitesimal volume gives:

$$F_{A0} dX_A = -r_A dV \tag{8.50}$$

The elementary volume is $dV = Sdz$, where $S = \pi d^2 / 4$ and d the reactor diameter. By introducing the specific molar flux of the reference reactant $A, \widetilde{F}_{A0} = F_{A0} / S$, the characteristic equation of a PFR can be written in differential form as:

$$\frac{dX_A}{dz} = \frac{-r_A(X_A)}{\widetilde{F}_{A0}} \tag{8.51}$$

The equation (8.51) can be integrated analytically or numerically for simple reactions in isothermal conditions to get the reactor volume or the *space-time* defined as $\tau = V / Q_{v0}$.

$$V = F_{A0} \int_0^{X_{A,f}} \frac{dX_A}{-r_A(X_A)} \quad \text{or} \quad \tau = c_{A0} \int_0^{X_{A,f}} \frac{dX_A}{-r_A(X_A)} \tag{8.52}$$

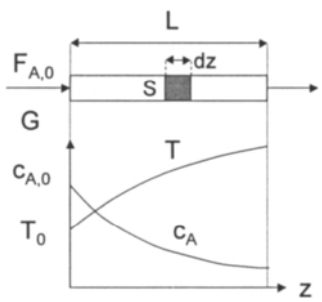

Figure 8.3 Illustration of a Plug Flow Reactor

For multiple reactions, the set of the stoichiometric independent reactions must be integrated simultaneously. Molar extent of reaction is more convenient as reaction variable, at best by reference to the total mass flow $\xi_{mi} = \xi_i / m$. The mass balance equations become:

$$\frac{d\xi_{mi}}{dz} = \frac{r_i(\xi_{m1}, \xi_{m2}, ...)}{\widetilde{G}}\ ,\quad i = 1,2, ..., R \tag{8.53}$$

where $\widetilde{G} = G/S = \rho u_z$ is the mass flux, G being the total mass flow rate, also the

product between mass density ρ and linear velocity u_z.

For non-isothermal operation the heat balance equation must be considered. It is easy to demonstrate that the equation giving the temperature profile may be written as:

$$\frac{dT}{dz} = \frac{1}{\widetilde{G}C_p}\sum_{i=1}^{R}(-r_i)(-\Delta H_{R,i}) - \frac{4U}{\widetilde{G}C_p d}(T - T_a) \tag{8.54}$$

The heat involved in each independent reaction is the product of reaction rate ($-r_i$) by the heat of reaction ($-\Delta H_{R,i}$). The heat transferred is proportional with the overall heat transfer coefficient U and the temperature difference (T-T_a) between the reaction mixture and the thermal agent. Hence, the solution of the equations (8.53-54) will produce profiles of concentrations and temperature.

The computation methods described above require the knowledge of reaction kinetics. Unfortunately, this is not the case in a large number of cases, particularly in an evaluation project. In this case *shortcut* methods are handy, in which the reactor volume may be estimated from information about the residence time. The following definitions of the reaction time are mostly used:

- Space-time τ as the ratio of reactor volume V by the inlet volumetric flow $Q_{v,o}$

$$\tau = V / Q_{V,0} \tag{8.55}$$

- Space-velocity as the reciprocal of the space time:

$$SV = 1/\tau \tag{8.56}$$

Three measures for space-velocity (measured in hour^{-1}) in are commonly used:

- LHSV (liquid) = (inlet liquid flow rate at STP[1]/ reactor volume);
- GHSV (gas space velocity) = (inlet gas flow rate at STP/reactor volume);
- WHSV (weight space velocity) = (inlet mass flow rate / mass of catalyst).

In order to avoid severe errors attention has to be paid to the units used in the above definitions. If the reaction volume can be reasonably estimated by short-cut calculation, then some hydrodynamic constraints, as the allowable pressure drop, or minimum / maximum fluid velocities, are other elements used to asses the final sizing.

8.3.2 Performance of ideal reactors in simple reactions

Let's consider the reaction $A \rightarrow products$ with the kinetics $-r_A = kc_A^n$. Figure 8.4 shows a graphical qualitative comparison between the volumes of a CSTR and a PFR needed to reach the same conversion. It may be observed that for a *n-th* order reaction a PFR needs always a smaller volume than a CSTR, the difference being significant at high conversion of A. The explanation is that in a CSTR the reaction rate is lower than in a PFR, being limited at the value of the final concentration.

[1] STP stands for standard temperature an pressure

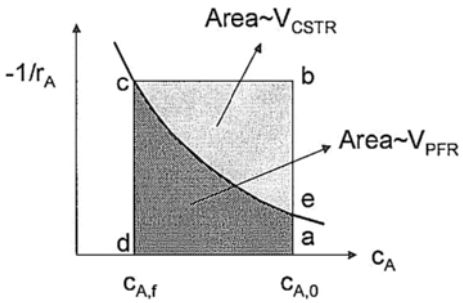

Figure 8.4 Qualitative comparison of CSTR and PFR reactors

Figure 8.5 presents a quantitative comparison for first-order and second-order reactions. It may be observed that at low conversions, say below 30%, the difference in volumes is small. The choice between CSTR and PFR is determined by other considerations, as the need of mixing for a better contact, heat transfer rate, safety, or mechanical technology. However, the difference in reaction volumes becomes considerable at conversions larger than 90%. For a first-order reaction at X_A=0.99 the ratio V_{CSTR}/V_{PFR} is 10, while for a second-order reaction this ratio becomes 100.

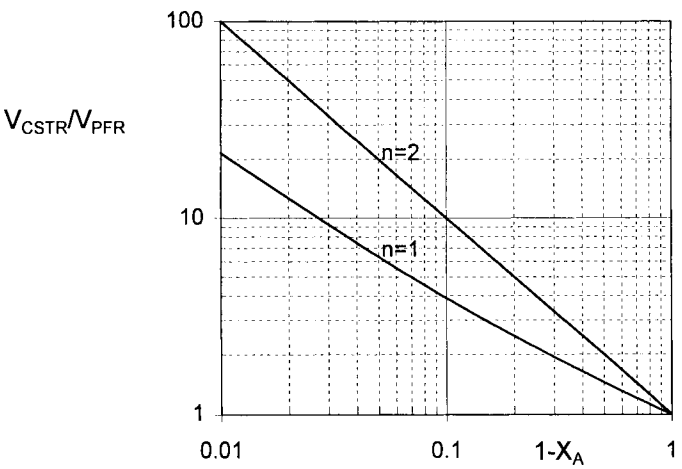

Figure 8.5 Comparison of CSTR and PFR for first and second-order reactions

A question arises: how to reduce this difference? The solution consists of using a series of CSTRs instead a single PFR. Since the reaction rate is higher in each intermediate volume, finally a much higher productivity than in a single equivalent reactor is obtained (Fig. 8.6). At limit, an infinite series of CSTRs behaves as a single PFR of the same volume.

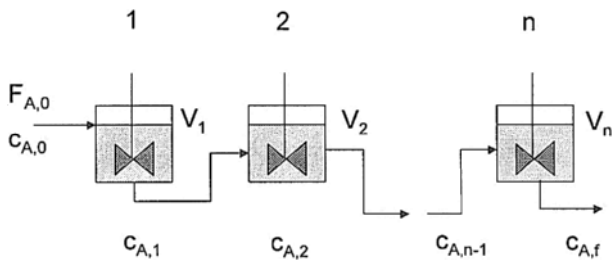

Figure 8.6 Series of CSTRs

Let's examine an isolated reactor l in a series. The characteristic equation is:

$$\frac{c_{A,l-1}}{c_{A,l}}\frac{Q_{V,l-1}}{Q_{V,l}} = 1 + (-r_{A,l})\frac{\tau_l}{c_{A,l}} \tag{8.57}$$

For first-order reaction and constant density mixture the analytical solution is:

$$\frac{c_{A,0}}{c_{A,N}} = \prod_{l=1}^{N}(1 + k_l\tau_l) \tag{8.58}$$

A graphical method can solve elegantly the design of a series of CSTR for any kinetics in the case of a single reaction. In a diagram $-r_A = f(c_A)$ lines with the slope $-1/\tau_l$ are drawn starting from c_{A0}. The segments needed to reach the final concentration c_{Af} give the number of reactors.

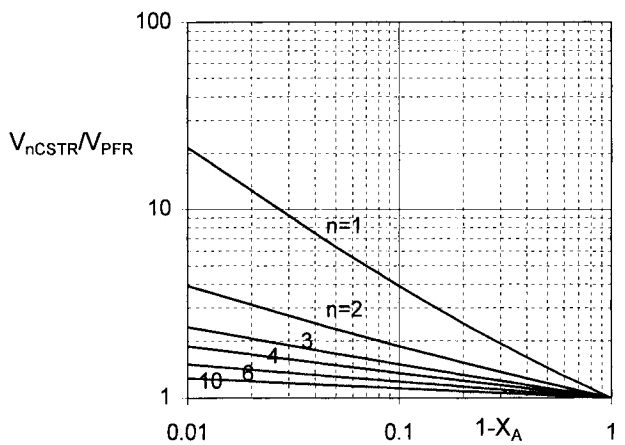

Figure 8.7 Comparison of performance of a series of n equal-size CSTRs and a PFR

Figure 8.7 illustrates the difference between a series of CSTRs and PFR for first-order reaction. Similar results may be shown for second-order reactions. Diagrams are presented in standard textbooks (Levenspiel, 1999). It may be observed that the improvement is considerably already starting with only two reactors. Hence, a series of CSTRs can replace advantageously a single large reactor, particularly when high conversions are desirable. The series of CSTRs may consist of individual units, or compartments arranged in the same unit.

8.3.3 Performance of ideal reactors in complex reactions

The relative performances discussed before, valid for single reactions, consider only the productivity as comparison criteria. In the case of multiple reactions the issue is the selectivity to the desired product.

a. Parallel reactions

Consider the following parallel reactions:

$$A \rightarrow P \ , \quad r_P = k_1 c_A^{\alpha}$$

$$A \rightarrow R \ , \quad r_R = k_2 c_A^{\beta}$$

P is the desired product, while R is a waste. The relative rate of formation of P to R is:

$$\frac{r_P}{r_R} = \frac{k_1}{k_2} c_A^{\alpha-\beta} \tag{8.59}$$

The selection of a suitable reactor can be analysed by means of the following heuristics:

- If the desired reaction has a higher reaction order than unwanted reaction ($\alpha > \beta$) a high reactant concentration is favourable; PFR or batch reactors are suitable.
- If the desired reaction has lower reaction order than the unwanted reaction ($\alpha < \beta$), the reactant concentration should be kept low. CSTR at high conversion should be chosen, although the required reaction volume is large.
- If $\alpha = \beta$ the concentration has no effect. The only way to control the product distribution is by modifying the ratio k_1 / k_2. The activation energies of the competing reactions should be examined. If $E_1 > E_2$ the reaction temperature should be maximised. If $E_1 < E_2$ the reaction temperature should be kept low. However, in this situation much more efficient is to search a suitable catalyst.

b. Series reactions

Consider the first-order reactions $A \xrightarrow{k_1} P \xrightarrow{k_2} R$, where P is the main product and R the by-product. The formation of P or of any other intermediate is maximised when fluids of different compositions at different stages of conversion are not allowed to mix.

Therefore, PFR or batch reactor will give a better yield of P as CSTR. In the first case, the maximum concentration of P is given by:

$$c_{P,max} / c_{A0} = (k_1 / k_2)^{k_2/(k_2-k_1)} \tag{8.60}$$

as well as the optimum residence time:

$$\tau_{p,opt} = ln(k_2 / k_1)/(k_2 - k_1) \tag{8.61}$$

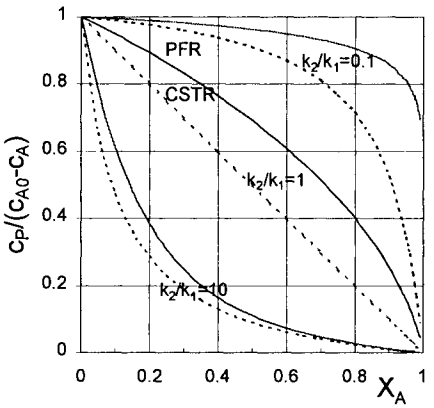

Figure 8.8 Comparison of selectivity in CSTR and PFR

Figure 8.8 gives a comparison of selectivity in CSTR and PFR models. PFR gives always a better selectivity. The advantage is significant if the secondary reaction is slower than the main reaction. When the by-product formation is fast then the mixing pattern has less importance. Low conversions give always better yield in intermediates. However, a large amount of unconverted reactant has to be recovered and recycled. The cost of separations may be determinant in the overall plant economics. Thus, the reactor selection should be evaluated against the cost of separations.

c. Series-parallel reactions

As example, we examine the reactions:

$$\begin{aligned} A + B &\xrightarrow{k_1} P \\ P + B &\xrightarrow{k_2} R \end{aligned} \tag{8.62}$$

The designer has a wide choice in manipulating variables and mixing patterns. However, these reactions can be analysed in terms of their constituent reactions. The optimum contact device for favourable product distribution is the same as for the constituent reactions. (Levenspiel, 1999). If P is desired, the above reaction system can be analysed by analogy with the series reaction $A \rightarrow P \rightarrow R$. In this case PFR gives always a higher yield in intermediate, the feeding policy of B being irrelevant.

As mentioned, selectivity is the key issue in selecting a chemical reactor for multiple reactions. Typically, high selectivity might be obtained at low conversion, but this implies a large amount of reactant to be recycled. Heuristics do not offer simple solutions. Again, the design of the reactor should be seen not isolated, but in the context of the separations with recycles The type and the size of reactor, as well as the operating parameters should be optimised against the cost of separations. This is possible by taking advantage from the optimisation capabilities offered by the flowsheeting programs.

8.3.4 Non-ideal reactor models

Continuous stirred tank and plug flow are ideal mixing patterns. Real reactors may deviate considerably from these models. The following aspects could affect the behaviour of a real reactor:

- Residence time distribution (RTD).
- The state of aggregation (micro- and macro-fluids).
- The earliness and lateness of mixing.

The two latest factors are difficult to handle, so that we may assume as workable hypotheses micro-fluid state and perfect mixing of reactants at the reactor inlet. It remains the problem of the residence time distribution. This can be solved by adopting one of the following methods:

- *Compartment model.* A real reactor may be approximated by the combination of zones with ideal mixing patterns, as perfect mixing or plug flow, connected by streams (Figure 8.9). The volume of different zones and the corresponding flows can be optimised to fulfil some criteria of productivity or selectivity. The idea has been developed in the recent years in a much more sophisticated manner. Ideal models may be assembled in a 'superstructure', from which the final configuration are determined by means of optimisation techniques. This topic will be discussed later in this chapter.
- *Tank-in-series model.* A series of CSTRs can be used to describe moderate deviations from the plug flow. The approach is much simpler than dispersion models, and can be easy implemented in a process simulator.

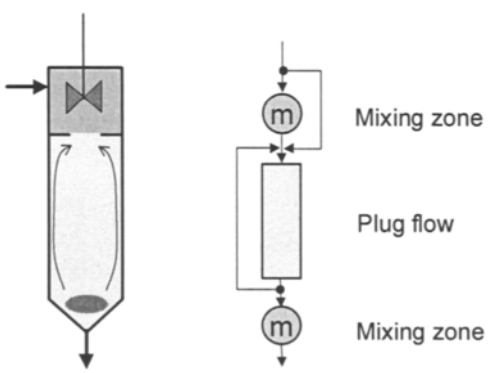

Figure 8.9 Modelling of a real reactor by compartments with ideal mixing pattern

8.4 REACTORS FOR HETEROGENEOUS SYSTEMS

In the case of a heterogeneous reaction the overall process rate must consider the kinetics of both chemical and physical steps. If a very slow step can be identified, this controls in generally the global reaction rate. More often, the analysis should consider several limiting steps, both of physical and chemical nature. Therefore, the computation of the reaction rate in heterogeneous systems requires information that is hardly available at the conceptual stage.

Flow modelling of each phase is another difficult problem. Simplified assumptions are often not realistic. The hold-up of the reacting phase is particularly important, depending on the design and hydrodynamic characteristics of the reaction device.

Therefore, the analysis of heterogeneous reactions is a complex topic, out of the scope of this book. We limit the discussion only at basic aspects regarding the selection of the reactor, as well as the simulation of the reactor system at conceptual design stage.

8.4.1 Solid catalysed reactions

1. Kinetics

a. Rate of catalysed reaction

A catalysed reaction is a result of several steps involving adsorption on active sites, reaction between sites and desorption from sites. Following Langmuir-Hinselwood-Hougen-Watson (LHHW) approach, the reaction rate has the form:

$$-r_A = \frac{(\text{kinetic term})(\text{driving force})}{\text{adsorption term}} \tag{8.63}$$

In design is more rational to replace a multi-constant formula by a local valid first-order kinetics, which can be combined easy with other rate controlling steps.

b. Pore diffusion combined with surface kinetics

The pore diffusion can affect the reaction rate. Let's consider an isothermal particle. The actual reaction rate can be found by correcting the above surface reaction by an effectiveness factor ε defined as:

$$\varepsilon = \frac{\text{actual reaction rate}}{\text{surface reaction rate}} \tag{8.64}$$

The effectiveness factor can be determined as function of particle geometry L, effective pore diffusion coefficient D_{eff} and the kinetic constant k. These can be put together in a physical parameter called 'Thiele modulus' defined as $L\sqrt{k/D_{eff}}$. Analytical expressions and graphical representations are available elsewhere (Levenspiel, 1999).

c. Film temperature resistance

Exothermic reactions might display effectiveness factors larger than one because of the temperature gradient across the gas film. The calculation is complicated, but the assumption of isothermal particle is conservative for conceptual design.

d. Mass transfer resistance

Mass transfer across an external film may play a role in the case of very fast reactions, as combustions, or in the case of catalyst coated on surface. Correlations based on dimensionless number are available for a large spectrum of physical situations.

2. Types of reactors

a. Gas-solid catalytic reactors

Fixed bed reactors

Figure 8.10 presents various types: (a) single packed bed (b) multi-bed arrangements, (c) multi-tubular reactor. Single-bed type is suited for adiabatic operations, preferably for endothermic reactions. Multi-bed reactor is better suited for reversible exothermal reactions, as methanol or ammonia synthesis, where after-stage cooling is necessary to move away from equilibrium. Multi-tubular heat exchanger enables better temperature control, and is recommended in the case of high exothermal reactions.

The design of such gas-solid catalytic reactors can be approximated by a pseudo-homogeneous model with gas phase in plug flow. In the case of very exothermic reactions accounting for radial dispersion of heat and mass might be useful to prevent excessive particle overheating. The reaction time must find a compromise with the hydrodynamic design, namely the maximum gas velocity and pressure drop.

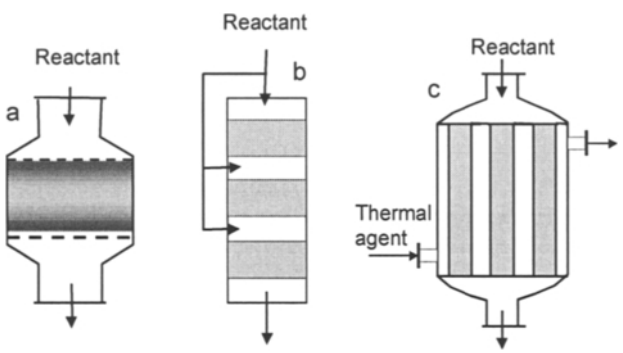

Figure 8.10 Types of fixed-bed catalytic reactor

Fluidised bed reactors

Intense mixing in a fluidised bed gives high mass & heat transfer rates, leading to good temperature control. Figure 8.11 presents two types: (a) stable catalyst, and (b) catalyst that needs regeneration. The last type is used in Fluid Catalytic Cracking (FCC) of hydrocarbon. The description of different models can be found in Levenspiel (1999).

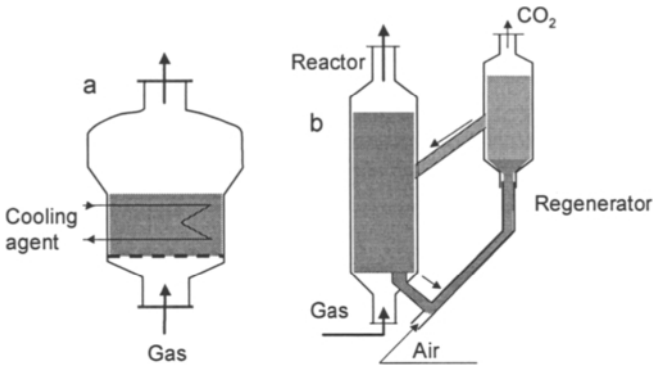

Figure 8.11 Fluid bed reactors

b. Gas/Liquid reactors on solid catalyst

The following discussion refers to the reaction:

$$A(gas) + {}_bB(liquid) \xrightarrow{catalyst} products \qquad (8.65)$$

Figure 8.12 presents the main types. Packed-bed reactor (a) is similar with an absorption column, where the packing can posses catalytic properties (coated catalyst), or host catalyst in special arrangements, as for example tea-bags. In the trickle-bed reactor (b) the gas dissolved or dispersed in liquid flows downwards through the bed of catalyst in co-current with the liquid phase. This reactor is suited for high-pressure operation and large ratios gas/liquid. In the last two devices, the catalyst dispersed in liquid as very fine particles is brought in contact with the gas either in a slurry bubble column (c), or in an agitated slurry reactor (d).

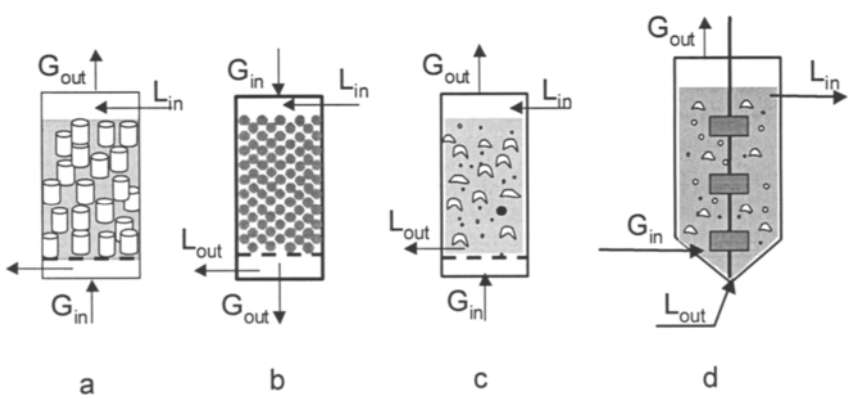

Figure 8.12 Types of gas/liquid reactions catalysed by solids

8.4.2 Heterogeneous fluid/fluid reactors

Here we will pay attention to the gas-liquid reactors. The reaction takes place usually in the liquid phase. Three main types of contact may be distinguished following the phase ratio: (1) gas bubbles dispersed in liquid, (2) liquid drops dispersed in gas, and (3) gas and liquid in film contact. In the first category we may cite gas-liquid bubble columns, plate or packed absorption columns, agitated tanks, agitated columns, static mixer columns, pump-type reactors. As examples in the second class we may name spray columns or liquid injection systems. The third category can be used with very exothermic reactions or viscous liquids.

The heterogeneous process can be seen as a combination of physical absorption with chemical reaction. The reaction zone can penetrate in the liquid phase, if the reaction is relatively slow, or takes place only at the interface, if the reaction rate is infinite. The chemical reaction can accelerate considerably the pure physical process. The ratio of actual process rate by the physical process rate is known as *enhancement factor* E. In the case of a bimolecular reaction the enhancement factor can be expressed as function of Hatta number $Ha = \sqrt{kc_B D_{Al}} / k_{Al}$, where k is the chemical kinetic constant, c_B the liquid-phase concentration of the reactant B, D_{Al} the diffusivity of gas through the liquid film, and k_{Al} the film mass transfer coefficient in the liquid phase.

8.5 THERMAL DESIGN ISSUES

8.5.1 Temperature profile

a. Optimum temperature profile

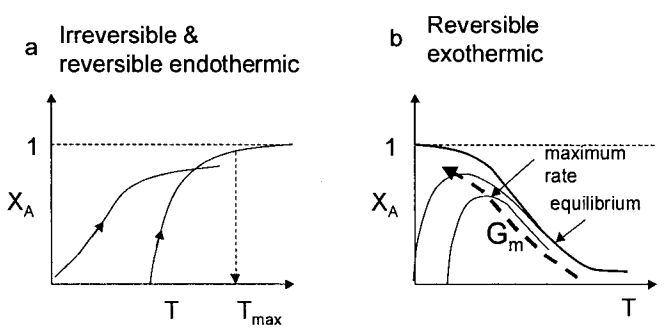

Figure 8.13 Optimal temperature profiles

The temperature profile should maximise the reaction rate to ensure maximum productivity, but respecting safety and other technological constraints. For *simple reactions* the best path is the isothermal profile, both for irreversible reactions and

endothermic reversible reactions (Figure 8.13-a). As mentioned, in the case of the reversible exothermic reactions the equilibrium conversion decreases with the temperature. Consequently, the reaction should start at the maximum allowable temperature, and decrease continuously or stage-wise along a path that gives a reaction rate close to optimum (Figure 8.13-b). For this reason the design of reactor for exothermic reversible reactions is a challenging optimisation problem.

The treatment of *multiple reactions* is more complex, because it involves not only the objective of optimal productivity, but also the desired selectivity. The optimal temperature path in a reactor can be found by computer simulation. As a qualitative guideline, it should be kept in mind that high temperature favours reactions with higher activation energy, while low temperatures is recommended for reactions with low activation energy. Let's consider the following consecutive-series first-order reactions:

$$A \xrightarrow{k_1, E_1} P \xrightarrow{k_2, E_2} S$$

$$A \xrightarrow{k_3, E_3} R$$

P is the desired product. If $E_1 > E_2$ and $E_1 > E_3$, high temperature is recommended. If E_1 is the lowest, then low reaction temperature should be applied. If $E_1 > E_2$ but $E_1 < E_3$ the reaction should start at higher temperature, and decrease with conversion. If $E_1 < E_2$ but $E_1 > E_3$ then the reaction should start at lower temperature, and increase afterwards.

b. Adiabatic operation

In an adiabatic operation, there is a simple relation between the variation of temperature rise and conversion. In addition, this is independent of the type of reactor. Consider a homogeneous reaction of the type A $\rightarrow$ products . The feed with the mass throughput G enters the reactor at T_1. The mixture leaves the reactor at T_2. The inlet molar flow rate of the reactant A is $F_{A0} = (G/\rho)c_{A0}$, where ρ is the density, and c_{A0} the initial concentration. The following energy balance may be written:

$$GC_p^1(T_1 - T_0) = GC_p^2(T_2 - T_0) + F_{A0}X_A(-\Delta H_R) \tag{8.66}$$

T_0 is a reference temperature, not very far from T_1 and T_2. Further we assume that the mass heat capacity is almost constant, so we may write $C_p^1 = C_p^2 = C_p$. It follows immediately the relation:

$$\Delta T = \Delta T_{ad} X_A \tag{8.67}$$

where ΔT_{ad} is the *adiabatic temperature change* defined by:

$$\Delta T_{ad} = \frac{(-\Delta H_R)}{\rho C_p} c_{A0} \tag{8.68}$$

Hence, a good approximation in an adiabatic operation is that the temperature variation is proportional with the adiabatic temperature change multiplied by conversion.

The adiabatic temperature change ΔT_{ad} is an important characteristic in designing chemical reactors. As the relation (8.68) indicates, ΔT_{ad} depends on the heat of reaction, the heat capacity of the mixture, as well as on the reactant concentration in feed. Fig. 8.14 presents typical temperature profiles. For both endothermic and exothermic reactions, the use of a large amount of inert brings the operation close to an isothermal regime, but the reactor productivity decreases by dilution. Therefore, use of inert may be uneconomical. Another solution could be imagined, as the use of intermediate heating (endothermic reactions) or intermediate cooling (exothermic reactions).

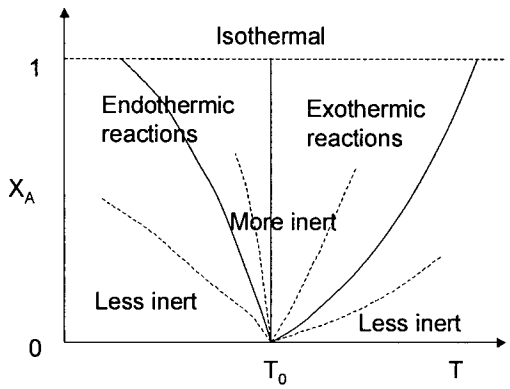

Figure 8.14 Temperature profiles for adiabatic operation

The heat of reaction developed by an exothermal reaction in an adiabatic reactor can save energy by means of a feed-effluent-heat exchanger (FEHE) device, as in the case of the HDA process. Even if PFR is stable as stand-alone unit, it may become unstable in such energy recovery loop. This problem will be analysed in Chapter 13 as an example of interaction between reactor design, energy saving and control.

c. Non-adiabatic operation

The polytropic mode makes use of a thermal agent. The temperature profile inside the reactor can deviate more or less from the (ideal) constant temperature, depending on the rate of the heat transfer to the cooling agent. If the heat transfer is too low, a *hot spot* may occur, which in general is dangerous for operation.

A useful representation of the thermal regime is the X_A-T diagram. By dividing the relation (8.54) by (8.51), and by taking into account (8.68), the following equation is obtained for the conversion-temperature profile:

$$\frac{dX_A}{dT} = \frac{1}{\Delta T_{ad} - \dfrac{4Uc_{A0}}{\rho c_p d[-r_A(X_A,T)]}(T - T_a)} \tag{8.69}$$

Figure 8.15 displays several trajectories for an exothermic reversible reaction. The optimal reaction rate is located close to the equilibrium curve. The points A, E, G, H

correspond to several feed temperatures. Let's consider a higher feed temperature (point A). Initially the reaction rate is high, the second term in the denominator of the equation (8.69) is nearly zero, so that the slope dX_A / dT is close to $1/\Delta T_{ad}$. As a result, the temperature increases with an initial adiabatic trend. As the reaction advances the difference between the two terms becomes smaller, while the slope dX_A / dT becomes larger. When the two terms are equal, the slope goes to infinity the temperature reaching a maximum. The profile exhibits a *hot-spot* given by the relation:

$$T - T_a = \frac{\rho c_p d}{4Uc_{A0}}(-r_A)\Delta T_{ad} \tag{8.70}$$

After reaching the maximum, the second term becomes larger than the first one, and the slope dX_A / dT becomes negative. The temperature decreases steadily, although the conversion still increases, up to the final point D. It may be observed that a trajectory of type ABCD is close to the optimum reaction rate. If the inlet temperature is somewhat lower (point E) the temperature profile still shows a maximum, but the reactor is operating globally at a lower reaction rate. If the feed temperature is low, as indicated by the points G or H, the temperature profile decreases monotonically. The profile is almost isothermal, but globally the reaction rate is low, and in consequence a large reactor volume is needed.

Hence, trajectories exhibiting maximum temperature, as ABCD or EFD, are more economical than isothermal profiles. This should be obtained not by less intensive heat transfer, but by selecting suitable temperatures for the feed and the thermal agent. Naturally, the maximum reactor temperature should be acceptable. But more important is to check that the proposed design does not exhibit an excessive *parametric sensitivity*, which can lead to a complete destabilisation of the operation. This aspect, together with other safety topics, will be discussed in the next section.

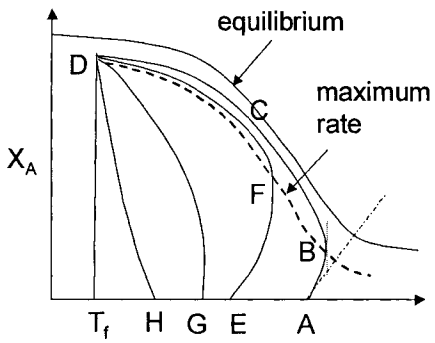

Figure 8.15 Conversion-temperature trajectories for exothermic reversible reaction in non-adiabatic operation

8.5.2 Stability of the thermal regime

In this section we will discuss basic aspects regarding the stability of the thermal regime of chemical reactors. More material could be found in specialised books, as in the monograph of Carrbery and Varma (1987).

1. Parametric sensitivity

The concept of parametric sensitivity designates the behaviour of a plug flow reactor in the case of high exothermic reactions with respect of some parameters characterising its thermal regime. As typical parameters we may cite initial concentration of the reactant(s), feed temperature T_0, and cooling agent temperature T_a.
Figure 8.16 shows qualitatively the behaviour of a PFR. The temperature profiles correspond to a feed temperature of 340 K, and the thermal agent temperature between 300 and 342.5 K. Up to 335 K, the temperature profiles shows a gradual variation. If T_a has lower values, say below 330 K, the temperature decreases further, meaning that in fact there is no reaction. Contrary, higher T_a can start the reaction and give a satisfactory conversion over the whole reactor length. However, above a certain value of T_a the temperature profile becomes very sensitive with the feed temperature. Thus, when T_a increases from 335 to 337.5 K an excessive temperature rise (hot-spot) appears at 420 K. In this case a modification of T_a with 2.5 K gives an increase in the reactor temperature of 80 K. For 5 K variation in T_a the hot-spot rise is of 100 K!
The situation described above is not acceptable for operation. Therefore, hot-spot occurrence is very likely with high exothermic reactions, and must be avoided by a proper design and selection of operating parameters. Computer simulation is a powerful method that can be used to detect such behaviour.

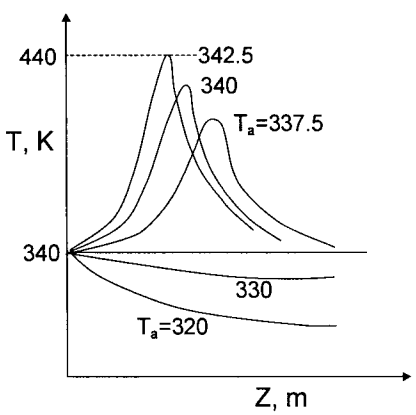

Figure 8.16 Parametric sensitivity of a PFR

2. Multiple steady states

The intersection of the material balance and energy balances gives the *stationary operation points* of a chemical reactor. In the most cases, there is a single operating point, or a single stable steady state. However, there are a number of cases displaying

multiple steady states. In other words, the reactor could operate in several points, depending on the variation of some parameters during the operation. Some states could be stable, but some states could be unstable. The reactor design should be adapted such to ensure that the desired stable-state will be always reached, even for large variations in the operating parameters. The operation around unstable points should be avoided. Working in an unstable point is in principle possible, but the stabilisation implies a costly control and safety system. Note that safety is more important than any other economic or performance consideration in designing chemical reactors. The occurrence of multiple steady states should not be limited to only stand-alone analysis, but incorporating the effect of recycles. Chapter 13 will discuss this topic in more detail.

The occurrence of multiple steady states can be illustrated at best by a CSTR in which a high exothermic reaction takes place. A simple method is to examine separately the behaviour of the two terms of the energy balance: heat generated by reaction, and heat transferred from the reactor. The heat generated is proportional with the reaction rate and the thermal effect:

$$Q_G = V(-\Delta H_{R,A})[-r_A(X_A,T)] = (-\Delta H_{R,A})F_{A0}X_A \tag{8.71}$$

For a first-order reaction $-r_A = kc_{A0}(1-X_A) = k_o \exp(-E/RT)c_{A0}(1-X_A)$. From the characteristic equation of a CSTR we obtain:

$$X_A = \frac{k_0\tau \exp(-E/RT)}{1+k_0\tau \exp(-E/RT)} \tag{8.72}$$

where $\tau = Vc_{A0}/F_{A0}$ is the residence time. It follows that the heat generated can be expressed as function of temperature and conversion by the relation:

$$Q_G = F_{A0}(-\Delta H_{r,A})\frac{k_o\tau \exp(-E/RT)}{1+k_o\tau \exp(-E/RT)} \tag{8.73}$$

Similarly, in the case of a first-order reversible reaction $A \underset{k_2}{\overset{k_1}{\leftrightarrow}}$ we find:

$$Q_G = F_{A0}(-\Delta H_{r,A})\frac{k_o\tau \exp(-E/RT)}{1+k_{1,0}\tau \exp(-E_1/RT)+k_{2,0}\tau \exp(-E_2/RT)} \tag{8.74}$$

Numerical exploration of the equations (8.73-74) shows that the curves Q_G-T have a *S*-shape for irreversible reactions, and a maximum for reversible reactions (non-represented). The shape is more complex in the case of multiple reactions, because simultaneously exothermic or endothermic reactions in the individual steps.

The heat transferred displays a much simpler trend, being in general a linear function of temperature. We may distinguish two contributions:

- Sensible heat of the reaction mixture $Q_{T1} = Gc_p(T-T_0)$.
- Heat transferred to the thermal agent $Q_{T2} = UA_t(T-T_a)$, with T_a constant.

Hence, the heat transferred is given by:

$$Q_T = Gc_p(T - T_0) + UA_t(T - T_a) \tag{8.75}$$

Plotting Q_T against T shows a family of lines that can be shifted up and down by means of T_0 or T_a. Modifying the heat transfer coefficient and the heat transfer area makes change the slope. With these elements we may examine how multiple steady states might occur. The intersection of Q_G and Q_T gives the temperature of the stationary states, which can be further used to compute conversion and concentrations. Figure 8.17 presents three typical situations:

- Low conversion state, when either the temperature T_a is too low, or the product UA_t is too high.
- High conversion state, which may occur at higher T_a or lower UA_t.
- Three or more steady states. In the case of a first-order reaction there are three steady states, while in the case of a first-order consecutive reaction there are up to five stationary points.

It is important to note that the behaviour of these steady states is not identical with respect to inherent disturbances in operating conditions, as for example feed reactor temperature, composition or flow rate of the feed, or temperature and flow rate of the cooling agent, etc. Some are insensitive to such variations, in the sense that after the disturbance vanishes the system comes back naturally in the original state. These are *stable stationary states*, as the points A and C in Fig. 8.17. In the case of the point B the situation is essentially different. This is an *unstable stationary state* because in the absence of a control action small disturbances will move the system either to the high conversion state (reaction ignition), or to the low conversion state (reaction extinction). This type of behaviour is dangerous for operation and must be avoided.

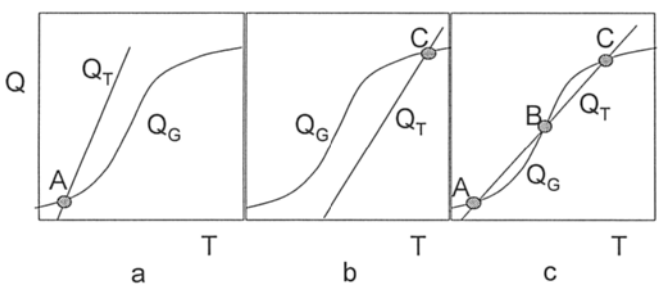

Figure 8.17 Stationary steady-states for a CSTR for an irreversible exothermic reaction

A physical explanation of the multiple steady states occurrence can be found by examining the slope of the curves Q_G and Q_T against T in the stationary points, as presented in Figure 8.18. Consider the low conversion point A (Figure 8.18a). If a disturbance makes decrease the reactor temperature, such as $T<T_A$, then the heat generated becomes larger than the heat transferred, $Q_G>Q_T$. If the disturbance disappears, then the reactor comes back naturally to the point A. Contrary, if $T>T_A$ then $Q_G<Q_T$, and the reactor cools down. Thus, the point A is stable, because it recovers itself after a disturbance. The same demonstration is valid for the point C. Generalising the above result, the necessary condition for stability is that the slope of the heat transferred to be larger than the slope of the heat generated:

$$\frac{dQ_G}{dT} < \frac{dQ_T}{dT} \tag{8.76}$$

The behaviour of the mid-state (point B) is different. If the temperature decreases below T_B with a small amount ΔT it can be seen that the heat generated by reaction is unable to bring the temperature back when the disturbance disappears. Because $Q_G < Q_T$. the temperature has the tendency to decrease even more. The operating point will move finally in the low conversion point. It is said that the reaction dies out. On the contrary, when the reaction temperature increases by ΔT, because $Q_G > Q_T$ the temperature will increase steadily up to reaching the stationary point of high conversion. It may be observed that the unstable point is characterised by the condition that the slope of heat generated by reaction be larger than the slope of heat transferred:

$$\frac{dQ_G}{dT} > \frac{dQ_T}{dT} \tag{8.77}$$

The above analysis regards only the steady state behaviour. In consequence, no indication is given about the evolution of the system in time. The time behaviour is important particularly in the case of the unstable steady states. Therefore, a more rigorous analysis of stability must take into account a dynamic model. Two approaches can be applied. The first one is to study the behaviour to small disturbances by using a linearised model developed around the stationary point. The model consists of differential equations for which standard numerical methods can be used. The second approach consists of studying the influence of parameters that may affect significantly the qualitative behaviour of the system over a larger range of variation by using the techniques of *bifurcation analysis*. Chapter 13 presents some results obtained by applying this last technique in studying the behaviour of chemical reactors in recycle systems (Bildea and Dimian, 1998).

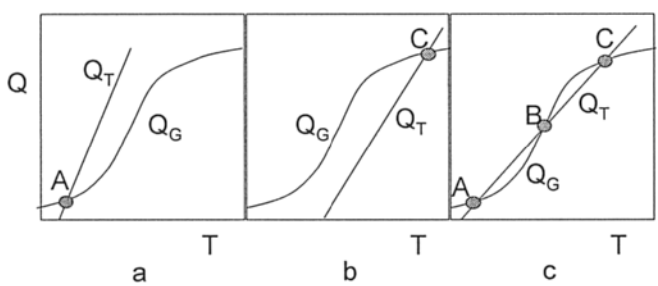

Figure 8.18 Stable and unstable steady states: the slope condition

Note that the auto-thermal PFR reactor (preheat of inlet reactant by the outlet reaction mixture) exhibits similar behaviour with CSTR. Even if the PFR alone is stable, the positive feedback of heat through the recovery heat exchanger makes the system unstable. The stabilisation can be obtained by introducing a heat source that keeps constant the feed reactor temperature (see also the Chapter 13).

8.5.3 Types of thermal design

This section deals with issues regarding the thermal design of chemical reactors, which will be examined following the two main types, mixed and plug flow reactors.

a. Mixed reactors

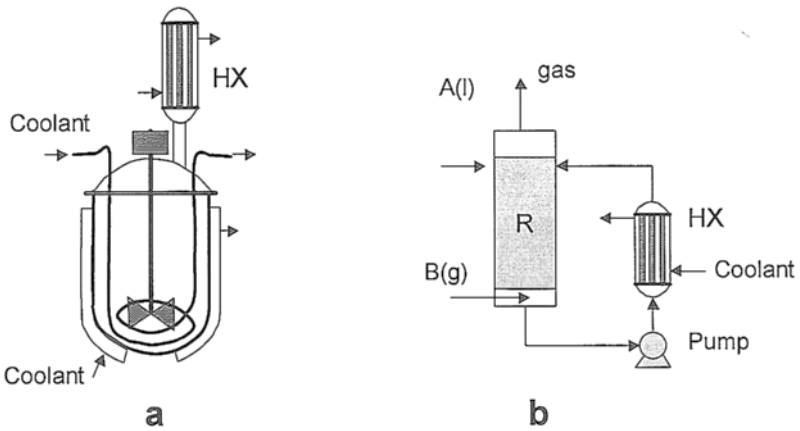

Figure 8.19 Heat transfer devices for mixed reactors

The main advantage of a mixed reactor is high intensity of heat and mass transfer. Constant temperature is the usual way of conducting a reaction in laboratory. There are many reasons to extrapolate this mode of operation at industrial scale. Fig. 8.19 illustrates two solutions are applicable to liquid-phase reactions .

The transfer of the heat of reaction may be achieved by means of an external jacket, or/and by the use of an internal heating/cooling coil. In a more efficient set-up the thermal agent circulates in a semi-closed loop, in which the temperature of the thermal agent is regulated by make-up from a constant temperature source. In some very exothermic reactions, as polymerisation, the operation at the bubble point of the mixture is possible. The cooling takes place by the vaporisation of a solvent or of a reactant. The vapour phase is condensed in an external heat exchanger and refluxed back.

A very efficient heat transfer may be achieved by pumping the reaction mixture via an external heat exchanger. This solution is also applicable to a plug flow reactor. If the recycle rate is high, the global behaviour will be close to a mixed reactor.

b. Plug flow reactor

Plug flow reactors are applied mainly for gas-phase reactions. Heat transfer coefficient inside the reactor tube usually controls the overall heat transfer. High turbulent flow regime is recommended. However, the fluid velocity is constrained by the allowable pressure drop, by the feasible reactor length, catalyst attrition, etc. Figure 8.20

illustrates two types, pipe-tube and heat exchanger reactor. Pipe reactor is suitable when the gas velocity should be high, as in the case of cracking of hydrocarbons, typically between 30 to 50 m/s. Fixed bed and tubular heat exchanger is recommended when the gas velocity should be kept low, as when using solid catalysts. In this case the superficial gas flow rate is typically between 10 to 30 cm/s.

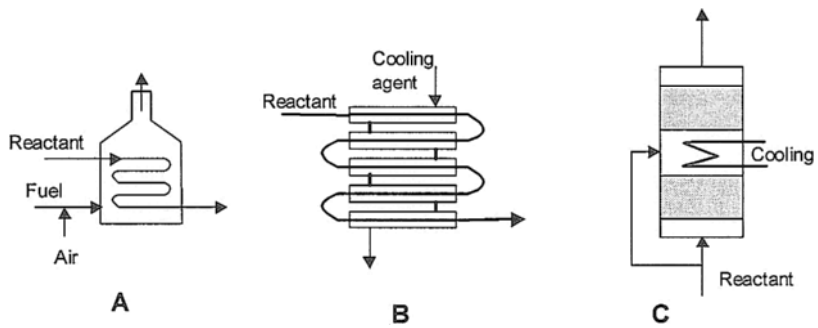

Figure 8.20 Types of thermal design for PFR

8.6 SELECTION OF CHEMICAL REACTORS

A central issue in process design is the selection of the best reactor that could meet the process requirements before to start the flowsheet development. An 'ideal' reactor configuration should conciliate process operability with productivity requirements. In this respect we may mention:

- Safe operation within the feasible space of temperature, pressure, concentration and residence time.
- Environmental acceptability.
- Good controllability properties: stable operation and easy rejection of disturbances.
- Acceptable flexibility to feedstock quality. Capacity to handle large variations in throughput.
- Maximum selectivity to desired products and minimum waste production.
- Constant product quality.
- Low capital and operating costs.

Some preliminary information should be collected before starting the evaluation. The following checklist may be of help.

- Write down the network of chemical reactions.
- Determine the number of independent reactions.
- List by-products and impurities.
- List quality requirements, minimum tolerable impurities.
- Compile physicochemical data: physical state of reactant, reaction enthalpy and Gibbs free energy in standard conditions.
- Specify the operating conditions, as temperature and pressure.

- List safety problems, as flammability and explosion limits.
- Study chemical equilibrium issues, as conversion, effect of temperature and pressure, reactants' ratio.
- Study selectivity issues linked with conversion.

8.6.1 Reactors for homogeneous systems

Taking into account the elements discussed before, we may formulate some guidelines for reactor selection. The strategy may be applied also for heterogeneous reactions described by pseudo-homogeneous models, as some gas-solid catalyst reactors, or gas-liquid reactions with reaction in the liquid phase.

1. Continuous versus batch reactors.
Continuous processes are preferred for large-scale production of commodities or intermediates, as in basic organic, inorganic, petrochemical and polymer industries. The boundary might be placed between 5000 to 10000 tonne/year. Batch reactors are more difficult to control. Therefore, continuous processes might be suitable even for small rates of dangerous products, which could be at best produced and consumed on site, and not stored and transported. Semi-batch processes may also be suitable for temperature sensitive reactions.

2. CSTR versus PFR reactors
CSTR can offer intense heat and mass transfer. Beside, this reactor is compatible with the manner of which most of the reactions are carried out in laboratory. PFR brings the advantage of productivity, but here the mixing is detrimental. Thus, PFR is not the best when high heat and mass transfer is required. Hence, the designer is confronted with the dilemma "to mix or not to mix"! To answer this question, two aspects should be examined mainly: 1) the contact mode of reactants, and 2) the magnitude of the heat of reaction. The first aspect may be solved by pre-mixing, either in separate devices, or when feeding the reactor. The second problem is solved in principle better in a mixed reactor, but it can be treated also conveniently in a PFR if sufficient specific heat transfer area is available (small tube diameter).

With respect to an isothermal operation we may formulate the following rules (adapted from Levenspiel, 1999):

Rule 1. For single reactions, minimise the reaction volume by keeping the concentration as high as possible for reactant whose order is $n>0$, otherwise keep the concentration low. Some application tips may be distinguished:

a. For normal reactions where $n>0$, CSTR requires a larger volume than PFR. The difference increases with the conversion, particularly in the region of high conversions, and is also larger for higher reaction orders.

b. The use of a series of CSTRs, either as individual units, or assembled in a compact construction, can diminish the required total reaction volume, bringing closer to the volume of a PFR for a sufficient large number of units.

c. One of two CSTRs followed by a PFR might also be seen as an interesting alternative that minimises the reaction volume.

d. At low conversions, up 30%, the difference between CSTR a PFR is not relevant as performance. The selection can be done on the base of cost, but also on controllability and safety reasons. Hence, in a PFR the reaction can be stopped easier, but simply cutting the feed and flushing the reactor with inert. A CSTR would require much more time.

Rule 2. For reactions in series, to maximise any intermediate, do not mix fluids that have different concentrations of the reactant and intermediates. PFR gives the most of all intermediates.

Rule 3. For parallel reactions to get the best product distribution, keep in mind that low reactant concentration c_A favours the reaction of lowest order, while high c_A favours the reaction of highest order. If the desired reaction is of intermediate order then c_A should be intermediate. If the reaction orders are the same, the product distribution is not affected by concentration, and the only solution is to search a suitable catalyst.

Rule 4. Complex reactions can be analysed by means of simple series and parallel reactions. In the case of series-parallel reactions of first-order, the behaviour as series reactions dominates. A PFR reactor is more advantageous for the production of the intermediate component.

Rule 5. High temperature favours the reaction with larger activation energy. Reactions with small activation energy are slightly affected, so that low temperature is preferred.

3. Thermal design.

The technical solution depends on the sign of the thermal effect, endothermic or exothermic, as well as of its magnitude. The following systematisation may be applied.

a. Endothermic reactions.

The reaction temperature should be maximised to ensure high reaction rate. The following reactor types may be considered:

- Adiabatic reactors. Premix the reactant with an inert heat carrier, fluid or solid, which can be recovered and recycled.
- Non-adiabatic reactors. Use heating from an external source, as for example:
  - Preheat and reaction coil placed in a furnace, as for hydrocarbon cracking;
  - Shell-and-tube heat exchanger, usually the reaction taking place in tubes.

b. Exothermal reactions. In the case of CSTR the designer should ensure that the operation does not occur in an unstable steady state (except special cases), or there is not danger of runaway in the case of PFR. The following solutions may be considered:

- CSTR with cooling by external jacket and/or cooling coil.
- CSTR operating at the mixture boiling point and external condenser.
- CSTR or PFR with external cooling loop.
- Adiabatic PFR with inert dilution. Provide quench after reactor to prevent overheating and thermal decomposition.
- PFR with external cooling, either as long length/diameter tube (coil) or as shell-and-tube heat exchanger.

8.6.2 Reactors for heterogeneous systems

The selection of a reaction system for multiphase reactors is a complicated matter that cannot be covered in the limited space of this book. Here we mention the comprehensive paper of Krishna and Sie (1994) addressing this topic.

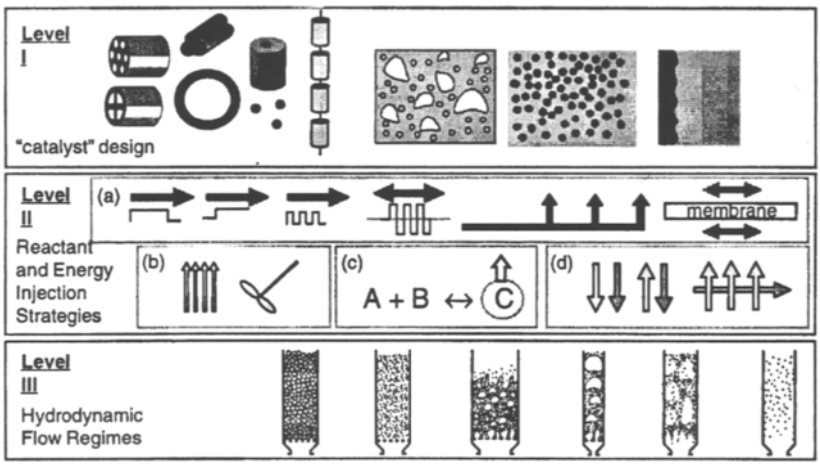

Figure 8.21 Strategy for multiphase reactor selection (after Krishna & Sie, 1994)

The three-level strategy (Fig. 8.21), consists of the following type of activities:

- Catalyst design strategy.
- Injection and dispersion strategies.
- Choice of hydrodynamic flow regime.

The first phase, called 'catalyst design', studies the kinetic problem, namely the rate-limiting step and measures to enhance it. For example, in the case of a solid catalyst the design variables are the particle size, its shape, porous structure and distribution of active material. For gas-liquid systems the decisions concern the choice between gas-dispersed or liquid-dispersed systems, and provisions of an appropriate ratio between liquid-phase bulk flow and liquid-phase diffusion layer.

The second level deals with the contact of reactants. It consists of several strategies:

- Reactant and energy injection strategy, as one-shut (batch), continuous pulsed injection, reversed flow, staged injection, and use of a membrane.
- Choice of the optimum state of mixedness.
- Choice between in-situ separation of products and post-reaction treatment.
- Injection of energy against in-situ production.
- Contacting flow pattern as co-, counter-, and crosscurrent contacting of phases.

The third level deals with issues regarding the details of heat and mass transfer phenomena. Here the choice is between different hydrodynamic regimes in multi-phase flows, as dispersed bubbly flow, slug flow, or churn-turbulent flow for gas-liquid systems, or dense-phase transport vs. dilute-phase transport for gas-solid systems.

The application of this strategy is worthwhile particularly for exploring innovative reaction systems that goes beyond the combination of classical mixed and plug flow models. From the above presentation, it can be observed that more attention is paid to the problem of combining the reaction and separations in a compact device (process intensification), as reaction with distillation, extraction, membrane diffusion, etc.

EXAMPLE 8.1 Selection of a chemical reactor

Ethylbenzene (EB) is currently produced by alkylation of benzene with ethylene, primarily via two routes: liquid-phase with $AlCl_3$ catalyst, or vapour-phase in catalytic fixed bed reactor (Ullmann, 2001). Examine the differences, as well as advantages and disadvantages of these routes. List pros and cons in selecting suitable reactors.

Solution.

1. Chemical reaction network

The alkylation of benzene with ethylene is described by a network of complex reactions. The main reaction is:

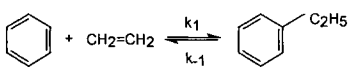

The reaction needs Lewis-acid type catalysts. Higher polyalkylbenzenes are formed by successive series reactions, as for example the formation of diethylbenzene.:

$$C_6H_6 + C_2H_4 \underset{k_{-2}}{\overset{k_2}{\rightleftharpoons}} C_6H_5\text{-}(C_2H_5)_2$$

Note that diethylbenzene has three isomers in orto-, meta-, and para- ring positions. Up to six substitutions at the benzene ring might be theoretically possible. Propylene present in ethylene as impurity may also produce cumene and higher alkylates as by-products. Using an excess of benzene can improve the yield by converting the polyalkylbenzene into ethylbenzene, as for example:

$$C_6H_5\text{-}(C_2H_5)_2 + C_6H_6 \underset{k_{-3}}{\overset{k_3}{\rightleftharpoons}} 2C_6H_5\text{-}C_2H_5$$

Hence, the alkylation of benzene with ethylene consists of a complex network of reversible reactions. Globally the reaction may be seen as parallel with respect of ethylene and benzene, and series with respect of polyalkylbenzenes.

2. Chemical equilibrium

Modern simulators can calculate the equilibrium of complex reactions by the minimisation of Gibbs free energy of the reaction mixture. Here we present results obtained with the module RGibbs of Aspen Plus. An appropriate thermodynamic model is a cubic equation of state, as Peng-Robinson.

Let's start with the equilibrium of the main reaction for a molar ratio 1:1. Figure 8.22A presents the equilibrium conversion on the interval 500-700 K, and pressures of 1, 10, 20, and 40 atm. It may be observed that almost complete conversion of benzene is possible, but the temperature should be kept lower than 500 K. The equilibrium conversion decreases with the temperature, because the reaction is exothermic. Higher pressure can increase significantly the equilibrium conversion, allowing higher reaction temperature and higher reaction rate.

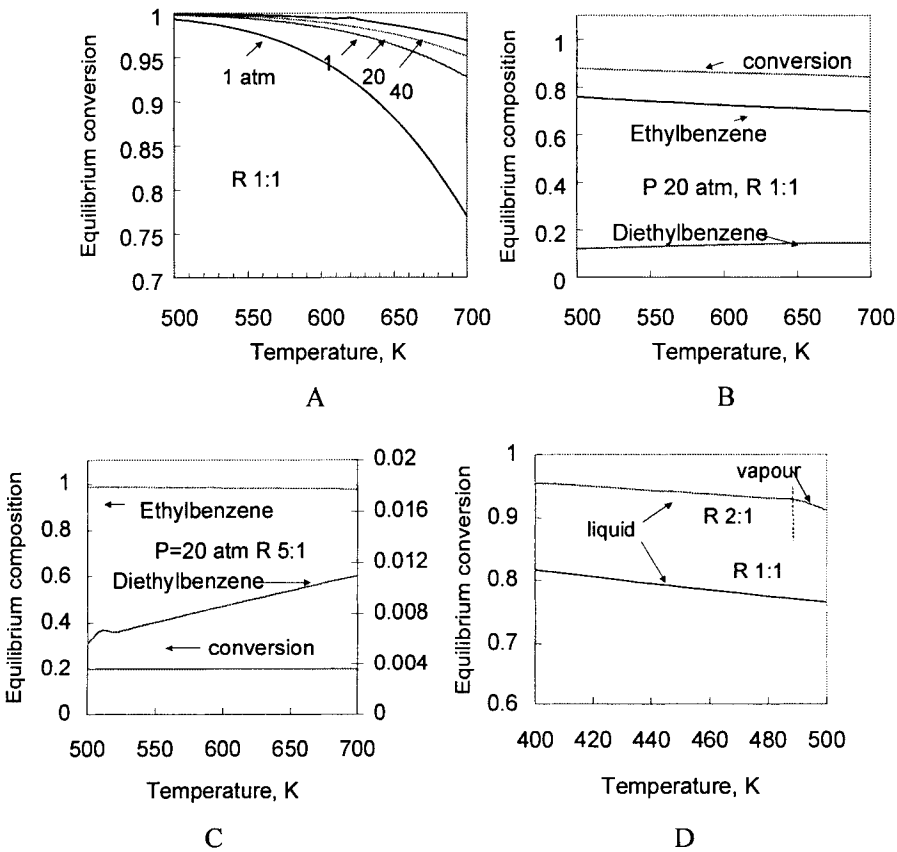

Figure 8.22 Chemical equilibrium by the alkyklation of benzene with ethylene

Now we consider a mixture of four components: benzene, ethylene, ethylbenzene and diethylbenzene. Figure 8.22B presents the equilibrium composition at a ratio of reactants 1:1 and 20 atm. The above picture changes considerably. The equilibrium conversion of benzene drops under 80%. The amount of ethyl-benzene at equilibrium drops also significantly, because of diethylbenzene. On the contrary, the temperature seems not to play a role. Hence, we must include in our analysis secondary reactions. The problem is that we would need kinetic data to assess the selectivity.

Fortunately, the thermodynamics can help again. What happens if we would consider an excess of benzene? Figure 8.22C presents results for a benzene/ethylene ratio of 5:1 at 20 atm. It may be seen that the selectivity in ethyl-benzene increases considerably, over 98%. The benzene conversion per pass is low, of 20%, signifying high recycle, but this is the price for high selectivity.

Improving the yield can be obtained by treating the recycled poly-alkyl-benzenes with an excess of benzene. Figure 8.22D illustrates that a ratio benzene /di-ethyl-benzene of 1:1 is insufficient, but at 2:1 an equilibrium conversion higher than 95% may be obtained. Note that at 20 bar and below 200 °C the reaction takes place in a single liquid phase, after which a second vapour phase appears.

Summing up, the thermodynamics teaches us that the following elements should be taken into account when selecting and designing a reactor system for EB synthesis:

- To get high conversion use higher pressures, larger than 20 bar, and lower temperatures, under 500 K.
- Use an excess of benzene (4:1 to 5:1) to improve the selectivity. Consider complete consumption of ethylene.
- If poly-alkyl-benzenes are formed, further improvement in the yield of EB can be obtained by reversible conversion with benzene.

3. Catalyst

Firstly, Lewis acid catalyst as $AlCl_3$, $FeCl_3$, or $ZrCl_4$ can be considered. Aluminium chloride catalyst is a complex of $AlCl_3$ in benzene with ethyl chloride as promoter, and gives fast reaction rates. The problem is that the removal of $AlCl_3$ from the final product and its recycle implies costly steps and waste formation. Another catalyst in this category is BF_3/alumina commercialised by UOP Alkar process. Solid-phase silica-alumina catalysts, as zeolite ZSM-5 developed by Mobil, can be successfully applied. Note that the reaction mechanism is different from the $AlCl_3$ catalysis. Ethylene molecules are adsorbed onto Broensted acid sites, and the activated complex reacts further with benzene. This reaction mechanism gives less polyethylbenzenes, so that a transalkylation reaction is not necessary. Vapour phase, as well as liquid phase zeolite may be applied, depending on the catalyst properties.

4. Kinetics

The first alkylation step is much faster than the subsequent steps, because the alkyl groups decrease the activity of the aromatic ring. As an order of magnitude, the reaction rates for the first, second and further substitutions are of 1: 0.5: 0.25: 0.1: 0.1: 0.1.

5. Heat effect and thermal regime

The reaction is moderate exothermic with ΔH_R = -114 kJ/mol. A measure of exothermicity is the adiabatic temperature rise. Table 8.1 gives some values calculated for an inlet temperature of 400 K and 1 atm. The adiabatic temperature rise for the stoichiometric mixture is considerable (441.6 K), but the dilution with benzene in the ratio 5:1 makes drop it to 144.6. If diluted ethylene feedstock is considered, the

adiabatic rise diminishes further, but less compared with benzene dilution, because much lower molecular weight. Hence, the reaction needs a heat transfer device, except for very diluted ethylene feedstock and high benzene recycle.

Table 8.1 Adiabatic temperature rise by the benzene alkylation

Case	Feed composition	F (kmol/h)	G (kg/h)	Cp (kJ/kg/K)	T_{out}-T_{in}
1	R =1	2	106.5	2.24	441.6
2	R=5	6	418.6	1.74	144.6
3	R=5, 25% ethane	7	448.7	1.77	132.5
4	R=5, 75% ethane	9	508.8	1.82	113.6

6. Secondary reactions and product specifications

Ethylbenzene is used mainly for the manufacture of styrene. Among impurities, diethylbenzene is very important, because dehydrogenation to divynilbenzene, which is harmful in polymerisation. It is worth to keep in mind that the formation of troublesome impurities should be prevented by the design of the reaction system. In this respect the catalyst plays a determinant role. Zeolite-type catalysts should give less polyalkylbenzene. The use of an excess of reactant can help to shift the product distribution to higher yield in ethylbenzene. Another possibility is to use a separate reactor for transalkylation. The trade-off between of a larger recycle of benzene and the use of a secondary reactor is a matter of optimisation.

7. Reactor selection

With the above elements the following reaction systems may be considered:

A. Liquid-phase alkylation using $AlCl_3$ catalyst (heterogeneous or homogeneous system).
B. Vapour-phase alkylation with BF_3/alumina catalyst.
C. Vapour-phase zeolite catalyst.
D. Liquid-phase zeolite catalyst.

Table 8.2 presents comparatively the four reactor types proposed above. Liquid-phase alkylation was practiced in the past, but is nowadays completely obsolete, mainly because of pollution problems. Vapour-phase alkylation (UOP *Alkar* process) was popular up to 1970, when Mobil/Badger process based on ZMS-5 synthetic zeolite catalyst was launched. This process dominates the market nowadays, but is in competition with the liquid-phase process based equally on zeolite catalyst proposed by UOP/Lummus. The two processes have similar performances. The selection depends greatly on the catalyst behaviour, price and regeneration cost. We would prefer the last, for the following reasons:

- Lower temperature is more favourable from equilibrium viewpoint, implying less benzene recycle;
- Liquid-phase reaction gives also higher productivity compared with a gas-phase reactor;
- A simpler flowsheet and a better heat integration, because the absence of vaporisation/condensation steps before and after the reactor.

Table 8.2 Reactor selection by the benzene alkylation

		A	B	C	D
1	Reactor type	Stirred tank/ Bubble column	Tubular	Fixed bed	Trickle bed
2	Operating conditions	1-5 bar, 100-130 °C	25-35 bar 130-150 °C	400-450 °C 20-30 bar	< 200 °C 20 - 30 bar
3	Ethylene feed	> 90%	Diluted	Diluted	Concentrated
4	Benzene/ feed ratio	3 - 3.5	5 - 7	> 4	> 4
5	Transalkylation reactor	Yes	Yes	No	Yes
6	Catalyst handling	Removal and recovery	Recycle	Regeneration	Regeneration
7	Selectivity	Good	Good	Very good	Good
8	Sensitivity to impurities	High	Moderate	Low	Low
9	Environment	Corrosion/ Water Waste	Corrosion	No corrosion/ No waste	No corrosion No waste
10	Productivity	Good	Good	Good	Very good
11	Thermal regime	Isothermal/External cooling	Adiabatic	Adiabatic/ Cooling	Adiabatic/ Cooling
12	Materials	Special	CS	CS	CS
13	Reactor Cost	High	Moderate	Moderate	Moderate
14	Catalyst cost	High	Low	High	High
15	Selection	Obsolete	Fair	Good	Very good

We are tempted to proceed a little bit further, and examine the development of the whole flowsheet in relation with the reaction system. Let's suppose that the feedstock is of high purity ethylene and benzene. Because recycling a gas is much more costly than a liquid, we consider as design decision the total conversion of ethylene. The benzene will be in excess in order to ensure higher conversion rate, but also to shift the equilibrium. The equilibrium calculation can predict with reasonable accuracy the composition of the product mixture for given reaction conditions. Then polyalkylates, mainly diethylbenzene can be reconverted to ethylbenzene in a second reactor.

Hence, the reaction section will have two reactors, alkylation and transalkylation. The alkylation reactor should be operated at higher pressure where the solubility is high enough to ensure a homogeneous reaction. The reaction temperature may be selected such to allow cooling by steam generation. In this case a temperature in the range of 130-150 °C can produce low-pressure steam of 3 to 6 bar. Higher temperature would be more interesting, because higher value of the medium pressure steam, and its possible utilisation as heating agent for the distillation section. Thus, the process might be designed to be energetically self-sufficient.

For the development of the separation section we will examine the composition and the thermodynamic behaviour of the outgoing reaction mixture. This contains benzene, ethylbenzene and polyethylbenzenes. The separation sequencing is simple because the mixture is zeotropic and the difference in the normal boiling points of components is large. A first distillation column takes off benzene for recycle, a second one separates

the main product, and a third column recovers polyethylbenzenes for transalkylation. Figure 8.23 present the final flowsheet.

In conclusion, this example emphasises important issues in selecting a reactor:

1. Before any other consideration, the analysis of stoichiometry is necessary. This must include secondary reactions, as well as reactions generated by the existing impurities in the original feed. The analysis of chemistry should take into account constraints regarding the purity specifications in the final product.
2. Chemical equilibrium calculations may reveal essential features in design, particularly the feasible pressure/temperature range, as well as achievable composition space.
3. The selection of the operating conditions and the reactor design is subordinated to high selectivity, not only by maximising the amount of desired product, but also minimising or preventing the formation of components difficult to remove later.

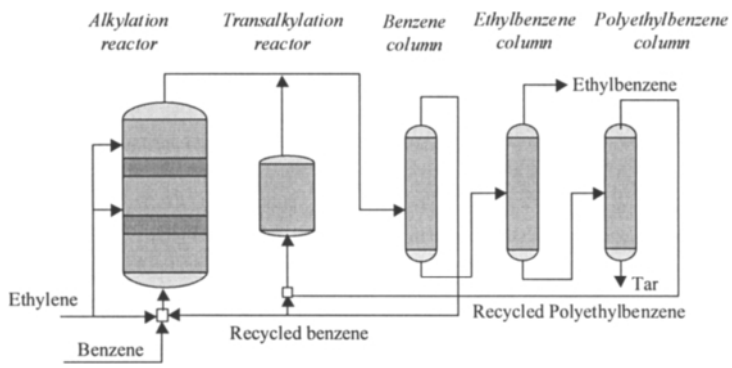

Figure 8.23 Ethylbenzene manufacture by liquid-phase alkylation of benzene

8.7 SYNTHESIS OF CHEMICAL REACTOR NETWORKS

The methods described so far for developing a reactor system start with the proposal of a device, either as single reaction space or as combination of zones. The solution is further evaluated by design and performance calculations. This approach is suitable in the case of simple reactions, where the difference between the two limiting models, mixed flow and plug flow is easy to express quantitatively. In more complex cases, as multiple reactions in homogeneous systems or multi-phase reactions, the selection and the design of an optimal reaction system is not easy. High productivity, requesting high per-pass conversion, is usually in conflict with low selectivity, which increases the cost of separations. The trade-off depends on a large number of variables, and is guided by heuristics rather than by rigorous evaluation. Without a systematic approach the evaluation of a large number of alternatives is necessary.

The synthesis problem of a chemical reactor network may be defined as follows. *Given* the reaction stoichiometry and kinetic expressions, initial feeds, reactor targets (productivity, selectivity, flexibility), technological constraints, *find* the optimal reactor network structure, as well as sub-optimal alternatives. The following elements should be determined:

- Feasible design space in term of temperature, pressure and concentrations
- Flow pattern, system's elements (zones), and their connection
- Size of zones and optimal distribution of flows
- Energy requirements and optimal temperature profile.

Therefore, in the first place the process synthesis should solve a structural problem, the configuration of the optimal reactor system. Then detailed design and refinement can follow. If there are several candidates close to optimum, these could be assembled in a superstructure and submitted to structural optimisation.

As it can be observed from the above discussion, the objective of such approach would be not to replace the principles of designing chemical reactors, but to facilitate the invention of more complex reaction systems. Some researches started in the recent years, but a real breakthrough in the design practice has not been achieved yet. This area is at the edge of the advanced research. Here we present only a brief description of two advanced topics, Attainable Region concept and Optimisation methods. For more details the reader is referred to the book of Biegler, Grossman and Westerberg (1998).

8.7.1 Attainable Region concept

Attainable Region (***AR***) is a systematic geometric method for the synthesis of a complex chemical reactor network. The concept has been developed in the last 15 years, starting with the pioneering works of Glaser and Hildebrand (1987). The visit of the website **www.wits.ac.za** (University of Witwatersrand, South Africa) may serve both as introduction and update in this topic.

The synthesis problem is the following: given a feed state and a number of fundamental processes, as mixing, chemical reactions, heating or cooling, find the best combination of these processes that will built-up the optimal chemical reactor, as well as the optimal operating conditions. Note that the objective function is usually of economic nature, but it may include safety or environmental elements.

The traditional way is to consider a (large) number of combinations of units, usually CSTRs or PFRs, and compute their performances for various designs. This method is tedious and never ensures that the best reactor has been found. Contrary, ***AR*** tries to give an answer from a different perspective. Firstly, it looks at the fundamental processes that may occur in the reacting system. The analysis enables to find a region where all the possibilities for conducting the reaction could be found. This is used to obtain the optimum layout and the optimum operating conditions. Then designing and sizing the chemical reactor is a downstream activity.

Before entering into the presentation of conceptual issues, some introductory elements are necessary.

- The *fundamental processes* that may be considered in synthesis of a reaction system are physical and chemical phenomena as, mixing, reaction, separation, and heat or

mass transfer. Later these phenomena can be materialised in reactors or unit operations that are already available, but also as innovative designs.

- The state of the system is characterised by *state variables*. These describe the fundamental processes, but it may include also variables from the objective function.
- Process vectors give the instantaneous change in state variables if a fundamental process occurs.
- Attainable Region has the property of *convexity*. Figure 8.24 gives a geometrical explanation. It is said that a region is convex if containing two points *A* and *B*, contains all the points of the segment *A-B*. The region is concave if the segment connecting A and B goes through the complement of the region. In other words, in a convex region all the vectors point-out into the region, or they are tangent at most to its boundary, or zero. A concave region can be transformed in a convex one by adding a 'convex hull'.

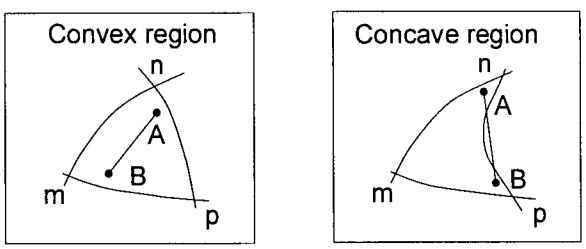

Figure 8.24 Convex and concave regions

In the discussion that follows we will consider a homogeneous reaction system where three types of fundamental processes are the most interesting:

- Mixing. By this operation two fluids of states c and c* produces a fluid with the state $\overline{c}$ given by the *lever arm rule*, as $\overline{c} = \alpha c + (1-\alpha)c^*$. α is a weighting factor such that $0 \le \alpha \le 1$. We can describe also a mixing by a vector $\mathbf{v} = \mathbf{c} - \mathbf{c}^*$ that points-out from the state c to the state c*. As state variables obeying a mixing law we may cite composition, enthalpy and residence time. Note that mixing as defined before can take place only in a convex region.
- PFR. The reaction rate at constant density is a vector tangent to the trajectory of component concentration, because the length variation can be translated in time.
- CSTR. The mixing vector **v** is collinear with the scaled reaction vector because $c - c^* = \tau r(c)$.

The construction of the Attainable Region

It is important to note that when using ***AR*** technique we are interested in constructing only the boundary of ***AR*** (∂AR). Any other interior point can be achieved by mixing points from the boundary. Sometime an interior point could be preferred because of

economic optimisation or technical feasibility. However, ∂AR will represent always the best performance.

A definite methodology to find the Attainable Region for given fundamental processes is not available. A trial and error procedure is necessary. However, the ***AR*** technique is supported by a powerful test procedure. The candidate region must respect the following necessary conditions, as demonstrated by the works of Glasser, Hildebrand (1997):

1. The region includes all the feed points.
2. No process vectors on the boundary of the region point out of the region.
3. No stationary point with mixing as process exists in the complement of the attainable region.

The first condition states that the feed must be included in the ***AR***, because it will deliver a product even without processing. Other possibility is by-pass the feed around the reactor. This operation modifies the residence time, and in consequence can shift the performance of the reactor system.

The second condition ensures that a candidate ***AR*** is convex. The process vector must point inwards, be tangent or zero. If a process vector points out of the region, then a possible extension could be imagined. This condition is particularly powerful when mixing is allowed as fundamental process. If by mixing boundary points the resulting vector points out then the region is not ***AR***, and must be extended.

The third condition can help to extend a candidate region that might fulfil the first two conditions. The stationary point with mixing is in fact a CSTR. If such point can be found outside the candidate region, this means that the Attainable Region has not been yet found, and an extension is possible. This condition can be satisfied if the system feed and maximum rate reactors (both absolute and relative) have been considered.

Example

The concept of ***AR*** will be illustrated by means of an example developed originally by Glasser and Hildebrand (1987). The problem consists of finding the best reactor network that maximises the amount of B product formed by the following reaction scheme (van de Vusse):

$$A \xleftrightarrow{k1,k2} B \xrightarrow{k_3} C$$
$$2A \xrightarrow{k_4} D \qquad (8.78)$$

The desired product B is formed by a reversible reaction from A, and consumed by a consecutive irreversible reaction to C, and is also in competition with the by-product D. Hence, only the species A and B are of interest.

The kinetic constants are as follows: k_1=0.01 s^{-1}; k_2=5 s^{-1}; k_3=10 s^{-1}; k_4=100 m^3/kmol.s. As fundamental processes we consider mixing, perfect mixed reaction (CSTR) and reaction with no mixing (PFR).

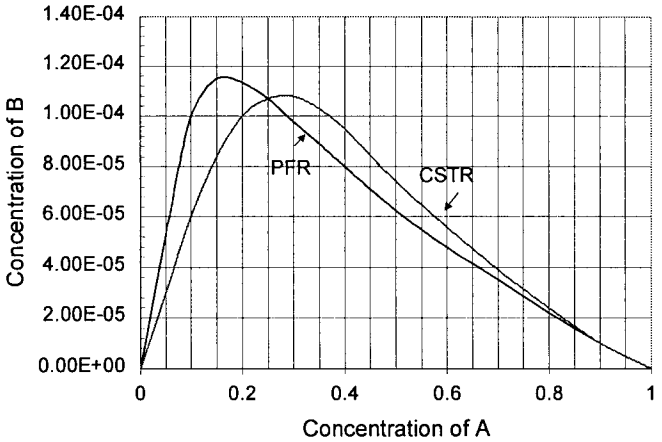

Figure 8.25 State-space representation of van der Vusse reaction for PFR and CSTR

In a first attempt, we will analyse the design problem based on the classical chemical reaction engineering. Note that the equilibrium of the reaction $A \longleftrightarrow B$ is shifted to the left, such that a small amount of B would appear. Because of the series reaction $B \rightarrow C$ the amount of B would be even smaller. It may be observed that the reaction rate A to D is very high compared with A to B. From this point of view, a small concentration of A (high conversion) would give a higher concentration of B. A CSTR would be suitable, but it will require a much larger volume than a PFR.

The analysis can be performed quantitatively by means of methods explained in the section 8.3. We consider individual PFR and CSTR with the pure A as feed of c_{A0} = 1 kmol/m^3. The concentration of all species can be obtained as function of residence time. With this information we can plot a state-space diagram c_B-c_A, as shown in Figure 8.25. It may be seen that a PFR gives a somewhat higher concentration of B at c_A around 0.15 (conversion 0.85), while CSTR gives an optimum concentration of B at c_A around 0.3 (conversion 0.7). Thus, taking into account the performance of ideal reactors it comes out that a PFR is preferred. Now the question is if we can find a better reaction system.

Let's examine in more detail the behaviour of a single PFR, as shown in Fig. 8.26, where the scale has been modified for better visibility. The trajectory of the reaction in the c_B-c_A space may be found directly from the obvious relation:

$$dc_B / dc_A = r_B /(-r_A) \tag{8.79}$$

In other words, the tangent to the reaction trajectory of species B and A in a PFR is given by the ratio of the corresponding reaction rates. It may be seen that at the left side, up to the point X, the region seems to obey the property of convexity. Vectors linking two points of the boundary point inwards the region. If for example two PFRs are connected in parallel, as figured by the points a and c, then the amount in B in the mixed product is inferior to that produced by a single PFR, as indicated by the point b. At the right of the point X the situation is different: better selectivity can by obtained in

two parallel PFRs (points d and f), compared with a single PFR (point e) The conclusion is that the PFR region is concave, and may be extended.

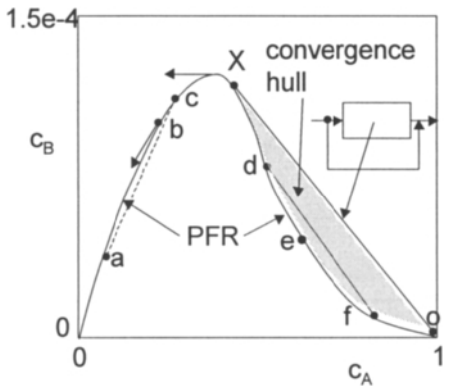

Figure 8.26 Correction of concavity by means of a 'convex hull'

We may consider the extension of the region by means of segments that fill-in in the concave domain. The full correction to convexity can be obtained by building what could be called a 'convex hull'. This can be obtained graphically by means of the segment *OX*. Note that *X* may be located as the point where the maximum rate of formation of B is recorded. It may be also observed that a point on the segment OX represents a PFR with bypass, the position depending on the fraction of feed split. It can be seen that a PFR with bypass gives a better selectivity than any PFR or combinations of PFRs up to the point *X*.

Summing up, we have obtained a candidate ***AR***. This obeys the first two conditions, because it contains the feed, and is convex. The question is if it satisfies also the third condition? The answer is no. Indeed, we have seen that a CSTR starting from the feed gives a better selectivity than a PFR. Thus, we should consider firstly a CSTR.

We will re-examine the Figure 8.25, where PFR and CSTR trajectories are displayed starting from the same feed. It may be seen that there is a large overlap in the behaviour of the two reactors. However, CSTR gives a better selectivity at lower conversion, while PFR gives a higher selectivity at higher conversion. We can proceed as before by adding a convex hull at the right of the CSTR region, starting with the feed. This can be obtained by drawing the tangent *OP*, as indicated in the Figure 8.27A. Moreover, the vector *OP* represents in fact a CSTR, because of the relation:

$$(c_{B0} - c_B)/(c_{A0} - c_A) = r_A / r_B \tag{8.80}$$

The point P is located as the maximum rate of formation of *B* related with the consumption of *A* in a CSTR. Points on the line *OP* represent a CSTR with by-pass, where the ratio of the direct feed and by-pass may be found by the lever rule.

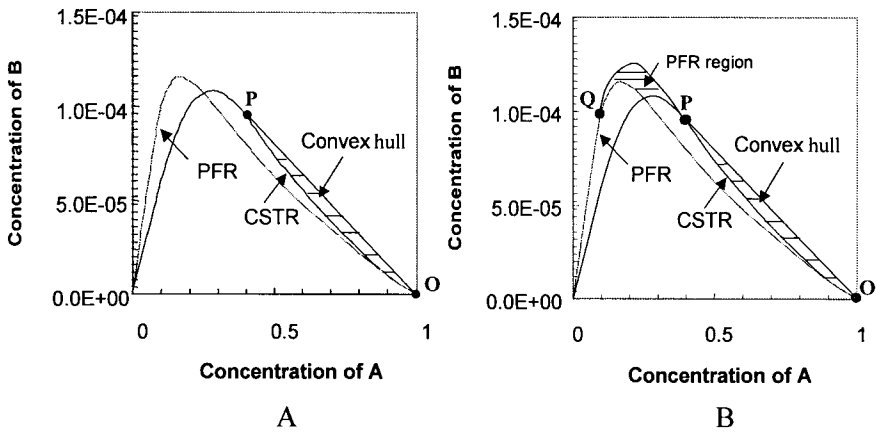

Figure 8.27 Construction of the Attainable Region

However the region at the left of the point *P* is not convex. But we may continue from the point *P* with a PFR, as indicated in Fig. 8.27B. The computation is done by simply integrating the differential equations of a PFR, this time input concentrations supplied by the exit of the CSTR. The new augmented region is convex. This time all three conditions are fulfilled. No other mixed reactors can be found above the boundary that could give a higher amount of B. This is the final Attainable Region.

After obtaining the Attainable Region, in fact drawing only its boundary, the synthesis of the reaction network is easy. Figure 8.28 displays possible configurations. Up to 60% a single CSTR with by-pass gives the best selectivity. The highest selectivity of the all reaction systems is obtained with a combination CSTR-PFR. The graphical construction gives the intermediate conversion, and enables to determine the size of the two reactors. The CSTR has to be sized to reach a conversion of 60 %, followed by a PFR to complete the reaction up to a conversion of 78%.

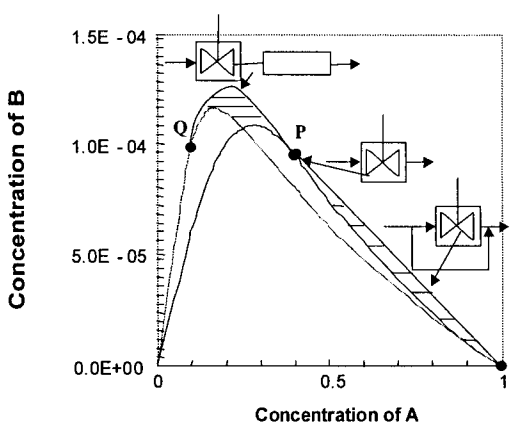

Figure 8.28 Possible configurations for the reaction system

Hence, the combination CSTR-PFR gives a higher yield in B that could be obtained with either single CSTR or PFR, as well as with other CSTRs or PFRs arrangements, in series or parallel. In general, the proposed combination is the best configuration of the all-imaginable combinations of CSTR and PFR reactors. The last result is important, and illustrates the power of the Attainable Region approach. Now we are sure that a better reactor cannot be obtained, and the search of other systems is not necessary.

As it has been shown, in ***AR*** approach the construction of the boundary is essential. Feinberg and Hidebrandt (1997) demonstrated that the boundary of attainable region could be assembled only by means of combinations of PFRs, CSTRs, and DSRs (differential side-stream reactors). The calculation of these elementary reactors is simple. The construction of an ***AR*** is not complicated, if the analysis is restricted at two dimensions. Moreover, 3-D representation could be visualised relatively easy with an appropriate computer tool. In the case of systems of higher dimensions the method relies rather on numerical techniques, and is not easy to apply.

The ***AR*** method has been extended to more complex system, as non-isothermal reactions, catalytic reactions, polymerisation reactors, or combination with separations. Other important applications of Attainable Region are in the field of optimisation and planning of experiments. More information can be found by consulting the above cited website.

8.7.2 Optimisation methods

The synthesis of chemical reactors by means of optimisation methods is another systematic approach in the field of chemical reaction engineering developed by process systems community. The synthesis problem consists of finding the optimal reactor network and its flow pattern, as well as the best energetic policy, for given chemistry, rate laws and systems constraints. This research area is relatively recent. Among representative papers, we can mention Kokossis & Floudas (1990, 1994, 1995), as well as Biegler and co-workers (1997). As mentioned in Chapter 7, when making use of structural optimisation there are two problems: generate a superstructure imbedding the optimal network, and find the true global optimum.

The first problem is the key issue. The immediate approach is to see the reactor synthesis as the inverse problem of the decomposition of a real reactor in compartments of ideal mixing patterns. Thus, the chemical reaction network would consists of a combination of ideal models, CSTR's and PFR with connections and by-pass streams.

In addition, we can consider the differential stream reactor (DSR) as a generalisation of PFR model, in which the inlet and outlet streams enter or leave at different side points. In practice DSR can be met as cold-shot reactors for methanol and ammonia synthesis, or as multi-feed tubular reactor for gas-phase ethylene polymerisation. However, the approach is not restricted to homogeneous systems. In fact, the most incentive is the field of heterogeneous reactor when several phases (gas, liquid, solid) are involved.

In an early attempt Kokossis and Floudas (1990, 1994) proposed the use of a redundant MINLP superstructure that includes several CSTR's, and recycles. Integer variables are used to manage the selection of reactors and their connections. It is clear

that the solution of the problem is extremely difficult, because of high non-linearities typically for reaction systems.

To progress in the generality of the approach the combinatorial dimension of the problem should be kept reasonable. Balakrishna and Biegler (1992) had the idea to use the **AR** method for rationalising the generation of superstructure by an approach that the authors call "MINLP targeting method". In this way two problems are solved, the extension of **AR** approach to more than two dimensions, and a drastic simplification of the superstructure. It is worthy that the superstructure has no recycles but only a series-parallel structure, and contains just two types of reactors, CSTR and DSR. The principle of this approach is illustrated in Fig. 8.29. The superstructure consists of assembling modules of fixed configuration. The number of modules is increased successively and the new superstructure is solved. The procedure stops when no further improvement in the objective function is obtained. In this way the reactor network is developed starting with a simple description, and adding elements of complexity up to achieving the optimal structure. This is a fundamental difference with earlier approaches, where the superstructure was super redundant. In addition, the construction of the superstructure avoids non-monotonic behaviour protecting against premature termination of the algorithm.

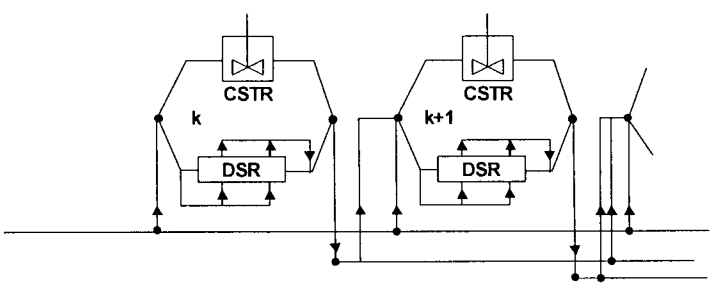

Figure 8.29 The superstructure of a MINLP targeting model

The algorithmic methods for reactor synthesis can be extended, in principle to the whole flowsheet. Two directions have been investigated:

- Simultaneous synthesis of the reactor/separator/recycle system. The cost of separations and recycle affects the economic trade-offs. The optimal reactor would be somewhere between maximum yield (minimum recycles) and maximum selectivity (minimum separations).

- Simultaneous optimisation of reactor design and heat integration around it. The optimal reaction temperature profile inside and around the reaction system should take into consideration opportunities for heat integration.

For more detail about these topics, and in general about the use of optimisation method in Process Synthesis, the reader could consult the book of Biegler et al. (1997). The books of Floudas (1995) and Grossmann (editor, 1996) are recommended as introduction in the field of optimisation methods including MINLP techniques.

8.8 FURTHER READING

The material offered in this chapter is only a condensed treatment of basic elements of chemical reactor engineering needed to approach a process design problem. The reader should have already a good knowledge of this discipline. As study or refreshment material, we recommend in the first place the classical textbooks due to Levenspiel (recent edition in 1999) and Fogler (1992). Other remarkable books have been published by Carberry (1976), Westerterp, van Swaaij and Beenackers (1984), as well as by Froment and Bishop (new edition in 1990). More advanced treatment of different subjects in chemical reaction engineering can be found in the monograph edited by Carberry and Varma (1987) with contributions of experts in each field.

Practical insights, calculation methods and numerical examples can be found in the books of Rase (1977) and Rose (1981), as well as in Walas (1995). Regarding chemical kinetics issues, important both for process development and design, we recommend the books of Smith (1981) and Walas (1995).

8.9 REFERENCES

Carbery, J. J., 1976, Chemical and Catalytic Reactor Engineering, McGraw-Hill

Carrberry, J. J., A. Varma, 1987, Chemical Reaction and Reaction Engineering, Marcel Dekker

Biegler, L. T., I. E. Grossmann, A. W. Westerberg, 1997, Systematic Methods of Chemical Process Design, Prentice Hall

Doraiswamy, L. K., M. M. Sharma, 1983, Heterogeneous Reactions: Analysis, Examples and Reactor design, two volumes, Wiley

Feinberg, M., D. Hildebrandt, 1997, Optimal reactor design from a geometric viewpoint, Chem. Eng. Science, 52(10), 1637-1665

Floudas, C. A., 1995, Non-linear and Mixed-Integer Optimisation: Fundamentals and Applications, Oxford University Press

Froment, G. F., K. B. Bischoff, 1990, Chemical Reactor Analysis and Design, Wiley

Fogler, H. S., 1992, Elements of Chemical Reaction Engineering, Prentice-Hall

Glasser, D., C. Crowe, D. Hildebrandt, 1987, A geometric approach to the steady flow reactors. The attainable region and optimisation in concentration space, I&EC Research, 26(9), 1803

Glasser, D., D. Hildebrandt, 1997, Reactor and process synthesis, Computers Chem. Engng., Vol. 21, s775

Grosmann, I. E. (Editor), 1996, Global Optimisation in Engineering Design, Kluwer Publ.

Hildebrandt, D., D. Glasser, C. Crowe, 1990, The geometry of attainable region generated by reaction and mixing, I & EC Research, 20(1), 49-58

Hildebrandt, D., L.T. Biegler, 1995, Synthesis of reactor network, FOCAPD '94, AIChE Symp. Series

Levenspiel, O., Chemical Reaction Engineering, 3rd edition, Wiley, 1999

Kokossis, A. C., C. A. Floudas, 1990, Optimisation of complex reactor networks, I. Isothermal operations, Chem. Eng. Sci., 45(3), 593; 1994,
II. Non-isothermal operations, 1994, Chem. Eng. Sci., 49(7), 1037

Krishna, R., S. T. Sie, Strategies for multiphase reactor selection, 1994, Chem. Eng. Sci., vol. 49, 24A, 4029-4065

Rase, H. F., 1977, Chemical Reactor Design for Process Plants, 2 volumes, Wiley

Rose, L. M., 1981, Chemical Reactor Design in Practice, Elsevier

Smith, R., 1981, Chemical Engineering Kinetics, McGraw-Hill

Ullmann, 2001, Encyclopedia of Chemical Technology

Walas, S. M., 1989, Reaction Kinetics for Chemical Engineers, Butterworths

Walas, S. M., 1995, Chemical Engineering Handbook of Solved Problems, Gordon & Breach

Westerterp, K. R., W. P. M. van Swaaij, A. A. Beenackers, 1984, Chemical Reactor Design and Operation, Wiley

Chapter 9

SYNTHESIS OF AZEOTROPIC SEPARATION SYSTEMS

9.1 Graphical representations for ternary mixtures
- 9.1.1 Residue Curves Map
- 9.1.2 Distillation Curves Map
- 9.1.3 Right-angle triangle diagrams
- 9.1.4 Separation regions

9.2 Homogeneous azeotropic distillation
- 9.2.1 Separations in one distillation field
- 9.2.2 Extractive distillation
- 9.2.3 Separation in two distillation fields

9.3 Heterogeneous azeotropic distillation

9.4 Combined processes
- 9.4.1 Distillation combined with extraction
- 9.4.2 Distillation combined with adsorption
- 9.4.3 Distillation combined with membrane permeation

9.5 Design issues
- 9.5.1 Shortcut method for zeotropic mixtures
- 9.5.2 Minimum reflux in ternary distillation
- 9.5.3 Design methods for non-ideal systems

9.6 Further reading

9.7 Summary

9.8 References

The separation of mixtures involving azeotropes has been considered until recently a difficult problem. Today systematic methods are available, which can stimulate greatly the designer's creativity in discovering new entrainers and novel flowsheets, or by combining distillation with other separation techniques.

As shown in the Chapter 7, the separation of a complex liquid mixture can be split in two large sub-problems: zeotropic and azeotropic mixtures. In the last case the problem can be reduced to the treatment of ternary mixtures, the azeotrope plus the entrainer. Therefore, we may define the following elementary separation problem:

> Given the mixture *AB*, forming *minimum* or *maximum azeotrope*, find a suitable *entrainer E* and *feasible separation sequences* that can deliver *A* and *B* of high purity, at least one operation being distillation. The entrainer may be present already in the mixture, or being added and recycled.

It is clear that the above problem adopts a systems viewpoint focusing on the feasibility of the separation, and not on the detailed design of separators.

We start the chapter by explaining the graphical thermodynamic representations for ternary mixtures known as Residue Curve Maps. The next section deals with the separation of homogeneous azeotropes, where the existence of a distillation boundary is a serious obstacle to separation. Therefore, the choice of the entrainer is essential. We discuss some design issues, as entrainer ratio, optimum energy requirements and finite reflux effects. The following subchapter treats the heterogeneous azeotropic distillation, where liquid-liquid split is a powerful method to overcome the constraint of a distillation boundary. Finally, we will present the combination of distillation with other separation techniques, as extraction or membranes.

9.1 GRAPHICAL REPRESENTATIONS FOR TERNARY MIXTURES

9.1.1 Residue Curves Map

Let's consider the following experiment: a ternary mixture of composition x_A, x_B, x_C is submitted to simple differential distillation at constant pressure, as depicted in Figure 9.1-left. The time-evolution of the liquid composition describes a *residue curve*. Suppose that at the time t, the pot contains L moles of liquid of composition x_i. If the vapour with the equilibrium composition y_i is removed at the rate V, then the component material balance over the time dt gives:

$$\frac{d(Lx_i)}{dt} = L\frac{dx_i}{dt} + x_i\frac{dL}{dt} = -Vy_i \tag{9.1}$$

Further, we introduce the dimensionless time $\theta = Vt/L$. Since $dL/dt = -V$, $y_i = K_i x_i$, the liquid composition is described by the relation:

$$\frac{dx_i}{d\theta} = (K_i - 1)x_i \tag{9.2}$$

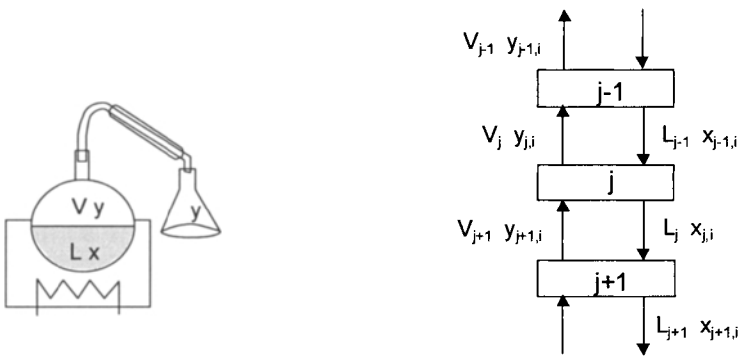

Figure 9.1 Residue curves and distillation lines analogy

The integration of the equation (9.2) is easy, but in each point the equilibrium constants K_i has to be calculated by a suitable thermodynamic model, as function of pressure, temperature and composition. The trajectory obtained in this way starting with an arbitrary initial concentration describes a *residue curve*. The assembly of trajectories of liquid composition forms a *Residue Curves Map* (RCM).

Figure 9.2 presents a RCM for an ideal zeotropic system: benzene/toluene/ethyl-benzene[1] in the form of an equilateral triangle. Pure components are set in vertices, while the sides describe binary mixtures. The space inside the triangle contains all possible ternary mixtures. Note that the boiling points of the pure components at the pressure of separation are marked in vertices. On the contrary, the boiling temperatures of the intermediate mixtures cannot be given explicitly, but their evolution during the distillation is clearly indicated by arrows.

We adopt here the convention that the direction of a trajectory points-out from lower to higher temperatures. For example, on the segment representing the binary mixture the trajectory is oriented from the light to the heavy component. The shape of the residue curves depends on the relative volatility of components. It may be observed that in Fig. 9.2 all the residue curves have the same vertices as origin and terminus. More specifically, all the trajectories emanate from the benzene corner and terminate in the ethyl-benzene vertex. These species are the lowest and the highest boilers, respectively. The vertex of toluene is only an intermediate destination, where the residue curves enter from the benzene and leave to the ethyl-benzene. Note that the residue curves do never intersect each other.

The assembly of residue curves having as origin and terminus the same points forms a *distillation region*. Hence, a zeotropic mixture displays always a single distillation region. On the contrary, if azeotropes are present several distillation regions can exist.

---

[1] The RCMs in this chapter have been computed by Aspen Plus and exported to EXCEL .

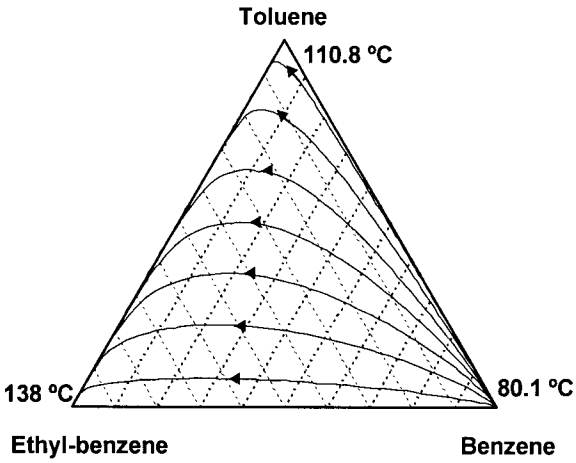

Figure 9.2 Residue Curve Maps for a zeotropic system

After this example, we may introduce the *characteristic points* of a RCM (Fig. 9.3). *Node* is a point where the residue curves can start or terminate. *Saddle* is an intermediate destination, in which the trajectories enter from one direction and leave to another one. We adopt here the convention that a node is *stable* if the residue curves converge on it. Thus a stable node designates implicitly a high boiler. A node is *unstable* if the trajectories diverge from it, and therefore designates a low boiler. Saddle points are intermediate boilers. In Figure 9.2, benzene is an unstable node, ethyl-benzene is a stable node, while toluene is a saddle. The behaviour of nodes and saddles can be treated theoretically by analogy with non-linear systems. The concept of characteristic points is important in classifying the azeotropic mixtures.

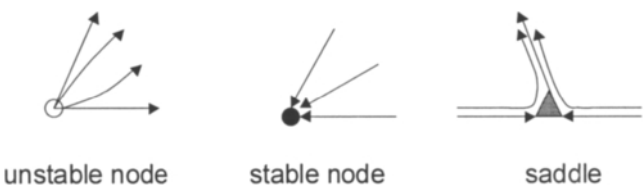

Figure 9.3 Types of characteristic points

Figure 9.4 displays RCMs for some typical azeotropic mixtures. Figure 9.4a presents the mixture acetone (56.2 °C) / benzene (80.1 °C) / heptane (98.4 °C). Acetone and heptane form a minimum boiling azeotrope with nbp of 55.1 °C, which is the lowest boiler. It may be observed that the residue curves emanate from the azeotropic point, take the direction to the benzene/heptane edge, and then deflect to the heptane vertex. Binary azeotrope and heptane are unstable and stable nodes, respectively. Acetone and benzene are saddles. In this case there is a single distillation region, as for zeotropic mixtures, but the shape of the residue curves is peculiar.

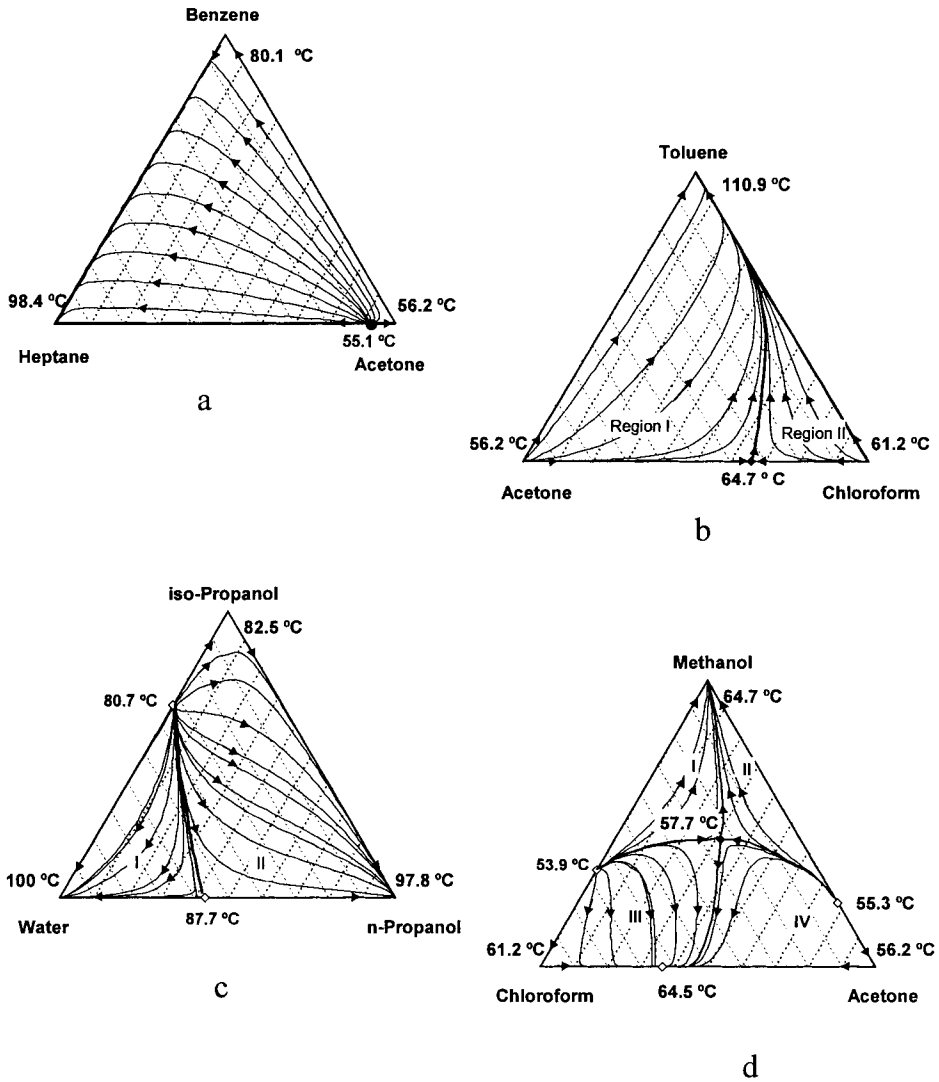

Figure 9.4 Residue Curve Map for some azeotropic systems

Figure 9.4b displays the RCM for the mixture acetone (56.2 °C) / chloroform (61.2 °C) / toluene (110.8 °C). The first two components give a maximum-azeotrope (nbp 64.7 °C), but boiling lower than toluene. There are two unstable nodes (acetone and chloroform), one stable node (toluene), and a saddle (azeotrope acetone-chloroform). The residue curves can emanate either from the acetone or from the chloroform vertices, but all terminate in the toluene vertex. The direction of trajectories shows clearly the separation of the

concentration space in two regions: Region I formed by the curved triangle acetone/toluene/azeotrope, and Region II in the remaining part.

Hence, the family of all residue curves that originate from one fixed composition point and terminate into another fixed composition point defines a distillation region. Two adjacent regions are separated by a *separatrix*. In this book we called it simply *distillation boundary*.

Distillation boundaries appear because of the existence of one or several azeotropes between the components of a mixture. A distillation boundary links a node with a saddle. Note that in Figure 9.4b the boundary has a noticeable curved shape. The curvature of distillation boundaries plays a decisive role in the feasibility of the potential separation sequences.

Figure 9.4c presents the RCM for the mixture iso-propanol (82.5 °C) / n-propanol (97.8 °C) / water (100 °C). The two alcohols give minimum-boiling azeotropes with water, the boiling points being 80.7 °C and 87.7 °C. Now there are five characteristic points. A distillation boundary appears between the two azeotropes, the first being (unstable) node, the second being a saddle. N-propanol and water are stable nodes, but located in different distillation regions, while iso-propanol is a saddle.

Finally, Figure 9.4d illustrates a more complex situation, the mixture acetone/ chloroform/methanol, with four azeotropes (three binaries and one ternary). There are four distillation regions. Note that the ternary azeotrope is a saddle.

From the above examples, it may be concluded that simple thermodynamic information, as boiling points of pure components and azeotropes, is sufficient to sketch the main features of a RCM, as the direction of trajectories and distillation boundaries. However, drawing correctly the curvature of boundaries needs accurate knowledge of phase equilibrium.

The geometric properties of a RCM allow its simple sketch. Figure 9.5 shows the construction for the mixture methyl-isopropyl-ketone (MIPK), methyl-ethyl-ketone (MEK) and water. Firstly, the position of the binary azeotropes and of the ternary azeotrope is located. Then the boiling points for pure components and azeotropes are noted (Fig. 9.5a). The behaviour of characteristic points (node or saddle) is determined by taking into account the direction of temperatures. Finally, straight distillation boundaries are drawn by connecting saddles with the corresponding nodes (Fig. 9.5b).

The consistency of a RCM with the azeotropic data can be verified by a theoretical test (Doherty and Malone, 2001), expressed by the following relation:

$$4(N_3 - S_3) + 2(N_2 - S_2) + (N_1 - S_1) = 1 \tag{9.3}$$

N_i and S_i are the number of nodes and saddles, respectively, involving exactly i species from the ternary mixtures. For example, in Figure 9.4c N_3=0, S_3=0, N_2=1, S_2=1, N_1=2, S_1=1, and 4(0-0)+2(1-1)+(2-1)=0+0+1=1. In the Figure 9.4d we have N_3=0, S_3=1, N_2=3, S_2=0, N_1=1, S_1=2, and 4(0-1)+2(3-0)+(1-2)=-4+6-1=1.

In this way, qualitative diagrams for the assessment of distillation regions can be drawn. A complete classification can be found in Perry (Seader et al., 1997).

Before closing this topic, we must stress the importance of the thermodynamic data in getting reliable RCMs. The adequacy of models and the accuracy of interaction parameters must be checked always. Wilson is very accurate for homogeneous

mixtures. UNIQUAC and NRTL are sufficiently accurate in a large number of cases. A supplementary advantage is that these models can be applied for both VLE and LLE. Specifying systematically VLLE as option for flash calculation avoids unreliable azeotrope prediction. Different sources of equilibrium data should be tested. UNIFAC should be used only for exploratory purposes.

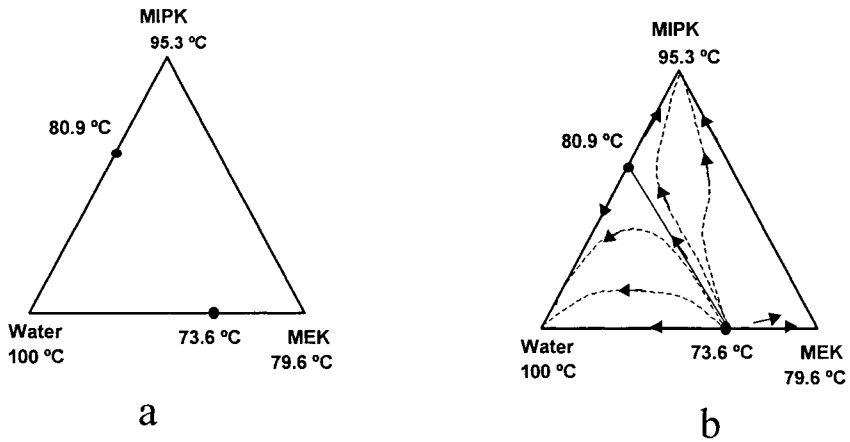

Figure 9.5 Sketching a Residue Curve Map from characteristic points

9.1.2 Distillation Curves Map

We can imagine another experiment, in which a distillation column equipped with trays is operated at total reflux (Fig. 9.1b). The component material balance between two successive trays gives:

$$V_{n+1}y_{n+1,i} = L_n x_{n,i} \tag{9.4}$$

Because at total reflux $V_{n+1} = L_n$, one gets:

$$y_{n+1,i} = x_{n,i} \tag{9.5}$$

Hence, for each component the concentration of a vapour rising from the tray $(n+1)$ equals the concentration of the liquid flowing from the tray n. This relation defines a *distillation curve* as the locus of the tray compositions at total reflux. A *distillation curve map* (DCM) can be generated easily by choosing a tray liquid composition $x_{n,i}$, and stepping up and down by a series of bubble and dew points.

As before, tracing the DCM of a ternary mixture involving azeotropes may lead to one of more distillation regions. Numerical investigation demonstrates that distillation and residue curves are, in general, close to each other. In fact, both are related with the variation of concentration in a distillation column operated at infinite reflux, RCM for a packed column, and DCM for a trayed column.

When the distillation boundary is almost straight the difference between RCM and DCM is negligible. When the distillation boundary exhibits a high curvature, the differences might be of significance. Because neither RCM nor DCM offers a safe basis to predict the extent of boundary crossing, this difference has no practical consequence when using methods based on the equilibrium-stage concept.

9.1.3 Right-angle triangle diagrams

A RCM can be represented as a right-angular triangle, more practical for sketching separation sequences. The following convention is adopted (Doherty & Malone, 2001):

a. Pure components: lowest-boiler on top, intermediate-boiler on bottom-left, highest-boiler on bottom-right.
b. Azeotropes. A binary azeotrope is represented by a number, which is:
   0: no azeotrope,
   1: binary minimum-boiling azeotrope, node;
   2: binary minimum-boiling azeotrope, saddle;
   3: binary maximum-boiling azeotrope, node;
   4: binary maximum- boiling azeotrope, saddle.
   Ternary azeotrope: m (minimum), M (maximum) or S (intermediate).

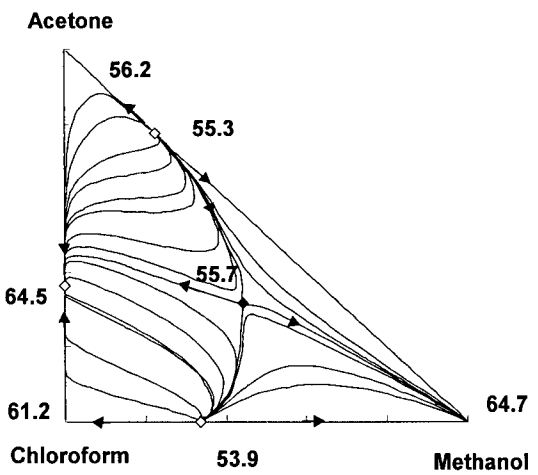

Figure 9.6 Residue Curve Map in a right-angle ternary diagram

Figure 9.6 shows the RCM for the mixture acetone/chloroform/methanol, for which the class is 311-S. The first digit represents the max-azeotrope acetone/chloroform, the second the minimum-azeotrope chloroform/methanol, the third the minimum-azeotrope acetone/methanol. The letter S signifies the ternary saddle azeotrope. More RCMs are presented in Perry (1997), from a total of 125 configurations.

9.1.4 Separation regions

A separation region defines the part of a RCM where the separation of a mixture in products is feasible. Figure 9.7 presents the generation of separation alternatives for the zeotropic mixture benzene, toluene, and ethyl-benzene. Point F is the initial feed. Figure 9.7-left shows the 'direct sequence', in which the first column recovers the light component (benzene) in top. The separation is represented by the segment b_1d_1. Note that the position of d_1, close to the vertex of benzene, denotes high purity, while the position of b_1, practically on the edge toluene/ethyl-benzene, indicates high recovery. A second split separates the medium-boiler (toluene) in top from the high-boiler (ethyl-benzene) in bottoms.

The graphical representation makes use of the following rules:

- Feed F and products, d_1 and b_1, must be collinear,
- The ratio distillate to bottoms respects the *lever rule*, that is $D/B = \overline{Fb_1} / \overline{Fd_1}$.

A second alternative, called 'indirect sequence', is depicted in the Figure 9.7-right. In the first split the pure high-boiler is recovered completely as bottoms, followed by the separation of the light and medium components. Note that the two alternatives make use of *simple distillation columns*, with one feed and two products. A suitable design can fulfil any type of feed composition and purity specifications.

Let's examine another alternative. For example, the first split might be 'sloppy', meaning that both distillate and bottoms contain a large amount of the intermediate component. This would imply two more splits, in total three simple columns, obviously uneconomical. In consequence, the second column should deliver all three components, including the intermediate as side-stream. This scheme seems unusual, but it may be in fact more economically when the two columns are heat-integrated.

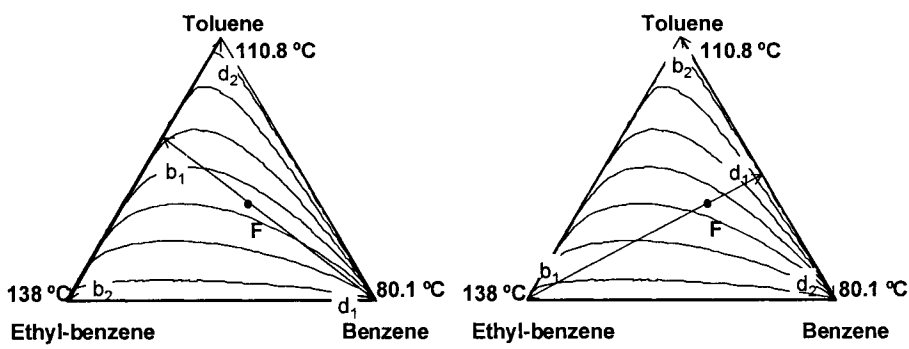

Figure 9.7 Direct and indirect distillation sequences

Hence, the RCM representation allows the designer to identify the *feasible separations*. In the case of zeotropic mixtures if the separation is possible at total reflux, then it is certainly feasible at finite reflux, the problem being only finding a

suitable column design, as number of stages and reflux. This reasoning is not in general valid for azeotropic separations! For azeotropic mixtures the effect of reflux and of the mass transfer on the separation of azeotropic mixtures is an issue not yet satisfactory understood, but of the greatest importance in practice. For instance, in azeotropic distillations there is a minimum and a maximum reflux to achieve a given product purity. This topic will be developed later (see Example 9.2).

Figure 9.8 presents the separation of a zeotropic ternary mixture in somewhat more detail. A feasible solution is obtained when the material balance line d_1-F-b_1 intersects a residue curve passing through the points d_1 and b_1. This is the case with the couple d_1-b_1, but also with the couple d_2-b_2. The couples d'-b' (direct sequence) and d"-b" (indirect sequence) represent limiting situations in which one pure component is completely recovered, either as the most volatile, or as the heaviest.

These limiting points allow the definition of *separation regions* as the space of attainable products (Fig. 9.9). Thus, the region of all possible concentrations for the top product may be visualised by the shaded curved triangle Afd". The top distillate can vary between pure *A* (d'-direct sequence) and the mixture *A/B* (d"-indirect sequence), the other limit being the residue curve passing through the feed. Similarly, the region of attainable bottoms is delimited by the curved triangle CFb'.

Hence, it is important to keep in mind that in the case of zeotropic ternary mixtures the feasibility of separations does not depend on the feed composition. This can be performed in a sequence of two simple columns, either as 'direct' or as 'indirect' sequences. The choice is a matter of optimisation or constrained by technological reasons.

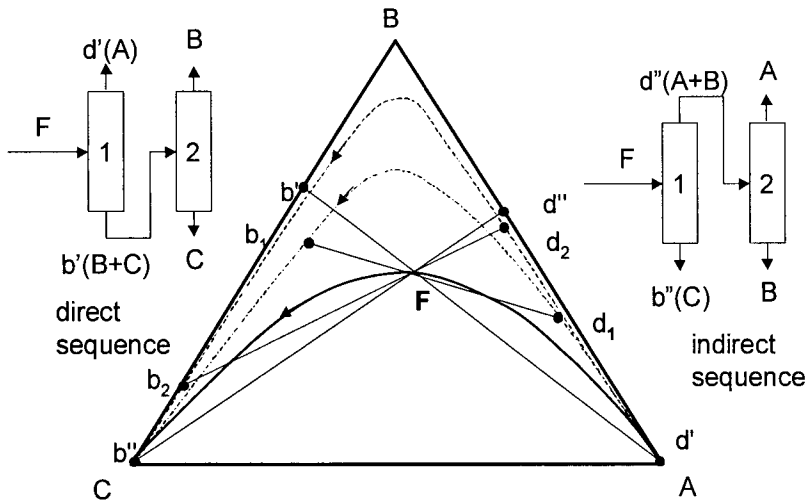

Figure 9.8 Separation alternatives in a Residue Curve Map

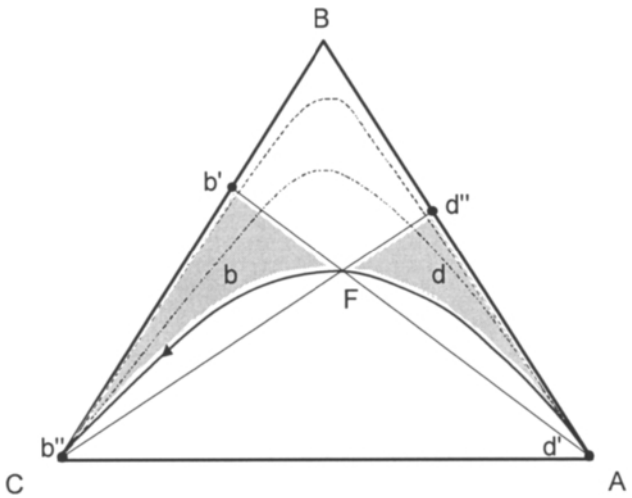

Figure 9.9 Separation regions for a ternary zeotropic mixture

When the components *A* and *B* form a homogeneous azeotrope the situation is fundamentally different. It is clear that the recovery of both high purity *A* and *B* in a single column is not possible. The use of an entrainer is necessary. This will change the relative volatility of components creating opportunities for separation. Obviously, the entrainer must be recycled, if it is not a component already present in significant amount in the original mixture. It may be observed that at least two distillation columns are necessary: a first one to recover the first pure component, and the second one to recover the other component and recycle the entrainer.

At this point, it is important to make a clear distinction between *homogeneous and heterogeneous azeotropic distillation.* In the first situation, at every separation step all the azeotropes are homogeneous. In the second case, the process involves a second liquid phase, usually in the separation of the top distillate by liquid-liquid decanting. Intuitively, the separation by homogeneous azeotropic distillation would be preferable, so we will examine it in the first place.

The trajectories of the residue curves in homogeneous azeotropic distillation can give two pictures:

- No distillation boundary.
- One or more distillation boundaries.

The absence of a distillation boundary seems rather uncommon, but it may be encountered in practice (see Example 9.1). The occurrence of distillation boundaries in the RCM is more likely. The feasibility of the separation of pure components will depend on the type of RCM. Moreover, the shape of the distillation boundary plays a crucial role in feasibility.

Figure 9.10 illustrates a situation in which *A* and *B* form a maximum azeotrope, with *C* the highest boiler. *A* and *B* are unstable nodes, *C* is a stable node, while the *AB* azeotrope is saddle. Consider an *AB* mixture rich in *A* as represented by the point f_1.

After mixing with the entrainer *C*, the new feed becomes the point m_1. The mixing operation is represented by the segment f_1-*C*, the position of m_1 depending on the ratio entrainer/initial mixture given by the lever rule. Suppose that we would like to separate *A* of good purity by a first split. The distillate is described by the point d_1 close to the vertex of *A*. The bottom product is marked by the point b_1 collinear with d_1 and m_1. Both d_1 and b_1 will be situated on the same residue curve. In addition, the position of b_1 must obey a hard constraint imposed by the distillation boundary: it cannot go beyond. Thus, high purity *A* can be obtained, but the maximum recovery is dictated by the distillation boundary.

Now, the second split, represented by the segment d_2-b_2 has no other choice as to separate the azeotrope *AB* in the top and the entrainer *C* in the bottom. Thus, it is not possible to obtain pure component *B* by this technique. Similarly, it is not possible to obtain pure *A* from a feed rich in component *B* (point f_2). The separation regions are represented by shaded curved triangles.

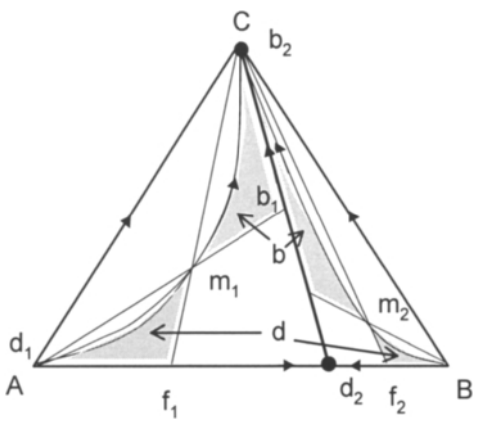

Figure 9.10 Distillation regions when components *A* and *B* are separated by a straight distillation boundary

At this point, a question arises. Could we overcome the constraint of a distillation boundary? The answer is not easy. In any case, the selection of a suitable entrainer is the key element. The number of columns involved in the separation sequence is not very important, because it can be either two or three. On the contrary, the recycle policy of the entrainer and of intermediate mixtures plays a major role. Sometimes the location of feeds, as for example the original mixture and the entrainer in the first column, may have also an effect on the overall feasibility. These issues will be developed in a lager extent in the next sections.

If a suitable solvent cannot be found, the problem should not be abandoned. The combination of azeotropic distillation with other separation techniques can offer better solutions than painful separation by only distillation.

9.2 HOMOGENEOUS AZEOTROPIC DISTILLATION

The problem is finding feasible separation sequences for breaking the binary azeotrope *AB* by using only homogeneous distillation. There are two possibilities:

1. Both pure products *A* and *B* belong to the same distillation field. There is no distillation boundary between the components to be separated.
2. The pure products *A* and *B* are separated by a distillation boundary, and they belong to different distillation fields. The distillation boundary must be sufficiently curved, such that one split can cross it.

9.2.1 Separations in one distillation field

9.2.1.1 Entrainer selection

In the subsequent presentations, we will consider that *A* is more volatile as *B*. The entrainer must be selected such that both components to be separated belong to the same distillation field. The *AB* azeotrope must be a node, stable or unstable, or in other words does not belong to a distillation boundary. Criteria for entrainer selection have been proposed by Doherty & Caldarola (1985), and are given in Table 9.1. The choice is organised as function of the azeotrope type and the relative volatility of the entrainer. Note that the mentioned requirements are minimum. Additional azeotropes may exist.

A first choice, valid for both minimum and maximum azeotropes, would be a medium-boiler entrainer. Such condition is difficult to fulfil in practice because in the most cases the species forming azeotropes have close boiling points. However, such entrainers can be found (see Example 9.1).

In addition, for a minimum *AB* azeotrope the entrainer may be: 1) low boiler that forms medium-boiling maximum azeotrope with *A*, and 2) maximum boiler. The last case is quite special, and it is known as *extractive distillation*. For maximum *AB* azeotrope, the entrainer may be high-boiler that forms medium-boiling minimum azeotrope with *B*. It should be noted that is difficult to find entrainers giving opposite azeotropes with *A* or *B* with respect to the original *AB* azeotrope. Hence, the choice of an entrainer generating separations in one distillation field is in practice limited.

Table 9.1 Criteria for entrainer selection for separations in one distillation field

Entrainer *C*	Minimum *AB* azeotrope	Maximum *AB* azeotrope
Low boiler	Medium-boiler maximum azeotrope with *A*	No
Medium boiler	Yes	Yes
High boiler	Yes (Extractive distillation)	Medium-boiler minimum azeotrope with *B*

Examples of suitable RCMs for azeotropic separation in a single field are given in Fig. 9.11. For a feasible sequence, *A* and *B* but not both must be a saddle, except in extractive distillation, when both *A* and *B* are saddles. Two columns are sufficient for

separation, either as direct or indirect sequence. The first column separates one product and a mixture with the entrainer. The second column allows the separation of the second component, and the recycle of the entrainer, either pure or as azeotrope with *A* or *B*. In general, the entrainer and the original mixture can be merged in the same feed. A notable exception is the extractive distillation.

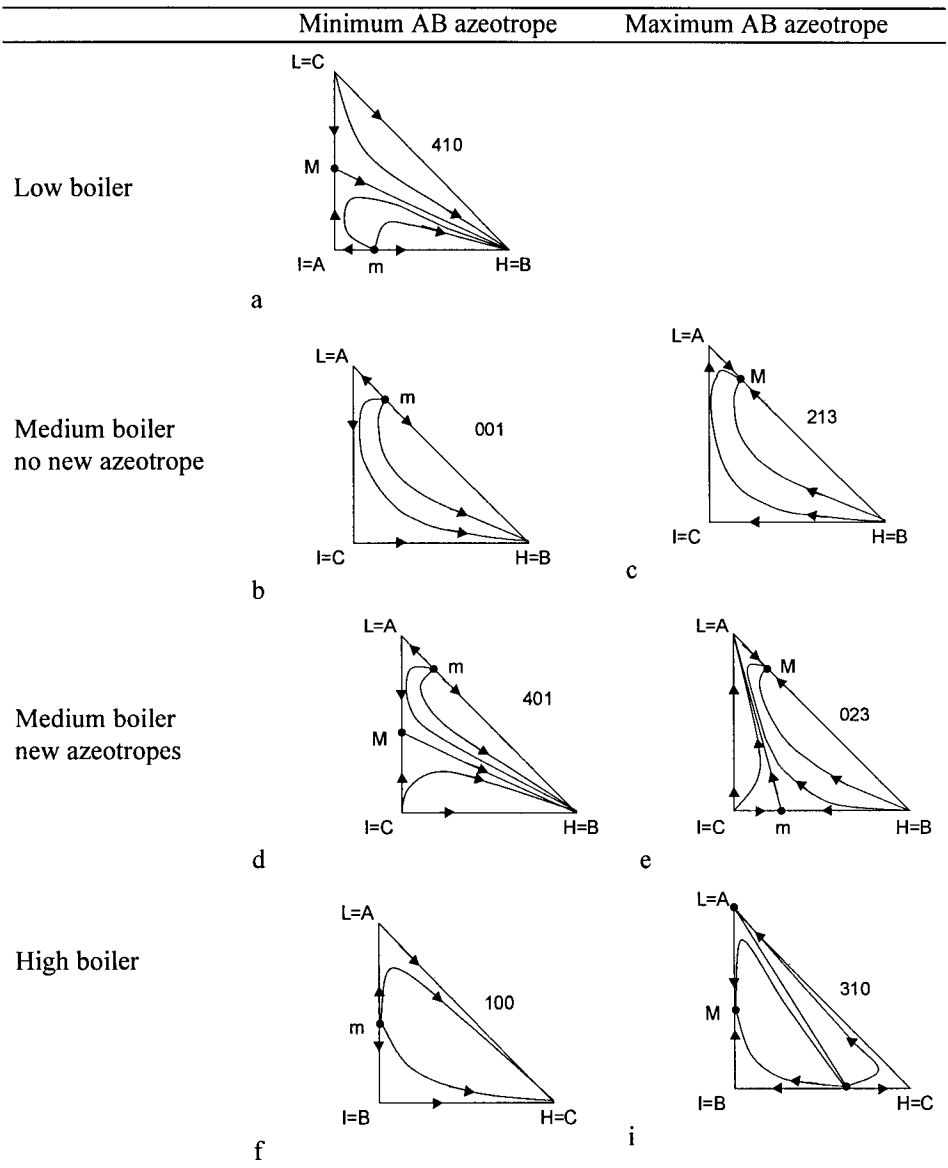

Figure 9.11 Feasible Residue Curve Maps for separating AB azeotrope with the entrainer E by azeotropic distillation in a single field

9.2.1.2 Sequencing of splits

Let's consider the separation of a binary minimum azeotrope *AB* with a medium boiling entrainer *C* (Fig. 9.12). Note that the *AB* azeotrope and the component *B* are nodes, while both *A* and *C* are saddles. The separation regions for the first split are delimited by direct and indirect sequences, respectively. If the boiling points of *A* and *AB* azeotrope are not too close, *A* can be obtained as distillate, even if it is a saddle! Rooks et al. (1998) has given recently a consistent explanation; the split is feasible when the concentration profiles of both rectification and stripping zones points to the same common saddle, in this case the component C.

As an exercise, the reader could examine the separations based on the RCM's drawn in Fig. 9.11, either as direct or as indirect sequence. Note that the products are always of type node-saddle, with the notable exception of the case f (extractive distillation), where the both products are saddles. The entrainer can be recycled either as overhead or as bottoms. The last alternative should be preferred from an energetic viewpoint.

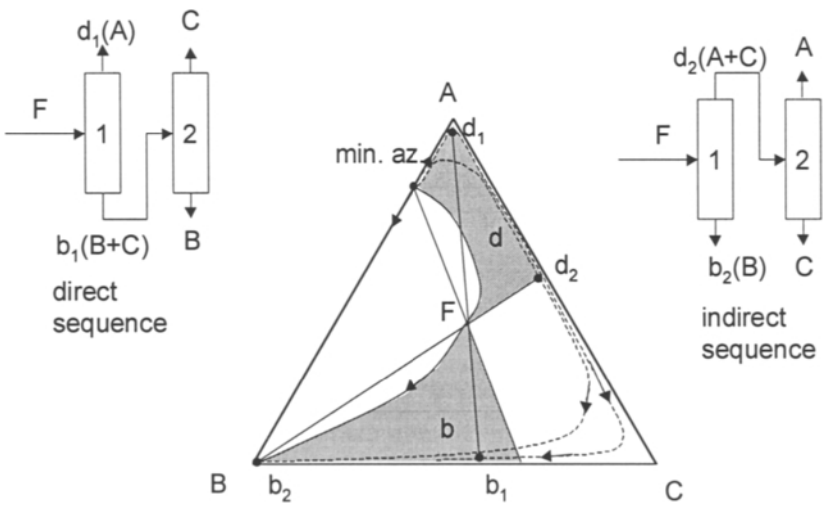

Figure 9.12 Separation of an azeotropic mixture in one distillation region

---

EXAMPLE 9.1 Separation of the azeotrope acetone/heptane using benzene

Acetone and heptane give at normal pressure a minimum-boiling azeotrope with 89.8 % mole acetone and nbp 55.1 °C. Examine the feasibility of separation with benzene as entrainer by both direct and indirect sequences. Compare the attainable purity.

Solution. Let's consider a mixture acetone/heptane of azeotropic composition. The RCM acetone/heptane/benzene has been presented already in the Figure 9.4a. There is only one distillation region. The heavy component, heptane, is a stable node. The other

node (unstable) is the binary azeotrope acetone/heptane. The entrainer benzene is medium-boiler and saddle.

Split sequencing follows the representation sketched in Figure 9.12. Direct sequence gets acetone as distillate in the first split, and heptane as bottom product in the second split. In indirect sequence heptane can be recovered as bottoms from the first split, while acetone is obtained as top distillate from the second split.

At the first sight, the direct sequence should be more favourable as energetic consumption, because of the large amount of acetone in the initial mixture. On the other hand, the indirect sequence should give higher purity acetone, because the second split is a zeotropic binary acetone/benzene. Note that in both sequences the entrainer is recycled as bottoms.

Computer simulation gives more insights. Table 9.2 presents some results obtained with ASPEN Plus. The direct sequence is more difficult, particularly the first split, where about 80 stages are necessary to get 99.8% purity acetone.

It is important to observe that in the direct sequence the first column has two feeds: binary mixture in lower position, and entrainer in higher position, somewhat similar with an extractive distillation! Thus, the feasibility of the first split illustrates the rule of 'common saddle' mentioned. Both distillate and bottom products point to the same saddle, in this case the benzene. Surprisingly, high purity products can be achieved with a relatively low entrainer ratio of 0.4.

In indirect sequence, the first split is much easier (35 trays), and the amount of entrainer is lower (0.08). In the second split, however, the situation is less favourable. Equilibrium diagram *y-x* shows difficult separation of pure acetone, because very low relative volatility with respect to benzene. However, the same high purity of 99.8% acetone can be obtained. It is important to note that the feed should be placed near to the reboiler, so that the second column is practically a stripper. The recycled entrainer benzene may contain a small amount acetone, which helps to get high purity products. The energetic consumption is slightly below the direct sequence, because low amount of entrainer. Hence, contrary to expectations, the indirect sequence has better indices, both as hardware and energetic consumption.

Table 9.2 Simulation results for the separation acetone/heptane with benzene

	Direct sequence	Indirect sequence
Ratio entrainer/mixture	0.4	0.08
Column 1:		
- stages	80	35
- location azeotrope/entrainer	55/35	22
- reflux ratio	4	1.9
Column 2:		
- stages (feed location)	50 (40)	35(33)
- reflux ratio	9	4.43
Purity acetone	99.8	99.8
Purity heptane	99.99	99.99
Reboiler duty	0.134+0.124=0.258 MW	0.086+0.145=0.231 MW

9.2.2 Extractive distillation

Extractive distillation is the most used separation method of azeotropes by homogeneous distillation with important applications in industry (see Table 7.31). Extractive distillation consists of using a high boiling component as mass separation agent (entrainer or solvent). The separation is of type direct-sequence (Fig. 9.13). The main product is obtained from the first column as top distillate, while the other component (co-product) leaves in the bottoms with the solvent. The second column distillate the co-product and recover the entrainer. Note that the product is not always the most volatile species. In fact, the role of entrainer is to change significantly the relative volatility of the components to be separated.

The extractive distillation column has always two feeds: the entrainer is sent to the upper position, few stages below the top, eventually slightly sub-cooled, while he mixture is fed in the lower position. The entrainer flows downwards in counter-current with the vapour, absorbing selectively the component that will leave in bottoms.

Let's examine the case of breaking the azeotrope ethanol/water with ethylene glycol. The flowsheet was given in Fig. 7.28. The RCM plot is given in Fig. 9.13-left. It can be observed that both products are saddles, which is typical for extractive distillation.

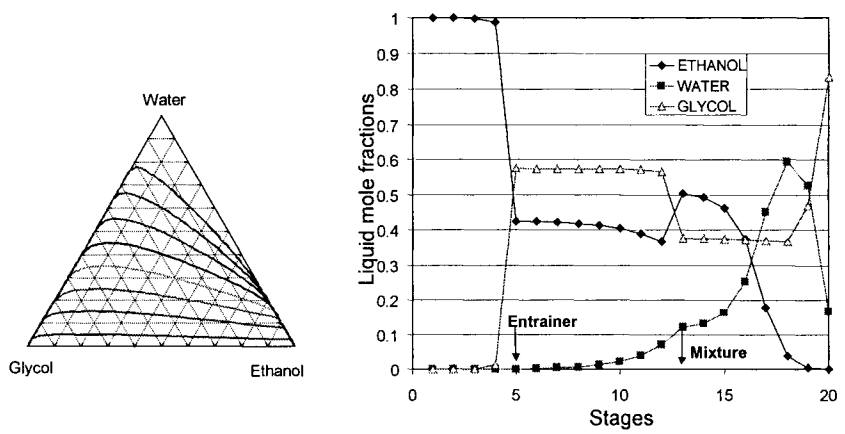

Figure 9.13 Concentration profiles in an extractive distillation column

The behaviour of an extractive distillation column (Fig. 9.13-right) shows notable differences with respect to a simple column. The concentration profiles show that the column can be divided in three zones: rectification, mid-section and stripping. In the top section, the separation takes place between the product (ethanol) and the entrainer. Because large differences in boiling points only few stages are necessary. In the mid-section is the co-product (water) whose concentration changes significantly. In fact, water from the vapour-phase is absorbed into glycol. For this reason Stichlmair (1999) suggests that more appropriate would be to designate this method by 'extractive-absorption'. Note also that in extractive distillation the reflux has minimum and maximum values. More information can be found in Doherty & Malone (2001).

9.2.3 Separation in two distillation fields

The process can take place in two distillation fields when the distillation boundary between the components to separate is highly curved. An important issue is the location of feasible products. Figure 9.14 illustrates the case when *AB* gives maximum-boiling azeotrope, but lower than the entrainer *C*. There is a curved distillation boundary connecting the vertex *C* (node) with the *AB* azeotrope (saddle). Consider a ternary feed *F* close enough to the concave side. At infinite reflux both top and bottom products must be located on the same residue curve, and in the same distillation field, either on the concave or on the convex side of the separatrix. In Fig. 9.14 these can be the couples d_1-b_1 or d_2-b_2, but not d_1-b_2! Note that crossing the boundary is possible, but only from the concave side!

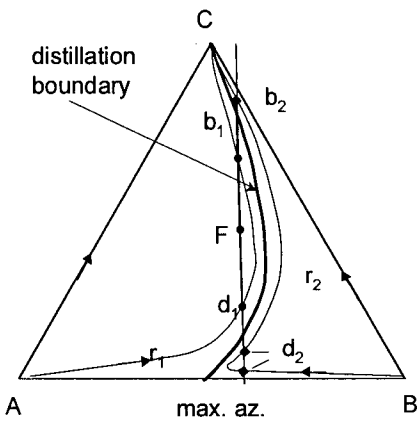

Figure 9.14 Feasible products by crossing a curved distillation boundary at infinite reflux

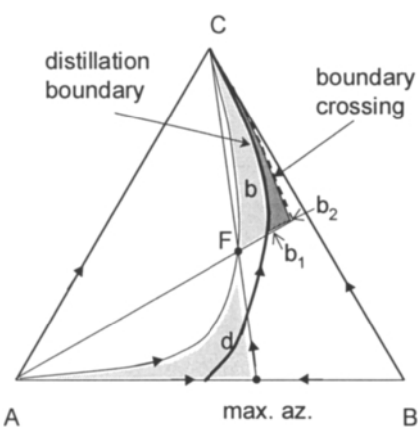

Figure 9.15 Separation regions with a curved distillation boundary

Let's see a separation at very high reflux. The separation regions are depicted in Figure 9.15, bounded by the direct and indirect sequences, as well as by the residue curve passing through the feed. In direct sequence after the first split the bottoms, figured by the point b_1, is on the separatrix. Then, the second split using b_1 as feed can cross the boundary, since it is on the concave side, leading finally to recover *A* and *B* (see later Fig. 9.16). However, note the boundary can be crossed already in the first split at finite reflux, giving a bottom product designated here by b_2. In this way, at finite reflux the feasibility region may be larger than predicted by the analysis at infinite reflux! Therefore, the infinite-reflux design may be considerate as conservative.

9.2.3.1 Entrainer selection

The selection of an entrainer with boundary crossing is based on the observation that in a RCM both constituents *A* and *B* are nodes, stable or unstable. In other words, both *A* and *B* can be separated either as overhead or bottom products. Table 9.3 gives a list of recommended heuristics for entrainer selection (Stichlmair and Fair, 1999). In all cases, the distillation boundary must be highly curved, although 'how much curved' is not exactly known at the present time. The simplest choice is a low boiler for a minimum *AB* azeotrope, and a high boiler for a maximum *AB* azeotrope.

Table 9.3 Criteria for entrainer selection for systems with boundary crossing

Entrainer *C*	Minimum *AB* azeotrope	Maximum *AB* azeotrope
Low boiler	The entrainer has to boil lower than the minimum *AB* azeotrope.	New maximum azeotropes with both *A* and *B*. At least one has to boil higher than the *AB* azeotrope.
Medium boiler	New minimum azeotrope with *A*, the low boiling component.	New maximum azeotrope with *B*, the high boiling component.
High boiler	New minimum azeotropes with both *A* and *B*. At least one has to boil lower than the *AB* azeotrope.	The entrainer has to boil higher than the maximum *AB* azeotrope

9.2.3.2 Sequencing of splits

The feasibility of a separation process with boundary crossing is still a subject of research. Although numerous simulation studies predict that a highly curved distillation boundary could be easily crossed, the experimental material to prove it is very insufficient. A more conservative approach (Doherty & Malone, 2002) asserts that schemes with boundary crossing would require a large number of stages and high entrainer ratio. On the other hand, Springer & Krishna (2002) demonstrated experimentally the possibility of crossing the distillation boundary at finite reflux in many situations, including almost straight boundaries. They give a theoretical explanation by means of non-equilibrium stage modelling. In the absence of systematic studies a more careful position seems logical. However, the search of innovative solutions should take into account that crossing boundary may be possible.

Infinite reflux design

The design based only on the assumption of total reflux and of large (theoretically infinite) number of plates is called usually ∞/∞ analysis. The sequencing requires the following rules when crossing the distillation boundary (Doherty et al., 1985, Stichlmair, 1992):

1. Feed must be sufficiently close to the distillation boundary, on the concave side.
2. Both products A and B must belong to the same residue or distillation curve, which can be either on the same side with the feed, or on the other side.

On this basis, separation alternatives with maximum three or minimum two columns can be generated.

9.2.3.3 Three columns alternative

Figure 9.16 presents a first sequence for breaking a maximum boiling azeotrope (*AB*) with a high boiler *C* when the mixture *AB* is richer in *A*. The initial mixture is f_1. After mixing with *C*, the feed m_1 is obtained. In the first split, the distillate d_1 can recover *A* at high purity. The bottoms b_1 will consist of a mixture *B/C* with some *A*. Note again that d_1, m_1, and b_1 are located on the material balance line. In addition, d_1 and b_1 belong to the same residue curve, in the left distillation field. Therefore, this split has not crossed the distillation boundary, but the point b_1 can be pushed very close to it.

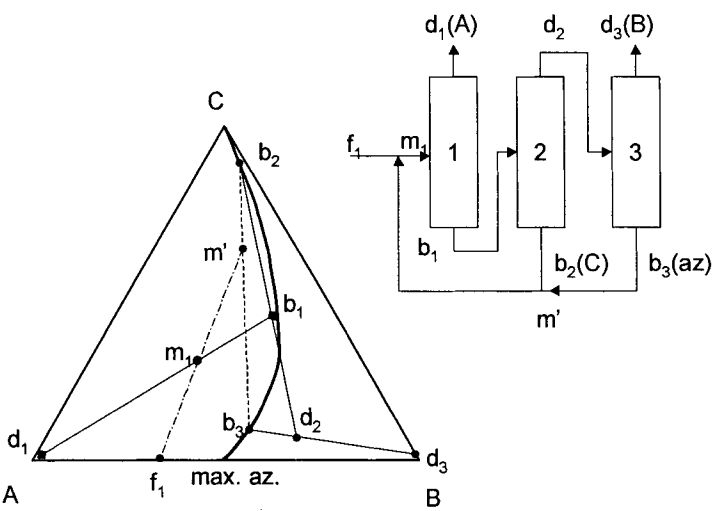

Figure 9.16 Separation of acetone and chloroform with toluene (Alternative 1).

Three columns sequence for separation in two distillation fields. The first split is sharp.

On the contrary, the second split will cross the boundary, so that the products d_2 and b_2 jump on the convex side. The column can be designed to deliver *C* as bottoms and an *AB* mixture as top product. Further, the component *B* can be recovered at high purity as top distillate, while the azeotrope *AB* is recycled. Thus, the sequence has three columns.

Both components are recovered as top distillate, because they are the origin of the residue curves. The entrainer is recycled as bottoms.

As an exercise the reader could examine the situation when the initial feed has an excess of *B*. The first split will take place in the right-side region. By clever recycle of the entrainer and mixing with the *B*-rich mixture from the first split, again a three-column sequence can be generated.

Figure 9.17 displays a second alternative. The first column may be designed to give a 'sloppy' split. The points b_1 and d_1 are on the same residue curve, and inside the same distillation region. Because d_1 can be brought practically on the side AB, the next binary split will produce high purity *A* and *AB* azeotrope, which is recycled. The point b_1 is at a small distance from the side BC, depending on the shape of the distillation border. As a result, the third split can recover *B* and deliver the entrainer to be recycled. Hence, this alternative seems to be interesting, but limited with respect to achievable purity. Fortunately, crossing the distillation boundary already in the first split can increase the purity, as it will be demonstrated later in this section.

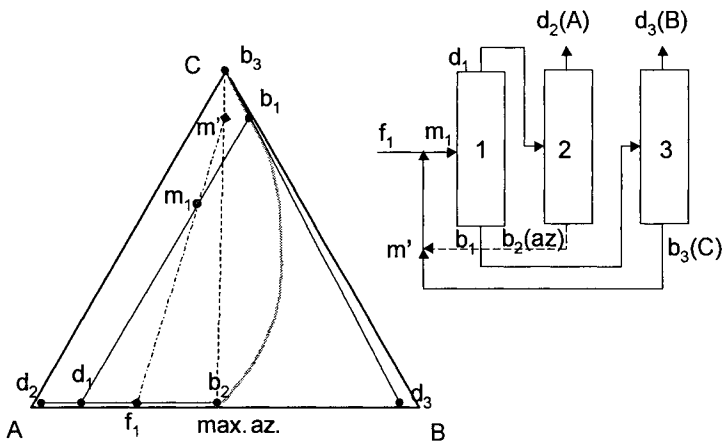

Figure 9.17 Separation of acetone and chloroform with toluene (Alternative 2).
Three columns sequence for separation in two distillation fields. First split sloppy.

Two columns sequence

The process may be simplified to a sequence with only two columns, as displayed in Figure 9.18, leading to a third alternative. The feed m_1 may be shift close to the vertex *C* by increasing the amount of solvent. The point b_1 will move very near to the side BC, making possible a quasi-binary separation b_2-d_2.

A convincing application of two columns sequence is the split of the azeotrope ethanol (A) / water (B) with tetrahydrofurane (C), as proposed by Stichlmair (1999). Figure 9.19 depicts qualitatively the split sequencing. The entrainer is a low-boiler forming a minimum azeotrope with water (az_1, nbp 64.2 °C) below the boiling point of the original water-ethanol azeotrope (az_2, nbp 78.2 °C). There is also an azeotrope tetrahydrofurane-ethanol (az_3, nbp 65.9 °C), but this is not essential. Water and ethanol,

as well as the water-tetrahydrofurane azeotrope, are nodes. The entrainer self and the water-ethanol azeotrope are saddles. The rules of feasibility given in Table 9.3 are respected. In this case, water and ethanol can be taken as bottom products, while the entrainer is recycled as azeotrope with water. Note that the distillate d_1 is on the concave side of the boundary, while the products d_2 and b_2 are on the other side.

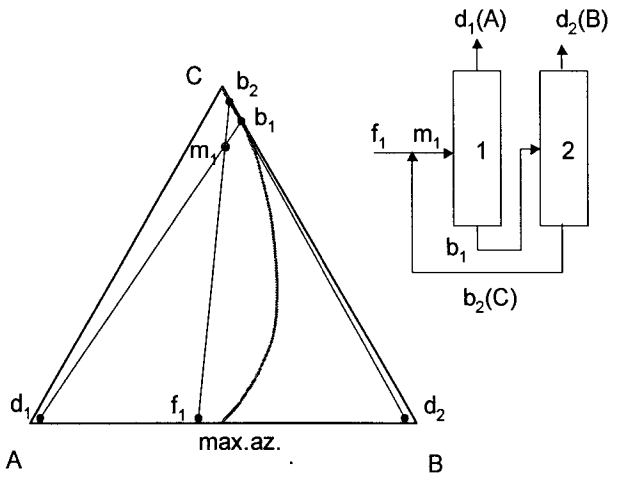

Figure 9.18 Separation of acetone and chloroform with toluene (Alternative 3). Two columns sequence for a separation in two distillation fields.

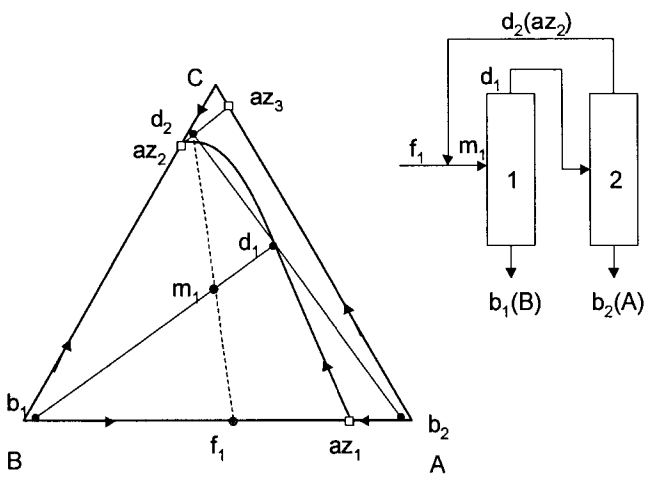

Figure 9.19 Breaking the ethanol-water azeotrope with tetrahydrofurane by a two columns sequence. The process takes place in two distillation regions.

Finite reflux design

Feasible separation alternatives identified at total reflux remain valid for finite reflux. However, if the distillation boundary at infinite reflux has a strong curvature, it can be crossed at finite reflux (Wahnschafft and Westerberg, 1992). This means that the top and bottom products may belong to different residue curves in different distillation regions. Thus, it seems that we might speak about an *effective distillation border* that is a function of reflux. There is no simple way to predict it, but its extent can be framed by simulation. This topic will be illustrated in the next example.

EXAMPLE 9.2 Split of the azeotrope acetone/chloroform with toluene

Acetone and chloroform forms a maximum-boiling azeotrope. Toluene, a high boiler, seems to be a suitable entrainer following the criteria given in Table 9.3. Examine by simulation the feasibility of different alternatives. Evaluate the influence of different design elements on product purity. Consider 50 kmol/h mixture with 30% chloroform and 70% acetone.

Solution. Here we present results obtained with ASPEN Plus version 10.1. Figure 9.4b presented already the RCM drawn with the NRTL model. Acetone and chloroform are both unstable nodes, toluene is a stable one, the maximum-boiling azeotrope acetone-chloroform being a saddle. The distillation boundary shows a strong curvature.

The tree alternatives have been already presented for the separation of such mixture. Alternative 1 (see Fig. 9.16) has three columns. Figure 9.20 presents the concentration profiles in the first column after flowsheet convergence. The column has 50 theoretical stages, with the feed mixture-entrainer on stage 20, and the entrainer/feed ratio of two. The reflux is set at 3.5. The distillation takes place in a single distillation field, at the left of the distillation bondary. The rectification part works mainly to separate the binary acetone-chloroform, the entrainer concentration being negligible. A jump in concentration takes place around the feed. Below, over several stages in the stripping zone the toluene remains constant, while the acetone decreases significantly. By approaching the distillation boundary, the profile bows to toluene.

The concentration profile of the second column shows that this works completely on the right side of the distillation border, even if the feed seems to be on the left side. The concentration profile follows closely the residue curves. The third column is a binary separation, without much interest. Hence, the simulation indicates that the separation sequence designed in a RCM by ∞/∞ analysis is feasible and leads to high purity products. Sizing and optimisation of columns can be done by standard procedures.

The flowsheet convergence deserves a comment. Closing the recycle has to cope with the accumulation of different components. Make-up of the recycled component is always necessary to get convergence. For example, a splitter may remove completely the toluene, while an external feed gets it back. A controller could manipulate the external flow such the difference between exit and make-up toluene goes to zero.

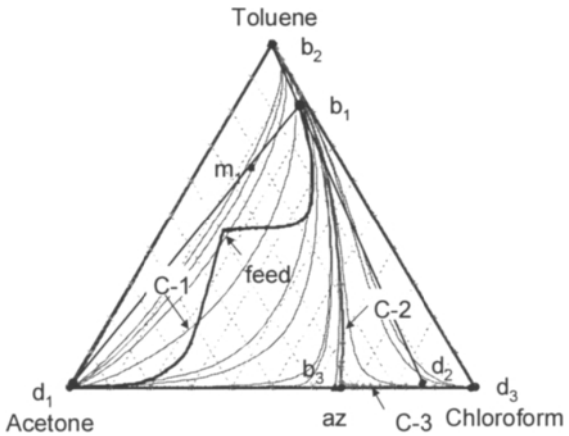

Figure 9.20 Separation of acetone and chloroform with toluene (Alternative 1)
The first split is sharp. The process takes place in two distillation regions, but the concentration profiles do not cross the simple distillation border.

Alternative 2 has also three columns, as depicted in Fig. 9.18. From ∞/∞analysis we expect the presence of a small amount of acetone in chloroform, because of the constraint set by the separatrix. Fortunately, chloroform purity is better at finite reflux. In fact, the distillation border can be crossed in the first column, as demonstrated by the concentration profile in Fig. 9.21. The bottom product is free of acetone, high purity chloroform being obtained by a simple binary distillation.

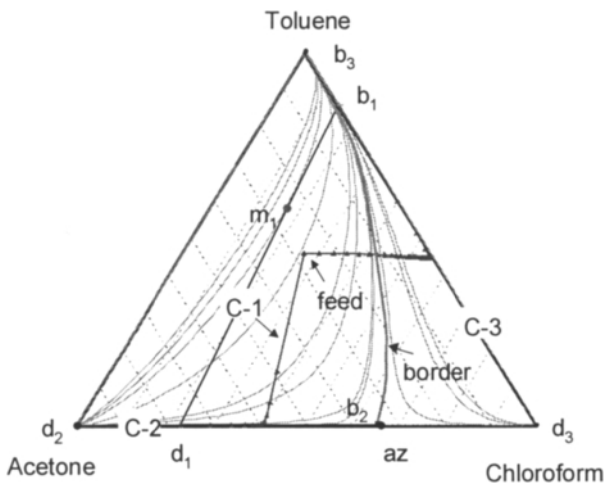

Figure 9.21 Separation of acetone and chloroform with toluene (Alternative 2).

Three columns, first split sloppy. The simple distillation border is crossed in the first column.

Alternative 3 (see Fig. 9.16) has only two columns. The first split could deliver high purity acetone, while the second split would give chloroform with acetone as impurity. The graphical representation predicts that chloroform purity would not exceed 98% for a reasonable amount of entrainer. Again, computer simulation gives a much better solution. The concentration profile for the first column (Fig. 9.22) shows clearly that the distillation border is crossed at finite reflux, and high purity can be obtained in the second split.

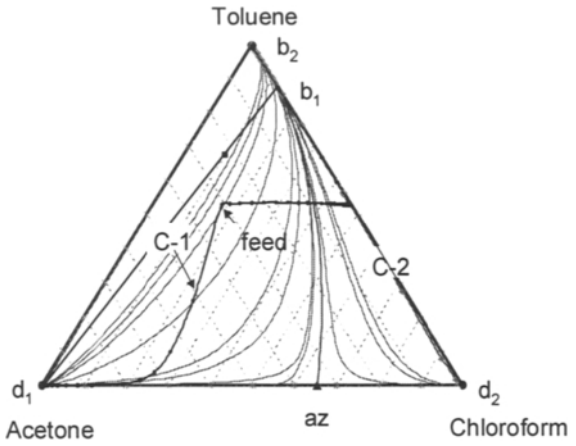

Figure 9.22 Separation of acetone and chloroform in two columns (Alternative 3). The simple distillation border is crossed in the first column.

Elements affecting purity.

Purity can be managed mainly by means of two factors: entrainer and reflux ratios. For given purity there is a minimum entrainer ratio. This can be determined from a RCM plot. The influence of reflux is subtler. In the case of azeotropic systems, we may have a minimum and a maximum reflux ratio giving the same purity.

Figure 9.23a displays curves of constant purity as function of reflux ratio and entrainer flow rate, when distillate rate and number of stages are constant. The sequence has two columns (Alternative 3). Two situations are examined, low and high purity of chloroform. It can be observed that there is a minimum entrainer ratio to achieve a given purity. For the same entrainer ratio there are minimum and maximum reflux ratios. At low purity, there is a wider range for reflux, while at high purity the variation is limited.

Figure 9.23b shows curves at constant purity as function of reflux and number of stages, keeping the entrainer ratio constant. The existence of a minimum number of stages for desired purity is clearly indicated. When the column has more stages than minimum, there are two steady states for the reflux necessary at given purity.

The above behaviour is unusual, in contrast with zeotropic systems, where the purity improves always by increasing the reflux. The explanation may be found in a dilution effect by solvent at higher reflux, making that its effect on the relative volatility of components drops too.

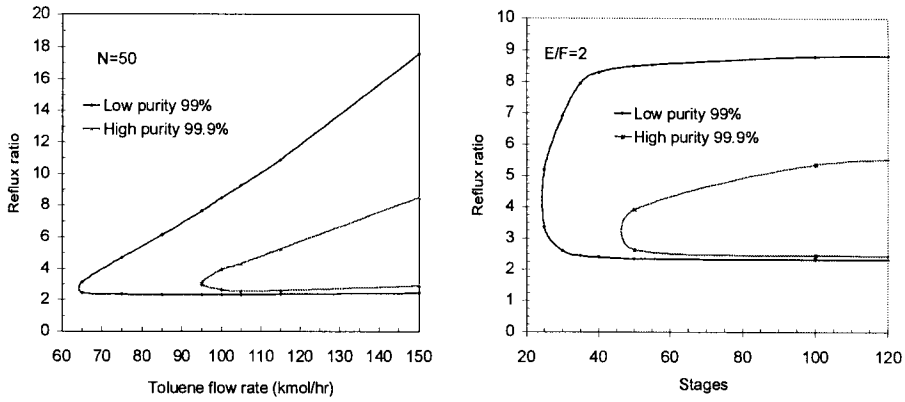

a b

Figure 9.23 Dependence of chloroform purity on entrainer, reflux and number of stages. Mixture acetone/chloroform with 70% acetone, feed rate 50 kmol/h, two columns sequence.

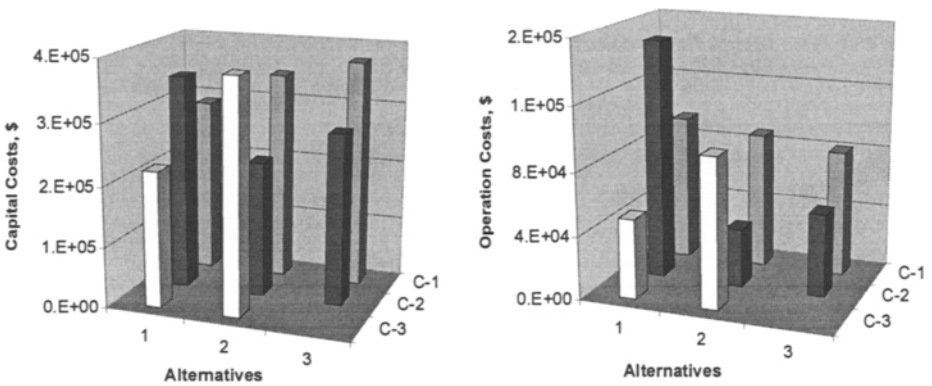

Figure 9.24 Capital and operation costs for three separation alternatives

Economic evaluation.

Finally, it is interesting to compare the three alternatives from economic point of view. Figure 9.24 presents capital and operation costs. The most expensive columns in term of capital are those crossing the boundary, as well as for separating the binary chloroform/toluene. The alternative with two columns is the cheapest. It has also the lowest operation costs. The first alternative is the most expensive in operation.

With these elements, the alternatives can be compared on the basis of Total Annual Cost (Fig. 9.23). By far, the best alternative has only two columns. The alternative with a sloppy split is ranked in the second place, because of cheaper operation.

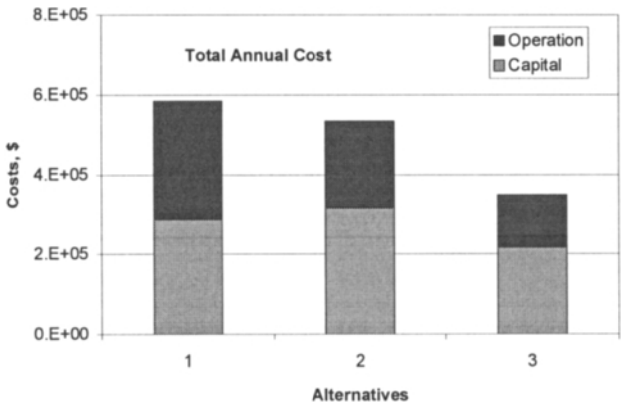

Figure 9.25 Total Annual Cost for three separation alternatives

9.3 HETEROGENEOUS AZEOTROPIC DISTILLATION

In heterogeneous azeotropic distillation liquid-liquid phase splitting helps to overcome the constraint of the distillation boundary. As example we will handle ethanol recovery from a water/alcohol mixture by using a generic entrainer.

Figure 9.26 shows the RCM. There are three minimum-boiling azeotropes, as well as a ternary azeotrope, the lowest-boiler. Pure components and ternary azeotrope are stable nodes, while binary azeotropes are saddles. Ethanol and water are both nodes, but in different distillation regions. The distillation boundary being almost straight, it cannot be 'crossed' by homogeneous distillation. Other strategy should be investigated.

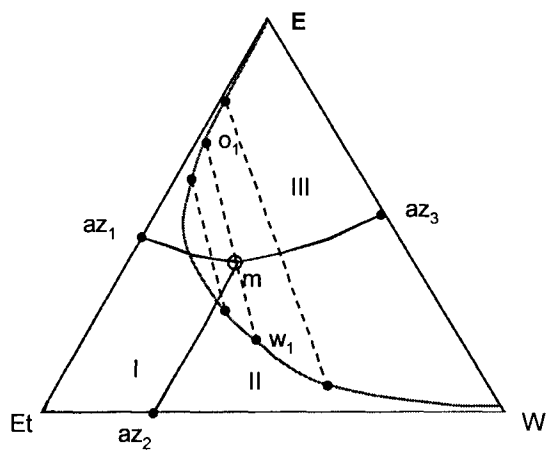

Figure 9.26 General Residue Curve Map for a ternary ethanol-water-entrainer

It may be observed that the ternary azeotrope *m* falls inside the heterogeneous region. Thus, an overhead vapour of this composition splits by decantation in two phases, one rich in entrainer o_1, other in water w_1, the ethanol being distributed in both. Moreover, o_1 and w_1 are in different distillation regions. By clever mixing with other streams, these streams can produce feasible feeds for ethanol and water recovery columns, by overcoming the constraints of the distillation boundaries. Hence, liquid-liquid decantation creates opportunities for the separation of an azeotropic mixture.

With these elements, we can sketch a separation sequence (Fig. 9.27). We may start with an initial feed close to the azeotropic composition (point F). The column receives as reflux the organic phase o_1 and recycled mixture F_R such to produce the overall feed f_1 situated in the distillation region I. Ethanol and ternary azeotrope are nodes. The top distillate is a vapour of composition y_1 that must fall in the heterogeneous region. The liquid-phase composition of the top stage should be in the homogeneous region.

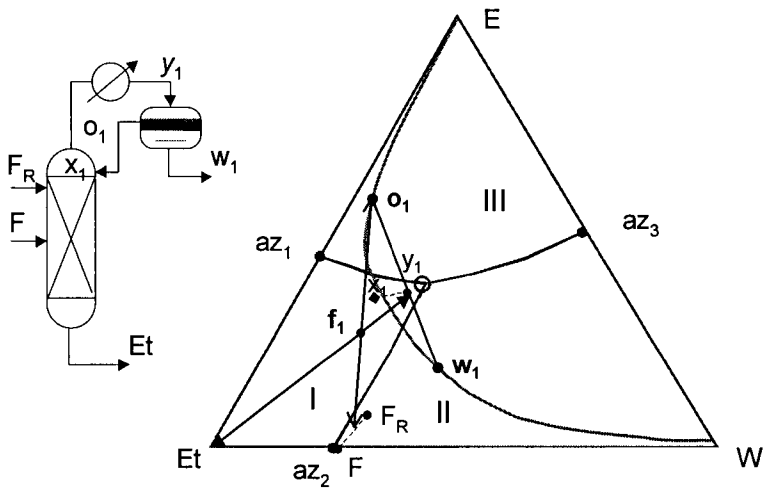

Figure 9.27 Separation of ethanol by azeotropic distillation

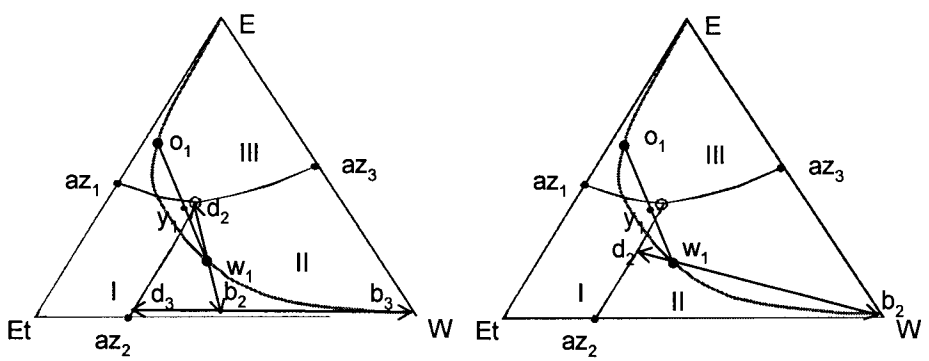

Figure 9.28 Alternatives for water removal

The other stream w_1 is located in the region II, where water and ternary azeotrope are nodes. Here, two possibilities appear. A sequence of two columns can be used (Fig: 9.28-left), the first taking the ternary azeotrope as top distillate, and the second split separating water and binary azeotrope az_2. In the second alternative (Fig. 9.28-right), with appropriate design a single column is necessary in which the water can be obtained directly as bottom product. The top distillate is a mixture enriched in ethanol containing some water and entrainer that can be recycled either in decanter or as feed in the ethanol column.

On this basis several flowsheet alternatives can be depicted. Figure 9.29 depicts only the alternative with two columns, one for ethanol recovery, whereas the other one is for water removal and alcohol concentration. Note that this flowsheet accepts relatively concentrated solutions. The concentration can be done in a separate column, so that the flowsheet contains a maximum of three columns.

From the above discussion it can be observed that the initial diluted feed can be sent to the water-column and not to the ethanol recovery column (azeotropic distillation). In consequence, this alternative has only two columns, and has been occasionally presented as innovative. Doherty & Malone (2001) discusses in detail all the alternatives discovered along the time using benzene as entrainer. The tw0-column sequence is not the most economical because of large entrainer recycle and expensive columns. It seems that the two-column sequence with prefractionator, in total three units, offers the best compromise between investment and operation (solvent recycle) costs.

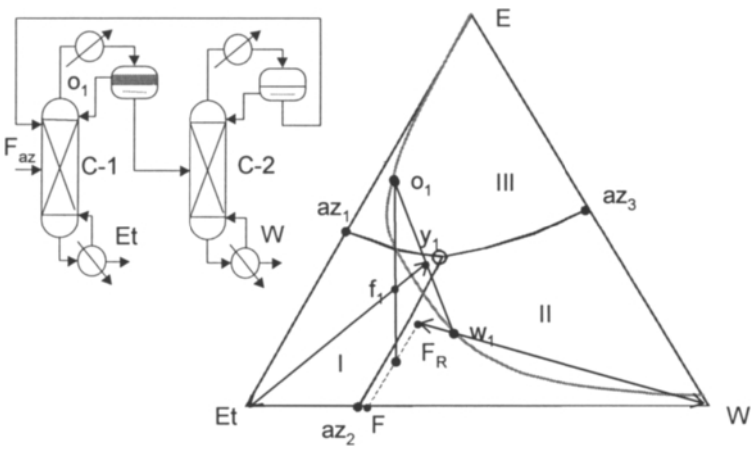

Figure 9.29 Flowsheet for separating ethanol from water by heterogeneous azeotropic distillation

We mention also that this type of separations could exhibit high non-linear behaviour, as multiple steady-states (Widago and Seider, 1996). This might explain some difficulties to obtain robust convergence in simulation.

EXAMPLE 9.3 Recovery of ethanol by heterogeneous azeotropic distillation

The azeotrope ethanol/water can be broken by azeotropic distillation with benzene. Examine by simulation the feasibility of a two-column alternative. Study the influence of different design elements on the achievable purity.

Solution. Ethanol (nbp 78.4 °C) and water (nbp 100 °C) form a minimum boiling azeotrope (nbp 78.2 °C and 10 % mole water). If benzene (nbp 80.1 °C) is selected as entrainer, the new azeotropes have the following characteristics at normal pressure:

- Binary homogeneous minimum boiling with ethanol (67.7 °C, 44.6 % mole E);
- Binary heterogeneous minimum boiling with water (69.3 °C, 29.8 % mole W);
- Ternary heterogeneous minimum boiling (64.1 °C, 27.5 % mole E, 19.4 % mole W).

The RCM (Fig. 9.30) was calculated by ASPEN Plus version 10.2 using UNIQUAC with interaction parameters from both VLE and LLE. The azeotropes are predicted with good accuracy. However, LLE computations show some difficulties near the plait point. The simple distillation boundary has moderate curvature, bowed to the ternary azeotrope, with the concavity to the water region. Ethanol is stable node in the region I, where the unstable node is the ternary azeotrope. These are potential products of the column (C-1). A temperature difference of about 14 °C is sufficient for economic separation. However, the azeotrope water/ethanol (saddle) is at only 0.2 °C from the boiling point of ethanol, so we expect difficulties. In the region II, the nodes are water and ternary azeotrope. Here should work the column (C-2). The only way to bridge the two distillation regions is by liquid-liquid splitting.

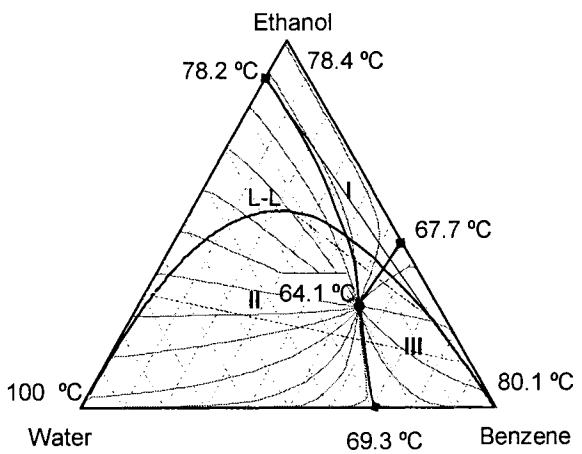

Figure 9.30 RCM for the mixture ethanol/water/benzene

Consider 1000 kg/h alcohol/water mixture of 90% weight fraction ethanol. The flowsheet is the same as in Fig. 9.29. The simulation of the ethanol column has to cope

with the difficulty of L-L splitting. For this reason, it was simulated as a stripping column, combined with a three-phase decanter. The thermodynamic option was UNIQUAC with VLE parameters for column, and LLE parameters for decanter. Accurate LLE is the key feature in convergence. Also, the feed of the column (C-1) should be very close to the simple distillation boundary, or inside the region I.

The ethanol column (C-1) has practically only stripping zone. Fig. 9.31-left shows composition profile both for liquid and vapour phase. The examination of the composition profiles highlights the role of the entrainer. In the zone close to the top the benzene extracts the ethanol in the liquid phase, and as a result increases the volatility of water, so that on lower stages the water is completely removed. In the lower part practically only the binary ethanol/benzene remains. The distillation trajectory starts from the ternary azeotrope, goes along the ethanol/ benzene saddle and terminates in the ethanol vertex. Because the boiling point of the azeotrope ethanol-water is close to the pure ethanol, the profile could easily jump to the ethanol/water azeotrope. Consequently, the design and operation of the column (C-1) is very sensitive.

Column (C-2) removes the excess of water in bottoms and delivers a concentrated mixture ethanol/water with small amounts of entrainer as top distillate. The column is fed near the top with the water-phase mixture from the decanter. The concentration profile (Fig. 9.31-right) shows clearly the role of this column as simply concentrator of ethanol. Therefore, if the feed is diluted it would be rational to enter it directly into the water column. Thus, a two-column alternative is workable. Note that in this flowsheet (Fig. 9.29) the top distillate from (C-2) is returned into the first column and not into the decanter! This operation is more efficient saving about 50% entrainer amount. The above process delivers high recovery and high purity ethanol (99.812%, 280 ppm benzene, 1600 ppm water). The ratio entrainer/ethanol is 9.44 mol/mol.

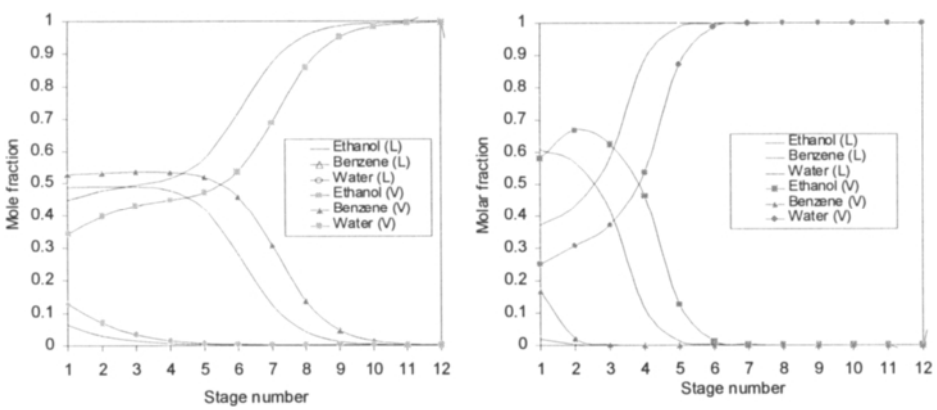

Figure 9.31 Composition profile for azeotropic separation ethanol/water with benzene

9.4 COMBINED PROCESSES

The combination of distillation with other separation techniques can overcome the difficulty in finding a suitable entrainer. Some methods will be analysed hereafter. The book of Stichlmair and Fair (1999) may be consulted for more information.

9.4.1 Distillation combined with extraction

Liquid-liquid extraction can be used to recover one of the components to be separated, as well as the entrainer to be recycled. A typical process is the separation of cyclohexane/benzene, with nbp's at 80.8 °C and 80.1 °C and minimum-boiling azeotrope at 77.6 °C (Seader and Henley, 1998). If acetone is used as entrainer (nbp 56.2 °C), then an azeotrope appears between acetone and cyclohexane (nbp 53.1 °C). RCM shows a distillation boundary between the components to be separated (Fig. 9.32). To simplify the process, consider an initial azeotropic mixture. After mixing with entrainer the feed f_1 is separated in two products, benzene in bottoms and acetone-cyclohexane azeotrope in top. From the last mixture cyclohexane can be extracted with water. Finally acetone and water are separated by simple distillation.

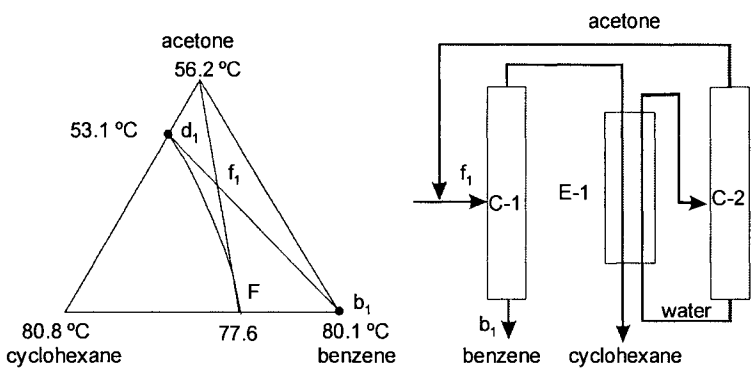

Figure 9.32 Combining distillation and extraction for the separation of cyclohexane and benzene

9.4.2 Distillation combined with adsorption

Adsorption is an effective technique to break an azeotrope. The separation makes use of molecular sieve adsorption, and can take place either in vapour or in liquid phase. Unlikely a process using a MSA that could contaminate the final product, here absolute purity product is obtained. Figure 9.33 depicts a process for pharmaceutical-grade ethanol (Stichlmair and Fair, 1999). After pre-concentration in the column C-1 operating at a pressure slightly above normal, the vapour distillate with the azeotropic composition is fed to the adsorption device. Here the water is retained, producing a vapour that consists of pure ethanol. This may be used to heat the second distillation

column C-2, which operates under vacuum and receives the water-rich effluent from the regeneration phase. Hence, the absorption is conducted in a cycle of three phases: adsorption, regeneration and pressure built-up.

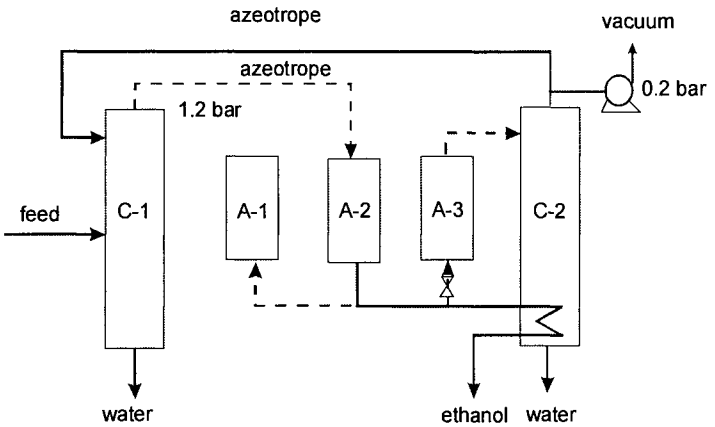

Figure 9.33 Distillation combined with adsorption

9.4.3 Distillation combined with membrane permeation

Membrane permeation is an emerging technique that can be efficient in breaking azeotropes. As example, we can give again the separation of ethanol from water. A suitable flowsheet is presented in Fig. 9.34. After pre-concentration in the column C-1, the azeotrope is fed to a membrane. The pressure on the inlet-side is higher, while the other side is connected to a vacuum line. Several stages are necessary to go beyond the azeotropic composition, with intermediate heating to compensate the vaporisation through permeation. The final ethanol-rich retentate is fed in a second column C-2 for advanced purification by distillation. Ethanol is recovered as a bottom product, while the top distillate having azeotropic composition is recycled to membrane permeation.

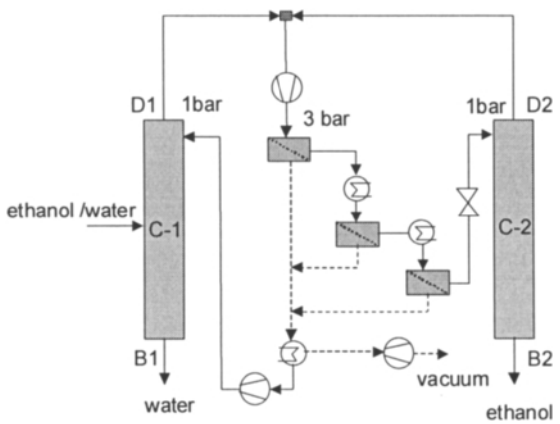

Figure 9.34 Distillation and membrane permeation (Stichlmair and Fair, 1999)

9.5 DESIGN ISSUES

9.5.1 Shortcut method for zeotropic mixtures

The two important design elements of a distillation column are the number of theoretical stages N, and the reflux R ratio. If the mixture is zeotropic, they are related, as illustrated in Fig. 9.35-a. There is a minimum number of theoretical stages N_{min}, as well as a minimum reflux R_{min}, both depending on the sharpness of separation. For zeotropic mixtures with n-components, the shortcut design procedure known as Fenske-Underwood-Gilliland (FUG) method is well-established (Perry's handbook, 1997).

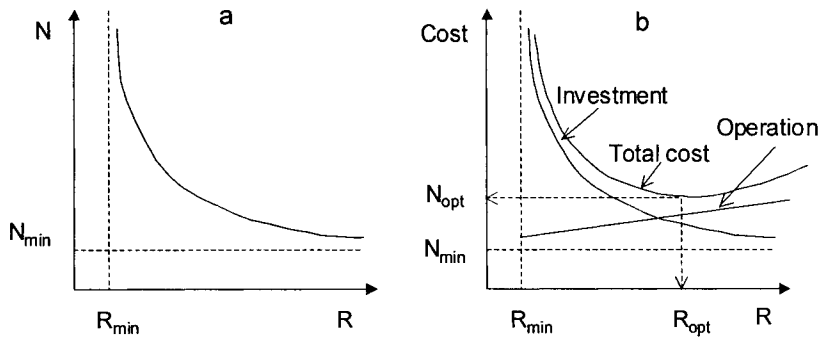

Figure 9.35 The relation between the number of stages and reflux

FUG procedure consists of the following steps:

1. Formulate specifications. For a new column these are usually the split on the key components and R/R_{min}, ratio of reflux to minimum reflux.
2. Calculate the minimum number of stages. Specifications are formulated as distillate and bottom rates and compositions, denoted by D, B, x_D and x_B, respectively from which the Fenske equation gives:

$$N_{\min} = \log\left[\left(\frac{Dx_D}{Bx_B}\right)_l\left(\frac{Bx_B}{Dx_D}\right)_h\right] / \log\alpha \tag{9.6}$$

where α is the mean relative volatility of key components.

3. Determine the minimum reflux by the Underwood method:

$$\sum_i \frac{\alpha_i (x_{i,D})_m}{\alpha_i - \theta} = R_{\min} + 1 \tag{9.7}$$

$$\sum_i \frac{\alpha_i x_{i,F}}{\alpha_i - \theta} = 1 - q \tag{9.8}$$

In the above equations α_i is relative volatility with respect to a reference component, and q is the thermal condition of the feed (1 for bubble-point, 0 for dew-point). Because the feed composition is known, θ may be found by iterations from the second equation. Then R_{min} is determined directly from the first equation.

4. Use Gilliland correlation to calculate N from R, or R from N:

$$\frac{N-N_{\min}}{N+1}=1-\exp\left[\left(\frac{1+54.4\Psi}{11+117.2\Psi}\right)\left(\frac{\Psi-1}{\Psi^{0.5}}\right)\right] \tag{9.9}$$

where $\Psi=(R-R_{\min})/(R+1)$.

Optimum reflux can be in principle determined by taking into account investment and operation costs. The column cost is roughly proportional with the number of stages N. The cost of utilities depends on the maximum vapour flow in the column, proportional with R+1. Consequently, the optimisation of the function $N(R+1)$ versus R can supply a good estimation of actual optimum reflux, as shown in the Fig. 9.35-b. In practice, the optimal reflux takes values between 1.2-1.5 R_{min}. Alternatively, the actual number of theoretical stages may be considered twice the minimum one.

9.5.2 Minimum reflux in ternary distillation

The concept of minimum reflux is more complex in azeotropic distillation, because of the high non-ideal behaviour and distillation boundaries. For the special case of ternary distillation, the analysis may be simplified. It is useful to mention that the minimum reflux is linked with the concept of *distillation pinch*. This represents a zone of constant phase composition, so that the driving force becomes very small. Consequently, the number of necessary stages for separation goes to infinite. Similarly, there is a minimum reboil rate. In this respect, three classes of limiting separations may be distinguished (Stichlmair and Fair, 1999). Figures 9.36 to 9.38 present concentration profiles obtained by simulation with an ideal system benzene-toluene-ethyl-benzene.

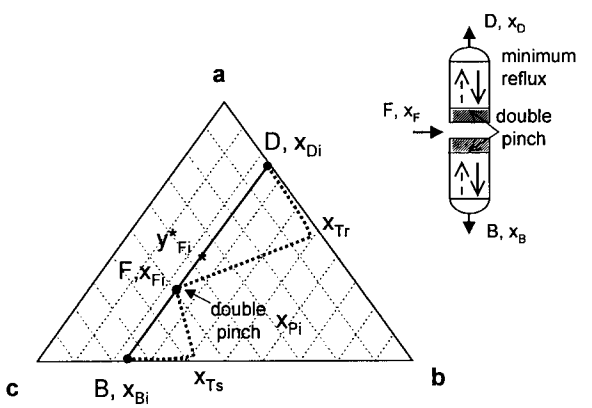

Figure 9.36 Preferred separation of a ternary mixture

In the first class, called *preferred separation*, the mid-component is distributed approximately evenly between the two products. There is a double pinch zone, above and below the feed (Fig. 9.36). Material balance line and concentration profile intersect at the feed point. The reflux ratio has the lowest value of all possible separations. Hence, the preferred separation is the most favourable in ternary systems.

In the second class, the distillate is of high purity in low boiler. The rectification section operates at a reflux above minimum, while the stripping section may operate at minimum reboil. There is only one pinch, below the feed (Fig. 9.37). The concentration profile does not intersect the mass balance line, the pinch being shifted upwards to the right. This situation is characteristic for the first column in direct sequence.

In the third class of separations (Fig. 9.38), the bottom product is enriched in high boiler. Now, the stripping section operates at higher reboil, while the rectifying section may be kept at minimum reflux. There is a pinch zone above the feed. Both the concentration profile and the pinch shift downwards. This situation is typical for the first column of an indirect sequence.

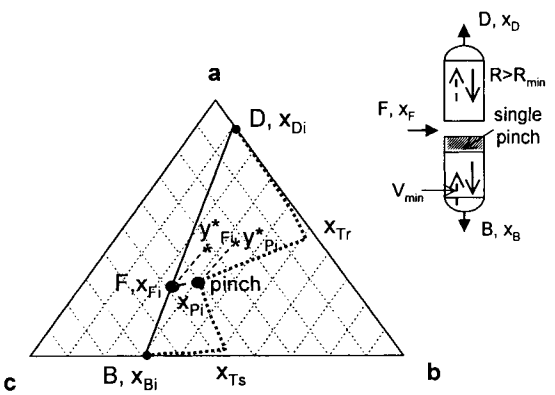

Figure 9.37 Separation of an overhead fraction rich in low boiler

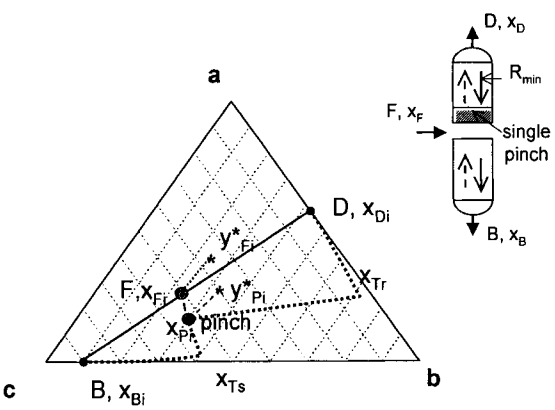

Figure 9.38 Separation of a bottom product rich in high boiler

When the ternary mixture is an azeotropic one, supplementary aspects must be considered, as the strong variation of volatilities with composition, as well as the existence of distillation boundaries. The design of such distillation column can be handled better by means of new tray-by-tray methods, as it will be explained below.

9.5.3 Design methods for non-ideal systems

Among the new methods for designing distillation columns dealing with non-ideal systems the Boundary Value (BV) method has received a large acceptance (Doherty & Malone, 2001). The principle is explained in Fig. 9.39, where the components A, B. C are in the decreasing order of volatility. Consider a simple column one-feed two-products. The calculation consists of tray-by-tray solution of the material and energy balances starting from the composition specifications on distillate and bottoms. Supplementary specifications are the reflux ratio L/D and the reboil V/B. In this way, separate profiles for stripping and rectification and stripping sections can be obtained (Fig. 9.39-left). If the profiles intersect then the column is feasible. By minimising the distance between profiles the number of stages and feed location can be obtained.

The BV method can be used to calculate the minimum flows. In Fig. 9.39-right the reflux and boilup ratios has been reduced close to minimum values. Pinch zones can be identified where the composition changes very little on successive stages. In this case the profiles just intersects at the feed position. Below minimum flows the profiles will not intersect. In Fig. 9.39-right a saddle pinch can be identified in the rectifying profile. This profile corresponds to the minimum reflux in a 'direct sequence', since the distillate is practically pure component A. The minimum reflux is practically independent of the bottoms composition. Similarly, a minimum reboil ratio can be identified. The determination of the minimum number of stages is subtler, since the composition of the top distillate and bottoms are not independent.

Hence, the BV method can be used for the design of the distillation columns dealing with the separation of non-ideal mixtures. The method is implemented in some software, as Aspen Split (AspenTech) and Distil (Hyprotech).

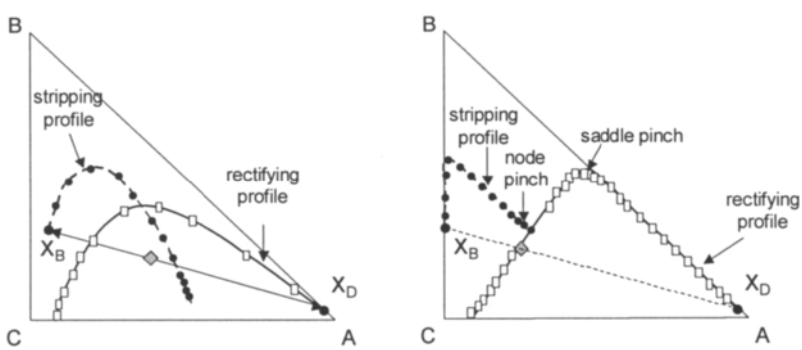

Figure 9.39 Drawing composition profiles by the Boundary Value Method

9.6 FURTHER READING

The conceptual design of distillation systems has received a particular attention in the recent years, by the publication of some remarkable books. The first that we mention is Separation Process Principles by Seader & Henley (1998), a significant upgrade of an already remarkable textbook on equilibrium-staged separations. However, modern RCM methods are explained only in a succint manner with emphasis on applications. The reader will find more information about new separation methods that are complementary to distillation, or can replace it in some cases.

A noteworthy book devoted exclusively to distillation has been published recently by Stichlmair & Fair (1999). Both authors are known as major scientific contributors in the field of distillation and absorption, the first in the area of conceptual design methods, the second in the are of internals design. The topics are very clearly explained and application oriented. The concise manner allows sufficient space to scientific issues regarding unsolved problems.

Another recent book dedicated to the conceptual design of distillation systems has been published by Doherty and Mallone (2001). The authors are well-known by outstanding contributions in the field. Emphasis is given to process synthesis aspects, namely to the new methods based on residue curve maps, as well as to the innovative use of Reactive Distillation.

In the area of process synthesis we may mention also two large reviewers due to Westerberg and Wahnshafft (1996), from a scientific perspective, and of Siirola (1996), from a practical perspective.

The presentation in this chapter was based on equilibrium-stage concept. Actually, there is a debate about the usefulness of such concept against more realistic rate-based models. At least the screening of alternatives can be done with the equilibrium-stage methods presented here. However, the designer should be aware that the solution of an industrial problem involves the consideration of the mass-transfer and hydrodynamics aspects. Therefore, each time when possible rate-based models should be used for final column design. These models involve detailed knowledge of sizing, geometrical characteristics and transport properties that is not usually available at a conceptual design stage. Reliable data are available only for standard internals and usual mixtures. The extrapolation of such data to innovative solutions should be carefully examined. Commercial programs are available for using rate-based models in the design of distillation columns, as for example ChemSep (Taylor & Kooijman) distributed by CACHE and Ratefrac from AspenTech. The theoretical basis of these models can be found in the excellent book of Taylor & Krishna (1996).

In the area of engineering practice the outstanding monographs of Kister dedicated to design (1992) and operation (1993) remain among the most comprehensive works.

The above references demonstrates that the old field of distillation still offers good subjects for research and development. Distillation remains the most used separation technique in chemical engineering.

9.7 SUMMARY

The conceptual design of distillation systems involving high non-ideal mixtures can be managed nowadays by means of systematic methods. These new methods combine the insight capabilities of graphical thermodynamic tools based on Residue Curve Maps with the power of computer simulation. The main ideas are:

Residue Curve Map (RCM) is a suitable thermodynamic representation for the conceptual design of distillation systems, particularly for ternary mixtures involving azeotropes. Residue curves represent the time evolution of the liquid-phase composition in a batch distillation still, being similar with the liquid-concentration profile in a packed distillation column at infinite reflux. Similarly, a Distillation Curve Map (DCM) describes the concentration profile on the stages of a distillation column operated at infinite reflux. RCM and DCM representation give similar results in conceptual design.

RCM is characterised by fixed composition points, which are the pure components and the azeotropes. The family of all residue curves that originate from one fixed composition point and terminate at another fixed composition point defines a *distillation region.* Two adjacent distillation regions are separated by a *distillation boundary.* The curvature of the boundary plays an important role in designing separation sequences.

3. Pure components and azeotropic data are sufficient to sketch the main characteristics of a RCM. However, accurate thermodynamic modelling is needed for design. Erroneous prediction of azeotropes will compromise the whole conceptual work. A typical fault is the confusion between homogeneous and heterogeneous azeotropes when interaction parameters from VLE and LLE data are mismatched. Because the curvature of the distillation boundary plays a major role, its accurate draw requires high quality thermodynamic data.

4. The elementary problem analysed in a RCM is the separation of high-purity components from an A/B binary mixture by means of a Mass Separation Agent (entrainer). The key issue is the entrainer selection that will produce a favourable RCM for breaking the azeotrope. In this respect a major decision is the application of only homogeneous azeotropic distillation, or considering also heterogeneous azeotropic distillation.

5. The separation by homogeneous azeotropic distillation is severely constrained by distillation boundaries. The major concern is the place where the process takes place, namely in one or two distillation regions. The first situation is similar with zeotropic systems, but finding a suitable entrainer is problematic. In the second case, the distillation boundary has to be crossed. Since insufficient theoretical and experimental research is available, this is not guaranteed by only simulation. Heuristics have been formulated for the both situations for the proper entrainer selection.

6. Heterogeneous azeotropic distillation offers in principle wider possibilities. Liquid-liquid split helps to cross the distillation boundary. However, the process might be very sensitive, because of a more complex thermodynamic behaviour.

7. When the distillation is not feasible or uncertain, the combination with other separation techniques is recommended.

9.8 REFERENCES

Bossen, B. S., S. B. Jorgensen, R. Gani, 1993, Simulation, design, and analysis of azeotropic distillation operations, Ind. Eng. Chem. Res., 32, 620-633

Doherty, M., F., G., A. Caldarola, 1985, Design and synthesis of homogeneous azeotropic distillations, Ind. Eng. Chem. Fundam., 24, 474-485

Doherty, M., F., M. Malone, 2001, Conceptual design of distillation systems, Mc Graw-Hill

Fidkowski, Z.T., M.F. Doherty, M. F. Malone, 1993, Feasibility of separations for distillation of nonideal ternary mixtures, AIChEJ, 39(8), 1303-1321

Fien, G., Y.A. Liu, 1994, Heuristic synthesis and shortcut design of separation processes using Residue Curve Maps: A rewiew, Ind. Eng. Chem. Res., 33, 2505-2522

Laroche, L., N. Bekiaris, H.W. Andersen, M. Morari, 1992, Homogeneous azeotropic distillation: separability and flowsheet synthesis, I. E. Chem. Res., 31, 2190-2209

Kister, H.Z., 1990, Distillation Operation, McGraw-Hill

Kister, H.Z., 1992, Distillation Design, McGraw-Hill

Koehler, J., P. Poellmann, E. Blass, 1995, A review on minimum energy calculation for ideal and nonideal distillations, AIChEJ, 43 (4), 1003-1020

Rooks, R. E., Julka, V., Doherty, M. F., Malone, M. F., 1998, Structure of distillation regions for multicomponent azeotropic mixtures, AIChEJ, 44(6), 1382-1391

Springer, P. A. M, S. van der Molen, R. Baur, R. Krishna, 2002, Experimental verification of the Maxwell-Stefan formulation in describing composition trajectories during azeotropic distillation, Trans IChemE, vol. 80, Part A, 654-665

Seader, J. D., E. J. Henley, 1998, Separation Process Principles, Wiley

Seader, J. D., J. J. Siirola, S. D. Barnicki, 1997, Distillation, in Perry's Chemical Engineers Handbook, 7th edition, McGraw-Hill

Sirola, J. J., 1996, Industrial applications of chemical process synthesis, Adv. Chem. Engng. Vol. 23, 1-62

Stichlmair, J. G., J. R. Fair, 1999, Distillation, Principles and Practice, Wiley-VCH

Stichlmair, J. G., J. R. Herguijuela, 1992, Separation regions and process for zeotropic and azeotropic ternary distillation, AIChEJ, 38 (10), 1523-1535

Taylor, R., Krishna, R., 1993, Multicomponent Mass Transfer, Wiley

Wanshafft, O. M., J. W. Koehler, E. Blass, A. W. Westerberg, 1992, The product composition regions of single-feed azeotropic distillation columns, Ind. Eng. Chem. Res., 31(10), 2354-2362

Westerberg, A., W., O. Wahnshafft, 1996, The synthesis of distillation-based separation systems, Advances in Chemical Engineering, vol. 23, Academic Press

Widago, S., W. D. Seider, 1996, Azeotropic distillation, AIChE J, 42(1), 99-130

PART IV

PROCESS INTEGRATION

This Page Intentionally Left Blank

Chapter 10

PINCH POINT ANALYSIS

10.1 Introduction
- 10.1.1 Basic concepts
- 10.1.2 The overall approach

10.2 Targets for energy recovery
- 10.2.1 Composite Curves
- 10.2.2 Pinch Point Principle
- 10.2.3 Balanced Composite Curves
- 10.2.4 Stream segmentation
- 10.2.5 Data extraction
- 10.2.6 Targets for energy and capital

10.3 Placement of utilities
- 10.3.1 Threshold problems
- 10.3.2 Multiple utilities
- 10.3.3 Variable temperature utilities

10.4 Design of the Heat Exchanger Network
- 10.4.1 Topological analysis
- 10.4.2 HEN design in the grid diagram
- 10.4.3 Stream splitting
- 10.4.4 Reducing the HEN
- 10.4.5 Network optimisation

10.5 Mathematical programming

10.6 Design evolution

10.7 Extensions of the pinch principle

10.8 Summary of Pinch Point Analysis

10.9 References

10.1 INTRODUCTION

Energy saving is a major issue in sustainable development. Thanks to the effort of several researchers, a methodology was developed in the decade 1980-90 under the label *Pinch Point Technology*. Some key concepts have been published at the end of 1970, but Linnhoff and co-workers have the merit of the most important contributions. They published the first 'Guide for Optimal Use of Energy in Process Industries' in 1982 (republished in 1994) where the concept of *Process Integration* was introduced. Since, Process Integration evolved to a paradigm of process design, which addresses not only energy saving but other important systemic issues (see Chapter 1). Today the label *Pinch Point Analysis* designates the systematic research of innovative solutions in the area of energy saving (Linnhoff et al., 1994).

Pinch Point Analysis

Pinch Point Analysis (PPA) is an extension of the second principle of Thermodynamics to the energy management of the whole plant. PPA deals with the optimal structure of the heat exchange between the process streams, as well as the optimal use of utilities. Among benefits we mention:

1) Assess the reference basis of an energy saving project, namely:
- Minimum Energy Requirements (MER), as heating and cooling loads for utility system, for a minimum temperature approach ΔT_{min} assumed at Pinch;
- Maximum energy saving by process/process heat exchange;
- Capital and operation costs needed by MER.

2) Set optimal targets before the detailed design of the heat exchanger network:
- Design targets for the Heat Exchangers Network (HEN), as the total heat exchange area and the number of units for achieving MER;
- Nature and amount of utilities needed for satisfying the optimal loads;
- Integration on heat saving with power generation.

3) Suggest modifications in technology and process design with significant impact on saving energy, as:
- Optimisation of the operating parameters of reactors and separators;
- Heat integration of distillation columns;
- Optimal placement of heat engines and heat pumps, etc.

PPA makes use intensively of conceptual graphical tools. The concept of *Pinch* has proved a generic value, being extended to the management of other valuable resources, as water, solvents and hydrogen (Linnhoff et al., 1994).

In parallel with PPA, a different approach was developed, based on *Mathematical Programming* (MP). Grossman, Floudas and co-workers have brought significant contributions (see the references). Nowadays the two approaches are largely complementary, PPA as conceptual tool while MP as automatic design tool.

Specialised packages for implementing Pinch Point Analysis are available, as SUPERTARGET™ (Linnhoff/KBC), ASPEN Pinch™, HEXTRAN™(Simsci). The synthesis of a heat exchanger network by mathematical programming may be handled by means of packages based on the generic environment GAMS™.

10.1.1 Basic concepts

Composite and Grand composite curves

The most fundamental concepts in Pinch analysis are *Composite and Grand Composite Curves*. Composite Curves (Fig. 10.1-left) visualises the flow of heat between the hot and cold process streams selected for heat integration. A composite curve is obtained by plotting the cumulative enthalpy of streams, cold or hot, against temperature. The relative position of the composite curves depends on the minimum temperature difference ΔT_{min} between cold and hot streams. This sets also the Pinch position as the place where the heat transfer between the hot and cold streams is the most constrained.

Composite Curves enable to determine directly the Minimum Energy Requirements (MER) from stream data without ever calculate heat exchangers. These are the minimum hot Q_h and minimum cold Q_c utility required for driving the heat exchanger network, with a minimum driving force of ΔT_{min} at Pinch.

The *Pinch principle* states that any design where heat is transferred across the Pinch will require more energy than minimum requirements. Consequently, the heat recovery problem is divided into two subsystems, above and below the Pinch.

The same information can be used for drawing the diagram *Grand Composite Curve* (Figure 10.1-right). Here the difference between the enthalpy of the hot and cold streams is plotted against a conventional shifted temperature scale. This representation identifies the possibilities of heat recovery by internal process/process exchange, as well as the optimal selection and placement of utilities.

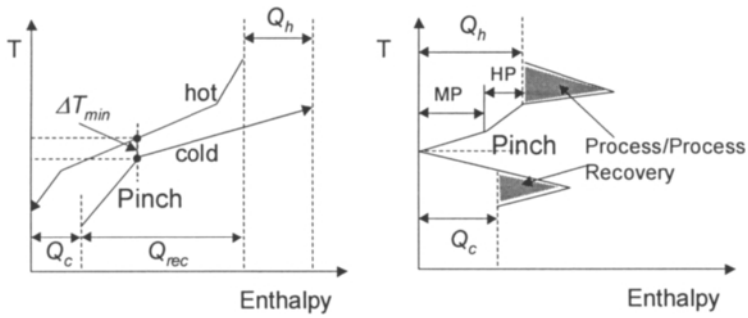

Figure 10.1 Composite Curves, Pinch Point, and Minimum Energy Requirements

Supertargeting

Energy costs increases roughly proportional with ΔT_{min}, while capital costs (heat exchangers) decrease more sharply than proportional (Fig. 10.2). S*upertargeting* consists of setting design targets for the whole process by an overall optimisation procedure well ahead the detailed sizing of heat exchangers.

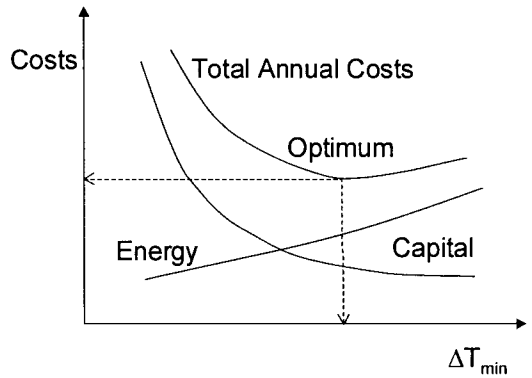

Figure 10.2 Targeting of energy and capital costs before HEN design

Grid Diagram

Grid diagram (Fig. 10.3) designates a working frame for developing the *Heat Exchanger Network* (HEN). The bubbled stick linking two streams in Fig. 10.3 symbolises a heat exchanger. The development of HEN is based on feasibility rules that form the *Pinch Design* method. HEN developed for MER is optimal when both energy and capital costs are considered. Additional reduction in capital costs may be obtained by removing small units. This operation might transfer heat across the Pinch, and as a results makes increase the total consumption of utilities.

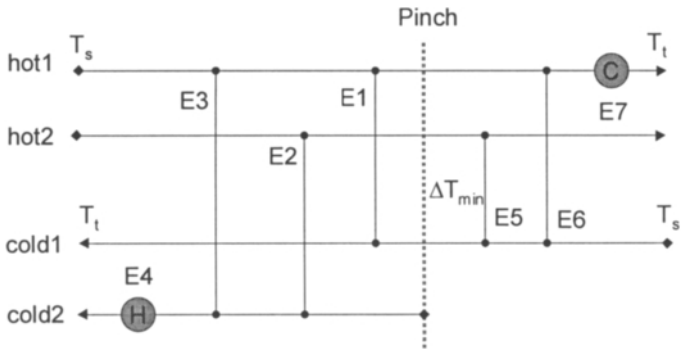

Figure 10.3 The Grid Diagram enables to develop the Heat Exchanger Network

Appropriate Placement

To ensure energy saving, the position of unit operations with respect to Pinch must respect the rules of the *Appropriate Placement*. For example, a heat engine has to be placed either above or below the Pinch, but not across it. Distillation columns should not be placed across the Pinch. Contrary, a heat pump is optimally placed across the Pinch. This subject will be discussed in more detail in the Chapter 11.

Plus/Minus Principle

The visualisation of heat exchange opportunities by the composite curves, combined with the rules of Appropriate Placement, can suggest changes in process design with significant effects on the energetic efficiency. In this way, Pinch Point Analysis becomes an empowering tool for Process Synthesis. *Plus/Minus principle* consists of some rules that can reduce the consumption of both hot and cold utilities. Figure 10.4 presents an example. Originally a distillation column is placed across the Pinch, the reboiler above, and the condenser below (dotted curves). Note that the reboiler is considered a cold stream! By lowering the pressure, the reboiler moves from above to below the Pinch. Thus, a cold stream is removed from above the Pinch (minus) and placed below (plus). Hence, a reduction in both hot and cold utilities is obtained. Consequently, the distillation column can run at zero net utility consumption, compared with the previous situation.

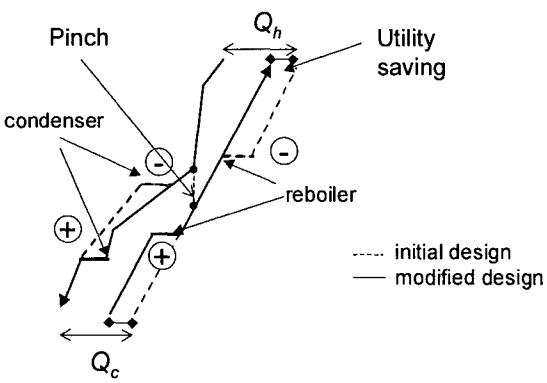

Figure 10.4 Plus/Minus principle

Balanced Composite Curves and Grid Diagram

Balanced composite curves are similar with those discussed above, with the difference that now the utilities are considered as streams. Since the utilities covers any imbalance between the streams selected for integration, the enthalpy balance is closed. Moreover, the design of the heat exchangers is done in the balanced grid diagram.

10.1.2 The overall approach

Pinch Point Analysis starts with the input of data. The first step is the extraction of *stream data* from a flowsheet simulation, which describes typically the material balance envelope (Reactors and Separators). Proper selection and treatment of streams by segmentation is a key factor for efficient heat integration. The next step is the selection of utilities. Additional information regards the partial heat transfer coefficients of the different streams and segments of streams, and of utilities, as well as the cost of utilities and the cost laws for heat exchangers.

After the input of data the next step is *targeting*, which consists of finding the optimal ΔT_{min} as a trade-off between energy and capital costs. On this basis targets for MER can be determined, as well as the overall heat exchange area and the number of units. If the economic data are not reliable, selecting a practical ΔT_{min} is recommended.

Then, the Appropriate Placement of unit operations is checked. This may suggest some design modifications by applying the Plus/Minus principle. Utility options are tested again. Capital costs are trade-off against energy costs. The procedure may imply iteration between targeting and process revision. Significant modifications could require reviewing the flowsheet simulation.

The iterative procedure is ended when no further improvement can be achieved. Note that during different steps of the above procedure the individual heat exchangers are never sized, although information about the heat transfer coefficients of participating streams are required. Only after completing the overall design targets the detailed sizing of the Heat Exchanger Network can take place. Optimisation can be used to refine the design. Then the final solution is checked by rigorous simulation.

Summing-up, Pinch Point Analysis consists of a systematic screening of maximum energy saving that can be obtained in a plant by internal process/process exchange, as well as the optimal use of the available utilities. The method is capable to assess optimal design targets for Heat Exchanger Network well ahead the detailed design of the equipment. Furthermore, PPA may suggest improvements in the original design that could enhance significantly the energetic performance of the process, from changes in the parameters of the operational units to structural modifications in the flowsheet.

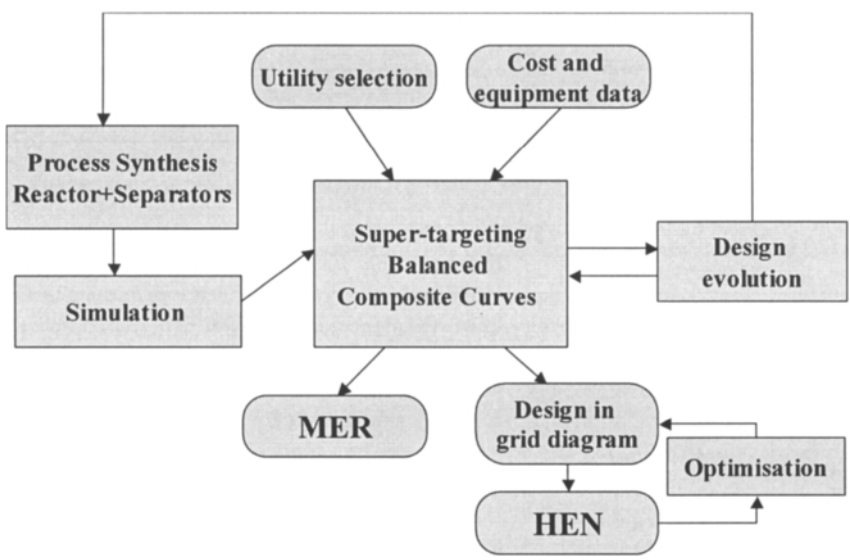

Figure 10.5 Overall approach in designing a Heat Exchanger Network by Pinch Point Analysis

10.2 TARGETS FOR ENERGY RECOVERY

10.2.1 Composite Curves

Stream data

Table 10.1 presents the stream data chosen to illustrate the construction of the Composite Curves. The following minimum elements are necessary:

- Stream or segment temperatures: supply T_s, and target T_t.
- Heat capacity of each stream or segment, defined as $CP=\Delta H/\Delta T$, where ΔH is the enthalpy variation over the temperature interval ΔT. Conversely, the enthalpy change of a stream segment is:

$$\Delta H = CP \times (T_t - T_s) \tag{10.1}$$

The hypothesis of constant CP is fundamental in PPA. If the enthalpy-temperature relation is not linear, then the stream must be 'segmented'. Note that in the relation (10.1) CP is in fact the term $F \times CP$ (mass flow rate by the mass heat capacity).

Table 10.1 Stream data for Composite Curves

Stream	Name	T_S °C	T_t °C	CP kW/C	ΔH kW
1	**hot1**	220	60	100	-16000
2	**hot2**	180	90	200	-18000
3	**cold1**	50	150	150	15000
4	**cold2**	130	180	400	20000
	Total				**1000**

The heat balance of the streams in the Table 10.1 shows an excess of 1000 kW. However, adding 1000 kW cold utility is not sufficient. The second law of Thermodynamics requires a minimum temperature difference between hot and cold streams. Consequently, the real energetic consumption is much higher.

Composite Curves

Composite Curve (CC) displays the cumulated enthalpy of all streams, hot or cold, available in a temperature interval between the extreme supply and targets temperatures. The formula to calculate the relation enthalpy-temperature is:

$$H = H_0 + \sum_i [\sum_j (CP_j)]_{i-1}^{i} \Delta T_i \tag{10.2}$$

CP_j's are the heat capacities of the active streams in the temperature interval ΔT_i. The value H_0 can shift the position of the composite curve. The partition in temperature intervals is based on the analysis of stream population. For the streams in Table 10.1, there are three intervals for the hot streams, and three for the cold streams (Fig. 10.6).

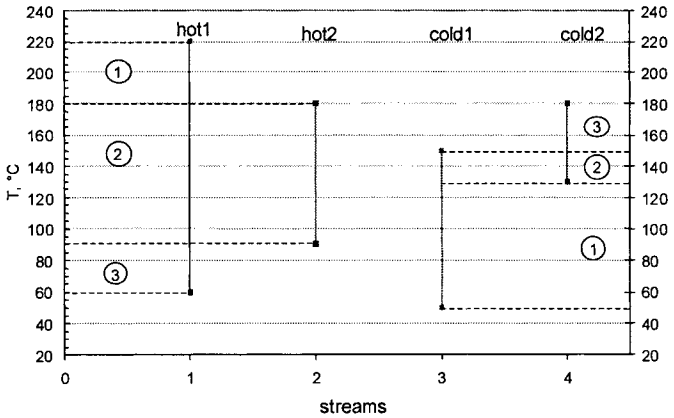

Figure 10.6 Temperature intervals of hot and cold streams

Figure 10.7 explains the graphical construction of the *hot Composite Curve*. The two streams, **hot1** and **hot2**, are represented by the segments ab and cd with CP_1=100 and CP_2=200 kW/°C, respectively. The total enthalpy variation is $\Delta H_h=\Delta H_1+\Delta H_2=$ 16000+18000=34000 kW. The interval between the target and supply temperatures is divided in three subintervals: 60-90, 90-180 and 180-220 °C. In each interval the overall *CP* can be obtained simply by adding the *CP*'s of the active streams. For instance, in the first and third interval there is only **hot1**, so that *CP*=100. In the second interval both **hot1** and **hot2** are active, therefore $CP=CP_1+CP_2$=300. Thus, each change in the slope of the composite curve corresponds to the entry or to the exit of a stream. Slope close to zero (horizontal position) means very high *CP*, as in the case of phase transitions.

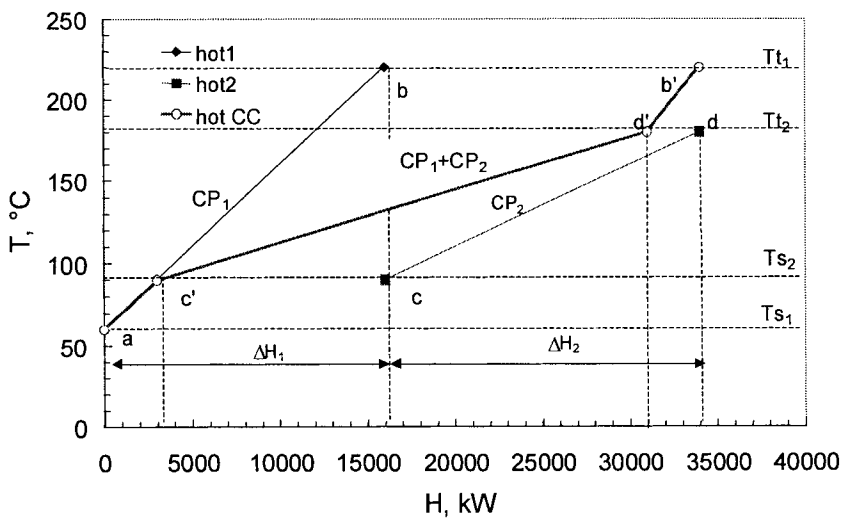

Figure 10.7 Construction of a hot Composite Curve

The same method can be applied to draw the *cold Composite Curve* (Fig. 10.8). There are three temperature intervals, 50-130, 130-150, and 150-180 °C, where CP_3=150, CP_3+CP_4=550 and CP_4=400. The enthalpy is ΔH_c=ΔH_3+ΔH_4= 15000+20000=35000 kW.

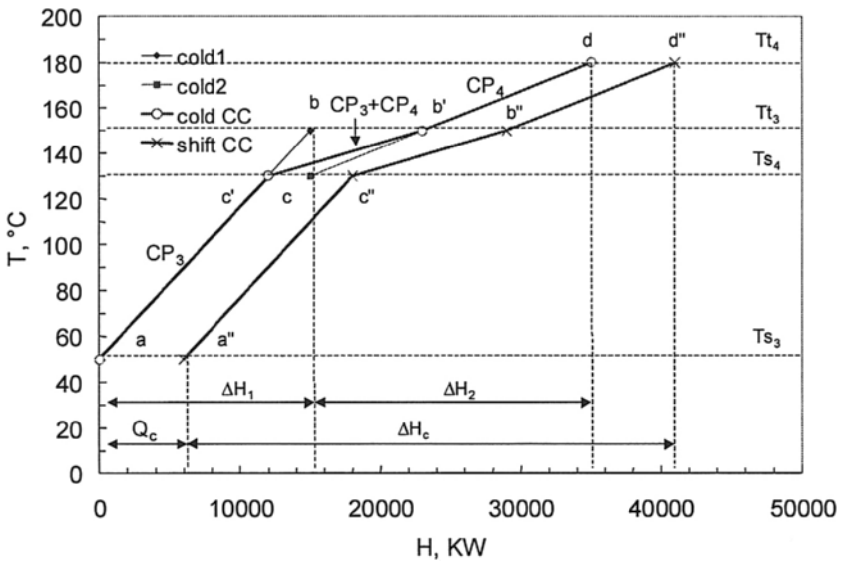

Figure 10.8 Construction of a cold Composite Curve

Both composite curves can be plot on the same diagram (Fig. 10.9). The hot CC may keep the original position. The cold CC shifts to the right by adding an amount of heat such to achieve ΔT_{min}. For ΔT_{min}= 10 °C Q_c= *6000* kW and Q_h=*7000* kW. The Pinch is situated between 130 and 140 °C.

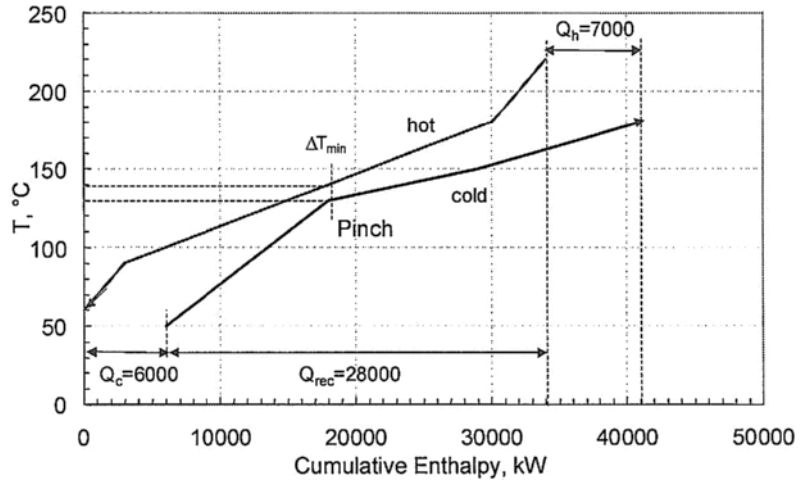

Figure 10.9 Composite Curves

In this way, the graphical representation has identified two fundamental elements of a heat integration problem:

1. Minimum temperature approach at Pinch, ΔT_{min}.
2. Minimum Energy Requirements (MER) as utility targets for heat recovery.

MER and ΔT_{min} are interdependent as illustrated in the Fig. 10.10. If ΔT_{min} is set to 15 °C, the hot CC keeps the same place, while the cold CC shifts to the right. One gets graphically Q_c=7500 and Q_h=8500 kW. The Pinch is located at 130-145 °C. Note that both utility requirements have increased with 1500 kW. In the first case the heat available for recovery was 28000 kW, while in the second case 26500 kW. Hence, increasing ΔT_{min} makes necessary more utilities and diminishes the energy saving.

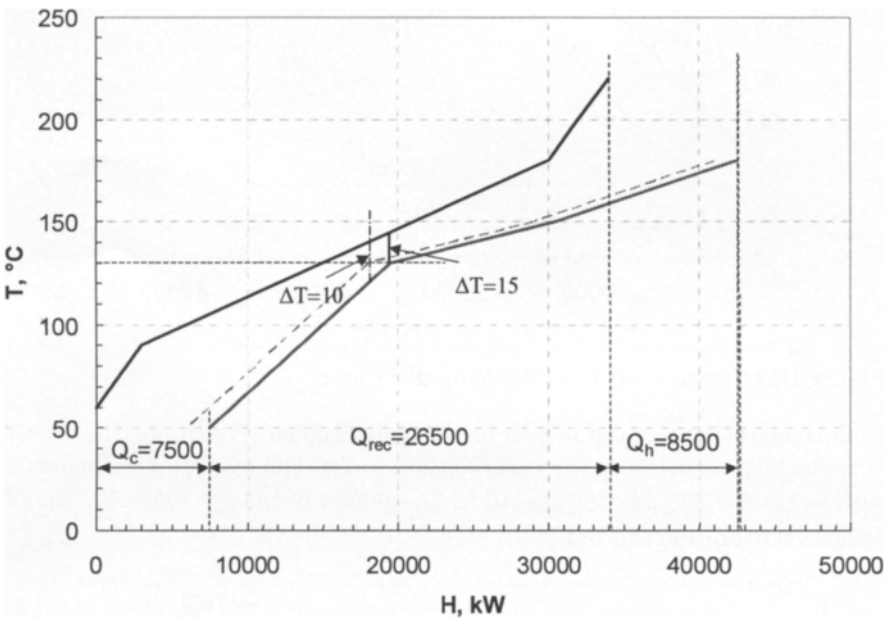

Figure 10.10 Shifting the composite curves modifies ΔT_{min} and utility targets

Problem Table algorithm

When investigating the heat integration between hot and cold streams available in a temperature interval, we must ensure that the driving force is at least equal with ΔT_{min}. Linnhoff and Flower (1978) solved elegantly this problem by means of a method designated by *Problem Table* algorithm.

Firstly, the temperature scale is modified such to accommodate a minimum driving force ΔT_{min} (Fig. 10.11). Hot streams are represented on the left scale. Cold streams are plotted on the right scale, where the temperature is shifted with ΔT_{min}, say by convenience with 10°C. Both hot and cold streams can be referred to *shifted temperature scale*, where the hot stream temperatures are moved down with $\Delta T_{min}/2$, and the cold stream temperatures shifted up with $\Delta T_{min}/2$.

Secondly, temperature intervals for heat integration are identified. In the above example, there are six temperature intervals. The first is delimited by the supply temperature of **hot1** (220 °C), as well as by the target temperature of **cold2** (180 °C). The shift temperatures are 215 °C and 185 °C, corresponding to an interval ΔT=30 °C. The next interval appears because of the entry of stream **hot2**. The shift temperature varies from 185 °C to 175 °C. The third interval corresponds to the exit of **cold1**, etc.

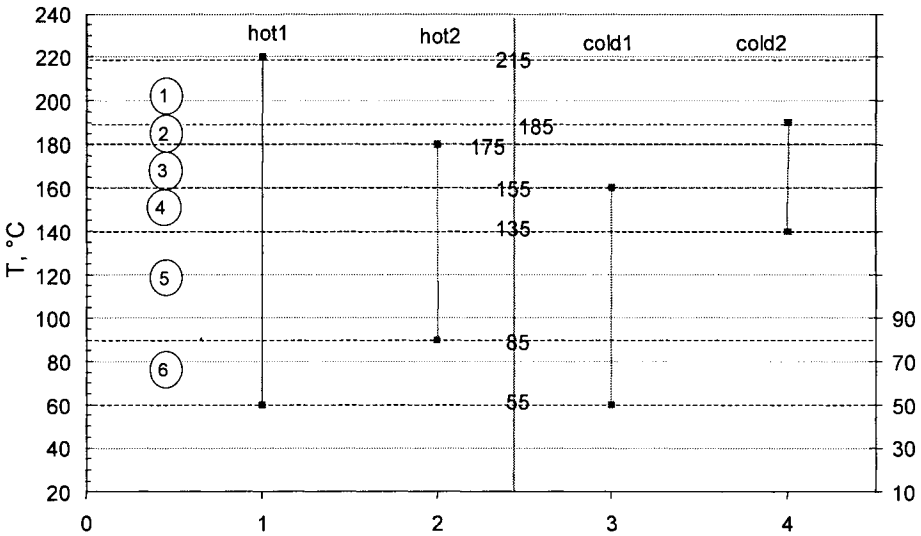

Figure 10.11 Shifted temperature scale

The next step is the set-up of the 'Problem Table'. Figure 10.12 gives a sample from an EXCEL™ workbook. The first three columns contain hot and cold stream temperatures, as well as shifted temperatures. Column four gives the temperature intervals. Column five gives the ΔT_{in}'s. Columns five to nine indicate the active streams necessary for CP calculation: zero for inactive streams, -1 for hot active streams, and 1 for cold active streams. This information can be related to the Table 10.1 for computing the CP's of each interval, as given in the column CP_{in}. Finally, the enthalpy variation of each interval is found by multiplying each CP by ΔT_{in}.

The last column gives a qualitative message: negative value signifies heat surplus, positive value means deficit. Excess heat can be removed by cold utility, while deficit heat can be covered by hot utility. Obviously, this approach would mean poor use of energy. Instead, we should try to combine the heat content of different temperature intervals. Thus, the deficit of cold streams can be covered with the surplus of the hot process streams, and only the unbalanced amount by hot utilities. Finally, this strategy allows the identification of the maximum recoverable energy by process-process heat exchange, and of the minimum amount of hot and cold utilities needed to cover the heat balance. It is important to note that the condition of a minimum temperature approach between coupled hot and cold streams must be fulfilled, but only in a restricted zone, of the Pinch. Far from the Pinch, the temperature difference could be larger than ΔT_{min}.

Thot	Shift T	Tcold	Interval	ΔT_{in}	CP_1	CP_2	CP_3	CP_4	CP_{int}	Delta H	Heat
220	215	210									
			1	30	-1	0	0	0	-100	-3000	surplus
190	185	180									
			2	10	-1	0	0	1	300	3000	deficit
180	175	170									
			3	20	-1	-1	0	1	100	2000	deficit
160	155	150									
			4	20	-1	-1	1	1	250	5000	deficit
140	135	130									
			5	50	-1	-1	1	0	-150	-7500	surplus
90	85	80									
			6	30	-1	0	1	0	50	1500	deficit
60	55	50									

Figure 10.12 Problem Table algorithm

The coupling of intervals can be found by organising the flow of heat in a cascade manner. In a first trial (Fig. 10.13-left) we assume that no heat is transferred from the hot utility. The first interval has an excess of 3000 kW that can be transferred to the second one, resulting in a net enthalpy flow of 0-(-3000)=3000 kW. The second interval has a deficit of 3000 kW, so that the net heat flow after this interval becomes zero. Consequently, the first and second intervals match perfectly each other. The third interval has a deficit of 2000 kW, and at its exit a net heat flow deficit of 2000 appears, which would increase at –7000 kW on the fourth interval. Clearly, a negative heat flow cannot be cascaded further. Therefore, this solution is not feasible.

In a second trial we may consider a hot utility load of 7000 kW that could compensate the deficit noted before. The result of cascading heat flow can be seen in the Figure 10.13 right. After the first interval the net heat flow is 7000-(-3000)=10000 kW. The second interval delivers 10000-3000=7000 kW. The cascade of heat flow goes on until the lowest interval is reached. As it can be seen, now all the net flows but one are positive. The location where the heat flow is zero is the *Pinch Point*! The shifted temperature is of 135 °C, or 130-140 °C expressed in real stream temperatures.

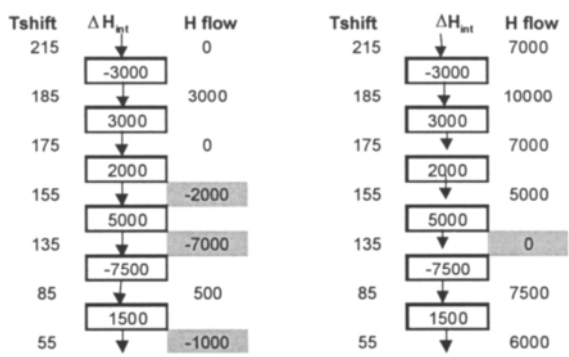

Figure 10.13 Cascade diagram

Grand Composite Curve

With the information issued from the Problem Table, we can draw the Grand Composite Curve (GCC). A composite curve is obtained by plotting the heat content of each temperature interval (x-axis) against shifted temperature scale (y-axis). As mentioned, the shifted temperature scale takes into account a difference of ΔT_{min} between hot and cold streams. Figure 10.14 presents *GCC* corresponding to the streams given in Table 10.1 for ΔT_{min}=10 °C. The following observations are of interest:

1. The Pinch Point divides the diagram in two regions, above and below the Pinch, in which the heat recovery problem can be analysed separately.
2. Above the Pinch there is need only for hot utilities. Below the Pinch only cold utilities must be used.
3. The 'pockets' of the grand composite curve designate possible heat recovery by process-process exchange.

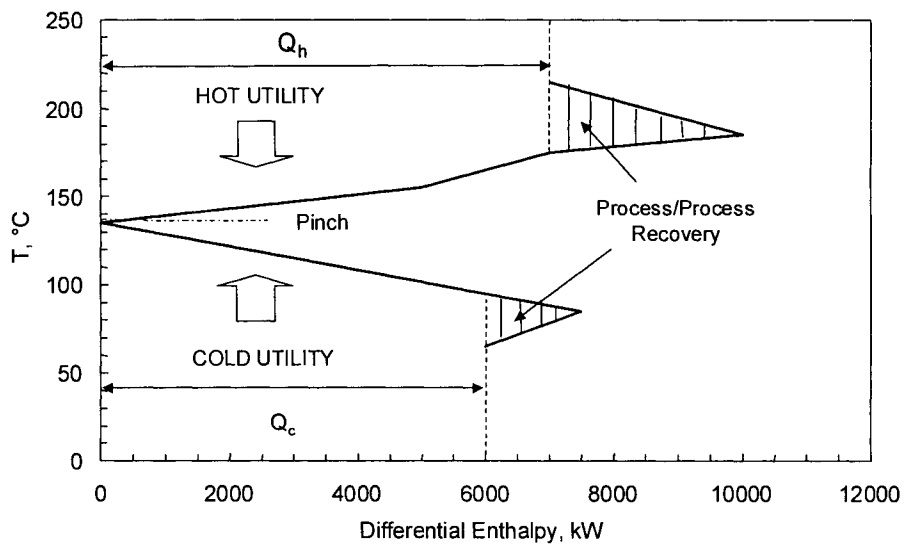

Figure 10.14 Grand Composite Curve

10.2.2 Pinch Point Principle

From the above example we learned that the Pinch separates the space of heat recovery into distinct regions, as represented in Fig. 10.15. The original problem is decomposed in two sub-problems, above and below the Pinch. Consequently, a *Pinch Point principle* can be formulated as follows (Linnhoff and Hindmarsh, 1982):

1. Do not transfer heat across the Pinch.
2. Do not use cold utility above the Pinch.
3. Do not use hot utility below the Pinch.

If there is heat flow across the Pinch, then the energy consumption is higher than minimum necessary. Both hot and cold utility consumption will increase with the same amount XP above the minimum targets. The Pinch equation is:

Actual Energy (A) = Target (T) + Cross-Pinch Energy flow (XP) (10.3)

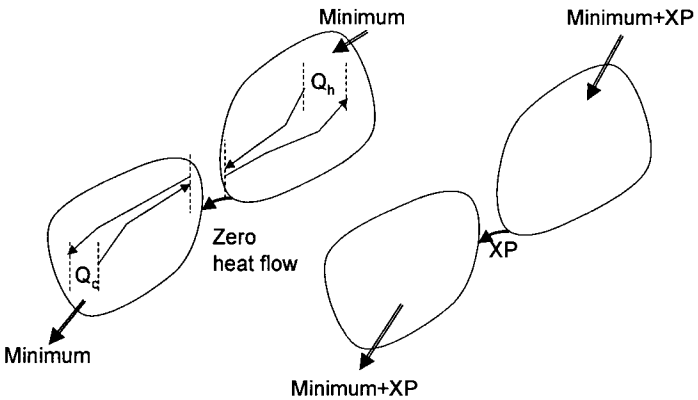

Figure 10.15 Pinch Point Principle

Thus, transferring heat across the Pinch is a double loss in energy. However, during the effective design of the heat exchanger network, the initial targets must be revised to accommodate constrains, as for example smaller number of units, or some imposed loads. The actual energy consumption could increase above the minimum targets, but the designer should try to keep the pinch violation as small as possible.

The temperature approach ΔT_{min} is a key variable in PPA. Recommended values are 10 to 20 °C in petrochemical industry, 20 °C in refining, but only 5 °C in cryogenics. More rigorously, ΔT_{min} can be determined by a *super-targeting* procedure, which performs an optimisation between the costs of utilities and of capital, as explained by the Fig. 10.2. Beside stream data, supplementary information is needed as:

- Type, temperature and costs of utilities.
- Partial heat transfer coefficients of streams (or of segments) and of utilities.
- Maximum heat transfer area of the heat exchangers.

As mentioned, because the energy targets increase linearly with ΔT_{min}, the cost of utilities follows the same trend. On the contrary, the capital cost decreases non-linearly with ΔT_{min}. Note that the cost function exhibits a jump when the number of units changes. Therefore, it is important to keep in mind that reduction in the number of units is by far more important for overall costs optimisation than the incremental reduction of heat transfer area.

10.2.3 Balanced Composite Curves

In balanced composite curves (Fig. 10.16) both utility and process streams are considered as usual streams. When more than one hot or cold utility is used, each

supplementary utility introduces a new pinch. Hence, we may have a main process Pinch and several utility Pinches. The selection of utilities may be guided by some heuristics. The simplest recommendations are:

1. Add heat at the lowest temperature level relative to the process Pinch.
2. Remove heat at the highest temperature level relative to the process Pinch.

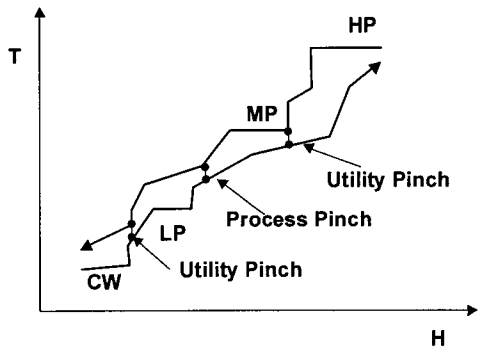

Figure 10.16 Balanced composite curves

10.2.4 Stream segmentation

The hypothesis of constant *CP* is the fundamental assumption in Pinch Point Analysis. In fact, the stream enthalpy is not strictly a linear function of temperature. This is particularly true for mixtures undergoing phase change. In this case we should decompose a *T-H* curve in segments of constant *CP*'s by an operation called *stream segmentation*. Let's examine the vaporisation/condensation of a pure component. We may define a virtual *CP* by considering a small temperature change, say 1 K (Fig. 10.17). Thus, the phase transition of a pure component stream may be represented by a (large) horizontal segment. In the case of a mixture we, can divide the stream in segments on which the *CP*'s are constant. Note that the segmentation has to be done always on the 'safe side', meaning that the segments should be placed below a hot stream, or above a cold stream (Fig. 10.18).

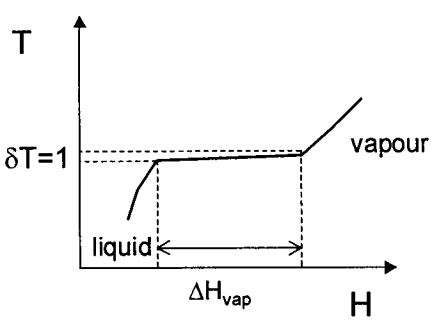

Figure 10.17 Phase transition

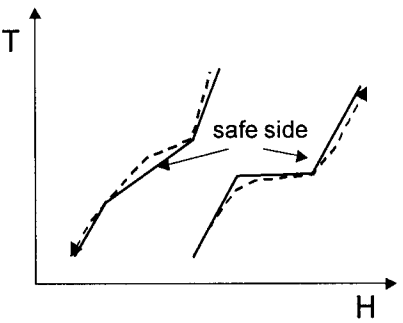

Figure 10.18 Stream segmentation

10.2.5 Data extraction

The selection of streams is determinant for efficient heat integration. Most of the studies are based on results issued from a process simulator. Automatic transfer of data to the Pinch software is a current feature of many simulation systems, commonly called 'data extraction', which sometimes is assisted by an expert system. However, the user should be aware about possible problems in heat integration caused by inappropriate stream extraction, even if it is computer-assisted. Hereafter some recommendations:

a. Check the accuracy of the thermodynamic model used for enthalpy calculation. Equations of state models often underestimate the enthalpy of phase transition.
b. Consider the plant decomposition in sections. The proximity of streams selected for integration is an important practical constraint. Furthermore, short path of the energy avoid time delays in control.
c. List carefully the process constraints. These must include controlled temperatures, as for example before reactors, separation flashes and distillation columns, for which heaters (furnaces) or coolers (refrigerant driven) are necessary. Some imposed heat exchangers may be eliminated from analysis.
d. 'Implicit' duties unimportant in simulation could become significant for heat integration, as those included in flashes.
e. Evaluate carefully the integration of chemical reactors, particularly for high exothermic reactions. Avoid the feedback of energy that might lead to multiple steady states and unstable behaviour.
f. In a first attempt do not consider the condensers and reboilers of the distillation columns, except if there is a particular incentive to save utilities by using process streams. These duties have a high energetic potential. However, the heat integration of separators with other process streams is limited by serious constraints on controllability. Use the plant or site utility system for such exchange.

10.2.6 Targets for energy and capital

As it was previously demonstrated, the Pinch Point principle enables to determine in a simple manner the load and cost of utilities for a given ΔT_{min}. These are minimum requirements that become targets in an energy saving project. The capital cost forms the other part of the targeting procedure. This is controlled by the following elements: equipment type, number of units, heat exchange area, number of shells, material of construction, pressure and pressure drop, piping and equipment layout.

Number of Heat Exchange Units

It can be demonstrated (see later in this chapter) that the number of the heat exchangers involving S streams, including utilities, is given by the simple relation:

$$N_U = S - 1 \tag{10.4}$$

If the Pinch is disregarded, then the above formula gives the total minimum number of units. For example for the streams given in the Table 10.1 we have N_U=(4+2)-1=5. If

the Pinch is considered, above the Pinch N_U=(3+1)-1=3, while below the Pinch N_U=(4+1)-1=4, in total 7 units. The difference is explained by the existence of two *loops*. The subchapter 10.3 will develop this topic.

Heat Exchange Area

Heat exchange area can be estimated from the balanced composite curves. The simplest is adopting the hypothesis of counter-current, as well as vertical heat transfer driving force. The total area $A_{1\text{-}1}$ is obtained by summing the differential heat-exchange area in different temperature intervals, as expressed by the relation:

$$A_{1-1} = \sum_{k}^{intervals} \frac{1}{\Delta T_{LMk}} \left(\sum_{i}^{hot} \frac{q_i}{h_i} + \sum_{j}^{cold} \frac{q_j}{h_j} \right) \tag{10.5}$$

In the above relation q_i or q_j are enthalpy variations over a temperature interval with a mean-logarithmic temperature difference ΔT_{LMk}. The notation h_i or h_j designates partial heat transfer coefficients, including fouling. Note that ΔT_{min} for process-utility heat exchangers may be different than for process-process heat exchangers.

Number of Shells

The number of shells can be determined simply by dividing the target of total area by the area of the selected type of heat exchanger. Shell-and-tube heat exchangers are sill the most used in process industries. The simplest is 1-1 type (1 shell pass, 1 tube pass), where the relation (10.5) is valid. There are situations when multi-pass heat exchangers are more advantageous, the most common being of type 1-2 (1 shell pass, 2 tube passes). The deviation from purely counter-current flow can be accounted for by means of the F_T factor. A practical value is F_T=0.9. Values lower than 0.75 should be avoided. The overall heat exchange area can be computed with the relation:

$$A_{1-2} = \sum_{k}^{intervals} \frac{1}{\Delta T_{LMk} F_{Tk}} \left(\sum_{i}^{hot} \frac{q_i}{h_i} + \sum_{j}^{cold} \frac{q_j}{h_j} \right) \tag{10.6}$$

The calculated area is increased by an oversizing factor of 10-20%. Then the number of shells can be found simply by knowing the area of single shell. The manufacture of shell-and-tubes heat exchangers is regulated by standards, the most known being the TEMA standards. Chapter 16 gives some guidelines.

Capital cost law

Simple cost law can be used to estimate the capital of a heat exchanger, such as:

$$Capital = A + B(Area)^{n} \tag{10.7}$$

The constants *A, B,* and *n* are function of the type of exchanger, pressure and material. The installed costs include insulation, piping and instrumentation. A usual assumption is that the network heat transfer area is divided evenly in a number of units, constrained by the

maximum shell area. Note that the capital costs must be aligned with the energy costs on annual basis. The simplest way is the assumption of a payback time, usually three years.

The above method gives reasonable results within 10% errors providing that the variation of the heat transfer coefficients is less than an order of magnitude (Smith, 1995). The search of preliminary targets can be summarised as follows:

1. Screen design options in conceptual design reflected in alternative material and energy balances.
2. Try different utility options with implications in both energy and capital costs.
3. Start preliminary process optimisation.

Thus, the targeting procedure makes possible a rapid estimation of energy and capital targets. This idea can be extended for designing a complete heat exchanger network by decomposing the plant in subsystems, where local integration may be applied (Polley & Heggs, 1999). The reduced number of streams leads finally to simple but reliable solutions, even if these might be considered as sub-optimal.

EXAMPLE 10.1 ΔT_{min} and minimum energy targets

Determine the optimal $\Delta T_{\min}$ and the targets for energy recovery with the streams listed in the Table 10.1. Consider as utilities cooling water at 20 °C and steam at 250 °C.

Solution.

1. Capital costs.

We use the values A=16000, B=3600, n=0.7 (Polley and Heggs, 1999), the cost being expressed in $/year. The area will be estimated as 1-1 shell-and-tube heat exchangers. We assume that the process streams have h_i of 0.5 kW/m^{2}K, plus 2.0 kW/m^{2}K for cooling water and 4 kW/m^{2}K for steam, all values including fouling resistances. Thermal effectiveness is 0.9. Maximum exchanger size is 500 m^2/shell. In addition we consider a payback time of 3 years and interest rate of 7.5%.

2. Utility costs.

The prices of utilities can be expressed on annual basis, for instance in $/(kWyear). From steam tables (Appendix F) at 250 °C the saturation pressure is 39.76 bar and the vaporisation enthalpy ΔH_v=1715.7kJ/kg. Consequently, the ton of steam has 1.716 GJ. The energy unit (kWyear) is equivalent with 1kJ/s×3600×8000= 28.8 GJ. Thus, the annual steam cost is 28.8/1.715=16.78×(cost of 1 ton steam). A price of 10 $/t gives 167.8 $/(kW year). This value might be compared with 0.0218 $/kWh=174.4 $/(kWyear) reported in reference. The price of water is 0.0015 $/kWh=12 $/(kWyear). However, in this example we consider the following prices: for steam 125 $/(kWyear), and for water 12.5 $(kWyear). Figure 10.19 presents the results of targeting obtained with SUPERTARGET™.

In this case the optimum ΔT_{min} is between 9 and 10 °C. The reader can check the values found for the energy targets, and verify that they increase linearly with $\Delta T_{min.}$ The capital costs decrease non-linearly.

This example gives the opportunity to draw some useful remarks:

- Targeting is sensitive to the cost data, particularly to the most expensive utility and to the exponent in the capital cost relation.
- In many cases when only area is variable the optimum is almost flat. Contrary, the objective function shows a sharp decrease by reducing the number of units.

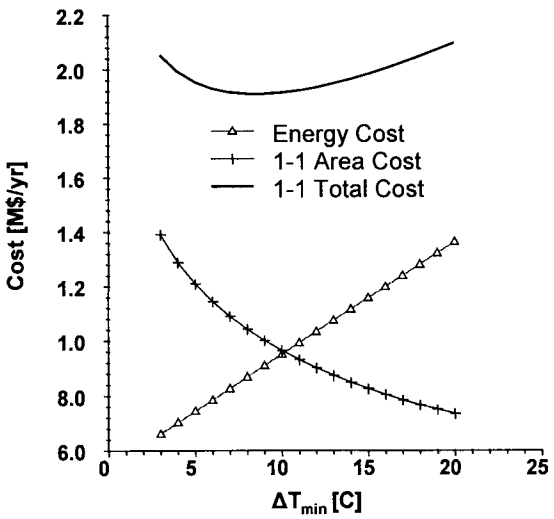

Figure 10.19 Targeting of ΔT_{min} by minimisation of capital and utility costs

10.3 PLACEMENT OF UTILITIES

This subchapter emphasises the advantage of selecting utilities well ahead the detailed design of heat exchangers. Again, a number of design decisions with great impact on the process economics can be taken at the targeting level.

10.3.1 Threshold problems

Not all heat recovery problems have a Pinch. Sometimes only hot or cold utility is required. Figure 10.20a illustrates a typical situation. Initially (right case), the analysis indicates a pinched problem with both hot and cold utilities. By lowering ΔT_{min} the cold composite curve shifts to the left up to a position where there is no need for hot utility. The value of ΔT_{min} when this situation occurs is called *threshold.* Lowering ΔT_{min} below the threshold leads to the need of a second cold utility, this time at the hot end. Similarly,

a problem with both hot and cold utility can turn into a problem that needs only hot utility below a threshold value of ΔT_{min} (Figure 10.20b). The above situations can be understood since utility requirements vary proportionally with ΔT_{min}. Hence, a problem apparently with both cold and hot utilities might hide a threshold problem.

Below the threshold ΔT_{min} the cost of energy remains constant. As a result, the trade-off between capital and energy can be considered only at ΔT_{min} values equal or above the threshold. Because the occurrence of utility at the opposite end increases the number of units, the probability of optimum near ΔT_{min} at threshold is more likely.

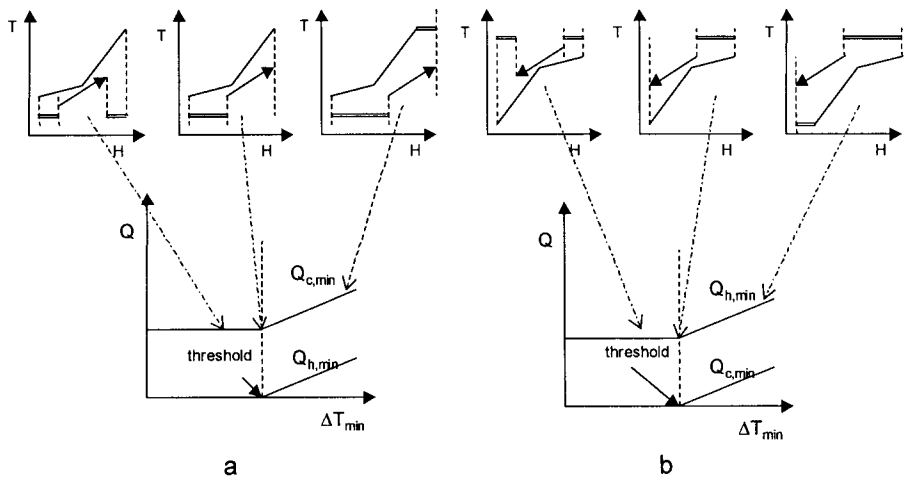

Figure 10.20 Threshold problems

Note that a threshold problem may turn into a pinch problem when multiple utilities are used. Figure 10.21 gives a graphical explanation. In Fig. 10.21 left the cold utility is covered by both cooling water (CW) and steam generation. A new utility Pinch occurs at steam-generation side. In Fig. 10.21 right, only hot utility is required. If the utility is covered by both high-pressure (HP) and low-pressure (LP) steam, then a new Pinch occurs at LP-process side. The only utility above this Pinch is HP steam. The design of HEN in a threshold problem keeps the same rules as for a normal pinch problem.

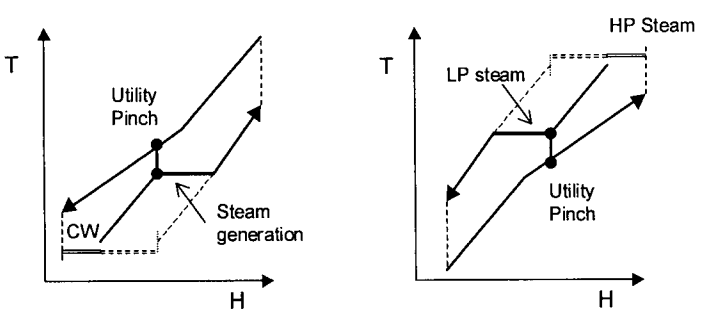

Figure 10.21 Threshold problem turned into a problem with utility Pinch

EXAMPLE 10.2 Threshold problem

Examine the targeting of the following streams:

	T_s, °C	T_t, °C	Duty, kW	*CP*, kW/°C	h_i, kW/m²K
hot1	220	60	16000	100	0.5
hot2	180	90	18000	200	0.5
cold1	40	150	38500	350	0.5

Utility and cost data are the same as for Example 10.1.

Solution. We use SUPERTARGET™ for targeting by varying ΔT_{min}. The plots indicate a threshold problem. Figure 10.22-left displays the utility consumption. Up to a $\Delta T^*_{min} = 20$, the threshold, there is no need for cold utility. Hot utility remains constant at 4500 kW. For $\Delta T > \Delta T^*_{min}$ a certain amount of cold utility is necessary, proportionally with the difference $\Delta T - \Delta T^*_{min}$. For example, for ΔT_{min}=25 °C Q_h=5000 kW and Q_c=500 kW, the difference remaining at 4500 kW.

Figure 10.22-right illustrates the costs of capital and energy, as well as the total cost. Capital cost is calculated as purely counter-current. Up to threshold both capital and energy costs are constant. There are three units: two process/process heat exchangers, plus a heater. After this point, a sudden increase in capital occurs due to a new unit, a cooler. From this point on, the problem is pinched. Capital cost decreases with ΔT_{min} because of larger driving force. Hence, it is advantageous to work below the threshold. HEN design will be solved in the Example 10.4.

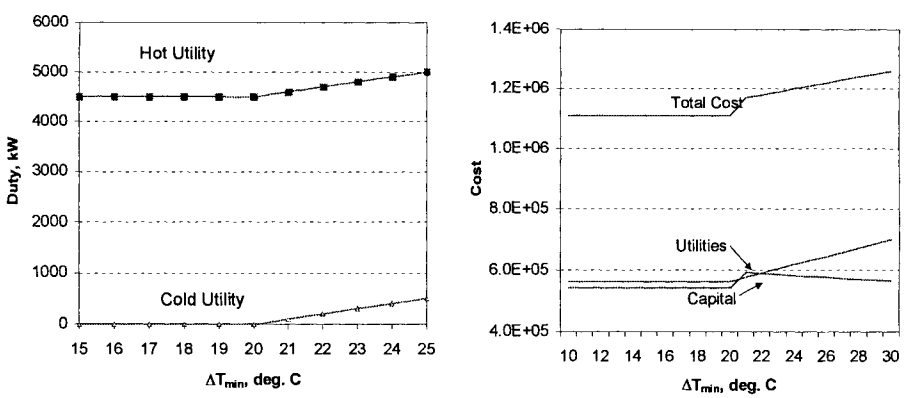

Figure 10.22 Targeting in the case of a threshold problem

10.3.2 Multiple utilities

Several hot or cold utilities may be used in a heat recovery project. GCC is the appropriate conceptual tool. Let's review the heat integration of the streams presented in Table 10.1. The same hot load as in Fig. 10.14 can be shared between two steam levels: high-pressure (HP) and low-pressure (LP) steam. In the GCC the solution is simple represented by horizontal segments placed at temperatures corresponding to their pressures, as in Fig. 10.23 for three steam levels. This feature makes possible to specify exactly the amount required by each utility. Simple targeting can be applied to optimise their amount if the prices are significantly different.

Similarly, the cold utility can be split into cold water and other cold utilities, as brine solution or refrigerant. Rising low-pressure steam is another possibility of cooling at temperatures above 100 °C! In this case, boiling feed water (BFW) is used to recover a part of energy by preheating. LP-steam can be upgraded at higher temperature by thermal compression. Each additional utility above the highest and coldest utilities introduces a new utility Pinch. A minimum temperature approach is required for each.

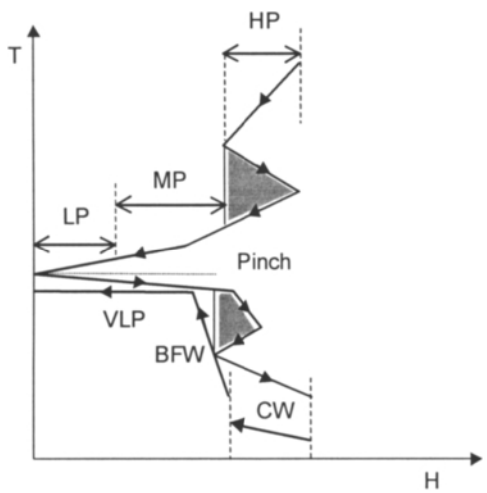

Figure 10.23 Multiple utilities

10.3.3 Variable temperature utilities

In this category we can consider flue gases, hot oil or other thermal fluids. The main problem is that the use of such utilities is more constrained with respect to the temperature level. Figure 10.24 illustrates two situations encountered when using flue gases for heating. Firstly, larger ΔT_{min} contribution utility-process must be assumed, say of 50 °C, because of poor heat transfer on the gas-side. Figure 10.24a presents the case when the constraint is the exit gas temperature. The graphical representation permits to visualise easily the stack losses. Increasing the theoretical flame temperature by air preheating or by low air excess can reduce the heat losses. Note that other factors as the Pinch can limit the flue gas temperature. This can be the process away from the Pinch,

as illustrated by the Fig. 10.24b, or the dew point of the acid components in the gas stack. As an exercise the user may examine the use of hot oil as thermal agent.

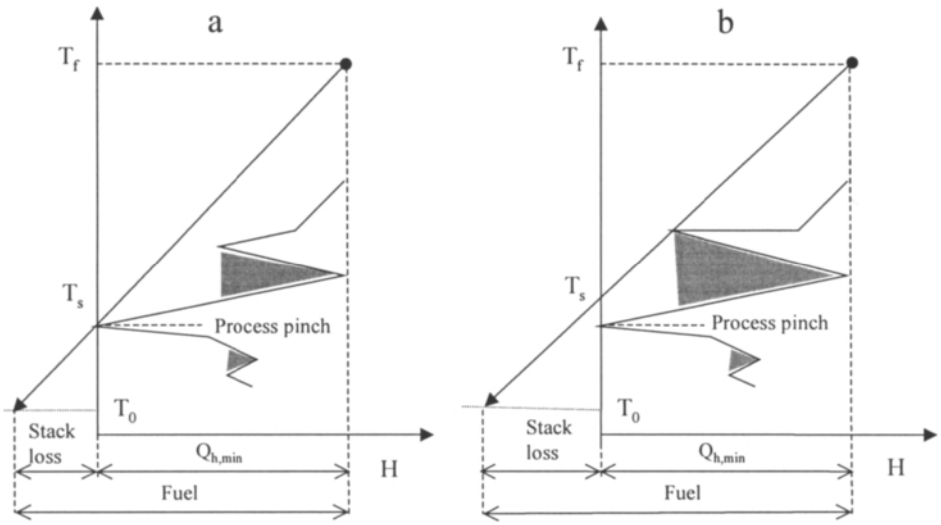

Figure 10.24 Flue gas as variable temperature utility. a) Constraint by process Pinch; b) limitations by a process away from the Pinch

10.4 DESIGN OF THE HEAT EXCHANGER NETWORK

The systematic procedure for designing the Heat Exchanger Network based on Pinch principle is designated as the *Pinch Design method* (Linnhoff et al., 1978, 1983). The methodology consists of the following steps:

1. Select streams for integration. Only streams useful for effective energy integration should be considered. Some simple rules could be mentioned:
   a. Examine the heat integration of reactors separately.
   b. In a first approximation do not consider reboilers and condensers.
   c. In the case of a larger flowsheet decompose the problem in subsystems, taking into account the proximity of streams.
2. Select utilities.
3. Estimate process/process saving and process/utility loads.
4. Construct Composite Curve and Grand Composite Curve. Identify process and utility pinches.
5. Determine targets for design: ΔT_{min}, Minimum Energy Requirements, number of units, capital and utility costs.
6. Construct the grid diagram.
7. Find the matches of heat exchangers by applying the rules of Pinch Design method.
8. Improve the design by eliminating small heat exchangers.

9. Optimise the Heat Exchanger Network.

The points 1 to 5 belong to the targeting procedure already presented. The points 6 to 9 form the core of the Pinch Design method that will be explained in the subsequent sub-chapters. Particularly the point 7 deserves more attention.

10.4.1 Topological analysis

Number of matches

It can be demonstrated that the minimum number of units (matches) N_E necessary to recover the energy between N_S process streams using N_U utilities is (Linnhoff, 1994):

$$N_E = N_S + N_U - 1 \tag{10.8}$$

If loops are presents in the network then the number of heat exchangers is given by the formula:

$$N_E = N_S + N_U - 1 + (\text{loops}) \tag{10.9}$$

Paths and Loops

The concepts of paths and loops are very useful for optimising a heat exchanger network. As noted, the application of the Pinch Design method generates redundancy in the number of units. Actually, reducing the number of heat exchangers can contribute more significantly in the cost saving than the incremental optimisation of the exchange area. Merging some units could violate the Pinch principle in the sense of increasing both hot and cold energy loads. In a number of cases an important reduction in capital may be obtained only with a marginal increase of energy above minimum requirements. This problem can be solved effectively by the approach explained below.

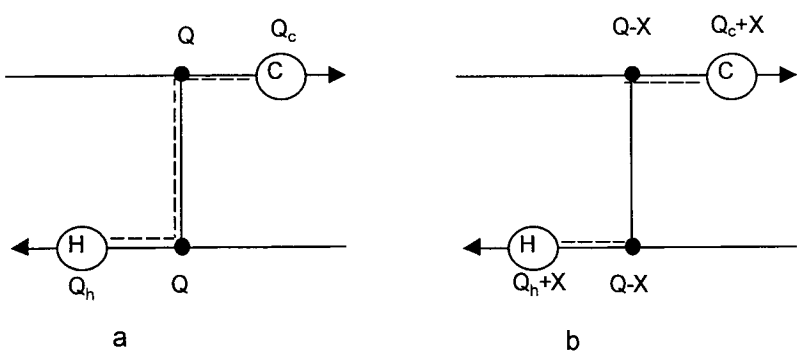

Figure 10.25 Concept of paths

Path means a physical connection through streams and heat exchangers for shifting energy between hot and cold utilities. Consequently, a path allows the modification of the temperature difference between the hot and cold streams. Figure 10.25 illustrates the idea. Initially the utility loads are Q_c and Q_h. In between there is a heat exchanger of duty Q_c (Fig. 10.25a). By rising Q_h with X units, the cold utility duty Q_c must rise

exactly with the same amount. Consequently, the heat exchanger duty becomes (*Q-X*), as in Fig. 10.25b. The outlet temperature of the hot side will decrease. The same happens with the outlet temperature of the cold side. Thus, the temperature differences at both ends are enlarged. Note that the heat exchangers outside the path are not affected, but well the utility heat exchangers.

Loop is a closed trajectory passing through several heat exchangers (Figure 10.26). Note that a loop can link several heat exchangers with the same utility. Changing a duty with X modifies the duties of the other exchangers with exactly the same amount, because conservation of energy. Setting the duty to zero eliminates the heat exchanger. The operation will change the temperatures of the units involved in the loop, and might lead to infeasible temperature profiles. Feasible ΔT can be restored if the loop is connected with both hot and cold utilities through a path. Example 10.4 will illustrate the approach, but after learning how to perform matches.

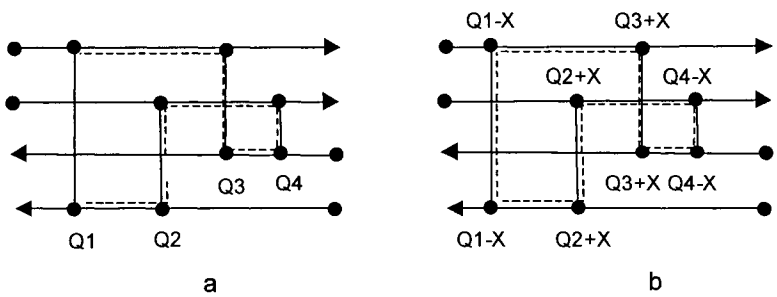

Figure 10.26 Concept of loops

10.4.2 HEN design in the grid diagram

The design of the Heat Exchanger Network takes place in the balanced grid diagram. This means that the utilities have been placed on the Grand Composite Curve. As illustrated by the Fig. 10.3, the hot streams run from left to right at the top, and cold streams run counter-currently at the bottom.

The Pinch split the diagram in two regions: above (at the left) and below (at the right) the Pinch. A vertical 'bubble headed' stick linking two streams represents a heat exchanger. Temperature and/or duty and area are also normally displayed.

The design starts at the Pinch, where the heat transfer is the most constrained. The match procedure has to respect some feasibility rules. Remember that in this context *CP* means (flowrate)x(specific heat capacity).

For a match above the Pinch, the following heuristic has to be respected:

$$CP_{hot} \leq CP_{cold} \tag{10.10}$$

Intuitively, the rule can be justified by the fact that above the Pinch there is need only for hot utility, such that the *CP*'s of cold streams must be greater than the *CP*'s of hot streams. A more accurate reason can be found in the fact that the temperature difference

(T_h-T_c) at the end looking to the Pinch is always smaller, at most equal to the temperature difference on the other side. It is also clear why the above rule is not so strict for a match away from the Pinch.

Similarly, below the Pinch the following heuristic holds:

$$CP_{hot} \geq CP_{cold} \tag{10.11}$$

Finally, the following relation can capture both heuristics:

$$CP_{in} \leq CP_{out} \tag{10.12}$$

Thus, for a match close to the Pinch, *CP* of the incoming stream must be smaller that the *CP* of the outgoing stream.

EXAMPLE 10.3 Heat Exchange Network design

Consider the streams given in the Table 10.1. Develop the Heat Exchanger Network in a grid diagram for Minimum Energy Requirements.

Solution. Figure 10.27 presents the grid diagram, on which stream supply and target temperatures, as well as the *CP*'s are marked. In Example 10.2 the Pinch was located at 130-140 °C for ΔT_{min}= 10 °C. We recall that the heat loads of streams were:

hot1	ΔH_1=100×(220-60)=16000	**hot2**	ΔH_2=200× (180-90)=18000
cold1	ΔH_3=150× (50-150)=-15000	**cold2**	ΔH_4=400× (130-180)=-20000

The targeting procedure found Q_h=7000 and Q_c=-6000 units. The process-process heat exchange can recover a maximum of 28000 units.

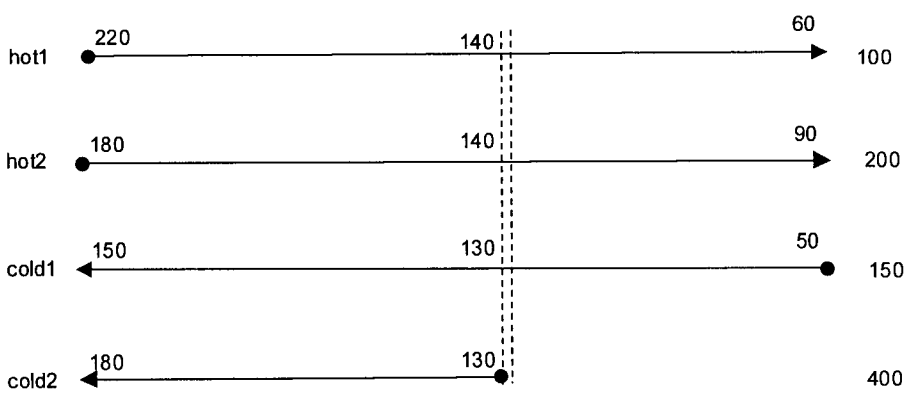

Figure 10.27 Grid diagram for Example 10.3

a. Region above the Pinch.

Figure 10.28 illustrates the approach. The investigation begins near the Pinch, keeping in mind the rule $CP_h \leq CP_c$. Matches that could tick-off streams completely are preferred. Let's consider firstly the streams **hot1** and **cold1**. The match rule is fulfilled. Moreover, the stream **cold1** is completely recovered. Hence, the first match **E1** looks as follows:

E1	*CP*	*T'*	*T''*	ΔT_{stream}	Duty
Hot side	100	170	140	30	3000
Cold side	150	150	130	20	3000
ΔT		20	10		

Note that at the cold-end facing the Pinch, $\Delta T''=\Delta T_{min}=10$ °C, while at the hot-end the temperature approach is sensible larger. Similarly, we can take the second match **E2** as **hot2/cold2**, because $CP_h=200 < CP_c=400$. Again, the whole stream **hot2** is recovered. Because duty is $Q_2=400\times(150-130)=8000$ units, the exit temperature of **hot2** is 140 °C. The third match takes the remaining of **hot1** with **cold2**. *CP* rule is respected, $CP_h=100 < CP_c=400$. Heat balance gives $Q_3=100\times(220-170)=400\times(162.5-150)=5000$ units. Because this match is far from Pinch, the temperature approach is larger than ΔT_{min} at the both ends. Finally, to close the heat balance we must place a heater on the stream **cold2**. The total enthalpy is $\Delta H_4=400\times(180-130)=20000$, and the heater load becomes $Q_4=20000-(8000+5000)=7000$ units. Summing up, there are four units above the Pinch.

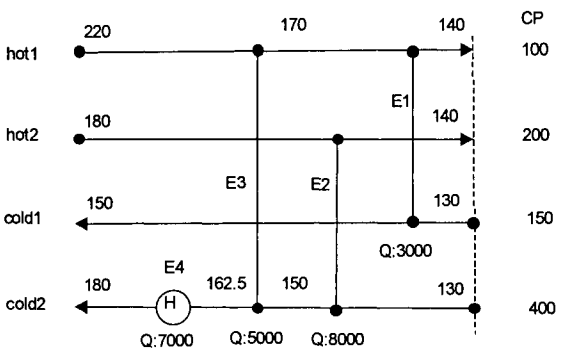

Figure 10.28 HEN above the Pinch

b. Region below the Pinch

The graphical construction of the network is given in Fig. 10.29. As before, we start at Pinch by keeping in mind that this time the matching rule is $CP_c \leq CP_h$. Firstly, we try to tick-off the stream **hot1**. The only available stream is **cold1**. Unfortunately, in this case the feasibility rule is not respected, because $CP_c=150 > CP_h=100$. Therefore, we have to consider the other stream **hot2**. Now $CP_c=150 < CP_h=200$, the match is feasible. We may tick-off the residual load of the stream **hot2**, such the match duty becomes 10000. The heat balance of **E5** is $Q_5=200\times$ (140-90)=150× (130-63.3)=10000.

The remaining 2000 units of **cold1** can be matched against **hot1** in **E6**, even if the *CP* rule is not respected. This is because the previous match has lowered the temperature of the cold outlet corresponding to the hot inlet (located at Pinch). For this heat exchanger the heat balance is Q_6=100×(140-120)=150×(63.3-50)=2000.
Finally, the residual load of **hot1** is rejected to the cooler **E7** with the duty Q_7=6000 units. Note that the placement of the cooler may create another alternative, by exchanging the place with **E6**. This choice may be motivated by technological reasons. In this case the cooler Q_7 could be coupled with a closed-loop heating system using pressurised water that could work between 70 and 130 °C.

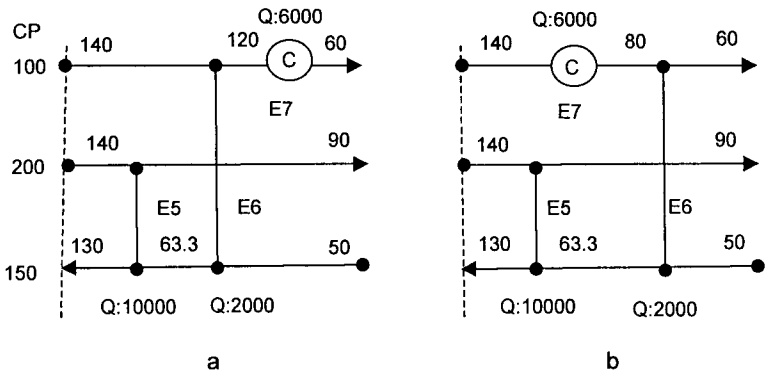

Figure 10.29 HEN below the Pinch

The Heat Exchanger Network assembling the subsystems is given in Fig. 10.30. This HEN corresponds to the maximum energy recovery thermodynamically possible for a given ΔT_{min}. However, this is not the most economical network, if the costs of both energy and heat exchangers are taken into account. The network can be further reduced.

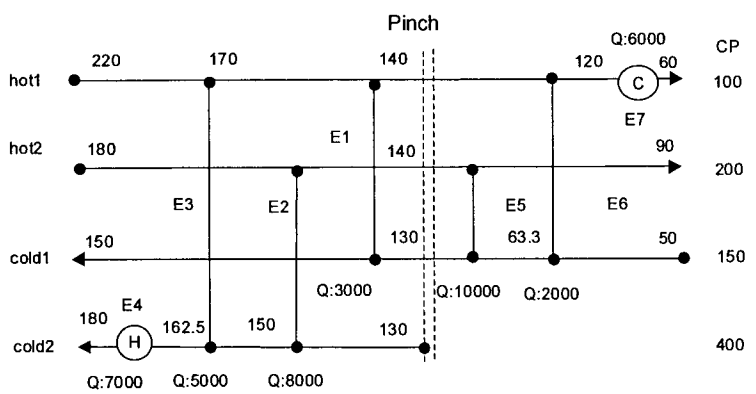

Figure 10.30 Overall Heat Exchanger Network (alternative 1)

Note that the solution is not unique. Figure 10.32 presents another alternative. Consider that the match **E5** (below the Pinch) involving **cold1** and **hot2** has a duty of only 4000. The remaining enthalpy of **cold1** is taken-off completely against **hot1** in the unit **E6**. Note that for this match the *CP* rule is not respected, since *CP1* < *CP2*. This is possible if the hot end is far from the Pinch. The remaining part of **hot2** is finally cooled in **E7**. The cooler **E7** moves from the stream **hot1** to the stream **hot2**. The change in temperatures can be read on the figure.

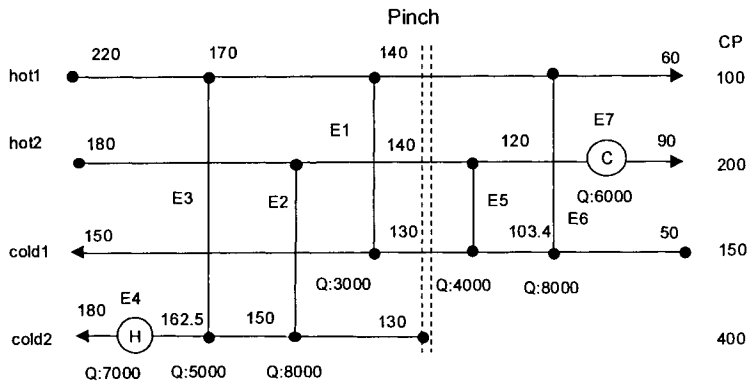

Figure 10.31 Overall Heat Exchanger Network (alternative 2)

10.4.3 Stream splitting

By stream splitting we can find practical solutions for cases where, apparently, the matches at Pinch are not feasible because the rules for *CP*'s do not hold. Some common situations are depicted in Figs. 10.32. The following explanations address the subsystem above the Pinch. Two situations will be examined:

a) The number of hot streams smaller than the number of cold streams.
In Fig. 10.32a-left there are two hot streams against one cold streams. Whatever *CP*'s might be, there are not sufficient cold streams, because above the Pinch we cannot use cold utility. Thus, in addition to *CP*'s rule a 'count rule' regarding the pairing of streams at Pinch must be satisfied. Above the Pinch, this rule is:

$$N_{hot} \leq N_{cold} \tag{10.13}$$

By splitting the cold stream in two segments two matches become possible. Moreover, the split must be done such to respect the CP's rule, as in Fig. 10.32a-right.

b) Count rule is satisfied, but not the *CP*'s rule.
Figure 10.32b-left illustrates this situation by one hot stream and two cold streams. The hot stream must be split in two parts such as the *CP*'s of hot streams becomes smaller than *CP*'s of the corresponding cold streams, as in the Fig. 10.32b-right.

It may appear also that the 'count rule' is satisfied, but the *CP*'s rule fulfilled only partially. In this case the largest cold stream should be split.

The analysis can be extended below the Pinch, where the 'count rule' becomes:

$$N_{cold} \leq N_{hot} \tag{10.14}$$

Considering that the hot and cold streams are *in* and *out* respectively, we may formulate the 'count rule' more generally as:

$$N_{out} \leq N_{in} \tag{10.15}$$

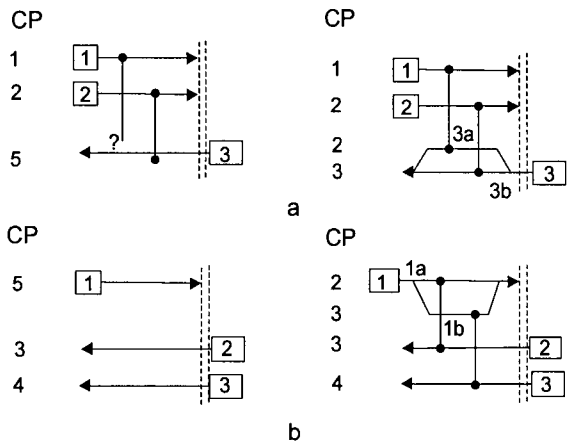

Figure 10.32 Principle of stream splitting at Pinch

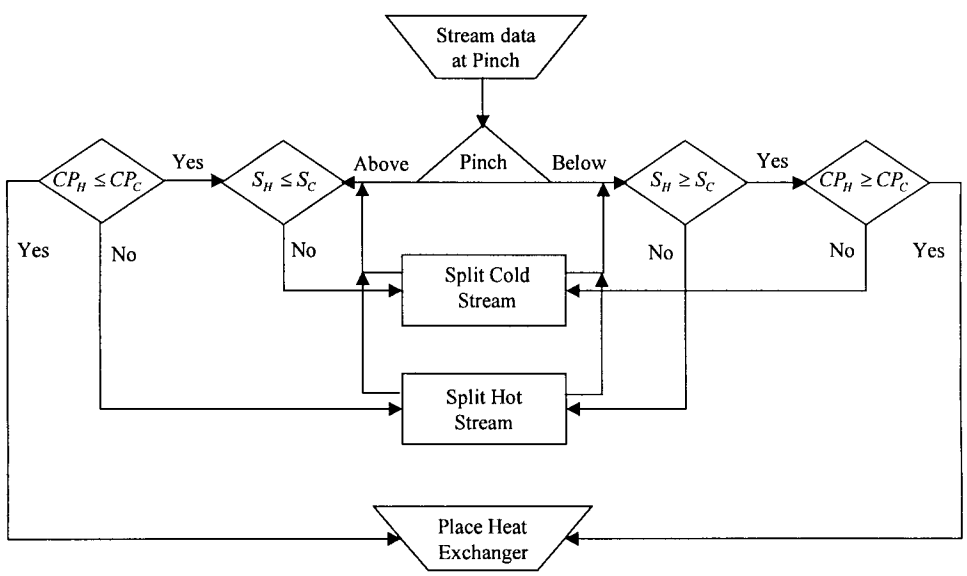

Figure 10.33 General HEN design procedure at Pinch

The above rules can be put together into a general design procedure at Pinch, as illustrated by the Fig. 10.33. Firstly, the stream count rule is checked. If not fulfilled, a first stream split is performed to balance streams, cold stream above the Pinch, or hot stream below the Pinch. Then the *CP*'s rule is checked for matches close to the Pinch. If not fulfilled, again stream splitting is executed, this time opposite to the first. Note that the above rules might be not respected away from Pinch.

EXAMPLE 10.4 Stream splitting

Develop a heat exchanger network for the streams given in the Example 10.2.

Solution. Figure 10.34 presents the grid diagram. We notice that there is only a cold stream, but three hot streams including the hot utility. There is no process Pinch. However, we may consider a utility Pinch on the cold side. In this case we select ΔT_{min} =15 °C, a lower value that the threshold of 20 °C, as calculated in the Example 10.2. Hence, we are at the left of the cold utility Pinch.

We may apply the same design method by starting with the matches at Pinch. The *CP* rule is respected, because the *CP*'s of the **hot1** and **hot2** streams entering the Pinch are smaller than the *CP* of the **cold1** leaving the Pinch. However, the stream count gives a problem: there are not enough cold streams. Because two hot streams, we need at least one cold stream more. The stream **cold1** should be split in two branches proportionally with the duty of streams **hot1** and **hot2** used for matching. Hence, the split fractions are 16/34 and 18/34 respectively. After matching, a mixer is necessary to recompose the stream **cold1**. Figure 10.34 presents the matches, with three units, as predicted by the topological analysis.

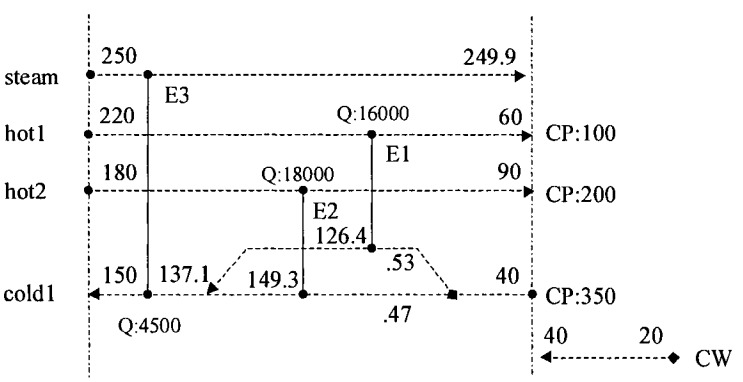

Figure 10.34 Example 10.4: streams and matches

10.4.4 Reducing the HEN

The synthesis of the heat exchanger network for Minimum Energy Requirements ensures the best energy recovery from thermodynamic point of view. However, taking into account the cost of heat exchangers could change the analysis substantially. The decomposition of the system in subsystem increases the number of units above those required by the first law analysis. The difference is given by the loops crossing the Pinch. Further reduction is paid by increasing both heating and cooling requirements. The trade-off depends on the costs of energy and of hardware in a particular situation. As a rule of thumb, the following two heuristics are recommended:

1. Break firstly the loop including the smallest heat exchanger.
2. Remove the unit with the smallest load in a loop.

The explanation is that the capital reduction for small units is by far more important for the same incremental area than for large units. For small heat exchangers the contribution of the fixed capital term, which accounts for installation, instrumentation, control, supervising and maintenance costs, can largely overcome the cost of area.

EXAMPLE 10.5 Reduction of the Heat Exchanger Network

The maximum energy recovery network found in the Example 10.3 has seven heat exchangers. First law analysis indicates a minimum number of five units because of four streams and two utilities. Two units could be removed. Identify the loops and redesign the network for ΔT_{min} =10 °C.

Solution. The original network is presented in Fig. 10.35. The smallest unit **E6** has a duty of 2000. Visual inspection can identify a loop passing through the units **E1** and **E6**. The next step is to suppress the unit **E6** by shifting its load to **E1**. The unit **E1** becomes **E1a**, its duty going from 3000 to 5000. This operation keeps constant the enthalpy balance of the streams **hot1** and **cold1**, but modifies the temperatures.

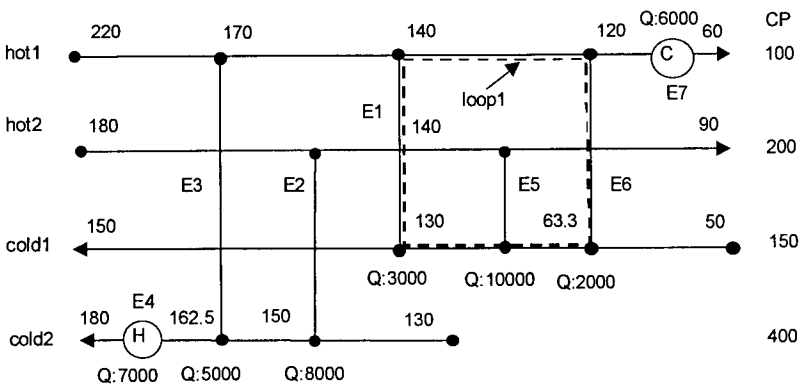

Figure 10.35 Network with minimum energy requirements

Figure 10.36 shows the situation after breaking the first loop. A simple heat balance around **E1** shows that the exit temperature of **hot1** changes from 140 to 120 °C, while the inlet temperature of **cold1** passes from 120 to 116.7 °C. The approach temperature at the cold-end becomes 3.3 °C, thus smaller than 10 °C. Restoring ΔT_{min} can be achieved by increasing simultaneously the utility loads, as depicted in Fig. 10.37. Indeed, there is a path linking the cooler **E7** with the heater **E4** through **E3**. It may be observed that by adding a duty of 1000 to **E7** will restore the exit temperature of **E1a** to 130 °C, while the temperature of the cold side remains unchanged. In this way a value of ΔT larger than 10 °C is achieved, such the match is feasible. Note that the duty of **E3** has been reduced with 1000, while the inlet temperature of **E3** passed from 162.5 to 160 °C. Hence, the reduction of a unit has been paid by reducing the amount of recovered energy by (1000/27000) ×100=3.7%.

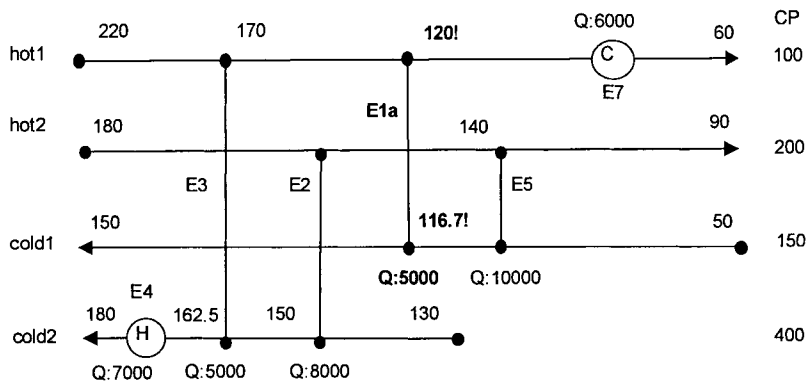

Figure 10.36 Breaking the first loop

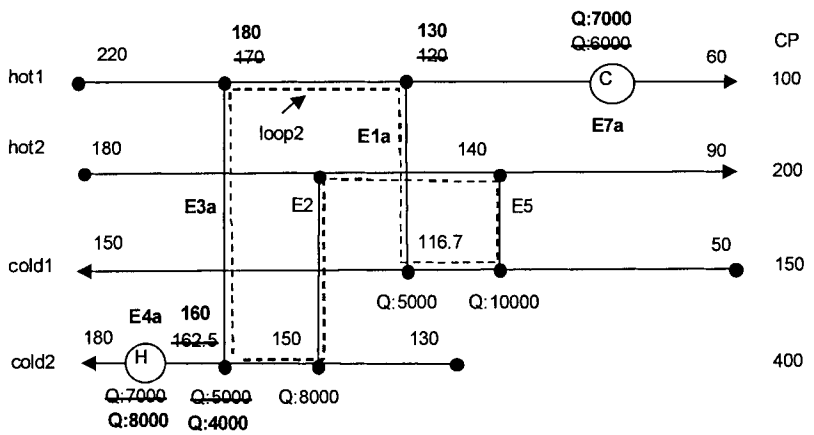

Figure 10.37 Restoring the temperature difference

The smallest unit is now the **E3a**. This is involved in a loop passing through the units **E3a-E1a-E5-E2**. We may combine **E3a** with **E1a**. Figure 10.38 shows the new temperatures after this operation. Note that the units **E2** and **E5** became **E2a** and **E5a**, because changed duties. The reader can check that the enthalpy balance is conserved. It may be seen that an infeasible temperature difference appeared at the cold-end of **E2a**, such as ΔT became –10 °C! For restoring it an increase in utilities is needed. It is easy to see that a supplementary load of 4000 will restore ΔT of **E2a** at 10 °C. Figure 10.39 displays the final network. There are now three process/process heat exchangers of loads 5000, 8000 and 10000, in total 23000 units. The utility consumption is 11000 units for cooling and 12000 units for heating. Hence, the loss in heat recovery is (4000/27000) ×100=14.8%.

As an exercise the user is encouraged to reduce the alternative 2 from Fig. 10.31. The final result is a HEN with 5 units, **E2**=8000, **E3**=1000, **E5**=15000, Q_c=10000 and Q_h=11000, with a ΔT_{min}=10 °C in E2.

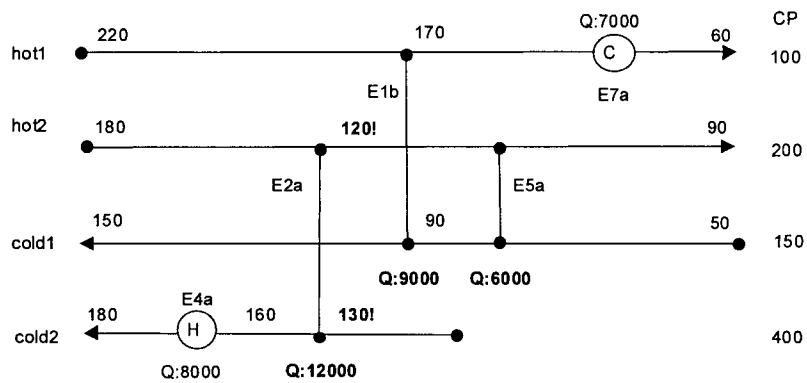

Figure 10.38 Breaking the second loop

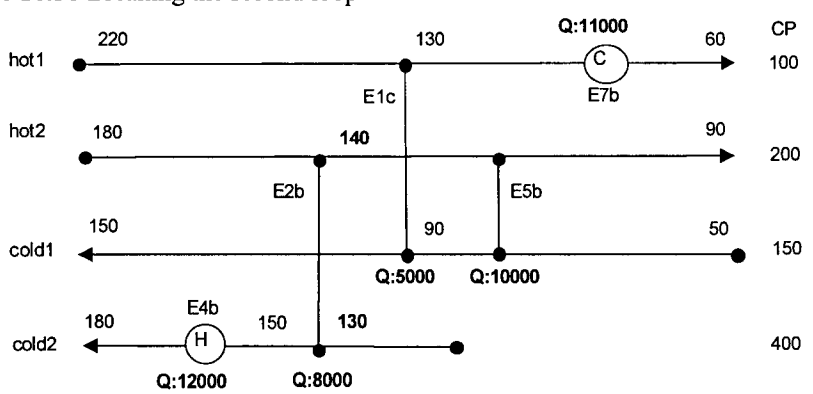

Figure 10.39 Final network with the minimum number of units

10.4.5 Network optimisation

As explained, the Pinch Design method generates a network with a certain degree of redundancy. The reduction of units can contribute to major saving in capital costs. However, more energy is necessary to inject into the network to restore infeasible driving forces. This task can be treated elegantly by optimisation.

Another application is the split of streams at Pinch in order to fulfil the feasibility criteria of matches. Some insights can be obtained from the grid diagram. However, the exact split fraction is a typical optimisation problem. The same is valid for splitting streams far from Pinch. Note that bypasses of streams around heat exchangers can be used for temperature control.

The above description shows that optimisation is a powerful method in handling the design of a heat exchangers network. Because the whole approach is founded on a linear enthalpy-temperature relation, the problem can be solved by Linear Programming (LP). The optimisation is essentially a parametric one, because the network structure is not affected. If the streams involved in matches are not longer constraint by the *CP*'s rule, as for matches away from the Pinch, then the optimisation becomes structural, and the problem is of type Mixed Integer Linear Programming (MINLP).

Optimisation is also a powerful manner for designing networks submitted to constraints. Usually these can be duties, inlet/outlet temperatures, area, heat transfer coefficients, and split and bypass fractions of streams. The approach is particularly powerful for revamping existing networks, where the number of old exchangers is by far larger than the new units to be inserted.

EXAMPLE 10.6 Network optimisation

Optimise the network for minimum energy requirements developed in Example 10.3 as Alternative 1 with data from the Example 10.1. The objective function is the total annual cost of both energy and capital.

Solution.

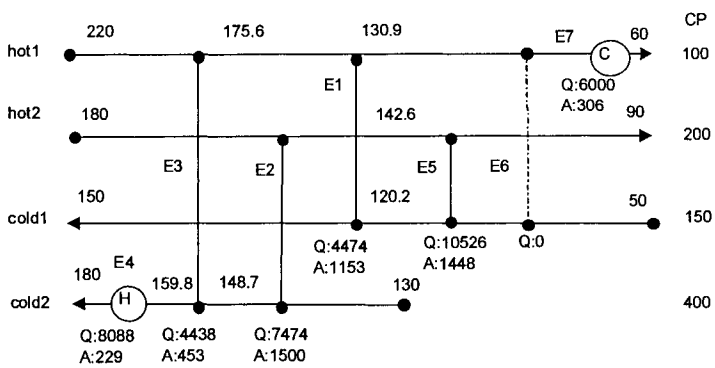

Figure 10.40 Optimised network for the Example 10.5

The heat exchanger area can be calculated in the hypothesis of counter-current 1-2 heat exchangers, as expressed by the relation 10.6. Then the cost of capital can be computed by considering a cost law. The number of shells is found straightforward by assuming a maximum area per unit of 500 m^2. The optimisation variable is the minimum temperature approach.

Figure 10.41 displays the optimised HEN found by using the design software SUPERTARGET™. A reduction in cost of about 10% is possible with respect of the MER network for ΔT_{min}=10 °C, but with the penalty of increasing the utility consumption with 15%. The reduction in total cost is explained by lower capital obtained by eliminating the heat exchanger **E6**. Note that ΔT_{min} is practically the same at 10.7 °C, but shifted between 130.7 and 120.2 °C.

10.5 MATHEMATICAL PROGRAMMING

Generally speaking, Mathematical Programming represents a class of alternative techniques that can be employed to solve energy saving problems. Numerous researches have been devoted to this subject. A good introduction in this area can be fund in the Chapter 16 of he book written by Biegler, Grossmann, and Westerberg (1998). He distinguished between *sequential* and *simultaneous* approaches.

The *sequential method* makes possible the development of partial optimised networks that satisfy one of the criteria among minimum utility, minimum investment or minimum number of units. Note that the solution of the minimum utilities may be seen analogue with the *transhipment problem* in linear programming (LP). Hot streams can be regarded as sources and cold streams as destinations. The heat can be transferred from sources to destinations through some intermediates exchange places, where a ΔT_{min} driving force must be ensured. This is equivalent with temperature intervals in the Problem Table algorithm, as it was formulated in the subchapter 10.2. The energy starts to flow from the hot utility source. The excess energy that cannot be transferred to cold streams can be cascaded at lower temperature intervals, and finally, to the cold utility. The result is a fully targeting of the recovery problem, as it was developed in section 10.3, where a Pinch can be clearly defined. Further, the problem can be extended to take into account physical matches by means of a Mixed Integer Linear Programming (MILP) algorithm. It is important to note that the solution may be not unique. There might be several networks for the same cost of utility and hardware. Conversely, the same network may have different distributions of heat loads if loops are present. It is worthy that the method can treat directly forbidden or imposed matches.

In the *simultaneous method* an existing superstructure is optimised rigorously by a Mixed Integer Non-linear Programming (MINLP). The modelling is based on a stage-wise build-up of the superstructure for each temperature interval. Within each stage potential heat exchange between any pair of hot and cold streams may take place. Accordingly, each stream is split and directed to match all cold streams, and reciprocally. In a first approximation the outlets of the exchangers are well mixed.

These are also optimisation variables. The number of stages can be put equal to the temperature intervals. Finding the number of matches is similar with the extended transhipment model. However, the constraint of the Pinch can be removed easier, and by consequence, leading to networks that minimise simultaneously units, capital and energy. Other structural features, as steam splitting and bypassing, can be considered.

In the past, Pinch Analysis and Mathematical Programming have been seen often as opposite. They are in fact highly complementary. Pinch Analysis remains an invaluable systematic investigation method, solidly anchored in Thermodynamics and based on simple intuitive graphical tools. It offers a step-wise global picture of the problem to be solved, suggest intermediate solutions, and therefore stimulate greatly the creativity. On the other hand, when the computations become tedious or excessive, the use of an automatic algorithmic tool is highly desirable. Hence, embedding Mathematical Programming into packages based on Pinch Point Analysis is the most efficient way to solve conceptual design problems in the field of energy saving.

10.6 DESIGN EVOLUTION

The most radical way to obtain substantial energy saving is to review the basic process design, namely the material balance envelope given by Reactor and Separators. Conversely, energy saving projects should also seen as an opportunity to bring important changes to the original process, from the revamp of some units to the debottlenecking of the whole plant.

Replacing the reactor is a hard decision, unlikely in an energy saving project. However, changing the reactor's parameters, particularly the temperature, might be possible when new operation mode can be envisaged, as for example switching on a new catalyst. Increasing the operating temperature of reactors is better for energy integration, particularly in the case of exothermal reactions.

The next important step is the revision of the distillation trains, above all the duties of reboilers and condensers, as well as the pressures and temperatures in top and bottoms. A simple list of these variables can identify possible thermal couplings between reboilers and condensers. If the thermal coupling is possible, the direct integration in the frame of a more complex distillation device should also be checked.

It should be keept in mind that only energy saving is never the ultimate goal. In fact, any process change should be investigated as a trade-off of both energy and capital costs. From a practical viewpoint, the targeting of subsystems based on the proximity principle can lead rapidly to a good integration that can be finally optimised without excessive effort. The last but not the least, the solution of a heat integration problem must always be examined from the point of view of operability and controllability.

There are two theoretical principles to consider in bringing conceptual changes with energy saving impact: *Appropriate Placement* and *Plus/Minus Principle* (Linnhoff et al., 1982, 1994). The first ensures an optimal use of energy provided that the placement of the unit operations in with respect to Pinch respects some rules. Chapter 11 will

present this topic in more detail. The second is based on the examination of the composite curves, and will be briefly comment here.

Plus/Minus principle states that a reduction in the utility requirements can be obtained if the following actions are taken (Smith, 1995):

- Increase the total hot stream load above the Pinch.
- Increase the total cold stream load below the Pinch.
- Decrease the total cold stream heat duty above the Pinch.
- Decrease the total hot stream heat duty below the Pinch.

An example has been given in the introductory part (Fig. 10.6). Figure 10.41 presents another example. A cold stream is removed from the region above the Pinch and placed below the Pinch. The shape of the cold composite changes accordingly. By removing a hot stream, the hot utility diminishes, and by exactly the same amount the cold utility load. Similarly, by moving a hot stream from the region below to above the Pinch reduces the cold utility load, and as a result the hot utility consumption. We may generalise the above observation as a generic heuristic in energy integration:

- Shift hot streams from below above the Pinch.
- Shift cold stream from above to below the Pinch.

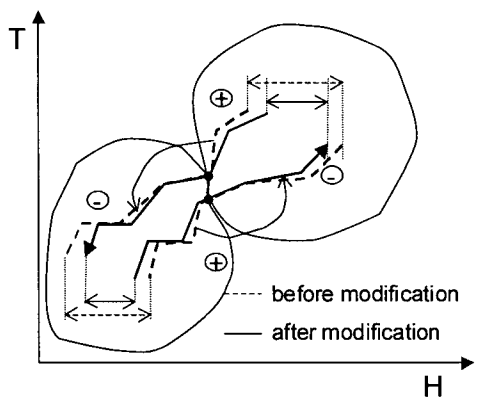

Figure 10.41 The use of Plus/Minus principle for energy saving

10.7 EXTENSIONS OF THE PINCH PRINCIPLE

By analogy with the energy saving, the Pinch concept has been extended to the treatment of other valuable resources in process industries as water, hydrogen or solvents. Saving process water is one of the most important issues in industry. Much more efficient use of water can be achieved by recycling it to the places for which is sufficiently clean, and not send it to the wastewater re-treatment. How to handle this in a systematic manner can be investigated by a method analogue to the thermal Pinch. The systematic investigation of wastewater management by Water Pinch has been

started with the paper of Wang & Smith (1994) and continued since with other co-workers. Similar with temperature-enthalpy composite curves, composite concentration curves can be built having as co-ordinate the concentration in contaminant versus the mass of contaminant (Fig. 10.42 left). The slope of each segment is inverse proportional with the stream flow rate; steeper slope means lower water flow rate. By taking into account the variation of contaminant in all the process streams, the water Pinch can be located. The slope of the line passing through this Pinch allows the identification of a minimum feasible overall water flow needed to supply the system (Fig. 10.42 right), which becomes a target for design. In this way the saving in process water can be precisely quantified. The water Pinch method has been developed to a mature technology that can be applied to industrial problems, namely by combination with MILP optimisation methods.

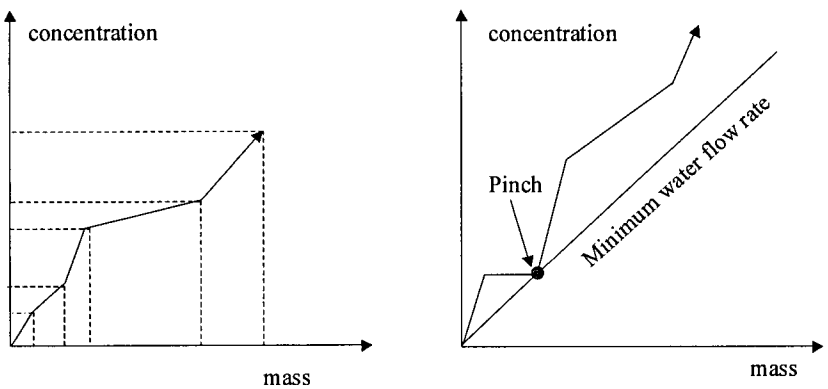

Figure 10.42 Water Pinch principle: concentration composite curve (left), targeting water consumption (right)

Another important application of the Pinch concept is the hydrogen management in refineries. Again, recycling hydrogen of convenient purity instead of high-purity hydrogen, can lead to important saving. The problem has been addressed recently by Towler et al. (1996) by means of Hydrogen Pinch.

The above examples suggest that mass-exchange operations could be treated by Pinch-modelling. However, unlike thermal Pinch, where the temperature is a general measure of the energy content, the identification of a unique measure of mass-exchange is difficult, because of large dimensionality of the problem. A general approach has been proposed by El-Halwagi and Manousiouthakis (1989) by means of the Mass Exchange Network concept, but its application in engineering calculations is difficult. However, practical solutions can be found in situations where lumping of components is possible, as in wastewater or emissions. These topics are developed in by El-Halwagi (1997) in this book over Process Integration in solving environmental problems.

The waste minimisation can take profit from Pinch Point Analysis. This issue is not mentioned here, but the reader can found more information in specialised works, as in

the series of articles of Petela and Smith (1991-92), as well as in the book written by Smith (1995).

However, the application of Pinch principle for optimising mass exchange networks cannot be so powerful as in heat integration, because of higher dimensionality of the problem in term of chemical species. On the contrary, this area is an example where optimisation techniques are more suitable, particularly of mixed integer non-linear programming (MINLP) type. The number of structural alternatives is rather limited by problem definition itself, whereas the number of streams and of components can be very large. In addition, a global optimisation can handle better the optimisation of costs of different operations and equipment involved in the mass exchange network. An example of such approach for waste minimisation has been published by Papalexandri, Pistikopoulos and Floudas (1994).

10.8 SUMMARY OF PINCH POINT ANALYSIS

1. Pinch Point Analysis is a systematic process design methodology consisting of a number of concepts and techniques that ensure an optimal use of energy. The Pinch is characterised by a minimum temperature difference ΔT_{min} between hot and cold streams, and designates the location where the heat recovery is the most constraint.
2. The fundamental computational tool is the Problem Table algorithm. This tool allows the identifications of the Pinch, as well as of targets for hot and cold utilities.
3. The net heat flow across Pinch is zero. Consequently, the system can be split into two stand-alone subsystems, above and below the Pinch. Above the Pinch there is need only for hot utility, while below the Pinch only cold utility is necessary. For given ΔT_{min} the hot and cold utility consumption identified so far becomes Minimum Energy Requirements (MER). No design can achieve MER if there is a cross-pinch heat transfer.
4. The partition of the original problem in subsystems may introduce redundancy in the number of heat exchangers. When the capital cost is high, it might be necessary to remove the Pinch constraint in order to reduce the number of units. The operation will be paid by supplementary energetic consumption, which has to be optimised against the reduction in capital costs. The result is that heat recovery problem becomes an optimisation of both energy and capital costs, constraint by a minimum temperature approach in designing the heat exchangers.
5. Stream selection and data extraction are essential in Pinch Analysis for effective heat integration.
6. The key computational assumption in Pinch Point Analysis is constant CP on the interval where the streams are matched. If not, stream segmentation is necessary.
7. The counter-current heat flow of the streams selected for integration may be represented by means of Composite Curves (CC). Another diagram, Grand Composite Curve (GCC) allows the visualisation of the excess heat between hot and cold streams. against temperature intervals. This feature helps the selection and placement of utilities, as well as the identification of the potential process/process matches.

8. The synthesis of a Heat Exchanger Network consists of three main activities:
   a. Targeting. Set a reference basis for energy integration, namely:
      - Minimum Energy Requirements (MER).
      - Utility selection and their placement.
      - Number of units and heat exchange area.
      - Cost of energy and hardware at MER.
   b. Synthesis of heat exchanger network (HEN) for minimum energy requirements and maximum heat recovery. Determine matches in subsystems and generate alternatives.
   c. Network optimisation. Reduce redundant elements, as small heat exchangers, or small split streams. Find the trade-off between utility consumption, heat exchange area and number of units. Consider constraints.
9. The improvement of design can be realised by Appropriate Placement and Plus/Minus principle. Appropriate Placement defines the optimal location of individual units against the Pinch. It applies to heat engines, heat pumps, distillation columns, evaporators, furnaces, and to any other unit operation that can be represented in terms of heat sources and sinks.
10. The Plus/Minus principle helps to detect major flowsheet modifications that can improve significantly the energy recovery. Navigating between Appropriate Placement, Plus/Minus Principle and Targeting allows the designer to formulate near-optimum targets for the heat exchanger network, without ever sizing heat exchangers.
11. Pinch Point principle has been extended to operations involving mass exchange. Saving water can be treated systematically by Water Pinch methodology. Similarly, the inventory of hydrogen in refineries can be efficiently handled by Hydrogen Pinch. Other applications of industrial interest have been developed in the field of waste and emissions minimisation. The systematic methods in handling the integration of mass-exchange operations are still in development. In this area the methods based on optimisation techniques are very promising.

10.9 REFERENCES

Biegler, L., I. E. Grossmann, A. Westerberg, 1998, Systematic Methods of Chemical Process Design, Prentice Hall

Duran, M. A., I. E. Grossmann, 1986, Simultaneous optimisation and heat integration of chemical processes, AIChEJ, 32, 123

Floudas, C. A., A. R. Ciric, I. E. Grossmann, 1986, Automatic synthesis of optimum heat exchanger network configuration, AIChEJ, 32, 276

El-Halwagi M. M., V. Manousiouthakis, 1989, Synthesis of mass exchange networks, AIChEJ, 35 (8), 1233-1244

El-Halwagi M. M., 1997, Pollution prevention through Process Integration. Systematic design tools, Academic Press

Linnhoff, B., B. Hindmarsh, 1983, The Pinch design method of heat exchanger networks, Chem. Engng. Sci., 38, 745

Linnhoff, B., D. W. Townsend, D. Boland, G. F. Hewitt, B. Thomas, A. R. Guy, R. H. Marsland, 1982 (1th edition), 1994 (2th edition), User Guide on Process Integration for the Efficient Use of Energy, The Institution of Chemical Engineers, UK

Linnhoff, B., 1993, Pinch Analysis. A-state-of-the-art overview, Trans. Inst. Chem. Eng., September, 501-522

Linnhoff, B., J. R. Flower, 1978, Synthesis of heat exchanger networks: Part I: Systematic generation of energy optimal networks, AIChEJ, 24(4), p. 633-642. Part II: Evolutionary generation of networks with various criteria of optimality, AIChEJ, 24(4), 642-654

Papalexandri, K. P., E. N. Pistikopoulos, A. Floudas, Mass exchange networks for waste minimisation, 1994, Trans IChemE, vol. 72, Part A, May, 279-294

Polley, G. T., P. J. Heggs, 1999, Don't let the Pinch pinch you, Chem. Eng. Progress, December, 27-36

Smith R., 1995, Chemical Process Design, McGraw-Hill

Smith, R., E. A. Petela, 1991-1992, Waste minimisation in process industries, The Chemical Engineer (UK), ibid. 1. The problem, 24-25, Oct. 1991, ibid. 2. Reactors. 17-23, Dec. 1991, ibid 3. Separation and recycle systems, 24-28 Febr. 1992, ibid 4. Process operations, 21-23, April 1992, ibid 5. Utility waste, 32-35, July, 1992

Towler, G. P., R. Mann, A. J. Serriere, C. M. D. Gabaude, 1996, Refinery hydrogen management: cost analysis of chemically-integrated facilities, Ind. Eng. Chem. Res., 35 (78), 2378-2388

Wang, Y. P., R. Smith, 1994, Wastewater minimisation, Chem. Eng. Sci., vol. 49, 981-1006

Chapter 11

PRACTICAL ENERGY INTEGRATION

11.1 Heat and Power Integration
- 11.1.1 Heat engines
- 11.1.2 Combined Heat and Power (Cogeneration)
- 11.1.3 Heat pumps
- 11.1.4 Refrigeration cycles

11.2 Distillation systems
- 11.2.1 Single columns
- 11.2.2 Heat pumps driven systems
- 11.2.3 Heat integrated columns
- 11.2.4 Thermally coupled columns

11.3 The integration of chemical reactors

11.4 Total Site integration

11.5 Summary

11.6 References

After the theoretical principles of Pinch Point Analysis this chapter continues with some major applications. We will develop the idea that the energetic performance of a unit operation in a process depends not only on its performance as stand-alone piece of equipment, but also upon the interactions with the other units.

The optimal behaviour of a unit operation in the context of a process can be formalised by means of the concept of *Appropriate Placement*. This concept consists of some rules regarding the position of a unit operation with respect to Pinch. In the subsequent sections we will analyse this topic for some major unit operations. A first section will be devoted to the integration of heat pumps and heat engines. An important issue is the combined production of heat and power. Then, we will present energy saving techniques for stand-alone and integrated distillation columns. In the case of high exothermal reactions the heat integration of chemical reactors offers good opportunities for supplying most of the energy needed in the plant or/and exporting the excess. The last topic is the concept of site integration, namely the optimisation of utilities and refrigeration loads.

11.1 HEAT AND POWER INTEGRATION

11.1.1 Heat engines

Thermodynamic background

A heat engine makes use of thermal energy to produce mechanical energy, designated usually as *shaft work*. Steam and gas turbines are the most important applications of heat engines in process industries.

Heat engine is a device that takes an amount of heat Q_1 from a source at the temperature T_1 and produces an amount of work W by rejecting an amount of heat Q_2 to a sink at the temperature T_2. The first law of thermodynamics states that the mechanical work delivered is simply:

$$W = Q_1 - Q_2 \tag{11.1}$$

In practice a heat engine operates in a cycle between a heat source and a heat sink. The second law states that the conversion of heat into work is never 100%. The maximum yield is achieved in a *Carnot reversible cycle* that consists of two adiabatic and two isothermal transformations. For such cycle the amount of work W produced from the heat source Q_1 is:

$$W = \eta_C Q_1 \tag{11.2}$$

The thermal efficiency η_C depends only of the absolute temperatures of the hot source and cold sink, as described by the simple relation (see Chapter 5):

$$\eta_C = 1 - T_2 / T_1 \tag{11.3}$$

More generally, the overall efficiency of a heat engine is:

$$\eta = W / Q_1 \tag{11.4}$$

Because of various losses the real efficiency is much lower than the real one, $\eta \leq \eta_c$.

For describing applications involving steam turbines the *Rankine cycle* is suitable, as represented in Fig. 11.1 in a *T-S* diagram. Initially, the hot source produces superheated steam at P_1-T_1 (point 1) submitted to expansion to produce shaft work. With appropriate design of the turbines, the expansion can be brought close to adiabatic (point 2). The conditions may be chosen to bring the point 2 near saturation, but preventing free-water. Then the vapour is totally condensed in a heat exchanger, which is the cold sink (point 3). The cycle is closed by rising the liquid water pressure to the original value P_1 (point 4), followed by pre-heating (point 5), and finally evaporation and superheating to the initial state (point 1). Note that the condensation step may be coupled with the heating of some unit operations, as distillation or evaporation. Therefore, the Rankine cycle is very attractive for energy integration.

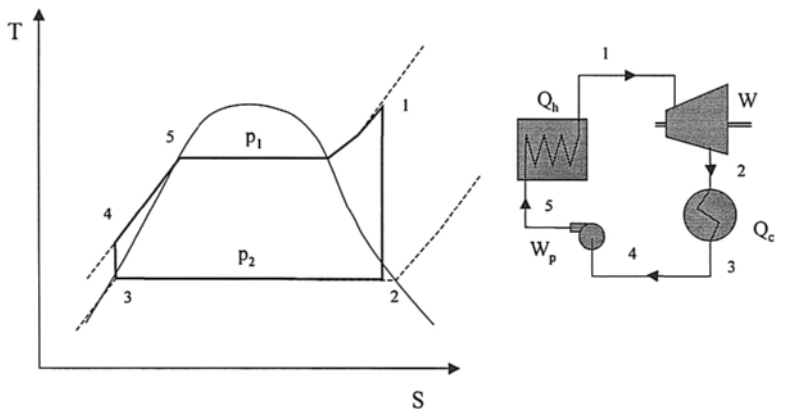

Figure 11.1 Rankine cycle

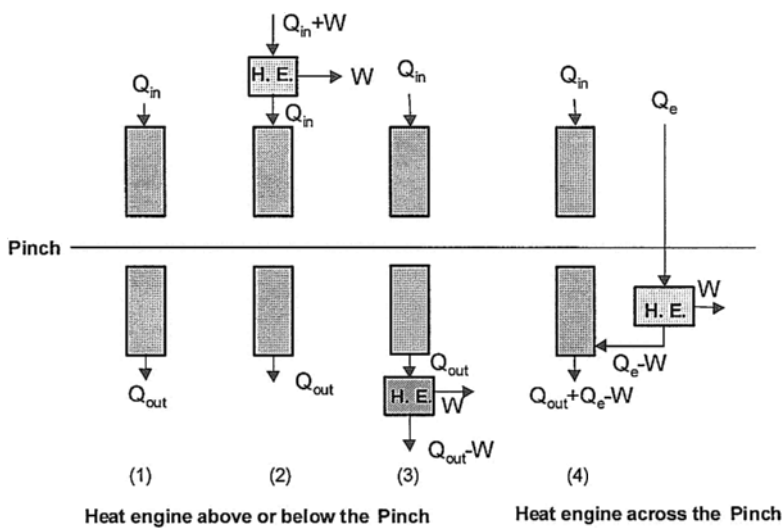

Figure 11.2 Appropriate placement of a heat engine

Appropriate placement

The correct placement of a heat engines is either above or below the Pinch, but not across it. Figure 11.2 gives the explanation. Initially the utility loads are Q_{in} and Q_{out}. If $Q_{in}+W$ is supplied to the heat engine, it is possible to deliver W shaft work and simultaneously Q_{in} heat. Because the injected energy is used entirely in the process, its efficiency becomes 100%! The same is valid for a heat engine placed below the Pinch.

When the heat engine is placed across the Pinch, an amount of heat Q_e supplied above the Pinch can be converted into the work W, but the rejected part Q_e-W is lost with the cold utility below the Pinch. Therefore, the placement of a heat engine across the Pinch must be avoided.

11.1.2 Combined Heat and Power (Cogeneration)

The combined production of heat and power in the frame of the same process is called *co-generation.* This technique offers opportunities for very efficient energy integration. The generated mechanical work or electricity can be used to drive compressors or heat pumps, while the heat can be used as hot utility. Two major applications will be examined.

1. Steam turbines

A steam turbine can be integrated as shown in Fig. 11.3. Initially, the boiler house generates high-pressure steam of duty Q_{HP}. This amount can be split into Q^*_{HP} and Q^*_W, the last term being converted into work and low-pressure steam, such as $W = Q^*_W - Q^*_{LP}$. Because the actual hot utility load is $Q_h = Q^*_{HP} + Q^*_{LP}$ one gets the amount of work:

$$W = Q_{HP} - (Q^*_{HP} + Q^*_{LP}) = Q_{HP} - Q_h \tag{11.5}$$

Without co-generation the utility consumption would be Q_{HP}. Therefore, the work W is get for free! The transformation of high-pressure steam in work has a theoretical efficiency of 100% when the rejected heat is used inside a process. Co-generation has proved to be cost effective in processes involving high exothermal reactions, but also as a method for valorisation of process waste.

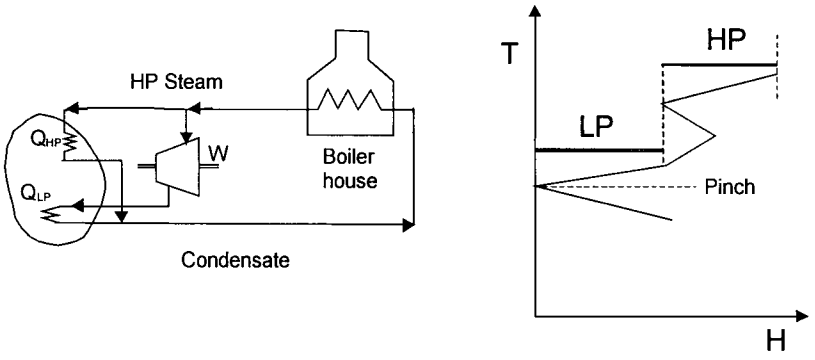

Figure 11.3 Combined power generation and heating with a steam turbine

2. Gas turbines

In the case of a gas turbine the process is not reversible. Figure 11.4 illustrates the principle of use. Hot gas produced by combustion is expanded through a gas turbine, which in turn drives a compressor or a power generator. For better efficiency the air is compressed and preheated. The overall engine efficiency depends on the gas temperature, process Pinch position, as well as on the shape of the composite curve.

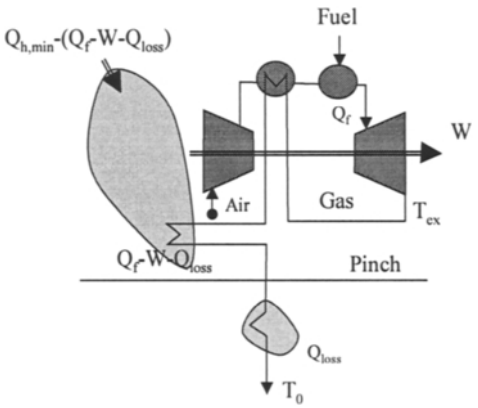

Figure 11.4 Combined power generation and heating with a gas turbine

---

EXAMPLE 11.1 Combined heat and power cycle

Examine the efficiency of a combined heat & power cycle that should supply the load required in the Example 10.3. Consider superheated steam at 60 bar and 540 °C. The stream for heating is extracted at a 50% ratio. Assume ideal Rankine cycle with steam exit pressure at 3 bar.

Solution. The hot load is of 7000 kW, the hottest stream being at 180 °C. If ΔT_{min}=30 °C is assumed for utility/process exchange, the minimum steam temperature is 210 °C, or a saturation pressure of approximately 20 bar. Thermodynamic properties of steam in different conditions as required by the problem are given below (see also Annex F):

	T, °C	Enthalpy (kJ/kg)			Entropy (kJ/kg/°C)	
		H_v	H_l	H_{vap}	S_v	S_l
Superheated steam 60 bar	540	3517.0	-	-	6.9999	-
Saturated steam, 20 bar	212.4	2799.5	908.8	1890.7	6.3409	2.4235
Saturated steam, 3 bar	180	2725.3	561.5	2163.8	6.9919	2.1379

Figure 11.5 presents the layout of a power & heat system following an ideal Rankine cycle. Consider 2 kg/s total steam at 60 bar split in the ratio 1:1 between only power and heat & power co-generation (point 1). After isentropic expansion from 60 to 20 bar the exhaust steam remains superheated at 360 °C, the enthalpy being h_2=3159.3 kJ/kg (point 2). The power delivered is $W_c = h_1 - h_2 = 3517.0 - 3159.3 = 357.7$ kW.

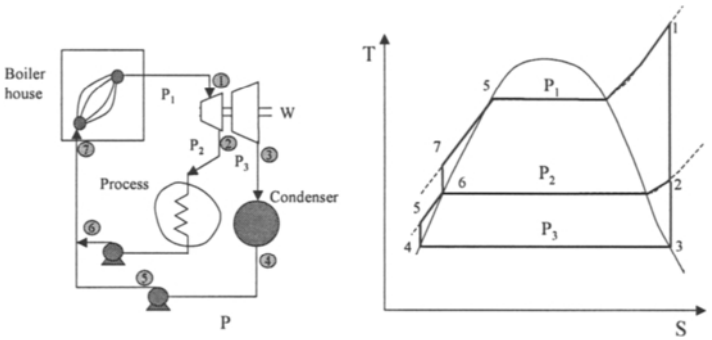

Figure 11.5 Co-generation and Rankine cycle for the Example 11.1

The heat available by condensation is $Q_h = 1*(h_2-h_6) = 3159.3-908.8 = 2250.5$ kW, so that the steam necessary for process heating is 7000/2250.5=3.33 kg/s.

If co-generation is taken into account, the useful energy per kg steam is W_c+Q_h= 357.7+2250.5=2608.2 kW (we neglect the power consumption for water recompression). The total heat consumed to bring the steam to the original state is: Q_1=3517-908.8=2608.2. Thus, for this part of the process the heat efficiency in an ideal cycle is 100%!

On the other hand, only power generation by steam expansion from 60 to 3 bar gives the work W_p = 3517-2725.3 =791.7 kW (point 1 to point 3, constant S). The thermal energy flow is Q_2=3517.0-561.5= 2955.5 kW, so that the thermal efficiency for only power generation is: η_p=791.7/2955.5=0.268.

By cogeneration the total useful heat flow is $Q_u = W_c+W_p+Q_h$ = 357.7+791.7+2250.5 = 3399.9 kW. The heat consumed is $Q_t = Q_1+Q_2$ = 2608.2+2955.5 = 5563.7 kW, so that the global thermal efficiency becomes η_{h+p}= 3399.9/5563.7 = 0.611>>0.268.

Thus, the above figures demonstrate that co-generation of heat and power could improve tremendously the energetic efficiency of an industrial process.

11.1.3 Heat pumps

Thermodynamic background

A heat pump is a device that operates in an opposite manner to a heat engine: takes the amount of heat Q_2 from a source at T_2 and delivers an amount Q_1 to a source at T_1 by spending W mechanical energy. Without losses the heat balance indicates that $Q_1 = Q_2 + W$. Classical examples are the domestic refrigerator, or the air-conditioning system. A heat pump can operate as a reversible cycle, so that Eq. (11.3) still holds.

The efficiency of a heat pump is characterised by a *coefficient of performance*, defined as:

$$COP = Q_1 / W = (Q_2 + W) / W \tag{11.6}$$

COP gives the amount of useful heat delivered by unit of mechanical work. Higher values means better heat pumping efficiency.

Figure 11.6 shows a typical vapour-compression cycle in a *T-S* diagram. Initially, the working fluid in liquid state (point 3) absorbs the amount of heat Q_2 from a source (evaporator) at P_2 and T_2 producing a vapour (point *4)*. Then the vapour is compressed to P_1 and T_1 by spending W work (point 1). Note that the point 1 is a superheated vapour. Then the vapour is cooled and transformed in liquid by condensation at constant pressure (point *2*). During this operation an amount of heat Q_1 is rejected to a sink (user). The cycle continues by restoring the low pressure and temperature state by expansion through a valve (point *3*). This operation gives a partial vaporised fluid. The liquid part passes again through evaporator delivering a saturated vapour (point 4). The vapour goes again to the compression in the next cycle.

Note that the fluid used in a vapour compression cycle should have large vaporisation enthalpy, moderate vapour pressure, as well as acceptable usage properties, as non-toxic, non-inflammable and non-corrosive.

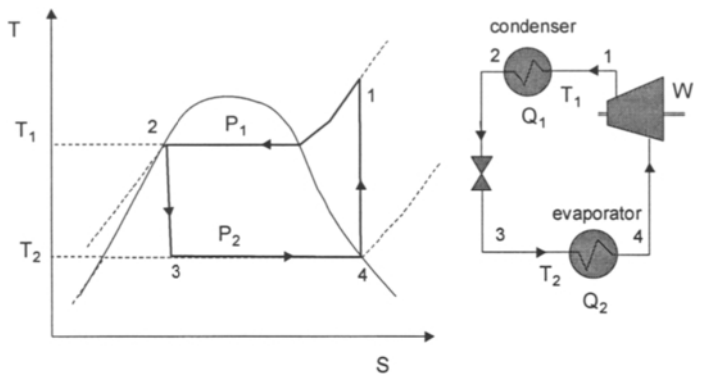

Figure 11.6 Representation of a heat pump

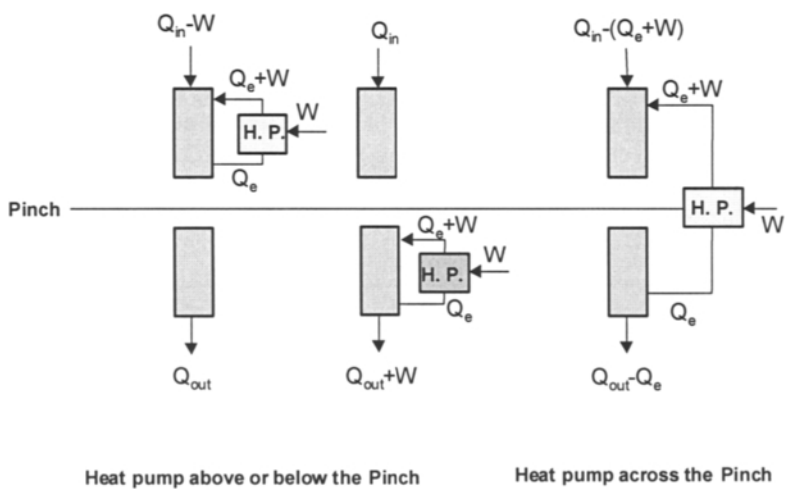

Figure 11.7 Appropriate placement of heat pumps

Appropriate placement

The best placement of heat pumps is across the Pinch (Fig. 11.7). If the heat pump is placed above the Pinch, the amount Q_e+W is reintroduced into the process, and the hot utility load decreases by W. This supplementary energy is more expensive than the thermal energy. On the contrary, if the heat pump is placed across the Pinch the device can take an amount Q_e from below the Pinch and bring it above the Pinch, such that both utility loads diminish by the same amount Q_e.

11.1.4 Refrigeration cycles

The industrial refrigeration systems are based on vapour compression cycles, and operate normally in more than one stage. Heat is absorbed at low temperature and rejected to the environment, or to another process. The only utilities are shaft work as source of energy, and water or air as cooling agents. The design of the refrigeration systems as stand-alone units is described in specialised books in Engineering Thermodynamics (Moran and Shapiro, 2000). However, Pinch Point Analysis can detect significant opportunities for energy saving and set optimal targets for shaft work directly from the process stream data (Linnhoff et al., 1994).

The performance of a refrigeration system can be characterised by a coefficient of performance COP_r that gives the ratio between the heat extracted Q_E and the shaft work consumed W:

$$COP_r = \frac{Q_E}{W} \tag{11.7}$$

An ideal refrigeration cycle could be based on a Carnot cycle, for which the ideal coefficient of performance is:

$$COP_r^{id} = \frac{T_C - T_E}{T_E} \tag{11.8}$$

T_C and T_E are condenser and evaporator temperatures on the side of the working fluid. As a rule of thumb, the ratio of ideal to actual coefficient of performance is around 0.6, so that the shaft work target for rejecting the amount of heat Q_E can be estimated roughly with the relation:

$$W = \frac{Q_E}{0.6}\frac{T_C - T_E}{T_E} \tag{11.9}$$

The energy integration of low-temperature processes may follow the general pattern of Pinch Point Analysis, namely the identification of the heat load targets and the placement of refrigeration levels. Then the power necessary to drive the refrigeration devices may be evaluated by applying established design rules. The above approach has the disadvantage of hiding opportunities for energy saving, this time in its high value form, for instance as electrical or mechanical energy.

A more efficient approach makes use of the concept of exergy (Linnhoff and Dhole, 1992). The CC or GCC plots can be redrawn into exergy composites by replacing the

temperature scale with the Carnot factor $\eta_C = 1 - T_0 / T$. The use of Grand Exergy Composite is displayed in Fig. 11.8. The refrigeration system supplies to the Heat Exchanger Network (HEN) the amount of exergy ΔEx_r by means of a multi-level refrigeration system. The amount of exergy ΔEx_p is supplied to the process. Clearly, ΔEx_r must be larger than ΔEx_p. The difference, denoted here by $(\sigma T_0)_{HEN}$, is the exergy loss in the HEN (including utility heat exchangers), proportional with the shaded area in Fig. 11.8. Thus the above graphical method allows a simple visualisation of opportunities for shaft work saving for different design alternatives.

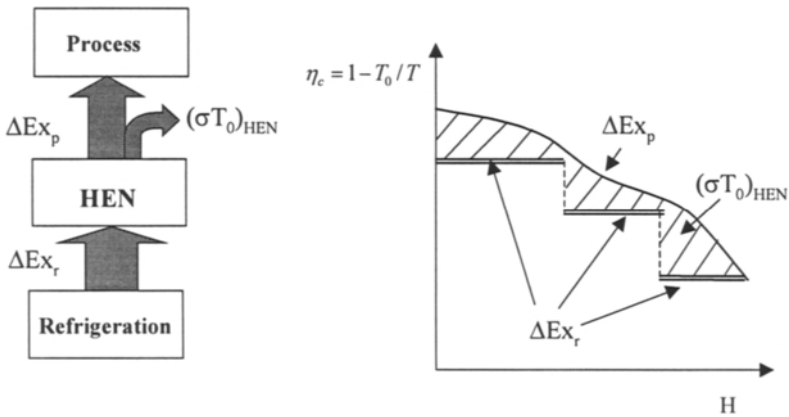

Figure 11.8 Exergy analysis in low-temperature systems

11.2 DISTILLATION SYSTEMS

Distillation remains the most used separation method, but is penalised by low thermodynamic efficiency in stand-alone operation. Therefore, energy saving in distillation is a priority topic in integrated process design. In this subchapter we present a number of techniques that can be applied to improve the energetic efficiency of distillation systems by integration with the whole process.

The efficiency of a distillation process can be rated against the minimum energy of separation. Consider a generic separation process in which *j* single-phase inlet streams containing *i* components are separated in *k* single-phase product streams. Let's denote the stream molar flow rate by F and the molar composition by z_i. The minimum (reversible) work of separations W_{min} is equal with the work that should be done by the surroundings on the system, when both would be at the temperature T_0. This may be expressed in terms of Gibbs free energy variation as:

$$-W_{min} = \sum_{out} F_k G_k - \sum_{in} F_j G_j \tag{11.10}$$

Taking into account that partial Gibbs free energy is given by $G_i = \mu_i^0 + RT \ln f_i$, one gets:

$$-W_{min} = RT_0\left[\sum_{out} F_k\left(\sum_i z_{i,k} f_{i,k}\right) - \sum_{in} F_j\left(\sum_i z_{i,j} f_{i,j}\right)\right] \tag{11.11}$$

Several cases will be examined. Thus, for an ideal mixture at low pressure the minimum work of separation is:

$$-W_{min} = RT_0\left[\sum_{out} F_k\left(\sum_i z_{i,k} \ln z_{i,k}\right) - \sum_{in} F_j\left(\sum_i z_{i,j} \ln z_{i,j}\right)\right] \tag{11.12}$$

For a non-ideal liquid mixture at near atmospheric pressure a similar expression is obtained, the molar fractions z_i being corrected by activity coefficients γ_i:

$$-W_{min} = RT_0\left[\sum_{out} F_k\left(\sum_i z_{i,k} \ln(\gamma_{i,k} z_{i,k})\right) - \sum_{in} F_j\left(\sum_i z_{i,j} \ln(\gamma_{i,k} z_{i,j})\right)\right] \tag{11.13}$$

The equation (11.13) indicates that a non-ideal mixture with positive deviations ($\gamma_i > 1$) requires less separation work than a mixture with negative deviations ($\gamma_i < 1$).

For the separation of a mixture in pure components the minimum separation work is:

$$-W_{\min} = RT_o \sum_j z_j \ln(\gamma_j z_j) \tag{11.14}$$

For a binary mixture the relation (11.14) becomes:

$$-W_{\min} = RT_o[z_1 \ln \gamma_1 z_1 + (1 - z_1) \ln \gamma_2 (1 - z_2)]$$

Numerical computations can show that the minimum separation work is rather small. For example, for a binary equimolar mixture the minimum ideal separation work in pure components at 298 K is W_{min}=0.6931 RT_o=1718 J/mol.

The actual separation process receives energy mainly as heat. The ability of heat to be converted into work is expressed by the exergy E, as the maximum amount of work that could be developed by a reversible Carnot engine receiving heat Q at T_b and rejecting the residual heat to the environment at T_0. The exergy associated to the heat transfer is:

$$\mathsf{E} = Q\left(1 - \frac{T_0}{T_b}\right) \tag{11.15}$$

For example, for a simple column receiving Q_R at the bottom temperature T_B and rejecting Q_C at the top temperature T_C the net separation work W_{net} is:

$$W_{net} = \mathsf{E}_R - \mathsf{E}_C = Q_R\left(1 - \frac{T_0}{T_B}\right) - Q_C\left(1 - \frac{T_0}{T_C}\right) \tag{11.16}$$

The thermodynamic efficiency of the separation can be obtained as:

$$\eta = \frac{W_{\min}}{W_{net}} \tag{11.17}$$

In many cases $Q_R = Q_C$, so that the relation (11.17) becomes:

$$W_{net} = Q_R T_0 (\frac{1}{T_C} - \frac{1}{T_B})$$

The temperature difference ($T_R - T_C$) is usually between 5 and 30 C, so from this point of view the losses in exergy are limited. In practice the temperature difference is even larger, because the heat is supplied from a source at $T_h > T_B$ and rejected to a cooling agent for which $T_c > T_C$. Moreover, if cooling water is used, then we may assume $T_c = T_0$, and the following approximate formula may be used:

$$W_{net} \cong Q_R (1 - T_0 / T_h) \tag{11.18}$$

From the above presentation it may be concluded that the increasing the thermodynamic efficiency of separations by distillation should consist primarily of reducing the heat requirement Q_R, as for example by optimising the reflux and the flow rate of mass-separation agents. Rejecting heat to the environment by condensation, as for example by cooling with air and water, represents important exergy losses. Therefore, the integration of distillation operations with the rest of the process should be systematically investigated.

EXAMPLE 11.2 Efficiency of a simple distillation process

Consider the separation of an equimolar mixture of 100 kmol/h methanol-water. The column is operated at normal pressure, and has 15 stages with the feed on the stage 7. The reflux ratio is 1.3. Examine the thermodynamic efficiency of this separation. Hot source is steam at 406.15 K, cold sink is cooling water at 298 K. How the energetic efficiency of separation could be improved?

Solution. Firstly, a simulation in ASPEN Plus is run, with Wilson as liquid activity option. Heat exchangers for feed preheating and product cooling are considered. The results are given below (component 1 methanol).

	Condenser	Reboiler
Temperature, K	337.8	377
Pressure, atm	1.0	1.20
Composition, x_1	0.997	0.008
Duty, kW	-1125	1147

The other heater/coolers are:

	T_s, K	T_t, K	Duty, kW
Feed preheat	298	351	138
Distillate cooler	337.8	298	-58
Bottoms cooler	377	298	-82

The activity coefficients in the initial mixture are γ_1= 1.11 and γ_2= 1.14. For the minimum work of separation one gets:

W_{min}=(100/3600) ×0.5755×2478.9=39.63 kW

In the most favourable situation the work for separation could be obtained by means of a Carnot engine operating between T_B, T_C and T_0=298 K. The net work would be:

$W_{net,0}$=1147× (1-298/377)-1125(1-298/337.8)=107.8 kW

The best thermodynamic efficiency for the given design would be:

$\eta_0=W_{min}/W_{net,0}$ = 39.63/107.8=0.367

The above value is not bad. In reality much more exergy is destroyed because of irreversibilities, particularly due to the cooling. For example, if we take into account only the hot utility for separation (feed preheating and reboiler) the total heat is Q_i = 138 + 1147 = 1285 kW. This could be extracted virtually from surroundings and converted by means of a Carnot cycle working between 298 and 406.15 K, for which the following work can been obtained:

$W_{net,1}$ = 1285×(1-298/406.15) = -342.2 kW

Thus, the thermodynamic efficiency in terms of availability of hot utility is:

$\eta_1= W_{min}/W_{net,1}$ = 39.63 / 342.2 = 0.116

This more realistic value is much lower than the previous one. We will search to improve it. Heat integration of feed and product streams could reduce the heat preheating. For ΔT_{min}= 10 °C one gets Q_h=32.8 kW and Q_c=22.5 kW. The total heat for separation can be reduced to 32.8+1147=1179.8 kW, giving W_{net}=1179.8(1-298/406.15) = 314 kW, and as result η = 0.126. The increasing in efficiency is about 10%, so that the improvement obtained by heat integration around the stand-alone column is marginal.

Next, we will examine another solution. Because the duty of reboiler and condenser are approximately equal, it could be interesting to use a heat pump. Suppose that the heat pump is designed with a very low temperature approach to reboiler and condenser, of 5 K. Hence, the heat pump works between 332.8 and 382 K. Using again a Carnot cycle, the energy of separation would be given by the relation (11.18):

$W_{net,2}$ = 1147×298×(1/332.8-1/382) = 134 kW

As a result, the energetic efficiency would rise to η_2 = 0.295, a significant improvement, close to the upper limit 0.367 determined above. In practice we should count a mechanical efficiency of 70%, so that the overall efficiency will drop to 0.21, still interesting.

Pumping over a large temperature interval is expensive in term of capital, as well as in term of energy, when this is exclusively from imported electricity. However, when cheap mechanical energy can be found, the use of heat pumping in distillation becomes a viable solution for energy saving.

11.2.1 Single columns

Consider a simple distillation column, one-feed two-products with total condenser. In a temperature-enthalpy diagram this can be depicted as a rectangular 'box' (Fig. 11.9). The upper and lower sides represent bottom and top products respectively, the segments being proportional to the reboiler and condenser duties. The inspection of temperatures and duties of simple columns gives a rapid idea about possible thermal coupling just by shifting the pressures. For example, the vapour distillate of a high-pressure column can supply heat to the reboiler of a low-pressure column, the same heat exchanger serving as condenser and reboiler.

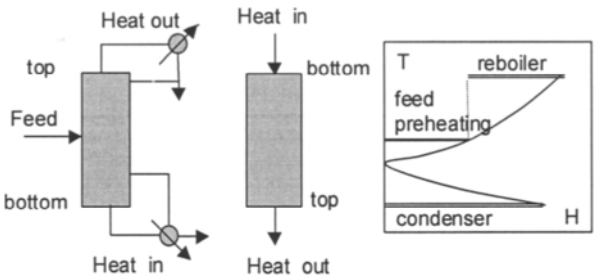

Figure 11.9 Representation of a simple distillation column

Appropriate Placement

The correct placement of a distillation column with respect to the background process is either above or below the Pinch, (Fig. 11.10). If the column is completely above the Pinch, the process can supply the heating load, while the condenser duty can be rejected back into the process at lower temperature. This operation does not modify the energetic requirements, but the distillation column will operate at zero energy cost! The same demonstration is valid when placing a column completely below the Pinch. On the contrary, both hot and cold utility consumption is increased for a distillation column placed across the Pinch. From practical viewpoint a distillation column can be moved in a direction compatible with better heat integration just by shifting the pressure.

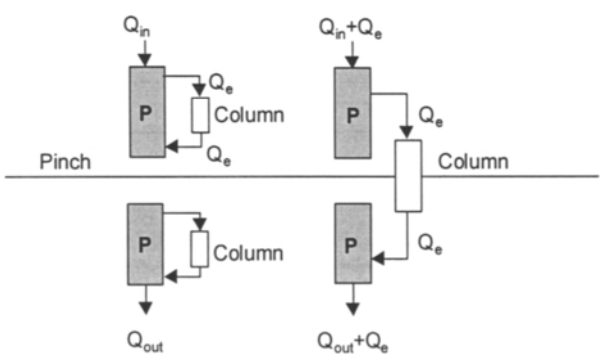

Figure 11.10 Appropriate placement of distillation columns

Column Profiles

A more refined approach consists of using the concept of Column Profiles (Dhole and Linnhoff, 1993). The counter-current vapour and liquid enthalpy traffic in a distillation column has large analogy with the Composite Curves. As a result, there is a Column Grand Composite Curve (CGCC), as is illustrated by the Fig. 11.11-left. Note again that the bottom and top products are placed at the highest and lowest position, respectively. These composite curves can be built from the enthalpy profiles obtained by rigorous simulation. Note that for a simple column the Pinch point is located in at the column feed. Fig. 11.11-right shows that the hot and cold utility loads can be placed at intermediate temperature levels as side-reboilers or side-coolers, similarly with placing multiple utilities on Grand Composite Curve. This possibility is exploited in the industry, the most salient example being the topping column in refining.

Column Profiles can be used to detect opportunities for energy saving, both with stand-alone and integrated units. The method is available in some packages, as in SuperTarget™. Some techniques for heat saving will be presented in the next sections.

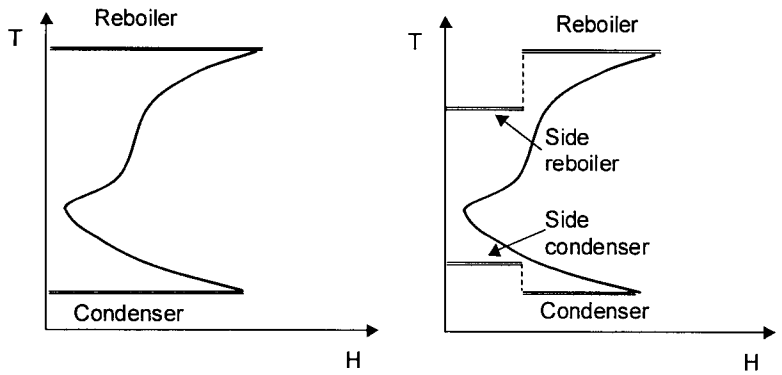

Figure 11.11 Enthalpy profiles and Composite Curves

1. Reducing the reflux.

CGCC can indicate if a reduction in reflux is possible (Fig. 11.12). At minimum reflux the Pinch touches the vertical axis. Obviously, both reboiler and condenser duties are reduced in the same proportion. Note that the reduction in reflux might be justified from a stand-alone operation point of view, but not necessarily when the integration with other units is considered, such as in the case of the heat integrated distillation columns (see later in this chapter).

2. Feed conditioning.

Inappropriate feed condition can be visualised by a large enthalpy variation near the feed. Excessively superheated feed could develop a large amount of vapour because of a flashing effect, dangerous for the hydrodynamics of internals. The same consequence may have an excessive sub-cooled feed, this time by a quenching effect. These situations can be easily

detected by examining the column profiles. Figure 11.13 depicts a situation where feed pre-heating would lead to a reduction in the load of reboiler.

However, the feed conditioning might affect the purity too. Partially vaporised feed increases both condenser duty and reflux in the rectification zone, and consequently gives higher purity of the top product. Sub-cooled feed will improve the purity of the bottom product by increasing the vapour flow rate in the stripping zone. Hence, partially vaporised feed will improve the separation of a heavy impurity by increasing the reflux, while sub-cooled feed gives a better removal of light impurities from bottoms by means of a higher vapour flow available for stripping! This effect is counterintuitive, since it would be expected that the partial vaporisation of the feed will help the separation of a light species.

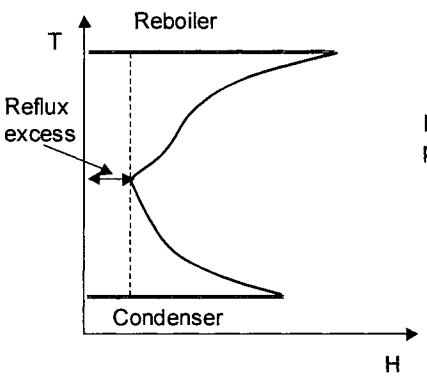

Figure 11.12 Scope for reflux reduction

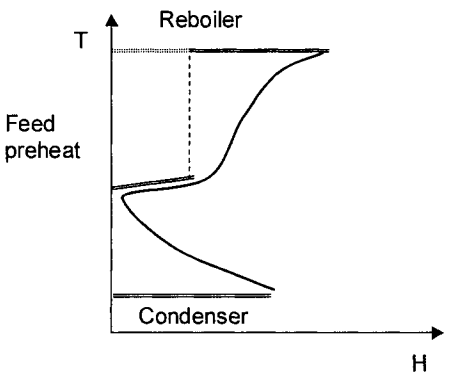

Figure 11.13 Feed conditioning

3. Side-stream heat exchangers: heaters, coolers, reboilers or condensers.

Heating and cooling at only the extreme sides of a distillation column is not always economical, particularly in the case of very high or very low temperatures. Appropriate placed side-stream heat exchangers can take over significant parts of the heating or cooling loads, with the advantage of using process streams or cheaper utilities.

The approach may be extended to detect opportunities for energy integration when several columns are considered, as illustrated by the Fig. 11.14. The traditional approach by *T-H* boxes suggests increasing the pressure of A, and using a side condenser in B (Fig. 11.14-left). The first modification could be not acceptable because implies further rise in the bottom temperature of the column A. The examination of column profiles may suggest other solutions. In the Figure 11.14-right the GCCC curves of the three columns are superimposed, with the profile of the column B reversed. It comes out that it is more rational to consider the condenser of the column A as a side-reboiler for the column B, as well as a part of the condenser of B as side-reboiler for the column C. In this case the integration of columns does not require changing the pressures. The solution can be optimised by rigorous simulation.

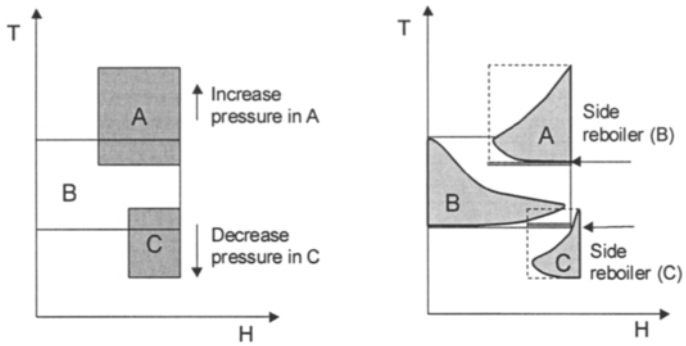

Figure 11.14 Column profiles help to develop complex distillation set-up

11.2.2 Heat pumps driven systems

Heat pumping can be a cost-effective solution for energy saving. A now classical example is the cryogenic purification of propylene by distillation (see Example 11.3). Several solutions will be examined.

A first possibility consists of using an *external heat pump* (Fig. 11.15). The heat taken from the condenser is raised at a sufficient high temperature by means of a compressor. Note that the working fluid may be chosen independently of separation mixture. It is easy to imagine another solution where the heat pump would connect not condenser and reboiler, but an intermediate cooler or reboiler (side integration). This combination would enable to manage better the temperature difference, as well as the variation of internal heat streams.

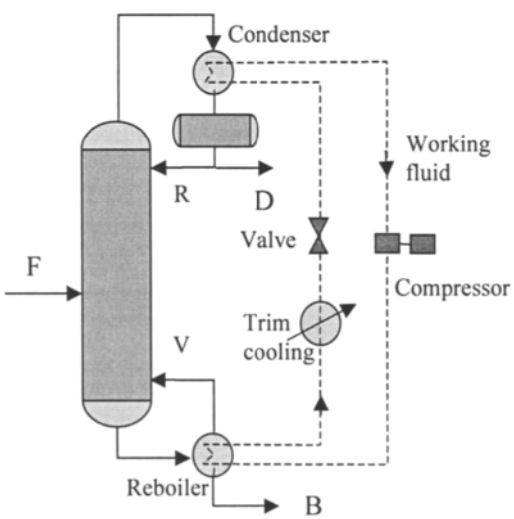

Figure 11.15 External heat pump

If the product is a high purity component, this can be used as working fluid. Two possibilities are offered. In the alternative with *heat pump of vapour distillate* (Fig. 11.16) the vapour overhead is heated-up by compression, and used to drive the reboiler. In the alternative with *heat pump of reboiler liquid* (Fig. 11.17), the bottom product is vaporised by expansion through a valve, evaporated by passing through the condenser, recompressed and injected as vapour in the base of the column. Hence, the first alternative has only reboiler, the second one only condenser. Note that the insertion of a cooler on the trajectory of the pumping fluid is necessary to ensure appropriate temperature before flashing and phase separation. Supplementary heat exchangers might be necessary to complete the thermal balance, but also for start-up and shut down.

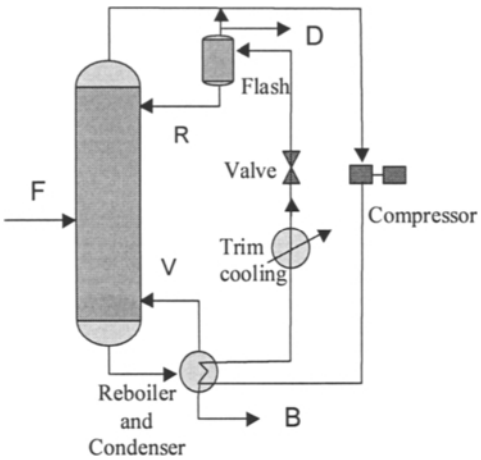

Figure 11.16 Heat pump with vapour distillate

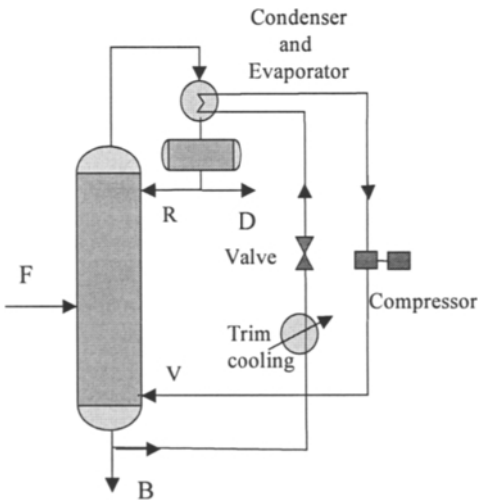

Figure 11.17 Heat pump with reboiler liquid

The implementation of a heat pump depends greatly on the local economic elements. The cost of the shaft-work is the most critical. Electricity is typically expensive, unless a special price is agreed. More attractive is the use of a gas turbine driven by low cost recovered fuel, as well as shaft work produced in combined heat and power cycles.

EXAMPLE 11.3 Heat pump driven system

The separation of propylene from propane is difficult, the difference in the boiling points being of about 5 K, and the relative volatility below 1.1. In conventional cryogenic distillation the column is operated at 16-19 bar with water condenser, or at 21-26 bar with air cooler. Large number of stages is required, between 150 and 200, as well as large reflux ratios, between 10 and 20. Propylene purity is of polymerisation grade over 99%. Examine the thermodynamic efficiency of heat pumping for saving energy.

Solution. We select the scheme with vapour distillate recompression. The following data are assumed:

- Feed: 100 kmol/hr C3/C3= with 40% C3=, T=298 K, P=12 bar.
- Column: 120 theoretical stages.
- Pressure: top 10 bar, column pressure drop 1.2 bar.

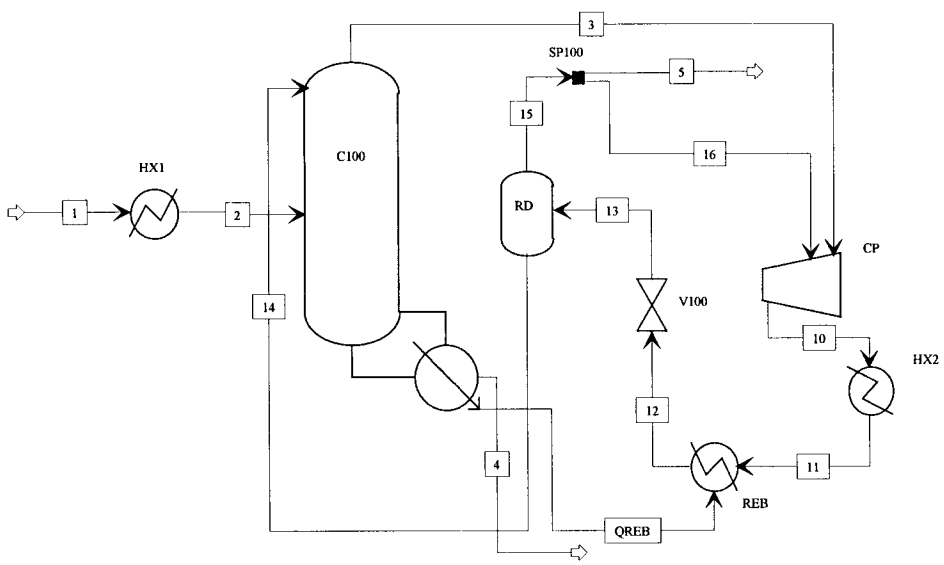

Figure 11.18 Simulation of a heat pump driven separation of propane/propylene

Figure 11.18 presents the flowsheet simulated with Aspen Plus. The distillation column C100 has only reboiler, linked by an energy stream with the heat exchanger REB. The compressor COMP increases the propylene pressure from 10 to 18 bar, sufficient to rise the temperature from 292 K to 328 K. In this way a gradient of about 24 K is created between the working fluid and reboiler. After condensation the propylene passes through a trim heat exchanger HX2. Its role is important in ensuring robust convergence, but also in practice for process control, because the suppression of the condenser removes a degree of freedom. Controlling the temperature of stream 12 at 306 K (33 °C) ensures sufficient liquid after the valve V100. The phase separation that takes place in the flash vessel supplies reflux for C100 and vapour distillate.

Table 11.1 presents some key results, as purity, energetic consumption and temperatures. Power consumption increases more than linearly with the purity. It is remarkable to note that the reboiler duty is by an order of magnitude higher than the power introduced by the compressor, in this case the only source of energy for separation. The ratio between heat duty used in the reboiler and the external mechanical work spent by the compressor is about 11. We may conclude that there is a real advantage to use heat pumping in this separation. A necessary condition is that the cost of mechanical energy should be low enough. This can be found in other sources than electricity, as for example gas turbines drives by recovered fuel.

Table 11.1 Key results by the simulation of propylene separation

Reboil ratio	Propylene purity	Reboiler duty, kW	Isentropic power, kW	Trim kW	Reboil duty to power	T top K	T bottom K	Tcompr K	Tout reboiler
12	0.9812	2900.5	250.0	-191.7	11.6	292.3	304.1	327.7	313.3
14	0.9902	3384.3	294.2	-252.9	11.5	292.3	304.1	327.6	314.1
16	0.9935	3865.8	338.1	-314.0	11.4	292.2	304.2	327.6	314.7
18	0.9954	4349.6	382.2	-375.2	11.4	292.2	304.2	327.6	315.2

11.2.3 Heat integrated columns

The methods for saving energy discussed so far were suited for the separation of essentially binary mixtures. In this section we will enlarge the treatment to multi-component mixtures. In Chapter 7 we discussed two alternatives, direct and indirect sequence. The unbalanced ternary mixtures can be better treated in sequences of heat-integrated columns. An interesting solution is a prefractionator followed by side-product column. The first column performs a separation in two binaries, A/B and B/C, sent as feeds to the second column. Here all three pure components are obtained, A and C as top and bottom products, and B as side-stream. It is interesting to note that the non-integrated prefractionator set-up needs roughly 30% less energy compared with the two-columns conventional arrangements (Smith, 1995). The reason is that the separation in

the prefractionator is not penalised by remixing effects, as it is the case with direct or indirect sequence. Further energy saving can be achieved by developing heat-integrated schemes, as it will be illustrated by the next example.

As general comment, we should add that the controllability of the heat-integrated scheme needs careful examination. By the coupling of units some manipulating variables disappear, as reboiler duty, or reflux flow rate. In addition, energy feedback could introduce unstable behaviour. When several alternatives offer similar energy consumption, the selection should be based on controllability properties rather on marginal energy saving. The next example illustrates this important topic.

EXAMPLE 11.4 Design and controllability of a heat-integrated distillation sequence

Consider the separation of an equimolar mixture of pentane (A)/hexane (B) /heptane (C) with a total flow rate of 150 kmol/h. The desired purity for A, B and C is of 0.99, 0.98 and 0.99. Study the design of a heat-integrated distillation scheme with prefractionator.

Solution.

Base case

As reference we consider the direct separation scheme. The design of columns was done in Aspen Plus by means of shortcut methods followed by rigorous simulation. The energetic consumption depends on the reflux ratio. We assume that the optimal R/R_{min} is 1.3, and column pressures of 2 and 1 bar with 0.2 bar pressure drop. Table 11.2 presents the results. Note that the initial feed temperature is 298 K, and therefore the reboiler duty of the first column includes feed preheating.

Table 11.2 Base case design (direct sequence) for separation of a ternary mixture

	Column 1	Column 2	Total
Stages (feed)	20 (8)	22 (10)	42
Reflux ratio (minimum)	1.3 (0.97)	1. 8 (1.35)	-
Condenser duty, MMkcal/h	0.675	0.972	1.647
Reboiler duty, Mmkcal/h	1.228	0.840	2.068

Heat integration schemes.

In the *forward heat integration* scheme (FHI) the top vapour of the prefractionator is used to heat the reboiler of the main column, and after condensation split in reflux and secondary feed for the main column (Fig. 11.19). The pressure in the prefractionator has to be high enough to ensure a temperature difference of minimum 10 K in the reboiler of the main column. In the *reverse heat integration* scheme (RHI) displayed in Fig. 11.20, the top vapour from the main column is used to drive the reboiler of the prefractionator. Note that this vapour is practically the pure component A. After condensation this stream is split in top product and reflux of the main column.

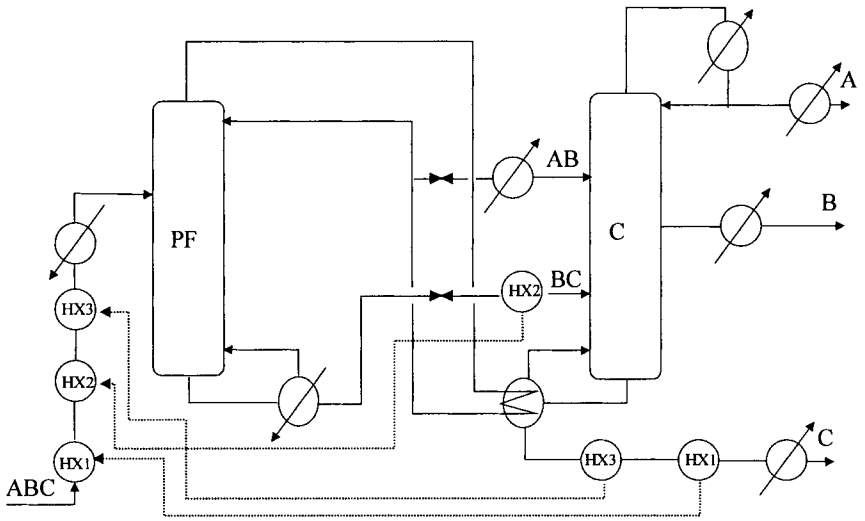

Figure 11.19 Forward heat integration

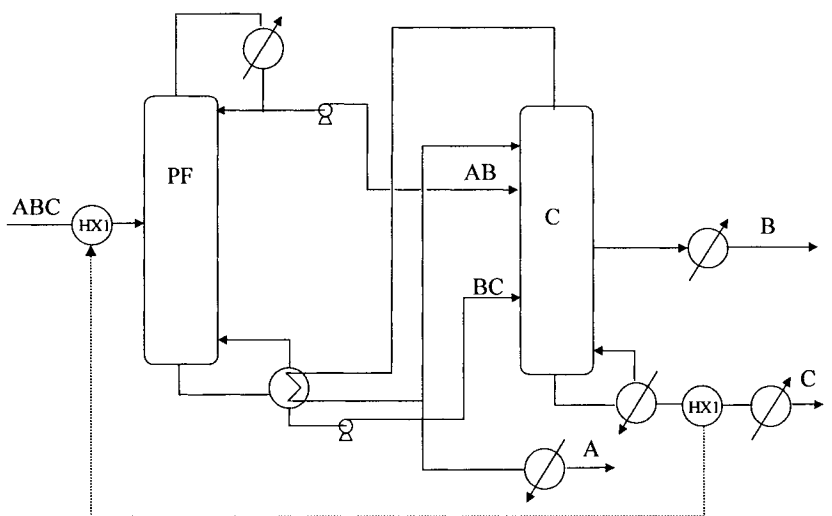

Figure 11.20 Reverse heat integration

It may be observed that in both cases the thermal coupling takes place by combining one condenser with one reboiler. Perfect matching of duties arises problems. A first solution is to install additional heat exchangers, but the capital cost increase could cancel the energy saving, because even small units have a non-negligible fixed-part cost. A second solution is to change the design of the column in a way that enables a perfect match of duties. Moreover, fewer trays for separation are needed. This solution was adopted here. Additional energy saving can be obtained by combining the feeds and products, as shown in the Figures 11.20-21.

Design alternatives.

Note that the amount of A (or C) that leaves the prefractionator with the bottom (or top) stream will end-up in the side-stream of the main column. Consequently, the maximum amount of A and C in the prefractionator bottom and top is 0.5 kmol/h, respectively. Therefore, the design of the prefractionator is critical for the achievable purities. Several specifications are possible.

Table 11.3 displays four design alternatives. In Design I the prefractionator performs a sharp separation A/C. In Design II, the amount of A and C in bottom and top of the prefractionator are closed to their maximum values, and as a consequence a sharp A/B and B/C split is required in the main column. Other options are: Design III, with high recovery of the heavy component, and low recovery of the light component, and Design IV, with low recovery of the heavy component and high recovery of the light component.

Table 11.3 Design alternatives for the prefractionator

	Design I	Design II	Design III	Design IV
Distillate (kmol/h)				
A	49.975	49.525	49.525	49.975
C	0.025	0.475	0.025	0.475
Bottom (kmol/h)				
A	0.025	0.475	0.475	0.025
C	49.975	49.525	49.975	49.525

The four design alternatives have different sizing characteristics, as given in Table 11.4. The pressure difference is of about 6 bar in FHI and 5 bars in RHI. In the both schemes the first design alternative has the tallest prefractionator, while the second one the shortest, the main column having practically the same number of stages. There is a difference in the theoretical number of stages required in each alternative, but this is not significant at industrial scale. We may observe that the total heating duty does not vary too much, being around 1.5 MMkcal/h. The maximum heating duty saving is of 30%.

However, if the above alternatives are similar with respect to energy consumption, they are very different as dynamic behaviour. It can be demonstrated by controllability analysis (see the section 13.6.2) that the forward heat-integration scheme is much easier to control, using only temperature measurements (Bildea and Dimian, 1999). The reversed heat-integration scheme needs a composition analyser of the side stream. The low-cost design with small prefractionator (Design I) has the best closed-loop performance.

This example demonstrates that the evaluation of controllability properties of a heat-integrated scheme is necessary. Very often the differences in energy saving between alternatives are marginal, while the differences in dynamics might be considerable.

Table 11.4 Characteristics of prefractionator/side stream column heat integrated system

	Design I		Design II		Design III		Design IV	
	PF	C	PF	C	PF	C	PF	C
Forward heat integration								
Reflux ratio	2.	3.39	1.96	2.35	2.14	2.40	1.55	2.17
Total stages	24	28	12	30	15	28	19	28
Feed tray (from top)	12	6, 20	6	6, 23	10	5, 20	8	6, 20
Side-stream tray		12		12		12		12
Top stage pressure (bar)	7.3	1	7.1	1	7.4	1	7.0	1
Reboiler duty, Mkcal/h	1.138	**1.052**	1.150	**1.068**	1.149	**1.081**	1.087	**1.008**
Condenser duty, Mkal/h	**1.052**	1.052	**1.068**	1.046	**1.081**	1.061	**1.008**	0.988
Feed preheat duty	0.455		0.442		0.493		0.432	
Total duty, Mkcal/h	1.593		1.592		1.642		1.440	
Reverse heat integration								
Reflux ratio	0.891	2.588	0.980	2.568	1.016	2.568	0.828	2.5
Total stages	20	34	10	35	15	35	15	35
Feed tray (from top)	10	7, 25	5	6, 26	9	6, 25	6	7, 26
Side-stream tray		15		15		15		15
Top stage pressure (bar)	1	5.95	1	5.4	1	5.6	1	5.75
Reboiler duty, Mkcal/h	**0.911**	1.558	**0.922**	1.542	**0.916**	1.543	**0.895**	1.539
Condenser duty, Mkal/h	0.858	**0.911**	0.886	**0.922**	0.869	**0.916**	0.853	**0.895**
Total duty, Mkcal/h		1.558		1.542		1.543		1.539

11.2.4 Thermally coupled columns

By *thermal coupling* the heat is transferred by direct contact between vapour and liquid flows that connect sections of different columns. This is a major difference with 'heat integrated columns', where the heat exchange takes place by condenser/reboilers. Hence, thermal coupled columns have a more complex behaviour. Figure 11.21 illustrates two basic arrangements with side-columns. The first is the *side-rectifier*, derived from a direct sequence. The second one is the *side-stripper* that corresponds to

an indirect sequence. In both cases a side-stream is picked-up from the main column and treated in a second column to separate the intermediate component B. The side-rectifier is placed below the feed, while the side-stripper is located above the feed to avoid the contamination with B of the product A and C, respectively. These thermal coupled arrangements are more efficient as conventional direct and indirect sequence.

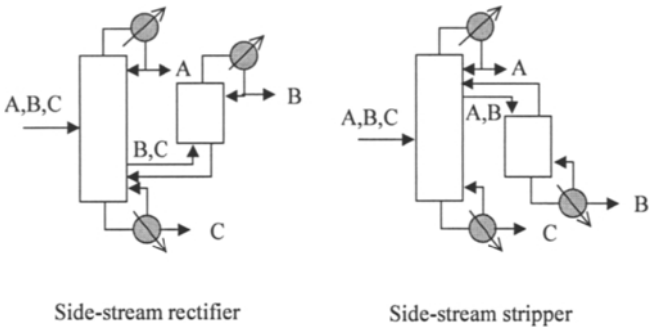

Figure 11.21 Thermally integrated side-stream columns

The prefractionator scheme can generate a thermal coupling arrangement. A first possibility known as the *Petlyuk column* is illustrated in Fig. 11.22 (left). The prefractionator performs enriching in A and C delivering two secondary feeds, vapour and liquid, for the main column. This receives also liquid reflux and vapour boil-up from the main column. Note that the prefractionator can be included physically in the separation space producing a *dividing wall column*, as depicted in Fig. 11.22 (right).

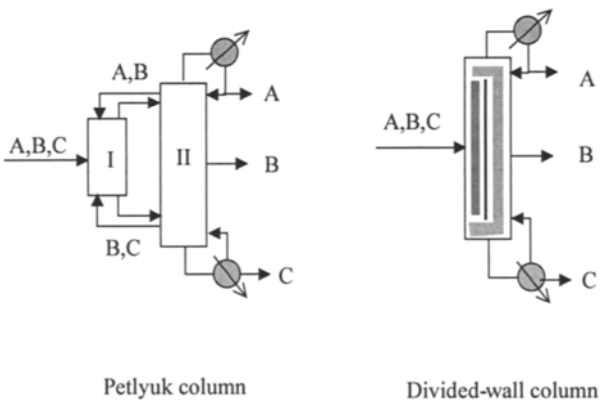

Figure 11.22 Thermally coupled columns

Petlyuk column has been extensively studied. The energy saving may be estimated roughly at 30% compared with simple columns, being more efficient than side-rectifier and side-stripper arrangements. However, the industry is reluctant. A reason is the difficulty to manage mechanical problems, as the split of the flows and the pressure drop between columns. More fundamental reasons seem to be the limitation in

achieving high purity, as well as the occurrence of multiple steady-states. By thermal coupling the pressures, temperatures and flows in columns become highly interdependent, making the design and control more difficult as with simple columns. It seems that the best application of a Petlyuk column is the separation of a ternary mixture with a large amount of middle component, when the purity is not crucial.

Contrary to expectations, it is divided-wall column that have received more attention from industry. Some dozen of applications have been recorded in the last years all over the world.

11.3 THE INTEGRATION OF CHEMICAL REACTORS

An exothermic reaction is a heat source. Accordingly to the general principle the appropriate placement is above the Pinch (Figure 11.23a). The minimum hot utility can be reduced by the amount of heat developed by the reaction, so $Q_{H,min} = Q_H - Q_R$. The minimum cold utility remains the same because no heat transfer across Pinch occurs. In contrast, the placement of an exothermic reaction below the Pinch is inappropriate, because leads to an increasing in the consumption of cold utility. Note also that in the case of an exothermic reaction the operating temperature should be maximised, in order to offer the highest driving force for the integration with the rest of the process.

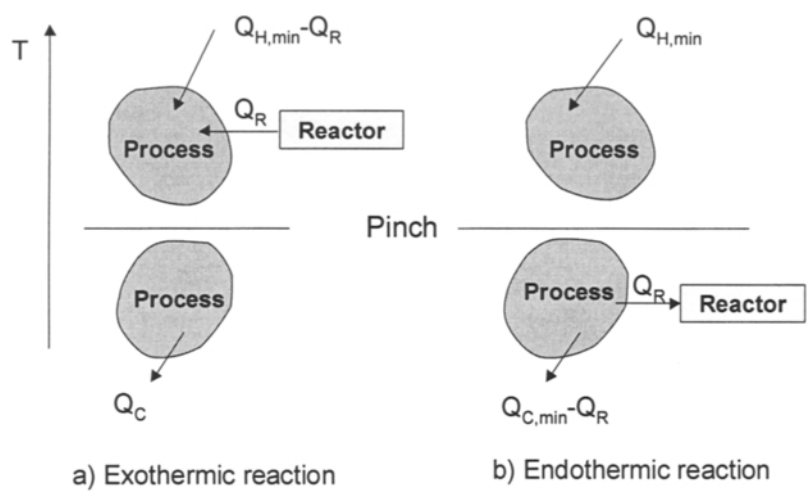

Figure 11.23 Appropriate placement of chemical reactors

In a similar way, the recommended placement of an endothermic reaction is below the Pinch (Figure 11.23b). This time the minimum cold requirements will diminish by the heat of reaction, such as $Q_{C,min} = Q_C - Q_R$. The integration should be done at the lowest temperature that still gives an economical reaction rate.

If the reactor placement is not appropriate, it is in general easier to change the process. Otherwise the revision of the whole reactor design is necessary. In this case the

system behaviour will be a significant factor in the reactor selection. The principle of local integration plays even a greater role. Safety and controllability requirements are much more harder for reactors than for separation units. It is therefore rational to use standard heat integration techniques with utility driven heat exchangers, which can act also as interface for export/import from the utility system. If the integration with process streams is feasible, providing trim heat exchangers for control ensures a more robust operation.

11.4 TOTAL SITE INTEGRATION

The concepts of Pinch Point Analysis can be extended from a single plant to an *industrial site*. Usually, several plants share the utility system, namely steam and water, and the same electricity supplier. The export/import of utilities via the site utility system is a simple way for integration, with significant economic advantages. For example, further expansion of the energy supply can be done in the central utility plant and distributed via the existing network. The optimisation of steam levels in individual plants is more profitable when the total site is considered.

The analysis of a site integration problem can be executed in diagrams known as *Total Site Profiles* (Linnhoff et al., 1994). Figures 11.24a-b present the Grand Composite Curves of individual plants. The GCC's are drawn in the classical *T-H* diagram, by freezing the 'pockets' where process-process recovery takes place, and by shifting the sink (above Pinch) and source (below Pinch) elements with $1/2\ \Delta T_{min}$ up and down, respectively. Then the shifted segments are combined in a Total Site Grand Composite Curve, with site source profile and site sink source profile, as shown in Fig. 11.24c.

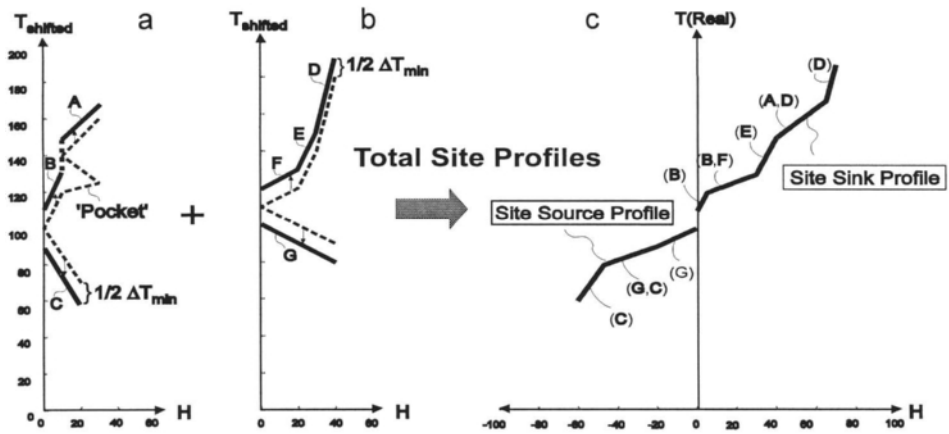

Figure 11.24 Total Site integration: constructing Source and Sink profiles from individuals GCCs (after Dohle and Linnhoff, 1993)

The representation of Total Site profiles can give a central view of the targets for fuel, turbine loads, and cooling, as it is shown in Fig. 12.25. The central cogeneration

plant supplies VHP steam that produces an amount of power W and HP steam, which further is fed in different processes noted here 1 to 6. In addition, there is a MP steam facility that recovers heat from certain processes and supplies to others. The excess heat is rejected to the site cooling water, which in turn is conditioned via cooling tower system.

Note that on the secondary right vertical axis, not the temperature, but the equivalent Carnot efficiency $\eta_C = 1 - T/T_0$ has been plotted. This second graph allows the designer the visualisation of the shaft work co-generated, proportional with the shaded area. This type of plot can be used to evaluate the benefit of integrating individual plants on site, before undergo major investments or process modification that can lead to significant saving in capital and energy.

Similarly, the problem of emissions can better be handled as a site integration problem. It is worth to note that the reduction in waste and effluents could increase the consumption in fuel, and as a consequence to increase gaseous emissions. The explanation is that larger steam consumption is needed for waste separations, which in turn is produced in fired boilers. Hence, there is a trade-off between process emissions and fuel related emissions.

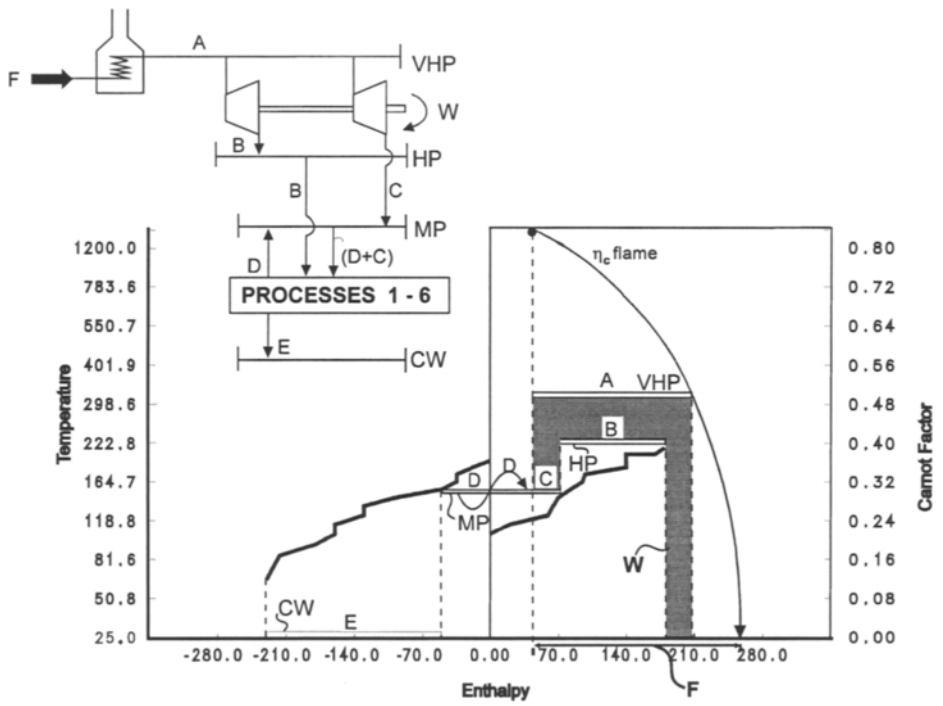

Figure 11.25 Total site targets for fuel, steam and power (after Dohle and Linnhoff, 1993)

11.5 SUMMARY

The most efficient energy saving can be obtained by examining the integration of different units in the context of the whole process rather than by improving individual performances. Appropriate Placement of units with respect to Pinch is the key concept in saving energy. Unit operations involving both sink and sources, as distillation columns and heat engines, must be placed on the same side of the Pinch, either above or below. Heat pumps should be placed across the Pinch. Otherwise, the correct placement for energy sources is above the Pinch, and of sinks below the Pinch.

Distillation is a major energy consumer. Saving opportunities can be obtained starting with the optimisation of energy around and inside the column, as by optimising the reflux, by appropriate feed conditioning, placement of side-heaters and coolers, etc. A finer assessment of different saving opportunities can be obtained by means of Column Grand Composite Curves. Heat pumping is a viable option for smaller temperature differences, and when cheap shaft work is available.

Thermal integrated columns offer significant savings, typically between 20-30%. The schemes with prefractionator are particularly interesting. Thermal coupled columns are promising, but still in research, although divided-wall column has known some success recently.

Exothermic reactions should be placed above the Pinch, while endothermic reactions below the Pinch, at the highest temperature possible. The appropriate placement should be considered among the criteria for chemical reactor selection.

Saving energy by very tight integration might enter in conflict with operability and controllability. The integration of design and control should be carefully examined.

Total Site Integration allows the identification of major opportunities for saving both energy and capital investment in new infrastructures. The approach involves careful analysis of the integrated plants by process simulation. Significant saving can be obtained by structural flowsheet modifications, or by reconsidering the site policy regarding energy and utilities.

11.6 REFERENCES

Bildea, C. S., A. C. Dimian, 1999, Interaction between design and control of a heat integrated distillation system with prefractionator, Trans. Inst. Chem. Engnrs., ChERD, vol. 77, Part A, 597-607

Dhole, V. R., B. Linnhoff, Distillation column targets, 1993, Comp. & Chem. Engng., vol. 17, No. 5/6, 549-560

Linnhoff, B., D. W. Townsend, D. Boland, G. F. Hewitt, B. Thomas, A. R. Guy, R. H. Marsland, 1994, User guide on process integration for the efficient use of energy, The Institution of Chemical Engineers, UK

Moran M. J., H. N. Shapiro, 2000, Fundamentals of Engineering Thermodynamics, 4th Edition, Wiley

Smith R., 1995, Chemical Process Design, McGraw-Hill

Chapter 12

CONTROLLABILITY ANALYSIS

12.1 Introduction

12.2 Modelling of dynamic systems
- 12.2.1 Mathematical models
- 12.2.2 Linear models
- 12.2.3 Linearization and perturbation variables
- 12.2.4 Laplace transform
- 12.2.5 Frequency response

12.3 Controllability analysis of SISO systems
- 12.3.1 Definitions
- 12.3.2 Characteristics of feedback control

12.4 Controllability analysis of MIMO systems
- 12.4.1 Stability
- 12.4.2 Directions in MIMO systems
- 12.4.3 Controllability measures

12.5 Decentralized control
- 12.5.1 Controllability measures for decentralised control
- 12.5.2 Methodology for input/output controllability analysis

12.6 References

12.1 INTRODUCTION

This chapter presents fundamental elements from the process control theory necessary in assessing the controllability of a design. It prepares also the computational tools used in Chapter 13 devoted to plantwide control. Prior knowledge is welcome. If the material is too difficult, the reader should go back to specialized undergraduate books. A concise presentation of the process control essentials viewed from process engineer's perspective has been recently published by Luyben & Luyben (1998). In the field of feedback control of multivariable systems with emphasis on controllability analysis we recommend the book of Skogetsad and Postletwhite (1998).

The controllability tools presented in here are based on the theory of linear systems, which is valid for relatively small disturbances around the stationary state. A non-linear approach, more suited for investigating the effect of large variations, will be developed in Chapter 13. The chapter starts with a brief introduction in process dynamics, followed by the properties of linear systems. The controllability analysis begins with SISO (single input/single output) systems and reviews the major concepts in feedback control. Then, the analysis is extended to MIMO (multi input/multi output) systems, with emphasis on decentralised control systems (multi SISO control loops), which is the most encountered in plantwide applications.

The preparation of a control strategy begins with a thorough steady-state analysis. Its objective is to investigate potential control structures (pairings), and to correct some weak points in the design, particularly in the magnitude of the manipulated variables. However, this is not sufficient. A dynamic controllability analysis is necessary to ensure a robust behaviour and satisfactory dynamic performance faced with given disturbances.

Naturally, the type of controller plays an important role. In this chapter we limit the analysis to classical PID controllers. These form over 90% of the control loops in industry. As mentioned, from a plantwide control viewpoint multi-SISO controllers are the most adapted. Naturally, we do not exclude more sophisticated MIMO control systems, as DMC or Model Based Control systems, but these are typically applied to stand-alone complex units, as FCC reactors, complex distillation units in refining, etc. Hence, the controllability analysis presented here aims more to get a conceptual insight in the dynamics of a process related to its design than to offer a high-performance control solution.

Outline of control system design

In the process control language the object upon a control system is applied is called often a 'plant'. This can be a single unit, or an assembly of several units, as two heat-integrated distillation units. However, when the control system design embodies the whole process and regards the interrelation between different units, we speak about plantwide control.

The design of a control system of a plant can be formulated as a procedure of several steps (Skogestad and Postletwaite, 1996):

1. Study the plant to be controlled and determine the control objectives.
2. Model the system and simplify the model, if necessary.
3. Analyse the model and determine its dynamic properties.
4. Decide which variables can be measured, which must be controlled, and which are manipulated variables. The last aspect implies an analysis of the available degrees

of freedom. In the most cases, the manipulated variables are the valves that can be inserted to vary flows of material streams or duties of energy streams.

5. Select the control configuration. In the case of multi SISO systems this step consists in the determining the pairing between controlled and manipulated variables.
6. Decide the type of controller to be used, for example P, PI or PID.
7. Specify the required performance of the control system.
8. Design the controller. In the case of a PID controller this step is equivalent to tuning the parameters.
9. Simulate the behaviour of the resulting controlled system.
10. Choose hardware and software for control system implementation.
11. Implement the control system, test and retune the control loops on-line.

Steps 8 and 9 are subject of process control courses. In practice, control systems are often designed considering only steps 1, 4, 5, 6, 10 and 11. This chapter focuses on systematic tools to assist the designer during steps 3 (*input-output controllability analysis*), 4, 5 and 6 (*control structure design*). Input-output controllability can be defined as the ability to achieve acceptable performance. For chemical plants, "performance" is regarded as reaching and maintaining desired equilibrium (set-point) values.

It should be noted that controllability is a property of the plant. Controllability can be improved by design changes. Therefore, the design of control systems might include a step 0, involving the design of the process itself. Controller and process should be considered as a unit. However, the process is more important. As Luyben noted (1998), we should see the Process Control with capital *P* and small *c*. A simple controller is often able to perform acceptable on a process that is easy controllable. By contrary, the finest controller could fail when applied to a poor design.

12.2 MODELLING OF DYNAMIC SYSTEMS

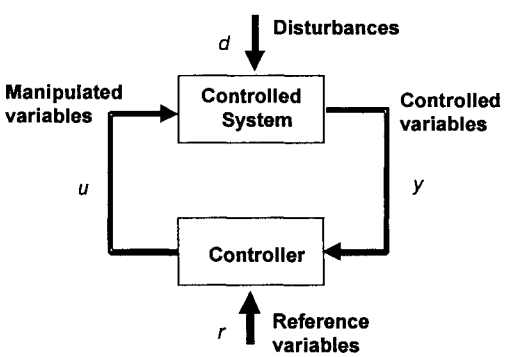

Figure 12.1 General structure of control systems

A dynamic system is described by a set of *state variables*. We are interested to keep some *controlled (output) variables* as constant as possible (the *regulator problem*), or to make them follow some desired trajectory in time, (the *servo problem*). We achieve these goals by changing some *manipulated (input) variables*. The device for adjusting the manipulated inputs to keep the controlled outputs at their desired values (*references* or *setpoints*) is called *controller*. There are also external variables that are not manipulated, but may influence the process dynamics by their inherent variations. They are called *disturbances*. The main job of a control system is to rejecting disturbances.

Throughout this chapter, we will use the following notations: x - state variables, u - manipulated inputs, d - disturbances, y - controlled variables, r - references.

12.2.1 Mathematical models

Nonlinear, *distributed parameter* systems are described by partial differential equations of the following form:

$$\frac{\partial x(\xi_i,t)}{\partial t} = f\left(x, \frac{\partial x(\xi_i,t)}{\partial \xi_i}, \frac{d^2 x(\xi_i,t)}{d\xi_i^2}, u(t), d(t), \xi_i\right)$$
$$y(t) = g\left(x(\xi_i,t)\right) \qquad (12.1)$$

The variables x are of intensive nature characterising the 'state' of a system, as temperature, pressure, and concentrations. The state variables are function of time, as well as of spatial coordinates ξ_i. The functions f and g are in general nonlinear.

The integration of the system 12.1 needs appropriate initial and boundary conditions (see also Chapter 4). For simulation purposes, the spatial coordinates in distributed parameter models must be discretised, for example, by finite differences, finite elements, or other techniques.

Lumped parameter systems are described by nonlinear differential-algebraic equations of the general form:

$$\frac{\partial x(t)}{\partial t} = f\left(x(t), u(t), d(t)\right)$$
$$y(t) = g(\,x(t)\,) \qquad (12.2)$$

with the initial condition $x(0) = x_0$.

Because the mathematical theory of nonlinear dynamic systems is complex, such models are used more for dynamic simulation purposes than for the analysis and design of control systems. Simpler models can be obtained by linearisation around a *nominal operating point*.

12.2.2 Linear models

Some issues from the theory of linear systems with immediate application in controllability analysis are further discussed. More details can be found in textbooks over control theory. The general form of linear models is:

$$\frac{dx(t)}{dt} = A \cdot x(t) + B \cdot u(t) + B_d \cdot d(t)$$
$$y(t) = C \cdot x(t) \tag{12.3}$$
$$x(0) = x_0$$

where A, B, B_d, and C are real matrices of appropriate dimension.

Sometimes both manipulated and disturbances are included in the input variables u. In this case, a simpler form of (12.3) is obtained:

$$\frac{d\,x(t)}{d\,t} = A \cdot x(t) + B \cdot u(t)$$
$$y = C \cdot x(t) \tag{12.4}$$

In the particular case of single-input/single-output (SISO) systems, the B and C matrices become column and row vectors, respectively:

$$\frac{d\,x(t)}{d\,t} = A \cdot x(t) + B \cdot u(t)$$
$$y = c^T \cdot x(t) \tag{12.5}$$

12.2.3 Linearization and perturbation variables

The nonlinear differential equations

$$\frac{d\,x(t)}{\partial\,t} = f\big(x(t), u(t), d(t)\big)$$
$$y(t) = g(\,x(t)\,) \tag{12.6}$$

can be transformed into linear differential equations by the following steps:

1. Find the nominal, steady-state operating point (x_s, u_s, y_s) by solving:

$$f\big(x_s, u_s\big) = 0$$
$$y_s = g(\,x_s\,) \tag{12.7}$$

2. Expand in Taylor series the nonlinear functions f and g, keeping only the linear factors:

$$f(x,u) = f(x_s,u_s) + \left.\frac{\partial f}{\partial x}\right|_s (x - x_s) + \left.\frac{\partial f}{\partial u}\right|_s (u - u_s) + \ldots \tag{12.8}$$

$$g(x) = g(x_s) + \left.\frac{\partial g}{\partial x}\right|_s (x - x_s) + \ldots$$

3. Substitute (12.8) in (12.9), observing that $\frac{d(x(t) - x_s)}{dt} = \frac{dx(t)}{dt}$:

$$\frac{d(x - x_s)}{dt} = \left.\frac{\partial f}{\partial x}\right|_s (x - x_s) + \left.\frac{\partial f}{\partial u}\right|_s (u - u_s) \tag{12.9}$$

and

$$y - y_s = \left.\frac{\partial g}{\partial x}\right|_s (x - x_s) \tag{12.10}$$

4. Introduce the perturbation (deviation) variables:

$$\tilde{x} = x - x_s, \tilde{u} = u - u_s, \tilde{y} = y - y_s \tag{12.11}$$

5. The linear model is:

$$\begin{aligned} \frac{d\tilde{x}(t)}{dt} &= A \cdot \tilde{x}(t) + B \cdot \tilde{u}(t) \\ \tilde{y} &= C \cdot \tilde{x}(t) \end{aligned} \tag{12.12}$$

where $A = \left.\frac{\partial f}{\partial x}\right|_s, B = \left.\frac{\partial f}{\partial u}\right|_s, C = \left.\frac{\partial g}{\partial x}\right|_s$ are Jacobian-type matrices.

Note: From now on, we will work with perturbation (deviation) variables. We will use the normal notation (*x, u, d, y,* without tilde ~).

Scaling

Consistent results in controllability analysis demand the use of *scaled* variables ($\hat{u}, \hat{d}, \hat{y}, \hat{r}$). Scaling consists of evaluating the magnitude of expected disturbances and reference changes, of available manipulated inputs, and of the allowed deviation of controlled outputs. Scaling is achieved by dividing each variable by its maximum expected or allowed change:

Δ_d - diagonal matrix containing the largest expected change in disturbances, $\delta d_{i,max}$

Δ_u - diagonal matrix containing the largest allowed input changes, $\delta u_{i,max}$

Δ_ε - diagonal matrix containing the largest allowed control errors, $\delta \varepsilon_{i,max}$

Δ_r - diagonal matrix containing the largest expected change of the reference values, $\delta r_{i,max}$.

The scaled model is obtained by expressing the unscaled variables in term of the scaled ones:

$$u = \Delta_u \hat{u} \ , \ d = \Delta_d \hat{d} \ , \ y = \Delta_\varepsilon \hat{y} \ , \ r = \Delta_\varepsilon^{-1} \Delta_r \hat{r} \tag{12.13}$$

The scaled model $\left(\hat{A}, \hat{B}, \hat{C}\right)$ is given by:

$$\hat{A} = A \ , \ \hat{B} = B \cdot \Delta_u \ , \ \hat{B}_d = B_d \cdot \Delta_d \ , \ \hat{C} = \Delta_\varepsilon^{-1} \cdot C \tag{12.14}$$

From now on, for more comfort, we will discard the sign ^ over the scaled variables.
In terms of scaled variables, the *control objective* is to keep the control error $|\varepsilon(t)| = |y(t) - r(t)| \le 1$, in spite of disturbances $|d(t)| \le 1$ and of reference changes $|r(t)| \le 1$, by using manipulated inputs $|u(t)| \le 1$.

12.2.4 Laplace transform

Laplace transformation allows an easier solution of ordinary differential equations. The Laplace transform of a function of time $f(t)$ is defined by:

$$L[f(t)] = \int_0^\infty f(t) \cdot e^{-st} dt \tag{12.15}$$

By this operation a time-dependent function is transformed into a function depending on the complex variable s.

Transfer matrix

When perturbation (deviation) variables are used, and the system is initially at steady state, the transfer function can be interpreted as the ratio between the Laplace transforms of the output and input variables:

$$y(s) = G(s) \cdot u(s) \tag{12.16}$$

A practical expression for the transfer matrix is obtained by applying the Laplace transform to the linear system (A, B, C):

$$\begin{aligned} sx(s) - x_0 &= Ax(s) + Bu(s) \\ y(s) &= Cx(s) \end{aligned} \tag{12.17}$$

After some algebraic manipulation, the Laplace transform of output vector is obtained as:

$$y(s) = C \cdot (sI - a)^{-1} \cdot x_0 + C \cdot (sI - A)^{-1} \cdot B \cdot u(s) \tag{12.18}$$

If the system is initially at steady state (x_0 = 0), the ratio between the Laplace transforms of output and input variables (the transfer matrix) becomes:

$$G(s) = C(sI - A)^{-1} B \tag{12.19}$$

The following observations are of significance:
1. For SISO systems, the *transfer function* can be calculated as $G(s) = c^T (sI - A)^{-1} b$.
2. For SISO systems, the transfer function is a *strictly proper* rational function, i.e. is ratio of two polynomials, the order of the denominator being larger than the order of the

numerator ($\lim_{s\to\infty} G(s) = 0$). For MIMO systems the transfer matrix contains strictly proper rational functions.

3. The disturbance transfer function (matrix), $G_d(s)$, can be defined in a similar manner. Then, the output of the liniar system

$$\frac{d\,x(t)}{d\,t} = A\cdot x(t) + B\cdot u(t) + B_d\cdot d(t) \tag{12.20}$$

$$y(t) = C\cdot x(t)$$

is given by:

$$y(s) = G(s)\cdot u(s) + G_d(s)\cdot d(s) \tag{12.21}$$

4. After transforming the equation into the Laplace domain and solving for output variables in term of s, we can transform back in the time domain by inverting the Laplace transform:

$$y(t) = L^{-1}[y(s)] \tag{12.22}$$

The most common method is called *partial fraction expansion.* The function to be inverted is written as a sum of simple functions:

$$y(s) = \sum_k y_k(s) \tag{12.23}$$

and

$$y(t) = \sum_k L^{-1}[y_k(s)] = \sum_k y_k(t)$$

Often, $y(s)$ appears as the ratio of two polynomials:

$$y(s) = \frac{Z(s)}{P(s)} = \frac{Z(s)}{(s-p_1)\cdot\ldots(s-p_N)} \tag{12.24}$$

which can be expressed as:

$$y(s) = \sum_k \frac{A_k}{(s-p_k)}, \text{ where } A_k = \lim_{s\to p_k}\left[(s-p_k)F(s)\right] \tag{12.25}$$

12.2.5 Frequency response

To give a physical interpretation of the transfer function, let consider a sinusoidal input to a linear and stable SISO system:

$$u(t) = u_0 \sin\omega t \tag{12.26}$$

where u_0 and ω are the magnitude and frequency, respectively. The output is also a sinusoid with the same frequency but shifted in phase (delayed) from the input:

$$y(t) = y_0 \sin(\omega t + \varphi) \tag{12.27}$$

The ratio y_0/u_0 and the phase shift φ can be obtained from the transfer function by inserting $s=j\omega$ and evaluating the magnitude and phase of the resulting complex number $G(j\omega)$:

$$\frac{y_0}{u_0} = |G(j\omega)| \quad \text{and} \quad \varphi = \angle G(j\omega) \tag{12.28}$$

$G(j\omega)$ is called the *frequency response* of the system described by $G(s)$. It shows how the system responds to sinusoidal inputs of frequency ω.

The magnitude of the frequency response, $|G(j\omega)|$ is called the *system gain.* Sometimes, the gain is given in units of decibel (dB) defined as A [dB] = 20 $\log_{10} A$. The argument of the complex number $\varphi = \angle G(j\omega)$ is called *phase.* A graphical representation is obtained by plotting the gain and the phase of the transfer function versus frequency (Bode diagram). As an example, Fig. 12.2 presents the Bode diagram for the transfer function $G(s) = \dfrac{s+2}{s^3+2s^2+3s+4}$.

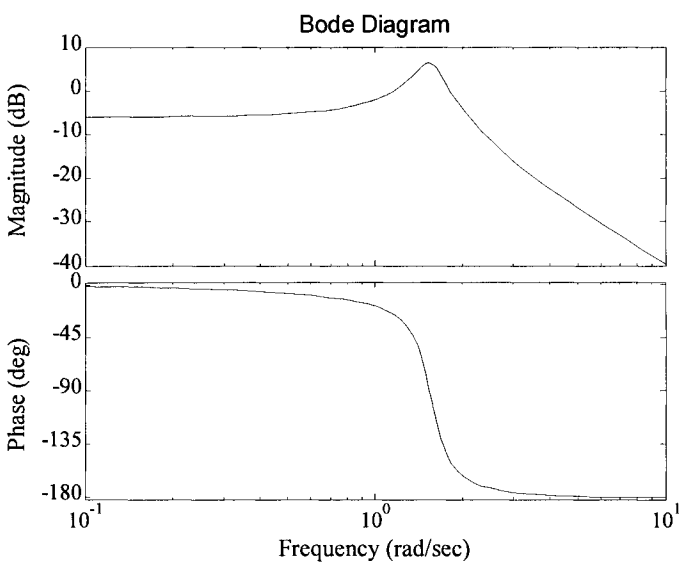

Figure 12.2. Bode diagram

When interpreting the frequency response, we will adopt the following point of view: high frequency means fast changing inputs; low frequency (in particular $\omega = 0$) signifies steady state. In the case of MIMO sistems, $G(j\omega)$ is a matrix. Its elements, $g_{ij}(j\omega)$ represent the sinusoidal response from input j to output i. The overall response to simultaneous input signals with the same frequency in several input channels is equal to the sum of individual responses:

$$y_i(\omega) = g_{i1}(j\omega)u_1(\omega) + g_{i2}(j\omega)u_2(\omega) + \ldots = \sum_j g_{ij}(j\omega)u_j(\omega) \tag{12.29}$$

where $y(\omega)$ denotes a sinusoidal signal with frequency ω.

12.3 CONTROLLABILITY ANALYSIS OF SISO SYSTEMS

12.3.1 Definitions

Figure 12.3 presents the block diagram of a real process in open loop. The plant is characterised by the transfer function $\boldsymbol{G}$ that links the inputs u and the outputs y', so that $y' = Gu$. A real process is also characterised by disturbances d. Their action on the output can be formally expressed by a transfer function $\boldsymbol{G_d}$ so that $y'' = G_d u$. The total output is $y = y' + y''$. It is desired to keep the output y at the reference r, whose values might change in order to fulfil operational requirements. The action of a setpoint change is similar to a disturbances characterised by a transfer function R. In consequence, the *control error e* may be written as:

$$e = y - r = Gu + G_d d - Rr \tag{12.30}$$

With these elements the definition of *input-output controllability* can be formulated as follows:

> Controllability is the ability to achieve acceptable control performance; that is, to keep the outputs (y) within specified bounds or displacements from their references (r), in spite of unknown but bounded variations, such as disturbances (d) and plant changes, using available inputs (u) and available measurements (y_m and d_m).

In other words, a plant is controllable if a controller exists (connecting plant measurements and plant inputs) that gives acceptable performance for all expected plant variations. It should be kept in mind that the controllability is independent of the controller type, but is a property of the plant (process) alone. It can only be affected by design changes.

The above definition of controllability does not specify the allowed bounds for the displacements or the expected variations in the disturbances; that is, no definition of the desired performance is included.

When we discuss controllability, we assume that the variables and models have been scaled as previously outlined, so the acceptable performance is defined as:

- Keep the control error $|\varepsilon(t)| = |y(t) - r(t)| \le 1$, in spite of disturbances $|d(t)| \le 1$ and reference changes $|r(t)| \le 1$ using manipulated inputs $|u(t)| \le 1$.

This definition can be interpreted from a frequency response point of view, i.e. considering sinusoidal disturbance $d(t) = d_0 \sin \omega t$. We then have:

- At each frequency the performance requirement is to keep the control error $|e(\omega)| \le 1$, for any disturbance $|d(\omega)| \le 1$ and any reference $|r(\omega)| \le 1$, using an input $|u(\omega)| \le 1$.

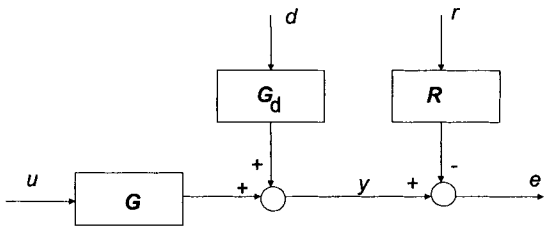

Figure 12.3 Block diagram of the plant

Feedback control

Figure 12.4 illustrates the principle of a feedback control system. The control system compares the value of the controlled variable (y) with the desired one (r). The control error is used to calculate the manipulated variable u that will bring the controlled variable y as close as possible to the setpoint r. The action of controller can be characterised by the transfer function K, so that the controller output / plant input is:

$$u = K(s)(r - y) \tag{12.31}$$

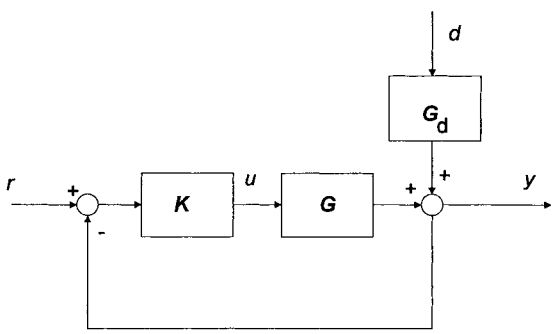

Figure 12.4 Block diagram of the control system

The plant model without control is

$$y = G(s)u + G_d(s)d \tag{12.32}$$

After replacing y = r, the Eq. 12.32 can be solved for the required value of the manipulated variable u as follows:

$$u = G^{-1}G_d d + G^{-1}r \tag{12.33}$$

From Eq. 12.33 it seems that perfect control is possible, if the disturbances d are known, and the models G_d and G are available. However, the disturbances G_d can not be measured, and a perfect plant model G is never available. Moreover, the plant model G must be inverted. For this reason, all factors that make difficult the calculation of G^{-1} (for example, a near-singular matrix G) are detrimental for control.

When the controller is implemented, the open-loop response becomes:

$$y = GKr + G_d d \tag{12.34}$$

The closed-loop response under feedback control becomes:

$$y = (I + GK)^{-1} GKr + (I + GK)^{-1} G_d d \tag{12.35}$$

The following notation and terminology are used:

- Loop transfer function: $L = GK$ (12.36)
- Sensitivity function: $S = (I + GK)^{-1} = (I + L)^{-1}$ (12.37)
- Complementary sensitivity function: $T = (I + GK)^{-1} GK = (I + L)^{-1} L$ (12.38)

The comparison of open and closed-loop responses (12.37) and (12.38) reveals that the sensitivity function S gives the reduction of sensitivity to disturbances, achieved by feedback control. It is evident that S =0 and T = 1 are desirable. In this way, the output follows perfectly the setpoint, and the process is not affected by disturbances. Both can be achieved by large controller gain, that is $K \to \infty$. However, large controller gain leads to instability, which sets limits on the achievable closed-loop performance.

12.3.2 Characteristics of feedback control

Bandwidth and crossover frequency

Loosely speaking, *bandwidth* may be defined as the frequency range [ω_1, ω_2] over which control is effective. In most cases we require tight control at steady state. Since ω_1=0 we call ω_2 the bandwidth. The word 'effective' may be interpreted in different ways, giving rise to different definitions of bandwidth. The interpretation we use is that control is effective if we obtain some benefit in terms of performance. For example, considering the interpretation of the sensitivity function S, we arrive at the following definition:

- The closed-loop *bandwidth* ω_B is the frequency where $|S(j\omega)|$ first crosses $1/\sqrt{2} = 0.707 \ \ (\approx -3dB)$ from below.
- The *gain crossover frequency*, ω_c, defined as the frequency where $|L(j\omega)|$ first crosses 1 from above, is also used to define closed-loop bandwidth. It has the advantage of being simple to compute, and usually gives a value close to ω_B.

Stability

Here we adopt the following definition valid for linear systems: a system is 'stable' if bounded input variations produce bounded output variations as t $\rightarrow\infty$; otherwise the system is unstable (Ogunnaike & Ray, 1994). One of the main issues in designing feedback controllers is stability. Let consider the response of a closed-loop system under proportional control, as deviation in output y vs. time (Fig. 12.5). If the controller gain is moderate ($K_c<K_u$) then y goes to zero after some oscillations. By increasing gain the oscillations intensify up to a point where they become sustained. This point correspond to the ultimate gain $K_c=K_u$. For $K_c>K_u$ the system becomes unstable.

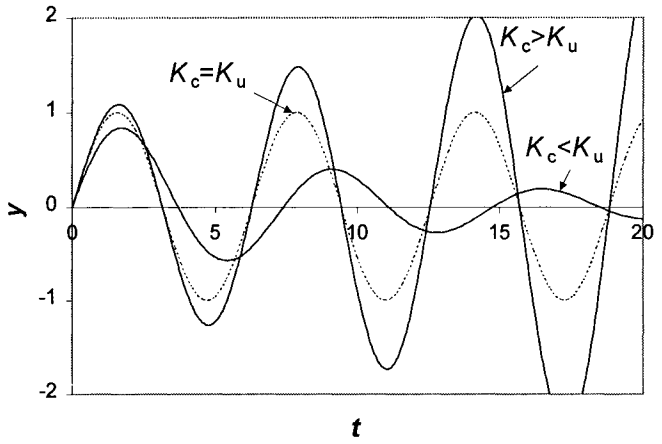

Figure 12.5 Typical time-domain response of stable and unstable systems

Two methods are commonly used to determine closed-loop stability:

1. Evaluate the poles of the closed-loop system, i.e. the roots of the function $1+L(s)=0$). The system is stable if and only if all the closed-loop poles are in the open Left Half Plane (LHP).
2. Plot the frequency response of $L(j\omega)$ in Bode diagram (Fig. 12.6). For open-loop stable systems $\angle L(j\omega)$ falls with frequency such that $\angle L(j\omega)$ crosses –180° only once at the frequency ω_{180}. *Bode's stability criterion* says that the closed-loop system is stable if and only if the loop gain $|L|$ is less than 1 at this frequency.

$$\left|L(j\omega_{180})\right| < 1 \tag{12.39}$$

- The *gain margin* GM is defined as:

$$GM = 1/\left|L(j\omega_{180})\right| \tag{12.40}$$

Thus GM is the factor by which the loop gain $|L(j\omega)|$ may be increased before the closed-loop system becomes unstable. The GM is thus a safeguard against steady-state gain uncertainty. Typically, we require GM>2.

- The *phase margin* is defined as:

$$PM = \angle L(j\omega_c) + 180 \tag{12.41}$$

PM tells how much phase-lag (time delay) we can add to *L(s)* at frequency ω_c before the phase at this frequency becomes –180 °, which corresponds to closed-loop instability. Typically, we require PM>30 °. It is important to note that by decreasing ω_c (resulting in a slower response) the system can tolerate larger time delay errors.

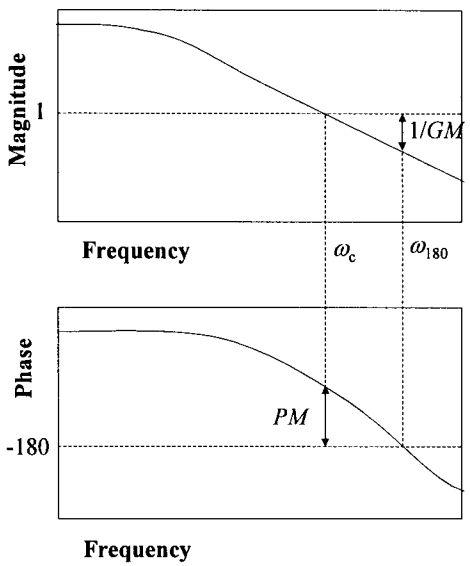

Figure 12.6 Bode diagram showing gain and phase margin

Performance of the control systems

Figure 12.7 shows some common measures used to assess the closed-loop performance, when a step setpoint change is applied. The *offset* represents the difference between the final, steady state values of the setpoint and the controlled variable. The *rise time* is the time from the change of the setpoint, until the controlled variable reaches the first time the new setpoint. The *overshoot* shows by how much the deviation exceeds the setpoint during the initial transient period. The *decay ratio* is the ratio between the magnitudes of two neighbour peaks in the response. The *settling time* is the time needed for the output to attain a nearly constant value, for example the final value +/- 2%. For a well-designed control system, the offset is zero, the decay ratio is about 1/4, and the rise time, overshoot and settling time have small values.

In addition, the performance may be evaluated by integrated the squared control error over some time interval, $ISE = \int_0^\infty [y(t) - r(t)]^2 dt$

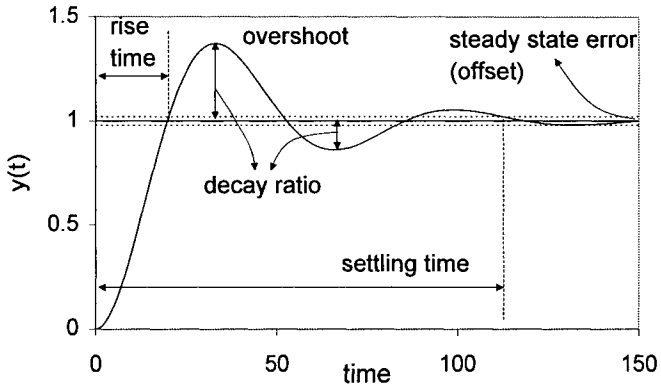

Figure 12.7. Performance of control systems

Limitations imposed by Right-Half-Plane (RHP)-zeros and time delays

RHP-zeros typically appear when we have competing effects of slow and fast dynamics. For example, the plant:

$$G(s)=\frac{1}{s+1}-\frac{2}{s+10}=\frac{-s+8}{(s+1)(s+10)} \tag{12.42}$$

has a RHP-zero at $z = 8$.

For a stable plant with n_z RHP-zeros, it may be proven that the output in response to a step change in input will cross zero (its initial value) n_z times. We have inverse response that is detrimental for control, because the controlled variable moves, initially, in the wrong direction. Therefore, in this case fast control is impossible.

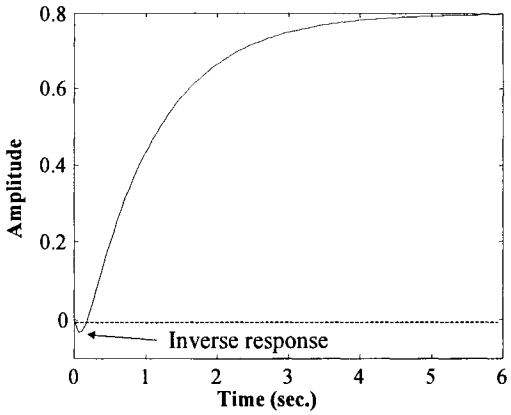

Figure 12.8 Inverse response

It is well known from classical root-locus analysis that as the feedback gain increases towards infinity, the closed-loop poles migrate to the positions of open-loop zeros. Thus, the presence of RHP-zeros implies high-gain instability.

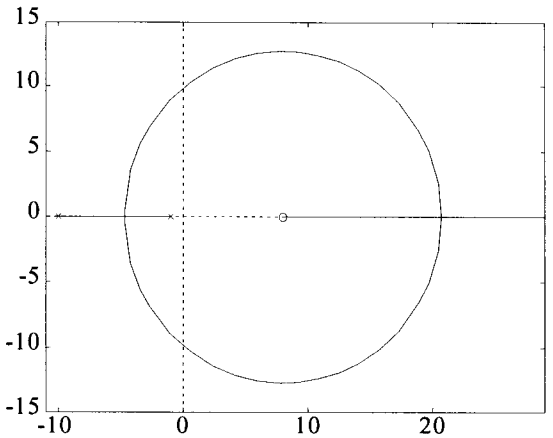

Figure 12.9 Root-locus plot

The polynomial approximation of the time delay (Padé) contains a RHP zero:

$$G(s) = e^{-s\theta} = \frac{e^{-s\frac{\theta}{2}}}{e^{s\frac{\theta}{2}}} \approx \frac{1 - s\frac{\theta}{2}}{1 + s\frac{\theta}{2}} \tag{12.43}$$

showing that time delays have detrimental effects, similar to RHP-zeros.

Limitations imposed by input constraints

In all physical systems there are limits to the changes that can be made to the manipulated variables. We want to know if the expected disturbances can be rejected and if we can track the reference changes, while maintaining $|u(t)| < 1$?

We replace $y = Rr$ in plant model $y = G(s)u + G_d(s)d$ and solve for the required input:

$$u = G^{-1}Rr - G^{-1}G_d d \tag{12.44}$$

For disturbance rejection ($r=0$, $d(\omega)=1$) the requirement $|u(\omega)| < 1$ is equivalent to:

$$\left|G^{-1}(j\omega)G_d(j\omega)\right| < 1 \quad \forall\omega \tag{12.45}$$

For setpoint tracking ($r=1$, $d=0$) the requirement $|u(\omega)| < 1$ is equivalent to:

$$\left|G^{-1}(j\omega)R\right| < 1 \quad \forall\omega < \omega_r \tag{12.46}$$

In addition, for an unstable plant with a real RHP-pole at $s=p$ we approximately need:

$$|G| > |G_d| \quad \forall \omega < p \tag{12.47}$$

Otherwise, the input will saturate when there is a sinusoidal disturbance $d(t) = \sin \omega t$, and we may not be able to stabilize the plant. Note that the frequency p may be larger than the frequency ω_d at which $|G_d(j\omega_d)| = 1$.

EXAMPLE 12.1 Controllability analysis of a chemical reactor

In this exercise, we will evaluate the controllability of a CSTR with heating jacket (Fig. 12.10). The reaction $A \rightarrow B$ is first-order, irreversible and moderate exothermic. Since the heat of reaction is not enough to achieve a temperature that gives high conversion, heat is provided by pressurised hot water (inlet temperature 383 K). Temperature measurements follow a first order dynamics with a time constant of 60 s. Valve dynamics is represented by first order elements with a time constant of 30 s. Study the controllability property of the SISO loop keeping the reactor temperature at set-point by manipulating the hot-water flow rate. Disturbances in reactor inlet temperature and reactor inlet concentration are expected.
The nominal values of the input variables are:
$F_0 = 0.006 \quad m^3/s$ feed flow rate, $c_0 = 0.84 \quad kmol/m^3$ feed concentration
$T_0 = 333\,K$ feed temeperature, $F_c = 0.003 \quad m^3/s$ heating agent flow rate

The following design data are known;
$V = 2\,m^3$ reactor volume, $\rho = 670\,kg/m^3$ density
$k_0 = 3.547 \cdot 10^9\,s^{-1}$ pre-exponential factor, $\frac{E}{R} = 10000\,K$ Arrhenius temperature
$\Delta H_R = -72.95 \cdot 10^6\,J/kmol$, heat of reaction, $C_p = 2445\,J/(kg \cdot K)$ specific heat
$V_c = 0.2 \quad m^3$ jacket volume, $UA = 5438\,W/K$ heat-transfer capacity
$C_{pc} = 4185\,J/(kgK)$ heating agent specific heat, $\rho_c = 1000\,kg/m^3$ heating agent density
$T_{c,in} = 383\,K$ heating agent inlet temperature

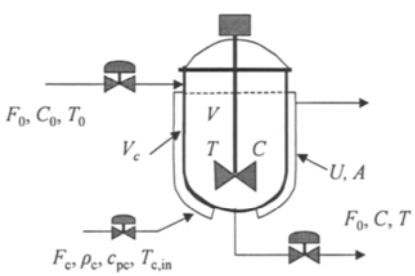

Figure 12.10 Physical scheme and notations for the control of a CSTR

Solution

The dynamic model consists of mass and energy balance:

$$V\frac{dC}{dt} = F_0(C_0 - C) - Vk_0 \exp\left(-\frac{E}{RT}\right)C$$

$$\rho C_p V\frac{dT}{dt} = F_0\rho C_p(T_0 - T) + V(-\Delta H_r)k_0 \exp\left(-\frac{E}{RT}\right)C + UA\left(T_c - T\right)$$

$$\rho_c C_{pc} V_c \frac{dT_c}{dt} = \rho_c C_{pc} F_c \left(T_{cin} - T_c\right) - UA\left(T_c - T\right)$$

The steady state operating point is obtained by setting the time derivatives to zero, and solving the resulting set of algebraic equations, $f(x,u,d) = 0$:

$c_S = 0.397 \quad kmol/m^3$, reactor concentration

$T_S = 361.2 \quad K$, reactor temperature

$T_{c,S} = 376.4 \quad K$, jacket temperature

Linearization around steady state gives the linear model:

$$\frac{dx}{dt} = \frac{d}{dt}\begin{bmatrix} c \\ T \\ T_c \end{bmatrix} = A\cdot\begin{bmatrix} c \\ T \\ T_c \end{bmatrix} + B\cdot\left[F_c\right] + B_d\begin{bmatrix} c_0 \\ T_0 \end{bmatrix}$$

$$y = T = C\cdot\begin{bmatrix} c \\ T \\ T_c \end{bmatrix}$$

where

$$A = \begin{bmatrix} -6.3\cdot10^{-3} & -1.19\cdot10^{-4} & 0 \\ 0.149 & -1.23\cdot10^{-4} & 1.66\cdot10^{-3} \\ 0 & 6.5\cdot10^{-3} & -2.15\cdot10^{-2} \end{bmatrix}$$

$$B = \begin{bmatrix} 0 \\ 0 \\ 33.0 \end{bmatrix}; \quad B_d = \begin{bmatrix} 3\cdot10^{-3} & 0 \\ 0 & 3\cdot10^{-3} \\ 0 & 0 \end{bmatrix}; \quad C = \begin{bmatrix} 0 & 1 & 0 \end{bmatrix}$$

Using scaled variables, the transfer function representation is given by:

$$y(s) = G(s)u(s) + G_d(s)d(s)$$

where

$$G(s) = \frac{\Delta_u}{\Delta_\varepsilon}C\left(sI - A\right)^{-1}B = \frac{6.84\cdot10^{-5}s + 4.34\cdot10^{-7}}{s^3 + 2.79\cdot10^{-2}s^2 + 1.44\cdot10^{-4}s + 2.75\cdot10^{-7}}$$

$$G_d(s) = \frac{\Delta_d}{\Delta_\varepsilon} C(sI - A)^{-1} B_d = \frac{\begin{bmatrix} 1.5 \cdot 10^{-2} s^2 + 4.18 \cdot 10^{-4} s + 2.05 \cdot 10^{-6} \\ 1.88 \cdot 10^{-5} s + 4.03 \cdot 10^{-7} \end{bmatrix}}{s^3 + 2.79 \cdot 10^{-2} s^2 + 1.44 \cdot 10^{-4} s + 2.75 \cdot 10^{-7}}$$

where

$\Delta_\varepsilon = 2K$, $\Delta_u = 0.0025\ m^3/s$, $\Delta_d = \begin{bmatrix} 10\ K & 0 \\ 0 & 0.084\ kmol/m^3 \end{bmatrix}$ are matrices containing the scaling factors.

The magnitude of the transfer functions **G** and $\mathbf{G_d}$ is plotted in Fig. 12.11 as function of frequency. At steady state, the magnitude of the both disturbance transfer functions exceed 1, therefore feedback control is necessary. The rejection of disturbance in feed concentration seems to be possible although with some difficulties, because $|G| > |G_{d,2}|$ but the difference is very small. In exchange it can be seen that the manipulated variable is not big enough to reject disturbances in feed temperature ($|G| < |G_{d,1}|$). The analysis predicts problems with the rejection this disturbance, and the necessity to review the design. Figure 12.12 shows the closed loop response, when the feed temperature is reduced from 333 K to 328 K. The controller succeeds to reduce the error to less than 2 K. However, the heating flow rate has to be increased from 0.003 m^3/s to 0.09 m^3 / s, that is by a factor of 30! This cannot be realized in practice.

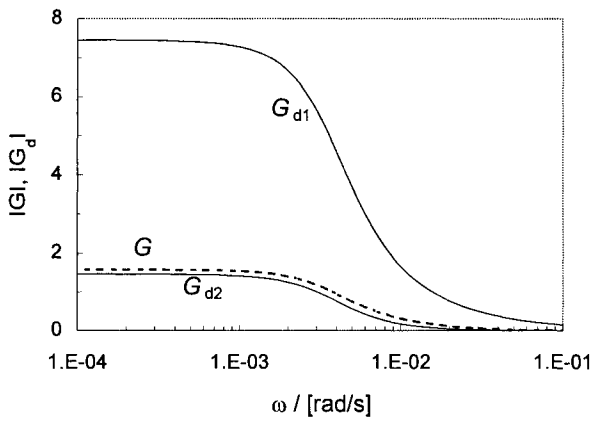

Figure 12.11 Magnitude of transfer functions for reactor cooling system, and disturbances (1- reactor inlet temperature, 2- reactor inlet concentration) vs. frequency

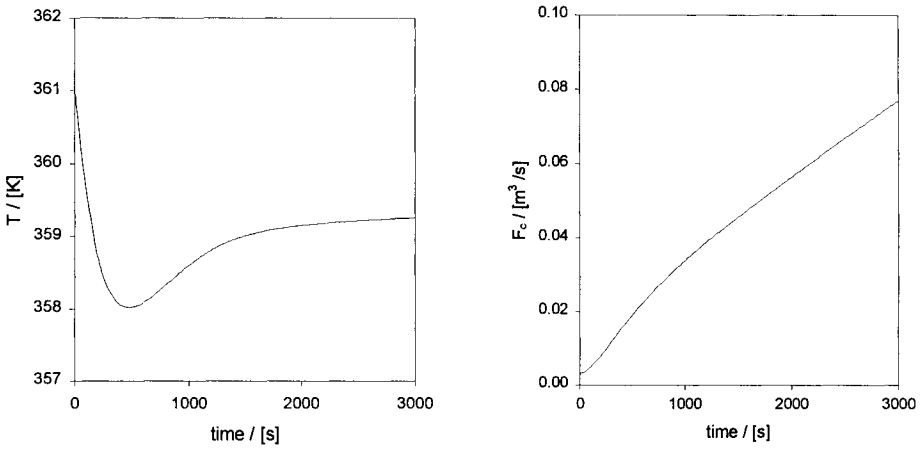

Figure 12.12 Left: Closed-loop response of the reactor temperature to a disturbance of 5 K in feed temperature; Right: Variation of the hot-water flow rate

In the second part we will demonstrate that the controllability can be improved by changing the design. Instead hot water we use hot oil with the temperature $T_{c,in} = 473$ K. Fig. 12.13 shows the new situation. Now both disturbances transfer functions are under the process function up to moderate frequencies. Disturbance rejection is possible, meaning that there is power enough in the external heating source that is less vulnerable to disturbances in feed temperature. However, fast temperature disturbance cannot be rejected at frequencies $\omega > 5 \cdot 10^{-3}$ rad/s where $|G| < |G_{d,2}|$, but unlikely in practice.

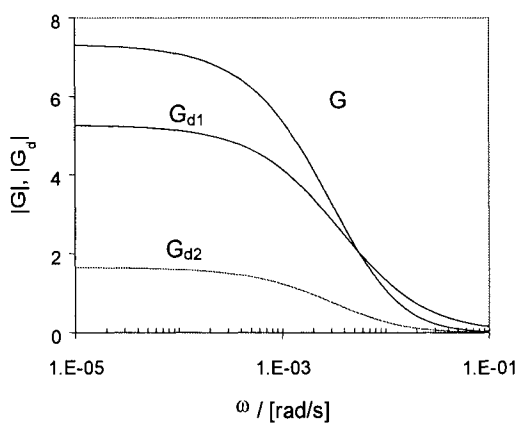

Figure 12.13 Process and disturbances transfer functions with hot oil as thermal agent

Hence, the process becomes controllable. Fig. 12.14 shows closed-loop simulation for 10 K decrease in the feed temperature. The results confirm the controllability analysis

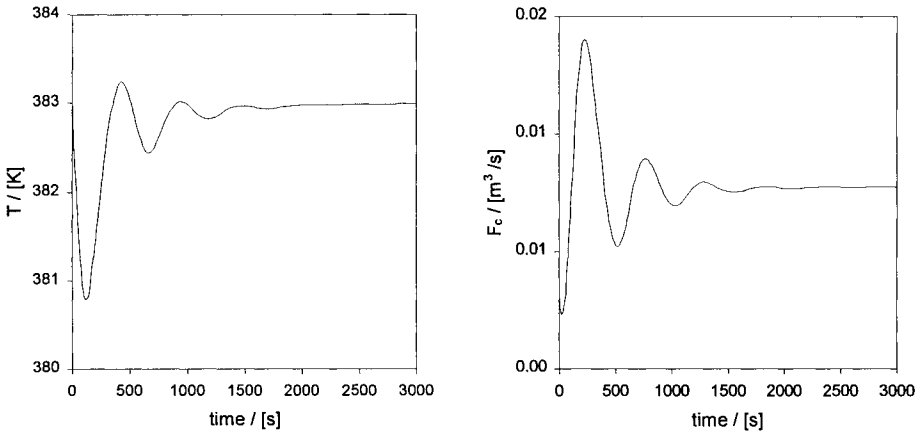

Figure 12.14 Closed-loop simulation results, for decrease of 10 K in the feed temperature.

12.4 CONTROLLABILITY ANALYSIS OF MIMO SYSTEMS

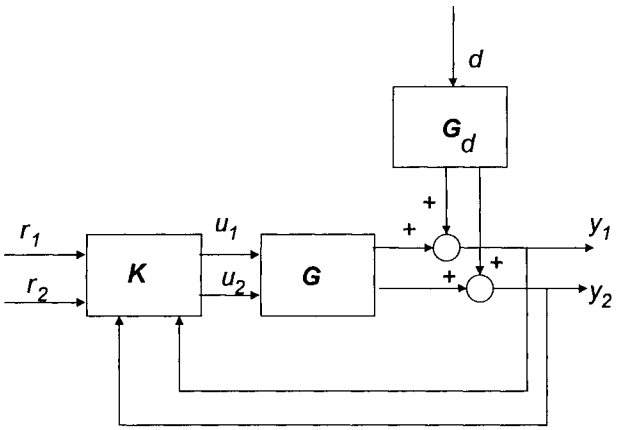

Figure 12.14 MIMO control system

In a multi-input multi-output (MIMO) control system (Fig. 12.14), there are several controlled variables (vector **y**) that should be kept on set-points (vector **r**) faced to disturbances (vector **d**) by means of appropriate manipulated variables (vector **u**). The feedback controller **K** provides the algorithm that will ensure the link between the manipulated (inputs) and controlled (outputs) variables. In this chapter we will consider a decentralised control system that makes use of multi-SISO control loops, which means that a single controlled variables is controlled by a single manipulated variable. This arrangement is typical for plantwide control purposes. However, there will be interactions between different loops. These interactions can be detrimental, or can bring advantages. Therefore, the assessment of interactions is a central issue in the analysis of MIMO systems.

12.4.1 Stability

The input/output dependency in a linear MIMO system can be described by the following relation:

$$\mathbf{y}(s) = \mathbf{G}(s)\mathbf{u}(s) + \mathbf{G}_d(s)\mathbf{d}(s) \tag{12.48}$$

This time **G**(s) and $\mathbf{G}_d$(s) are matrices that define the gain function of outputs with respect to the inputs and disturbances. If a multivariable controller is used the closedloop equation for (12.35) becomes:

$$\mathbf{y} = (\mathbf{I} + \mathbf{GK})^{-1}\mathbf{GKr} + (\mathbf{I} + \mathbf{GK})^{-1}\mathbf{G}_d\mathbf{d} \tag{12.49}$$

where now **K** designates a multivariable controller.

Again, poles and zeros are important for evaluating stability and controllability properties of the physical system. To find the poles of an open-loop MIMO system one can use the transfer function matrix or the state-space description. They are related by:

$$\mathbf{G}(s) = \frac{[\mathbf{C}Adj(s\,\mathrm{I} - \mathbf{A})\mathbf{B}]}{|(sI - \mathbf{A})|} \tag{12.50}$$

The poles of the transfer function and the eigenvalues of the equivalent system matrix in the state-space form are the same. The knowledge of poles is linked with stability. A multivariable system is stable if all the poles of the transfer function matrix lie in the left-half (LHP) plane; otherwise it is unstable.

The calculation of zeros is more subtle. Suppose that the transfer function matrix is square. The appropriate definition is that multivariables zeros are the poles of the inverse of the transfer function matrix (Ogunnaike & Ray, 1994):

$$\mathbf{G}^{-1}(s) = \frac{Adj\mathbf{G}(s)}{|\mathbf{G}|} \tag{12.51}$$

Thus, the roots of the equation $|\mathbf{G}(s)| = 0$ are the zeros of the determinant transfer function matrix **G**(s). For a non-square matrix the zeros of **G**(s) are those values that reduce its rank.

For closed-loop systems the characteristic equation for finding the poles is:

$$\det[\mathbf{I} + \mathbf{G}(s)\mathbf{K}(s)] = 0 \tag{12.52}$$

If any of the roots of the above equation are in the RHP the system is closed-loop unstable. The treatment of this problem by Nyquist or root locus plot is can be found in Luyben (1990).

To illustrate the topics of this section we will use as example a distillation column for the high purity separation of a benzene/toluene mixture. The following transfer function model in scaled variables represents the column's dynamics (Dimian, Bildea & Kiss, 2001):

$$\begin{bmatrix} x_D \\ x_B \end{bmatrix} = \frac{1}{7.9s+1}\begin{bmatrix} 2115 & -3045 \\ -2387 & 3495 \end{bmatrix} \cdot \begin{bmatrix} L \\ Q \end{bmatrix} + \frac{1}{7.9s+1}\begin{bmatrix} 403 \\ -469 \end{bmatrix} \cdot [F] \tag{12.53}$$

The system is stable because it has only one pole at -1/7.9 in LHP.

12.4.2 Directions in MIMO systems

For a SISO system for which $y = Gu$ the gain at a given frequency is:

$$\frac{|y(\omega)|}{|u(\omega)|} = \frac{|G(j\omega)u(\omega)|}{|u(\omega)|} = |G(j\omega)| \tag{12.54}$$

Thus, in a SISO system the gain depends on frequency, but is independent of the input magnitude.

For MIMO systems, the inputs and outputs are vectors, and therefore we need to "sum up" the magnitudes of the elements. If we select the vector 2-norm:

$$\frac{\|y(\omega)\|_2}{\|u(\omega)\|_2} = \frac{\|G(j\omega)u(\omega)\|}{\|u(\omega)\|} = \frac{\sqrt{y_{10}^2 + y_{20}^2 + \ldots}}{\sqrt{u_{10}^2 + y_{20}^2 + \ldots}} \tag{12.55}$$

The gain depends on frequency ω, it is independent of the input magnitude $\|u(\omega)\|_2$, but it depends on the *direction* of the input.

For the above distillation process, the steady state (s = 0) transfer matrix is $G = \begin{bmatrix} 2115 & -3045 \\ -2387 & 3495 \end{bmatrix}$; Consider the following inputs, having the same magnitude $\|u\|_2$=1, but different directions:

$$u_1 = \begin{bmatrix} 1 \\ 0 \end{bmatrix}; u_2 = \begin{bmatrix} 0 \\ 1 \end{bmatrix}; u_3 = \begin{bmatrix} 0.707 \\ 0.707 \end{bmatrix}; u_4 = \begin{bmatrix} 0.707 \\ -0.707 \end{bmatrix}$$

The corresponding output vectors are:

$$y_1 = \begin{bmatrix} 2115 \\ -2387 \end{bmatrix}; y_2 = \begin{bmatrix} -3045 \\ 3495 \end{bmatrix}; y_3 = \begin{bmatrix} -657 \\ 783 \end{bmatrix}; y_4 = \begin{bmatrix} 3648 \\ -4159 \end{bmatrix}$$

with the 2-norms:

$$\|y_1\|_2 = 3189; \|y_2\|_2 = 4635; \|y_3\|_2 = 1022; \|y_4\|_2 = 5532$$

12.4.3 Controllability measures

The controllability measures described in this section have a more general character. Measures applicable for square plants and decentralised control will be discussed in the next subchapter. The operations on matrices described below can be done easily with MATLAB, a specialised tool for analysing process control problems.

A. Singular Value Decomposition

Any matrix $G \in C^{l \times m}$ may be factorised by *singular value decomposition* (SVD):

$$G = U \cdot \Sigma \cdot V^H \tag{12.56}$$

where the matrices $U \in C^{l \times l}$ and $V \in C^{m \times m}$ are unitary ($U^{-1} = U^H$). The matrix $\Sigma \in C^{l \times m}$ has the following structure:

$$\Sigma = \begin{bmatrix} \Sigma_1 \\ 0 \end{bmatrix} \quad l \geq m$$
$$\Sigma = \begin{bmatrix} \Sigma_1 & 0 \end{bmatrix} \quad l \leq m \tag{12.57}$$

$$\Sigma_1 = diag\{\sigma_1, \sigma_2, \ldots, \sigma_k\}, \quad k = \min(l, m) \tag{12.58}$$

$$\sigma_k \in R^+$$

$$\bar{\sigma} \equiv \sigma_1 \geq \sigma_2 \geq \ldots \geq \sigma_k \equiv \underline{\sigma}$$

The unitary matrices U and V form orthonormal bases for the column (output) space and the row (input) space of G. The column vectors of u, denoted u_i are called *output singular vectors*. The columns of V, denoted v_i, are called *input singular vectors*.
Because:

$$G \cdot V = U \cdot \Sigma \tag{12.59}$$

for the *i-th* column:

$$G \cdot v_i = \sigma_i \cdot u_i \tag{12.60}$$

In other words, if the input has the direction of the *i-th* input singular vector v_i, then the output is in the direction of the corresponding output singular vector u_i, and the gain is equal to the corresponding singular value σ_i. Hence, the highest gain (for any input direction) is given by the maximum singular value ($\bar{\sigma}$), while the lowest gain is given by the minimum singular value ($\underline{\sigma}$).
For the distillation column example:

$$G(0) = \begin{bmatrix} -0.66 & 0.75 \\ 0.75 & 0.66 \end{bmatrix} \begin{bmatrix} 5626 & 0 \\ 0 & 21.95 \end{bmatrix} \begin{bmatrix} -0.57 & 0.82 \\ 0.82 & 0.57 \end{bmatrix}$$

This makes sense from physical point of view. The purity of products is sensitive (large singular value σ_1 = 5626) to simultaneous decrease of reflux and increase of boilup (input direction $[-0.57\ 0.82]^T$), which results in decreasing top purity and increasing bottom purity (output direction $[-0.66\ 0.75]^T$). However a simultaneous increase of reflux and boilup (in the input direction $[0.57\ 0.82]^T$) does not contribute much to purity increase (output direction $[0.66\ 0.75]^T$, singular value ($\sigma_1 = 21.95$)).

Minimum singular value

The minimum singular value[1] of the plant, $\underline{\sigma}(G(j\omega))$ is a useful measure for evaluating the feasibility to achieve acceptable control without input saturation. For scaled variables, we can achieve an output magnitude of at least $\underline{\sigma}(G)$ in any output direction, with a manipulated input of unit magnitude.

The requirement is that $\underline{\sigma}(G) > 1$ and preferably as large as possible. Minimum singular value can be used for the selection of the controlled outputs from a list of candidates paired with given inputs. It is desirable to have as outputs those that correspond to the highest minimum singular value.

Bandwidth in MIMO systems

We defined the bandwidth as the frequency up to which control is effective. For MIMO systems the bandwidth depends on directions. We have a *bandwidth region* between a lower frequency where the minimum singular value $\underline{\sigma}(S)$ reaches 0.707 (the low gain or worst-case direction) and a higher frequency where the maximum singular value $\overline{\sigma}(S)$ reaches 0.707 (the high-gain or best direction). If we want to associate a single bandwidth frequency for a multivariable system, then we consider the worst-case direction. The bandwidth defined this way is approximately equal to the frequency where $\underline{\sigma}(L(j\omega))$ crosses 1 (from above).

Condition number

The condition number γ of a $\boldsymbol{G}$ matrix is defined as the ratio between the maximum and minimum singular values:

$$\gamma(G) \stackrel{\Delta}{=} \frac{\overline{\sigma}(G)}{\underline{\sigma}(G)} \tag{12.61}$$

The larger is the condition number, the poorer the conditioning of the matrix. The condition number depends strongly on the scaling of inputs and outputs. Thus, we may consider a *minimized condition number*, defined by:

$$\gamma^* = \min_{D_1, D_2} \gamma(D_1 G D_2) \tag{12.62}$$

The condition number is a measure of input-output controllability. If the condition number is small, then the multivariable effects of uncertainties are not likely to be

[1] Minimum singular value is designated in some works by 'Morari Resiliency Index'.

serious. Large condition number might indicate sensitivity to uncertainties. When comparing several alternatives we would prefer those with smaller condition number.

B. Relative Gain Array

RGA provides a measure of interactions caused by decentralized control. Let assume that the input u_j controls the output y_i. Let the corresponding gain be: g_{ij} when the other loops are open, and $\hat{g}_{ij}$ when the other loops are closed, so that the other outputs are constant, except for the considered loop. By definition the element λ_{ij} of the RGA is given by:

$$\lambda_{ij} = \frac{g_{ij}}{\hat{g}_{ij}} = \frac{\left(\frac{\partial y_i}{\partial u_j}\right)_{all\ loops\ open}}{\left(\frac{\partial y_i}{\partial u_j}\right)_{all\ loops\ closed\ except\ for\ the\ u_j\ loop}} \qquad (12.63)$$

Mathematically, the relative gain array (RGA) of a non-singular matrix G is defined as:

$$RGA(G) = \Lambda(G) \stackrel{\Delta}{=} G \otimes \left(G^{-1}\right)^H \qquad (12.64)$$

where $\otimes$ denotes 'element-by-element multiplication'. $\left(G^{-1}\right)^H$ is the complex-conjugate transpose of the inverse of G matrix.

RGA has the following properties:

1. RGA is independent on input and output scaling.
2. The rows and columns of RGA sum to one.
3. The sum-norm of the RGA, $\|\Lambda\|_{sum} = \sum_{i,j} |\lambda_{ij}|$, is very close to the minimized condition number. This means that plants with large RGA elements are always ill-conditioned.

Consider a 2x2 system for which at steady-state the gains are K_{ij}. We may write:

$$y_1 = K_{11}u_1 + K_{12}u_2 \qquad (12.65)$$

$$y_2 = K_{21}u_1 + K_{22}u_2$$

It can be demonstrated that in the case of a 2x2 system the elements in the steady state RGA can be calculated by the following relation:

$$\lambda_{11} = \frac{1}{1 - \frac{K_{12}K_{21}}{K_{11}K_{22}}} \qquad (12.66)$$

The other elements are $\lambda_{22} = \lambda_{11}$, $\lambda_{21} = \lambda_{12} = 1 - \lambda_{11}$.

C. Disturbance direction and disturbance condition number

Consider a single (scalar) disturbance and let the vector g_d represent its effect on the outputs. The disturbance condition number γ_d or DCN is defined as:

$$\gamma_d = \frac{\left\| G^{-1} \cdot g_d \right\|_2}{\left\| g_d \right\|_2} \cdot \bar{\sigma}(G) \tag{12.67}$$

DCN provides a measure of how a disturbance is aligned with the plant. It may vary between 1 (disturbance in the "good" direction $\bar{u}$), and $\gamma(G)$ (disturbance in the "bad" direction $\underline{u}$), $\bar{u}$ and $\underline{u}$ being the output directions in which the plant has its largest and smallest gain, respectively. For the distillation column example, we obtain a disturbance condition number DCN = 2.63. This is close to 1, and very small compared to condition of the plant (CN = 256), meaning that the effect of the disturbance is well aligned with high gain direction of the plant (corresponding to maximum singular value)

D. Inputs for perfect control

For a square plant the input needed for perfect disturbance rejection is:

$$u = -G^{-1} G_d d \tag{12.68}$$

The worst-case single disturbance is $|d(\omega)| = 1$. Then, input saturation is avoided if all the elements of u are less than 1 in magnitude, that is:

$$\left\| G^{-1} g_d \right\|_{max} \leq 1 \quad \forall \omega \tag{12.69}$$

12.5 DECENTRALIZED CONTROL

A multivariable controller computes the value of each manipulated input based on the value of *all* controlled outputs. The design of multivariable controllers is not an easy task. Moreover, multivariable controllers requite accurate plant models. Therefore, most of process systems make use of a simpler structure, where the value of one manipulated is computed based on the value of *one* controlled output. This is called decentralized control, or multi-SISO. The decentralized controller has the following diagonal structure:

$$K(s) = diag\{k_i(s)\} = \begin{bmatrix} k_1(s) & & & \\ & k_2(s) & & \\ & & \ddots & \\ & & & k_{n1}(s) \end{bmatrix} \tag{12.70}$$

The design of a decentralized control systems involves two steps:

- The choice of pairings
- The design of each controller.

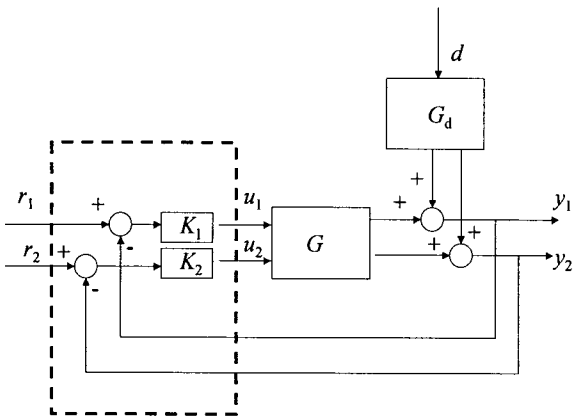

Figure 12.15 Decentralized control of MIMO systems

12.5.1 Controllability measures for decentralised control

RGA number

RGA is often presented as the method for pairing controlled and manipulated variables. In this respect some comments are useful:

1. If λ_{ij} is close to 1, then there is almost no interaction between control loops. The system is almost decoupled. Note that interactions are not necessarily bad, because interacting loops may help each other in rejecting disturbances.

2. Pairing on negative values $\lambda_{ij}(0) < 0$ is highly undesirable, because it means that the steady-state gain in "our" loop changes the sign when the other loops are closed.

3. Very large values of RGA indicate that the system can be quite sensitive to model parameters. The linearisation of the model should be checked carefully.

Luyben (1999) noted that RGA should be not considered as an effective tool in recommending pairing, but it can be seen more useful in avoiding poor pairing.

The RGA vs. frequency can be used to measure the diagonal dominance in multi-SISO control systems, by means of the simple quantity:

$$RGA\_number = \left\| \Lambda(G) - I \right\|_{sum} \tag{12.71}$$

Suitable pairings should give an *RGA_number* close to 0 at crossover frequency.

Niederlinski index

A simple method for avoiding poor pairing is based on the computation of the Niederlinski index. Note that integral action must be used in all controllers. It needs only the knowledge of the steady-state gains K_{ij}. The formula is:

$$NI = \frac{\det[K_{ij}]}{\prod_{j=1}^{N} K_{jj}} \tag{12.72}$$

The necessary but not sufficient condition for stability is that *NI* for the selected pairing be positive. For a 2 x 2 system, the RGA and Niederlinski index are equivalent. This is not true, however, for larger systems.

Performance Relative Gain Array

Let $\tilde{G} = diag(g_{ii})$ be the matrix containing the diagonal elements of G. The decentralized controller is diagonal $K(s) = diag(k_i)$ and each loop has the transfer function $L_i = g_{ii}k_i$.

At frequencies where feedback is effective, the sensitivity function is $S \approx \tilde{S}\,\Gamma$, where $\tilde{S}$ is the sensitivity of individual loops and

$$\Gamma \overset{\Delta}{=} \tilde{G}(s)G^{-1}(s) \text{ is called } \textit{Performance Relative Gain Array} \tag{12.73}$$

Γ is important when evaluating the performance with decentralized control. Consider a change in reference for the output j of magnitude R_j. Then, for acceptable reference tracking we must require for each loop i:

$$|1 + L_i| > |\gamma_{ij}| \cdot |R_j|, \forall i \tag{12.74}$$

Consequently, for performance is desirable to have small PRGA elements, at least at frequencies where feedback is effective. However, at frequencies close to crossover, stability is the main issue and we prefer to have γ_{ii} close to 1.

Closed Loop Disturbance Gain

Similarly to PRGA, the closed loop disturbance gain (CLDG) is defined as:

$$\tilde{G}_d(s) \overset{\Delta}{=} \Gamma(s) \cdot G_d(s) = \tilde{G}(s) \cdot G^{-1}(s) \cdot G_d(s) \tag{12.75}$$

Consider a single disturbance g_d and let g_{di} denote the i-th element of g_d. Then, for acceptable disturbance rejection ($|e_i| < 1$), we must require for each loop i:

$$|1 + L_i| > |\tilde{g}_{di}| \quad \forall i \tag{12.76}$$

In other words, $\tilde{g}_{di}$ gives the "apparent" disturbance gain as seen from loop i when the system is controlled using decentralized control. Thus, the condition to avoid input constraint follows directly:

$$|g_{ii}| > |\tilde{g}_{dik}| \quad \forall k \tag{12.77}$$

Taking the ratio between the closed loop disturbance gain $\tilde{g}_{di}$ (CLDG) and the disturbance gain g_{di} we obtain the *relative disturbance gain*, giving the change of disturbance gain caused by decentralized control.

$$\beta_i \overset{\Delta}{=} \frac{\tilde{g}_{di}}{g_{di}} = \frac{\left[\tilde{G}G^{-1}g_d\right]_i}{\left[g_d\right]_i} \tag{12.78}$$

12.5.2 Methodology for input/output controllability analysis

The methodology presented hereafter regards a MIMO system that can be handled by a combination of multi SISO loops. It is an input/output controllability being based on linear analysis tools. It can be applied to a stand-alone complex unit, as a distillation column, or to a flowsheet. In this later case it has the character of a decentralised (integral) plantwide control problem.

1. Problem definition

- Control objectives. It should be clear what are the control objectives, as for example, production change, quality specifications of products, minimisation of waste and emissions, etc. The basic inventory control (pressures, levels) should not be among the objectives, although this could interfere with the higher level control objectives, as mentioned.
- Process constraints. These constraints are defined by safety requirements, environmental regulations, product quality and equipment protection.
- Controlled variables (outputs). The selection of the controlled variables should be based on process engineering judgement, as well as the type and location of the measurements. In this case the controlled variables refer to quality control, as the purity of products from distillation columns, or having a plantwide character, as the concentration of key impurities on selected process streams, or temperatures regarding the reaction system, etc.
- Manipulated variables (inputs). These are available degrees of freedom left after considering the basic control. The selection of manipulated variables could also be the object of a local controllability analysis. A typical example is the use of SVD for the selection of the sensitive stage for inferential quality control in a distillation column.
- Disturbances. Disturbances must be defined in term of amplitude and frequency range. Setpoint changes, due to optimisation or/to design modifications could also be included.
- Scaling of variables and disturbances. Proper scaling is necessary for a meaningful computation of controllability indices.

2. Steady state controllability analysis

- Determine steady-state gains for plant, as well as for disturbances. An important problem here is the linearity and sensitivity of the inputs with outputs. This feature should be careful investigated by simulation. Good linearity over the control range

should be ensured. If the manipulated variables have not sufficient power on the controlled variables, they are excluded, or the design has to be changed.

- Try to get a global picture of the system behaviour, by computing the dependence of the state variables vs. operating parameters. You may find multiple steady states. Be aware that some of them are unstable.
- Estimate feasible pairing by relative gain array (RGA). Keep in mind some simple rules:
  1. Do not pair on negative RGA elements.
  2. Avoid pairing on high RGA positive elements, although this could mean rather high sensitivity to model than problems in controllability.
  3. Avoid very interactive loops, as RGA element close to 0.5 in a 2x2 system.
- Eliminate unfeasible pairing that gives a negative Niederlinski index.
- Evaluate the power of manipulated variables by SVD analysis. The best set is that giving the highest low singular value (MRI) and lowest condition number CN. Consistent scaling has to be used in comparing different alternatives.
- Rank the control alternatives. Prefer alternatives where the controlled and manipulated variables are physically close.

3. Dynamic flowsheeting

The job is not finished with steady state controllability analysis. Only dynamic simulation enables a reliable assessment of the control problem. The solution of the dynamic modelling depends on the dynamics of units involved in the control problem. Detailed models are necessary for the key units. The simplification of the steady-state plant simulation model to a tractable dynamic model, but still able to represent the relevant dynamics of the actual problem, is a practical alternative. Steady-state models can be used for fast units, as heat exchangers, or even chemical reactors with low inventory.

Before performing a controllability analysis, ensure the stability of the plant. The first step is to close all inventory control loops, by means of level and pressure controllers. Then, check the stability, by dynamic simulation. If the plant is unstable, it will drift away from the nominal operating point. Eventually, the dynamic simulator will report variables exceeding bounds, or will fail due to numerical errors. Try to identify the reasons and add stabilizing control loops. Often a simple explanation can be found in uncontrolled inventories. In other situations the origin is subtler. Some units are inherently unstable, as with CSTR's or the heat-integrated reactors. The special case when the instability has a plantwide origin will be discussed in Chapter 13.

4. Dynamic controllability analysis

Based on the non-linear plant model, a linear dynamic model is derived, either as a set of transfer functions (identification method), or as a state-space description. The last alternative is offered in advanced packages as ASPEN Dynamics^{TM}.

- Check once again the stability of the plant, by computing the eigenvalues of the **A** matrix in state space description or the poles of the transfer function.
- Check the pairing by computing the frequency-dependent RGA-number. If the pairing is correct, the RGA-number should drop to small values at high frequencies.

A value close to zero means quasi-independent SISO controllers.

- Scale the model. For each disturbance, obtain the frequency response. The range of frequencies to be considered in further analysis corresponds to disturbance transfer function larger than 1 in magnitude.
- Compute and plot comparatively the frequency–dependent closed loop disturbance gain (CLDG) and the magnitude of the transfer functions connecting manipulated inputs to outputs. Assess the "power" and "speed" of the manipulated variables.
- The previous step gives an indication of the controller tuning: the closed-loop disturbance gain (CLDG) should be smaller than the loop transfer function $[1+g_{ii}(s)k_i(s)]$ for each disturbance, where $g_{ii}(s)$ is the open-loop input/output transfer function, and $k_i(s)$ the controller model.
- Calculate the frequency-dependent disturbance condition number, and compare with the plant condition number.
- Optionally, the controllability performances can be estimated by performance relative gain array (PRGA) and relative disturbances gain (RDG).

5. Closed loop simulation

The control structures identified by the controllability analysis are tested by full non-linear simulation. Here the first task consists of implementing and tuning of controllers. The use of prescribed local control structures, or setting perfect control for fast loops simplifies this task and preserves the plantwide character of the analysis.

6. Design alternatives

If there are design alternatives, the procedure should be repeated and alternatives ranked. Design modifications may concern:

- (Re)sizing of units.
- Alternative flowsheet (recycle) structures.

A similar controllability analysis can be applied to solve various plantwide control problems, as the handling of impurities in a complex plant (see Case Study 3 in the Chapter 17). The next example will illustrate the main aspects of a controllability analysis by means of a distillation column.

EXAMPLE 12.2 Controllability analysis applied to distillation column

Analyse the feasibility of different control structures by a controllability analysis for a distillation column methanol-water. Consider the data of the EboAkademi pilot-scale column (Haggblom & Waller, 1992).

Solution

Firstly, a steady state simulation is built in AspenPlus. The feed stream consists of F = 200 kg/h containing 19.41 % mol methanol. The column has 15 trays. At the nominal operating point, reflux and reboiler duty are R = 60 kg/h and Q = 41.84 kW,

respectively. This gives x_D = 90.76 % mol methanol in distillate, and x_B = 98.68 % mol water in bottom. Disturbance of +/- 40 kg/h in feed flow rate are expected.

We consider sieve trays with a diameter d = 0.13 m. Reflux drum and column sump are sized by assuming residence times of 5 min and 10 min, respectively.

Steady state controllability analysis

Small disturbances of 0.5% around the nominal operating point are considered in distillate (D), reflux flow rate (L), reboiler duty (V), bottom product (B), and feed (F). The gain matrix is given below, where scaled values are marked by a star:

	ΔD	ΔL	ΔV	ΔB	ΔF
Δx_D	-0.01395	0.00686	-0.00455	0.00476	-0.00451
Δx_B	0.00168	-0.00082	0.00863	-0.00306	0.00197
Δx_D^*	-279.150	137.375	-73.823	214.616	-90.2017
Δx_B^*	33.719	-16.593	47.454	-137.957	39.4014

RGA is calculated from the gain matrix as $RGA = G \otimes G^{T}$. SVD analysis gives MRI, condistion number and disturbance condition number. MRI is the minimum value of Σ: $G = u \cdot \Sigma \cdot v$; $MRI = \sigma_{min}$. Condition number is $\gamma = \sigma_{max} / \sigma_{min}$.

For example, in the case of the LV structure the calculations are:

$$RGA^{LV} = G^{LV} \otimes G^{LV,T} = \begin{bmatrix} 137.375 & -73.823 \\ -16.593 & 47.454 \end{bmatrix} \otimes \begin{bmatrix} 0.0089 & 0.0031 \\ 0.0139 & 0.0259 \end{bmatrix} = \begin{bmatrix} 1.2313 & -0.2313 \\ -0.2313 & 1.2313 \end{bmatrix}$$

$$G^{LV} = u \cdot \Sigma \cdot v = \begin{bmatrix} -0.97039 & 0.24152 \\ 0.24152 & 0.97039 \end{bmatrix} \cdot \begin{bmatrix} 160.5028 & 0 \\ 0 & 32.984 \end{bmatrix} \cdot \begin{bmatrix} -0.85553 & 0.51774 \\ 0.51774 & 0.85553 \end{bmatrix}$$

Therefore: $MRI^{LV} = \sigma_{min} = 32.98$ and $\gamma = \frac{\sigma_{max}}{\sigma_{min}} = \frac{160.50}{32.98} = 4.86$

The steady-state controllability analysis for several structures is briefly given below:

Alternative	RGA	MRI	γ	γ*
DV	0.55	34.26	9.16	7.36
LB	0.81	58.14	4.55	1.089
LV	1.23	32.98	4.86	4.67
RV	1.28	34.25	6.40	6.20

The alternative **DV** has an RGA-element close to 0.5 meaning strong interaction, so this can be excluded. The other three structures behave somehow similar. RGA-element is close to 1, MRI is high, while γ is low but still higher than γ*. From steady-state controllability indices it seems that **LB** structure is the most suitable. The **LV** structure has very similar characteristics, although it seems to have some difficulties to reject feed disturbances. For this reason we will examine this structure in dynamic mode also.

Control structures

A one-feed two-product distillation column has five degrees of freedom, corresponding to five valves available: condenser duty and reboiler duties, as well as reflux, distillate, and bottom flows. Three degrees of freedom are used for inventory control. In one possible control configuration: condenser duty for pressure, distillate for level in the reflux drum, bottom flow for level in the sump.

The remaining two degrees of freedom can be used for composition control. In **LV** configuration the reflux rate controls the distillate purity, and reboiler duty controls the bottoms purity.

Dynamic Simulation

When exporting the steady-state solution file for dynamic simulation, Aspen dynamics provides inventory (i.e., level and pressure) controllers. However, the tuning of **P** level controllers is too tight, and need to be changed to 1 %/%.

Linear Model

Aspen Dynamics generates automatically a linear model by means of a Control Design Interface (CDI). The state space matrices **A**, **B**, **C**, **D** are saved as sparse matrices in ASCII files. These can be imported in MATLAB™ and used for further calculations.

Scaling

The following table is of help in defining the scaling factors:

Variables	Nominal value	Maximum/expected deviation
Controlled variables		
% methanol in distillate	0.9076	0.002
% water in bottoms	0.9868	0.002
Manipulated variables		
reflux flow rate (kg/hr)	60	40
reboiler duty (kW)	46.57	20
Disturbances		
feed flow rate (kg/hr)	200	40

Steady-state linear controllability analysis

The steady state transfer matrix obtained from dynamic simulation is:

$G(0) = -C \cdot A^{-1} \cdot B = \begin{bmatrix} 137.37 & -73.82 \\ -16.59 & 47.45 \end{bmatrix}$. It may be observed that the result is identical with the steady state analysis obtained by linearisation in Aspen Plus.

The scaled disturbance gain matrix at steady state is:

$G_d(0) = -C \cdot A^{-1} \cdot B_d = \begin{bmatrix} 0.90 \\ -19.16 \end{bmatrix}$.

Since one element is larger than 1 in magnitude, implementing control for disturbance rejection is necessary.

The magnitude of inputs can be determined as follows:

$$u = G(0)^{-1} \cdot G_d(0) = \begin{bmatrix} 0.26 \\ 0.49 \end{bmatrix}$$

Both inputs are less than 1; the manipulated variables are powerful enough.

For pairing the RGA at steady state is calculated:

$$RGA(0) = G(0) \otimes G(0)^T = \begin{bmatrix} 1.231 & -0.231 \\ -0.231 & 1.231 \end{bmatrix}.$$

The same values from steady state analysis are obtained, which confirm the pairing x_D-L and x_B-V. In addition the RGA elements are small, so the effect of modelling errors is not serious.

The SVD analysis gives the results:

$$G(0) = u \cdot \Sigma \cdot v, \text{ with } \Sigma = \begin{bmatrix} 160.50 & 0 \\ 0 & 32.98 \end{bmatrix} \text{ and } \gamma = \frac{\sigma_{max}}{\sigma_{min}} = 4.86.$$

The smallest value $\sigma_{min} = 32.98$ value is large, so that the plant is well-conditioned.

Dynamic controllability analysis

The primary information in dynamic controllability analysis is similar to the steady-state analysis, namely the gains for manipulated variables and disturbances on the controlled variables, this time plotted against frequency. This can be obtained from a state-space description (matrices **A**, **B**, **C**, **D**) or by identification.

Figure 12.16-left illustrates the open loop gain for manipulation, L and V, on the controlled variables x_D and x_B. Figure 12.16-right shows the scaled gains produced by a disturbance in feed. On the range where $|G_d|$ is less than one the rejection do not need control. In this case the disturbance in feed $|G_{d,1}| \sim 1$ seems not to affect the distillate composition, but $|G_{d,2}| >> 1$ indicates that control for purity of bottoms is needed. Indeed, from the control problem definition the distillate purity is loose, while the purity of bottoms is much more strict.

Another insight can be obtained by examining closed loop disturbances gain (CLDG) elements against the corresponding open loop gain, as illustrated by the Fig. 12.17. For both controlled variables the open-loop gain is much higher that the closed-loop disturbance gain, therefore the disturbances should be easily rejected.

The ability to the proposed pairing to handle the disturbance can be investigated by means of RGA-number. RGA-number is below one over a large frequency range, showing that the control by the proposed pairing is effective (Fig. 12.18-left). The same conclusion can be drawn by plotting condition number γ and disturbance condition number γ^* against frequency (Fig. 12.18-right). Condition number is higher than disturbance condition number, suggesting a good control structure.

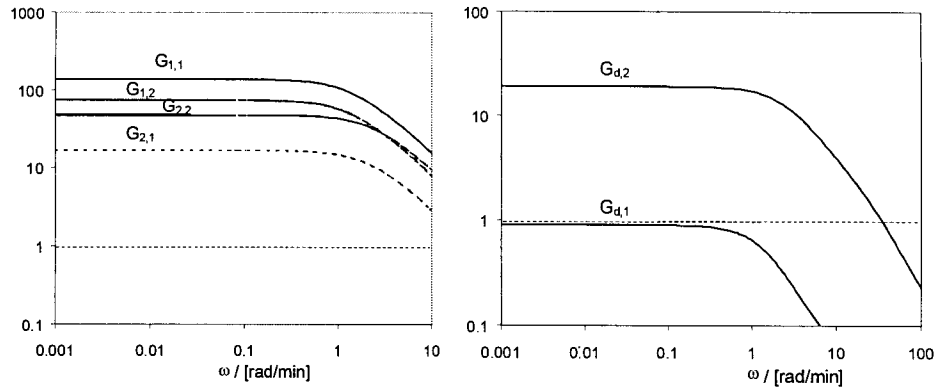

Figure 12.16 The gains in open loop for manipulated variables and feed disturbance

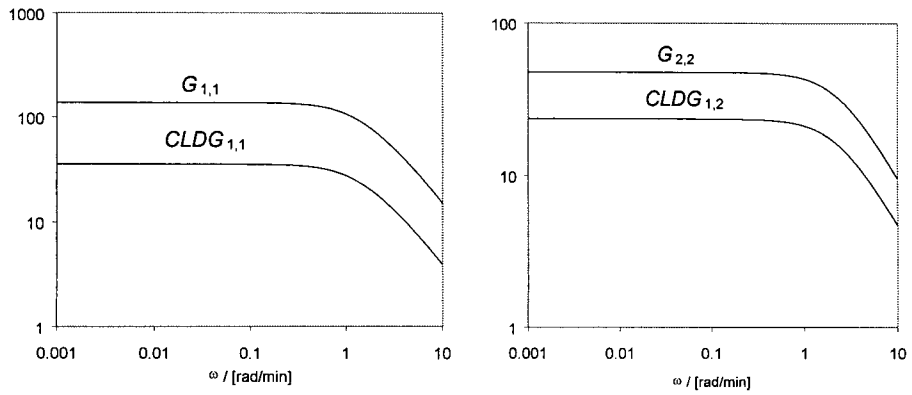

Figure 12.17 Closed loop disturbance gain against loop gain

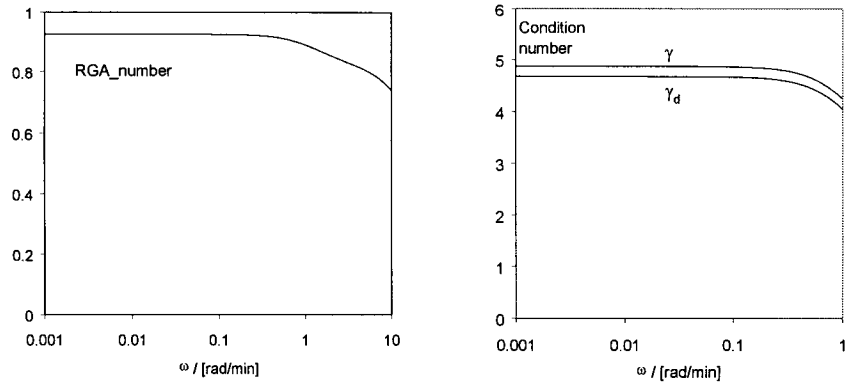

Figure 12.18 RGA number and Condition number against frequency

Finally, the results of controllability analysis are checked by closed loop dynamic simulation. Figure 12.19 displays the time variation of the distillate and bottom purity as fraction from the full scale for a disturbance of 40 kg/h (20%) in the feed flow rate. Both controllers are of PI-type with K_C=1 and reset time of 20 minutes. It may be observed that both disturbances are rejected conveniently, despite a very large disturbance. Controlling the purity of distillate is easier than of the bottoms, which confirms the controllability analysis.

The above example was limited to a single disturbance, the feed flow rate. Other disturbances could be feed composition, or feed temperature, etc. When several disturbances arrive in the same time then we may speak about 'directions'. It could happen that the control system would reject easier (or more difficult) a combination of disturbances. A convenient measure of the ability of the control system to handle such situations is the 'cost of disturbances' (Lewin, 1996).

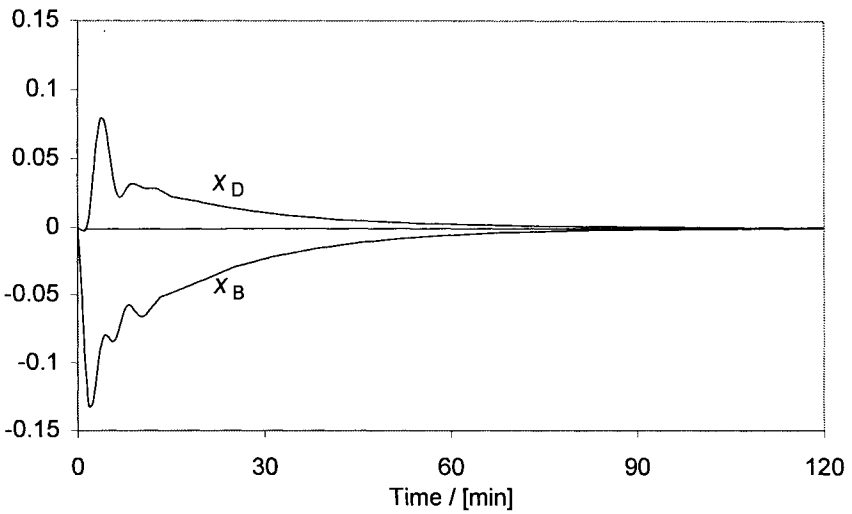

Figure 12.19 Closed loop response of methanol-water distillation column

In conclusion, this chapter reviews the basics of the controllability analysis in view of a better use of steady state and dynamic simulation for integrating design and control. The measures presented makes use of information that is easy to obtain by simulation, providing that the modeling is realistic and accurate for the purpose of investigation.

For a deeper insight in control aspects the reader is invited to consult some of the references given hereafter, at least the concise book of Luyben & Luyben (1997). Considering controllability as a built-in element of design is a new approach in process engineering, as well in teaching design. Beside this work, the only book dealing with this issue has been published by Seader, Seder, & Lewin (1999).

12.6 REFERENCES

Dimian, A. C., C. S. Bildea, A. Kiss, 2001, Advanced Process Integration, postgraduate course, University of Amsterdam

Haggblom, K. E., Waller, K. V., 1992, Control structures, consistency, and transformations in Practical Distillation, ed. W. Luyben, Van Nostrand Reinhold

Lewin, D. R., 1996, A simple tool for disturbance resiliency diagnosis and feed forward control design, Comp. & Chem. Engng., 1, 13-25

Luyben, W. L., 1990, Process Modelling, Simulation and Control for Chemical Engineers, 2nd edition, McGraw-Hill

Luyben, W.L., M.L. Luyben, 1997, Essentials of Process Control, McGraw-Hill, New York

Moore, C. F., 1992, Selection of controlled and manipulated variables, in Practical Distillation, ed. W. Luyben, Van Nostrand Reinhold

Marlin, T., 1995, Process Control: Designing processes for dynamic performance, McGraw Hill

Ogonnaike, B., W. H. Ray, 1998, Modelling and Process Control, Academic Press Seader,

Seider, W. D., J. D. Seader, D. R. Lewin, 1999, Process Design Principles: Synthesis, Analysis and Evaluation, Wiley

Skogestad, S., I. Postlethwaite, 1996, Multivariable Feedback Control, Analysis and Design, Wiley

Chapter 13

INTEGRATION OF DESIGN AND CONTROL

13.1 Introduction

13.2 Steady state design and controllability

13.3 Dynamic effects in recycle systems
- 13.3.1 Effects of recycles on the overall dynamics
- 13.3.2 Dynamics of interdependent units
- 13.3.3 Snowball effects
- 13.3.4 Feasibility of control structures in recycle systems

13.4 Control of component inventory
- 13.4.1 Make-up policy of reactants
- 13.4.2 Control of impurities

13.5 Steady state nonlinear effects of material recycle
- 13.5.1 Modelling
- 13.5.2 Isothermal CSTR - Separator - Recycle
- 13.5.3 Two-reactants, second-order reaction
- 13.5.4 Adiabatic CSTR – Separator – Recycle

13.6 Dynamic effects of energy recycle
- 13.6.1 Heat integrated reactors
- 13.6.2 Heat integrated distillation

13.7 Plantwide control procedure
- 13.7.1 Outline
- 13.7.2 Application

13.8 Integrating plantwide control in Hierarchical Conceptual Design
- 13.8.1 Basic flowsheet structures
- 13.8.2 Approach

13.9 Summary

13.10 References

13.1 INTRODUCTION

Modern plants are characterised by complicated recycle structures due to high valorisation of raw materials and waste minimisation, as well as to energy integration. Conceptual process design must guarantee good inherent controllability characteristics.

The traditional approach in designing the control system of a process is to develop firstly an optimised steady state design, and then to implement control loops unit-by-unit, in a way that inspired the expression 'like the candles on a Christmas tree'. Often in the past, plants that looked wonderful on paper failed in operation, requiring costly revision of the conceptual basis. Therefore, an integrated approach of design and control is needed, which should begin at an early conceptual stage. The advent of powerful computation systems integrating both steady state and dynamic simulation capabilities makes today this wish realistic.

This chapter is devoted mainly to the control philosophy of the whole plant, what nowadays is called 'plantwide control'. Clearly, it is desirable to make use, as much as possible, of standard control loops at the unit level, because the global control strategy should be independent of the implementation and tuning of local controllers.

Plantwide control problems arise in the context of plants with recycles of mass and energy. Positive feedback effects complicate the dynamics because of interactions and non-linear phenomena, as multiple steady states and chaotic behaviour.

In the past, inserting large buffering capacities has been used to solve dynamic problems, as interactions between different plant sections, or variations in raw materials and throughput. In this way, the units should behave much as stand-alone with almost constant inflow, and their control could be assessed individually. The price of such approach was slow dynamics and higher operation costs. In addition, large storage capacities were potential sources of safety problems.

Nowadays the designers should try to eliminate unnecessary storage and surge capacities, but with clear understanding of implications on the operability of the whole plant. It might be expected that reduced buffers accelerate the dynamics, but increase sensitivity to disturbances. Thus, the assessment of interactions between units and the optimisation of inventories are key issues in modern process design. In addition, in modern design the plant should be responsive to large variations in throughput. Ideally, the plant should work smoothly 'on-demand' and avoid the storage of products waiting for a virtual client. This operating mode becomes imperious for hazardous chemicals.

The current practice has shown that there is a gap between process and control engineers. Filling this gap is a challenge for education. Only very recently plantwide controllability issues have been included in a book dealing with process design (Seider, Seader & Lewin, 1999). This chapter aims to give another perspective on the same subject, with emphasis on integrating controllability aspects in flowsheet synthesis.

The first topic developed in this chapter is the interrelation between steady state design and controllability. Particular attention will receive the generic structure Reactor-Separator-Recycle. We consider that material balance has priority in establishing the plantwide control strategy. That is why we will examine in the first place the effects induced by the recycle of mass. Particular attention will receive the feed policy of the reactants, as well as the handling of impurities, both fundamental plantwide control issues. Then we will examine the effect of recycling energy, with emphasis on heat

integrated reactors and heat integrated distillation columns. The last part will handle the development of plantwide control structures. Firstly, we will present a recent methodology that is applicable to existing plants (Luyben & Tyreus, 1999). Then we will exemplify a workable procedure for new designs based on the identification of basic flowsheet structures and their connection in a flowsheet.

It is assumed that the reader is familiar with the fundamentals of process control of the key unit operations, as reactors, distillation columns, etc. A concise description of essential topics in Process Control can be found in the recent book of Luyben & Luyben (1998). We also strongly recommend the recent monograph of Luyben and Tyreus on plantwide control (1999). Basic issues in dynamics and process control can be found in the classical textbooks of Stephanopoulos (1984), Luyben (1990), Marlin (1995) and Ray & Ogunnaike (1998).

It is useful to remember here three 'common sense' laws in process control (Luyben & Luyben, 1998):

1. The best control is the simplest one that will do the job.
2. You must understand the process before you can control it.
3. Liquid levels must always be controlled. However, the liquid surge level in a recycle system may float up and down between safe limits.

13.2 STEADY STATE DESIGN AND CONTROLLABILITY

It has been recognised for long time that the performance of a plant depends much more on its design characteristics than on the sophistication of the control algorithms. The practice showed also that the optimal steady state design is not always the best in operation. Only slightly more expensive alternative could posses much better dynamic properties, and become more profitable when the 'cost of time' is taken into account. Hence, there is always a trade-off between steady state economics and controllability.

From steady state point of view, the size of equipment should be kept as small as possible in order to minimise the capital cost and prevent safety risks. However, a too small volume increases the sensitivity to disturbances, and in the worst case can upset the operation. Therefore, the design should provide sufficient capacity to dump fluctuations, although an excessive value would give too long transients. Hence, the design of capacities is a matter of optimisation, both from steady state and dynamic viewpoint.

The capacity of a unit in mass-exchange or reactive operations is designated often in process dynamics by *holdup* or *inventory*. This can be expressed globally, or per components. As a rule of thumb, the volume of a liquid surge should be designed with a residence time between 5 and 10 minutes.

The trade off between design and controllability can be illustrated simply by an example from chemical reaction engineering. From textbooks we learn that a series of CSTR's is more advantageous than a single CSTR, because it needs a smaller total volume to reach a given conversion. Thus, steady state optimisation would consist of replacing a single large CSTR by a number of smaller CSTR's. This apparent advantage should be reviewed if the dynamic behaviour is examined. Figure 13.1 compares the time evolution of temperature for a single large reactor of 20 m^3 and a series of three

smaller reactors (3×1.85 m^3) at a step change in the heat release. The overshoot in a single large reactor can be limited to 1.5 °C, while the hot-spot in the first CSTR is of about 20 °C. It is obvious that this aspect must be considered in process design if the product quality depends strongly on temperature, as in the case of polymerisations. Thus, the optimal steady state design could be not the best from control viewpoint.

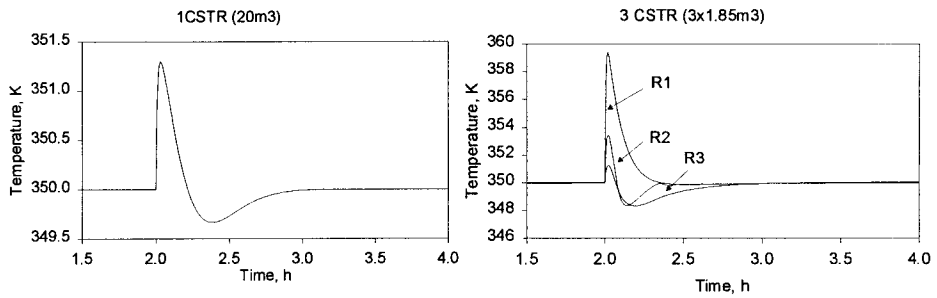

Figure 13.1 Temperature variation in one large CSTR and a series of smaller CSTR

Another important observation is that the design of a stand-alone unit and incorporated in recycle might be very different. We refer again to chemical reactors. Traditionally, the design considers fixed inlet conditions (flow rates, inlet temperature and concentrations) and desired performance (usually conversion and product distribution). The result is a reaction volume according to a desired mixing pattern. However, the design objective can change significantly when the reactor is examined in the context of a plant with recycles. The reactor must cope not only with small variations around the nominal operation point, but also with large variations in the plant throughput corresponding to a desired flexibility. The reactor inlet flow rate, including recycles, could vary significantly, but the reactor must ensure the transformation of each fresh reactant molecule entering the process. If not, accumulation of materials that occurs in various places can generate operation and control problems.

Therefore, a systemic approach is necessary in designing chemical reactors. In this chapter, we will demonstrate that a minimum reactor volume is required in a recycle system for flexible operation. Moreover, the nominal design should be placed sufficiently far away from the maximum sensitivity region of the relation conversion-reactor volume. It is worthy to note that multiple steady states are possible in the case of several recycles of reactants. The recycle of heat gives an even more complicated behaviour. Moreover, the stability and performance of the reactor system depends also on the control structures of other units. Hence, reactor design and feasibility of the control structures at the plant level should be examined simultaneously.

The example of CSTR reactor might suggest the idea that 'large is beautiful' from controllability point of view. This is not true, in general. When positive feedback is present because of a recycle of mass or energy, very efficient equipment might be not the most suitable. Typical example is the recovery of reaction heat for feed preheating by means of a feed-effluent heat exchanger (FEHE). A high-efficiency heat exchanger will increase the chance of unstable behaviour because of a stronger positive feedback of heat. Thus, the notion of 'small' or 'large' equipment should be seen as context dependent. This chapter will illustrate a quantitative treatment by non-linear analysis.

13.3 DYNAMIC EFFECTS IN RECYCLE SYSTEMS

13.3.1 Effects of recycles on the overall dynamics

The presence of recycles affects greatly the dynamic behaviour of a process compared with a sequential flowsheet. In general, the overall dynamic response shows longer time-constant and higher steady state gain than the individual elements.

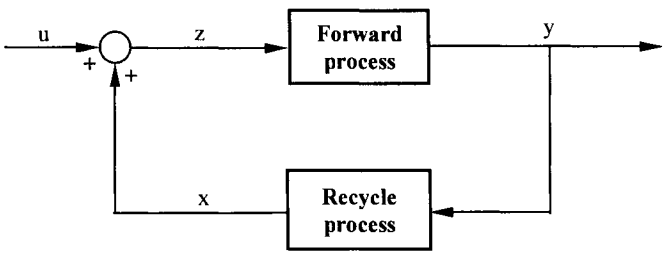

Figure 13.2 Plant with recycle

Let's consider coupled forward and recycle processes, as depicted in Fig. 13.2. In the absence of recycle, the forward process receives u as input and delivers y as output. With recycle the input becomes $z=u+x$, where x is the output of the recycle process. We assume that the dynamics of both processes is described by first-order ODE, as follows:

$$\tau_F \frac{dy}{dt} + y = K_F(u + x) \tag{13.1}$$

$$\tau_R \frac{dx}{dt} + x = K_R y \tag{13.2}$$

K_F, K_R and τ_F, τ_R are gains and time-constants for the forward and recycle process respectively. By differentiating the first equation and replacing the derivative dx/dt from the second, leads to a second-order linear ODE, whose characteristic equation is:

$$\frac{\tau_F \tau_R}{1 - K_F K_R} s^2 + \frac{\tau_F + \tau_R}{1 - K_F K_R} s + 1 = 0 \tag{13.3}$$

This relation can be put in a more convenient form as:

$$\tau^2 s^2 + 2\xi\tau s + 1 = 0 \tag{13.4}$$

In this way two dynamic characteristics of a process can be identified: the time-constant τ and the dumping factor ξ. For the first we get the expression:

$$\tau = \sqrt{\frac{\tau_F \tau_R}{1 - K_F K_R}} \tag{13.5}$$

As it may be observed, the overall process time-constant depends on the total gain through the recycle loop, which is the product of individual gains of the forward and

recycle processes. If $K_F K_R << 1$ (small loop gain) then τ is simply the geometric mean of individual τ_F and τ_R. If $K_F K_R$ approaches unity, then the global time-constant increases rapidly. For $K_F K_R \geq 1$ the process becomes unstable. The system is always stable for a negative recycle gain.

Figure 13.3 shows the time-domain response to a step change in input u for different values of recycle gain K_R, as well as K_F=1, $\tau_F = \tau_R$=1. It can be seen that increasing the recycle gain lead to more sluggish response. For larger recycle gain (K_R = 1.2), the system is unstable and the output y increases infinitely.

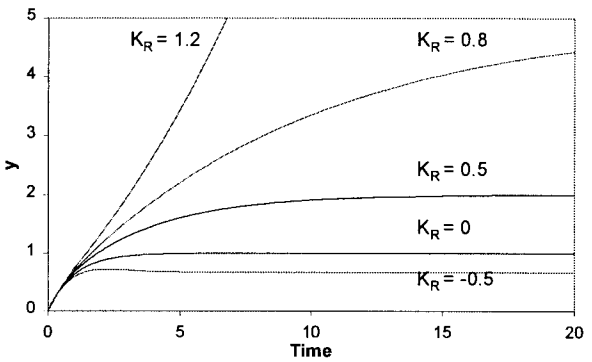

Figure 13.3 Effect of recycles on plant dynamics

Representing the roots of the characteristic equation in the complex domain offers a simple way to perform a stability analysis. The system is stable if and only if all the poles are located in the open left-half-plane (LHP). If there is at least one pole in the right-half-plane (RHP), the system is unstable. The representation is similar with the well-known *root-locus plot* used to evaluate the stability of a closed-loop system.

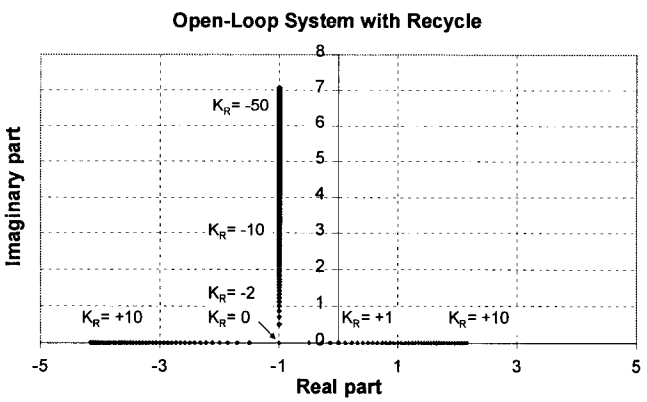

Figure 13.4 Analysis of the open-loop stability in the s-plane

Figure 13.4 presents the system discussed above, where both forward and recycle processes can be described by a first order lag. Without recycle (K_R=0), there is one pole

situated in the LHP at s = -1. When recycle is introduced, the system becomes second-order, and there are two poles. Increasing further K_R moves one of the negative poles closer to zero. Correspondingly, the time constant becomes larger and larger. When K_R=1, one pole reaches zero, and the system behaves as pure integrator. This pole shifts further in the RHP for recycle gains larger than unity, and the system becomes unstable. For negative values of K_R the poles become complex conjugate, the system is stable, and exhibits under-damped behaviour.

The above simple analysis highlights an important issue in process dynamics: the influence of positive and negative feedback on system's stability. Instability can occur in recycle systems due to *positive feedback* when the gain is larger than unity. We may give as example the recycle of energy developed by an exothermal reaction in an adiabatic PFR for feed preheating. Instability may occur because of the exponential increase in reaction rate with the temperature when this cannot be properly controlled (Bildea & Dimian, 1998). Another example is the recycle of impurities in a plant with recycles, whose inventory cannot be kept at equilibrium by the separation system (Dimian et al., 2000).

On the other hand, *negative feedback* can contribute to stabilise the system. Similar examples may be given, but now with negative gains. Thus, the temperature of high exothermal reactions can be controlled by recycling a part of the reaction mixture through an external cooler, or by partial vaporisation/condensation in an external condenser. The positive feedback due to accumulation of impurities can be eliminated by means of catalytic conversion.

13.3.2 Dynamics of interdependent units

Based on the above analysis we may state that the units involved in a recycle system are dynamically interdependent. As a result, their design, sizing, and control are correlated. For instance, a control structure that is perfectly valid for standalone operation might be inappropriate when the same unit is placed in a recycle structure. Further, we will examine this important issue by means of some examples.

A case of practical interest is a chemical reactor coupled with a separation section, from which the unconverted reactants are recovered and recycled. Let's consider the simplest situation, an irreversible reaction A→B taking place in a CSTR coupled to a distillation column (Fig. 13.5). Here we present results obtained by steady state and dynamic simulation with ASPEN Plus and ASPEN Dynamics. The reader is encouraged to reproduce this example with his/her favourite simulator. The species A and B may be defined as standard components with adapted properties. In this case, we may take as basis the properties of n-propanol and iso-propanol, and assume ideal phase equilibrium. The relative volatility B/A increases at lower pressures, being approximately 1.8 at 0.5 atm. We consider the following data: nominal throughput of 100 kmol/hr of pure A, reactor volume 2620 l, and reaction constant k=10 s^{-1}. For stand-alone operation the reaction time and conversion are τ = 0.106 hr and x_A = 0.36.

The design of the distillation column must take into account the operation in recycle. In a first approximation we use a shortcut design imposing as specifications in top 95% recovery of B and 0.01% of A. The purity of B in distillate is better than 99.8 %, while the fraction of B in bottoms is kept at less than 5 %. A number of 35 theoretical stages is found for $1.3R_{min}$, but we consider 40 stages to ensure some flexibility.

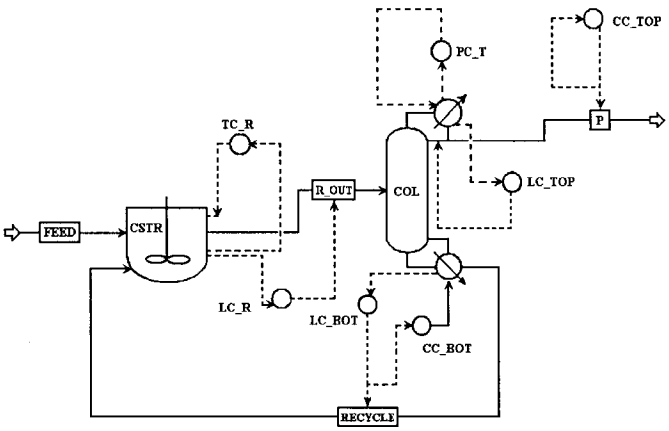

Figure 13.5 Control structure for the reactor/distillation recycle system

With these elements, ASPEN Plus can perform a sizing run and determine initial values for dynamic simulation, particularly the holdup on each tray. We select a diameter of 2.2 m and sieve trays with 50 mm weir height. Then the operation parameters, sizing elements and initial values are exported to ASPEN Dynamics.

In the first approach, we may consider a 'classical' standalone control structures, as displayed in Fig. 13.5. Reactor feed is on flow control (PI), and outlet stream on level control (PI). For the distillation column a classical inventory control is: column pressure with condenser cooling (PI), base level with bottom product (P), and reflux drum level with distillate (P). Quality control loops are top composition with reflux and bottom composition with reboiler duty, both as PI controllers.

Figure 13.6 presents the dynamic response for a 10% decrease of the feed flow rate. For comparison, the same response of a series reactor/column without recycle is depicted. Time constants can be estimated of about 2.5 hr and 8 hr, respectively. It is clear that the dynamics of the recycle system is much slower.

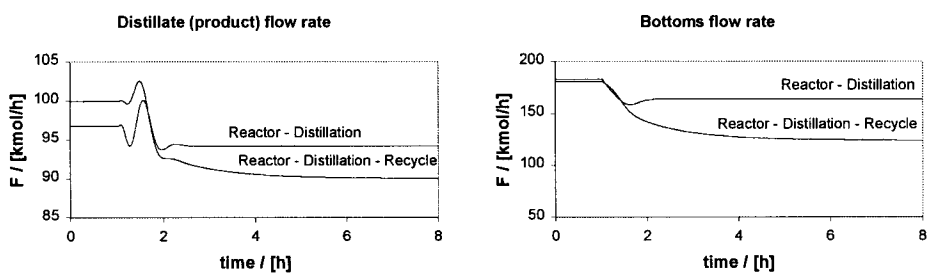

Figure 13.6 Closed loop response of a reactor - distillation column series

A simulation exercise can show the distillation column has more effect on the response than the reactor, because of higher order dynamics. Modifications on reactor, as increasing the kinetics and simultaneously reducing the volume, will improve only

marginally the whole dynamics. More efficient is to accelerate the dynamics of the distillation column by reducing the capacitive elements, as the number of stages. High efficiency trays bring only a limited improvement on dynamics. On the contrary, packed columns give faster dynamics but higher sensitivity to disturbances.

Another important aspect that we can learn from this example is the optimisation of a recycle system. If only the steady state operation is studied, the optimal plant consists from a small reactor coupled with a tall column, because usually the reactor is more expensive. If the cost of transient operation and off-spec products is taken into account, the steady state optimisation is no longer valid. Other sub-optimal designs might offer better dynamic performances, as for example somewhat larger reactor and shorter distillation column. The solution can be found by dynamic optimisation (Luyben, 1999).

13.3.3 Snowball effects

Snowball effect designates the situation in which small variations of a flowsheet variable, generally a flow rate at the inlet or outlet of a process with recycles, generates large variations of streams around some units inside the process (Fig. 13.7). It is worthy to note that snowball is essentially a steady state effect, and not a dynamic one, because at finite disturbance the amplification remains finite. However, some units cannot tolerate large fluctuations in flows, particularly the distillation columns. Therefore, the designer should avoid snowball effects already at the conceptual stage.

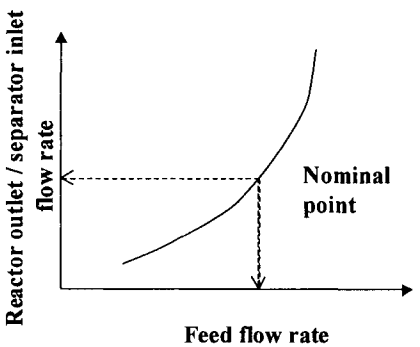

Figure 13.7 Increase in the recycle flow rate due to a snowball effect

Based on the analysis of several recycle systems, Luyben has formulated a useful heuristic: *A stream somewhere in a liquid recycle loop should be flow controlled.* This rule has proved a significant practical importance, particularly in recycle systems involving the control of inventory of several components. However, its implementation as control principle deserves more studies.

13.3.4 Feasibility of control structures in recycle systems

A perfect workable control structure for a stand-alone unit can become unfeasible because of interactions with other units by recycles. The opposite might also be true: an infeasible stand-alone control structure can become feasible when the interactions along

recycles are exploited. Clearly, when linking units in a structure, controlling the whole is different that just by adding the control of components. Strategies for the plantwide control will be discussed later in this chapter. Here we point out only some qualitative aspects regarding the influence of recycles on the two types of major equipment items: reactors and distillation columns.

Chemical reactors

The classical control structure for a CSTR presented in Fig. 13.5 (fresh reactant on flow control and reaction mixture on level control) is usual in stand-alone operation. However, it might be unfeasible in recycle systems (Luyben et al., 1999). It was found that fixing the outlet flow and allowing variable reaction volume between some limits could lead to better control. But as demonstrated in the section 13.5 the explanation is merely in too small reactor volume. Hence, the design of the reactor working in a recycle system should incorporate the effect of recycles.

Another remarkable example is the recycle of energy developed in an adiabatic PFR for reactants' preheating. Although the stand-alone PFR reactor is stable, in recycle it may become unstable. Consequently, control is needed to stabilise it. Moreover, the stabilisation depends on the design of the units involved in recycle. Section 13.6 develops more this issue.

Distillation columns

Let's consider a simple one-feed two-product distillation column. When examined as stand-alone item with a fixed feed, its control is typically a 5x5 multivariable problem. Among the five controlled variables three are for the basic inventory: pressure, level in reflux drum and reboiler. The two remaining are for quality control: purity of distillate and bottom products. The five manipulated variables are: distillate flow D, bottom product B, boilup V or reboiler duty Q_r, condenser duty Q_c and reflux flow L. The combination of controlled and manipulated variables may lead to several control structures. Here we present some typical situations useful for dynamic simulation.

Usually the column pressure is controlled by the condenser duty Q_c. Reflux drum level can be hold by either distillate D or reflux L. Here the so-called 'Richardson rule' is useful: *use the largest flow to control a level.* Base level can be hold with either the bottoms, or with the boilup (reboiler duty). Finally, there are two compositions left, of top x_D and of bottoms x_B, respectively, which can be controlled by the remaining manipulated variables. If both are simultaneously controlled, we speak about *dual composition* control. If only one is held constant, we have *single-end composition* control. Basic structures are depicted in Fig. 13.8. The first input controls x_D and the second x_B.

1. R-V: Reflux and Boilup. The levels in reflux drum and base are kept by distillate and bottoms. This structure may be interactive as dual composition control. As a single-end composition control it is one of the most used. In this case either reflux or boilup are kept constant at a value sufficient to ensure an acceptable variation in the composition of the uncontrolled product.
2. D-V: Distillate and Boilup. The levels are hold by reflux and bottom product, respectively. This structure is justified at high reflux ratio, when the distillate is too

small to control the level in the reflux drum. Because the composition is determined by reflux, it is desirable to accelerate the action of the level control loop. This can be achieved by setting the reflux on ratio with distillate and use the level controller to change this ratio.

3. RR-V: Reflux ratio (L/D) and Boilup. This structure is similar with R-V, but works better in dual composition control.
4. R-B: Reflux and Bottoms. In this case the base level is controlled by the heat input, which might create some problems because of inverse response.
5. RR-BR: Reflux ratio and Boilup ratio (V/B).

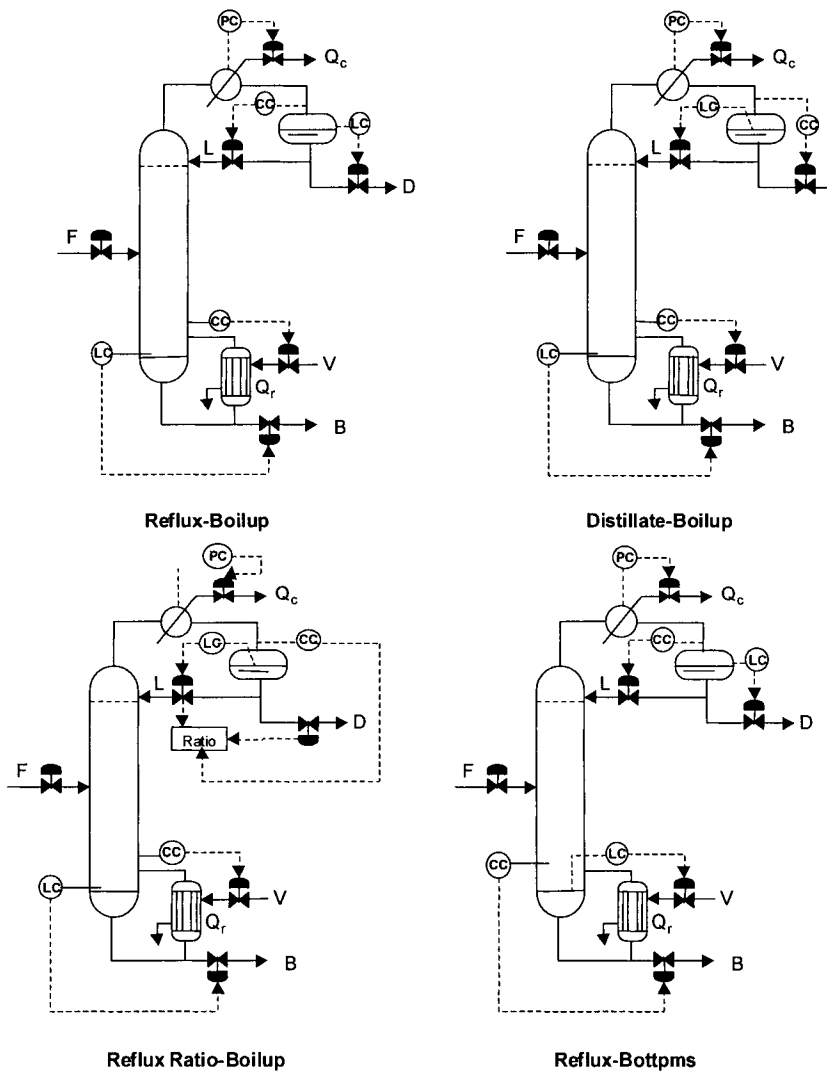

Figure 13.8 Control structures for distillation columns

When the distillation column is placed in a recycle, the interaction with other units must be taken into account, particularly with the reactor. The reactor is the place where significant changes in composition occur, which can lead to even larger variations in recycles. If these variations are too large, the disturbances sent to separators could reach magnitudes and frequencies that cannot be rejected properly. Thus, controlling the recycle streams can improve the dynamic behaviour of both reactor and separators.

EXAMPLE 13.1 Control of the distillation section of the HDA plant

Examine the control structure for the separation section of the HDA plant from plantwide perspective.

Solution.

Fig. 13.9 presents the flowsheet for the separation section of a HDA process. The first column is a stabiliser. The vapour distillate - a mixture of H_2, CH_4 with traces of benzene and toluene - can be used to hold constant the pressure. The quality of the bottom product is ensured by controlling a sensitive temperature in the top zone (inferential control) with the reboiler duty. Reflux and bottoms flow rates control the levels in reflux drum and sump, respectively.

The second column supplies benzene of high purity. One-point composition control is more robust in a recycle system. In inferential mode the heat input in reboiler controls a 'sensitive temperature' in the column. If the sampling point is placed in the stripping section, this control loop ensures good composition control of the bottom product. The reflux is set in ratio with the feed flow rate. For moderate disturbances, this allows good purity of distillate simultaneously with high recovery. The levels in the flash drum and in the base are hold by manipulating distillate rate and bottom product, respectively.

Finally, the control of recycle column is quite simple: distillate is taken-off by level control, reboiler duty is used to control the losses of toluene in bottom, and a bleed stream is paired on the reboiler-level control for the removal of the heavy impurities.

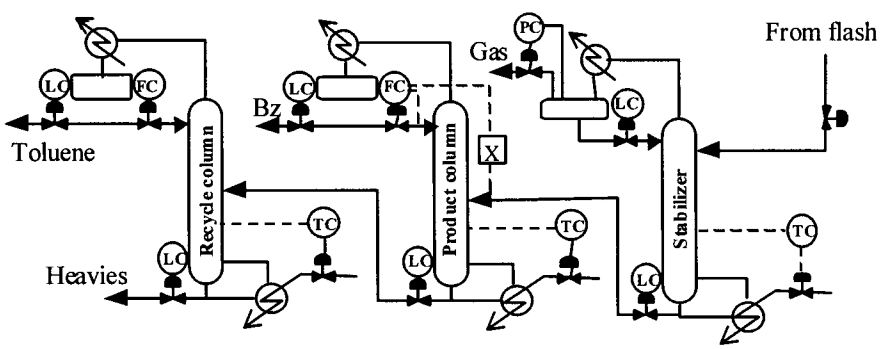

Figure 13.9 Control of distillation section in the HDA plant

13.4 CONTROL OF COMPONENT INVENTORY

We recall that in process dynamics the material content of a given volume is usually called 'inventory'. In recycle systems with chemical reactions the control of the components' inventory is a central issue in developing a plantwide control strategy. From this point of view we can distinguish two important aspects:

- Make-up policy of reactants.
- The handling of impurities.

13.4.1 Make-up policy of reactants

At steady state the chemical species must enter and leave the plant in a manner that satisfies perfectly the material balance. If chemical reactions are present, the make-up policy of the reactants must fulfil the stoichiometry of various chemical reactions. However, in practice the material balance of components has always a dynamic character. When several reactants are involved, not all can be fed on flow control. Firstly, because of inherent measurement errors and variability of raw materials, the reactants cannot be exactly counted in the stoichiometric ratio. Secondly, the reaction conditions are not constant. Accumulation will take place, and over longer period could lead to dysfunctions or even to plant upset. Somewhere in the plant the inventory of the reactants and products should be measured or estimated, and the make-up policy adapted accordingly.

The issue of reactant feed policy in recycle systems has been raised by Bill Luyben. Complete references and ampler presentation can be found in his recent book (1999). Here we will examine two typical situations involving a bimolecular reaction. In the first the reference reactant is completely converted, while the other one is recycled. The second case considers that both reactants are incompletely converted and recycled.

13.4.1.1 Incomplete reactant conversion

Let's consider a recycle system where a reaction of the type $A + B \rightarrow C$ takes place. The reaction rate is bimolecular and has the form:

$$v_{R,A} = kc_A c_B \tag{13.6}$$

Suppose that the reactant A is totally consumed. If the reaction rate is not infinite, the reactant B must be recycled at a convenient rate, in such a way that the resulting reaction rate leads to the total consumption of A. Therefore, we may speak about total conversion of the one-pass reactant, and partial conversion of the recycled reactant. Because the feed of fresh reactants must respect the stoichiometry, the feed policy of B must be adapted to fulfil the dynamic material balance. The above situation can be found often in industry, as for instance the synthesis of ethers from alchene-oxides and alcohols, the alkylation of benzene with ethylene or propylene to ethylbenzene or cumene, the addition of HCN to ketones, etc.

Figure 13.10 presents a first alternative. Both A and B feeds are on flow control according to the stoichiometric ratio. This control structure seems feasible on paper. In practice, as well as in simulation, it will not work. The reason is that the input/output material balance cannot be hold, even when small disturbances occur. Contrary, the

make-up policy displayed in Fig. 13.11 gives good results. Now only the reactant A (completely converted) is set on flow control. The fresh reactant B is fed in recycle after separation in a manner that fulfils the reaction stoichiometry. Therefore, the recycle flow rate of B can be set at a constant value, sufficient to ensure complete consumption of A, while the fresh B is fed on level control in a buffer tank. This control structure can handle moderate variations in throughput, of order of +/- 10%, depending on the reactor volume. At larger change the fixed recycle flow rate must be adapted accordingly. The next example will illustrate this feed strategy.

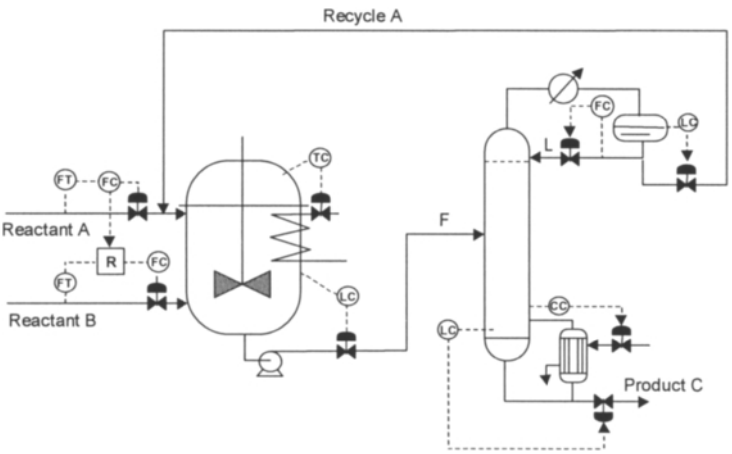

Figure 13.10 Feed policy for a recycle system with incomplete bimolecular reaction. Alternative A: both reactants on feed control

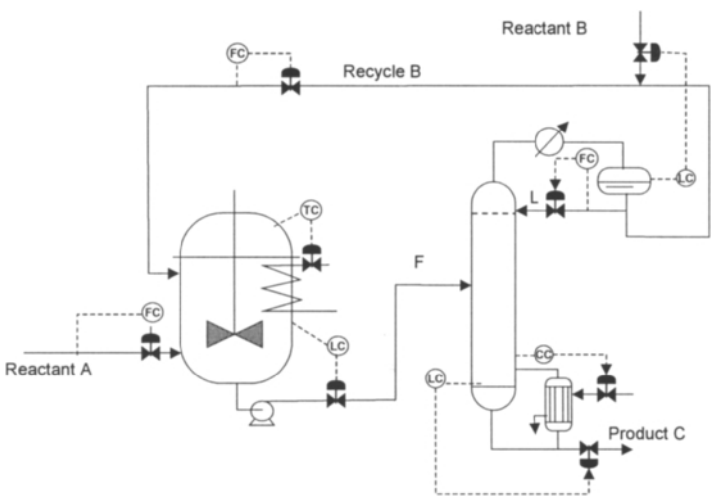

Figure 13.11 Feed policy for a recycle system with incomplete bimolecular reaction. Alternative B: make-up of partially converted reactant in recycle

EXAMPLE 13.2 Make-up control of addition of methanol to propylene-oxide

Consider the reaction of propylene-oxide with methanol leading to 2-methoxy-propanol:

$$\underset{(A)}{(CH_2-CH)O}-CH_3+\underset{(B)}{CH_3-OH}\rightarrow CH_2OH-\underset{(C)}{CH(OCH_3)}-CH_3$$

Examine alternative feed policies for a fresh feed of 10 kmole/h of A and B.

Solution. Propylene-oxide is a volatile hazardous species (nbp 35 °C) that cannot be recycled. The boiling points of the other two components are 63.5 °C for methanol and 129 °C for 2-methoxy-propanol. These can be separated easily by distillation. Thermodynamic analysis shows that the VLE behaviour is ideal. The reaction constant in Aspen is formulated as: $k=k_o(T/T_0)^n\exp(-E/R(1/T-1/T_0))$. For this exercise we consider $k_0=2\cdot10^7\ s^{-1}$, E=30000 cal/mol, T_0=1000 K and n=0. These values are realistic for an industrial plant.

We start by examining the feasibility of alternative feeding policies by steady state simulation in Aspen Plus. Figure 13.12 depicts the flowsheet. The key units are the reactor and the distillation column. We chose a PFR model, with 100% per-pass conversion of A. The reactant B is converted exactly in the same proportion as the amount of fresh A, but the excess is recovered by distillation and recycled. Further, we consider a distillation column with 10 stages and feed in the middle.

In the first alternative, both fresh reactants are set on flow control. This arrangement can be simulated simply by setting each flow rate at 10 kmol/hr. In this case the control of the reactor (plug flow) is not of significance. On the contrary, implementing control structures for the distillation column is necessary, because it determines the behaviour of the exit and recycles streams. Only two specifications are allowed. The first may be the quality of the bottom product, achieved by manipulating the boilup. The second one should be related to the overall material balance. The specification of the flow rate of the bottom product is unfeasible, because this cannot exactly match the input of reactants, unless its purity is extremely high. Another solution is to specify the ratio distillate/feed, and let the flow rates of the streams to be adapted by the convergence procedure. In this case we may define a ratio distillate/feed of 0.35, which gives about 50% recycle of B. If the purity in bottom is set at 99.9% the simulation fails. The same happens for 99.99%. Convergence is obtained only at very high purity, but because the amount of B tolerated in product is under the convergence error of the tear stream. This behaviour is unlikely in practice. Hence, the steady state simulation shows clearly that setting both fresh feeds on flow control does not lead to a controllable flowsheet.

Now, we try the second feeding alternative: the fresh input of the reactant B is adapted to fulfil the overall material balance. At steady-state, the amount of B supplied must be exactly the feed of A plus the loss in the bottom product. For this purpose the reactant B is fed now in recycle. A mixer unit is added to the flowsheet. The make-up of B is set such to achieve a constant partial flow rate of B at the mixer outlet, say at 15 kmole/hr. The column specifications have to be adapted to this situation. The specification of the bottom product purity can be kept. On the other hand, specifying the distillate flow rate would be in conflict with the fixed recycle. Another alternative is to

specify the flow rate of the bottom product, by considering the required purity. These specifications work well, suggesting a feasible plantwide control alternative.

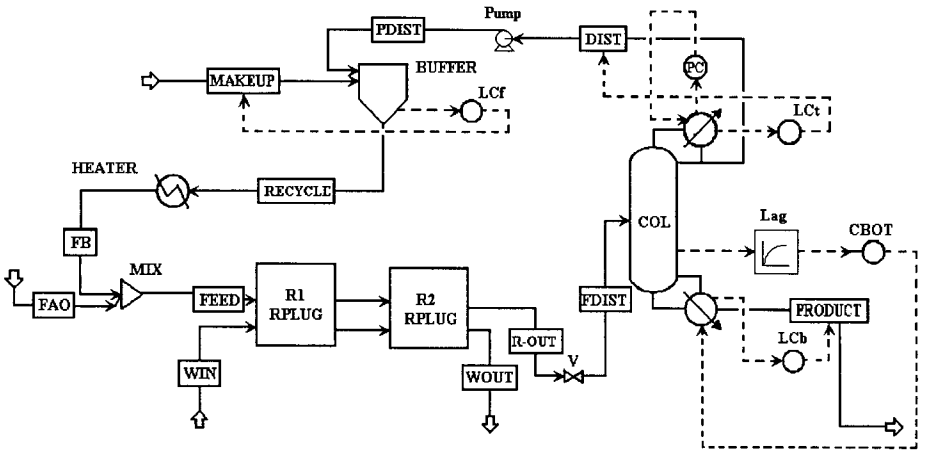

Figure 13.12 Flowsheet for bimolecular reaction with complete one-pass conversion of limiting reactant

Before starting the dynamic simulation, the sizing of units must be considered. The reactor is a long serpentine tube of 0.05 m diameter and 1000 m length. The high exothermic reaction develops an adiabatic temperature rise of 240 °C. The reactor temperature is kept between acceptable limits by means of hot water at 4 bar in co-current. A simulation exercise shows high sensitivity of the temperature profile inside the reactor with the inlet temperature of both reactant and thermal agent. Cold inlet temperatures, as well as too cold thermal agent can lead to severe hot spot on the first 50 m. This aspect, although highly interesting, is not developed here. Convenient results can be obtained by taking the inlet temperature of the thermal agent at 120 °C and heat transfer coefficient of 2000 W/m^2K. The temperature-rise is under 20 °C, while the reaction is kept at a good rate along the whole length. Complete conversion is achieved for propylene-oxide.

The reactor simulation with Aspen Dynamics sets some modelling constraints. In dynamic mode a PFR is transformed in a series of CSTR's. In order to get a reasonable model size, the number of elements is limited at 10 to 20. Therefore, we consider two PFR's in series. Because the temperature variation is the most important in the first zone, the first reactor has 100m and 20 elements. In the second zone the variations are almost linear, so that 10 elements for 900 m are sufficient.

Dynamic simulation of distillation column needs also tray sizing. We considered sieve trays with 0.4 m diameter of and 0.05 m static liquid height.

Manage properly the pressure is a key aspect in dynamic simulation. As shown in Chapter 4, Aspen Dynamics offers two possibilities: flow driven or pressure driven simulations. We selected the first possibility. We take care to specify all the items needed in dynamic simulation: pressure change units (pumps, valves), mixers and heat

exchangers. After performing the sizing in Aspen Plus, the results are exported to Aspen Dynamics. Figure 13.12 presents the flowsheet for dynamic simulation.

Let's take a look at the control loops. Now the make-up stream of reactant B is fed on level controller *LCf* of the buffer tank. The flow rate of the exit stream (Recycle) is set at a constant value by a simple specification on the stream's script. There are also two level controllers *LCt* and *LCb* for the top and bottom inventories of the distillation column, which manipulate the distillate and bottom products, respectively. Besides, the top column pressure is kept constant by means of the condenser duty. Quality control is implemented only for the bottom product, the reflux being fixed. We considered a composition measure with a first-order lag transmitted to a controller that manipulates the reboiler duty.

As it can be observed, we did not implement controllers on reactor. This is not necessary, because of the self-regulating mode of operation ensured by design and the choice of operating conditions. An important role in self-regulation plays the internal vaporisation of liquid mixture that protects the reactor from *runaway*. This situation was checked in steady state simulation by selecting an appropriate flash option. Unfortunately, this option was not available in dynamic simulation. However, the design was robust enough to ensure moderate temperature profile and very high conversion of propylene-oxide.

The tuning of controllers has been done by standard procedures, with final adjustment in the dynamic run. The proposed control structure shows remarkable robustness faced to different disturbances. The plant can face large changes in throughput for at least +/- 20%. However, the overall dynamics is slow. Figure 13.13 displays some trends.

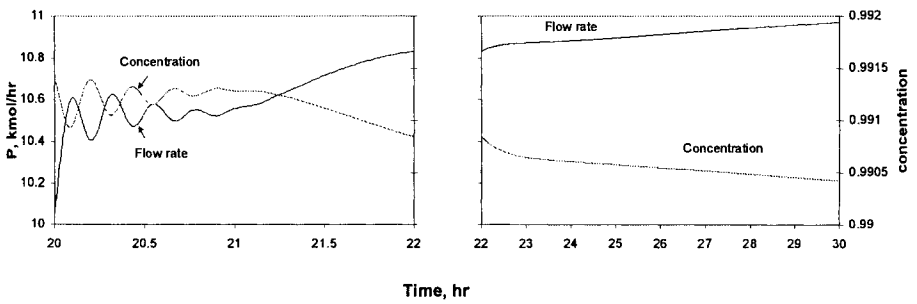

Figure 13.13 Time-profiles for flow and product concentration at large changes in throughput

Summing up, the above example demonstrates that the feed policy is a plantwide control problem. When several reactants are involved, only one can be set on flow control. The make-up of the other reactants must be implemented in a way that prevents a permanent accumulation (positive or negative) in the dynamic material balance. Thus, fixing the recycle flow of the second partner in a bimolecular reaction has proved to be an efficient method to stabilise the variability of recycle streams. However, this is not the panacea for feeding the reactants. The next section will bring supplementary insights.

13.4.1.2 Second order reaction with incomplete conversion of both reactants

This time both reactants are only partially converted. As before, we assume that distillation is the best separation method. There will be one of two recycles depending on the relative volatility of components.

1. Both reactants A and B are more volatile than the product C.

Only one distillation column is needed. At the first sight, because the consumption of the reactants in reactor follows the stoichiometry, their ratio would remain constant also in recycles. Consequently, one might think that both can be fed on flow control, taking care to respect the stoichiometry. As before, this control structure will not work in practice. Because the reactants are linked by the separation, their inventory cannot be determined separately. Moreover, the strategy consisting in putting one reactant on flow control and adjusting the make-up of the other one will not work either.

Figure 13.14 presents a suitable control structure for feeding. This time the reactant A is put on concentration control, while B is fed on level control. This structure keeps the advantage of measuring directly the production rate by integrating the feed variation over a period of time. However, a continuous measurement of concentration of A is needed, and this is not always obvious. Note also that the outlet reactor stream is held on flow control, in order to prevent a snowball effect. Increase or decrease in production can be achieved at best by manipulating the reactor temperature, which in turn will determine an automatic adjustment of the reactant feeds.

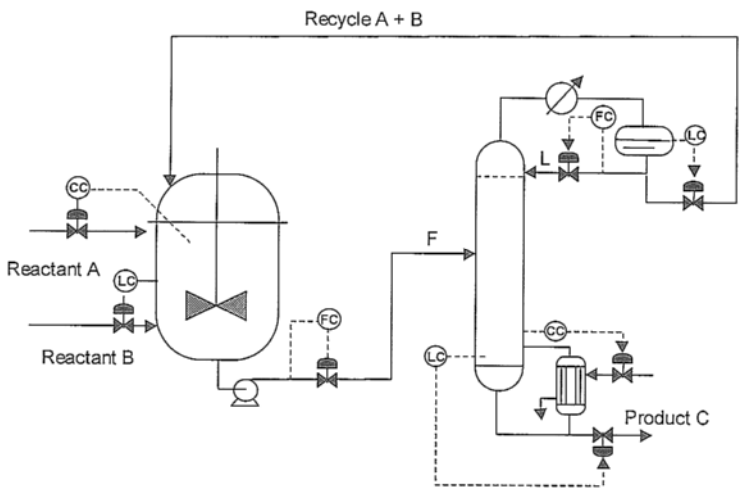

Figure 13.14 Feed policy for a second order reaction with recycle of both reactants from a single distillation column

2. The volatility of the product C is intermediate between A and B.

Two distillation columns are needed. Suppose that $\alpha_A > \alpha_C > \alpha_B$. Reactant B can be recycled as bottom product from the first column (indirect sequence), while the reactant A is recycled as top product from the second column. The product is obtained as

bottoms from the second separator. Luyben et al. (1999) have identified four control structures, which will be briefly commented.

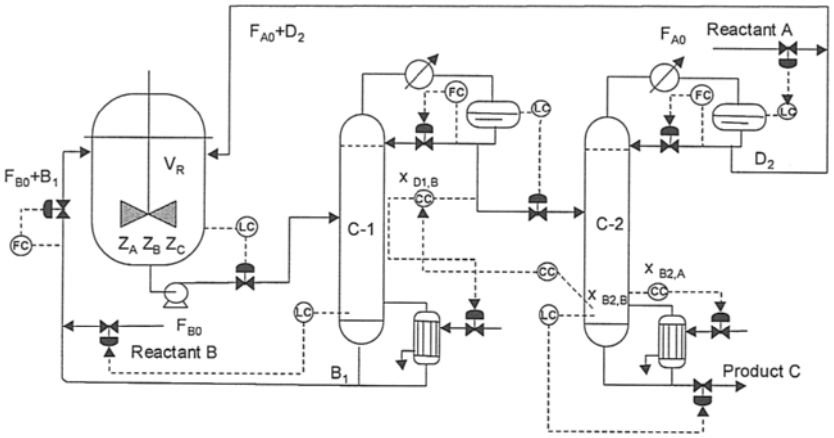

Figure 13.15 Control structure for bimolecular reaction with both reactants fed in recycles

Control structure CS1 shown in Fig. 13.15 makes use of the feed in recycles of both reactants. Recycles flow rates are also fixed on flow control. Note that the make-up of A and B may be done directly in the reflux drum and in the reboiler sump, respectively. The reactor outlet is put on level control. Single-point composition control and fixed reflux are used for distillation columns. Composition controllers can be co-ordinated by the composition measurement for the end product. This structure works well, but has the disadvantage of an indirect setting of production.

Another control structures can be developed. The structure called CS2 consists of feeding A on flow control, while B is set on level control. Although appealing and logical at the first sight, this structure does not work. This can handle only small disturbances in feed, of order of +/- 2%, but not larger variations. An imbalance in inventory occurs that lead to an upset of the system after a number of hours. Control structure CS3 keeps A on flow control, but replaces the input of B with the composition control. Again, this structure does not work. Finally, the control structure CS4 adds A on concentration control and B on level control, the reactor outlet being on flow control. This structure works well, but as CS1 it has the disadvantage of an indirect measure of production rate and requires a composition analyser.

A finer analysis permits to understand why CS2 and CS3 do not work. It may be observed that at constant temperature in the case of a bimolecular reaction the same reaction rate can be reached for different concentrations of z_A and z_B. The locus of constant reaction rate is a hyperbole (Fig. 13.16 left). Accordingly, for the same reactor inlet flow F we can have two steady states (Fig. 13.16 right). These are:

- Large concentration in A corresponding to a large recycle flow of A (stream D_2), and small concentration of B, corresponding to small recycle of B (stream B_1).
- Opposite, small concentration in A corresponding to a small recycle flow of A (stream D_2), and large concentration of B, corresponding to large recycle of B (stream B_1).

A stability analysis can show that the first situation leads to unstable behaviour. Consequently, when the limiting reactant is on flow control, its concentration in reactor should be small enough. Note that the control structure CS2 can be improved by introducing ratio control elements that can account for the amount of reactants in the two recycles.

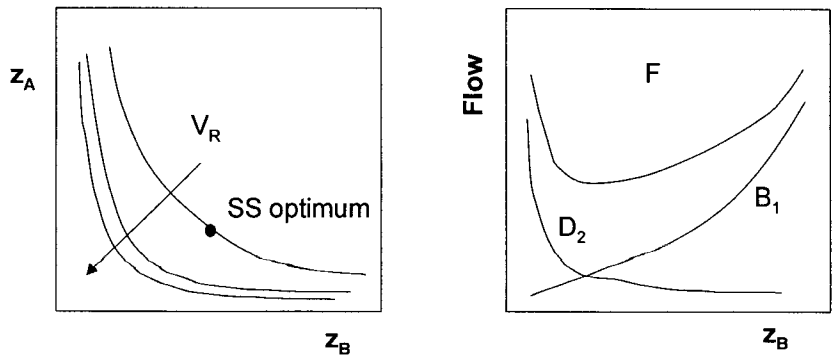

Figure 13.16 Multiple steady-states for bimolecular reaction

The above examples demonstrate in a simple manner that the feed policy of reactants in a plant is a plantwide control problem, particularly important for complex reactions with several recycles. Ideally the reactants should be introduced in amounts corresponding to the stoichiometry, including the formation of by-products and impurities. This is impossible by setting all the feeds by flow control in given ratios, not only because the measurements errors, but mainly because of variations in the reaction rate of different species due to various factors, temperature, catalyst activity, purity of feeds, etc. To this, it should be added the positive feedback of recycles. It can lead to excessive steady state sensitivity manifested by snowball effects, damageable for the operation of separation units, or in some cases to dynamic unstable behaviour. These phenomena are interrelated with the design of chemical reactor. When flexibility in production is required, the reactor volume should be sufficient large to cope with important variations in the reaction conditions. In addition for safety reasons the operating point should avoid regions where multiple steady states could exist, but ignored by designer. We reach again the conclusion that the design of a reactor should take into account the effect of recycles.

13.4.2 Control of impurities

The management of impurities is an issue of greatest significance in Process Design. Impurities affect the product quality, but also can generate troubles in operation and maintenance, and cause environmental damages. The inventory of impurities is a plantwide control problem, because it involves reactors and separators connected through recycles. Ideally, each component should be followed in each unit and each stream. Downs (1992) pointed out that the material balance must be preserved not only from an overall viewpoint, but also for each component. He presented a qualitative

method to solve this problem known as 'Downs drill'. This consists of preparing material balance tables for each component following the rule:

$$\{\text{Input}\} + \{\text{Generation}\} - \{\text{Output}\} - \{\text{consumption}\} = \{\text{accumulation}\}$$

The control of the accumulation can occur by *self-regulation*, or by manipulating process flows and operating conditions of units.

Figure 13.16 illustrates the difference between non self-regulating and self-regulating processes by means of a simple example. Suppose that a water supply system is fed through a storage tank. The feed F_1 is on flow control. In case *a* the flow F_2 to the process is pumped out at constant rate. Because the tank can become flooded or empty, the system is not self-regulating. In other words, the system integrates any imbalance between input and output. The process becomes *controlled self-regulating* if a level controller LC is put in place. If the inflow increases or decreases, the outflow will follow these variations perfectly at steady state, although dynamically with some delay and fluctuations. If the tank has an overflow then the process is *naturally self-regulating*. Note that putting both input and output on flow control, and setting their ratio to 1 as feed-forward controller is not practical, because of measurement errors.

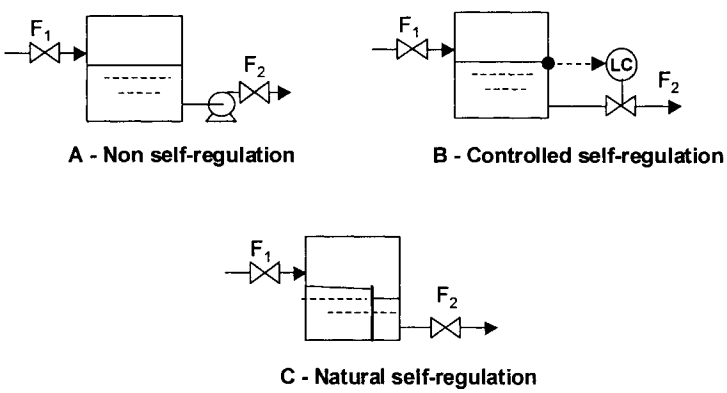

Figure 13.17 Principle of self-regulation

In a similar manner, the accumulation term can be driven to zero in gas-phase operations by means of controlled self-regulation that makes use of a pressure controller. Chemical reactions can also act as self-regulating when the accumulated component is a reactant, or if this is involved in an equilibrium reaction. When the accumulated component is a product, there is no mean to limit its inventory, except to manipulate an exit stream, or to cancel its generation. The above procedure is intuitive, and may be used for small-scale problems. However, it does not indicate how to solve systematically this problem, and how to include design elements in analysis.

A quantitative approach of the plantwide control of impurities has been proposed by Dimian et al. (2000). They demonstrate that the inventory of impurities in a large plant is a plantwide control problem that can be solved efficiently by managing positive and negative feedback effects, as well as by taking profit from interactions through recycles.

Chemical conversion is an effective way to counteract the accumulation of impurities due to positive feedback. Also, changing the connectivity of units may be used to modify the effect of interactions, for example by preventing an excessive increase in recycles due to snowball effects. Effective plantwide control structures may imply controlled and manipulated variables belonging to different but dynamically neighbouring units. The methodology to evaluate the dynamic inventory of impurities consists of a combination of steady state and dynamic flowsheeting with controllability analysis. This is used to assess the best flowsheet alternative and propose subsequent design modifications of units. Case Study 3 in Chapter 17 will present this problem in more detail.

13.5 STEADY STATE NONLINEAR EFFECTS OF MATERIAL RECYCLE

The nonlinearity of chemical processes received considerable attention in the chemical engineering literature. A large number of articles deal with stand-alone chemical reactors, as for example continuously stirred tank reactor (CSTR), tubular reactor with axial dispersion, and packed-bed reactor. The steady state and dynamic behaviour of these systems includes state multiplicity, isolated solutions, instability, sustained oscillations, and exotic phenomena as strange attractors and chaos. In all cases, the main source of nonlinearity is the positive feedback due to the recycle of heat, coupled with the dependence of the reaction rate versus temperature.

Nonlinear phenomena can be induced by material recycles. For examples, the plug-flow reactor (PFR) with recycle of a fraction of reactor's effluent can exhibit state multiplicity, sustained oscillations around a unique steady state and chaotic behaviour. If the material recycle has the temperature equal to the reactor effluent the true cause of the nonlinear phenomena is the material feedback.

Fig. 13.18 depicts reaction systems involving material recycles that are common in the industrial practice. The plant receives the feed F_0 of concentration c_0. The reactor effluent (F_2, c_2) is firstly processed by a separation section, and only afterwards recycled. Fixed composition of product (4) and recycle (3) streams is achieved by local control of the separation units. Hence, the composition at reactor inlet is not directly dependent on the reactor effluent. The temperature at the reactor inlet has a constant value by an upstream heat exchanger. This excludes the energy feedback. Such plant will be designated here by *Reactor-Separator-Recycle* system.

The analysis presented in this chapter is motivated by several plantwide control studies, which reported control difficulties due to the "snowball effect", when production changes were required. Moreover, the behaviour of Reactor-Separator-Recycle systems is relevant for integrating conceptual design and plantwide control because. Early during conceptual design, one reaches the stage when the recycle structure of the flowsheet is established. Accordingly, the reactor is the first unit to be examined in detail, because the chemical species present in the reactor effluent determine the separation section. Hence, reactor modelling, sizing, and control should be considered before separation is addressed. Thus, kinetic-reactor / black-box separation /recycle is the first quantitative model available.

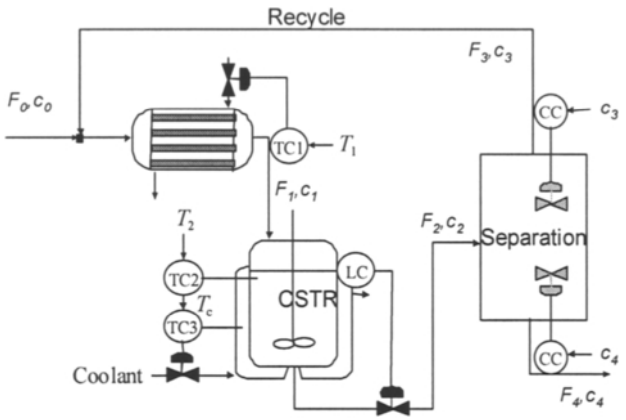

Figure 13.18 CSTR – Separator – Recycle systems

13.5.1 Modelling

The model used in this section neglects the time delays due to recycles and the capacity of the mixing vessels. Consequently, the model is obtained by the combination of the differential equations describing the dynamics of the reactor and the closed-loop separation. F and c are molar flow rate and reactant concentration, respectively. Dimensionless values are denoted by $f=c/c_0$ and $z=F/F_0$ with reference to process inlet. Subscripts follow the numbering explained in Fig. 13.18. When two reactants are involved, a second subscript is used. Because high purity product $c_4 = z_4 = 0$.

Reactor model

A dynamic model of a CSTR can be derived based on unsteady mass and energy balance (see Chapters 4 and 8). The model contains a few nonlinear differential equations, being amenable to analytic or numerical investigation. When n^{th}-order reaction is considered, the mass and heat balance equations can be written in the following dimensionless form:

$$\frac{dz_2}{d\tau} = \frac{1}{Da}\left[1 + f_3 z_3 - (1+f_3) z_2\right] - z_2^n \exp\left(\frac{\gamma\theta}{1+\theta}\right) \tag{13.7}$$

$$Le\frac{d\theta}{d\tau} = -\frac{1+f_3}{Da}\theta + Bz_2^n exp\left(\frac{\gamma\theta}{1+\theta}\right) - \beta(\theta - \theta_c) \tag{13.8}$$

The variables of the dimensionless model are: reactor outlet concentration (z_2), reactor temperature (θ), and time τ. The model parameters represent the activation energy (γ), adiabatic temperature rise (B), heat-transfer capacity (β), coolant temperature (θ_c), and Lewis number (Le). The recycle flow rate (f_3) and concentration (z_3) are state variable and

parameter of the separation model, respectively. The new and the most important parameter in this analysis is the *plant Damköhler number* (*Da*) given by:

$$Da = k\left(T_{ref}\right)\frac{V}{F_0}c_{ref}^{n} \tag{13.9}$$

Note that Eq. 13.9 makes use of F_0, the *plant feed* flow rate, and not of the reactor inlet flow rate.

Closed-loop separation model

In a simplified approach we consider a *separation section* where all the units are lumped in a black-box. The composition of the outlet streams is constant due to the local control. In practice, this is achieved by manipulating internal flow rates or by heat duties. Changing the flow rate or composition of the inlet streams is reflected by a gradual change of the flow rate of outlet streams. When complete reactant recovery is assumed ($z_4 = 0$), the simple model describing the dynamic behaviour of the recycle consists of a first-order differential equation:

$$\tau_S \cdot z_3 \frac{df_3}{d\tau} = \left(1 + f_3\right) \cdot z_2 - f_3 \cdot z_3 \tag{13.10}$$

where f_3 and τ_s are dimensionless recycle flow rate and time constant, respectively. The composition of the recycle stream z_3 is fixed by the local control system. Here we make the following remarks concerning the dimensionless model (Eqs. 13.7 to 13.10):

- Flow rate (F_1) and composition (c_1) of the reactor-inlet depend on the flow rate (F_3) and composition (c_3) of the recycle, and therefore cannot be used as references. For this reason, the dimensionless quantities are defined using the flow rate (F_0) and concentration (c_0) at the plant inlet. The *plant Damköhler number* obtained in this way is different from the classical definition that makes use of reactor inlet as reference.
- When a control loop keeps constant the reaction temperature, this can be used as reference, $T_{ref} = T_2$. When there is no reactor temperature control, but reactor-inlet temperature control, then $T_{ref} = T_1$.
- We consider the plant Damköhler number to be a varying parameter. The overall mass balance requires the equality of the feed (F_0) and product (F_4) flow rates, $F_0 = F_4$. Consequently, the plant Damköhler number accounts for production (F_0), reactor volume (V) and design uncertainty ($k(T_{ref})$).
- Each of the following variables appears in only one dimensionless variable: feed flow rate (F_0), heat transfer capacity (UA), coolant temperature (T_c), recycle concentration (c_3), reaction activation energy (E_A), and reaction enthalpy ($-\Delta H$). Thus, the effect of each one can be easily investigated.
- The reaction conversion (X) is a key result. It can be calculated as:

$$X = 1 - \frac{\left(1 + f_3\right) \cdot z_2}{1 + f_3 z_3} \tag{13.11}$$

13.5.2 Isothermal CSTR - Separator - Recycle

For n^{th}-order reaction $A \rightarrow products$ taking place in an isothermal CSTR-Reactor-Separator system, the dimensionless model Eqs. 13.7 and 13.10 reduces to:

$$\frac{dz_2}{d\tau} = \frac{1}{Da}\left[1 + f_3 z_3 - (1+f_3) z_2\right] - z_2^n \tag{13.12}$$

$$\tau_S \cdot z_3 \frac{df_3}{d\tau} = (1+f_3)\cdot z_2 - f_3 \cdot z_3 \tag{13.13}$$

The steady state model, obtained after dropping the time derivatives in Eqs. 13.12 and 13.13, has two steady state solutions:

$$(z_2)_{1,2} = \left(z_3, \frac{1}{z_3 \cdot \sqrt[n]{Da}}\right) \tag{13.14}$$

$$(f_3)_{1,2} = \left(\infty, \frac{1}{z_3 \cdot \sqrt[n]{Da} - 1}\right) \tag{13.15}$$

The steady state conversion is given by:

$$(X)_{1,2} = \left(0, \frac{z_3 \sqrt[n]{Da} - 1}{z_3\left(1 + \sqrt[n]{Da}\right) - 1}\right) \tag{13.16}$$

Figure 13.19 presents the conversion vs. plant Damköhler number, for two different reaction orders and different values of the recycle concentration. Solid and dashed lines refer to stable and unstable steady states, respectively. It is obvious that one solution is unfeasible, corresponding to zero conversion and infinite recycle flow rate (its stability is presented for $z_3 = 1$). The other one is feasible ($0 < X < 1$, finite recycle) if, and only if the following condition is fulfilled:

$$z_3 \cdot \sqrt[n]{Da} > 1 \tag{13.17}$$

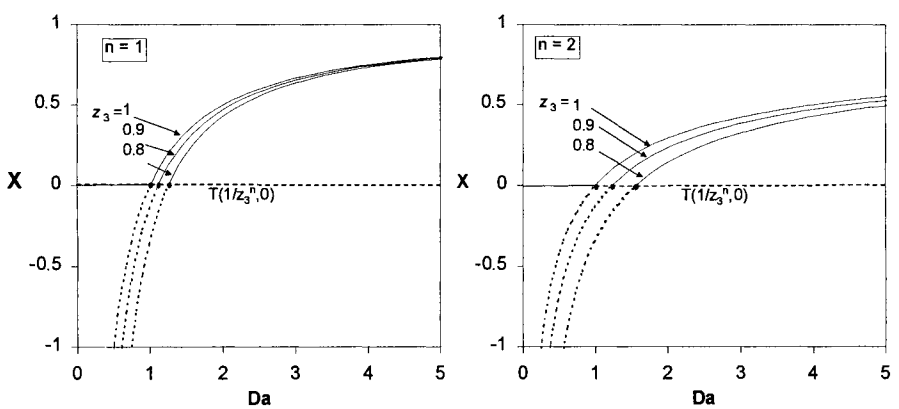

Figure 13.19 One– reactant, n^{th}-order reaction in isothermal CSTR –Separator –Recycle system

Such a feasibility constraint, characteristic to recycle systems, does not appear for stand-alone reactors. It can be explained by simple material balance reasons. The separation section does not allow the reactant to leave the process. Therefore, for a given a reactant input (F_0) either large reactor volume (V) or fast kinetics ($k(T_{ref})$) are necessary to consume entirely the reactant fed and avoid accumulation. These three variables are conveniently grouped in the plant Damköhler number. The factor z_3 accounts for the degradation of reactor performance due to impure reactant recycle. We note that a similar feasibility conditions also holds when the concentration of the reactant in the product stream is nonzero. Moreover, systems containing a purge stream of fixed flow rate have the same qualitative behaviour as the simple system described here. Finally, we remark that the condition 13.17 applies also to the system PFR – Separator – Recycle.

Interaction between design and control

The set of specifications used in the previous section (F_0, V, z_3, z_4) can be viewed as a conventional plantwide control structure, as displayed in Fig. 13.20a. Plant throughput is set by the reactant feed, the reaction volume is kept constant, and the separation section is dual-composition controlled. For this control structure, the feed disturbances affect the flow rate and composition of the reactor outlet/separation inlet. Hence, manipulated variables internal to separation section are used to reject the disturbances. As a result, disturbances are rejected mainly by changing the reaction conditions.

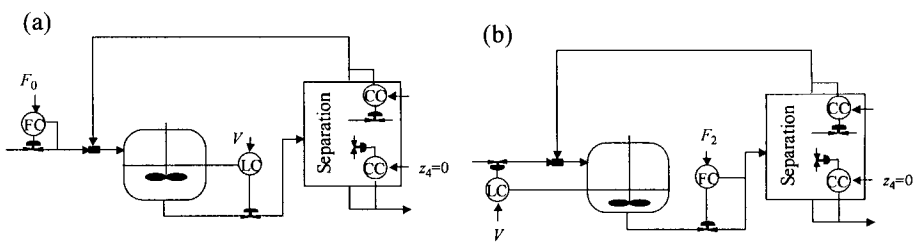

Figure 13.20 CSTR-Separator-Recycle: control structures

The CSTR-separator-recycle system was previously analysed in several plantwide controllability studies. Luyben (1994) pointed out that the conventional control structure exhibits high sensitivity to feed disturbances. He proposed as alternative (Fig. 13.20b) to keep the reactor outlet on flow control and to modify the plant throughput by changing the reaction conditions, either by allowing larger variation of the reactor volume or by modifying the temperature. This control structure is equivalent to the following set of design specifications: F_0, F_2, z_3, z_4. When disturbances affect the process, the load of the separation section changes only due to composition modification. In order to compare the conventional and Luyben's control structures, we perform a steady state sensitivity analysis for different values of the design parameters.

Let's F_0^* and V^* represent nominal feed flow rate and reaction volume. For the conventional control structure, Fig. 13.21-left displays the flow rate to separation vs.

reactant feed flow rate, for different values of the nominal Damköhler number $\left(Da^* = k \cdot V^* \cdot c_0 / F_0^*\right)$ and recycle stream purity (z_3). In the case of Luyben's structure, Fig. 13.21-right presents reactor volume ($V \neq V^*$) vs. reactant feed flow rate.

A sensitivity study demonstrates that systems with small reactor or slow reaction rate ($Da^* < 2$) are better controlled by the Luyben's structure. However, systems with large reactor or fast reaction rate ($Da > 3$) are better controlled by the conventional structure. To explain this fact, we recall that close to Da=1 the system is sensitive to Da. For the conventional control structure, the plant Da number represents a disturbance, as it contains F_0. Because low sensitivity is required, designs with Da large perform better. For the Luyben control structure, the plant Da number is a manipulated variable through the reaction volume V. Consequently, disturbances can be rejected with small effort if Da is small. It should be also noted that high purity separation (z_3 = 1) improves the performance of the conventional control structure. It is worthy to mention that the design analysed by Luyben (1994) had Da=1.12. Hence, poor performance of the conventional control structure is expected.

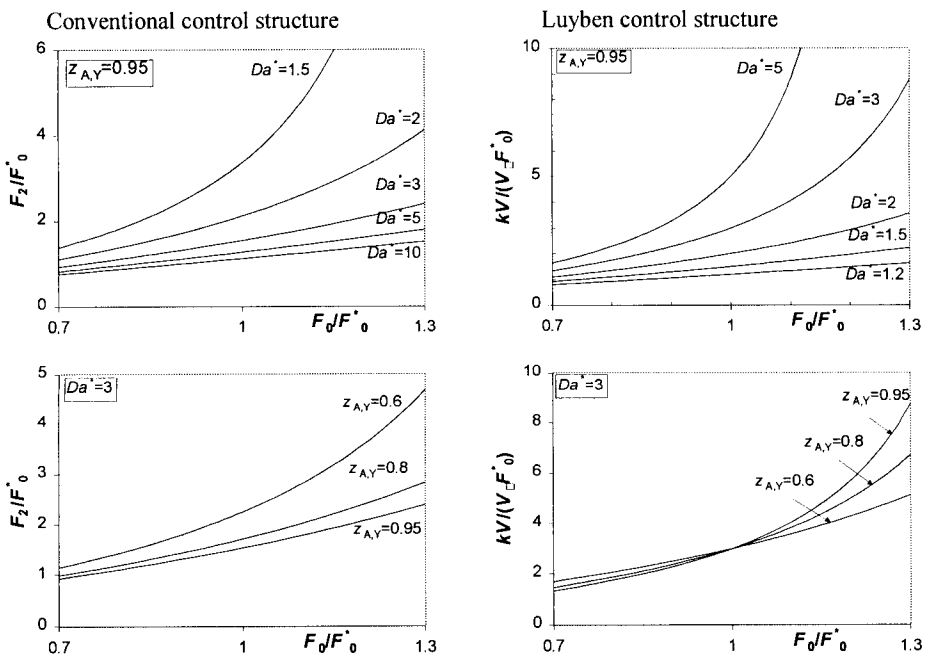

Figure 13.21 First-order reaction in CSTR-Separator-Recycle: sensitivity analysis for different control structures

The implementation of a variable-volume reactor could be seen as not practical, because the reactor is an expensive equipment item whose volume should be effectively used. In fact, sizing properly the reactor should ensure by design the required flexibility to large variations in throughput. However, the rule of limiting the variation of recycles

keeps its importance, but other solutions than controlling the reactor's outlet can be imagined.

13.5.3 Two-reactants, second-order reaction

This section analyses the second order reaction $A + B \rightarrow P$ taking place in an isothermal CSTR-Separator-Recycle system. When the reactants are completely recycled, feasible operation is possible only if the ratio of reactants in the feed matches exactly the stoichiometry. For this reason, only one reactant feed may be on flow control ($f_{A,0}$=1), while the feed flow rate of the second reactant ($f_{B,0}$) must be used to control its inventory. Two possible control structures are discussed (Fig.13.22): flow control of the recycle stream of one reactant, or of the reactor effluent, respectively.

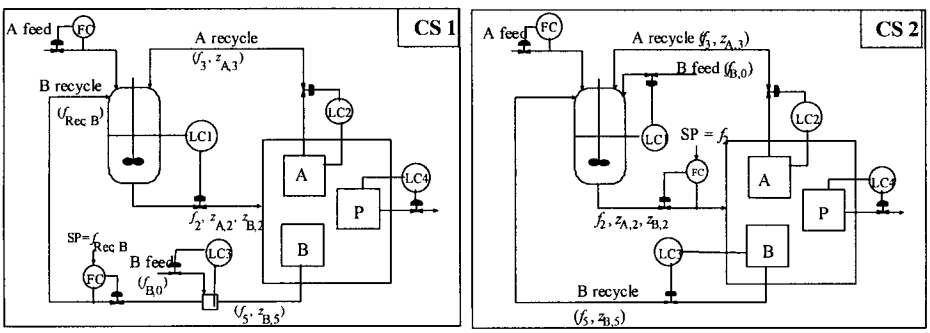

Figure 13.22 Two-reactants, second-order reaction in CSTR-Separator-Recycle system

The steady state model includes reactor and separation equations, as well as the relation for the feed flow rate of second component imposed by the control structures:

$$\text{CS 1: } f_{B,0} = f_{Rec,B} - f_5 \tag{13.18}$$

$$\text{CS 2: } f_{B,0} = f_2 - \left(1 + f_3 + f_5 - Da \cdot z_{A,2} \cdot z_{B,2}\right) \tag{13.19}$$

In both cases, two steady state solutions are possible. They have complex analytical expressions, not reproduced here.

The conversion of the key component, X_A, is presented in Fig. 13.23 for high purity separation ($z_{A,3} = z_{B,5} = 1$). For given values of the fixed flow rate ($f_{Rec,B}$ or f_2) and separation performance ($z_{A,3}$ and $z_{B,5}$), two feasible steady states exist when the plant Damköhler number exceeds the critical value corresponding to the turning point of the Da - X_A diagram. The following feasibility conditions can be derived:

$$\text{CS 1: } Da > Da^{cr} = 4\frac{f_{Rec,B}}{z_{A,3} \cdot z_{B,5}\left(f_{Rec,B} - 1\right)} \tag{13.20}$$

$$\text{CS 2: } Da > Da^{cr} = \frac{4}{z_{A,3} \cdot z_{B,5}} \left(\frac{f_2}{f_2 - 1} \right)^2 \tag{13.21}$$

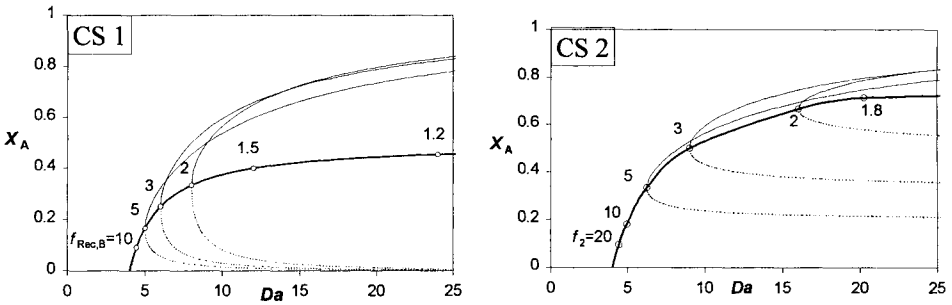

Figure 13.23 Multiple steady states of two-reactants, second-order reaction in isothermal CSTR-Separator-Recycle system

An important result of the above analysis is that a recycle system in which the reactor is designed near critical Da^{cr} can suffer from serious operability problems. If the reaction kinetics is over-estimated, or the feed flow rate deviates from the nominal design value, the operating point falls at the left of the turning point in the $Da - X_A$ map, in the region where no steady state exists. Infinite reactant accumulation occurs and the plant has to be shut down. This behaviour was confirmed by dynamic simulation using a more detailed model. We remark that is very likely to get a design in this high sensitivity region by steady state optimisation.

In Fig. 13.23 the lower steady state is unstable and has unusual behaviour: larger reactor gives lower conversion. The instability can be proved based on steady state considerations only, showing that the analogue of CSTR's slope condition is not fulfilled. Note that the low-conversion state is *closed-loop* unstable. Moreover, it is independent on the dynamic separation model. Because this instability cannot be removed by control, operation is possible when the following requirements, necessary but not sufficient, are met:

$$\text{CS 1: } X_A > \frac{1}{z_{B,5} \cdot f_{Rec,B} + 1} \tag{13.22}$$

$$\text{CS 2: } X_A > \frac{2}{2 + z_{A,3} \cdot (f_2 - 1)} \tag{13.23}$$

A dynamic model is needed to prove the stability of the upper solution branch, which is not guaranteed by Eqs. 13.22 and 13.23. More precisely, differences in the dynamics of recycles might lead to oscillatory behaviour, because of the violation of a dynamic stability condition. To check stability, a dynamic model is needed.

The lower limit of the conversion achievable at a stable operating point decreases as the flow rates increase (Eq. 13.22, 13.23) and Da^{cr} increases (Eq. 13.20, 13.21). Hence,

for a second-order reaction in isothermal CSTR there is a lower limit of the reactor size in a recycle system given by:

$$Da \cdot z_{A,3} \cdot z_{B,5} > 4 \tag{13.24}$$

13.5.4 Adiabatic CSTR – Separator – Recycle

Steady state behaviour

We start by recalling some results concerning the stand-alone adiabatic CSTR. Its steady state can be described by the following dimensionless equation, where the Damköhler number (Da^*) and adiabatic temperature rise (B^*) are calculated using the reactor-inlet flow rate (F_1) and concentration (c_1) as reference values.

$$-X + Da^* \cdot (1-X) \cdot \exp\left(\frac{\gamma B^* X}{1 + B^* X}\right) = 0 \tag{13.25}$$

It can be proven that Eq. 13.25 admits three solutions for $\gamma B^* > 4(1+B^*)$. Because usually B^* has small values, an approximate criteria for state unicity is $\gamma B^* < 4$.

The steady state model of the adiabatic CSTR-Separator-Recycle system is obtained by setting $\beta = 0$ and dropping the time derivatives in Eqs. 13.7 and 13.8. After some algebraic manipulations, the model can be reduced to one equation with one state variable X (the recycle of A is pure component so that $z_3 = 1$):

$$\begin{aligned} f(X, Da, B, \gamma) &= -X + Da \cdot X \cdot (1-X) \cdot exp\left(\frac{\gamma BX}{1+BX}\right) = \\ &= X \cdot g(X, Da, B, \gamma) = 0 \end{aligned} \tag{13.26}$$

Equation 13.26 has $X = 0$ as trivial solution, which will be disregarded in the following. The multiplicity features of the expression

$$g(X, Da, B, \gamma) = -1 + Da \cdot (1-X) \cdot exp\left(\frac{\gamma BX}{1+BX}\right) = 0 \tag{13.27}$$

are summarised below:

- The dependence of X vs. Da (including the unfeasible domain of negative conversion) is S-shaped. Therefore, for fixed values of B and γ, a range of Da values for which Eq. 13.27 admits three solutions (not necessarily with physical significance) does exist. The range of multiple steady states is bounded by two turning points.
- Multiple feasible states exist if at least one of the turning points is located in the region of positive conversion and the following condition is fulfilled:

$$B\gamma > 1 \tag{13.28}$$

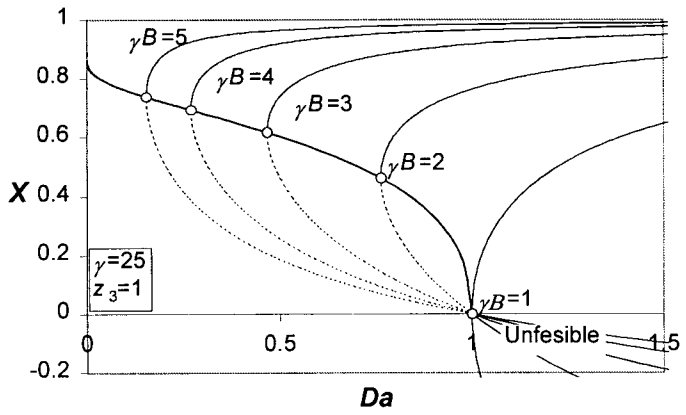

Figure 13.24 First-order reaction in adiabatic CSTR – Separator – Recycle system

Figure 13.24 presents X vs. Da, for fixed value of the activation energy $\gamma = 25$, and different values of the adiabatic temperature rise B. When $B\gamma > 1$, zero, two or one feasible steady state exist for $Da < Da^F$, $Da^F < Da < 1/z_3$, and $Da > 1$, respectively. When $B\gamma < 1$, a unique feasible steady state exists for $Da > 1/z_3$, which is exactly the feasibility condition obtained for isothermal reactor operation. Note that the multiplicity region of the adiabatic CSTR – Separator – Recycle system ($B\gamma > 1$) is larger compared to the stand-alone adiabatic CSTR ($B^*\gamma > 4$). An optimisation procedure might suggest a small reactor, corresponding to an operating point close to the turning point, but such system will be faced with operability problems.

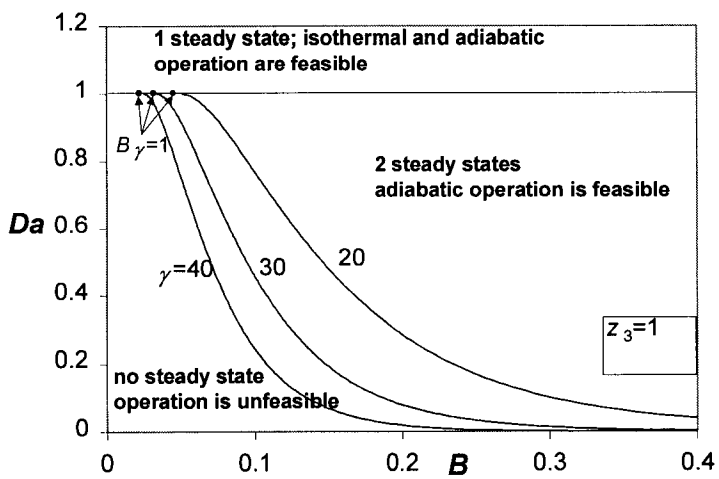

Figure 13.25 First-order reaction in adiabatic CSTR – Separator – Recycle system: Effect of activation energy (γ) and adiabatic temperature rise (B) on the extent of feasibility region

Figure 13.25 presents the locus of the turning points in a Da vs. B diagram, for different values of γ and $z_3 = 1$. For reactions with sufficiently high activation energy or adiabatic temperature rise ($B\gamma > 1$), the range of Da values for feasible operation ($Da > Da^F$) is larger, compared to the isothermal CSTR operation ($Da > 1/z_3$). This happens due to the occurrence of feasible steady states at the turning point. However, only one of the new steady states is stable, as discussed in the next section.

Dynamic behaviour

When multiple steady states exist, the low-conversion one is unstable (dashed-line in Fig. 13.24). This is independent of the dynamic separation model, but does not guarantee the stability of the high-conversion branch.

Instability of the low-conversion branch restricts the conversion that can be achieved in an adiabatic reactor. This can have practical consequences when low conversion is desired, for selectivity reasons. Stability condition is presented in Fig. 13.26 left, where the influence of recycle purity and activation energy on the coordinates (B, X) of the turning point are shown. For a given reaction (fixed B and γ), one can design an adiabatic reactor to operate in a stable Reactor – Separator – Recycle system only if the required conversion is in the upper part of the diagram. Note that the performance of the separation section (z_3) has a small influence, as illustrated in Fig. 13.26 right.

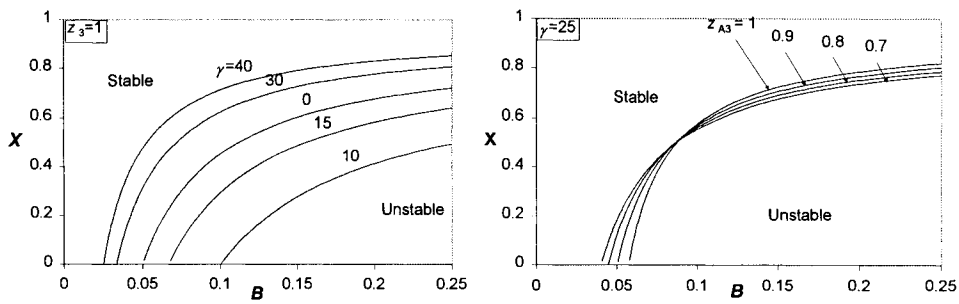

Figure 13.26 First-order reaction in adiabatic CSTR – Separator – Recycle system: Conversion achievable at stable operating points

Summing up, we may state that the interaction between Reaction and Separation systems through material recycles generates nonlinear phenomena. For all reactors a zero-conversion infinite-recycle steady state exists, but obviously, this is not realistic. Feasible steady states at conversion greater than zero appear when the reactor volume exceeds a critical value. Feasibility rules regarding the design of reactors in recycle systems can be formulated in term of dimensionless number that takes into account the reaction kinetics, the thermal effects, as well as the specifications of the recycle composition. Attention should be paid in designing chemical reactors to steady state stability in recycle systems. This aspect could set hard constraints to the conversion level for which the reactor should be designed.

13.6 DYNAMIC EFFECTS OF ENERGY RECYCLE

Saving energy by integration must be analysed also from the point of view of its effect on dynamics and control. Industrial practice showed that excessive heat integration could lead to poor dynamics or even inoperable plants. Hence, considering controllability aspects in designing energy saving systems is an essential topic.

The coupling of units creates new paths for the propagation of disturbances, while reducing the number of the degrees of freedom. The positive feedback of energy through recycle may lead to unstable systems even if the stand-alone units are stable.

Luyben et al. (1999) presented an interesting analysis of the relation between thermodynamics and process control by means of the *exergy destruction principle.* Thus, a responsive control is achieved when the *control system can alter significantly the rate of exergy destruction* (entropy generation). Here we have to solve a contradiction. Tight heat integrated systems are not likely to be responsive, when the control is ensured only by transferring the excess of energy from one location to another. On the other hand, quick responsive processes can be obtained at the expense of high entropy generation, or in other words of high inefficiency. Consequently, there is an optimal trade-off between the thermodynamic efficiency and operability, which is a task of an integrated design. For example, significant improvement in responsiveness can be obtained by using some (usually small) auxiliary utility-driven heat exchangers. From operability point of view, the utility system can manage control problems by cutting the paths for the propagation of disturbances when energy is recycled.

Similarly with the recycle of mass, the recycle of energy can induce non-linear phenomena that affect the whole plant. Practical solutions can be obtained by examining these aspects at the level of sub-systems. The next sections present two examples of practical significance: heat integrated reactors and heat integrated distillation columns.

13.6.1 Heat integrated reactors

In the case of highly exothermic reactions, the heat exchange between the effluent of an adiabatic reactor and the feed stream may be used for energy saving. A feed-effluent heat exchanger, abbreviated often as FEHE, is placed before the reactor. There are several reasons to include additional units as follows:

- A heater, as for example furnace, is required for start-up. Because positive feedback due to heat integration may lead to state multiplicity, the furnace duty can be manipulated in a temperature control loop to ensure stable operation.
- The heat excess must be removed in a cooler (steam-generator). Placing the steam-generator before the FEHE allows heat recovery at higher temperature and is therefore preferable in view of exergetic considerations.

In this way another structure is obtained, as presented in Fig. 13.27, which is more general for industrial applications. This will be called heat-integrated PFR. This generic structure has been studied by Bildea & Dimian (1998, 2000) from the point of state-multiplicity, stability, and controllability. The investigation has put in evidence the close link between design and controllability.

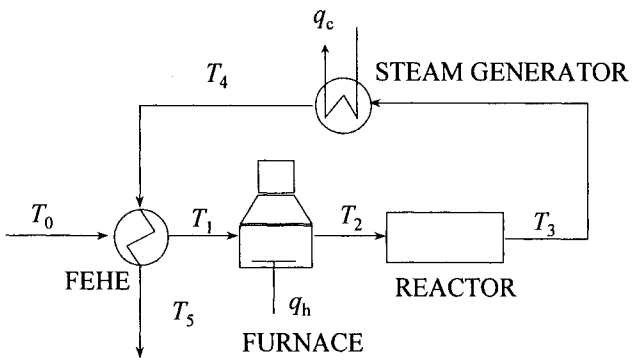

Figure 13.27 Heat-integrated plug-flow reactor

Four design alternatives of the heat-integrated HDA plant have been considered (Table 13.1). Design 1 has low-efficiency FEHE and operates in the unicity region, but close to the unicity/multiplicity boundary. Design 2 has high-efficiency FEHE, and therefore operates in the multiplicity region, at an unstable operating point. Each design has two alternatives. In alternatives 1A and 2A both the steam generator and the furnace duties are large. In the alternatives 1B and 2B, a small steam-generator is considered. Thus, the energy saving, expressed by the FEHE duty, increases from design 1A to 2B.

Table 13.1 Design alternatives of the HDA heat-integrated reactor

	Design 1A	**Design 1B**	**Design 2A**	**Design 2B**
Furnace duty,	large	large	large	moderate
Steam-generator duty	large	small	large	small
FEHE				
Hot side inlet (°C)	297	588	297	588
Efficiency, ε	0.28	0.28	0.745	0.745
Area	small	small	large	large
Hot side outlet temperature, T_1 (°C)	104.7	186	212.8	445.5
Cold side outlet temperature T_5 (°C)	223.8	435.6	102.7	181.9
Duty	small	moderate	moderate	large

Three control structures are considered:

- CS1: reactor temperature/furnace duty
- CS2: reactor temperature/bypass around FEHE
- CS3: reactor temperature/furnace duty, inlet furnace temperature/bypass FEHE.

The disturbances are (1) reactor feed, (2) steam generation duty, and (3) overall heat transfer coefficient because of the fouling of FEHE.

A linear controllability analysis can be performed using the measures presented in Chapter 12. The necessary condition to ensure control with given inputs is that for every disturbance the loop gain has to be greater than disturbances gains, such as:

$$|g_{ii}| > |\tilde{g}_{dik}|, \quad \forall k \tag{13.29}$$

As illustration of the approach, Fig. 13.28 presents loop and disturbance gains when furnace duty is the manipulated variable (control structure CS1). At low frequency, the condition 13.29 is fulfilled for the designs 1A and 2A. For the designs 1B and 2B, it is necessary to increase slightly the maximum allowed control action to avoid input saturation. In all cases, fast disturbances cannot be rejected at high frequencies. Feed flow rate is the most difficult disturbance. When steam-generator is designed for large load, a disturbance in its duty (design 1A and 2A) is difficult to reject. Because a fast change in FEHE heat transfer coefficient is not expected, we are concerned with only low frequency response, where the disturbance is easy to reject.

When bypass around FEHE is the manipulated variable (control structure CS2), the simulation shows that disturbances in the feed flow rate cannot be rejected. Disturbances in steam-generator duty can be handled only if the steam-generator duty is small (design 1B and 2B). Only designs 2A and 2B can cope with FEHE fouling.

Taking into account the overall behaviour, the design 2B with moderate furnace duty, small steam-generator and efficient FEHE performs the best.

This example demonstrates that the controllability of the heat-integrated reactors must be investigated in more detail before other design steps are undertaken. Non-linear behaviour puts serious constraints on conversion range and operating parameters, particularly on the temperature. The optimal conversion is not only a matter of trade-off between separation and recycle costs, but also a problem of control and operation.

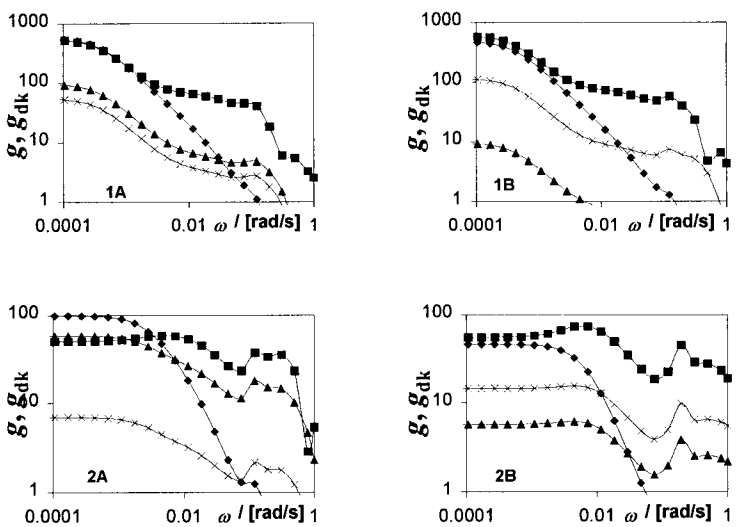

Figure 13.28 CS1 : Frequency-dependent loop and disturbance gains
♦ g (loop gain); ■, ▲, ×, g_{dk} (disturbances gain), k=1 (feed), 2 (duty), 3(heat transfer).

13.6.2 Heat integrated distillation

Heat integration of distillation columns can lead to significant energy saving. However, this should not penalise operability. In this section we will show how simultaneous design and control can solve conveniently this problem (Bildea and Dimian, 1999).

The integrated system discussed consists of prefractionator coupled to a side-stream main column. Figure 13.29 presents forward heat-integration with prefractionator at higher pressure. Vapour distillate is sent to heat-up the reboiler of the second column. In reverse integrated scheme the pressure in the second column is higher, the top vapour being used as heating agent in the reboiler of the first column.

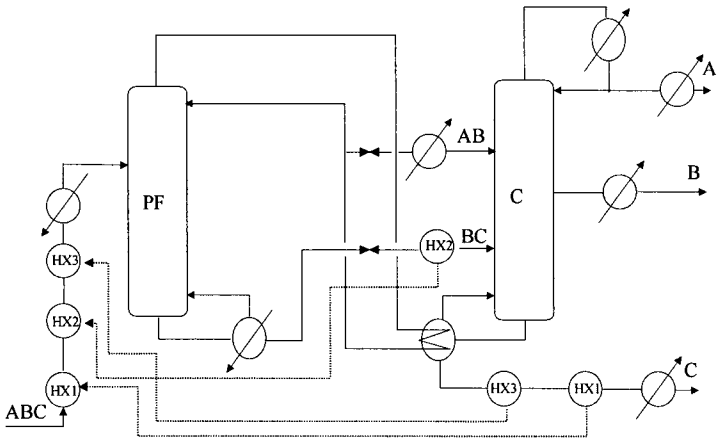

Figure 13.29 Prefractionator /side stream column with forward integration

As example, we consider the separation of an equimolar mixture of pentane/hexane/heptane with moderate purity requirements. Four designs are investigated for both forward and reverse heat-integration. Energy integration takes into account total match of reboiler and condenser of the first/second and second/first columns, respectively, as well as feed preheating with excess enthalpy of products. Design I considers tall prefractionator for sharp light/heavy split. Design II has shorter prefractionator for moderate light/heavy split. In the other cases, the prefractionator is designed for high recovery of the light, or of the heavy component, respectively. In all designs the number of stages varies significantly for prefractionator, but remains practically constant for the main column. The results can be summarised as follows:

- In all cases, the total energy consumption varies only slightly. Therefore, energy recovery cannot be a selection criterion between alternatives. However, the dynamic behaviour shows significant differences.
- Controllability indices, as Closed Loop Disturbance Gain (CLDG) and Performance Relative Gain Array (PRGA) predict in all situations better dynamic properties for the forward heat-integration scheme, compared with the reverse one. This behaviour is verified by closed loop simulation with the full non-linear model.
- For the preferred forward integration scheme an efficient control structure using only temperature measurements can be developed as shown in Fig. 13.29[1].
- The design with short prefractionator has, by far, the best performance.
- Reverse heat-integration scheme does not work with only temperature measurements. The system is controllable only if the concentration of the side-

[1] YC denotes ratio controller.

stream can be measured. Moreover, better disturbance rejection is possible with a sharp light/heavy split in the prefractionator.

It may be concluded that in general the forward heat-integration scheme is easier to control. A possible explanation may be the absence of a positive feedback of energy, which is very likely in the reverse heat-integration scheme.

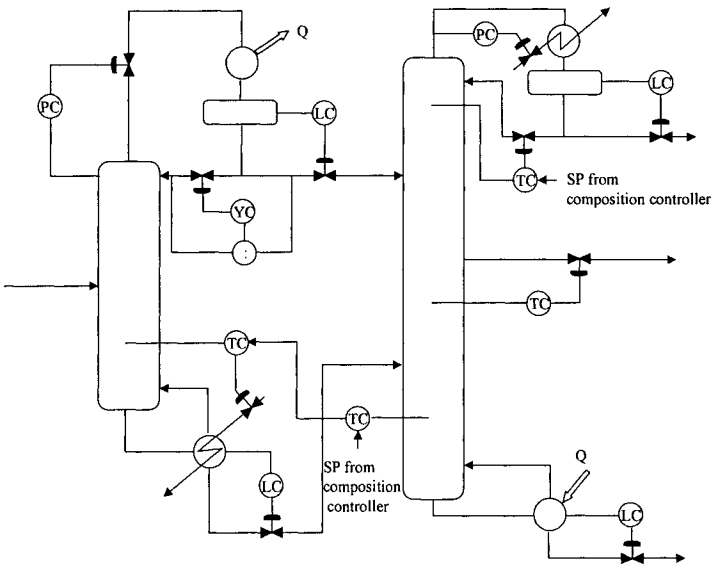

Figure 13.30 Control structure for forward heat-integration.

13.7 PLANTWIDE CONTROL PROCEDURE

In this section we present a heuristic plantwide control procedure proposed by Luyben and Tyreus (1999). The methodology is founded on considerable industrial experience, and it is illustrated in the original reference by relevant case studies. The procedure is applicable for existing flowsheets. The synthesis of flowsheets for desirable controllability patterns remains an open research topic.

13.7.1 Outline

The plantwide control procedure consists of nine steps briefly presented hereafter.

1. Establish control objectives

Assess steady state design and dynamic control objectives. The manipulations must have sufficient power to reject disturbances and drive the set points. The choice of the control objectives is essential, because different objectives may lead to different structures. Typically the plantwide control objectives could include reactor and separation yields, quality specifications, product grades, as well as constraints set by

environmental restrictions and safe operation. The nominal operation point must be selected preferably in the mid-range of the allowed variations.

2. Determine control degrees of freedom

Count the control valves. The number of control valves available in a process equals the degrees of freedom for control. Most of the valves will be allocated to the basic control features, as production rate, control of inventories (gas and liquid), product quality control, as well as safety and environmental constraints. The remaining valves can be used to enhance steady state economics or improve dynamic controllability. Additional manipulations can be obtained by bypassing heat exchangers or some separators.

3. Establish energy management system

In term of plantwide control the energy management has to fulfil two functions:
1. Remove exothermic heats of reaction. The elimination of excess heat directly to utility could lead to a more responsive but inefficient process. Transfer to another unit(s) via process stream(s) improves the energy efficiency, but might affect controllability. After all the excess heat will be dissipated to the utility system.
2. Prevent the propagation of thermal disturbances in the case of process-process heat integration. Excessive heat-integration might have as consequence long paths for disturbances and poor dynamic performance. The insertion of trim utility heat exchangers, as heaters or coolers, may help to solve this problem.

4. Set production rate

Establish the variables that dominate the productivity of the reactor and determine the most appropriate manipulator to control the production rate. A desired production rate can be achieved only by altering the reaction conditions, either directly or indirectly, and simultaneously by changing the fresh feed. To obtain higher production the overall reaction rate must increase too. By far, the temperature has the most important effect. When this cannot be modified, we can try other manipulators, as reactant concentration for liquid-phase reactions, or reactor pressure, for gas-phase reactions. The reaction rate can be also manipulated by catalysts or initiators.

The reactor can handle large variations in throughput if it has sufficient volume. A certain degree of oversizing will help the controllability. As we demonstrated, a minimum reaction volume is necessary for reactors involved in recycles.

The control strategy of feeds must ensure the amount of fresh reactants needed by stoichiometry. If the reaction is monomolecular, reactant on feed control may be feasible only if the reactor is large (high conversion). For bimolecular reactions, only one (limiting) reactant could be on flow control. The make-up policy for the other reactant should be adapted dynamically, preferably by feeding in recycle after separation.

5. Control product quality and handle safety, operational, and environmental constraints

Select the 'best' valves to control each of the product-quality, safety, and environmental variables. The above quantities must be tightly controlled for economic and operational reasons. The selection of the manipulated variables has to ensure good dynamic characteristics with respect to the controlled variables: small time-constants and dead-times, as well as large steady state gains. Considering quality control loops before overall material balance inventory is a distinctive feature of this plantwide control

methodology. The effect of magnitude of flow rates on variables defining product quality and vital process constraints must be carefully evaluated.

6. Fix a flow in every recycle loop and control inventories

Fix a flow in every recycle loop and then select the best manipulated variables to control inventories. A simple and effective way to prevent large changes in recycle flows (snowball) is fixing a flow in every control loop. Whenever level controllers set all flows in a recycle loop, wide excursions can occur in these flows because the total system inventory is not regulated.

Once fixed a flow in each recycle loop, one can determine what valve should be used to control each inventory variable. Inventory may be controlled with fresh reactant make-up streams but also with streams leaving the units. Liquid streams may be added to a location where the level varies with the amount of that component in the process. Similarly, gas fresh feed streams may be added to a location where the pressure gives a measure of the amount of that material in the process.

7. Check component balances

Identify how chemical components enter, leave and are generated (or consumed) in the process. Accumulation of chemical components in recycle streams can be a major reason of failure in control. A preventing method consists in tracing the paths and evaluating inventories for reactants, products and inert, as well as for sub-products and main impurities. This accounting operation can be done by means of a component table where input, generation, output and accumulation region are noticed.

Because the reactants are not allowed to leave the process with the product, they accumulate, if not consumed by the reaction. Excess reactant above stoichiometry at the reactor inlet must be ensured by recycle policy and not by fresh feed.

All products must have exit points from the system. Recycling a limited amount of products is allowed. As a consequence, tight control of purity of recycle streams is not in general a plantwide control issue.

Inert accumulation might be also a source of troubles. Typically, the inert is removed by purging a small fraction of a recycle stream. The purge rate is adjusted to keep the recycle composition between acceptable limits.

The flow rate of gaseous recycles is limited by the high costs of compressors. For this reason a gas recycle should be set constant at the highest value.

In the case of complex flowsheets with interaction between recycles, the handling of impurities can be formulated as a plantwide control problem and solved by means of controllability analysis.

8. Control individual unit operations

The control of units can be treated following effective structures proven by the industrial practice. However, if a unit is involved in a recycle, the control scheme should be reviewed and adapted. For example, dual-concentration control of distillation columns in recycles can be replaced by more flexible one-point concentration control.

9. Optimise economics or improve dynamic controllability

Establish the best way to use the remaining control degrees of freedom. After satisfying the basic control requirement described above, there are some degrees of freedom left.

These can be used either to optimise stead-state economic performance or to improve the dynamic response of the plant.

13.7.2 Application

HDA process will illustrate the above methodology. Figure 13.31 presents the flowsheet with control implementation, as suggested by Luyben and Tyreus (1999).

Step 1. Control objective: desired production rate of high-purity benzene. Constraints: feed ratio hydrogen/aromatics greater than 5, and reactor effluent quenched at 620 °C.

Step 2. There are 23 valves for control: two for fresh feed toluene and hydrogen; purge; furnace fuel; liquid quench; cooling water; two for gas and liquid outlets from flash; five for each distillation columns (steam, reflux, distillate, bottoms, cooling water).

Step 3. The reaction is exothermal. After process/process energy saving for feed preheating, the excess energy is rejected to the cooling water. Because the only reason of the furnace is to ensure constant inlet reactor temperature the first control loop is inlet reactor temperature/fuel inflow. To prevent the thermal decomposition of the product, a second loop keeps constant outlet reactor temperature by manipulating the quench stream.

Step 4. Production may be set by either supply or demand. Controlling the input of reactants (direct mode) is dynamically more convenient than setting the plant output (indirect mode). Here we prefer to control the production by the supply of reactants.

We have to identify dominant variables for changing the reaction rate. These may be inlet reactor temperature, pressure, and toluene concentration. Changing pressure is not recommended for safety reasons. Manipulating the inlet reaction temperature is also restricted. Changing the toluene inlet concentration would remain the only solution. At constant temperature, pressure and ratio hydrogen/toluene, the inlet concentration of toluene is also constant. Thus, apparently there is no way to manipulate the reaction rate!

A deeper insight shows that in this case there is no possibility to isolate the effect of temperature and concentration. In fact, both have a significant contribution in the reaction rate, and must be examined not at the reactor inlet, but inside the process. For example, increasing the reaction rate means that in the given reaction volume the reaction rate must be in average higher. Measuring 'directly' the reaction rate in the reactor would imply to measure several temperatures and concentrations inside the reactor, and apply a correlation model. This is not practical.

Fortunately, there is another possibility: use an indirect measure by means of the separation system itself! In fact, the separation system will recycle the amount of non-reacted toluene, which is a function of conversion. Thus, the solution is adding in the recycle an amount of fresh feed compatible with the achievable conversion. Hence, fixing the flow rate of a reactant in recycle proportional with the desired production is a feasible mean to change the production.

Thus, changing the production will consist of setting on flow control the valve for the recycle of toluene, but setting the make-up toluene on level control in the drum of the recycle column.

Step 5. The quality of the product, benzene, is determined by the amount of lights transferred from the stabiliser, as well as by the contamination with heavies. Therefore, the quality control in stabiliser is the advanced removal of lights from bottoms. The

separation is easy, and therefore the reflux may be simple set at a convenient value. Sensitive stage temperature(s) with bottoms purity may be found and coupled with the reboiler duty. The same is valid to control the purity of benzene and recycled toluene. Simple one-point concentration control with fixed reflux can be applied in all three columns. Note that steady state simulation must check a good linearity and sufficient magnitude of the input (reboiler duty). The control of benzene purity could work more efficient as cascade control configuration, where the set-point of the (secondary) sensitive temperature controller is supervised by the (primary) composition controller.

Step 6. The recycle flow rate of toluene, after separations and make-up, can be fixed at a value compatible with the achievable production. Similarly, the gaseous recycle can be set at fixed flow rate. This solution is also advantageous for compressor operation. Therefore, make-up of hydrogen can be set on pressure control.

Step 7. The material balance of toluene has been already discussed. Recycling toluene will not create accumulation as long as the reactor can convert the fresh feed. Small amounts can leave with heavies in the recycle column, but should be kept as low as possible. These losses will be compensated automatically by make-up in recycle.

Because benzene is a product, it is desirable to separate it completely. Small amounts might be recycled, and should not give troubles as long as the control of the distillation columns is robust. Small amounts are lost in purge and in the top of the stabiliser, where minimal losses can be achieved by low condenser temperature.

Methane is sub-product, but enters also as feed impurity. It goes almost completely in the purge. Small amounts dissolved in liquid after flash must be removed in the stabiliser. The inventory of hydrogen is subtler. The minimum amount to be fed is the stoichiometric amount relative to toluene. This ratio cannot be fulfilled, because there is no separation methane/hydrogen before recycling. Moreover, there is a hard constraint at the reactor inlet regarding the ratio hydrogen/toluene. Steady state simulation shows that specifying both excess of hydrogen and purge flow rate is incompatible with a strict control of the hydrogen/toluene ratio. In this case putting the purge on composition control will limit the accumulation of methane.

Di-phenyl is generated as by-product in a secondary reaction. The net amount formed in reaction must be removed as bottoms in the recycle column.

Table 13.2 summarises the material balance of components as discussed above.

Table 13.2 Component inventory table in HDA process

Component	Input	Generation	Output	Cons.	Accumulation
Toluene	Fresh feed	0	0	R1	LC in recycle column
Benzene	0	R1	Product (Stabiliser)	R2	CC in product column
Hydrogen	Fresh feed (excess)	2*R2	Purge (Stabiliser)	R1	PC in recycle gas loop
Methane	Fresh feed	R1	Purge (Stabiliser)	0	CC on gas purge
Di-phenyl	0	R2	Bottoms	0	TC in recycle column

Step 8. The control of distillation column can be implemented mainly by stand-alone considerations. Liquid inventories in the flash and separation columns have classical structure: base flow on level control. The liquid level in the flash drum is kept by the condenser cooling duty. Pressure is controlled by condenser duty in the production and recycle columns, but by vapour distillate in stabiliser.

Note that the reflux flow rate has been fixed in the all three columns. This solution avoids interactions that could occur if dual-composition control would be implemented.

Step 9. The above control loops represented the basic regulatory control. The remaining valves could be used for improving the yield or optimisation. In this case there is no remaining valve left. However, we may imagine a supervisory level of some controllers that can be effective in optimisation. Thus, the optimisation of yield can be realised only in the reactor. The inlet reactor temperature can be related with the quality of the hydrocarbon feedstock in order to give the best selectivity. Flash temperature is also an optimisation variable for limiting the losses in volatile components, as benzene and toluene. The set point of purge controller can also be related with the purity of the hydrogen fresh feed.

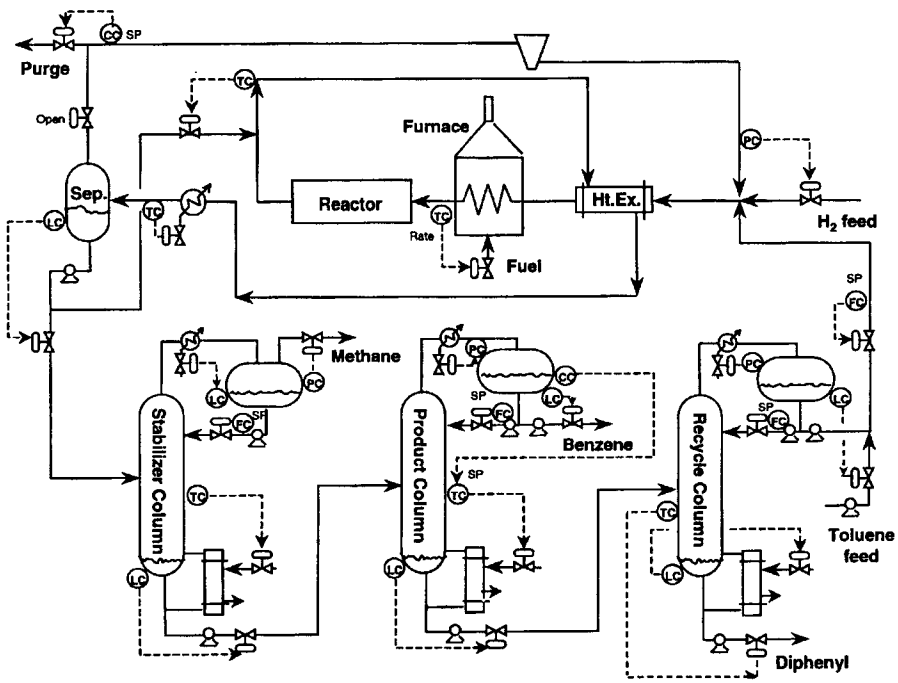

Figure 13.31 HDA process control strategy (after Luyben and Tyreus, 1999)

13.8 INTEGRATING PLANTWIDE CONTROL IN HIERARCHICAL CONCEPTUAL DESIGN

Using Hierarchical Approach for flowsheet synthesis as conceptual frame for implementing the process control structure has been initiated by Douglas et al. (1988), and continued by other researchers as Ponton & Liang (1993), and Lyman & Georgekis (1995). More recent Zheng et al. (1999) have reconsidered the hierarchical procedure for plantwide control system synthesis. However, because of richness of issues the integration of design and control in flowsheet development is still a research topic.

This chapter presents a simple synthesis-oriented approach methodology for integrating plantwide control in hierarchical conceptual design (Bildea, 2001). Two ideas are central:

1. Process plants can be represented by means of subsystems, called *basic flowsheet structures* (BFS). These can interact through material and energy streams. This representation reveals two steps for integrating conceptual design and plantwide control: design controllable BFS's, and couple the BFS's in such a way that a controllable system is obtained.
2. The main objective of plantwide control is to maintain the mass & energy balance of the plant. We remark that energy imbalances can be easily directed towards the utility system. Mass balance is more difficult to manage, because every species entering or formed in reactions (even traces!) must be consumed in reactions or find a way to leave the plant. Therefore, the mass balance must take into consideration the interactions throughout the whole plant, easier to handle at the level of subsystems. On the other hand, the control of energy integration can be solved locally, and/or by exchange with the plant utility system.

The earliest stage where controllability can be considered is when the recycle structure of the flowsheet has been designed. Design decisions concern the performance of reaction (conversion, selectivity) and separation sections (purity, recovery), as well as recycle policy. These will freeze the most important elements of the mass balance. At this level the reactor modelling, sizing, and control may be considered in more detail. Hence, the plant may be viewed as a Reactor–Separator–Recycle super-system.

13.8.1 Basic flowsheet structures

We consider that a process plant consists of several subsystems interconnected through material and energy streams (Figure 13.32) called *basic flowsheet structures* (BFS). Here local control objectives can be achieved using only manipulated variables that are interior to the BFS. Delimiting the BFS depends on what design and modelling details are available and how the control objectives are assigned. We consider that the basic flowsheet structure can be identified based on engineering judgment. Examples are heat-integrated reactors, complex distillation arrangements, azeotropic distillation with solvent recycle, etc.

The task of plantwide control is to harmonise the BFS's in such a way that the whole system operates in a required manner. This is achieved by changing the control objectives of the BFS. The controllability of the BFS is a necessary (but not sufficient)

condition for the controllability of the entire plant. Consequently, our approach to integrate design and control consists of two steps:

1. Design basic flowsheet structure with good controllability properties. This is possible for unit operations, where a lot of industrial experience exists. However, it is an open field of research more complex sub-systems.
2. Couple the BFS in such a way that a controllable system is obtained.

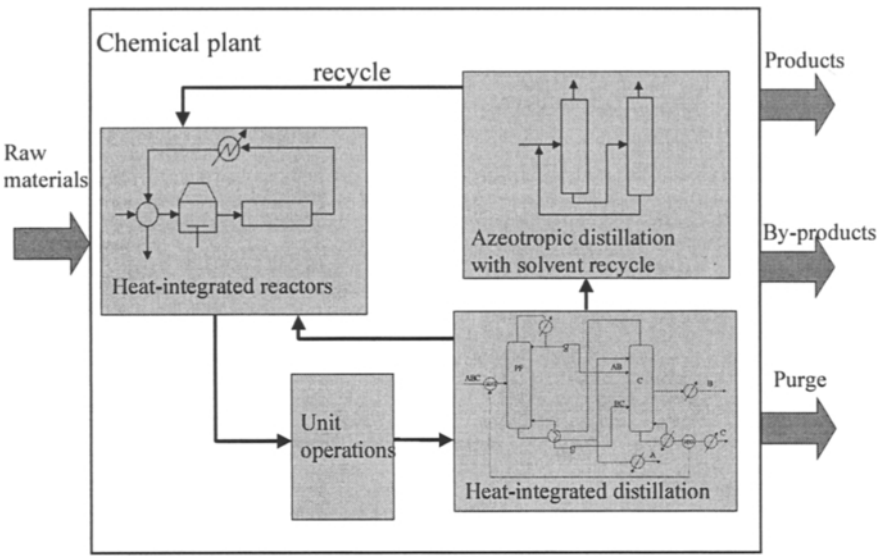

Figure 13.32 Systemic representation of chemical plants

13.8.2 Approach

1. Initial data

The design initial data concerns reactions' chemistry, raw materials, production rate, product specifications and economic constraints. Control-related data must specify the required production range, the product grades, and the variability of the raw materials.

2. Input-output

Typical design decisions at input/output regard feed purification, gas purge and recycle of by-products. They establish the number and the composition of product streams. One could be tempted at this stage to decide how to control the production rate. The analysis presented before demonstrated that setting all reactants on flow control gives difficulties. Moreover, the strategy depends on reactor design, separation performance and recycles. Hence, it is too early to take plantwide control decisions.

3. Recycle structure of the flowsheet

After the selection of the reactor and the specification of its performance the structure of recycles can be established. Separation sections are specified as product recovery or

purity. Additional units for recycling and conditioning fluids may be considered. Flow rate and composition of the streams are expressed in terms of several design variables, as conversion, recycle flow rate or composition, etc. In the hierarchical procedure, the values of these design variables are determined at the next level, when the cost of recycles and separations can be calculated more accurately. However, plantwide control structure may be considered.

First, several candidates for plantwide controlled variables may be identified. These are not assigned to a particular basic flowsheet structure, and therefore they have a true plantwide character. Examples are production rate, recycle composition, ratio between reactants at reactor inlet, etc.

Secondly, candidates for manipulated inputs can be found. When they are flow rates connecting BFS's, the choice affect the control of both upstream and downstream. As an example, it was proposed to keep reactant recycle on flow control and to change the setpoint of this loop when production changes are required. This implies that the inventory control of the upstream unit is in direction opposite to flow, while the inventory control of the downstream unit is in the direction of flow. Manipulated flows should be chosen with care to avoid over-specification with respect to plant mass balance. The set-points of the BFS's form another category of plantwide manipulated variables. Examples are reaction conversion, separation performance, etc.

The choice of the controlled and manipulated variables can be based on engineering judgement, or on methods that are more systematic. In any case we recommend those that regard in the first place the material balance. This gives valuable insight into the number of control degrees of freedom, functional controllability, I/O pairing for decentralized control.

The proposed control structures may be analysed by steady state simulation. In commercial simulators, unit operation input data or flow rate and composition of feed streams can be varied in order to meet some 'design specifications'. Although the design specifications are apparently similar to SISO feedback controllers, it does not mean that the final control structure has to be decentralized or the I/O pairing must be preserved. This approach is advantageous because the nonlinear character of the process remains intact.

Sensitivity analysis can show which plantwide manipulated inputs (setpoints of BFS control) are necessary. Variability of the streams connecting BFS indicates which disturbances must be rejected. In this way, the designer can identify control objectives of the basic flowsheet structures, and set them as explicit targets for design.

4. Separation system

Because of problem complexity, the separation system is usually decomposed into sub-systems, as vapour, liquid and solid separations. For each sub-system, there are systematic procedures to generate design alternatives. For many separation operations, there are procedures, supported by industrial experience, that lead to economical optimal design with good controllability properties. However, there are also many cases where design procedures for robust controllability are still needed.

5. Heat integration

Pinch Point Analysis can be used to develop heat integration schemes. Some could be optimal from the viewpoint of energy saving, but inoperable in practice. We adopt the

position that the heat-integration should be performed locally. When energy cannot be recovered by integration in one plant section, it should be used to generate steam or power, and exported this way to other sections. In any case, the designer should check that heat integration does not affect the process controllability.

The next example will revisit the plantwide problem of HDA plant, this time viewed as a process synthesis problem where flowsheet design and controllability are examined at the same levels of the hierarchical methodology.

EXAMPLE 13.3 Development of a control structure for HDA plant

Examine the development of a control structure for HDA plant discussed in Chapter 7. Supplementary data on design and steady state simulation are given in Case Study 1. The nominal production rate is 120 kmol/h benzene at a purity exceeding 99.8%. The feed streams are pure toluene and hydrogen. Production flexibility of ±25% is required

Solution. We have seen that the analysis of a plantwide control problem can begin at the level three, the recycle structure. In this case, two recycles have been identified:

- Gas recycle. Non-reacted hydrogen and methane is recycled to the reactor by means of a gas compressor. Purge is necessary to prevent methane build-up. The flow rate of the gas recycle is determined by the reaction conversion, as well as by the constraint of a strict ratio hydrogen/hydrocarbon at the reactor inlet.
- Liquid recycle. Non-reacted toluene is recycled to the reactor, after separating dissolved gases, benzene product and by-product (diphenyl).

At this level, considering an adiabatic tubular reactor and a furnace for feed heating up to the reaction temperature completes the flowsheet.

Further we will discuss the selection of controlled and manipulated variables. The recycle structure is presented in Fig. 13.33. At this level a simple mass balance with perfect separations and negligible side reactions can give valuable insight to the plantwide control problem. The equations are:

$$F_B = F_1 \tag{13.30}$$

$$y_{HP} = y_{H2} - \frac{F_1}{F_2} = y_{H2} - \frac{F_1}{F_P} \tag{13.31}$$

$$\frac{y_{H3}}{y_{T3}} = \frac{X}{F_1} \cdot \left(F_R \cdot y_{HP} + F_2 \cdot y_{H2}\right) \tag{13.32}$$

$$F_T = F_1 \cdot \frac{1-X}{X} \tag{13.33}$$

$$F_P = F_2 \tag{13.34}$$

F_j and y_{kj} denote the flow rate of stream j and the molar fraction of the k component (H – hydrogen, T – toluene) in the stream j, while X is the reaction conversion.

If production rate and hydrogen/toluene ratio at the reactor inlet (y_{H3}/y_{T3}) are set, Eqs. 13.30 to 13.34 have two degrees of freedom. Hence, two design variables must be specified, but not any combination is feasible. Douglas (1988) considers reactor conversion and purge composition as design variables and optimises the economic potential. We use his results ($X = 0.78$, $Y_{HP} = 0.424$) as a starting point.

Next we will examine potential controlled and manipulated variables. There are five potential controlled variables: production (F_B), hydrogen/toluene ratio (y_{H3}/y_{T3}), pressure, purge composition (y_{HP}), and conversion (X). However, some of them might be left uncontrolled. For example, conversion control is difficult, because of dead-time associated with a PFR. Moreover, it requires on-line composition analyser, which is not available or expensive. For these reasons, it would be desirable to develop a control structure in which controlling the reactor inlet temperature would be sufficient.

The following manipulated variables are available: toluene feed (F_1), hydrogen feed (F_2), gas recycle (F_R), purge (F_P) and furnace duty (q_h). Furnace duty may be used to control the reactor inlet temperature. The setpoint of this control loop may be coupled, in a cascade manner, with other variable from the previous list.

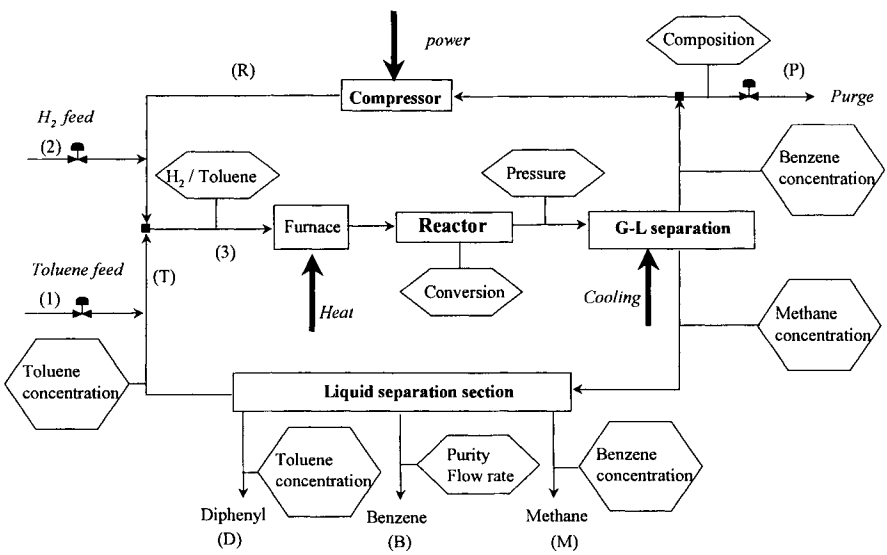

Figure 13.33 Recycle structure of the HDA plant

It should be observed that it is not rational to vary the gas recycle flow rate, because operating the compressor under its capacity is not economical. Moreover, hydrogen loss is minimized when the gas recycle is at maximum. For these reasons we consider in all control structures constant gas recycle.

Inspection of the mass balance equations gives more insight into control issues:

- The only way fed toluene can leave the system is as benzene. Hence, any strategy that will try to set the production rate without modifying the toluene feed will fail.

- The purge composition can be controlled using either the hydrogen feed or purge flow rate, but not both.
- The pressure is constant if the gas holdup remains constant. Because the number of moles of gaseous components does not change in the reaction, hydrogen feed and purge flow rates must be equal. Consequently, assigning one for purge composition control leaves the other for pressure control.

The remaining manipulated variable (set-point of the furnace duty) can be used to control either the conversion or the hydrogen/toluene ratio. Both controlled variables seem to be important. Low conversion means more utility consumption for separation, while high conversion affects reaction selectivity. Low hydrogen/toluene ratio leads also to undesirable by-products.

This way, a large number of control structures have been excluded from further analysis. Table 13.3 presents five control structures that were considered, denoted CS1 to CS5.

Table 13.3 HDA plant: candidate control structures.

Control structure	Hydrogen/Toluene ratio	Purge composition	Conversion
CS1	Hydrogen feed	-	-
CS2	Hydrogen feed	-	Setpoint of the furnace duty-reactor inlet temperature loop
CS3	-	Hydrogen feed	-
CS4		Hydrogen feed	Setpoint of the furnace duty-reactor inlet temperature loop
CS5	Setpoint of the furnace duty-reactor inlet temperature loop	Hydrogen feed	-

In all control structures, gas recycle flow rate is constant; toluene feed is used to set the production; purge flow rate is used to keep constant pressure.

The control structures have been evaluated by steady state sensitivity analysis with ASPEN PLUS, by means of design-specifications. Figure 13.34 presents the most important results.

- Without control, hydrogen/toluene ratio deviates considerably from the optimal value (Fig. 13.34a). Controlling purge composition (CS3, CS4) reduces the variability, but it is still bellow target at higher production rates.
- For all control structures, the hydrogen lost in purge is proportional with the production (Fig. 13.34b). When purge composition is controlled (CS3, CS4 and CS5), the hydrogen loss is less sensitive to production changes.
- Conversion (Fig. 13.34c) and reactor outlet temperature (Fig. 13.34d) strongly depend on the production when both y_H/y_T and y_{PH} are controlled (CS5). This may affect negatively the selectivity.
- For the design considered, CS5 requires high flexibility of separations (Fig. 13.34e). At the lowest production, the liquid separation section handles 90 kmol/h benzene, 55 kmol/h toluene. At the highest production, the mixture consists of 150 kmol/h benzene, 15 kmol/h toluene. However, the variability of the stream entering the separation section

can be reduced if the system is designed for lower conversion, for example X=0.5, as illustrated in Fig. 13.34f.

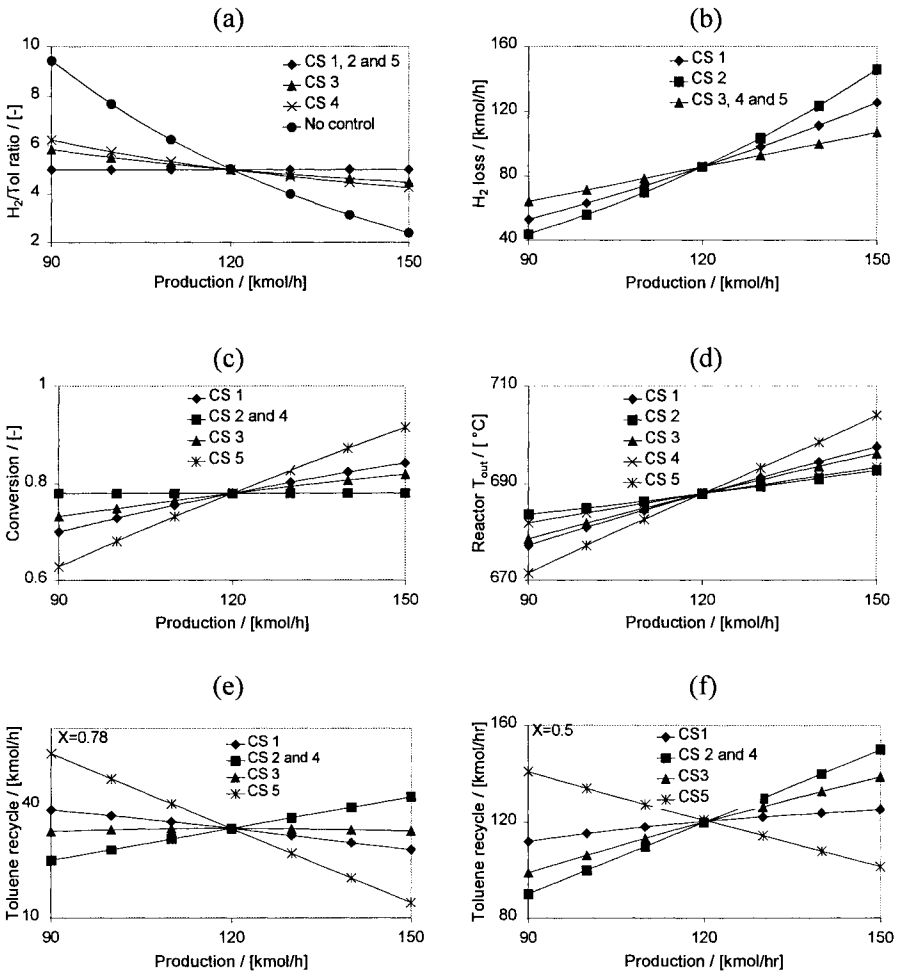

Figure 13.34 HDA plant. Control structure evaluation by steady state simulation

It may be concluded that there is no incentive to control the reactor conversion. Either the purge composition or the hydrogen/toluene ratio (but not both!) should be controlled. In the first case, the whole plant must be over-designed to work at a hydrogen/toluene ratio higher than necessary. In the second case, increased hydrogen loss at high production must be accepted. To control both variables, the plant must be designed for lower conversion and higher load of the distillation columns. Hence, the control structure CS1 has a minimum of disadvantages and will be further considered.

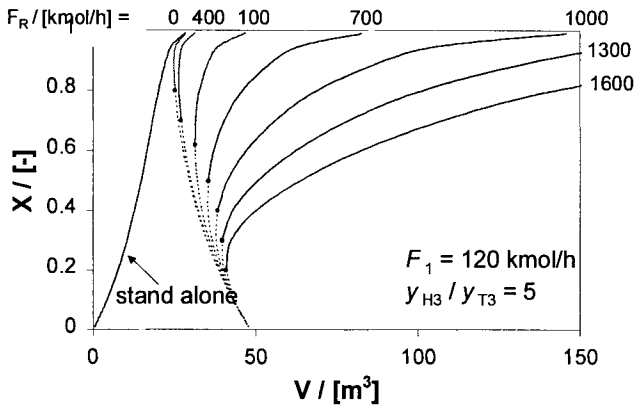

Figure 13.35 Conversion vs. reactor volume, for fixed hydrogen / toluene ratio and different values of the gas recycle flow rate

One could arrive at control structure CS1 based only on the mass balance equations and by the fact that conversion control is difficult. In this case, the requirement of good plantwide controllability is a constraint for further design optimisation. To illustrate this idea, the dependence of the conversion versus reactor volume is presented in Fig. 13.35, for fixed values of the gas recycle flow rate and hydrogen / toluene ratio. It is interesting to note that the system exhibits state multiplicity! The turning points of the volume/conversion diagrams represent the stability limit. The upper branch (high conversion) is stable, while the lower branch (low conversion is unstable). Note that it is possible to have moderate conversion (good selectivity) at stable operating point only if the gas recycle is large enough.

When the operating point is chosen by optimisation, the locus of the turning point should be seen be considered as a feasibility limit. Designs near the turning points are dangerous. Consider the stable operating point X=0.55, F_R=700 kmol/h. The reactor volume can be calculated, but the kinetic data is always uncertain. When the reaction rate is over-estimated, the real operating point falls at the left of the volume-conversion line, in the region where no feasible operating point exists. Then, although the control system does a perfect job, toluene accumulation occurs, leading to infinite recycle.

Separation system

The control of the distillation columns has been discussed in the Example 13.2. It should be remarked that the range of feed disturbances affecting the separation section was obtained as a result of the sensitivity analysis performed at the previous design level. This way, disturbance rejection can be set as a distinct design specification.

Heat-integration

Heat integration issues have been discussed in the section 13.6.1. Because one heat-balance constraint, two design decisions should be taken, for example FEHE efficiency and steam generator duty. They can be found by optimisation according to some economic criteria. However, it is known that auto-thermal reactors have complex, nonlinear behaviour, including state multiplicity, isolated solution branches and

sustained oscillations. Consequently, the design and control of the heat-integrated PFR should be analysed in a greater detail, as we did.

Dynamic simulation

Te mentioned control loops have been implemented in Aspen Dynamics (Fig. 13.37) that includes the control of the heat integration loop around the reactor (Fig. 13. 27) and of the separation system (Fig. 13.9). The following scenario was used to evaluate the performance of the control system: initially, the production rate is set to 120 kmol/h, after 2 hours, increased to 150 kmol/h, later, reduced in two steps to 90 kmol/h.

Figure 13.38 presents the results of the dynamic simulation. Large production increase or decrease can be easily achieved, while the product purity is held on specification. Reaction selectivity remains high, so that the production of heavies is minimised. The constraint related to hydrogen / toluene ratio is satisfied most of the time. Note that the reactor design is such that the operation point is on the upper stable branch in Fig. 13.35. In contrast, if the design is on the unstable branch, close to the turning point, then operability problems appears (Bildea et al., 2002).

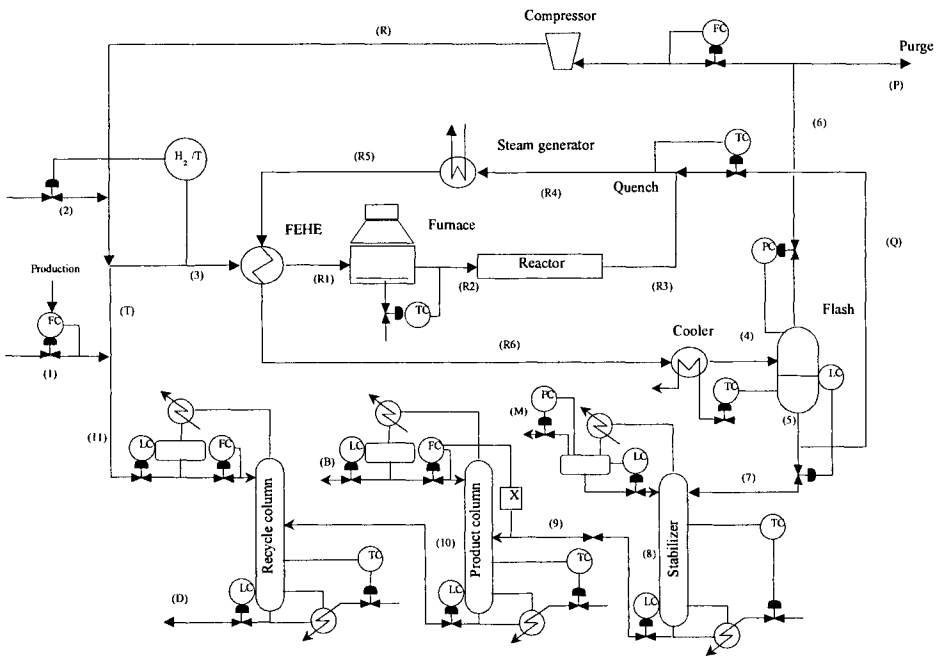

Figure 13.36 Plantwide control of the HDA plant

The example demonstrates that the interaction between reaction and separation systems through recycles can lead to steady state multiplicity and instability even if the stand-alone reactor has a unique stable state. Non-linear analysis is a powerful method to investigate this behaviour.

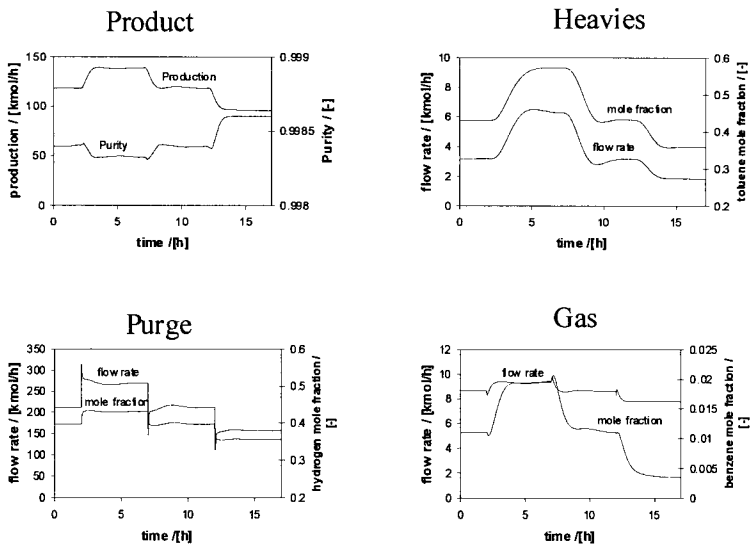

Figure 13.37 Dynamic simulation results

13.9 SUMMARY

Integrating controllability in design is more a process design issue than a process control problem. Optimum steady state design might be not the best for controllability. This situation could occur if the manipulated variables have not sufficient power, or if the holdup of reactors and of other capacitive items involved in recycles are too small. Controllability tools based on linear control theory can serve for examining controllability issues for small variations. For larger variations a non-linear analysis is more suited, since it allows the identification of multiple steady states or of regions of maximum sensitivity, where control difficulties could be met.

The recycle of mass and energy have important effects on the dynamics and control of complex plants. Positive feedback increases the time constant of units placed in recycle, the effect depending on the recycle gain. Larger gains can lead even to unstable behaviour. On the contrary, negative feedback has always a stabilising effect.

Snowball effects designate high sensitivity of recycle flows to small changes in input/output flows or in some parameters of units. The snowball is essentially a steady state effect, but the large magnitude of variations and the duration of transients can affect seriously the operation and control, leading eventually to plant upset. Therefore, the snowball effects must be avoided by design.

The feed policy of reactants is a plantwide control problem. Setting all reactants on flow control leads typically to conflicts in the dynamic material balance. Control problems can be identified even for monomolecular reactions carried out in the simple flowsheet CSTR-

separator-recycle, where the classical control structure based on the level control of reaction volume could not always work. The problem turns out to be in fact a combined reactor design and control strategy.

More elaborated make-up schemes are necessary for multi-reactant processes. If one reference reactant may be set on flow control, the make-up of others should be done in a way that satisfies the dynamic material balance. In this respect is important to note the Luyben's rule that *'a stream somewhere in a liquid recycle loop should be flow controlled'.*

A fundamental aspect highlighted in this chapter is that the design of chemical reactors has to consider the non-linear effects due to recycles of mass and energy. Thus, there is a minimum reactor volume for feasible operation, which for simple reactions can be expressed as a function of a 'plant Damköhler number'. For multi-molecular reactions multiple steady states can occur even in isothermal conditions, the type of reactor being less important than the stoichiometry. For non-isothermal operation multiple steady states can occur not only when using a CSTR, which gives such behaviour already as stand-alone (see Chapter 8), but even with a PFR, which itself is stable as standalone. Furthermore, it should be avoided to design the reactor near the maximum sensitivity region of conversion vs. reactor volume.

The control of waste and impurities is a key issue in developing a plantwide control strategy. The accumulation of impurities must be avoided by providing exit points in purges after transformation in benign materials. Obviously, the amount of waste should be minimised by design. The control system can help to solve the waste minimisation problem by its capacity to measure and control the dynamic inventory of components. Controllability tools can be used to solve this plantwide problem.

Heat integration of units should be done in such way that avoids control troubles due to unstable behaviour. Particular attention should be paid to reactors dealing with very exothermal reactions. Excessive feedback of heat is detrimental for controllability. Using the utility network for exporting/importing energy gives simple and robust solutions that preserve both energy efficiency and controllability. Similarly, simultaneous analysis of design and control has to be included in the heat integration of distillation columns. It is demonstrated that feed-forward heat integration of two distillation columns can be realised by using simple temperature controllers, but with appropriate design of columns.

The implementation of a plantwide control structure on a given design can follow a step-wise procedure (Luyben & Tyreus, 1999). The actions with plantwide character regard energy management, production rate, product quality, safety and environmental protection, and control of impurities.

The synthesis of a flowsheet with desired controllability pattern is a more complicated problem still in research. A practical approach is proposed based on the concept of basic flowsheet structures (BFS's). These are subsystems whose control objectives can be fulfilled by using internal manipulated variables. Then the BFS's are coupled in a way that leads to a controllable process. The priority is given to material balance. The integration of BFS's can be studied by steady state simulation by means of sensitivity analysis and of flowsheet controllers (design specifications). The hierarchical approach of design (Douglas, 1988) is employed as the general frame in developing simultaneously the flowsheet structure and the plantwide control strategy. Controllability analysis can be used to assess the feasibility of control structures. Dysfunctions can be corrected by adopting alternative control strategies or/and by changing the design.

13.10 REFERENCES

Bildea, C. S., A. C. Dimian, 1998, Stability and multiplicity approach to the design of heat-integrated PFR, AIChE Journal, vol. 44, 703-2712

Bildea, C. S., A. C. Dimian, 1999, Interaction between design and control of a heat-integrated distillation system with prefractionator, Chem. Eng. Research & Design (Trans. Inst. Chem. Eng.), vol. 77, A7, 597-609

Bildea, C. S., A. C. Dimian, P. Iedema, 2000, Interaction between design and control of heat-integrated PFR, Proceedings of ESCAPE-10, Elsevier, 169-175

Bildea, C. S., A. C. Dimian, P. Iedema, 2000, Nonlinear behaviour of Reactor-Separator-Recycle systems, Comp. & Chem. Engng., vol. 24, 209-217

Bildea, C. S., Integration of Design and Control by Nonlinear Analysis (PhD thesis), 2001, University of Amsterdam

Bildea, C. S., S. Cruz, Dimian, A. C., Iedema, P., 2002, Design of tubular reactors in recycle systems, Proceedings ESCAPE-12, Elsevier, 439-444

Dimian, A. C., A. J. Groenendijk, P. Iedema, 2001, Recycle interaction effects on the ontrol of impurities in a complex plant, 2001, Ind. Eng. Chem. Res., 40, 5784-5794

Downs, J., 1992, Distillation control in a plantwide control environment, in W. Luyben (ed), Practical Distillation Control, van Nostrand Reinhold, New York

Fisher, W. R., M. F. Doherty, J. M. Douglas, 1988, The interface between design and control, Ind. Eng. Chem. Res., 27, 597-611

Groenendijk, A. J., A. C. Dimian, P. Iedema, 2000, Systems approach for evaluating dynamics and plantwide control of complex plants, AIChE Journal, 41, 133

Luyben, W. L., 1990, Process Modelling, Simulation and Control for Chemical Engineers, McGraw-Hill, second edition

Luyben, W. L., M, L. Luyben, 1998, Essentials of Process Control, Mc-Graw Hill

Luyben, W. L., Tyreus, B., 1999, Plantwide Process Control, Mc-Graw-Hill

Lyman, P., C. Georgeakis, 1995, Plantwide control of Tennessee-Eastman problem, Comp. Chem. Eng., 19, 321

Marlin, T., 1995, Process Control: Designing processes for control systems for dynamic performance, McGraw Hill

Ogunnaike, B., W. H. Ray, 1998, Modelling and Process Control, Academic Press

Ponton, J. W., D. M. Liang, 1993, Hierarchical approach to the design of process control system, Chem. Eng. Res. Des., 70, 181

Seider, W. D., J. D. Seader, D. R. Lewin, 1999, Process Design Principles: Synthesis, Analysis and Evaluation, Wiley

Skogestad, S., I. Postletwaite, 1998, Multivariable Feedback Control, Wiley

Stephanopoulos, G., 1984, Chemical Process Control, Prentice Hall

Zheng, A. R., R. V. Mahajanam, J. M. Douglas, 1999, Hierarchical procedure for plantwide control system synthesis, AIChEJ, 45, 1255

PART V

DESIGN PROJECT

This Page Intentionally Left Blank

Chapter 14

PROCESS DESIGN PROJECT

14.1 Scope

14.2 Organisation

14.3 Process Integration courses
14.3.1 Undergraduate Process Integration course
14.3.2 Postgraduate Process Integration course

14.4 Process Integration project

14.5 Plant Design Project
14.5.1 Outline
14.5.2 Subjects

14.6 References

14.1 SCOPE

This chapter presents a framework for teaching modern Process Design by an integrated approach of methods and tools. The main educational object is the Plant Design Project. Guidelines are provided for developing courses and projects at both undergraduate and postgraduate levels.

Creativity is the distinctive feature of an engineer, and particularly of a designer. Process Design (PD) project is the activity in the curriculum where the student develops creative skills, consolidates the knowledge in chemical engineering and learns to work in a team committed to reach an objective in short time with limited data. In most cases the PD project is the last activity before graduation where the student learns the rigour of the engineer's profession. Without much experience she/he has to find solutions that could stand against proven processes.

In the past the perfection of details was often the goal of the design exercise, the creativity being something that would come after years of experience. This attitude could be explained by a narrow specialisation on technologies, some having an innovative character, as petrochemical products and polymers in the 1960-70, but since entered in the field of commodities. The educational system followed the same trend. The situation changed radically in the last years. Nowadays a chemical engineer should be able to do "anything". This means to be able to work in any industry or social activity asking for its skills. And there are a lot of opportunities. The explanation of this versatility can be found in the fact that the education of chemical engineer is oriented to solving problems by a multidisciplinary approach.

In the latest years the curriculum of many universities has migrated from specialisation on technologies to a more fundamental approach under the slogan 'back to basics'. Indeed, only mastering the fundamental knowledge offers a long-term basis for professional evolution. Continuous education over the whole professional life is the only solution for keeping pace with the fast changes of the modern society.

The challenges for engineering companies are greater than ever. Adaptability and responsiveness to uncertainties of the global market are key factors for competitiveness. Strict environmental regulations and severe safety norms set hard constraints that must be integrated in the core of the design project. Hence, creativity and rigour are today's key features of the chemical engineer profession.

Process engineering changed dramatically in the last years, above all because of information technology. Nowadays individual engineers can perform sophisticated calculations that needed before large teams of specialists in different areas. Database technology expands dramatically the flow of information inside and outside a company. Time-consuming activities, as equipment sizing and drawing, can be done much easier, so that more effort may be spent in innovative tasks.

Computer-based engineering tools have a huge impact on the profession of designer. A large part from the sizing methods based on empirical correlations, mostly originated from the period 1950-1970, are nowadays obsolete. New correlations are in many cases proprietary of consulting companies or equipment suppliers. More efficient is a 'direct' approach based on first-principle methods, in other words on the fundamental equations

of chemical engineering. A salient example is the use of Computer Fluid Dynamics in designing new devices for process intensification and environment protection. The detailed sizing of internals has lost in interest because it can be done much better with specialised packages. In consequence, the problem of equipment design shifted from sizing to functional design. This has to take into account not only the performance of stand-alone items, but also the interactions with the other units by a systems approach of the whole design problem. Therefore, in conceptual design the emphasis is on the optimal selection of equipment items from a number of alternative types for which suppliers can be found. From this point of view the formulation of appropriate *specifications sheets* is a key issue.

Summing up, today a student design project should be directed primarily to the development of creative skills, but without scarifying the reliability of the engineering solution. The project should focus not only on technical performance and economic efficiency, but also on issues of social significance, as sustainability and environment protection.

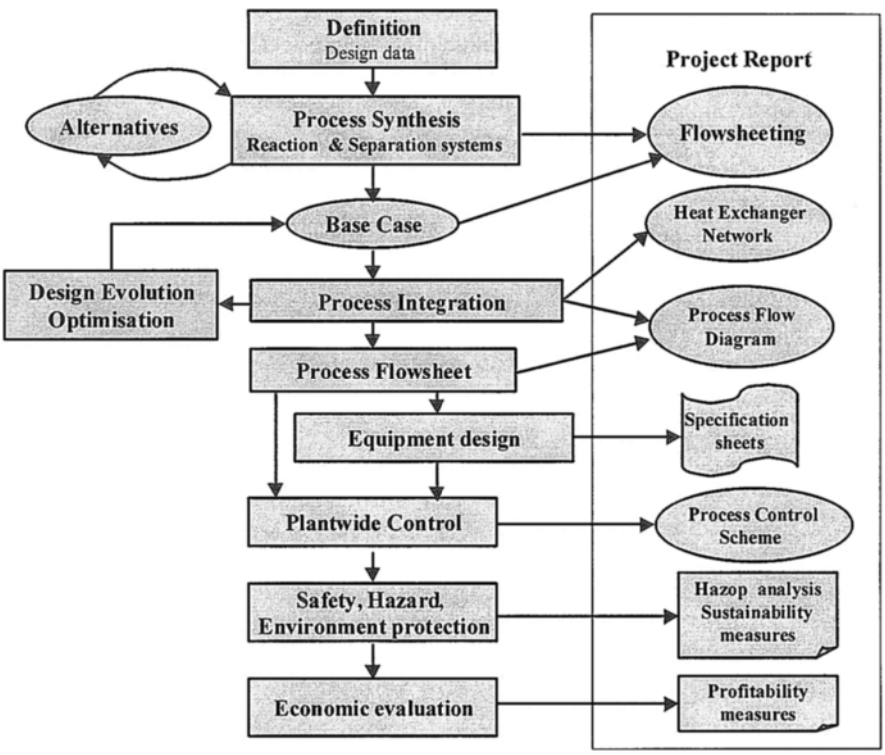

Figure 14.1 Outline of the Design Project

The outline of a process design project is illustrated in Fig. 14.1. More details will be given in the subsequent chapters. The following steps can be distinguished:

1. Define the design problem and collect sufficient data.
2. Generate flowsheet alternatives by applying Process Synthesis methods. The basic flowsheet structure is given by the Reactor and Separation systems. These form the material balance envelope that is the basis for further development. Use flowsheeting to get insights into different conceptual issues, as well to evaluate the performance of different alternatives.
3. From competing alternatives select a good 'base case' and improve it by using the techniques of Process Integration. Determine targets for utilities, process water and mass separation agents, as well as for the equipment design. Optimise the final flowsheet.
4. Select the equipment items, perform sizing, and collect the key characteristics as 'specification sheets'.
5. Examine plantwide control aspects, including safety, environment protection, flexibility with respect to production rate, and quality control.
6. Minimise waste and emissions. Assess process sustainability.
7. Estimate capital and operating costs. Execute the economic evaluation focused on profitability.
8. Elaborate the design report. Defend it by public presentation.

More details about this approach will be given in the following sections. It is worthy to mention also some teaching principles, as for example:

- Make use of the systems viewpoint in defining a design problem.
- Employ systematic methods in solving a design problem.
- Stimulate the reasoning in terms of design decisions and alternatives.
- Employ computer simulation as the main tool for analysis and design.
- Make use efficiently of information technology through Internet.
- Use representative applications for learning systematic methods.
- Stimulate innovative solutions by challenging subjects.

14.2 ORGANISATION

The teaching of Process Design can be organised at two levels:

- Develop creativity and teach systematic methods by means of a dedicated Process Design course and of an introductory project.
- Consolidate the engineering skills in the frame of a full Plant Design project.

Many recent curricula in chemical engineering or industrial chemistry incorporate a course in Process Design. This course will be designated in this book by Process Integration, a label that reflects the modern trends in process engineering, as explained in Chapter 1.

Some observations are of interest regarding the organisation of a design project:

- Working in small teams of 2/4 students is the most efficient. The assignment should provide a clear scheduling of tasks and strict follow-up.

- The projects should be customised taking into account the level and motivation of the students. The projects involving industrial subjects are the best.
- The evaluation should be individual, although the group responsibility is required for the acceptance of the project.
- The report has to fulfil the requirements of logic, concise and clear development.
- The Plant Design project has to be defended by public presentation. Communication skills should be acquired by special training.

Preliminary knowledge is necessary before application for PI course and design project. The following courses could be considered as compulsory:

- Chemical and Engineering Thermodynamics*.
- Chemical Reaction Engineering *.
- Transport Phenomena.
- Separation Processes*.
- Unit Operations*.
- Process Dynamics and Control*.
- Safety and Environment Protection.

Courses marked by a star should have projects of smaller or larger extent. Particularly important are the projects in Thermodynamics, Chemical Reaction Engineering and Separation Processes, where the use of a simulator is welcome. However, the student should keep the ability to develop basic chemical engineering calculations without making use of sophisticated simulation programs, but by employing spreadsheets or generic mathematical tools. Particularly important is to develop analytical skills in performing material and energy balances, as for example described in the book of Himmelblau (1996).

14.3 PROCESS INTEGRATION COURSES

In this section we share the experience in teaching Process Integration (PI) courses in The Netherlands at both undergraduate and postgraduate levels for about 10 years.

14.3.1 Undergraduate Process Integration course

The course described below is based on four weeks full time, corresponding to 4×40=160 hours. The split between lectures and working classes depends on the teacher's choice, but we found that the ratio 40/120 is convenient. The content of a typical Process integration course is outlined in Table 14.1, with indication to chapters in the present book. Hereafter we mention some pedagogical issues.

The course starts by teaching the fundamentals of the steady-state flowsheeting by means of a simple case study, as the Example 2.1. The emphasis should be not on the manipulation of the simulator, but on generic topics as, degree of freedom analysis, formulation of feasible specifications, flowsheet control structures and treatment of recycles. Tracing the inventory of components is a valuable method in debugging convergence problems, but also to highlight the relation between material balance and plantwide control problems.

The chapter on Integrated Process Design presents the features of the systems approach and of systematic design methods. This chapter offers also the opportunity to discuss social issues as Sustainable Development and Production-integrated environmental protection.

Process Synthesis deals mainly with the invention of flowsheets by the Hierarchical Approach. In teaching this topic care should be given to pass throughout all the steps of the procedure, emphasising the role of design decisions in generating alternatives. The same is valid for the Process Integration project, where each step in flowsheet development has to be supported by a design decision. A distinctive feature of the hierarchical methodology presented in this book is the application of a knowledge-based approach in developing the separation system. Because the key role of the reactor, supplementary material is given in Chapter 8 with respect to selection and design from a systems viewpoint. Similarly, the synthesis of distillation sequences for non-ideal mixtures is treated in a separate chapter. However, this chapter is meant mainly for a postgraduate level.

Pinch Point Analysis develops the basic principles in performing energy integration. The presentation should focus on the targeting approach before detailed design of heat exchangers, as well as on the role of the appropriate placement of units with respect to Pinch. The application of the Pinch design method could become cumbersome if the problem is not properly analysed, namely in term of streams selection. This part needs training before to be used in the project.

Finally, the Economic Evaluation should be oriented from the beginning to profitability analysis, by identifying the design elements that have impact on the profitability measures.

Table 14.1 Undergraduate Process Integration course

Topics	Lectures	Working classes
Integrated Process Design	4 h (Ch. 1)	Environmental measures
Process Simulation	4 h (Ch. 2 & 3)	Simulation exercises
Process Synthesis	12h (Ch. 7 & 8)	Project PI
Pinch Point Analysis	8 h (Ch. 10)	Working classes / Project PI
Practical Energy Integration	8 h (Ch. 11)	Project PI
Economic Evaluation	4 h (Ch. 15)	Project PI

14.3.2 Postgraduate Process Integration course

A postgraduate education system for designers named "Two-year Advanced Design Study" has been developed in The Netherlands to respond the demands of modern process engineering (Grievink et al., 2002). The key objective is to learn the modern process design principles, including the systematic methods and computer tools. The course on Advanced Process Integration and Plantwide Control (Dimian et al., 2002) is an example. The course is followed optionally by a project between two and four weeks. Table 14.2 presents the outline with reference to chapters from this book.

In the present globalisation environment the students come from different countries with different backgrounds. For this reason a 'sequential' teaching system is not longer

appropriate. More efficient is a 'direct access' system, where the knowledge is adapted and customised to the classroom's needs. The distinctive feature of this postgraduate course is the integration of dynamics and control in the process design methodology. Particular attention is given to the use of controllability analysis as design tool, as well as to the development of a plantwide control strategy. The advanced investigation of these aspects becomes possible by the integration of simulation tools, namely of steady state and dynamic flowsheeting.

Table 14.2 Advanced Process Integration and Plantwide Control course

Day	Topics	Lectures	Working classes
1	Process Simulation	Ch. 2 & 3	SS flowsheeting
2	Dynamic Simulation	Ch. 4	Dynamic simulation
3	Process Synthesis.	Ch. 7	Azeotropic distillation
	Non-ideal distillation systems	Ch. 9	systems
4	Integration Design and Control	Ch. 11	Controllability analysis
5	Plantwide Control	Ch. 12	Dynamic simulation

14.4 PROCESS INTEGRATION PROJECT

The scope of the Process Integration project is to develop an innovative approach of a process design problem. The teaching objective is to incite the students to produce original flowsheets rather than imitate proven technologies. The emphasis is on learning the methodology for flowsheet development and suitable systematic methods for the design of subsystems. The student should understand why several competing technologies could exist for the same process, and be able to identify the key design decisions that have been produced different flowsheets. Thus, the creativity is the major goal at this level. A more rigorous engineering approach will be trained during the Plant Design project.

A typical content of a Process Integration project is given in Table 14.3. The timing corresponds to 80 hours or two weeks full time for a group of two students. In preliminary stages of material balance the use of a spreadsheet should be encouraged. In later stages of flowsheet development the use of simulator is welcome, but taking care not transforming the project in the solution of a simulation problem.

Table 14.3 Content of a Process Integration project

1. Project definition
1.1 Product definition and commercial interest
1.2 Product specifications and plant capacity
1.3 Alternative chemical routes
1.4 Commercial competing processes
1.5 Product, raw materials and utilities costs
1.6 Safety and environmental requirements
1.7 Site selection

2. Reaction system
2.1 Chemistry and industrial stoichiometry
2.2 Heat of reaction
2.3 Chemical equilibrium
2.4 Catalyst and chemical kinetics
2.5 Reactor selection
3. Process synthesis
3.1 Input/Output material balance (S)
3.2 Input/Output Economic Potential (S)
3.3 Recycle structure of the flowsheet
3.4 Material balance with recycles (PS)
3.5.Economic Potential with recycles (S)
3.6 General structure of the separation system
3.7 Vapour separation system
3.8 Liquid separation system using splitters
4. Process simulation
4.1 Thermodynamic analysis (PS)
4.2 Reactor modelling (S, PS)
4.3 Preliminary simulation of the flowsheet (PS)
4.4 Separation system (PS)
4.5 Stream report
5. Energy integration
5.1 Selection of streams for heat integration
5.2 Selection of utilities
5.3 Input data: streams and utilities
5.4 Targets of energy integration (PPA)
5.5 Design of Heat Exchanger Network (PPA)#
6. Evaluation
6.1 Critical comparison with existing processes
6.2 Future improvements

S – spreadsheet; PS – process simulation; PPA – pinch point analysis; # - optional

14.5 PLANT DESIGN PROJECT

14.5.1 Outline

The objectives of a Plant Design Project (PDP) are:

- Develop the conceptual design of a process at a level of feasibility and performance close to the industrial reality.
- Assess the environmental impact and propose measures to improve it.
- Evaluate the economics and profitability.
- Educate the teamwork and the management of time.
- Improve the communication skills.

Unlike the PI project where the emphasis was on generating flowsheet alternatives, in the Plant Design Project the subject is selected from existing competing technologies. However, the rationale of the flowsheet design has to be retraced by a rigorous revision of the conceptual levels and of the appropriate design decisions at each design step.

Table 14.4 presents a typical content of a PDP, but this may be adapted to meet specific teaching needs. The efficiency and the robustness of the engineering solution are this time central features. The project is demanding both as content and intensity, so the work should be done at best by groups of 3-4 students. Typical duration is between 10 to 12 weeks full time. The tasks should be planned in such a way to allow parallel working. For example, writing the final report should start from the first week by incorporating the information at the right place in the outline. Sharing efficiently tasks and information allows the team to complete the project in time, despite difficulties.

Table 14.4 Content of a Plant Design project

1. Project Definition
1.1 Requirements: products, raw materials, production rate, specifications
1.2 Site selection
1.3 Alternative chemical routes
1.4 Commercial competing processes
1.5 Short description of the selected technology
1.6 Prices: products, raw materials, utilities
2. Chemical Reaction Analysis
2.1 Chemical reaction network
2.2 Thermo-chemistry
2.3 Chemical equilibrium analysis
2.4 By-products and impurities
2.5 Catalyst production and regeneration
2.6 Material Safety Data Sheets of main components
2.7 Process constraints: safety, toxicity, odour, waste
3. Thermodynamic Analysis
3.1 Physical properties of pure components
3.2 Phase equilibria of representative mixtures
4. Process Synthesis
4.1 Input/Output structure
4.2 Chemical reactor analysis
4.3 Recycle structure of the flowsheet
4.4 Separation systems
4.5 Preliminary Process Flow Diagram
5. Material and Energy balances
5.1 Input/Output material balance
5.2 Approximate material balance with recycles
5.3 Detailed simulation with rigorous units
5.4 Stream report
6. Energy Integration (Pinch Point Analysis)
6.1 Selection of utilities
6.2 Energy integration around the reaction system
6.3 Energy integration of distillation columns
6.4 Streams selection for heat integration

6.5 Heat and Power co-generation 6.6 Water cooling and refrigeration systems 6.7 Heating agent systems 6.8 Heat Exchanger Network design 6.8 Revised Process Flow Diagram
7. Equipment Selection and Sizing 7.1 Chemical reactor 7.2 Distillation columns 7.3 Heat exchangers 7.4 Transport of fluids 7.5 Cooling and refrigeration systems 7.6 Storage vessels 7.7 Handling of solids
8. Process Control and Instrumentation 8.1 Plantwide Control analysis 8.2 Process Control of main units
9. Safety and Loss Prevention 9.1 Main process hazards 9.2 Risk analysis
10. Environmental Analysis 10.1 Air pollution sources 10.2 Waste disposal 10.3 Wastewater treatment
11. Economic Evaluation 11.1 Market analysis 11.2 Total Capital Investment 11.3 Total Operating Costs 11.4 Profitability analysis
12. Critical evaluation 12.1 Summary of results 12.2 Sustainability measures 12.3 Conclusions
13. Documents and drawings 13.1 Process Simulation Diagram 13.2 Process Flow Diagram 13.3 Stream Report 13.4 Equipment specification sheets
14. Appendixes 14.1 Literature survey: articles, patents 14.1 Supplementary information: computer files, etc.

The project starts by an intensive research of data. Literature research is time consuming, although this is more efficient today because of Internet. The problems generated by the chemistry should be analysed before any design step. A comprehensive description of the chemical reaction network, as well as the availability

of data about the selectivity of different steps is of greatest importance. Most of the separation difficulties come from the removal of by-products and impurities that affect the specifications on product purity. In addition, the problems arisen by the use of auxiliary chemicals have to be analysed, as solvents, acid or basic neutralising agents, or catalyst. Health and safety properties of the main components and by-products must be listed as Material Safety Data Sheets, for which many data are available on Internet. Different physical properties of species and mixtures can be found in CRC Handbook (2000), as well as in the Landolt- Börnstein collection of physical data.

Thermodynamic modelling is of crucial importance for reliable design. Our experience, shared by colleagues from other universities (Jimenez & Bañares-Alcántara, 2002), shows clearly that there is a gap between the general knowledge taught in Physical Chemistry courses and the its application in the calculation of physical properties and phase equilibria by means of process simulation. That is why this book contains two chapters on generalised thermodynamic methods and phase equilibria, which can be used as material for a short course in Applied Thermodynamics, or for upgrading the knowledge by individual study. Other important preliminary issues in design are thermo-chemistry and chemical equilibrium.

As mentioned, the process synthesis section should retrace the rationale of flowsheet development by applying the Hierarchical Approach, as explained in Chapter 7. Deviations from the standard flowsheet are encouraged. This is necessary because often the flowsheets described in the open literature are either oversimplified or being based design decisions that could be not longer valid in the context of the actual design.

Developing a good material balance is a milestone of the project. Reliable and accurate simulation of Reactor-Separations-Recycle system is necessary. The simulation should start by combining stoichiometric models for reactor with shortcut models for separations. These can be upgraded in rigorous units after closing the recycle loops. In addition, considerations about the stability of the reaction system could be studied. Because of the importance of the chemical reactor, we recommend the study of Chapter 8 dealing with the reaction engineering from the viewpoint of Process Synthesis. Basic elements for the synthesis of separation systems are discussed in Chapter 7, namely for zeotropic mixtures. More advanced issues that address non-ideal mixtures are presented in Chapter 9. Note that the use of simple distillation columns is sufficient at this stage. The need for complex columns should be a result of process integration.

The next step is the energy integration by applying Pinch Point Analysis and techniques for energy saving. The selection of streams should be carefully examined from the point of view of their potential for heat exchange. Instead of listing all the streams, more efficient is the strategy of local integration. The analysis should start around the chemical reactor. If the reaction is highly exothermal, there are opportunities for saving energy for separations and/or exporting energy to other users on site. The analysis of distillation columns can identify potential thermal coupling or opportunities for making use of complex columns.

After solving the integration of key units, the analysis could proceed with other process streams by applying the targeting principle. As a result the Minimum Energy Requirements of the process can be identified. The analysis in Balanced Grand

Composite Curve could suggest modifications in the flowsheet design leading to energy saving. After completing the analysis by targeting approach, the design of the Heat Exchanger Network can follow by applying the Pinch design method. The whole analysis will lead to a revised flowsheet. This flowsheet should be simulated as a final proof for the correctness of design.

After flowsheet development, the next step consists of equipment selection and sizing. Chapter 15 contains guidelines about the design of the main equipment items, as reactors distillation columns and heat exchangers. More information about equipment design can be found in specialised books, as Coulson & Richardson (1993), Perry (1997), Woods (1995), Sandler & Luckewicz (1987), etc. Note that the flowsheeting systems incorporate sizing capabilities. However, the report should indicate clearly the assumptions in performing the calculations, as for example the type of tray and the position of the operating point with respect to flooding in the case of a distillation column. Accordingly, the sizing characteristics should be clearly described for each equipment item. We recommend the use of specification sheets in the format employed by the engineering companies (see examples in Coulson & Richardson, 1993).

For the correct estimation of capital investment a complete list of the equipment items is needed. Note that some units lumped in the simulation blocks or neglected as unimportant must be explicitly listed as equipment items, and sized accordingly. Typically these are storage tanks and reservoirs, furnaces and heating systems, special pumps and devices for the transportation of solids, dryers, filters, evaporators, centrifuges, cyclones, etc. These items should be added on the final Process Flowsheet Diagram.

The chapter on Process Control should focus on plantwide control problems as safety, change of the production rate and product quality. Control schemes for individual units are well documented, but these should be adapted to the particular situations.

Emphasise should be set on safety and loss prevention issues. The Hazop study could follow the guidelines from Coulson & Richardson (1993). More information about this topic may be found in Crowl & Lowvar (1990), and other specialised references.

The environmental analysis consists of evaluating the risks on health and environment, even if prevention measures have been incorporated in design. The requirements formulated in project definition should be examined on the base of the proposed solutions. For example, the cost of antipollution measures should be added to the operating costs, and their impact on profitability estimated. For this section we recommend the book of Allen & Rousselot (1997).

The economic evaluation of the project should be oriented to profitability analysis, as explained in Chapter 14. The estimation of capital investment and operation costs is necessary, but the figures are only intermediate steps to profitability measures. These should be compared with similar processes, or other industrial projects, on a longer-term vision based on a lifecycle analysis. The economic analysis can be done at best with a spreadsheet.

The project concludes with a synthesis of the main results, as material and energy consumption, capital-investment, profitability indices and sustainability measures. The critical analysis should review the main requirements and possible improvements.

Good quality graphics should be used to illustrate all the design issues. The tables should contain sufficient information to support the design, but not irrelevant data. A comprehensive plant stream table is compulsory. Reworking the tables provided by simulator is often necessary.

The Plant Design project should be defended by public presentation. The final mark should take into consideration both the quality of the technical work, as well as the capacity of the team to convince the audience and the examination commission about the merits of the project.

14.5.2 Subjects

Table 14.5 presents a sample of subjects that can be solved by means of public information. Most of the subjects are of petrochemical nature, more suited for the fully application of the methodology developed in this book. However, processes in speciality chemicals, biotechnologies or environmental engineering could be envisaged. The list contains also examples of design problems based on the internal scientific research.

The basic technological information for most of the subjects can be found in Encyclopaedias of industrial chemistry, as Ullmann's and Kirk-Othmer, or can be based on more specialised books, as Myers (1997) and Gary & Handwerk (1994). Efficient bibliographical research can be done nowadays on Internet, but the students should learn to search selectively and efficiently the information really needed.

Assigning a variety of subjects could arise some scepticism. However, our experience showed great interest and motivation of students. The results were surprisingly good even in the case when the students arrived with some weaknesses in the initial skills. The reason is that the design project is the occasion of a substantial revision of the knowledge acquired in fundamental chemical engineering courses, whose usefulness is now obvious. Particularly, the challenging character of the design problem produces a substantial improvement in motivation, and a net enhance of the individual performance. Care should be paid to keep the computer use focused on solving the design problem. Failure and frustration could arrive for various reasons, as interruption in work, communication gap between team members and insufficient staff support. Teamwork management is another useful element that the students appreciate during this high value educational activity.

Table 14.5 Student projects

No.	Process	Observations
1	Acetone/Phenol via Cumene	
2	Acetylene purification	Absorption in methanol/n-octane/NMP
3	Acrylonitrile by Propylene amonoxidation	Sohio process
4	Benzene alkylation to Ethylbenzene and Iso-propylbenzene	Several processes: Vapour-phase, Liquid-phase or Reactive Distillation

5	Benzene and Xylenes from Toluene	Toray process
6	Butadiene by selective oxidation	Innovative process
7	Benzoic acid by tar upgrading	Research
8	Cyclohexanone from Phenol	Research
9	Dimethylterephtalate by Xylene oxidation	Huels/Witte process from p-xylene
10	Polymer-grade ethylene by pyrolysis of hydrocarbon feedstocks	Stone & Webster, ABB Lummus,
11	Etylene Oxyde	Shell Chemicals
12	Butadiene extraction from C4 fracion	Comparative study of several solvents
13	Fatty esters hydrogenation	Research (Brands et al., 2001)
14	HF Alkylation of C3/C4 fractions	UOP and Philips Petroleum processes
15	Methanol from synthesis gas	Low and medium pressure process
16	Selective butadiene hydrogenation	DSM process
17	Polymerisation processes: PE, PP, PVC, Polystyrene, SAN	Use Aspen-Polymer Plus™ for specific polymerisation reaction models
18	PCB supercritical water oxidation	Internal research
19	Vinyl Acetate synthesis	Acetic acid/ethylene/oxygen process
20	Vinyl Chloride Monomer	1. Balanced process, see Case Study 3 2. Stauffer process

14.6 REFERENCES

Allen, D. T., K. S. Rosselot, 1997, Pollution prevention for Chemical Processes, Wiley

Brands D, A. C. Dimian, A. Bliek, 2002, Supercritical hydrogenolysis of fatty esters. 1. Thermodynamics. 2. Process development, J. Am. Oil. Chem. Soc., vol, 79, 75-91

Crowl, D. A., Lowvar, J. F., 1990, Chemical Process Safety, Prentice Hall

CRC Handbook of Chemistry and Physics, 2000, CRC Press

Himmelblau, D. M., 1996, Basic Principles and Calculations in Chemical Engineering, Prentice Hall

Gary, J. H., Handwerk, G. E., 1994, Petroleum Refining. Technology and Economics, 3nd Ed., Marcel Dekker, NY

Kirk-Othmer Encyclopaedia for Chemical Technology, 1991, 4th Ed., Wiley

Landolt-Börnstein, Zahlenwerte and Functionen, Springer Verlag

Meyers, R. A., 1997, Handbook of Petroleum Refining Processes, 2nd Ed., McGraw-Hill

Perry's Chemical Engineer's Handbook, 1995, 7th edition

Sandler, H, J, Luckewicz, E. L., Practical Process Engineering, 1987, McGraw-Hill

Sinnott, R. K, in Coulson & Richardson, 1993, Chemical Engineering, vol. 6, Pergamon Press

Ullmann's Encyclopaedia of Chemical Technology, 2000

Woods, D. R., 1995a, Process Design and Engineering Practice, Prentice Hall

Woods, D. R., 1995b, Data for Process Design and Engineering Practice, Prentice Hall

Chapter 15

ECONOMIC EVALUATION OF PROJECTS

15.1 Introduction

15.2 Basic concepts
- 15.2.1 Prices
- 15.2.2 Capital and operating costs
- 15.2.3 Cash flow

15.3 Time-value of money
- 15.3.1 Compound interests
- 15.3.2 Annuities
- 15.3.3 Annualised capital costs
- 15.3.4 The effect of inflation

15.4 Capital costs
- 15.4.1 Elements of capital costs
- 15.4.2 Estimation of capital investment
- 15.4.3 Cost indexes
- 15.4.4 Capital depreciation

15.5 Operating costs
- 15.5.1 Elements of operating costs
- 15.5.2 Estimation of operating costs
- 15.5.3 Simplified model for estimating operating costs

15.6 Profitability Analysis
- 15.6.1 Traditional profitability indices
- 15.6.2 Simplified profitability analysis
- 15.6.3 Modern profitability measures
- 15.6.4 Discounted Cash Flow Rate of Return
- 15.6.5 Summary of profitability measures

15.7 Further reading

15.8 References

15.1 INTRODUCTION

The moment of truth of any design is the economic analysis. A good project should ensure rapid return of the investment and good profitability over the expected lifetime, comparable with other industrial or financial projects. Characteristic for the modern process design is the fact that the conceptual design itself incorporates the basic elements of the economic analysis. For example, in the synthesis of flowsheet by Hierarchical Approach explained in Chapter 7, the Economic Potential is used to eliminate unfeasible routes in early stages, and for ranking flowsheet alternatives in later stages. Moreover, the economic optimality is imbedded in the objective function that controls the synthesis of subsystems, as the separation system or heat exchanger network. In other words, the paradigm of modern Process Integration allows the development of an optimal design both from technical and economical point of view.

From the perspective of integrated design the economic analysis of a project should be seen in the first place as an assessment of process profitability. This should not require the revision of the flowsheet structure and of the basic equipment items. If this happens, the conceptual design methodology was not properly applied.

Nowadays, sophisticated computer packages interfaced with process simulation and engineering database systems can support the economic analysis of a design project from initial stages to its completion. These tools contain capabilities for design and mechanical sizing of process equipment, databases with information about materials of construction, as well as data about suppliers and prices. In this way rapid and accurate estimation of capital-investment is possible for smaller or larger projects, at any level of detail required. The engineer can focus on the conceptual and decisional aspects of his work. One of the most known software in the economic analysis of design projects is ICARUS Process Evaluator® interfaced with Aspen Plus.

As with process simulation, however, complicated economic computations might obscure basic features, and most of all the decisional levels and the sources of uncertainty of different elements. That is why is important to know the fundamentals of an economic analysis and to pass throughout the main steps before let a computer to do an essential sophisticated job.

The conceptual design of a process is the most responsible for the success or failure of the whole project. Therefore, an unfortunate decision at this stage will be paid later at much higher cost. The economic evaluation of the conceptual design stage is often called *preliminary cost estimation.* This is also the object of the present chapter.

The chapter starts by introducing the basic concepts of an economic analysis, as prices, breakdown of the capital and manufacturing costs, profit, as well as the formation of cash flow. Because the time-value of money plays a central role the next section presents some basic elements of financial methods. Two other sections deal with the detailed estimation of capital and operation costs. Simplified equations based on typically cost ratios can be used for quick estimations. These ratios are also helpful for the control of more detailed computations. The chapter ends with a more detailed description of the profitability analysis, both by traditional and modern methods. Note that the methods developed in this chapter can be applied using spreadsheets.

15.2 BASIC CONCEPTS

15.2.1 Prices

The economic analysis of a design project starts early in the conceptual design with the evaluation of an Economic Potential (*EP*). Thus, at the Input/Output level this is:

EP (Input/Output) = value of products – cost of raw materials – environmental expenses = selling-price × production rate – purchasing-price × raw materials amount – environmental expenses

This first step involves crucial cost elements, as the *selling price of products* and *purchasing price of raw materials*, which by far dominate the profitability of any chemical process. If this information is not reliable from the beginning, it will blur the whole analysis, whatever the accuracy of other costs could be.

Characteristic for Chemical Process Industries is the burden of raw materials in the manufacturing costs, typically between 50 and 60%. As a result, the profit of chemical processes depends heavily on the market of raw materials. In addition, the weight of the shipping fees in the product cost must be also carefully examined for remote suppliers.

In the case of commodities, as fuels, plastics or fertilisers, the raw materials are intermediate chemicals produced from more basic raw materials, as oil, natural gas or minerals. For example, the production of polyolefin is integrated on a petrochemical platform with refining and other basic chemicals. The combination of several processes on a large industrial site is a typical feature of chemical industry that determines in large extent the profitability of a particular plant.

Selling prices for existing products are controlled by the market and easier to estimate. They are more stable on a longer period. It should be stressed that the price of a chemical product depends on its application properties, mainly of purity. Ensuring high-value product specifications by design can bring a significant commercial advantage even with relatively expensive raw materials.

15.2.2 Capital and operating costs

From the point of view of a designer the costs involved in a project can be classified in two major categories: (1) Capital costs and (2) Operating costs.

Capital costs regard the equipment and the infrastructure needed to realise physically the plant. The main part is the *fixed-capital* (F_C). Here we count the cost of the land and site development, the expenses necessary to design the plant, to purchase the equipment, to erect the plant and ancillary buildings, as well as various contingencies. Besides *working-capital* (F_W) is necessary for starting-up the production including manufacturing expenses for the first months of production.

Operating costs are linked directly with process operation. Here the most important position is the cost of raw materials. The second large expenses are the energetic utilities. Operating costs include also the maintenance of equipment, as well as

manpower, labour, administrative overhead, sales, provisions, etc. Detailed description and estimation methods for both categories will be given later in this chapter.

Another classification, more appropriate for accounting, divides the costs associated with the manufacturing process in two types: (1) Fixed costs and (2) Variable costs.

Fixed costs are independent of the production rate, as capital charges, labour and overhead salaries, insurance, periodic maintenance and taxes.

Variable costs are proportional with the production rate, as raw materials, various chemicals, utilities and transport costs, but also some royalties and maintenance costs.

The common measure of different costs is money. Therefore, a *profitability analysis* must take into account the *time-value of money*. The practical way to evaluate the profitability is to forecast the evolution of the cash flow over a longer period of time, theoretically over the plant lifecycle. The next section will discuss in more detail the formation of the cash flow.

15.2.3 Cash flow

Different elements describing the formation of the cash flow are shown in Fig. 15.1. These originate from three categories:

- Capital sources and sinks,
- Total Capital Investment,
- Operating costs.

Capital sources include credits and loans from banks, stocks, etc., as well as the net cash flow from selling the products. The sinks are the repayment of credits and of different debts, as well dividends to shareholders.

Total Capital Investment (*TCI*) contains fixed and working-capital. The first is recovered over several years by means of a depreciation charge D. The second is consumed in the first year of operation. It is important to note that depreciation of the fixed-capital is regulated by law and depends on the taxation system of each country. The depreciation charge is typically 10-20% of the fixed-capital. This topic of particular importance in cash flow formation will be developed in the section 15.3.4.

Operating costs C_o include all expenses regarding the manufacturing process, as raw materials, utilities, manpower, contingencies, etc. (see later in this chapter), excluding the depreciation of the fixed-capital.

With these elements, the cash flow calculation can follow the procedure outlined below. The definition of the terms could be slightly different, and should always be checked for comparative studies. In this text we adopt the approach of Peters & Timmerhaus (1991). A more elaborated treatment written by Holland & Wilkinson can be found in Perry (1997).

1. Firstly, the *gross profit GP* can be calculated as the difference between revenue from sales S and operating costs C_o:

$$GP = S - C_o \tag{15.1}$$

Following the above definition the gross profit excludes the depreciation.

2. Next, a *net profit before tax* P_{bt} may be determined by deducting the depreciation from the gross profit:

$$P_{bt} = GP - D = S - (C_o + D) \tag{15.2}$$

3. Because tax must be paid for every profit, the *net profit after tax* P_{at} is:

$$P_{at} = P_{bt}(1-t) = [S - (C_o + D)](1-t) \tag{15.3}$$

where t denotes the *legal tax rate.*

4. Finally, the depreciation must be reintegrated. The *net cash flow CF* becomes:

$$CF = P_{at} + D = [S - (C_o + D)](1-t) + D = (S - C_o)(1-t) + D \times t \tag{15.4}$$

The result shows that the cash flow can be calculated simply as the gross profit after tax $(S - C)(1-t)$ plus the depreciation multiplied by the tax rate, the term $D \times t$. That is why the last term is often seen as a *tax credit* on capital depreciation.

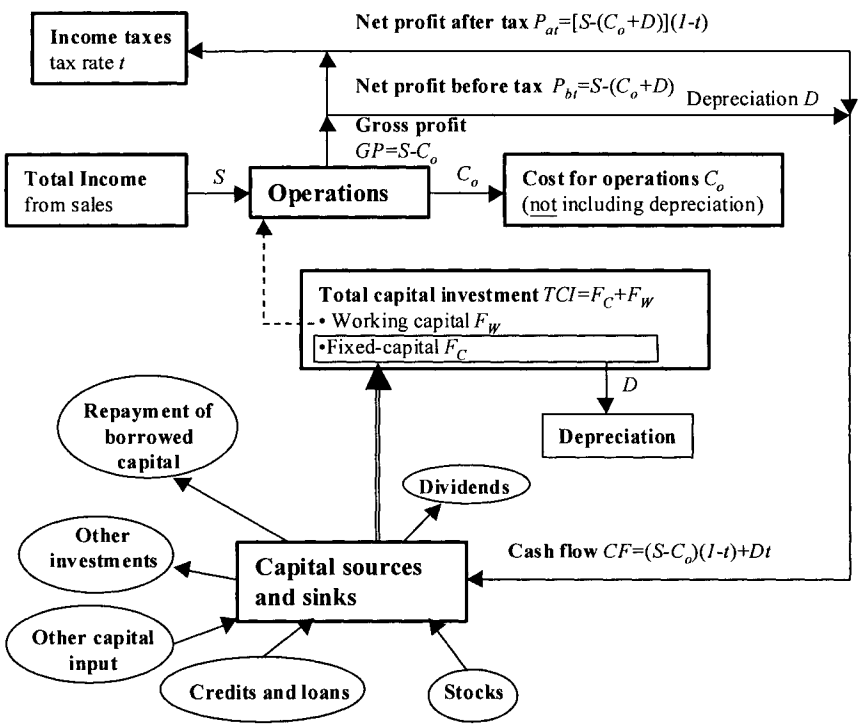

Figure 15.1 Formation of profit and cash flow (after Peters & Timmerhaus, 1991)

As the relation (15.4) suggests, the depreciation of the fixed-capital might be an important source of cash flow, although this is not created in the manufacturing process. Suppose that the sales are S=1000 k€ and the operation costs C_o=600 k€. The gross profit would be GP=400 k€. If the tax rate is 40% then the taxes on GP would be of

160 k€. Assume now fixed-capital depreciation of D=200 k€. The net profit before tax is P_{bt} =400–200 =200 k€. The income tax is 0.4×200=80 k€. The tax reduction is 160–80=80 k€. Therefore, capital depreciation could be a significant source of tax saving, particularly for short write-offs periods. The depreciation politics plays an important role in process profitability, as it will be discussed later in this chapter.

The above calculation method gives a 'spot' value of the cash flow, or averaged over time. In a profitability analysis it is necessary to estimate the evolution of the cash flow over a longer period of time, which inevitably should take into account *the time value of money*. Figure 15.2 presents the graph of *cumulative cash flow* over the project lifecycle[1]. This starts by buying the land (AB). It follows the period of fixed-capital investment indicated by the segment BC. Working-capital (CD) is needed to start the production. The total capital investment is represented by the segment OD and includes working and fixed-capital, as well as the cost of the land.

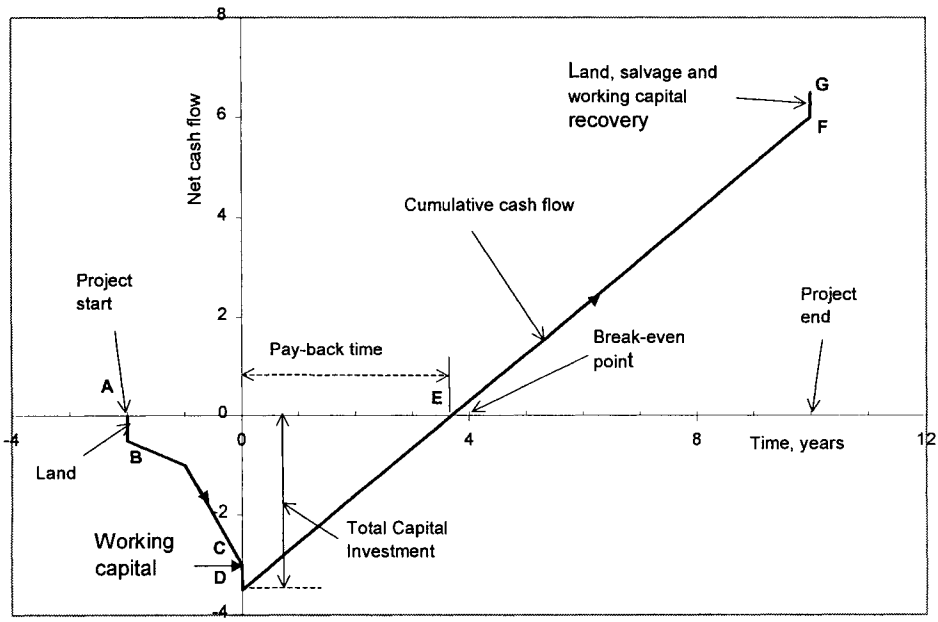

Figure 15.2 Cumulative cash flow over plant lifecycle

The repayment of the initial investment starts with the first production, which is considered the time zero. The cash flow will cumulate over the years up to the point where the production stops. The initial capital investment can be recovered at the end of the lifecycle as a *salvage value*. In the first phase of operation the cash flow is used

[1] The term 'project' is used here in a larger sens than process design, including plant realisation and operation, in general a profit generation activity implying capital and operating costs.

to pay back the total investment. Consequently, the negative cumulative cash flow diminishes to zero at the *break-even point* (E). The time interval necessary for reimbursing the initial capital investment is an important economic index called the *payback time.*

The above representation based on the cash flow analysis over a longer period gives a comprehensive image of the profitability from the point of view of the financial operations incurred by the manufacturing process. An important feature of cash flow is that it takes into account the variability in time of different cost elements, as prices, interest rate, market behaviour, depreciation politics, etc.

However, the above cash flow analysis is deterministic. Therefore, a more realistic treatment should include some elements of *risk analysis.* This consists of the identification, quantification, evaluation and acceptance of risks. The subject concerns more the management of projects and therefore it is out of the scope of this book. More material about risk analysis can be found in specialised references, as in Haimes (1998).

As an illustration of the above concepts we will examine the selling price that ensures a profitable operation. If the product price cannot be found from reliable market data, or when the product is new, then making use of simply profitability indicators, as Return On Investment (*ROI*), allows a quick estimation.

EXAMPLE 15.1 Estimation of a profitable selling price

A new plant for a speciality chemical is designed for a production of 1000 tonne/year. Estimate a profitable selling price that would give a *ROI* after tax of minimum 20%. The following data are assumed:

- Total capital investment *TCI*=1000 k€, with fixed-capital F_C =800 k€ and working-capital F_W =200 k€. The depreciation is straight-line over eight years.
- Annual operating costs C_o =200 k€/year.
- Tax rate t=0.35.

Solution.

ROI after tax is defined as the ratio between the profit after tax and the total capital investment (fixed plus working-capital), as follows:

$$ROI_{at} = P_{at} / TCI = [S - (C_o + D)](1-t)/(F_C+F_W)$$

For the net profit after tax we get $P_{at} = ROI_{at} \times TCI = 0.20 \times 1000 = 200$ k€/year.
Linear depreciation over 8 years gives D = 800000/8 = 100 k€/year.
Applying eq. 15.3 leads to the relation: 200 = [S– (200+100]×(1–0.35).
We get S= 607692,- €. Hence, a profitable selling price should be at least 608 €/tonne.

15.3 TIME-VALUE OF MONEY

Two major questions are of interest when examining the opportunity of an investment:
- What is the value of an amount of money (capital or earnings) over a longer period of time?
- What is a good policy of reimbursing a credit?

15.3.1 Compound interests

To answer the first question consider a bank deposit whose present value is P. What is its value after n years? Suppose that the annual interest rate i is constant. After the first year we get $P(1+i)$, after the second year $P(1+i)^2$, etc. After n years the future value F becomes:

$$F = P(1+i)^n \tag{15.5}$$

Conversely, the present value of a future expense F is:

$$P = F/(1+i)^n \tag{15.6}$$

The relation (15.5) is known as the *compound-interest formula*. The relation (15.6) is the reciprocal that allows the comparison of different options on the same basis, the present value. A simple numerical exploration shows that the variation of the future value F over years depends strongly on the interest rate. Figure 15.3 presents the evolution of a monetary unit over 20 years at different interest rates. The time-value of money change considerably, particularly for higher interest rates and longer times.

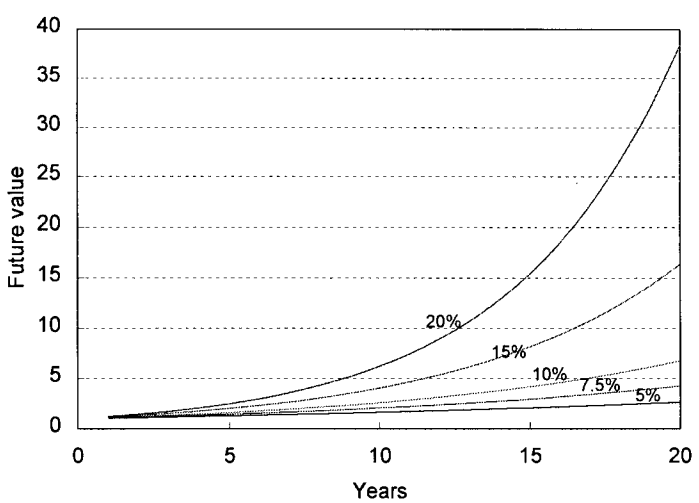

Figure 15.3 Value of unit currency function of time at different interest rates

A more accurate illustration of the future and present values is presented in Table 15.1. Thus a placement at 10% brings 46.4 % more value after five years, while the same amount of money left sleeping has only a value of 0.683 after five years.

Table 15.1 **Future and present values for a monetary unit at different interest rate**

Year		0	1	2	3	5	10
5%	*F*	1	1.0500	1.1025	1.1576	1.2763	1.6289
	P	1	0.9524	0.9070	0.8639	0.7835	0.6139
10%	*F*	1	1.1000	1.2100	1.3310	1.4641	2.5937
	P	1	0.9091	0.8264	0.7513	0.6830	0.3855

It is clear that large investments are rational when the interest rate is low enough in a stable macro-economic environment. This situation is typical for process plants that have a very long life, typically between 20-30 years. Contrary, smaller investments could accept higher interests, particularly for payback periods shorter than three years.

15.3.2 Annuities

The second question concerns the repayment of a loan or something equivalent, as mortgage or life insurance. Let's consider the opposite problem: what is the capital accumulated by investing regularly an amount R for which an interest rate i is received? The accumulated value consists of a series of n regularly payments, called *annuity*. In an ordinary annuity the payments occur at the end of each period, so it will accumulate interests on $(n-1)$ periods. Thus the partial capital generated by the first payment is $R(1+i)^{n-1}$. The second payment brings $R(1+i)^{n-2}$, etc. The lumped sum accumulated after the last payment is:

$$S = R(1+i)^{n-1} + R(1+i)^{n-2} + ... + R(1+i)^1 + R$$

Multiplying both terms by $(1+i)$ and subtracting the original expression leads to:

$$S = R\frac{(1+i)^n - 1}{i} \tag{15.7}$$

The term $[(1+i)^n - 1]/i$ is designated commonly as *series compound-amount factor*. For example, saving in a bank account a monthly deposit of 100 € at an annual rate of 5% over 40 years will bring a cumulative amount of 152602 €. This amount is by far more substantial than 48000 € saved over the sane period in a 'piggybank'. Referred to the initial time, this would be worth only 21676 € if the inflation rate is 5%.

The analysis presented above is also important to evaluate the depreciation of equipment. Let's denote by S is the difference between the purchasing and scrapping values. By assuming an interest rate i and a depreciation period n, the annual charge of depreciation as constant payments R can be computed as follows:

$$R = S\left[\frac{i}{(1+i)^n - 1}\right] \tag{15.8}$$

EXAMPLE 15.2 Equipment depreciation

An equipment has been purchased for 12000,- € with the intention of selling it after five years. A scrap value of 2000 € is expected. Calculate the profitability of renting the tool at 300,- €/month. The annual interest rate is of 10%.

Solution. The annual depreciation rate calculated with the equation (15.8) is:

R=[12000–2000]×0.1/(1.10^5–1) = 1638 €/year

This value shows that 1638 €/yr should be accumulated yearly in a depreciation fund at annual interest of 10% to account for the decrease in the equipment value. For this reason this type of depreciation is known as *sinking-fund method.* Note that the purchasing and scrap value are referred to the same present value. Thus, rent the equipment could bring 300×12= 3600 €/year, an amount that would cover largely the depreciation.

15.3.3 Annualised capital costs

In the accounting practice the operating and capital costs must be expressed on a common basis. The first are normally reported on yearly basis. With the capital the situation is different. We may consider that the capital is borrowed over a period of time, usually between five and ten years, the repayment will be done following a fixed sum called *annuity*. Suppose that the present value of the invested capital is P. If invested at a fixed interest rate i over n years, this will produce an equivalent amount F, as given by the equation (15.6). The reimbursement by yearly payments A can be expressed by the equation (15.7), so we may write $F = P(1+i)^n = A[((1+i)^n - 1)/i]$. It follows that the present value of the invested capital is:

$$P = A\frac{(1+i)^n - 1}{i(1+i)^n} \tag{15.9}$$

Conversely, the annual reimbursement becomes:

$$A = P\frac{i(1+i)^n}{(1+i)^n - 1} \tag{15.10}$$

The term multiplying A in equation (15.9) is called *present-value series factor*, while the term multiplying P in (15.10) is called *annualisation* or *capital-recovery factor.*

Table 15.2 presents some illustrative values. For example, to get revenue of 1000 each year over five years an amount of 4329.5 must be initially invested at 5%. For a mortgage of 1000 at 5% over five years the reimbursement is 231/y.

Table 15.2 Present-value series and capital-recovery factors

Present-value series factor					
Interest rate / year	1	2	3	5	10
5%	0.9524	1.8594	2.7232	4.3295	7.7217
10%	0.9091	1.7355	2.4869	3.7908	6.1446
15%	0.8696	1.6257	2.2832	3.3522	5.0188
Capital-recovery					
Interest rate / year	1	2	3	5	10
5%	1.0500	0.5378	0.3672	0.2310	0.1295
10%	1.1000	0.5762	0.4021	0.2638	0.1627
15%	1.1500	0.6151	0.4380	0.2983	0.1993

Table 15.3 presents a synthesis of financial calculations at 5% annual interest rate. Let's see the situation after three years. The significance of figures is:

- A single deposit of 100 will produce a value of 115.8 after three years.
- An amount of 100 is only 86.38 as present value after three years.
- An annuity of 100 will produces a future value of 315.3 after three years.
- To accumulate a capital of 100 after three years the annuity saving is 31.72.
- Annuity of 100 gives after three years a present worth of 272.3.
- A mortgage of 36.72 paid at the end of each year reimburses a credit of 100.

Table 15.3 Financial computations

Years	Single payment		Uniform series of payments			
	Compound-amount factor	Present-value factor	Compound-amount factor	Sinking-fund factor	Present-value factor	Capital-recovery factor
	$P \to F$ $(1+i)^n$	$F \to P$ $(1+i)^{-n}$	$A \to F$ $\frac{(1+i)^n - 1}{i}$	$F \to A$ $\frac{i}{(1+i)^n - 1}$	$A \to P$ $\frac{(1+i)^n - 1}{i(1+i)^n}$	$P \to A$ $\frac{i(1+i)^n}{(1+i)^n - 1}$
1	1.050	0.9524	1.0	1.0	0.952	1.05
2	1.103	0.9070	2.050	0.4878	1.859	0.5378
3	1.158	0.8638	3.153	0.3172	2.723	0.3672
5	1.276	0.7835	5.526	0.1809	4.329	0.2309
10	1.629	0.6139	12.578	0.0794	7.722	0.1295
15	2.079	0.4810	21.579	0.0463	10.380	0.0963
20	2.653	0.3769	33.066	0.0302	12.462	0.0802

EXAMPLE 15.3 Invest or reimburse a loan

A revamping project needs 1000000,- € investment. Someone has the idea to put the whole money in a bank account at 10% annual interest rate and ask for a loan at the same rate, but with monthly payments. Examine the feasibility of this proposal.

Solution. Firstly, let's see what a placement in a bank account can earn. Suppose that a placement at 10% for 5 years is found. The future value of the sum can be calculated with the Eq. 15.5 as F=1.0E6×(1+0.1)^5= 1.464E6 €.
On the other hand, we may consider a credit of one million paid monthly at an yearly interest rate of 10 % over five years (10/12 monthly interest over 60 months). The equation (15.9) can be used to calculated the annuity as follows:

A=1.0E6×(0.1/12)(1+(0.1/12))^{60}/[(1+(0.1/12))^{60}–1] ×12=1.0E6×0.25496=254960 €/year

Note that 0.25496 is the annualised factor that should be used to spread a present value over five years. The payments will give a lump sum of F'=254960×5=1.2748E6 €. The difference F-F' is the gain 1.464-1.275=0.189 million €. It may be observed that borrowing might be more advantageous than spending the own money, at the condition that the interest rate of return be equal or greater than the credit. Unfortunately, the banks know the answer to the above question.

15.3.4 The effect of inflation

Inflation affects considerably an economic analysis. Higher inflation rate is dissuasive for investors because the time-value of money declines rapidly. However, over a longer period of time a parallel trend between inflation and banking interest rate has been observed. This effect leads to a much more stable trend of the effective rate $i_{eff} = i - i_{Inf}$. For example, in Western Europe the decade 1990-2000 has been characterised by low inflation rate, between 1.5 and 3 %, and credits between 5.5 and 7%. The difference gives an effective interest rate almost constant of 4%.

The time-value of money is lowered by the effect of inflation. The future value becomes:

$$F = P\frac{(1+i)^n}{(1+i_{Inf})^n} \cong P\left[(1+i_{eff})^n\right] \tag{15.11}$$

The relation (15.11) is similar with (15.9), but the interest rate is diminished by the inflation rate. Contrary, the zero-time value is different, as follows:

$$P = \frac{F}{(1+i)^n(1+i_{Inf})^n} \cong F[1+(i+i_{Inf})]^{-n} \tag{15.12}$$

In this case the inflation is cumulative with the interest rate. The inflation diminishes the revenues, but accelerates the reimbursement of credits. The last effect discourages the investors, so finally both effects are negative.

15.4 CAPITAL COSTS

15.4.1 Elements of capital costs

A *grass-root plant* is defined as a complete plant erected on a new site. The area confining the plant is designated by the *battery limit* (BL). This area excludes facilities for large storage, general utilities and administrative buildings. *Total Capital Investment* (TCI) designates the amount of funds needed to design, build, and operate the plant, and is the contribution of two main categories, fixed-capital and working-capital.

Fixed-capital

The capital for designing and building the plant ready for start-up represent the *fixed-capital*, and includes *direct costs* and *indirect costs*. Table 15.4 presents the details.

Table 15.4 Breakdown of fixed-capital items (after Peters & Timerhaus, 1991)

Direct costs
1. Purchased equipment All equipment listed on flowsheet, surplus equipment, and spare parts. Inflation cost allowance.
2. Purchased-equipment installation.
3. Instrumentation and Control Purchase, installation, calibration, computer system.
4. Piping, valves and insulation.
5. Electrical equipment.
6. Buildings Process buildings, auxiliary buildings, maintenance, shops, building services.
7. Yard improvements Site development, roads, railroads.
8. Service facilities Utility plant and distribution, refrigeration plants, waste disposal, water treatment, fire protection. Non-process equipment and services. Distribution packaging.
9. Land
Indirect costs
1. Engineering and supervision. Design and engineering fees, administration, etc.
2. Construction expenses. Temporary constructions, personnel fees
3. Contractor's fees.
4. Contingency.

Working-capital

A plant needs *working-capital* in the first months of the manufacturing process. Typical elements are the costs for start-up, raw materials and other chemicals, work in progress and finished product inventories, accounts receivable from shipments, cash on hand for payroll and other debts. Raw material inventory should ensure approximately one-month production. The inventory of products should be limited to some days. Just-in-time production would mean only the storage of products waiting for shipment.

In preliminary estimations the working-capital may be approximated as a fraction of fixed-capital:

$$F_W = kF_C \tag{15.13}$$

The coefficient k depends on the type of product. It might be taken 0.05 for simple products, 0.15 for petrochemicals, and 0.30 for sophisticated products. In some contractor estimations a coefficient of 0.10 is added for start-up costs. Hence, the following formula can be used for calculating the total capital investment (*TCI*):

$$TCI = F_C + F_W = (1+k)F_C \tag{15.14}$$

The result is that only the fixed-capital needs to be determined more accurately.

15.4.2 Estimation of capital investment

The methods used to estimate the capital investment depends on the degree of accuracy required by the project and on the available data. An accuracy of +/- 5% can be achieved by means of a *detailed-item estimation*, in which equipment costs are computed from detailed sizing and material specifications. This method can be applied at best by using specialised computer package, as ICARUS™.

Hereafter we present a simpler method, used in *preliminary cost estimations*, known as *percentage of delivered-equipment cost* (Peters & Timmerhaus, 1991), or *detailed factorial method* (Sinnott, 1993). The fundamental element is the cost of *basic* equipment identified at the conceptual design stage, which includes the main items as reactors, mixers, separators, heat exchangers, intermediate storage vessels, compressors, pumps, filters, centrifuges, furnaces, dryers, etc.

The cost of an individual equipment item C_i^e may be estimated by means of a factorial relation of type:

$$C_i^e = C_{i,0}^e \times F_{\mathrm{m}} \times F_p \times F_t \tag{15.15}$$

$C_{i,0}^e$ is the reference price of the standard type, usually manufactured from carbon steel and designed for moderate temperatures and pressures. The reference price can be determined by means by means of public correlations or from vendor information. Generalised diagrams for cost estimation are presented in the Appendix *A* for some major equipment items, as vessels, internals of distillation columns, heat exchangers, etc. Note that correction factors account for material (F_m), pressure (F_p), and

temperature (F_t). Table 15.5 presents values that might be considered when specific information is missing.

For example, the cost of a distillation column can be assembled from the cost of elements: vertical cylindrical vessel, plus internals (trays or packing), reboiler, condenser, and reflux drum. The height of the shell can be determined from the number of trays and inter-stage height. The column diameter can be found by hydraulic calculations based on the flooding point. In this way, the volume of the cylindrical part can be easily evaluated. The volume of auxiliary vessels, as drum and reboiler, can be estimated from the residence time, typically of 10 minutes.

The cost of more complex equipment items, as reactors, furnaces, dryers, or filters can be estimated for preliminary design by means of a global quotation called the *capacity ratio method.* The cost is expressed by a power-law correlation as:

$$C_2^e = C_1^e (S_2 / S_1)^n \tag{15.16}$$

C_1^e and C_2^e are the costs at the capacities S_1 and S_2, respectively. The exponent n depends on the type of equipment. It is closed to 0.6 for vessels and heat exchangers, but can rise to 1 or greater for more sophisticated mechanical devices, as centrifuges. The value of 0.6 is accepted as a rough rule for extrapolation.

Table 15.5 Correction factors for material, pressure and temperature

Material	F_m	Pressure, atm	F_P	Temperature, °C	F_T
Carbon steel	1.0	0.005	1.3	-60 : 600	1.3
Bronze	1.05	0.015	1.2	0 - 300	1.0
Aluminium	1.075	0.05	1.1	100 - 200	1.05
Cast steel	1.11	0.5-5	1.0	600	1.1
Stainless steel	1.28-1.5	50	1.1	2000	1.2
Hastelloy C	1.54	200	1.2	2000	1.0
Monel	1.65	400	1.3	2000	1.0
Nickel/Inconel	1.71	400	1.3	1000	1.0
Titanium	2.0	400	1.4	2500	1.0

The central element in fixed-capital estimation is the *Purchased Cost of Equipment* (*PCE*). This can be determined simply by the addition of costs of individual items:

$$PCE = \sum_i C_i^e \tag{15.17}$$

The other cost contributions, either as direct or indirect costs, are expressed by means of factors f_i relative to the purchasing cost of basic equipment. Table 15.6 presents some mean values, ordered by the type of process: fluids, fluids and solids, or solids (Peters & Timerhaus, 1991). The reference year is 1990. The factors F1 to F9 designate *direct costs*, while the factors F10 and F11 regard *indirect costs*. The factors F12 and F13 allow the estimation of contractor fees and unforeseen events. The factors F6 to F9 considers only plant extensions and improvement of an existing site, and not grass-root

investments. In consequence, the method presented is valid for the estimation of capital costs in the area known as *Internal Site Battery Limits* (ISBL). The application of the ratios leads finally that the *TCI* can be obtained simply with the relation:

$$TCI = F_C + F_W = (\sum_i f_i) \times PCE \tag{15.18}$$

The interesting result is that the total cost of the investment can be expressed simply by a constant multiplying the purchasing cost of equipment *PCE*:

$$TCI = K_p \times PCE \tag{15.19}$$

The constant K_p depends on the type of process. Following the figures assumed, K_p is 5.69 for processes involving only fluids, as in petrochemistry and refining, 4.87 for processes with fluid/solid operations, and 4.55 for processes with only solids.

Table 15.6 Ratio factors for estimating fixed-capital investment based on purchasing cost of basic equipment *PCE* (after Peters & Timmerhaus, 1991)

Item	Fluids	Fluids-Solids	Solids
F1 - purchase cost of basic equipment	1.0	1.0	1.0
F2 - equipment installation	0.47	0.39	0.45
F3 - instrumentation and control#	0.18	0.13	0.09
F4 - piping #	0.66	0.31	0.16
F5 - electrical#	0.11	0.10	0.10
F6 - building, including services*	0.18	0.29	0.25
F7 - yard improvement*	0.10	0.10	0.13
F8 - service and utilities facilities*	0.70	0.55	0.40
F9 - land*	0.06	0.06	0.06
Direct costs	3.46×*PCE*	2.93×*PCE*	2.64×*PCE*
F10 - engineering and supervision	0.33	0.32	0.33
F11 - construction expenses	0.41	0.34	0.39
Indirect costs	0.74×*PCE*	0.66×*PCE*	0.72×*PCE*
F12 - contractor fee (~ 5% fixed costs)	0.21	0.18	0.17
F13 - contingency (~ 5% fixed costs)	0.42	0.36	0.34
Fixed-capital	4.83×*PCE*	4.13×*PCE*	3.87×*PCE*
Working-capital (~15% total capital)	0.86	0.74	0.68
Total capital investment	5.69×*PCE*	4.87×*PCE*	4.55×*PCE*

including installation; * omitted for minor extensions or retrofitting

Table 15.7 presents order-of-magnitude investment costs for some chemical process plants at the horizon of 1990. The scaling-rule based on the 0.6 power is reasonable and suggests that large-scale capacities are more advantageous. Small added value chemicals, as sulphuric acid and methanol, need considerable less specific investment compared with higher value products, as polymers. In refining large units are favoured, particularly for FCC, delayed coking and alkylation.

Table 15.7 Typical investments for process plants (after Peters & Timmerhaus, 1991)

Process	Capacity 1000t/year	Fixed-capital Millions $	$/tonne	Power, *n*
Chemical commodities				
Sulphuric acid	100	3	32	0.65
Methanol (steam reforming of methane)	60	13	200	0.60
Ammonia (steam reforming of methane)	100	24	240	0.53
Ethylene (refinery gases)	50	13	260	0.83
Chlorine (electrolysis)	50	28	550	0.45
Acetic acid (carboxylation of methanol)	10	6	650	0.68
Ethylene oxide	50	50	1000	0.78
Glycol (ethylene and chlorine)	5	15	2900	0.75
Polyethylene (high-density)	5	16	3200	0.65
Refining				
Distillation vacuum (65% vap.)	100	19	200	0.70
Distillation atm. (65% vap.)	100	32	320	0.90
Hydrotreating	10	3	320	0.65
Thermal cracking	10	5	500	0.70
FCC	10	16	1600	0.42
Alkylation (H_2SO_4)	10	19	1900	0.60
Coking (delayed)	10	26	2600	0.38
Reforming (catalytic)	10	29	2900	0.60

15.4.3 Cost indexes

The economic data fluctuates strongly. However, over a longer period of time some trends can be characterised by curves or equations. The update of the cost data can be done in a simple manner by means of *cost indexes*, as follows:

Present value = Reference value (actual index/reference index) (15.20)

Two of the most used cost indexes are briefly presented below.

1. *Marshall and Swift* equipment cost.

This index can be used for updating the cost of individual equipment items. Weighting factors take into account the contribution of eight industries, where chemicals have a weight of 48, refining 22, and rubber & plastics 8. The value of 100 is the basis for 1926. This index is updated monthly and published in *Chemical Engineering* magazine. M & S index was 1095 for mid 2002. Table 15.8 gives some values, while Fig. 15.4 gives the trend over the last 13 years, together with linear and quadratic regression equations. R^2 value closer to one indicates a better correlation. Although quadratic regression is statistically better, the linear extrapolation is safer.

Table 15.8 The evolution of Marshall & Swift cost index

Year	1926	1969	1988	1990	1992	1998	2000	2001
M&S	100	280	852	915	943	1061	1098	1095

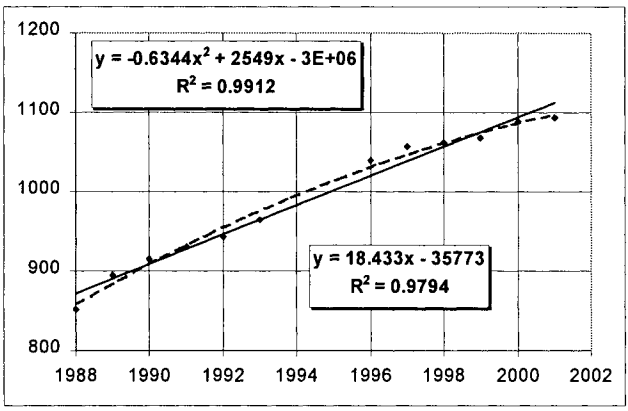

Figure 15.4 The evolution of Marshall & Swift factor in the period 1988-2001

2. *Chemical Engineering Plant* cost.

This index contains information about the construction costs. Four major components are weighted by factors accounting for equipment, installation, engineering and supervision. The equipment is further sub-divided in fabricated equipment, process machinery, pipes and valves, instrumentation and control, pumps and compressors, support, insulation and paint. The reference is 100 in 1957. As its name indicates, this index is updated monthly in the journal *Chemical Engineering*. It can be seen that the cost evolution on longer term is not linear, although on shorter time this could be assumed as a working hypothesis. The correlation equation is given only as an illustration.

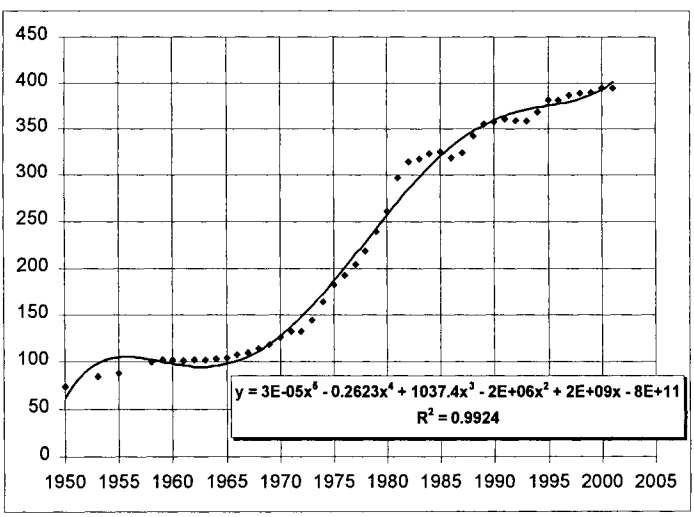

Figure 15.5 Chemical Engineering Plant Cost index from 1950 to 2002 (after Chemical Engineering magazine , Jan. 2002, pp. 62-70)

15.4.4 Capital depreciation

Depreciation is the procedure that takes into account the contribution of the fixed-capital in the cost of the final product. In the same time depreciation is a manner to consider the obsolescence of the working tool. The value of an equipment item starts to decline right from the moment when it has been paid. This phenomenon can be expressed quantitatively by a specific allowance, which is called *depreciation.* Another interpretation is that the depreciation is a manner to transfer the value of the capital into the cost of products or services. For this reason the depreciation should be included in a certain way in the operating costs.

The consideration of depreciation as a cost has several advantages. Firstly, it enables to determine realistically the expenses and the amount of profit that can be saved from taxation. Secondly, it provides an accounting procedure to recover the initial capital investment. Thirdly, it allows for the replacement of the obsolete capital by new investments. In this respect an accelerated depreciation stimulates the renewing of the production tools and can contribute to improve greatly the competitiveness.

On the other hand, the shareholders, who see the value of their property diminishing rapidly, perceive rapid capital depreciation less favourably. Thus for investors a long-term depreciation is more desirable. On the other hand, the authorities could see very fast depreciation rate as an attempt to escape paying taxes. Therefore, the depreciation is subject of legal regulations, but also subject of political decisions. The accounting system has its procedures too. Shortly, depreciation is a complicated issue in practice.

We should also note that maintenance and repairs of capital goods is not normally incorporated in depreciation, but well in the operating costs.

A manufacturing tool or property has a residual value at the end of its service, and might be sold to another user. The money obtained by sale is denoted as the *salvage* value. When the tool cannot be sold but only disposed or dismantled one speaks about the *scrap* value. Because of environmental reasons, the scrap value should be negative. It might be very high, as in the case of nuclear plants or very toxic chemicals.

The procedure for accounting the depreciation follows rules specific to each country. However, from conceptual viewpoint we may consider two categories, linear and accelerated depreciations.

In the *straight-line method*, the depreciable capital is split in equal parts over the estimated service life. The value of depreciation is simply given by:

$$D = (\mathrm{V}_i - V_s)/n \tag{15.21}$$

V_i and V_s are initial and salvage values, respectively, and n is the time of operation. This form of depreciation is preferred in quick estimation computations.

Accelerated depreciation can be obtained by the *declining-balance method.* This consists of applying a fixed-percentage factor f on the property value each year. For example, the depreciation in the first year is $d_1 = V_i f$, in the second year $d_2 = V_1 f$, etc. After n years the salvage values becomes $V_s = V_i(1-f)^n$, from which we get for the fixed-percentage factor the relation:

$$f = (1 - V_s / V_i)^{1/n} \tag{15.22}$$

The application of the declining method could lead to depreciation rates that might be seen too high by the legal authority. A method that avoids this drawback, called *double-declining method*, consists of putting f twice the straight-line depreciation factor. In this way a sharper depreciation in the early years of service occurs. This method might be useful to account for the downgrading of high-tech equipment, as automation and computer hardware.

Depreciation of capital falls under the authority of governmental tax agencies. The assets are categorised in classes of different lifetimes, as for example 3, 5, 7, 10, 15 and 20 years. The depreciation factors are adapted to reflect the most rational replacement policy from taxation viewpoint. As illustration, in USA the tax reform act from 1986 defined a Modified Accelerated Cost Recovery System (MACRS). Process equipment falls in 5-year class, as shown in the following table:

Year	1	2	3	4	5	6
fj	0.20	0.32	0.192	0.1152	0.1152	0.0576

Half years are considered at the beginning and the end of the project. The depreciation is the strongest in the first three years, when 70% of capital is written-off.

EXAMPLE 15.4 Depreciation costs

A piece of equipment has a purchase value of 50000 €. After a service of 10 years, it could be sold at a present value of 5000 €. Determine the book value after 5 years of service by straight-line, declining balance and double declining methods.

Solution.

a. By straight-line the annual depreciation is: d=(50000 – 5000)/10 = 4500 €/year. After five years the asset value is V_a = 50000-5×4500=22500 €.

b. By declining-balance method the fixed-percentage factor is: f=1-(5000/50000)$^{1/10}$= 0.2589. The book value after five years is V_a = 50000×(1-0.2589)^5=11178 €, much lower than previously.

c. By the double-declining method the linear depreciation factor is doubled. Thus f=0.2. The book value after five years becomes $V_a = 50000 \times (1-0.2)^5 = 16383$ €. This value is somewhat intermediate between the first two.

15.5 OPERATING COSTS

The fees necessary to manufacture and deliver the product give the second big category of costs, called here *operating costs*. Similar denomination is 'total product costs' (Peters and Timmerhaus, 1991), or manufacturing costs in other books. There are different levels of accuracy in estimating the operation costs.

15.5.1 Elements of operating costs

The operating costs may be divided in two main parts: manufacturing costs and general expenses. *Manufacturing costs* can be broken further into *direct production costs*, *fixed charges*, and *plant overhead* costs. Sometimes the term operating costs designates only manufacturing costs. *General expenses* include administration, distribution and marketing, research and development, as well as financial charges.

I. Manufacturing costs

A. Direct costs

1. Raw materials.
2. Operating labour.
3. Direct supervisory and clerical labour.
4. Utilities.
5. Maintenance.
6. Operating supplies.
7. Laboratory charges.
8. Patents and royalties.

B. Fixed costs

1. Depreciation.
2. Local taxes.
3. Insurance.
4. Rent.

C. Plant overhead costs: Safety and protection, Plant and payroll overhead, Control laboratory, Packaging, Storage facilities.

II. General expenses (supplementary costs)

A. Administrative costs

1. Executive salaries and clerical wages
2. Engineering and legal costs
3. Communications.
4. Office maintenance.

B. Marketing, distribution and selling

1. Sales office.
2. Marketing and advertising.
3. Shipment.

C. Research and Development

D. Financial interests

More details about individual items can be found in specialised works. Here we will discuss only some key positions.

Raw materials could represent up to 50-60% of the total operation costs. The cost of raw materials is time variable and highly uncertain. Sources of prices are specialised journals as *Chemical Market Reporter*, and more recently on Internet sites. Freight and transportation fees should be included.

Utilities (steam, water, refrigerants, natural gas, liquid fuel, electricity, etc.) can be determined accurately from the material and energy balance obtained by simulation. The heat integration study can estimate the lowest energetic consumption. Then the real consumption can be determined to allow a margin for operation, typically by using an oversizing of 20-25%. Electricity consumption must be included in the case of compressors, blowers, high pressure pumps, vacuum systems, very viscous liquids, pneumatic transportation, mixing vessels, and in general for power intensive operations. The prices of utilities depend heavily on the country, as well on the facilities offered by the industrial site. Combined heat and power production could offer much lower prices. As a rough approximation, the costs of utilities might represent 10 to 20% of the total operating costs. Appendix B contains more information about utility prices.

Operating labour designates the cost of human operators involved in plant operation. Chemical industry employed many people in 1960-70, but nowadays much less because of automation and supervision by computers. Estimation from old sources is obsolete. At best, the manning of a process may be estimated by inspecting the flowsheet, and paying attention to different operations, as reaction, separation, filtration, waste water treatment, etc. Table 15.9 presents some guidelines. The working time is 40 hr/week. In practice due to different events, illness, vacation, training, etc., five shifts should be provided for each operator position.

Wages are difficult to estimate. The situation is very variable from country to country, particularly regarding the special allowances for employees, but also the employer contributions to social security. The reference for social contribution is often the minimum salary. Table 15.10 gives some data for European countries. The computation should also take into account different allowances, as well as social security charges paid by the company.

Table 15.9 Direct labour requirements

Unit operation	Worker/unit/shift
Reactor: batch, continuous	1, ½
Distillation columns	1/3-1/2
Dryers: spray, rotary	1, ½
Filter (vacuum)	¼
Centrifuge	1/4-1/2
Evaporator	¼

Table 15.10 Minimum and median monthly salary in some European countries#

Country	Minimum salary, €	Average salary, €	Ratio
Netherlands	1057	2157	0.49
France	1030	1716	0.60
Spain	414	1150	0.36
UK	922	2316	0.398

OECD sources, basis 01/01/1999

15.5.2 Estimation of operating costs

Table 15.11 presents data for the estimation of operating costs based on the above decomposition. The basis is the material and heat balance from flowsheeting, as well as the operating labour. This checklist can be used to compute the operating costs for profit and cash flow calculation. Note that the depreciation charge should be excluded, if it is accounted separately.

Table 15.11 Estimation of the total operating costs (after Peters & Timmerhaus, 1991)

Costs	Typical values
Manufacturing costs = direct costs + fixed charges + plant overhead costs (MC)	
1. Direct costs (DC)	
Raw materials	From material balance (10-50%)TOC
Operating labour (OL)	From manpower (10-20% TOC)
Direct Supervisory	20% OL
Utilities	From energy balance (10-20% TOC)
Maintenance and repairs	10% F_C
Operating supplies	1 % F_C (6%OL)
Laboratory charges	10-20% OL
Patents and royalties	0-6% TOC
Total DC	~ 60% TOC
2. Fixed costs (FC)	
Depreciation#	10% F_C for equipment, 2-3% F_C for buildings
Local taxes	1-4% F_C
Insurance	0.5-1% F_C
Rent	8-12% from rented land and buildings
Total FC	~ 10-20% TOC
3. Plant overhead (OVHD)	50-70 % from operating labour or 5-15 % TOC It includes general and payroll overhead, medical and safety services, restaurant, lab, storage, etc.
Total manufacturing costs = DC+FC+OVHD	80-90% TOC

General expenses (SARE)##	
Administrative Costs	15% OL, or 2-6 % TOC (executive salaries, clerical wages, legal fees, office supplies, communications)
Distribution and selling	2-20% TOC
Research and Development	5% TOC
Financial interests	0-10 % F_C
SARE	10-20% TOC or 2.5% from Revenue
Total operating costs = MC+SARE	TOC
Product cost = Annual operating cost/Annual production rate	

Do not include in operating costs if accounted separately in the cash flow
Sales, Administration, Research and Engineering

15.5.3 Simplified model for estimating operating costs

A simplified cost model can be deducted based on the breakdown of costs shown in Table 15.11. The total operating cost TOC can be expressed as the sum of manufacturing costs (*MC*) and general expenses (*SARE*):

$$TOC=MC+SARE \tag{15.23}$$

The first term is calculated as the contribution of direct costs (*DC*), fixed costs (*FC*) and plant overhead (*OVHD*) as

$$MC=DC+FC+OVHD \tag{15.24}$$

Direct costs are composed from the costs of raw materials (*RM*), utilities (*Ut*), operating labour (*OL*), direct supervision and clerical labour (*Ds*), maintenance and repairs (*Mt*), operating supplies (*Os*), laboratory charges (*Lab*), patents and royalties. We may neglect the last term. By using the factors in Table 15.10 we obtain:

$$DC = RM+Ut+OL+0.2OL+0.1F_C+0.01F_C+0.15OL = RM+Ut+1.35OL+0.11F_C \tag{15.25}$$

Fixed costs are given by depreciation (excluded in this case), local taxes (ignored), insurance and rent. For the last two terms we take the approximation

$$FC = 0.03F_C \tag{15.26}$$

The plant overhead include management and payroll overhead that cam be related with the operating power *OL*, as well as safety and maintenance fees that can be related with the fixed-capital. For the first we may take 60% from the charges involved in direct costs, while for the second 2.5% from fixed-capital. So we have approximately

$$OVHD=0.81OL+0.025F_C \tag{15.27}$$

SARE costs can be approximated by 2.5% from the revenue (*S*). Summing the terms in equation 15.23 leads to

$$TOC=RM+Ut+2.16OL+0.165F_C+ 0.025S \tag{15.28}$$

The cost of operating labour can be further refined taking into account that 4.5 shifts are needed for an operator position. The average salary of a Dutch worker in year 2000 can

be found from the Table 15.10 by considering 12 months plus one month extra allowance, and 2.5% annual increase 2000/1999. One gets a gross salary of 28750 €, or 129340 € for an operator position. The labour cost can be approximated by

$$OL=28750\times\text{Operators (€/yr)} \tag{15.29}$$

For even simpler calculations the estimation of the labour costs could be eliminated by assuming 10% of TOC. The relation (15.28) becomes:

$$TOC=1.11(RM+Ut)+0.183F_C+0.028S \tag{15.30}$$

It is clear that the accuracy of the simplified equations is limited by the uncertainty in the numerical values of factors assumed for different costs.

15.6 PROFITABILITY ANALYSIS

Before entering into the subject it is worthy to review the definition of the terms in the computation of cash flow and profitability measures (Table 15.12). The profitability measures should be calculated on after-tax basis (net values) to ensure a consistent comparison. A typical tax rate is 35%.

The revenue is the total income from sales, or the total savings. Gross profit is revenue minus cash expenses without accounting for depreciation. All expenses are the cash expenses adding the depreciation. The net profit before tax is the revenue minus all expenses. Income taxes are paid on the net profit. Accordingly, the cash flow has to reintroduce the depreciation. This is done in practice by an internal transfer of value in the accounting system. The net cash flow is the net profit after tax plus the depreciation.

Thus, again the depreciation plays an important role in cash flow calculation. Presenting the results in terms of gross profit without depreciation gives the impression of a better profit margin. On the other hand considering higher depreciation rate allows more tax saving and larger cash flow. It can be shown that the profitability is maximised when the depreciation can be done quickly.

Table 15.12 Definition of elements entering in a profitability analysis

Revenue = Total income (or total savings) Gross profit = Revenue – Cash expenses (w/o depreciation) All expenses = Cash expenses + Depreciation Income tax = (Revenue - All expenses) ×tax
Net profit before tax = Revenue – All expenses
Net profit after tax = Revenue – All expenses – Income tax = (Revenue – All expenses)×(1-tax rate)
Cash flow = Net profit + Depreciation = Revenue – Cash expenses – Income tax Cash flow = (Revenue – All expenses) × (1-tax rate) + Depreciation Cash flow = (Revenue - Cash expences) × (1-tax rate) + Depreciation×tax rate= = Gross profit + Depreciation×tax rate

15.6.1 Traditional profitability indices

Rate of Return measures

Rate of Return on Investment (*ROI*) is defined as the annual profit generated by a unit of invested capital, as expressed by the relation:

$$\%\ ROI = (\text{Annual Net Profit/Invested Capital}) \times 100 \tag{15.31}$$

The terms can be expressed in different ways, which might create confusion. The annual net profit may be considered before or after tax. Sometimes the net profit in the third year after start-up is used. The invested capital may be referred to the original total capital investment, fixed-capital, depreciated investment, average investment, or something else. The operating costs could include the depreciation in the fixed costs.

Sometimes a minimum profit on capital is required before the investment becomes worthwhile. The minimum profit is included as a fictitious expense. The return should be larger than zero to make the investment attractive.

If fixed-capital is taken as reference the rate of return of the fixed-capital is:

$$ROI_C = \frac{NP}{S}.\frac{S}{F_C} = (\text{Earnings as percentage sales}) \times (\text{Turnover ratio}) \tag{15.32}$$

Turnover ratio $= S / F_c$ represent the ratio of gross sales to the fixed-capital investment. The reciprocal $CR = F_c / S$ is called *capital ratio*. For chemical industries the turnover ratio is about one. Values up to 5 are common for very efficient processes. Reducing both fixed and working-capital can increase the turnover ratio. More productive fixed-capital can be obtained by more compact flowsheet design and higher productivity of equipment by process intensification. Lower working-capital implies reducing inventories by Computer Integrated Manufacturing and 'Just-In-Time' delivery.

EXAMPLE 15.5 Rate of Return on Investment

A project requires fixed-capital of 850 k€ and working-capital of 150 k€. It is expected that the annual income will be of 900 k€ and the expenses (including depreciation) of 600 k€. Consider a tax rate of 35%. Calculate the rate of return before and after taxes. How *ROI* would change when a minimum annual return on investment before taxes of 15% is required?

Solution.

a. The total capital is 850 + 150 = 1000 k€

The profit before taxes is 900 – 600 = 300 k€/year.

The rate of return before taxes is given by ROI_{bt} = 300 /1000 = 30%.

b. After taxes the net profit is 300×(1-0.35) = 195 k€/year .

The rate of return after tax becomes ROI_{at} = 195 /1000 = 19.5%.

It can be noticed that between the two modes of *ROI* there is a considerably difference.

c. The minimum profit required is 0.15×1000 = 150 k€/year.

The expenses are 600 + 150 = 750 k€/year. The profit before taxes is 900-750=150 k€, and after taxes 150×(1-0.35) = 97.5 k€/year. We get for the return rate of investment 97.5/1000 = 9.75%. This value shows that the investment could bring much more than 15% required, and therefore is very attractive.

Payback time

Payback time (*PBT*) is defined as the minimum length of time theoretically necessary to recover the initial capital investment based on the average profit and average depreciation. The average profit is calculated from income minus operating costs excluding depreciation. The initial capital investment is generally the original depreciable fixed-capital. In a first approximation the effect of time-value of money may be neglected, so that computation can be done as follows:

$$PBT' = \text{Fixed-capital} / (\text{avg. profit} + \text{avg. depreciation}) \quad (15.33)$$

By another method the objective of a minimum rate of return could be considered. A minimum interest rate is chosen, for example equal with the banking interest. The annual cash flow is corrected for the present value. The calculation formula becomes:

$$PBT'' = (\text{Depreciable fixed-capital} + \text{interests on total capital investment}) / (\text{profit} + \text{depreciation})_{ct.\ annuity} \quad (15.34)$$

The payback time including a target for the rate of return will be longer, but more advantageous for projects making most of the profit in the early years.

The payback time can be identified more accurately on a cash flow diagram as the time interval from the plant first production to the break-even point. By definition, this index cannot measure the performance of a project after paying the initial investment. For large plants, as in petrochemistry and refining, the payback time should be between seven and ten years. This measure is much smaller for high-tech processes, as in speciality chemicals biotechnologies. For small-scale projects, as revamping or energy saving, typical values for the payback time are 2 to 3 years, sometimes shorter.

EXAMPLE 15.6 Payback time

An energy integration project may save 500 k€/year in utility, but requires investment in new heat exchangers of 1000 k€. The project life is 10 years. Calculate the payback time with investment financed by internal resources, and when the capital is borrowed at 10% interest rate.

Solution.

a. With linear depreciation the annual charge is 1000/10 = 100 k€/year. Payback time excluding interests is *PBT'*=1000/(500+100)=1.66 years.

b. The capital is reimbursed by annuity. Each year a factor of $i(1+i)''/[(1+i)''-1]$ is accounted for depreciation. From Table 15.2 an factor of 0.1627 is found. The annuity is 0.1627×1000=162.7 k€/year. The actual money paid is 1627 k€. The payback time with payment of interests becomes: $PBT'' = 1627 / (500 + 162.7) = 2.46$ years.
Although gives a somewhat longer payback time the second solution is viable.

15.6.2 Simplified profitability analysis

The simplified cost models developed for total capital investment and operating costs allows a quick analysis of profitability. For instance, the gross profit before taxes can be obtained by subtracting total operating costs *TOC* (Eq. 15.30) from sales *S*:

$$GP = S - TOC = 0.972S - 1.11(RM + Ut) - 0.183F_C \tag{15.35}$$

The equation 15.35 can be further simplified by using the following ratios:

$$\alpha = \frac{Ut}{TOC} \quad \beta = \frac{F_c}{S} \quad \gamma = \frac{RM}{S} \quad \delta = \frac{D}{F_C} \tag{15.36}$$

The factors defined before have the following significance:
α: maximum fraction of utilities from the total operating costs,
β: capital ratio, or reciprocal of turnover ratio (see equation 15.32),
γ: raw material to sales ratio,
d: depreciation charge.
From the equation (15.35)-(15.36) we obtain:

$$\frac{GP}{S} = \frac{0.972 - 1.11\alpha - 1.11\gamma - 0.183\beta}{1 - 1.11\alpha} \tag{15.37}$$

The left member of the above equation is the gross profit reported to sales, also designated by *profit margin*. Let us consider some typical values, as $\alpha = 0.1$, $\beta = 1$, $\gamma = 0.40$. For these values we obtain $GP/S = 0.3092$ or 30.92%.

The ratio between the prices of selling products and of raw materials is a subject of debate in an economic analysis. It would be desirable to have an idea about the minimum feasible ratio for given operating costs. A simple measure is the payback time. By applying the Eq. 15.33 we get:

$$PBT = \frac{TCI}{PB + D} = \frac{(1+k)F_c}{PB + \delta F_c} \tag{15.38}$$

We may consider k=1.25 that includes working capital and plant start-up expenses. δ is the capital charge depending on the depreciation policy. Dividing by S and denoting PBT=τ leads to the equation:

$$\tau = \frac{1.25\beta}{\frac{GP}{S} + \delta\beta} = \frac{1.25\beta}{\frac{0.972 - 1.11\alpha - 1.11\gamma - 0.183\beta}{1 - 1.11\alpha} + \delta\beta} \tag{15.39}$$

and finally:

$$\gamma = 0.8757 - \alpha - 0.165\beta - (0.9 - \alpha)\beta\left(\frac{1.25}{\tau} - \delta\right) \tag{15.40}$$

Feasible ratios sales to raw materials can be explored for different payback periods. Selecting $\alpha = 0.1$ and $\beta = 1$ leads to the results in Table 15.13.

Table 15.13 Price ratio of products to raw materials

τ	2	3	4	5	6
$S/RM=1/\gamma$	5.24	2.8	2.27	2.04	1.91

It may be seen that payback times shorter than three years requires *S/RM* ratios higher than three, while for payback times greater than five, as for large petrochemical or refinery plants, *S/RM* ratios less than two can be obtained. Equation (15.10) indicates also that the minimum ratio *S/RM* can be reduced by increasing the sales at fixed-capital (raising the turnover ratio) or by diminishing other variables costs, as the cost of utilities.

15.6.3 Modern profitability measures

The representation of the cash flow over the project's lifecycle, as depicted in Fig. 15.1, gives a more convenient image of the process profitability as the static measures described before. In the first stage - design, plant erection and start-up - the project creates the basis for the future earnings, but accumulates debts. In the second stage, operation, the plant starts to supply products and receive income. The revenues must overcome the expenses and deliver an acceptable profit. A first objective is to payback the initial investment. The second one is to obtain a good profit, which in practice means a higher rate of return, better if the money was invested in another operation, say in a saving account or in low-risk shares.

Thus, a more modern concept of the profitability analysis should consider the project as a source of profit as any other business. Capital and operating costs are only intermediate figures as inputs of a profitability analysis.

Net Present Value

By net present value analysis the cash flow CF_n earned in different years n is brought to the present value $CF_{n,0}$ by using a compound-interest formula:

$$CF_{n,0} = \frac{CF_n}{(1+i)^n} \tag{15.41}$$

Besides the current expenses, the cash flow must pay the total capital investment *TCI*. If the project lifetime is *T* and the interest rate is *i*, the cumulative cash flow expressed as *net present value* (*NPV*) will be:

$$NPV = \sum_{n=1}^{n=T} \frac{CF_n}{(1+i)^n} - TCI \tag{15.42}$$

The interest rate *i* in Eq. 15.42 can be selected as representative for the company, close to similar projects, or imposed as minimum acceptable. From profitability point of view the objective of a project is to maximise the net present value *NPV*. This implies not only recovering the initial investment, but also generating sufficient added value after the breakeven point. In this way *NPV* appears as a measure of the total value that could be achieved over a longer time. However, the analysis depends on the assumed value of the interest rate. This limitation can be removed by reference to the maximum achievable performance, the discounted rate of return.

A profitable project should realise a positive *NPV* for a sufficient high interest rate, say 10%. When several projects are compared, the best is the one bringing the highest *NPV*. If *NPV* is negative, the economic analysis should review the elements of the cash flow and identify saving measures. *NPV* evolution can also indicate when the project does not bring sufficient value, and therefore the plant should be retrofitted or stopped.

15.6.4 Discounted Cash Flow Rate of Return

Discounted cash flow rate of return (*DCFRR*) is a measure of the maximum interest rate that a project could afford just by paying the total capital investment at the end of its life. Other synonyms are used, the most popular being the Internal Rate of Return (*IRR*)[2].

Mathematically, *DCFRR* can be determined as the interest rate for which the Net Present Value at the end of the project lifetime becomes zero:

$$NPV = \sum_{n=1}^{n=T} \frac{CF_n}{(1+r)^n} - TCI = 0 \tag{15.43}$$

In equation (15.43) *r* denotes *DCFFR*. This may be found by trial-and-error, easy to do with a spreadsheet. Higher *DCFRR* means more profitable project.

Intuitively, *DCFRR* might be seen equivalent with the maximum interest rate of money borrowed to finance the project under the condition that the net cumulative cash flow over the project lifetime would be just sufficient to pay all principal and accumulated interests. In order to obtain consistent comparison, it is recommended to use after-tax values corrected for inflation. Hence, *DCFRR* is a synthetic measure of process profitability.

---

2 Other similar methods or names are Profitability Index, Interest Rate of Return, True Rate of Return, Investor's Rate of Return

Capitalised costs

Reduction of capital costs is a strong incentive in design practice. When competitive projects have similar *NPV* and *DCFRR*, the projects having the lowest capital investment should be preferred. This measure is useful in conceptual design when competitive processes might have similar flowsheets, but with alternatives for some key items. A typical example is the chemical reactor, a heavy investment normally subcontracted, for which different technology suppliers could be considered.

Capitalised costs represent the amount of money that should be available for the initial capital investment plus the funds necessary to generate sufficient interest accumulation for the perpetual replacement of the equipment. If the operating costs do not vary, the alternative giving the lowest capitalised costs will be selected.

The computation of capitalised costs can follow the pattern of annuity payment. The following equation is obtained:

$$K = C_V + \frac{C_R}{(1+i)^n - 1} = \frac{C_R(1+i)^n}{(1+i)^n - 1} + V_s \tag{15.44}$$

K is the capitalised costs, C_V the original cost of equipment, C_R the replacement cost, and V_S the salvage value. Note that $(1+i)^n/[(1+i)^n - 1]$ is the capitalised-cost factor.

15.6.5 Summary of profitability measures

It is worthwhile to review the advantages and shortcomings of the controllability measures presented before, and to make some comments and recommendations.

The fixed-capital investment is an (rough) indication of the technical performance of the process design. Comparison with competitive and similar processes is necessary. Lower capital investment is a definite advantage, but it does not in itself a guarantee for profitability in operation.

Rate of return indices gives an indication over the performance of an investment. It shows the fraction of the invested capital that can be recovered by the annual profit. Care should be taken in the definition of terms, as the profit before or after tax, including or excluding depreciation. The disadvantage is that it is only a static measure, at a given time or in average conditions, but it says nothing about the time evolution of profitability. This index can be used for assessing small projects.

Payback time shows the shortest period for capital recovery. It has the same disadvantage of rate of return index, giving no information about later years. For small projects payback period bellow three years is typical.

The indices based on discounted cash flow, as *NPV* and *DCFRR*, are more suitable for assessing the long-term profitability, as in the case of grass-root plants or significant retrofitting. However, the assessment will be not better than the accuracy of forecasting the cash flow. However, since the cash flows for the later years are highly discounted, the overall figures will be less affected by longer-term uncertainty. *NPV* has the advantage of showing clearly the real profit in each year, and when the project should be stopped. *DCFRR* is a synthetic measure of the maximum profitability, but has the disadvantage of ignoring the capital and cash flows as amounts and history.

The influence of different factors subject to uncertainty can be assessed by a *sensitivity analysis*. The most probable values are attributed to the base case. Then alternatives are generated by allowing errors in each factor, as for example variations in prices for raw materials, products or utilities, or different interest rates. The discounted cash flow analysis can determine which are the cost elements having the strongest influence on the *NPV* and *DCFRR*, and which are unimportant. This type of analysis is relatively simple to be done with a spreadsheet. The formulation of the problem in term of ratios can bring useful insights.

Risk analysis methods should be also considered in long-term projects or/and involving a large amount of capital. The forecast of cash flows can make use of statistics. Details can be found in Holland & Wilkinson (Perry, 1997).

EXAMPLE 15.7 Economic evaluation of a project

A feasibility study estimated a capital of 100 million €, from which 10% working-capital and 90% fixed-capital spread over three years as follows: 30, 50, and 10 million €. The plant lifetime is 15 years. Table 15.2 gives the forecast of revenue and operating costs (excluding depreciation) in millions €. The revenue in the last year includes the salvage of capital. Consider a tax rate of 35%. Analyse the profitability of this project.

Solution.

Table 15.14 presents the computations done with a spreadsheet. Revenue and operation costs (excluding depreciation) are given in columns two and three. The depreciation is assumed straight-line, in this case 90/15 = 6 mil. €/year. The gross profit *GP* is obtained by subtracting operation costs from revenue. The net profit *NP-bt* (before tax) is the gross profit minus depreciation. The net profit *NP-at* (after tax) is calculated by applying the factor 0.65 on the *NP-bt*. The cash flow is obtained from the net profit after tax by adding the depreciation. Column eight presents the cumulated cash flow, plotted in Fig. 15.14. The break-even point is reached after three years.

Column nine presents the discounted cash flow (present value) for an interest rate of 15%. The highest profit is reached in the third year, but it declines rapidly later. Already after nine years the linear trend in cash flow starts to fall. Retrofitting the plant would be rational after 12 years, or it should be closed.

The last two columns show how to determine *DCFRR*. By trial-and error it is found *DCFRR* of 32.1%. This is the maximum interest rate that this project could deliver, a rather high figure that predicts that the project would be very profitable, namely because of the high profit in the early years. The profitability indices are:

- Rate of return. The annual net profit after tax is the average of the column six, respectively 23.4 mil €, so that we have: ROI=23.4/(90+10) = 0.2346 or 23.4%.
- Payback time. The net profit before tax is in average 36 mil. €. PBT = 90/(36+6) = 2.14 years. With the net profit the payback time is PBT=100/(23.4+6)=3.06 years, a value close to that determined from the cash flow diagram.

Table 15.14 Profitability analysis

1	2	3	4	5	6	7	8	9	10	11	12
Year	Rev.	Op. Costs	*GP*	*NP-bt*	*NP-at*	*CF*	*CCF*	*PV* 15%	*NPV* 15%	*PV* 32.1%	*NPV* 32.1%
-3							0		0		
-2						-30	-30		-30		
-1						-50	-80		-80		
0						-20	-100		-100		-100
1	70	40	30	24	15.6	21.6	-78.4	18.78	-81.22	16.35	-83.65
2	100	60	40	34	22.1	28.1	-50.3	21.25	-59.97	16.10	-67.55
3	120	60	60	54	35.1	41.1	-9.2	27.02	-32.95	17.83	-49.72
4	130	70	60	54	35.1	41.1	31.9	23.50	-9.45	13.50	-36.22
5	140	80	60	54	35.1	41.1	73	20.43	10.99	10.22	-26.00
6	150	90	60	54	35.1	41.1	114.1	17.77	28.76	7.73	-18.27
7	160	90	70	64	41.6	47.6	161.7	17.89	46.65	6.78	-11.49
8	150	90	60	54	35.1	41.1	202.8	13.44	60.09	4.43	-7.06
9	140	90	50	44	28.6	34.6	237.4	9.84	69.92	2.82	-4.23
10	130	90	40	34	22.1	28.1	265.5	6.95	76.87	1.74	-2.49
11	120	90	30	24	15.6	21.6	287.1	4.64	81.51	1.01	-1.48
12	120	90	30	24	15.6	21.6	308.7	4.04	85.55	0.76	-0.72
13	110	90	20	14	9.1	15.1	323.8	2.45	88.00	0.40	-0.31
14	100	90	10	4	2.6	8.6	332.4	1.22	89.22	0.17	-0.14
15	100	90	10	4	2.6	8.6	341	1.06	90.27	0.13	-0.01

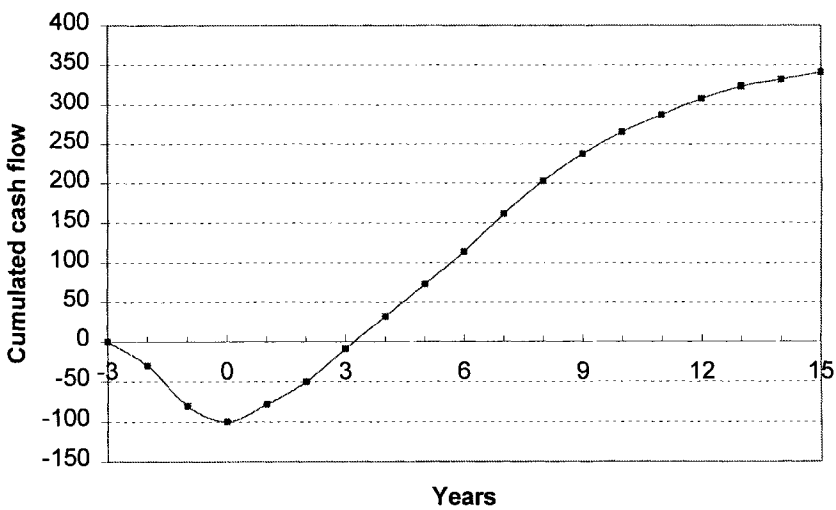

Figure 15.6 Cash flow forecast over the plant lifetime

15.7 FURTHER READING

A thorough presentation of fundamentals of an economic analysis for process design can be found in the classical book of Peters and Timmerhaus (1991). In addition this book contains detailed information about the cost of chemical equipment. A concise but useful treatment can be found in Coulson & Richardson volume 6 (1993). The part on economics in Douglas (1987) is particularly well written from the viewpoint of a designer. The chapter written by Holland & Wilkinson for Perry's Handbook 7th edition (1997) contains an extended description of the modern concepts of profitability, a comprehensive estimation of manufacturing and fixed-capital costs, as well as an introduction in the accounting and cost control concepts. The economic evaluation of projects from the perspective of the Institution of Chemical Engineers-UK may be found in Allen (1991).

15.8 REFERENCES

Allen D. H., Economic Evaluation of Projects, 1991, Institution of Chemical Engineers
Douglas, J. M., Conceptual Design of Chemical Processes, 1988, McGraw-Hill
Holland, F. A., Wilkinson, J. K., Process Economics, 1997, in Perry's Chemical Engineers Handbook, 7th edition, McGraw-Hill
Guthrie, K. M., Data and Techniques for Preliminary Cost Estimation, March 1964, Chemical Engineering, 76, 114-142
Guthrie, K. M., 1974, Process Plant Estimating, Estimation and Control, Craftsman
Haimes, Y., 1998, Risk Modelling, Assessment and Management, Wiley
Peters M. S., Timmerhaus, K. D., 1991, Plant Design and Economics For Chemical Engineers, 4th edition, McGraw-Hill
Sinnott, R. K., in Coulson & Richardson's Chemical Engineering, vol. 6, second edition, 1993

Chapter 16

EQUIPMENT SELECTION AND DESIGN

16.1 Reactors
16.1.1 Flow reactors
16.1.2 Stirred tank reactors
16.1.3 Mechanical design of vessels

16.2 Separators
16.2.1 Distillation columns
16.2.2 Absorption columns
16.2.3 Sizing separation columns
16.2.4 Extraction equipment
16.2.5 Membrane separation processes

16.3 Heat exchangers design
16.3.1 Heat transfer fluids
16.3.2 Heat transfer coefficients
16.3.3 Pressure drop calculation
16.3.4 Temperature driving force
16.3.5 Shell-and-tubes heat exchangers
16.3.6 Air cooled heat exchangers
16.3.7 Compact heat exchangers

16.4 Transport of fluids
16.4.1 Compressors
16.4.2 Pumps

16.5 References

The use of simulators has changed dramatically the design of process equipment. Traditional short-cut methods have been replaced by computer methods that can be executed in a fraction of second on PC's. For equipment design a large number of specialised packages are available either as stand alone or interfaced with the flowsheeting systems. However, the designer should be aware at any time about the modelling and sizing principles, and be capable to diagnose pitfalls and shortcomings. These are also situations in which the designer should be able to get quick but reliable estimations of equipment sizing with little data and without simulator.

This chapter is limited to key process equipment regarding chemical reactors, separators and transport of fluids, which cover the largest part of a design project. More material can be found in general purpose works as Perry (1997), Coulson & Richardson vol. 6 (Sinnot, 1994), Ullmann's Encyclopedia (1993), or in design books mentioned as references.

16.1 REACTORS

Reactor selection and computational methods have been discussed in Chapter 8. The design of chemical reactors consists of the following steps:

- Selection of the type of reactor.
- Volume calculation based on reaction kinetics or on known residence time.
- Geometrical arrangement of internals in a convenient manner for hydrodynamics.
- Hydraulic calculations such to match allowable pressure drop, velocity of fluids, and residence time.

16.1.1 Flow reactors

In shortcut methods the reactor volume may be approximated from information about the residence time, expressed either as LHSV, GHSV or WHSV (see section 8.3.1). Technological constraints, as allowable pressure drop, heat and mass transfer, catalyst attrition, etc., are other elements that lead to the final geometric characteristics. An important design parameter is the fluid superficial velocity (phase volumetric flow divided by cross-area). Recommended values are:

- Gas-phase reactions: 30-50 m/s (low pressures), 10-20 m/s (high pressures);
- Gas over catalytic bed: 0.10-0.30 m/s depending on catalyst size, allowable pressure drop, attrition resistance of catalyst pallets;
- Fluid bed: usually twice the minimum fluidisation velocity;
- Gas in absorption columns: 1 m/s in sieve or packing tray
- Gas in trickle bed reactors: 0.10-0.20 cm/s;
- Liquids or supercritical fluids in tubular reactors: 0.5-3 m/s;
- Liquid in trickle bed reactors: > 1 cm/s.

Table 16.1 gives some examples of residence time and/or space velocities. A larger list compiled by Walas can be found in Perry (1997). Useful information about different processes and sizing methods are given in Ullmann's Encyclopedia.

Table 16.1 Residence times in industrial reactors (adapted from Perry, 1997)

Process	Type	Phase	Catalyst	T, °C	P, atm	Residence time or space velocity
Acrylonitrile (air, propylene, ammonia)	FL[1]	G	Solid	400	1	4-5 s
Alkylation (C4)	CSTR[2]	L	H_2SO_4	5-10	2-3	5-40
Benzene (toluene)	TU[3]	G	None	<740	38	48 s
Butadiene	FB[4]	G	Solid	750	1	0.1-1
Caprolactam	CSTR	L	Homog.	80-110	1	0.25-1 h
Cracking, fluid catalytic	Riser	G	Solid	530	2-3	2-4 s
Hydrocraking (gas oils)	FB	LG	Solid	350-420	100-150	1-2 LHSV
Cyclohexane (benzene)	FB	G	Solid	150-250	25-50	0.7-2
Cyclohexanone (cyclohexanol)	MT[5]	G	Solid	250-350	1	4-12
Ethylene	TU	G	None	550-750	2-7	0.5-3 s
Etylene chlohydrine	CSTR	LG	None	30-40	3-10	0.5-5 min
Hydrogene (methane, steam)	MT	G	Solid	790	13	5.4 s
Methanol (CO, H_2)	FB	G	Solid	350-400	340	5000 GHSV
Nitrobenzene	CSTR	L	Homog.	45-95	1	30-40 min
Phtalic anhydride (o-xylene, air)	MT	G	Solid	350	1	1.5
Styrene (etylbenzene)	MT	G	Solid	600-650	1	7500 GHSV
Vinyl chloride (ethylene, Cl_2)	FL	G	None	450-550	2	0.5-5 s
Vinyl acetate (ethylene+CO)	TO[6]	LG	Solid	130	30	1 h liq., 10 s gas

1 - Fluid bed; 2 - Continuous stirred tank reactor; 3 – Tubular; 4 – Fixed bed; 5 – Multi-tubular; 6 – Tower reactor

Consider the case of a catalytic reactor characterised by a recommended value of WHSV to achieve a commercial conversion. By the definition we have:

$$WHSV = G_0 / W_c \tag{16.1}$$

where G_0 is the total mass flow rate at the reactor inlet, and W_c the amount of catalyst. The mass of catalyst can be easily calculated, and further the reaction volume as

$$V_R = G_0 / (\rho_c \times WHSV) \tag{16.2}$$

where ρ_c is the catalyst bulk density. The geometry of the reaction volume should be arranged in a manner compatible with the hydrodynamics. Assuming an inlet gas velocity u the geometric characteristics as cross-area A_T, diameter D and length L_R can be calculated as:

$$A_T = G_0 / \rho_G u\,,\ D = \sqrt{4A_T/\pi} \text{ and } L_R = V_R / A_T \tag{16.3}$$

where ρ_G is the gas density at the inlet conditions.

The next step is to check if the fluid velocity is acceptable for the minimum/maximum pressure drop, as well as for good mass and heat transfer. For fixed bed reactors a practical particle diameter is between 3 and 5 mm. The pressure drop across a bed of particles can be calculated by means of the general equation:

$$\frac{dp}{dz} = f\frac{\rho_G u^2}{g d_p} \tag{16.4}$$

f is a friction factor that can be estimated by the Ergun[1] equation:

$$f = \frac{1-\varepsilon}{\varepsilon^3}\left(A + B\frac{1-\varepsilon}{\mathrm{Re}_p}\right) \tag{16.5}$$

The Reynolds number is defined as $\mathrm{Re}_p = d_p G/\eta_G$, ε being the void fraction of the catalytic bed. For non-spherical particles an equivalent diameter is defined as $d_p = 6V_p/S_p$, where V_p and S_p are volume and surface. In the absence of experimental data the void fraction of packed bed of spheres can be estimated by:

$$\varepsilon = 0.38 + 0.073\left[1 + \frac{(D/d_p - 2)^2}{(D/d_p)^2}\right] \tag{16.6}$$

The constants in the Ergun's equation depend on the hydrodynamic regime. For example, if Re/(1-ε) < 500 then A=1.75 and B=150. For larger Reynolds values the correlation of Hicks[2] (1970) can be used:

$$f = 6.8\frac{(1-\varepsilon)^{1.2}}{\varepsilon^3}\mathrm{Re}^{-0.2} \tag{16.7}$$

The minimum pressure drop to ensure uniform distribution of reactants is of about 0.02 bar/m for fixed beds, and of 0.07 bar/m for trickle beds.

For industrial pellets the heat and mass transfer coefficients can be calculated simply by relations valid for spherical particles in static conditions: $Nu = 2$ and $Sh = 2$. The obtained values are conservative for preliminary design.

16.1.2 Stirred tank reactors

Geometry

The geometry of a stirred tank is determined by the aspect ratio *H/D* (height by diameter). The ratio *H/D* is typically 2 to 3. The actual reactor volume is calculated by

1 Ergun, S. Fluid through packed beds, Chem. Eng. Progr., 48(2),89, 1952

2 Hicks, R. E., Pressure drop in packed beds of sphere, Ind. Eng. Chem. Fundam., 9, 500, 1970

considering a filling factor of 0.7 to 0.8. The vessel diameter can be approximated from the volume of the cylindrical part $V = (\pi/4)D^2H$. For more accurate calculation the volume of the head should be considered (Table 16.2).

Table 16.2 Volume of heads for tank reactors

Head type	Height	Volume
Ellipsoidal	$D/4$	$\pi D^3/24$
Hemispherical	$D/2$	$\pi D^3/12$
Conical		$\pi h(D^2 + d^2 + Dd)/12$
		h - height, d - diameter of the small end

Mechanical mixing

The mixing device is an important element in designing stirred tank reactors. Perry's handbook or the monograph of Tatterson (1991) can be consulted for the selection of mixers. A good presentation can be found in McCabe et al. (1992).

The following types are commonly applied:

- Radial mixers: flat-blade impellers and turbines
- Radial/axial mixers: pitched bladed and marine propeller
- Low viscosity mixers: paddle, anchor and helical ribbon.

Turbines are smaller multi-blades mixers, which can be hub-mounted flat-blade type, straight or curved, or disc-mounted flat blade (Rushton) type, of generally six blades.

Impellers and paddle are larger slower-speed mixers with two or four blades. Both mixer types are almost universal for low and moderate viscosity. The flat-blade turbine has a predominant radial action being suited for turbulent mixing, as in the case of gas-liquid dispersions. The pitched-blade mixer and the marine propeller are appropriate for axial mixing.

The speed of such mixers is between 1800 and 400 rpm, higher for smaller volume, and lower for larger volumes. Baffles can be used to reduce the vertex formation that diminishes the active volume. For low viscous liquids (10^{-3} to 1 Ns/m^2) turbines, impellers and propellers are suitable. For viscous liquids, above 10^2 Ns/m^2, anchor and helical ribbon agitators are recommended.

The power consumption of a mixer is characterised by the power number N_P defined as:

$$N_P = \frac{P}{n^3 D_a^5 \rho} \tag{16.8}$$

The power number can be correlated as function of dimensionless numbers as:

$$N_P = \psi(\mathrm{Re}, Fr, S_1, S_2, \ldots S_n) \tag{16.9}$$

Dimensionless groups are Reynolds - $\mathrm{Re} = nD_a^2\rho/\eta$, Froude - $Fr = n^2 D_a / g$, while S_1 to S_n are geometrical similarity ratios. The notations are: D_a - mixer diameter, n- rotation speed, ρ - liquid density and η - viscosity.

The flow in mixed tanks can be characterised by two distinct regimes: laminar (Re < 10), and fully turbulent (Re > 10000). In laminar flow there is a linear relation between power and viscosity expressed by $N_P = K_L / \mathrm{Re}$. As a result the power can be determined with the following relation:

$$P = K_L n^2 D_a^3 \eta \tag{16.10}$$

In un-baffled stirred tanks, a vortex formation occurs at Reynolds larger than 300. This phenomenon should be avoided by working in laminar regime, or by using baffles in turbulent mixing (Re > 10^4). Because $N_P = K_P$ the following relation is obtained:

$$P = K_T n^3 D_a^3 \rho \tag{16.11}$$

Note that for Newtonian fluids in turbulent regime the mixing power is independent of viscosity.

Table 16.3 Constants for calculating mixing power in baffled tanks

Mixer type	K_L	K_T	Geometry
Turbines			
Six-blade disk[3]	65	5.75	S_3=0.25, S_4=0.2
Six-curved blades[4]	70	4.80	S_4=0.2
Four-pitched blades of 45° [3]	44.5	1.27	S_4=0.2
Propeller three blades			
Pitch 1.0[4]	41	0.32	
Pitch 1.5[3]	55	0.87	
Flat paddle, two blades[4]	36.5	1.70	S_4=0.2
Anchor[3]	300	0.35	

The constants K_L and K_T are constants specific to each type of mixer, for laminar and turbulent regime, as given in Table 16.3. The conditions of geometrical similarity are given by means of ratios $S_1 = D_a / D_t$, $S_2 = h_a / D_t$, $S_3 = L / D_a$, $S_4 = W / D_a$, $S_5 = B / D_t$ and $S_6 = H / D_t$. D_a and D_t are the diameters of mixer and of tank, respectively. H and h_a are height of the liquid, and of the distance of mixer with respect to bottom. L is the horizontal length of the turbine blade of width W. B is the baffle width. Recommended values for S_1 are 0.33 for turbines and propellers, 0.6 for paddle and 0.95 for anchor mixers. Usually S_2=0.33, S_3=0.25, S_4=0.2, S_5=0.1, S_6=1.

[3] Oldshue, J.Y., Fluid Mixing Technology, 1983, McGraw-Hill, 1983
[4] Rushton, J. H., Ind. Eng. Chem., 1952, vol. 44, p. 2931

Heat transfer

The partial heat transfer coefficient bulk-liquid/wall in an agitated vessel can be calculated by means of relations similar to the following:

$$Nu = C\,\mathrm{Re}^{0.66}\,\mathrm{Pr}^{0.33}\left(\frac{\eta}{\eta_w}\right)^{0.14} \tag{16.12}$$

C is 0.36 for jacketed vessels and 0.87 for cooling coils. (η/η_w) is a correction factor for viscosity variation between bulk and wall, usually negligible.

16.1.3 Mechanical design of vessels

A chemical reactor is a vessel manufactured from metal, often stainless steel or high resistant alloys. A minimum wall thickness is required to resist to different loads, and mainly to internal pressure. Accurate mechanical calculation of process equipment is a matter of mechanical engineering, and out of the scope of this book. Here we present only simple relations that permit the evaluation of weight and cost of vessels in a preliminary economic analysis. More information about mechanical design can be found in Coulson & Richardson (1993).

For a cylindrical shell of diameter D the minimum thickness δ for an internal design pressure P_i can be found with the relation:

$$\delta = \frac{P_i D}{2\sigma_d - P_i} \tag{16.13}$$

The design stress σ_d can be obtained from tables as function of temperature, as the Table C1 in Appendix C. Alternatively, the design stress can be estimated as the tensile strength σ_r divided by a safety factor S, for which typical values are from 2.5 to 4. The tensile strength σ_r is about 360 N/mm^2 for carbon steels and 500 N/mm^2 for stainless steels.

For spherical vessels the minimum thickness is given by

$$\delta = \frac{P_i D}{4\sigma_d - P_i} \tag{16.14}$$

The design pressure P_i is 10% above the working pressure.

In the case of vessels subject to vacuum, the shell buckling could occur because of elastic instability. A critical pressure P_b can be approximated by:

$$P_b = 2.2E(t/D_o) \tag{16.15}$$

where E is the Young modulus, t the wall thickness and D_o the outside diameter. Stiffness rings are welded to prevent the collapse of the metal sheet.

Beside the resistance to internal pressure, a minimum wall thickness is required to ensure that the vessel resists to deformation due to its own weight, to incidental loads,

as well as safety margin against corrosion, as given in Table 16.4. Note that for low pressures the minimum thickness calculated by the resistance to pressure could be much less than the values recommended in Table 16.4. Thus, minimum thickness is sufficient to ensure the resistance to internal pressure.

Table 16.4 Minimum thickness of cylindrical vessels

Vessel diameter (m)	Minimum thickness (mm)
1	5
1 to 2	7
2 to 2.5	9
2.5 to 3	10
3.0 to 3.5	12

16.2 SEPARATORS

16.2.1 Distillation columns

The two important design elements of a distillation column are the number of theoretical stages N, and the reflux R ratio. For a zeotropic mixture there is a minimum number of theoretical stages $N_{\min}$ at infinite reflux, as well as a minimum reflux $R_{\min}$, at infinite number of stages, as illustrated in Fig. 9.35. For binary mixtures the classical McCabe method gives useful insights into design. For n-components mixtures the Fenske-Underwood-Gilliland (FUG) procedure is the standard shortcut design method. However, the final solution should always be tested by rigorous simulation.

Optimum reflux can be in principle determined as a trade-off between investment and operation costs. The column cost is roughly proportional with the number of stages N. The cost of utilities depends on the vapour flow, proportional with the reflux plus distillate, $R+1$. Consequently, the optimisation of the function $F_R = N(R+1)$ versus R leads to a convenient approximation of the optimum reflux. In practice, the optimal reflux takes values between $1.1\text{-}1.5\,R_{\min}$, the most probable being 1.2-1.3. Alternatively, the actual number of theoretical stages may be taken twice the minimum number $N_{\min}$.

In the case of azeotropic and extractive distillation there is a minimum and maximum reflux to achieve a given purity. Design issues for such mixtures have been presented in Chapter 9.

McCabe-Thiele method for binary mixtures

The classical McCabe-Thiele method can be applied for the preliminary design of columns separating quasi-ideal binary mixtures in products with moderate purity when the volatility is larger than 1.5. It is also suitable for multi-component mixtures when the key components are adjacent. The method is based on the assumption of constant molar overflow.

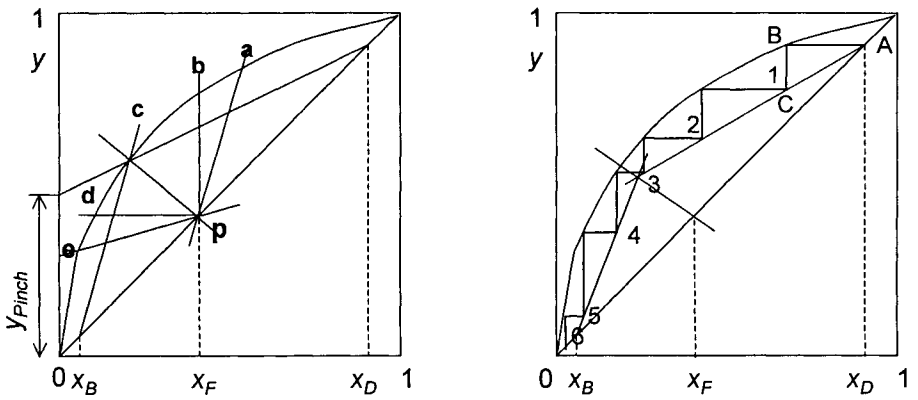

Figure 16.1 McCabe-Thiele graphical method

Left: Drawing the feed line: a - cold feed, b – liquid saturated feed, c – partial vaporized feed, d – saturated vapour feed, e – superheated vapour;
Right: Finding the number of equilibrium stages; ABC – top plate with total condenser.

The standard McCabe method that consists of the following steps (Fig. 16.1):

1. Trace the equilibrium diagram *y-x*. Place the points charactering feed x_F, distillate x_D and bottoms x_B.
2. Determine the feed condition *q*. This signifies the moles of liquid going to the stripping zone from one mole of feed, and can be found as follows:
   - Liquid at bubble point $q = 1$,
   - Vapour at dew point $q = 0$,
   - Mixture with vaporised fraction *f*, $q = 1 - f$, and therefore $0 < q < 1$,
   - Cold feed $q = 1 + C_{PL}(T_b - T_F)/\Delta H_V > 1$,
   - Superheated feed $q = -C_{P,V}(T_F - T_d)/\Delta H_V < 0$.

In the above relations $C_{P,L}$ and $C_{P,V}$ are the molar heat capacity of liquid and vapour, ΔH_V is the molar vaporisation enthalpy, while T_F, T_b, T_d are the actual feed temperature, feed bubble point and feed dew point.

3. Trace the feed-line as the equation

$$y = -\frac{q}{1-q}x + \frac{x_F}{1-q}$$

Make use of the property that the *q*-line cross the diagonal at $x = x_F$ and has the slope $-q/(1-q)$, as illustrated by Fig. 16.1-left. If the feed is at bubble point (recommended) the feed line is a vertical passing through x_F. If the feed is saturated vapour the feed line is a horizontal passing through $y_p = x_F$.

4. Determine the minimum reflux ratio. This can be located by the position of the operating line from x_D that intersects the feed-line on the equilibrium curve. The slope of this line is $R_{\min}/(R_{\min}+1)$ and the ordinate at $y_{Pinch} = x_D/(R_{\min}+1)$

5. Assume an operating reflux ratio by using the rule $R = (1.2 \div 1.3)R_{\min}$

6. Trace the operating lines. For a liquid feed at saturation the equations are:

- Rectification zone: $y - x_D = \dfrac{R}{R+1}(x - x_D)$

- Stripping zone: $y - x_W = \dfrac{R}{R+F}(x - x_W)$

The simplest method is to start with the rectification zone by drawing the corresponding line from the point $x = x_D$ and find the intersection with the q-line. Then the operating line for the stripping zone is simply joining this point with x_W.

7. Determine the number of theoretical stages by as the number of segments of a stepwise line that can be traced between the operating lines and the equilibrium curve starting from the top or from the bottom of the column. The graphical construction allows also the identification of the feed plate.

As example Fig. 16.1-right shows the determination of the number of stages when the feed is partially vaporised.

McCabe-Thiele method helps the identification of design troubles that could arrive with non-ideal mixtures when the equilibrium curve shows inflection points, as displayed in Fig. 16.2.

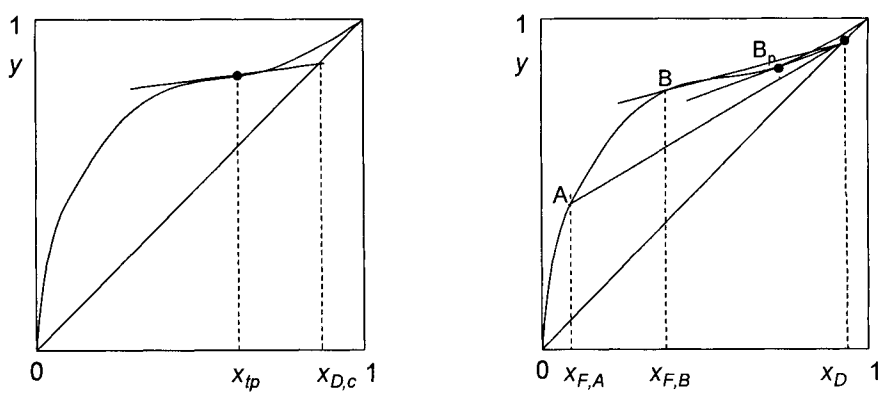

Figure 16.2 McCabe-Thiele method for mixtures showing equilibrium curves with tangent pinch. Left: Position of tangent pinch and critical distillate composition. Right: Minimum reflux and feed composition; A - feed pinch control, B – tangent pinch control

At the inflection point, designated by *tangent pinch*, the composition is x_{tp}, and the tangent intersects the diagonal at $x_{D,c}$ (Fig. 16.2-left). This composition is the

maximum purity that can be obtained without be affected by the inflection of the equilibrium curve. For purities higher than $x_{D,c}$ the minimum reflux and feed composition are interrelated (Fig. 16.2-right). In the case *A* the minimum reflux is controlled by the feed pinch. In the case *B* the minimum reflux at feed pinch is infeasible. The minimum reflux is controlled by the tangent pinch, as indicated by the point B_p, actually much larger than with reference to feed pinch. In conclusion, it is problematic to achieve high purity with a mixture displaying tangent pinch. Distillation should be coupled with other operation, as for example with liquid-liquid extraction.

Low volatility binary mixtures: Smoker equation

When the relative volatility is low, below 1.3, the number of theoretical stages could become very large, above 100. Graphical methods are tedious. In this case an algebraic method can be applied known as the Smoker method. The derivation starts with the assumption that the operation line is straight:

$$y = sx + c$$

and phase equilibrium can be described the Fenske equation

$$y = \alpha x / [(1 + (\alpha - 1x)]$$

α being the relative volatility. By eliminating y leads to the relation:

$$s(\alpha - 1)x^2 + [s + b(\alpha - 1) - \alpha]x + b = 0 \qquad (16.16)$$

The second-degree equation (16.16) has a positive root $k = x^+$ between 0 and 1. By setting $x^* = x - k$ it can be demonstrated that the number of stages is given by:

$$N = \log\left[\frac{x_0^*(1 - \beta x_n^*)}{x_n^*(1 - \beta x_0^*)}\right] / \log\left(\frac{\alpha}{sc^2}\right) \qquad (16.17)$$

where

$$c = 1(\alpha - 1)k \qquad (16.18) \qquad \beta = \frac{sc(\alpha - 1)}{\alpha - sc^2} \qquad (16.19)$$

Then the number of stages can be calculated for each section as follows:

a. Rectifying section

$$x_0^* = x_D - k\,,\ x_n^* = x_F - k\,,\ s = R/(R+1)\,,\ b = x_D/(R+1) \qquad (16.20)$$

b. Stripping section

$$x_0^* = x_F - k\,,\ x_n^* = x_B - k\,,\ s = \frac{Rz_F + x_D - (R+1)x_B}{(R+1)(x_F - x_B)}\,,\ b = \frac{(z_F - x_D)x_B}{(R+1)(x_F - x_B)} \qquad (16.21)$$

If the feed is not liquid at saturation the feed composition is replaced by $z_F^* = \frac{b + z_F/(q-1)}{q/(q-1) - s}$.

Multicomponent mixtures: Fenske-Gilliland-Underwood method

The procedure consists of the following steps:

1. Formulate specifications. For a new column these are usually the split of the key components and $R/R_{\min}$ or N/N_{min}.
2. Calculate the minimum number of stages with the Fenske equation.

$$N_m = \log\left[\left(\frac{Dx_D}{Bx_B}\right)_l\left(\frac{Bx_B}{Dx_D}\right)_h\right] / \log\alpha \tag{16.22}$$

where D, B, x_D and x_B are formulated distillate and bottoms flow rates rates and compositions, while α is the mean relative volatility of key components.

3. Determine the minimum reflux by solving the equation (Underwood method):

$$\sum_i \frac{\alpha_i (x_{i,D})_m}{\alpha_i - \theta} = R_m + 1 \tag{16.23}$$

$$\sum_i \frac{\alpha_i x_{i,F}}{\alpha_i - \theta} = 1 - q \tag{16.24}$$

In the above equations α_i is relative volatility with respect to a reference component, and q is the thermal condition of the feed (1 for bubble-point, 0 for dew-point). Because the feed composition is known, θ may be found by iterations from the second equation. Then $R_{\min}$ is determined directly from the first equation.

4. Use the Gilliland correlation to calculate N from R, or R from N:

$$\frac{N - N_m}{N+1} = 1 - exp\left[\left(\frac{1 + 54.4\Psi}{11 + 117.2\Psi}\right)\left(\frac{\Psi - 1}{\Psi^{0.5}}\right)\right] \tag{16.25}$$

where $\Psi = (R - R_m)/(R+1)$.

16.2.2 Absorption columns

Shortcut calculation for designing absorber and stripper can be performed by using group methods. The contact device is seen as counter-current cascades of N adiabatic stages (Fig. 16.3). The component vapour and liquid flow rates leaving and entering a stage at equilibrium are $v_i = Vy_i$ and $l_i = Lx_i$, while L and V are the flow rates of vapour and liquid phase, respectively. The system has no degrees of freedom. Consider an adsorption column. The problem is to determine the fraction of the gas absorbed by a

given solvent flow rate in a device of N stages, or to find the number N of stages for a desired absorption fraction. The original derivation is designated as the Kremser method, but there are several improvements documented in specialised references.

The non-absorbed fraction of the solute ϕ_A is related with the number of stages by the relation:

$$\phi_A = \frac{A_e - 1}{A_e^{N+1} - 1} \tag{16.26}$$

$A_e=L/KV$ is the average effective absorption factor of each component, whereas $K=y/x$ is the gas-liquid equilibrium constant.

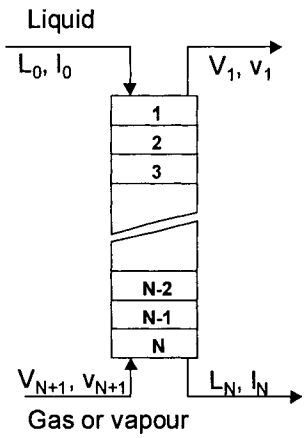

Figure 16.3 Cascade of stages for absorption or stripping operations

An analogue equation holds for stripping of volatiles components from a liquid stream by means of an inert. The non-stripped component fraction ϕ_S is given by

$$\phi_S = \frac{S_e - 1}{S_e^{N+1} - 1} \tag{16.27}$$

This time an average stripping factor is defined as $S_e=KV/L$.

Group methods are limited to dilute systems, where K-values could be considered as constant. In the case of more concentrated mixtures we recommend the use of computer methods. Attention has to be paid care to correct description of gas-liquid equilibrium. The use of asymmetric convention for K-values could overcome the drawback of using the Henry-law for concentrated solution (see Chapter 6). In the case of absorption with chemical reaction the methods based on the integration of mass transfer equations are recommended. Some specialised simulation packages have capabilities in this area.

16.2.3 Sizing separation columns

Tray or packed columns

Tray columns are used generally for diameters larger than 1 m. They accept a large variation of *turndown*, defined as the ratio of vapour flow rate at normal operating point to the minimum throughput, as well as large variation in the ratio vapour to liquid. In this respect valve trays are preferred over sieve trays. Tray columns can operate at very variable liquid load, from very low to very high. The holdup on trays can be designed to be low, as for thermal unstable chemicals or vacuum operation, or high, as for reactive distillation columns. Occasionally, heaters or coolers can be mounted on trays. Because of larger liquid holdup the tray columns are less sensitive to disturbances in flows and composition, and more robust in control than packed columns. The dynamics is however, slower. The features mentioned are significant advantages. Probably the most important disadvantage of plate columns is the pressure drop, typically 6-7 mbar per tray, which becomes critical at a large number of trays and low pressure. This aspect is also to consider for systems showing tendency to foaming.

Three types of trays dominate the market: sieve, valves and bubble-cap. Numerous commercial shapes exist. Sieve trays are low-cost in purchasing and maintenance, and robust in operation, can be designed for high throughput, but are penalised by a relatively low turndown, of about 2:1. The resistance to fouling is good, the entrainment moderate. The pressure drop can be lowered below down to 3 to 4 mbar. The market share of sieve trays is about 25%.

Valve trays keeps the feature of sieve trays, but have the important advantage of a higher vapour turndown of 4 to 5 or more. They are not suitable for separations where high probability of fouling exists. Valve trays dominate the market with about 70% of the applications, although they are 2-3 times more expensive than sieve trays.

Bubble-cap trays are considered obsolete, but still used in some occasions, for example at extremely low liquid load, or for conducting reactive distillation, where high holdup and longer residence time are necessary. They are very sensitive to fouling and expensive in maintenance.

Random packed columns are traditionally employed for low throughput applications when the diameter is below 1 m. New structured packings have pushed this limit to much larger values. The small pressure drop, typically 0.5-1 mbar per HETP is a significant advantage over tray columns. The low liquid holdup allows the treatment of thermally sensible components, but has a disadvantage of higher sensitivity to disturbances in control. The operation is flexible with respect to gas load, but it is very constrained with respect to the liquid flow rate. Packed column operate between a minimum liquid load required for uniform distribution, and a maximum load imposed by the flooding limit. The resistance of packed columns to fouling is limited, but in turn they behave better against foaming. Ceramic or plastic packing resist better to corrosion. New structured packing is available today in a variety of shapes, covering a large area of applications, as in fine chemicals processes and reactive distillation.

Real number of stages

In the approach based on equilibrium stages the number of real stages can be found by dividing the number of theoretical plates N_T by an overall efficiency E_o:

$$N = N_T / E_o \tag{16.28}$$

A very conservative value for overall efficiency is 0.5. More realistic values are in the range 0.7 to 0.8. There are a lot of correlations for overall efficiency. Doherty & Malone (2001) give the following equation based on O'Connell[5] experimental data:

$$E_o = 0.24 + 0.76\exp(-\sqrt{\alpha \frac{\eta}{\eta_0}} \tag{16.29}$$

where α is the relative volatility and η the relative viscosity of the liquid referred to water (η_0=10^{-3} Ns/m^2). Note that the relation has been developed originally for bubble cap trays, and is slightly conservative for sieve and valve trays. It can be applied equally for distillation and absorption. Kister (1992) found that the O'Connell correlation is the most convenient for preliminary design.

For packed columns the stages can be converted in equivalent packing by means of the height equivalent to a theoretical plate (HETP). Following Eckert (1988) for random packing the value of HETP is practically independent of the physical properties of fluids, but depends on the size of packing. For example, for Pall packing the HETP is 0.3 m for 25-mm, 0.45 for 38-mm and 0.6 m for 50 mm rings. A safety factor of 30 to 50% should be considered to account for the maldistribution of liquid. For hydraulic and efficiency reasons the packed columns are used for tower diameters less than 1 m.

Hydraulic design of trays columns

The hydraulics of a tray column shows a complex picture (Fig. 16.5). The ratio of vapour to liquid flow rates should be situated in a region of satisfactory operation. This region is constrained by undesired phenomena, as weeping, entrainment, entrainment flooding, and downcomer flooding. Weeping and flooding set lower and upper bounds for vapour velocity. It is desirable to work at high vapour velocity to reduce both diameter and column cost.

The hydraulic design of distillation columns consists primarily in determining the *flooding point*, where the vapour velocity becomes excessive such that leads to a dramatic increase in pressure drop. Usually the hydraulic design of trayed columns regards only the flooding of the active bubbling area. The operating point is selected typically at 70-80% with respect to the maximum load. Note that at higher pressures, when the density of vapour phase becomes important, there is a danger of flooding in downcomer, in the sense that the liquid could be pushed back and prevent to flow downwards. Provide larger downcomer area is necessary in such situation.

---

5 Connell, H. E. Trans. AIChE 42, 741-755, 1946

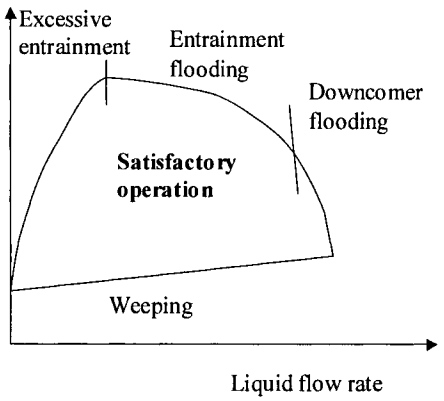

Figure 16.4 Tray hydraulics

The flooding mechanism is complex, depending on the type of tray. The *L/V* ratio and the column's pressure are the key factors. As illustrated in Fig. 16.5 at low pressures the entrainment flooding is the main limiting factor of column capacity, while at higher pressures the flooding in downcomer should be taken into consideration. More details about this issue can be found in Kister (1992).

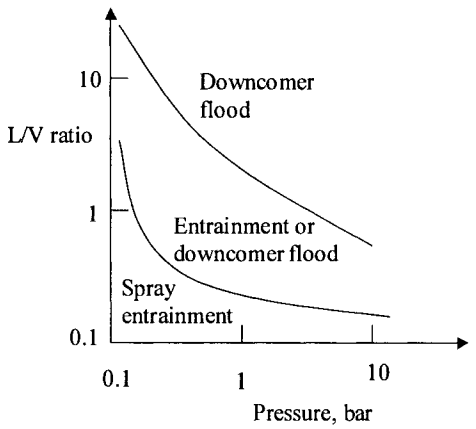

Figure 16.5 Flooding mechanism (after Kister, 1992)

Entrainment flooding is the most common. Among different methods the correlation proposed by Fair (1961)[6] found a wide acceptance. Fig. 16.7 presents a generalised plot in terms of *capacity factor* C_F that includes the flooding velocity u_{nf}

$$C_F = u_{nf}\left[\rho_V/(\rho_L - \rho_V)\right]^{0.5}(20/\sigma)^{0.2} \qquad (16.30)$$

6 Fair, J. R., Petro/Chem Eng. 33 (10), p. 45, 1961

versus a *flow factor* defined by

$$F_{LV} = L/V\left(\rho_V / \rho_L\right)^{0.5} \tag{16.31}$$

The gas velocity at flooding u_{nf} is referred to the net area, which is the tower cross-section A_T minus the area occupied by downcomer. In the above correlation ρ_L and ρ_V are the density of the liquid vapour and phase, L and V being the flow rates in mass units. The correlation includes a correction for superficial tension σ with respect to a reference value of 20 dyn/cm. The flooding in downcomer is more difficult to capture. The downcomer should be sized such to ensure a good hydraulic seal and sufficient liquid aeration. In practice this condition is fulfilled by taking the downcomer area as 10 to 12% from the cross-section, as well as the tray spacing of about 0.6 m.

The pressure drop can be determined as the contributions of dry plate, static liquid height, weir liquid crest and residual head. For approximate design the following relation is sufficient:

$$\Delta p = 1.5 h_w \rho_L g \tag{16.32}$$

where h_w is the weir height. The weir height is typically 40 to 60 mm for columns above atmospheric pressures, but much lower for vacuum operation (6 to 12 mm).

The manufactures of internals can supply devices of higher performance than the usual sieve and valve trays, optimised for given liquid/vapour traffic and physical properties of phases.

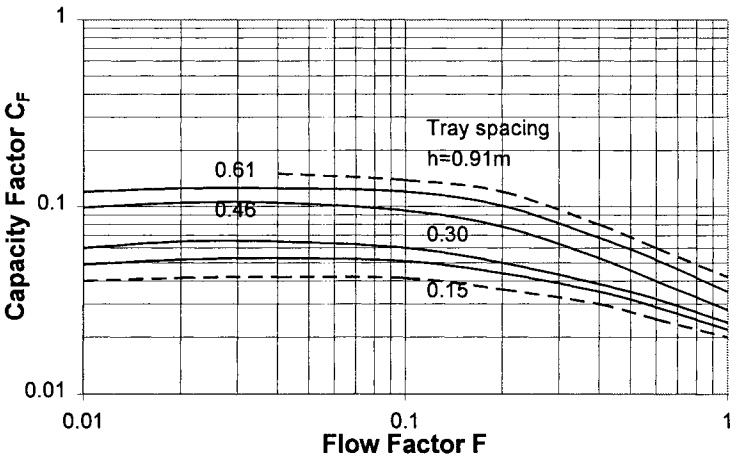

Figure 16.6 Flooding correlation for trays (adapted from Perry, 1997)

Hydraulic design of packed columns

Table 16.5 shows geometric and hydraulic characteristics of some common random packing, as Raschig and Pall rings, Intallox saddles, but including more modern shapes as IMTP and Mellapack. Note that the use of appropriate internals for support and fluid distribution could be more important for the overall efficiency than HETP (Kister, 1992). A single packing zone should not be higher than 8-10 times the tower diameter.

Table 16.5 Characteristics of some common packings (after Perry, 1997)

Packing	Size mm	Bulk density kg/m^3	Area m^2/m^3	Porosity	Packing factor, F_p m^{-1}
Raschig rings (ceramic)	13	880	370	0.64	1900
	25	670	190	0.74	492
	38	675	128	0.73	310
	50	660	95	0.74	210
Pall rings (metal)	25	480	205	0.94	183
	38	415	130	0.95	131
	50	385	115	0.96	89
Intalox saddles (C)	25	672	253	0.73	302
	38	625	194	0.76	170
	50	608	118	0.79	131
Intalox metal saddles IMTP®	25	352	230	0.97	135
	40	237	154	0.97	79
	50	150	98	0.98	59
Sulzer (metal gauze)	BX	-	492	0.90	69
Mellapack	500X	-	500	0.91	25
	250 X	-	250	0.95	8

Structured packing is nowadays largely used in industry because of lower pressure drop and higher mass transfer efficiency. There are numerous types. Following Kister (1992), structured packing has a definite advantage over modern random packing only at low liquid loads (< 20 gpm/ft2).

A generalised pressure drop correlation for determined the flooding point has been proposed by Eckert (1988) , and is displayed in Fig. 16.8. The ordinate is expressed as capacity at flooding $C_f = u_f^2 \eta_L^{0.1} F_p / \rho_V (\rho_L - \rho_V) g$. The packing behaviour is characterised by the *packing factor* F_p . Metric units are used with liquid viscosity in centipoise and g=9.81 m/s^2. The abscise is formulated as a flow factor given by $(L/V)/\sqrt{\rho_V /(\rho_L - \rho_V)}$, where L and V are in mass units. The plot allows the calculation of the superficial gas velocity at flooding u_f .

For the same packing size smaller F_p signifies higher capacity. For example IMTP of 25 mm has $F_p = 135$ while Raschig rings of 25 mm have $F_p = 492$. It comes out that IMTP packing allows 1.9 times more throughput.

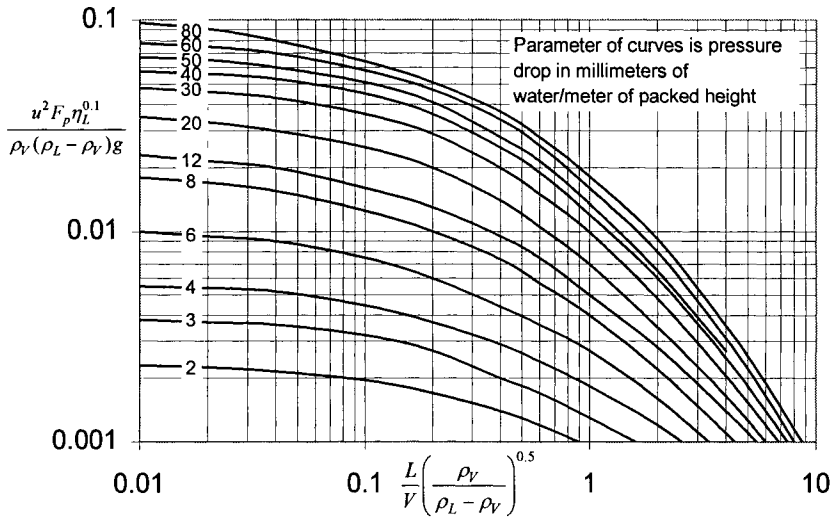

Figure 16.7 Flooding correlation for packed columns (after Eckert, 1988)

Condenser and reboiler

The duties of condenser and reboiler of a distillation column fed with liquid at saturation are approximately equal if the molar enthalpy of vaporisation of components is not too different. The condenser duty can be calculated as:

$$Q = D(R+1)\Delta H_c \tag{16.33}$$

where D is the distillate rate, R the reflux ratio and ΔH_c the enthalpy of condensation.

The sizing of the vessels around the column is based on allowable residence times. For the reflux drum and reboiler sump the residence these are of 5 to 10 minutes. The choice between kettle and thermosiphon reboilers could be justified by the observation that the last gives less trouble in operation (Kister, 1992).

16.2.4 Extraction equipment

The design of separators based on L-L extraction should be done outside the flowsheeting calculations, except situations where relatively diluted solutions are handled. Both LLE prediction and the calculation of the number of stages is more difficult as with distillation or absorption systems. The methods are essentially graphical and based on representations in triangular diagrams. These methods are well documented in specialised references, as Seader & Henley (1998). Note that shortcut methods for extraction devices have been developed by analogy with the Kremser method for adsorption-stripping columns.

The equipment for liquid-liquid extraction shows a large diversity. The following categories can be identifies:

1. Stage-wise equipment (mixer-settlers).
2. Continuous (differential) contact devices:
   a. Spray towers
   b. Packed columns
   c. Perforated plate columns
   d. Mechanically agitated columns: rotary-disk contactor (RDC), Scheibel, Kühni tower, Karr-reciprocating plate tower
   e. Pulsed columns
   f. Centrifugal extractors.

From these types the most interesting for industry are mixer-settlers, perforated plate columns, and mechanically agitated columns. In selecting the device attention should be paid to difference in density of phases, variation of superficial tension, and viscosity. Mixer-settlers can be designed as compacted vessels combining mixing and settling zones. The design of continuous contact systems is much more complex, but it can be done taking into account the hydrodynamics of the dispersed flows and the mass transfer kinetics from and to drops. The mass transfer factors define the capacity and performance of the extraction device. For details see Seader & Henley (1998), as well as the L-L extraction chapter written by Robins & Cusack in Perry (1997).

16.2.5 Membrane separation processes

The separations of gas and liquid mixtures by using membranes are emerging techniques. These include gas permeation, perevaporation, reverse osmosis, dialysis and electrodialysis. The membranes can be classified in two large categories, porous and non-porous materials. Gas permeation is the most interesting for large scale applications, as separation of hydrogen from refinery gases, adjustment of H_2/CO ratio in synthesis gas, air separation in oxygen and nitrogen rich gases, recovery of methane from biogas, etc.

In principle, the sizing of membranes consists of determining the cross-sectional area needed to achieve specifications with respect to recovery and selectivity of components. The mass flux calculation of a component N_i follows the expression:

$$N_i = \overline{P}_{M_i} \times (driving\ force) \tag{16.34}$$

$\overline{P}_{M_i}$ is the *permeance*, which is defined as the ratio of permeability P_{M_i} to membrane thickness l_M :

$$\overline{P}_{M_i} = \frac{P_{M_i}}{l_M} \tag{16.35}$$

In commercial applications the permeability is expressed in *barrers* defined as

1 barrer = 10^{-10} cm^3 (STP).cm/(cm^2.s.cmHg)

Permeability depends both on the adsorptive properties of the component and the diffusion through support. As an approximation the following relation to estimate the permeability of porous membrane when Knudsen diffusivity prevails:

$$P_{M_i} = \frac{\varepsilon}{RT\tau}\left[\frac{1}{1/D_i + 1/D_{K_i}}\right]$$

where D_i is the molecular diffusion coefficient, D_{K_i} is Knudsen diffusivity, ε the porosity, and τ the tortuosity.

The calculation of membranes is based on a number of empirical data regarding both membrane and fluid properties. More information can be found in Seader & Henley (1998), as well in the chapter devoted to alternative separations in Perry (1997).

Again, we should recall that membranes should not be used for high purity and large throughput, where other techniques are superior, mainly cryogenic distillation or Pressure Swing Adsorption. The energetic calculation has shown that the energy consumption for separating gases by membranes is not inferior compared with distillation, except when the gas is already at high pressure and low purity of product is acceptable.

16.3 HEAT EXCHANGERS DESIGN

The design of heat exchangers is based on the general equation:

$$Q = UA\Delta T_m F \tag{16.36}$$

where the notations have the following significance:

Q - heat exchanger duty (kW);

U - overall heat transfer coefficient (kW/m^{2}K);

A - heat exchange area (m^2);

ΔT_m - mean-temperature differences between the hot and cold fluids (K)

F_T - correction factor that accounts for crossing driving force effects.

Heat exchanger design by hand is tedious. Very convenient are computer programs as B-JAC, HTRI/HTFS or HEXTRAN interfaced with flowsheeting software. The understanding of some basic design principles is necessary, which is the scope of this section. Besides standard textbooks more technical information can be found in the monograph of Hewitt et al. (1994), as well as in the well-known guide of Linnhoff et al. (1994).

16.3.1 Heat transfer fluids

Water

Water is the most used heat transfer fluid. Critical pressure and temperature of water are 220 bar and 373.14 °C. As steam water is a valuable heating agent below 200 °C, where the saturation pressure is about 24 bar. Superheated steam can be used above the saturation limit. Liquid water is excellent for cooling purposes, and sometimes is used

for heating at mild temperature, below 100 °C. For higher temperatures special thermal fluids are more suitable than water.

Salt brines

Brines designate liquids used as heat transport agents between a remote heat source and the refrigeration systems. Salt brines are water solutions of inorganic salts. For example, NaCl solutions could be used down to -10 °C, but these are corrosive. Instead aqueous $CaCl_2$ solutions (concentration of maximum 25%) are preferable down to -20 °C. Salt brines have low purchase cost but are expensive in operation. Antifreezes described below are preferable.

Glycol solutions

Ethylene and propylene glycols as aqueous solutions of different concentrations are suitable for lower temperature applications. Ethylene glycols can be used in principle down to -35 °C, but in practice is limited to the range 10° / -10 °C because of high viscosity. Propylene glycol has the advantage to be non-toxic. Other antifreeze fluids, as methanol and ethanol solutions arise safety and toxicity problems.

Thermal fluids

The category of thermal fluids designates special molecules or mixtures for carrying out heat transfer operations over a large temperature interval but at reasonable operating pressures. As example, Table 16.6 shows the properties of some thermal fluids produced by Dow Chemicals. The most known Dowtherm A is a mixture of diphenyl oxide/diphenyl capable of working as liquid or vapour up to 400 °C at a maximum pressure of 10 bar. Other fluids are based on mixtures of heavy hydrocarbons. Silicones are excellent liquid heating/cooling media over a wide temperature range, as for example between -100 °C and 400 °C. More information can be found on the Internet sites of producers.

Table 16.6 Properties of some thermal fluids

Fluid	Composition	Temperature range °C	P_{sat} max.temp. bar	$Cp^{\#}$ kJ/kgK	$\rho^{\#}$ kg/m^3	$\eta^{\#}$ cP
Dowtherm A	$(C6H5)_2O$ / $(C6H5)_2$	L 15 ÷ 400 V 257÷ 400	10.6	1.556 2.702	1062 680	5 0.13
Dowtherm J	Alkylated aromatics	-80 ÷ 315	11.9	1.571 3.012	933.6 568.2	9.98 0.16
Dowtherm Q	Alkylated aromatics	L -35 ÷ 330	3.4	1.478 2.586	1011 734	46.6 0.2
Syltherm 800	Siloxane	-40 ÷ 400	13.7	1.506 2.257	990 547	51 0.25
Syltherm XLT	Siloxane	-100 ÷ 260	5.2	1.343 2.264	947 563	78 0.18

- values at minimum and maximum temperatures

Inorganic salts

The most used salt is molten mixture of the eutectic $NaNO_2$ (40%)/$NaNO_3$ (7%) /KNO_3 (53%). The service temperature is between 146 °C (melting point) and 454 °C.

Refrigerants

Refrigerants are substances that can remove heat from a body or process fluid by vaporisation. Ammonia (R717) seems to be again a popular refrigerant after years of decline in favour of chlorinated hydrocarbons (CFC's). Because of damaging the ozone layer, the CFC's are nowadays banned. New refrigerants based on hydrochlorofluorocarbons (HCFC) have been developed in the recent years, although these are not completely inoffensive. Thermodynamic properties of new HCFC can be found in Perry (1997). One of the most recommended is R 134a for replacing R12.

16.3.2 Heat transfer coefficients

The overall heat transfer coefficient between two fluids separated by a wall is the reciprocal of the overall resistance to heat transfer, obtained as the sum of individual resistances. These include the heat transfer through the fluid films (inside and outside), conductive heat transfer through the wall, as well as the resistance of fouling deposits on the both sides. Accordingly, the following relation can be used to calculate the overall heat transfer coefficient for a cylindrical tube:

$$\frac{1}{U_0} = \frac{1}{h_i} + \frac{d_o \ln(d_o / d_i)}{2\lambda_w} + \frac{d_o}{d_i}\frac{1}{h_i} \tag{16.37}$$

U_0 is the overall heat transfer coefficient based on the outside area, h_i and h_o are inside and outside heat transfer coefficients including fouling, d_i and d_o inside and outside diameter, while λ_w is the thermal conductivity of the tub wall material. Diameter correction can be neglected for thin walls.

The partial heat transfer coefficients depend on the hydrodynamic regime of the flow (turbulent, laminar, intermediate), as well as on the physical property of the system, particularly viscosity and thermal conductivity. The partial heat transfer coefficients h is obtained from the Nusselt number as:

$$h = Nu \times l / \lambda \tag{16.38}$$

where l is a characteristic length, as for example the tube diameter d , and λ is the thermal conductivity of the fluid. Nusselt is given by the general equation:

$$Nu = C\,\mathrm{Re}^{\alpha}\,\mathrm{Pr}^{\beta}\,\Gamma_g^{\gamma}\Gamma_p^{\delta} \tag{16.39}$$

Reynolds number is an indication of the hydrodynamic regime and can be calculated as:

$$\mathrm{Re} = \frac{ul\rho}{\eta} \tag{16.40}$$

where u is the fluid velocity, ρ the density and η the dynamic viscosity. Prandtl number includes only physical properties:

$$\mathrm{Pr} = C_p \eta / \lambda \tag{16.41}$$

Γ_g and Γ_p are invariants of geometry and physical properties. For other geometries the general formula (16.39) holds, but the characteristic length is replaced by a hydraulic diameter d_e= 4 × (cross-sectional area for flow) / (wetted perimeter).

For fully turbulent regime in pipes Re should be larger than 10^4. The hydraulic design should be such to ensure turbulent regime with reasonable pressure drop. This is possible by adapting the geometry of the heat exchange device, as for example the number of passes through tubes or the baffle spacing in a shell-and-tubes exchanger. When Re < 2300 the hydrodynamic regime is laminar and the heat transfer is governed by conduction.

The heat transfer coefficient for flow of liquids and gases in pipes in turbulent regime can be estimated accurately by means of the equation:

$$Nu = 0.027\,\mathrm{Re}^{0.8}\,\mathrm{Pr}^{0.33}\left(\frac{\eta}{\eta_p}\right)^{0.14} \tag{16.42}$$

By taking into account the relation 16.11 it follows that the heat transfer is inverse proportional with the viscosity to the power 0.47 ($\sim\eta^{-0.5}$) and to thermal conductivity to the power 0.67 ($\lambda^{2/3}$). High viscosity liquids have lower heat transfer coefficients, and therefore increasing the temperature has a favourable effect. For gases temperature the effect is opposite, since the viscosity of gases increases with temperature. A gas of exceptional conductivity is hydrogen, which gives coefficients higher by an order of magnitude than the usual gases. Note that for liquids in convection the heat transfer coefficient is in the range 300-3000 W/m^{2}K, while for gases the values are in the range 30-300 W/m^{2}K, function of pressures from lower to higher values.

In the laminar regime the following relation is convenient:

$$Nu = 1.83(\mathrm{Re}\,\mathrm{Pr})^{0.33}\frac{d_e}{L_t}\left(\frac{\eta}{\eta_p}\right)^{0.14} \tag{16.43}$$

For the condensation of vapours the following relation can be applied:

$$h_c = C\lambda\left[\frac{\rho_L(\rho_L - \rho_V)g}{\eta\Gamma_V}\right] \tag{16.44}$$

where h_c is heat transfer coefficient of the condensation film, , η and λ are the viscosity and thermal conductivity of the condensate, while ρ_L and ρ_V are the densities of liquid and vapour. Γ_V is the mass loading per tube and per unit of wetted perimeter in kg/m s. This is calculated as follows:

- $\Gamma_V = G / L_t$ for condensation outside horizontal tubes;

- $\Gamma_V = G / \pi d_e$ for condensation outside vertical tubes.

The constant C is 0.95 for horizontal single tubes, 0.75 for tubes in a bundle, and 0.926 for vertical tubes.

For condensers and evaporators where counter-current vapour/liquid flow occurs, the tube diameter should be checked against flooding (Sinnott, 1993):

$$\left[u_V^{1/2}\rho_V^{1/4} + u_L^{1/2}\rho_L^{1/4}\right] < 0.6[gd_t(\rho_L - \rho_V)]^{1/4} \tag{16.45}$$

where u_V and u_L are the superficial velocity of vapour and liquid.

Table 16.7 shows typical values for partial heat transfer coefficients that can be used in preliminary design. The assumed values should be checked in the final design. Particularly attention should be given to the situations involving two-phase mixtures, hydrogen-rich gases and condensation of vapours with non-condensable gases.

Table 16.7 Partial heat transfer coefficients

Fluid	h (W/m^{2}K)	Fluid	h (W/m^{2}K)
Gases		*Boiling liquids*	
Gases low pressure	20-80	Boiling water	1500-2000
Gases high pressure	100-300	Boiling organics	800-1300
Hydrogen-rich gases	80-150		
Liquids		*Condensing vapour*	
Water turbulent regime	1500-3000	Condensing steam	4000-5000
Dilute aqueous solutions	1000-2000	Thermal fluids	2000-3000
Light organic liquids	1000-1500	Organics	800-2000
Viscous organic liquids	500-800	Organics with NC	500-1500
Heavy-ends	200-500	Refrigerants	1500
Brines	800-1000		
Molten salts	500-700		

NC: non-condensables

Taking the fouling into consideration is important in designing heat exchangers. Table 16.8 gives values for the fouling resistance expressed as equivalent partial transfer coefficients. Note that for thicker walls from stainless steel the resistance across the metal is significant and should be included in the overall heat transfer coefficient.

Table 16.8 Fouling as equivalent heat transfer coefficient

Fluid	Fouling (W/m^{2}K)
Cooling water (towers)	3000-6000
Organic liquids & light hydrocarbon	5000
Refrigerated brine	3000-5000
Steam condensate	3000-5000
Steam vapour	4000-10000
Condensing organic vapours	5000
Condensing thermal fluids	5000
Aqueous salt solutions	1000-3000
Flue gases	2000-5000

The combination of different situations leads to the overall heat transfer coefficient listed in Tables 16.9-12. Note that fouling is included.

Table 16.9 Overall heat transfer coefficients for Shell-and-tubes heat exchangers

Hot fluid	Cold fluid	U (W/m^2K)
Heat exchangers		
Water	Water	800-1500
Organic solvents	Organic solvents	100-500
Light oils	Light oils	100-400
Heavy oils	Heavy oils	50-300
Gases	Gases	10-50
Coolers		
Organic solvents	Water	250-750
Light oils	Water	350-900
Heavy oils	Water	60-300
Gases	Water	20-300
Water	Brine	600-1200
Organic solvents	Brine	150-500
Gases	Brine	15-250
Water	Natural gas mixture with hydrogen	500-800
Water or brine	Gases moderate pressures	100-200
Heaters		
Steam	Organic solvents	500-1000
Steam	Light oils	300-900
Steam	Heavy oils	60-450
Steam	Gases	30-300
Dowtherm	Heavy oils	50-300
Dowtherm	Gases	20-200
Flue gases	Steam or hydrocarbon vapours	30-100
Condensers		
Steam	Water	1000-1500
Organic vapours	Water	700-1000
Organics vapours high NC, A	Water	100-500
Organics vapours low NC, V	Water	250-600
Thermal fluid vapours	Tall oil	300-400
Tall oil, vegetable oil vapours	Water	100-250
Vaporisers		
Steam	Aqueous diluted solutions	1000-2000
Steam	Light organics	1000-1500
Steam	Heavy organics	600-900
Evaporators		
Steam	Sea water (long tube falling film)	1500-3000
Steam	Sea water (ling tube rising film)	700-2500
Steam	Sugar solution (agitated-film)	1000-2000

Table 16.10 Overall heat transfer coefficients for air-cooled heat (bare tube basis)

Process fluid	U (W/m²K)
Water cooling	500
Light organics cooling	400-500
Fuel oil cooling	150
High viscous liquid cooling	40-100
Hydrocarbon gases, 3-10 bar	60-200
Hydrocarbon gases, 10-30 bar	300-400
Condensing hydrocarbons	400-600

Table 16.11 Overall heat transfer coefficients for jacketed vessels

Jacket	Vessel	U (W/m²K)
Steam	Aqueous solutions (glass-lined CS)	500-1000 (300-500)
Steam	Light organics (glass-lined CS)	250-800 (200-400)
Steam	Viscous solutions (glass-lined CS)	50-300 (50-200)
Water, brine, thermal fluid	Aqueous solutions (glass-lined CS)	250-1500 (150-450)
Water, brine, thermal fluid	Light organics (glass-lined CS)	200-600 (150-400)
Water, brine, thermal fluid	Viscous solutions (glass-lined CS)	100-200 (50-150)

Table 16.12 Overall heat transfer coefficients for immersed coils in agitated vessels

Coil	Pool	U (W/m²K)
Steam	Diluted aqueous solutions	500-1000
Steam	Light oils	250-500
Steam	Heavy oils	150-400
Water or brine	Aqueous solutions	400-700
Light oils	Aqueous solutions	200-300

NC: non-condensables

16.3.3 Pressure drop calculation

Pressure drop calculation in heat exchangers is based on the Fanning-Darcy equation:

$$\Delta p = \xi \frac{L}{d_{eq}} \frac{u^2 \rho}{2} \tag{16.46}$$

The equivalent diameter is given by $d_{eq} = 4S/P$, where S is the cross section and P the perimeter of the flow, L is the path length, and ξ is a friction factor expressed as function of Reynolds number and device geometry. Heat transfer and pressure drop calculations are interrelated. Higher fluid velocity is necessary to ensure intensive heat transfer, but this could lead to excessive pressure drop. As a rule of thumb the velocity should be in the order of 1-3 m/s for liquids with normal viscosity and density, and between 10-30 m/s for gases at normal pressures.

16.3.4 Temperature driving force

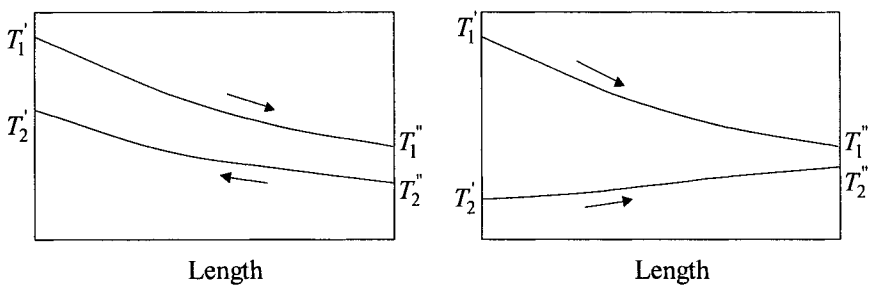

Figure 16.8 Temperature profiles in 1-1 heat exchanger

The temperature difference in a heat exchanger varies from point-to-point. Ideally the basic design equation $dA = dQ/U\Delta T$ should be integrated over different heat exchange zones to obtain the total heat exchange area. This is indeed done in CAD packages by methods based on *zone analysis*. For preliminary design the heat exchange area is determined by taking into account a logarithmic-mean temperature difference ΔT_m, called also LMTD, and a correction factor F_T as shown by Eq. 16.36. The computation of ΔT_m is based on the temperature differences at the two ends of the heat exchanger, the hot side $\Delta T' = t_1' - t_2'$ and the cold side $\Delta T'' = t_1'' - t_2''$. Fig. 16.8 displays the temperature profiles for ideal counter-current (left) and co-current (right) flows. The following formula is valid for both arrangements.

$$\Delta T_m = \frac{\Delta T' - \Delta T''}{\ln(\Delta T'/\Delta T'')} \tag{16.47}$$

The correction factor F_T accounts for the deviation from the ideal pattern due to reversed or *cross-flow*, when the hot fluid outlet temperature is below the cold fluid outlet temperature (for profiles see Fig. 16.9). F_T is less than 1. Graphical correlations are available in specialised books, as in Perry (1997). For 1-2 shell-and-tubes exchangers the following analytical formula can be applied:

$$F_T = \frac{\sqrt{R^2+1}\ln[(1-S)/(1-RS)]}{(R-1)\ln\left[\dfrac{2-S[R+1-\sqrt{R^2+1}]}{2-S[R+1-\sqrt{R^2+1}]}\right]} \tag{16.48}$$

where $R = \Delta T_1 / \Delta T_2 = G_2 C_{p,2} / G_1 C_{p,1}$, and $S = (T_2'' - T_2')/(T_1' - T_2')$.

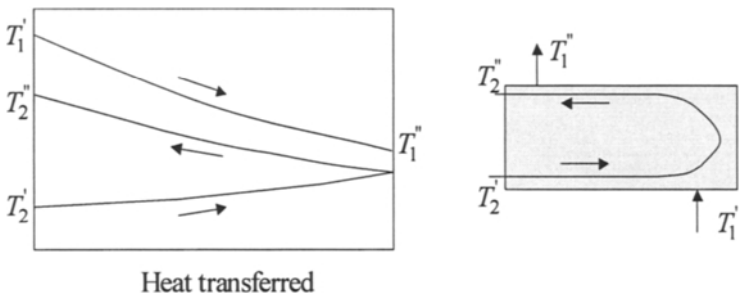

Figure 16.9 Temperature profiles for 1-2 heat exchanger

16.3.5 Shell-and-tubes heat exchangers

The shell-and-tube heat exchangers share more than 60% from the heat exchangers market. The design is well established. Figure 16.11 displays the American TEMA (Tubular Exchanger Manufacture Association) standards that are largely accepted (for details see Perry, 1997). The codification makes use of three letters that indicates the type of stationary head, shell and rear head, respectively. One of the most common type is AES or AEL that designate removable channel and cover (A), one-pass shell (E) and fixed tube sheet (L) or floating-rear (S). A similar type is BEM but with bonnet-type cover. The type A is preferred when fouling in tubes is likely. The types NEN designates channel integral with tube sheets and removable cover.

In preliminary design the problem is the selection of the right type of exchanger and its sizing that complies with design specifications. Conversely, the design should be developed such to use as much as possible standard heat exchangers. The designer should decide which side, shell or tube, is appropriate for each fluid, and find a compromise between heat-transfer intensity and maximum pressure drop. For example, cooling water passes usually through tubes in low-pressure condensers. When the flow velocity is insufficient to ensure high transfer coefficient more than one-pass is recommended, as 2, 4, or 6 passes. However, at higher pressures the tubes are more appropriate for condensing, while the cooling water is better fed in the shell side, where the fluid velocity can be manipulated by means of baffles.

Some rules for fluid allocation are mentioned briefly:

1. Corrosion: most corrosive fluid to the tube-side.
2. Fouling: fouling fluids in tubes.
3. Fluid temperatures: high temperature fluid in tubes.
4. Pressure: high-pressure fluids in tubes.
5. Pressure drop: lower pressure drop can be obtained in one or two passes.
6. Condensing steam and vapour at low pressures: shell side.
7. Condensing gas-liquid mixtures: tube-side with vertical position.
8. Stainless and special steels: corresponding fluid in tubes.

Allowable pressure drop is one of the key design parameters. This is in general of 0.5 to 0.7 bar for liquids, occasionally larger for tube-side flow, and of 0.1 for gases.

The shell diameter depends on the number of tubes housed, as well as the limitations set by pressure and temperature. The diameter may vary between 0.3 and 3 m. High values are valid for fixed-tube sheet. If removable bundle is necessary then the shell diameter is limited to 1.5 m.

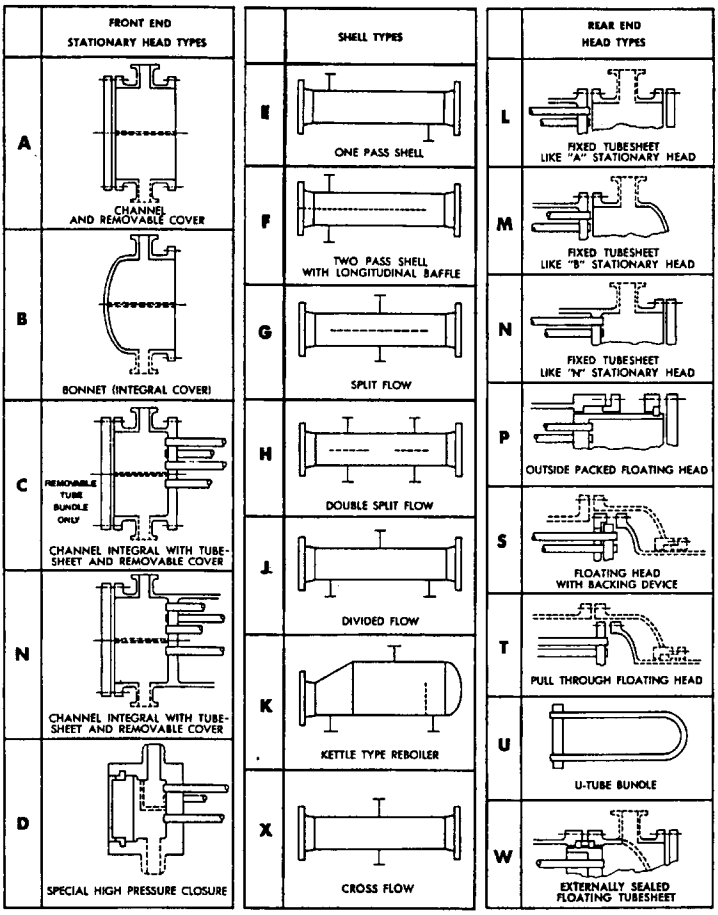

Figure 16.10 Type of shell-and-tubes heat exchangers following TEMA standards (reproduced from Perry's Chemical Engineers Handbook)

Tube size is designated by outside diameter O.D.) x thickness x length. Diameters are normalised in inch or mm. Examples are 1/4, 3/8, 1/2, 5/8, 3/4, 1, 1¼, and 1½ inches. Tubes of 3/4 in or schedule 40 (19/15 mm), as well as 1 in (25/21 mm) are the most used. Tube lengths may be at any value up to 12 m, the more common values being of 6, 9, and 10 m.

Triangular layout of tubes is the most encountered. The tube pitch is 1.25 times the outside diameter. Exact tube counting can be obtained by means of specialised design programs. For preliminary calculations the number of tubes can be found by means of relations based on the factor $C = (D/d) - 36$, where D and d are bundle and tube outside diameters, respectively. The total number of tubes N_t can be calculated by means of the following relations (Perry, 1997):

1 tube pass: $N_t = 1298 + 74.86C + 1.283C^2 - 0.0078C^3 - 0.0006C^4$

2 tube pass: $N_t = 1266 + 73.58C + 1.234C^2 - 0.0071C^3 - 0.0005C^4$

4 tube pass: $N_t = 1196 + 70.79C + 1.180C^2 - 0.0059C^3 - 0.0004C^4$

6 tubes pass: $N_t = 1166 + 70.72C + 1.269C^2 - 0.0074C^3 - 0.0006C^4$

As illustration Table 16.13 shows some layouts for ¾ and 1 inch O. D. tubes.

Table 16.13 Shell and tubes layout

Shell	One pass		Two-pass		Four pass	
I. D., in	¾ in O.D.	1 in O.D.	¾ in O.D.	1 in O.D.	¾ in O.D.	1 in O.D.
8	37	21	30	16	24	16
12	92	55	82	52	76	48
15 ¼	151	91	138	86	122	80
21 ¼	316	199	302	188	278	170
25	470	294	452	282	422	256
31	745	472	728	454	678	430
37	1074	674	1044	664	1012	632

Note that double-pipe heat exchangers are widely used for smaller flow rates. When the heat transfer coefficient outside is too low, a solution consists of using longitudinal finned tubes as extended surface.

16.3.6 Air cooled heat exchangers

Air-cooled heat exchangers are employed on large scale as condensers of distillation columns or process coolers. The approach temperature - the difference between process outlet temperature and dry-bulb air temperature - is typically of 8 to 14 °C above the temperature of the four consecutive warmest months. By air-humidification this difference can be reduced to 5 °C. Air cooled heat exchangers are manufactured from finned tubes. Typical ratio of extended to bare tube area is 15:1 to 20:1. Finned tubes are efficient when the heat transfer coefficient outside the tubes is much lower than inside the tubes. The only way to increase the heat transferred on the air-side is to extend the exchange area available. In this way the extended surface offered by fins increases significantly the heat duty. For example, the outside heat transfer coefficient increases from 10-15 W/m^{2}K for smooth tubes to 100-150 or more when finned tubes are used. Typical overall heat transfer coefficients are given in Table 16.10. The correction factor F_T for LMTD is about 0.8.

16.3.7 Compact heat exchangers

Compact heat exchangers (CHEs) are characterised by high efficiency in reduced volume, but much higher cost. If area density of the shell-and-tubes heat exchangers can achieve $100 m^2/m^3$, the compact heat exchangers have significantly higher values, between 200 and 1500 m^2/m^3. However, because of higher cost, the CHEs are employed in special applications. Some common types are briefly presented.

Plate heat exchangers

These devices are similar with plate filters. Because of small cross section, intensive heat transfer can be realised, as for example from 400 W/m^2K with viscous fluids up to 6000 W/m^2 K for water. Gasket plate devices are the most common. The effective area per plate can be larger than 1 m^2. Up to 400 plates can be assembled in a frame. However, the operation is limited to 30 bars and 250 °C. Plate heat exchanger are intensively used in food and pharmaceutical industry, but less in chemical industries. Welded plate heat exchangers are similar. The operation can rise to 80 bars and 500 °C, but cleaning is problematic.

Plate-fin heat exchangers are manufactured by assembling plates separated by corrugated sheets, which form the fins. The plates are made from aluminium sealed by brazing. The operation of these devices requires clean fluids. The main applications can be found in cryogenic and natural gas liquefaction for pressures and temperatures up to 60 bars and 150 °C.

Spiral plate exchangers

Spiral plate exchangers are usually of two types: spiral-plate and spiral-tubes. Very intensive heat transfer can be achieved, with transfer area per unit up to 250 m^2. The operation is limited to 20 bars and 400 °C. However, the cost of such devices is high.

16.4 TRANSPORT OF FLUIDS

16.4.1 Compressors

In computer simulation the (ideal) compression work in adiabatic operation is calculated usually as the variation in enthalpy of the gas mixture between initial state P_1, T_1 and final state P_2, T_2 (see also eq. 5.20):

$$W_s = F_G\left[H(P_2,T_2) - H(P_1,T_1)\right] \tag{16.49}$$

where F_G is the mass gas flow rate and H is the mass gas enthalpy. Eq. 16.49 is completed with the condition of isentropic compression $S_1(P_1,T_1) = S_2(P_2,T_2)$. The enthalpy and entropy of a gas mixture in different conditions of pressure and

temperature can be determined accurately from a PVT relation, for example by using an equation of state or three-parameter corresponding states law (see Chapter 5).

Another possibility used for shortcut calculations with unary gases is based on the analogy with an ideal gas. The first law for an open system gives $dH = \delta Q + VdP$. If the transformation is adiabatic $\delta Q = 0$ and $dH = VdP = dW_s$. The shaft work becomes $W_s = \int_{P_1}^{P_2} VdP$. Introducing the heat capacity ratio $\gamma = C_P / C_V$ the theoretical power for a single stage compressor can be obtained as:

$$W_s = F_G RT_1 \frac{\gamma}{\gamma - 1}\left[\left(\frac{P_2}{P_1}\right)^{(\gamma-1)/\gamma} - 1\right] \tag{16.50}$$

The temperature variation is given by $\frac{T_2}{T_1} = \left(\frac{P_2}{P_1}\right)^{(\gamma-1)/\gamma}$.

For larger pressure differences multi-stage compression are needed. The overall work in staged compression with intermediate cooling is significantly lower than in a single stage. The pressure interval between the initial pressure P_0 and the final pressure P_N can be split in N equal compression ratios such as $R = \left(P_N / P_0\right)^{1/N}$. If after each stage the gas is cooled at T_1, then the total power is obtained by summing the partial power of stages, leading to:

$$W = F_G RT_1 \frac{N\gamma}{\gamma - 1}\left[\left(\frac{P_2}{P_1}\right)^{(\gamma-1)/\gamma N} - 1\right] \tag{16.51}$$

The real shaft power is obtained by dividing the theoretical power by compression efficiency, generally 0.75, and by transmission efficiency, generally 0.8 to 0.9.

The selection of the type of compressor depends on pressure drop, type of fluid and gas flow rate (Table 16.14). For low pressures and smaller flow rates blowers and centrifugal fans are used. Multistage turbo-compressors are applied for higher pressures and larger flow rates. For very high pressures reciprocating compressor are used. The cost of a reciprocating compressor is about 30% more expensive than similar centrifugal type. For a more complete discussion see Perry (1997).

Table 16.14 Guidelines for compressor selection

Type	Maximum Speed (rpm)	Maximum capacity (m^3/h)	Compression ratio	Maximum pressure, bar
Axial flow fan	1000	150000	0.35	2
Turbo blower	3000	10000	0.3	1.5
Turbo compressor	10000	150000	3.5	100
Reciprocating	300	100000	3.5	5000

For vacuum production reciprocating, rotary positive displacement and liquid ring pumps can be used to pressures from 200 to 10 mmHg. Alternatively steam ejectors can be used when water self is a product, as in evaporation of aqueous solutions. The residual pressures can be lowered under 1 mmHg by using several ejectors in series.

16.4.2 Pumps

The power for pumping can be found by multiplying the volumetric flow rate Q_V by the total pressure head ΔP_t:

$$P = Q_V \Delta P_t \tag{16.52}$$

The pressure head includes the pressure difference between the supply and storage points, the pressure due to height difference, as well as the pressure drop due to friction:

$$\Delta P = (P_2 - P_1) + (h_2\rho_2 - h_1\rho_1)g + \lambda \frac{L}{d^5} \frac{8}{\pi^2} \frac{Q_V^2}{\bar{\rho}_L} \tag{16.53}$$

The friction coefficient in the transmission lines is given in general by the relation:

$$\lambda = C\,\mathrm{Re}^m \tag{16.54}$$

Recommended values for Newtonian liquids are C=0.16 and m=-0.20.

16.5 REFERENCES

Doherty, M., M. Malone, 2001, Synthesis of Distillation Systems, McGraw-Hill

McCabe, W. L., Smith, J. C., Harriott, P., 1992, Unit Operations of Chemical Engineering, 5th ed., McGraw-Hill

Eckert, J. S., 1988, Design of Packed Columns, in Handbook of Separation Techniques (editor A. Schweitzer), McGraw-Hill

Kister, H. Z., 1992, Distillation Design, McGraw-Hill

Linnhoff, B., D. W. Townsend, D. Boland, G. F. Hewitt, B. Thomas, A. R. Guy, R. H Marsland, 1982, 1994 (2th edition), User Guide on Process Integration for the Efficient Use of Energy, The Institution of Chemical Engineers

Hewitt, G. F., Shires, G. L., Bott, T. R., 1994, Process heat transfer, CRC Press

Perry's, Chemical Engineers Handbook, 7th ed., 1997

Seader, J. D., Henley, E. J., 1998, Separation Process Principles, Wiley

Sinnot, R.K, Coulson & Richardson's Chemical Engineering vol. 6, 1993

Stichlmair, J. G., J. R. Fair, 1999, Distillation, Principles and Practice, Willey-VCH

Taterson G. G., 1991, Fluid Mixing and Gas Dispersion in Agitated Tanks, McGraw-Hill

Ullmann's Encyclopaedia of Industrial Chemistry, 1990

Walas, S., 1977, Chemical Reactors, in Perry's Handbook of Chemical Engineers

Chapter 17

CASE STUDIES

17.1 Design and simulation of HDA plant
17.1.1 Flowsheet development
17.1.2 Preliminary design and simulation
17.1.3 Optimisation of material balance
17.1.4 Energy integration
17.1.5 Rigorous steady-state simulation

17.2 Dynamic simulation of the HDA plant
17.2.1 Plantwide control strategy
17.2.2 Control of the heat integrated reaction loop
17.2.3 Control of the separation section
17.2.4 Control of the flash
17.2.5 Plantwide control of the HDA plant

17.3 Control of impurities in a complex plant
17.3.1 Methodology
17.3.2 Process description
17.3.3 Plant Simulation Model
17.3.4 Plantwide control problem
17.3.5 Steady state controllability analysis
17.3.6 Dynamic controllability analysis

17.4 References

17.1 DESIGN AND SIMULATION OF HDA PLANT

HDA process has been used in several chapters of this book, particularly in developing the hierarchical approach of process synthesis. Here we present a complete treatment of the aspects raised before, which may serve also as a guide on how to use simulation throughout a design project.

17.1.1 Flowsheet development

The main reaction is the transformation of toluene to benzene in the presence of hydrogen. By-products are diphenyl, naphtalene and other heavy hydrocarbons.

$$Toluene\ (T) + H_2\ (H) \rightarrow Benzene\ (B) + CH_4\ (M) \tag{17.1}$$

$$Benzene \leftrightarrow Diphenyl\ (D) + H_2 \tag{17.2}$$

The reaction conditions are temperature 620-700 °C and pressure 25-35 bar. High excess of H_2 is necessary at the reactor entry to prevent coke formation. Here we consider that keeping a constant ratio hydrogen/toluene of 5/1 is a requirement of technology. Raw materials are pure toluene and H_2 with 5 % CH_4. Benzene product should be over 99.9 % purity.

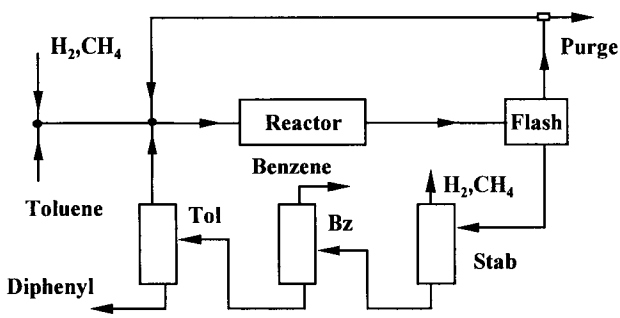

Figure 17.1 Simplified flowsheet for the HDA process

Figure 17.1 presents a simplified flowsheet, as developed in Chapter 7. Fresh raw materials mixed with recycled toluene and hydrogen is heated up to the reaction temperature. The reaction takes place in an adiabatic plug flow reactor. The reactor outlet is quenched with recycled hydrocarbon to prevent coke formation. Finally, the reaction mixture is cooled at 33 °C, and separated in a flash vessel in gas and liquid.

The gaseous stream contains hydrogen and methane with traces of benzene and toluene. The secondary product, methane, should be recovered before recycling hydrogen. This would imply a costly cryogenic distillation or membrane unit. In this case a simpler solution is to use a purge. However, the loss in hydrogen must be completed with an excess in feed. The recycle of hydrogen must also ensure a constant

ratio hydrogen/hydrocarbon at the reactor inlet. Thus, the excess of hydrogen in feed and the loss in purge are linked through the material balance. This feature has important consequences on both design and control of the whole plant.

The liquid stream contains benzene and toluene, as well as heavy impurities, mainly diphenyl, with traces of dissolved gases. The gaseous components are removed in a stabiliser, followed by the separation of the liquid mixture by distillation either as two-column sequence (benzene production and toluene recycling), or as single side-stream column.

The existence of two recycles sets an optimum for the reaction conversion. Higher conversion minimises the gas recycle cost, but increases the cost of liquid separations because of by-products and impurities. Economic Potential indicates that the optimal conversion should be between 70 and 80%.

17.1.2 Preliminary design and simulation

Energy integration is not necessary in preliminary design, so that the analysis can handle only the material balance.

17.1.2.1 Reaction section

The simulation of the reactor can be treated based on 1) stoichiometry and/or yield correlation, 2) kinetics for the main reaction and chemical equilibrium for the second, and 3) kinetics for the main reaction, followed by stoichiometry or yield correlation for secondary reactions.

We considered the following kinetic equation for the main reaction (Douglas, 1988):

$$r_1 = k_1 c_T c_H^{1/2} = 6.3e+10 exp(-52000/RT) \quad \text{kmol/m}^3\text{s} \tag{17.3}$$

Selectivity of the secondary reaction is:

$$S = 1 - 0.0036/(1-x_T)^{1.55} \tag{17.4}$$

S being the fractional amount of benzene transformed in di-phenyl, and x_T toluene conversion.

The reaction rate becomes commercially interesting above 620 °C, but the reaction temperature is limited to 710 °C. Because the adiabatic temperature rise is of about 70°C, the maximum inlet temperature is considered 640 °C.

17.1.2.2 Separations

There is no short-cut method for stabiliser, but this can be easily simulated as a distillation column with vapour distillate. The feed should be sent close to the top. For the separation benzene/toluene and toluene/di-phenyl a short-cut method as Fenske-Underwood-Gilliland can be used. R/R_{min}=1.2 or N/N_{min}=2 may be taken in a preliminary design. Note that the use of design models in preliminary simulation makes converge easier the recycles by guarantying the specifications. Obviously, the short-cut design must be reliable in order to fulfil later the specifications in rating mode.

17.1.2.3 Simulation

This case study has been simulated with ASPEN Plus™ and Aspen Dynamics™ version 10.1, but the approach remains valid for other software (Fig. 17.2).

A first issue is the thermodynamic modelling. For the high-pressure part including the stabiliser, an equation-of-state model is appropriate, as for example Peng-Robinson or Soave-Redlich-Kwong. A specific model for hydrocarbons, as Chao-Seader or Grayson-Streed, may be used equally for the low-pressure part.

The PFR model is built-up by using a kinetics for the main reaction followed by selectivity computation by inline-FORTRAN. Preliminary design considers an inlet temperature of 630 °C, and the conversion per pass of 0.7. By taking into account the effect of recycles, a reaction time of about 80 seconds and a volume of about 100 m^3 is found. The following geometry is proposed: diameter 2.8 m, length 16m. These values indicate that the reaction rate is very slow compared with other thermal cracking reactions. The linear velocity is of about 0.2 m/s, a very low value for homogeneous gas reaction, but normal for a solid catalyst reactor. Alternatively, several reactors in parallel might be considered.

Heating and cooling of streams to and out the reactor are simulated in preliminary design by simple heat exchangers. Quench has been simulated by a 'design-specification' that keeps the temperature at 620 °C by manipulating the flow rate of a splitter after the flash. A pressure drop of 3 bars is assumed for the whole gas line.

The liquid separation section may be simulated initially as a black-box. Rigorous units can be considered later after convergence of recycles.

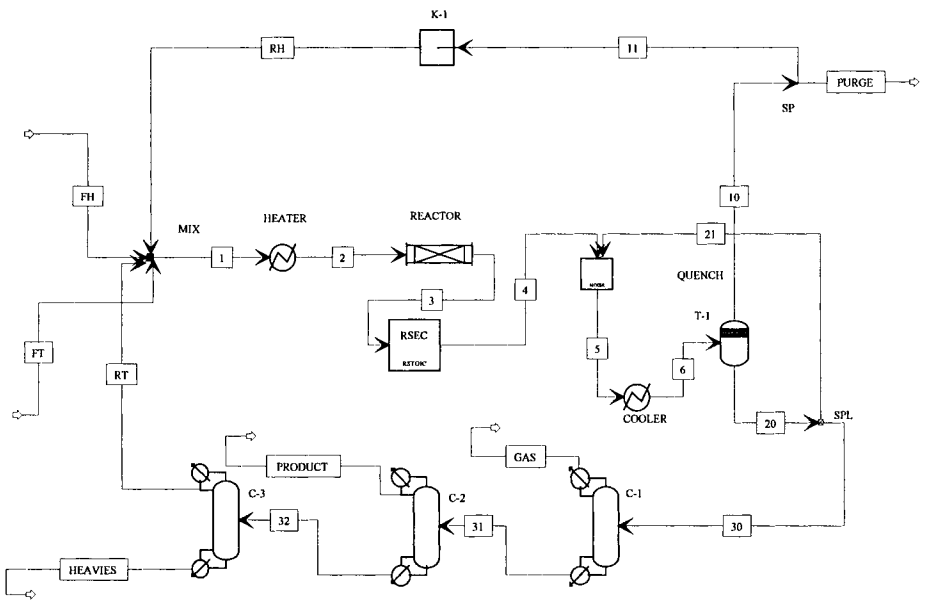

Figure 17.2 Preliminary Process Simulation Diagram

An important feature in this problem is that the material balance of the recycle system must be adapted to fulfil the constraint of a given ratio hydrogen/toluene at the reactor inlet. This has been done by means of a design specification, where the manipulated variable is the fresh feed of hydrogen.

A debatable point is the specification of purge. Fixing a purge flow rate or composition is not feasible, because of incompatibility with the overall material balance (see feasible specifications in Chapter 3). On the contrary, setting the purge as split ratio leads always to convergence. Note that in this study we have chosen to keep constant the flow rate of the gas recycle. This is rational, because the compressor is an expensive piece of equipment, which operates preferably at constant flow rate, close to the maximum capacity.

17.1.2.4 Preliminary material balance

The objective of preliminary simulation is to obtain a good operation point from material balance viewpoint. Table 17.1 presents the main streams of the simplified flowsheet. Fresh feed toluene of 125 kmol/h corresponds to a production of about 120 kmol/h benzene. The gas recycle has been set at 1500 kmol/h. With the constraint of a hydrogen/toluene ratio mentioned, the fresh hydrogen flow is 223.9 kmol/h. The feed of reactor is simply obtained by adding the first four columns of the Table 17.1. Thus the partial flow rate of toluene before the reactor is 0+125+1.22+48.63=174.8 kmol/h. Hence, the toluene conversion is (174.8-50.1)/174.8=0.713. The above hydrogen excess gives a molar fraction of hydrogen in purge of 0.434.

Table 17.1 Preliminary material balance

	Feed H	Feed T	Rec. H	Rec. T	R out	Product	Heavies	Purge	Gas
Temp. C	37.90	50	42.6	33	677.3	33	33	33	33
Pres. bar	37.5	37	35	32	34	32	32	32	32
Flow, kmol/h	235.7	125	1500	48.634	1909.3	120.24	1.61	230.43	8.42
Toluene	0	125	1.22	48.63	50.1	0.01	0.05	0.19	0
Hydrogen	223.91	0	650.36	0	749.52	0	0	99.91	0.80
Benzene	0	0	9.086	0	133.84	120.23	0	1.40	0.01
Methane	11.78	0	839.33	0	975.87	0	0	128.94	7.60
Diphenyl	0	0	0	0	0	0	1.56	0	0

17.1.3 Optimisation of material balance

At this point we may proceed by introducing more rigorous units, and refine the material balance. However, it will be interesting to consider the optimisation problem. There is obviously a trade-off of conversion, recycle flow rate and fresh-hydrogen feed that should be examined with respect to the Economic Potential. A preliminary screening of the optimal conversion has been presented in Chapter 7. The degradation of selectivity at conversion above 0.8 sets an upper limit already at the Level 2 of the Hierarchical Methodology. At the Levels 3 and 4 the cost of recycles sets a lower limit. Consequently, the objective function is the Economic Potential at the Level 4, with gas and liquid recycles, the optimisation variables being those affecting the production, as reactor length and reaction inlet temperature, as well as the gas recycle flow rate and the fresh hydrogen feed.

17.1.3.1 Objective function

Economic Potential is the income obtained from selling products and by-products, minus expenses, which include both the cost of raw materials and operating costs. Material costs are determinant, but submitted to large uncertainty. The difference between the prices of toluene and benzene should be sufficient to ensure a profitable process (Table 17.2). As noted in Chenier[1], the price of toluene should be at least of 132 $/tonne. In the 1990 decade the price of benzene oscillated between 1 and 2 $/gallon, or between 260 and 520 $/ton. Sub-products, heavies, gas purge and gas distillate, may be used as fuel in the process itself. It is rational to consider prices comparable with the replaced commercial fuel.

Table 17.2 Prices for HDA process

	Benzene	Toluene	H_2	Heavies (liquid fuel)	Purge (Gas fuel)	Gas
Price, $/tonne	350	170	1000	50	50	50

We consider an annual operation time of 8150 h. With the above data the Economic Potential regarding only the materials is 6.741.469 $/yr.

In the second step we introduce cost elements sensitive to recycles. For gas recycle we should account for the cost of compression plus compressor depreciation, both on annual basis. For liquid recycle we should consider the operating costs of the distillation column plus the recovery of investment. Preliminary heat integration around the chemical reactor has a feed-effluent heat exchanger (FEHE), as well as a furnace, necessary for start-up and control (Figure 17.3). A rigorous analysis will be present in the next section.

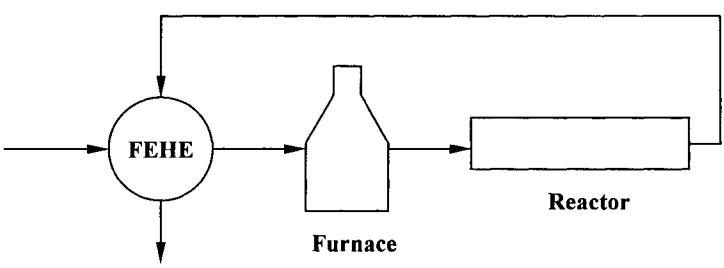

Figure 17.3 Preliminary heat integration around the chemical reactor

Equations suitable for analytical computation of installed cost of vessels, heat exchangers, compressors, and column internals may be found in the Annexe A. We consider a Marshall & Swift factor XMS=(M&S/280)=3.786, corresponding to year 1999. Three years payback time is assumed. In-line FORTRAN instructions given

[1] Chenier, P. J., Survey of industrial chemistry, 2nd edition, VCH, 1992

below (Table 17.3) illustrate the approach. Note that the retrieved values are in metric units, while the cost equations are originally in English units. As explained in Chapter 3, in the optimisation procedure the design-specification 'hydrogen/toluene ratio equal to five' has been transformed in constraint, another manipulated variable (hydrogen feed) being added to the list of the optimisation variables.

Table 17.3 Cost equations introduced as in-line Fortran in the optimisation procedure

Category	Cost equations
Raw Materials	VP=0.35*PBZ+0.05*FUEL+0.05*PG RM=0.17*GT+1*GH EP2=8150*(VP-RM)
Reactor: 50 bar, carbon steel diameter (DR), length (RL)	CR=XMS*101.9*(DR/0.303)**1.066*(RL/0.303)**0.802 *(2.18+1.6)
Compressor: centrifugal, adiabatic operation brake-power (HPCP), net-work (ECP)	CCOMP=XMS*517.5*(HPCP/0.736/0.9)**0.82*3.11 CEL=8150*ECP*0.10 CC=CCOMP/3 + CEL
FEHE heat exchanger: outlet temperature 520 °C. duty (QFEHE). U (200 kcal/h.°C), DTM (50 °C)	AFEHE=1E6*QFEHE/200/55 CFEHE=XMS*101.3*(AFEHE/0.0929)**0.65*3.61
Furnace: duty (QFEHE).	CF=XMS*5520*(DUTYF/0.252)**0.85*(1.27+1.5)
Liquid separations (only product column) Diameter 1.5 m. Number of stages (SBZ) Height (m) = (SBZ+2)*0.6. Stage efficiency 0.7. Cost of internals: 20D $/tray. Cost of heat exchangers: 200000 $.	HCOL=(SBZ/0.7+2)*0.6 CCOL=XMS*101.9*(1.5/0.303)**1.066*(HCOL/0.30)** 0.802*(3.18) CBZ=CCOL+2000*SBZ/0.7 CSEP=200000+CBZ
Objective function	EP3=EP2-CC-CF/3-CFEHE/3-CSEP/3 Constraint 1: outlet reactor temperature below 710 °C. Constraint 2: Hydrogen/toluene at reactor inlet set to 5.
Range of the manipulated variables	Reactor length: 16 - 19 m Reactor temperature: 620-640 C Recycle flow rate: 1400 - 2100 kmol/h Hydrogen feed: 200 - 300 kmol/h

17.1.3.2 Sensitivity

Before any optimisation, it is highly recommended to investigate the feasibility by a sensitivity study. Figure 17.4 presents the variation of the economic potential as function of gas recycle and reactor length. It may be observed that the optimum is reached at the maximum reactor length and high recycle flow rate. It is interesting to note that the purge concentration does not vary too much, floating around 0.4. This confirms that there is not need to design the plant for constant purge concentration, but rather for constant (high) gas recycle flow.

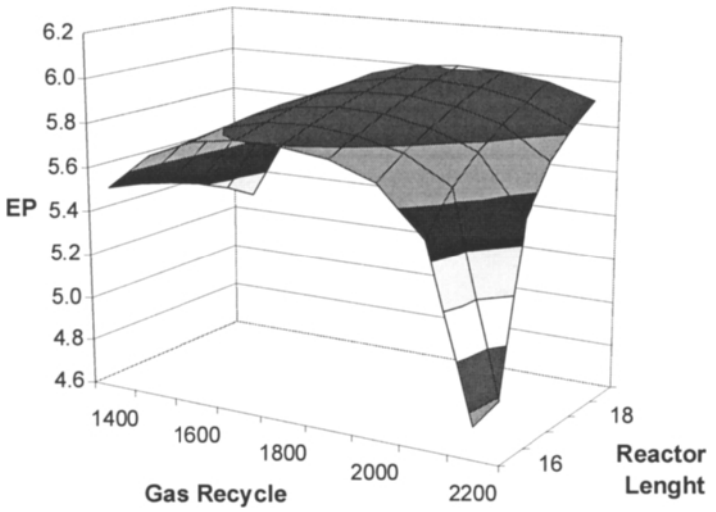

Figure 17.4 Sensitivity of objective function with respect of gas recycle and reactor length

17.1.3.3 Optimisation

ASPEN Plus makes use of an SQP algorithm for optimisation. The final results are:

Optimal economic potential: EP=6.35E6 $
Reactor length: RL=19 m (maximum)
Temperature: TR=640 C (maximum)
Recycle flow rate: RH=2191.4 kmol/h (2300 max)
Hydrogen flow rate: FH=201.62 kmol/h

The optimal reaction conversion is 0.646, and the purge hydrogen concentration of 0.35. Note that higher operation costs bring the optimum to higher conversion, lower recycle rate and higher fresh hydrogen flow rate, but the effect is limited. Thus, if the operation costs increase by a factor of four, then the optimal values are RL=19 m, TR=633.5 °C, RH=1615 kmol/h, FH=214.4 kmol/h, which corresponds to a conversion of 0.75, and a purge concentration of 0.386.

The robustness of the solution may be checked by means of *sensitivity analysis*. An important issue is that the 'optimal' design should be able to handle large variations in throughput. Table 17.4 presents three cases: the nominal operating point and +/- 12% variation in throughput. When increased production is required, the inlet reactor temperature must be to maximum, the recycle flow rate going to the upper boundary, while the fresh hydrogen feed increases more than proportional. Thus, increase in throughput is paid by more hydrogen loss in purge. Two situations are presented when the throughput decreases: a shorter reactor and lower gas recycle, but a higher consumption of hydrogen (column three), as well as a longer reactor with a larger recycle, but smaller hydrogen excess (column four). The last is compatible with the optimal design.

In conclusion, the optimal plant design should have a reactor length of 19 m, maximum inlet temperature of 640 °C, and gas recycle flow rate of 2300 kmol/h. The compressor should be operated at its maximum capacity, but the distillation columns should be sized to cope with higher loads at increased throughput. There is not necessary to keep constant the purge concentration in hydrogen. A sensitive manipulated variable in changing the production is the make-up of hydrogen. Setting the compressor at its maximum capacity will contribute to minimise the excess of hydrogen. Note that an increased production is realised by a lower conversion per pass! This result is somewhat counterintuitive.

Table 17.4 Optimal design and flexibility

Feed toluene	kmol/h	125	140	110	110
Reactor length	m	19	19	16	19
Inlet temperature	°C	640	640	630.2	640
Feed hydrogen	kmol/h	201.6	234.4	200.0	170.9
Recycle hydrogen	kmol/h	2191.4	2300	1690.6	2000
Conversion	-	0.646	0.641	0.6	0.66
Hydrogen in purge	-	0.35	0.374	0.42	0.328

The above analysis reveals some special features of process optimisation.

1. In a multi-variable optimisation problem most of the variables are on the boundary of constraints or very close to it.
2. Because the material costs play the most important role, the optimal solution moves to the region in which the loss in selectivity is the lowest.
3. If the cost of recycles is not excessive, the optimum moves to lower conversions. The cost of gas recycles could be higher than of liquid recycles.
4. A relatively big reactor is necessary to ensure a good flexibility in production. The units involved in recycles should be oversized accordingly. The problem of the proper reactor size in recycles, and particularly in the HDA process, has been treated rigorously by Bildea et al. (2002). The design of the reactor should avoid the region of maximum sensitivity situated around the turning point in a conversion-Damköhler Diagram (see Chapter 13).
5. A compressor in a recycle should be operated at its maximum capacity.

17.1.4 Energy integration

Here we adopt the principle of integration of sub-systems. We do not consider the heat integration of the reactor loop with the liquid separation system for controllability reasons. The excess of heat can be exported to the utility network, eventually to be re-imported as steam for the distillation section at adequate pressure levels.

17.1.4.1 Reactor system

In the first step we examine the possibility of heat integration of streams around the reactor. In a first approach we may disregard the quench. Table 17.5 presents the stream population for an operating point at a conversion of about 77 %.

Table 17.5 Stream population for heat integration around the reactor

	T_s , °C	T_t, °C	ΔH kW	MCP (W/kg/°C)
Reactor inlet	42.5	630	18600	31.74
Reactor outlet	677.5	33	-20100	31.18

The overall balance gives an excess of 1500 kW, so the problem does not require hot utility. There is need only for cold utility (cooling water). Thus, feed preheating may be covered exclusively by the exothermic reaction and save a significant amount of energy. However, a furnace is necessary before reactor to ensure constant temperature. The reactor outlet is quenched at 620 °C. Assume that the furnace has to preheat the reaction mixture from 520 °C to a reaction temperature of 630 °C. By simulation we find a duty of 3800 kW. The new stream population for heat integration becomes:

Table 17.6 Streams for integration without furnace

	T_s , °C	T_t, °C	DH (kW)	CP (W/kg/°C)
R_preheat	43.5	520	14800	31.0
R_outlet	620	33	20100	33.7

The problem requires again only cold utility. Besides cooling water we may consider steam generation at 250 °C (40 bar). For ΔT_{min}=10 °C the targeting procedure leads to cold utility requirements of 5300 kW. This is exactly the furnace duty plus the initial cooling duty (3800+1500=5300).

Figure 17.5 presents the heat network design in a grid diagram with SUPERTARGET™. Note that a Pinch is introduced at 250/260 °C by the hot utility. On the left side there are two matches: the steam generator (SG), and the first feed pre-heater (HX1). On the right side there are also two matches: a second feed pre-heater (HX2), and a final cooler (COOL). Figure 17.6 shows more clearly the flowsheet of the heat integrated loop around the chemical reactor (*alternative A*).

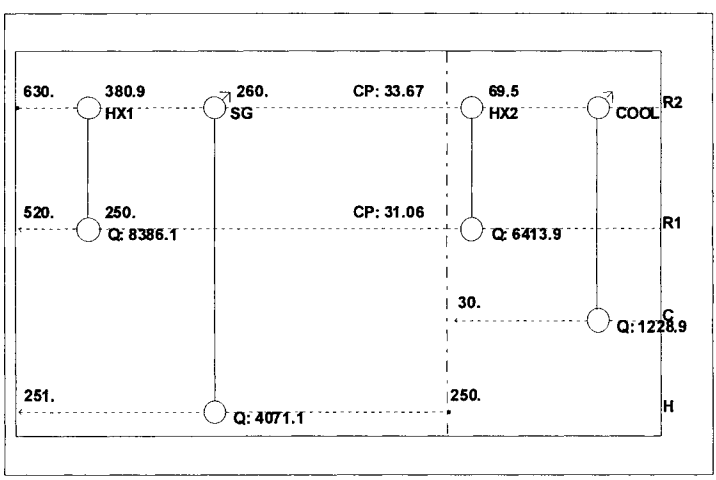

Figure 17.5 Heat exchanger network design around the reactor

There is also an *alternative B* with only a single pre-heater HX1 and a steam generator (SG). Both alternatives have been simulated successfully, the operating points being very close. Table 17.6 presents duties and temperatures for the heat exchangers. In both cases the process/process heat exchange is of about 14800 kW. *Alternative A* delivers 4000 kW high-pressure steam, and requires cooling water of about 1270 kW. In *alternative B* the steam production is lower of about 22%, while the cooling duty increases in the same proportion. Hence, the first alternative offers better heat integration, by a better use of the driving force between the hot and cold streams.

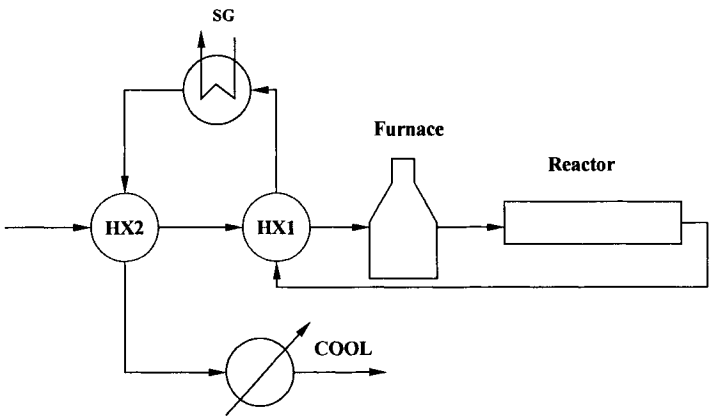

Figure 17.6 Heat integrated reactor loop

Table 17.7 Comparison of alternatives for heat integration of the chemical reactor

	Alternative A		Alternative B	
Feed preheating	HX1:	HX2:	HX1:	
	620 → 387 °C	267 → 72 °C	533 → 91.2 °C	
	244 ← 529 °C	43.5 ← 244 °C	43.5 ← 520 °C	
	Q: 8370 kW	Q:6400 kW	Q: 14790 kW	
Furnace	520 → 630 °C	Q: 3800 kW	520 → 630 °C	Q: 3800 kW
Steam generator	620 → 533 °C	Q: 3275 kW	387 → 257.5 °C	Q: 4000 kW
Cooler	72 → 33 °C	Q: 1270 kW	91.2 → 33 °C	Q: 2050

17.1.4.2 Liquid separation section

The synthesis of the liquid separation system for the HDA process has been discussed in Chapter 7. The flowsheet consists of three columns: C-1 (stabiliser), C-2 (production), and (C-3) recycle. For the same operation point discussed before Table 17.8 presents some characteristics of the three columns. Note that a cooler (duty 730 kW) should be inserted before the column C-2 to bring the feed at its bubble point. The design is valid for a benzene purity of 99.8 %, as well as for a loss of toluene in Heavies of about 0.4%, imposed by the limitation of reboiler temperature in the recycle column below 200 °C.

Table 17.8 Simulation results for the separation section

	C-1	C-2	C-3
N_{stages}	6	31	7
R/D	R=200 kg/h	1.136	0.167
P_c, bar	11	1.1	1.1
T_c, °C	32	82.9	113.5
T_r, °C	193	124.9	189
Q_c, kW	35	2200	370
Q_r, kW	1160	2190	360

Let us examine the potential heat integration of the columns C-2 and C-3. The temperature difference between the reboiler of the first and the condenser of the second is small. Actually, the fluid in both units is practically the toluene. Rising the pressure of the column C-3 at 2 bar would ensure a difference of 20 °C for the thermal coupling. The saving is of about 16%. More advantageous is to consider a column with side-stream. If low purity benzene is accepted this is the best solution. If high purity benzene should be produced, the solution with two columns is more suitable.

17.1.5 Rigorous steady-state simulation

The above presentation leads to the flowsheet shown in Fig. 17.7. The scheme can be simulated now with rigorous units. The sizing of units is also of interest both for the economic evaluation, as well as for preparing the dynamic simulation. Results are available as stream table for the whole process, performance characteristics for units, as well as sizing elements. They can be exported to a spreadsheet, for editing specification sheets or for design purposes. The complete results are not shown here, but the user is encouraged to reproduce the above steps with his favourite simulator.

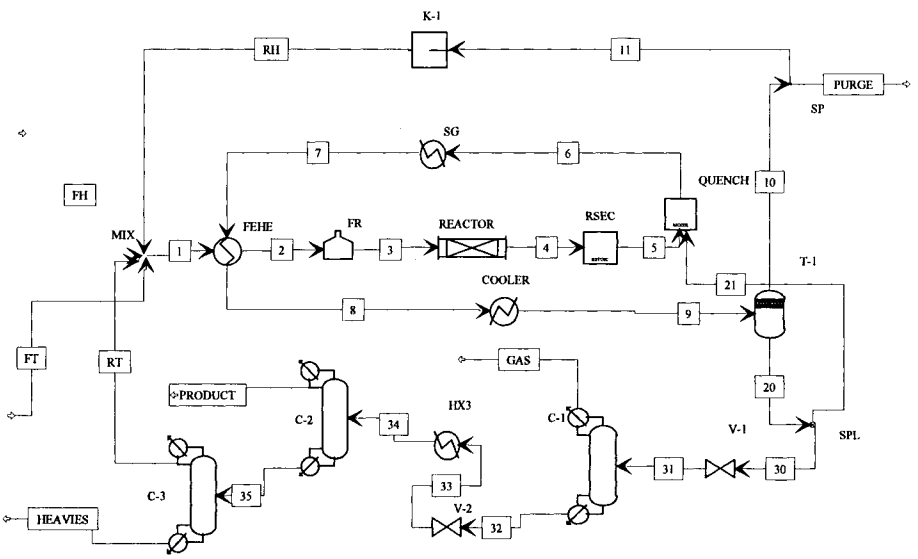

Figure 17.7 Steady-state flowsheet of the HDA plant

17.2 DYNAMIC SIMULATION OF THE HDA PLANT

After developing a robust steady-state simulation, the next step is the sizing of units whose dynamics is considered. Typically these are units with a significant material inventory, as flash vessels, distillation columns, and liquid-phase reactors. Heat exchangers, pumps and compressors may be considered in many situations as reaching fast steady state.

17.2.1 Plantwide control strategy

The plantwide control philosophy has been discussed already in Chapter 13, and illustrated by Fig. 17.8. The following plantwide control structures is proposed:

1. Production. In a first approach, toluene feed is set on flow control. This is the simplest solution that may work faced to a wide disturbance spectrum, if the reactor is large enough (see Chapter 13). Alternatively, the toluene may be fed in the liquid recycle as a make-up stream for keeping constant recycle rate. This solution may accommodate large throughput variations, but the production is set indirectly by modifying the set-point of the recycle accordingly. An even better solution is to keep constant the flow before the reactor, which now includes both fresh and recycled toluene.
2. Hydrogen make-up: hydrogen/toluene ratio kept on setpoint with the fresh hydrogen feed.
3. Reaction system: inlet reactor temperature with the furnace duty.
4. Gas recycle: keep constant the recycle flow rate close to the maximum compressor capacity.
5. Gas loop pressure: keep constant the gas pressure after flash by manipulating the purge flow.

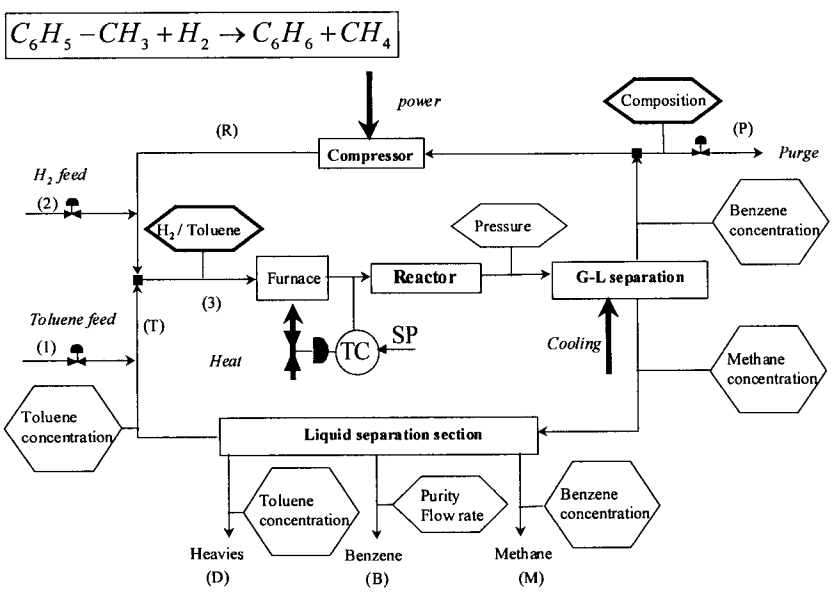

Figure 17.8 Plantwide Control of HDA plant

The control of units may follow the standard control structures applicable for stand-alone units. The HDA plant has been decomposed in several parts for an easier control implementation in Aspen Dynamics, as follows:

1. Heat integrated reaction loop.
2. Separation section.
3. Make-up of reactants.

17.2.2 Control of the heat integrated reaction loop

The flowsheet (Figure 17.9) contains a feed-effluent heat exchanger (FEHE), furnace, reactor, quench unit and steam generator. The following controllers can be considered:

- TC1: inlet reactor temperature with furnace duty,
- TC2: outlet reactor temperature with quench flow,
- PC1: outlet reactor pressure with outlet flow rate

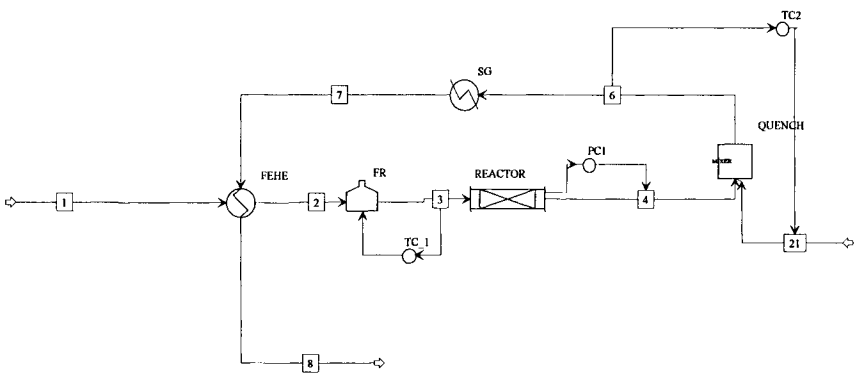

Figure 17.9 Control structure of the reaction section

The tuning may follow a simplified procedure. Let $\Delta\varepsilon_{max}$ and Δu_{max} be the maximum allowed control error and control action, respectively. Then the variable ranges are $y \pm \Delta\varepsilon_{max}$ and $u \pm \Delta u_{max}$, PI-controllers are used, with the gain $K_P = \Delta u_{max} / \Delta\varepsilon_{max}$, and integration time TI = 20 min. Table 17.9 presents the nominal operating point of the three controllers, at a nominal toluene plant throughput of 125 kmol/h.

Table 17.9 Nominal operating point of the reaction loop control

	PC1	TC1	TC2
y (output)	33.8 bar	630 °C	620 °C
$\Delta\varepsilon_{max}$	1 bar	5 °C	5 °C
u (input)	1984.6 kmol/h	3.46 Mkcal/h	59.5 kmol/h
Δu_{max}	1000 kmol/h	1.7 Mkcal/h	30 kmol/h

The robustness of the control scheme can be tested against disturbances. Steady-state simulation enable to define the spectrum of disturbances corresponding to different operation policies, as given in Table 17.10, for +/- 25 kmol/h. around the nominal value.

Table 17.10 Disturbances definition at the reactor inlet

	125 kmol/h (nominal case)	150 kmol/h	100 kmol/h
Component molar flow rates (kmol/h)			
Toluene	167.83	192.56	142.75
Hydrogen	839.18	962.84	713.75
Benzene	10.34	10.61	9.973
Methane	967.31	908.77	1035.08
Diphenyl	0.001	0.001	0

The performance of the control system is presented in Figure 17.10 for two disturbances, production increase to 150 kmol/h, as well as production decrease to 100 kmol/h.

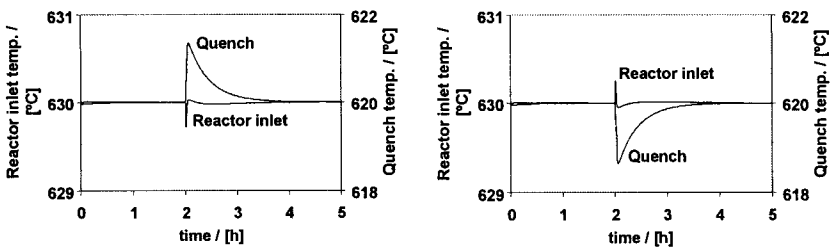

Figure 17.10 Response of the reaction system to disturbances in throughput

17.2.3 Control of the separation section

The control of the separation section is developed unit by unit by applying the standard control schemes for distillation units adapted to take into account the behaviour of the distillation column in a recycle environment.

Stabiliser. The control objective is the stripping of gases from liquid, but with minimum loss of benzene. A suitable control structure is:

- Reboiler level with bottom product.
- Reflux drum level with reflux flow rate.
- Column pressure with vapour distillate.
- Composition (inferential control) with reboiler duty.

Benzene column. The purity of distillate has to be over 99.9%, but no benzene is allowed in bottoms that could accumulate in recycle. One-point control of purity gives good results if the reflux flow rate is high enough. Setting a feed-forward scheme for reflux divided by feed allows good behaviour at large variations in throughput. The control configuration for the benzene column is:

- Level in reflux drum with distillate.
- Level in reboiler with bottoms.
- Condenser pressure with cooling water.
- Ratio reflux/feed constant with reflux flow rate.
- One point quality control: inferential concentration measurement (sensitive temperature in the rectification region) with reboiler duty.

Recycle column. This column operates more as a stripping. One-point quality control is sufficient.

- Level in reflux drum with distillate.
- Level in reboiler with bottom product.
- Condenser pressure with cooling water.
- One point quality control: inferential concentration measurement (sensitive temperature in the rectification region) with reboiler duty.

Aspen Dynamics provides implicit pressure PI-controllers, and sets the range of manipulated and controlled variables to [0, twice the nominal value]. Controller gain of 20 %/% and integration time of 12 min are used. These values are suitable. Contrary, the P level controller gain of 10 %/% seems too aggressive, and may be changed to 1 %/%.

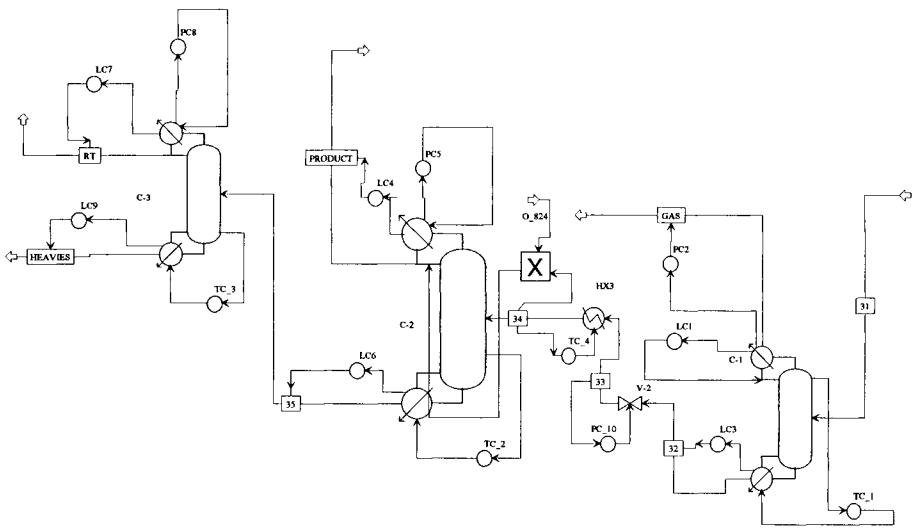

Figure 17.11 Control structure of the HDA separation section

Figure 17.11 presents the flowsheet with control implementation. Dynamic simulation showed that is essential to control the pressure after valve V2. Hence, a pressure controller PC_10 was added. It was difficult to control the condition of stream 34 using the heat exchanger HX3. For this reason, the temperature controller TC_4 is on "manual". Table 17.11 summarises the control structure of the separation section.

Table 17.11 Control structure for the separation section of the HDA plant

Item	Controlled variable			Manipulated Input			K_P	TI (min)
	Variable	Nominal value	Range	Variable	Nominal value	Range		
LC1	C-1 reflux drum level	0.925	0-1.85	Reflux	200	0-400	1	-
PC2	C-1 pressure	11	0-22	Vapour flow rate	8.63	0-17.25	20	12
LC3	C-1 sump level	1.25	0-2.5	Bottom flow rate	13500	0-27000	1	-
LC4	C-1 reflux drum level	1.875	0-3.75	Distillate flow rate	9271.4	0-18542	1	-

PC5	C-2 pressure	1.1	0-2.2	Condenser duty	-1.909	-3.82-0	20	12
LC6	C-2 sump level	1.625	0-3.25	Bottom flow rate	4233	0-8467.2	1	-
LC7	C-3 reflux drum level	1.3	0-2.6	Distillate flow rate	3849.1	0-7698.2	1	-
PC8	C-3 pressure	1.1	0-2.2	Condenser duty	-0.433	-0.866-0	20	12
LC9	C-3 sump level	1.625	0-3.25	Bottom flow rate	384.51	0-769	1	-
PC10	pressure	2	1.9-2.1	Valve opening	50	0-100	1	20
TC_1	C-1 tray 2 temperature	115.55	113.5-117.5	Reboiler duty	1.051	0.5-1.5	1	20
TC_2	C-2 tray 24 temperature	108.01	106-110	Reboiler duty	1.899	0.95-2.85	1	20
TC_3	C-3 tray 6 temperature	117.22	115-119	Reboiler duty	0.417	0.21-0.63	1	20

The disturbances seen at inlet of the separation section are available from steady state simulation. These are presented in Table 17.12. The following variables are of interest:

- Product flow rate and purity.
- Losses: benzene in stabiliser, and toluene in heavies.
- Product recycled (benzene in recycle).

Table 17.12 Disturbances for separation section of the HDA plant

	125 kmol/h (nominal case)	150 kmol/h	100 kmol/h
Component molar flow rates (kmol/h)			
Toluene	43.065	41.965	43.505
Hydrogen	0.701	0.851	0.551
Benzene	118.752	142.275	94.878
Methane	7.827	8.379	7.152
Diphenyl	1.742	2.731	1.048

Firstly, the performance of the control system is tested for a throughput increase with 20% (Fig. 17.12). The purity is only slightly affected, decreasing from 99.85% to 99.75%. However, the losses in benzene and toluene increase more than proportionally. This can be explained by an increased amount of sub-products that makes necessary to remove more useful components to respect specifications. Further reduction could be obtained by improving both the design and the control.

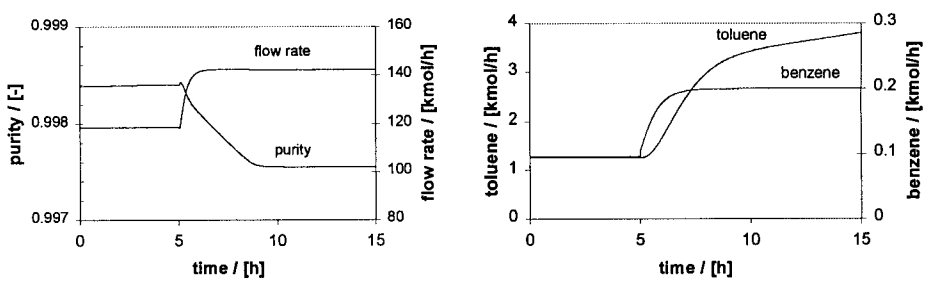

Figure 17.12 Response of the HDA separation section to an increase in production

Secondly, the effect of throughput decrease with 20% is investigated (Fig. 17.13). This time the purity is not affected, and the losses diminish.

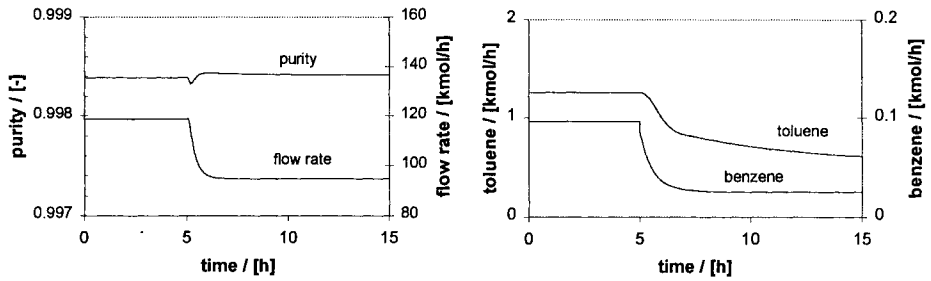

Figure 17.13 Response of the HDA separation section to a decrease in production

17.2.4 Control of the flash

The last subsystem to be analysed is the cooler and the flash vessel. This makes the connection between the reaction and separation sections. Figure 17.14 displays the control structure.

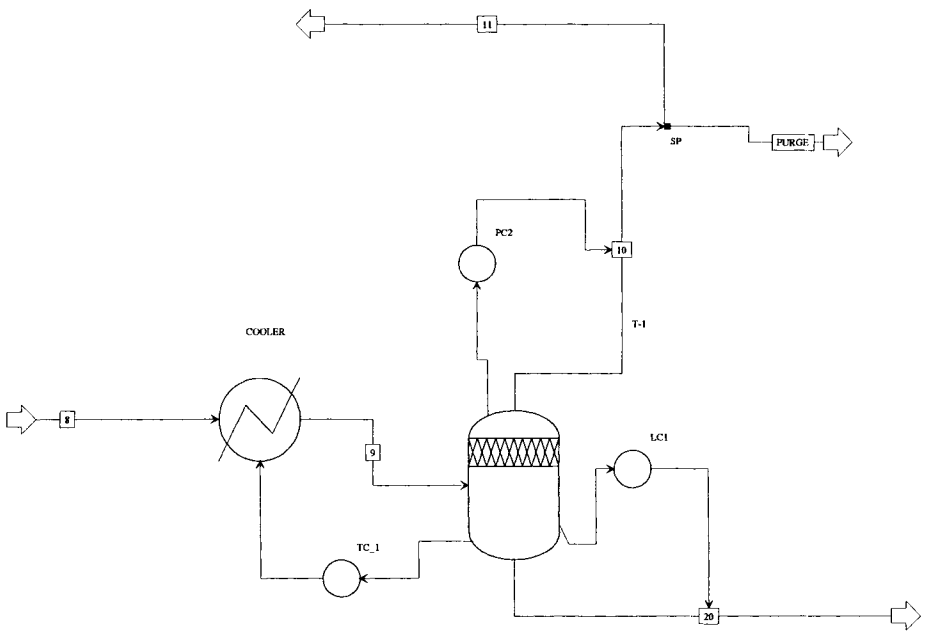

Figure 17.14 Control structure of the flash section of the HDA plant

For unknown reasons, Aspen Dynamics 10.1 does not allow the purge flow rate to be manipulated. Hence, vapour flow rate is used for pressure control. However, the gas recycle flow rate (stream 11) is set to the nominal value of 1600 kmol/h. The maximum

allowed control action (stream 10) is set to 100 kmol/h, which is about 50% of the purge flow rate. This ensures that the purge flow rate is always positive.

Table 17.13 Control structures of the flash section of the HDA plant

Item	Controlled variable			Manipulated Input			K_p	T_I (min)
	Variable	Nominal value	Range	Variable	Nominal value	Range		
LC1	Level	2.065	0-4.125	Liquid flow rate	18330	0-36660	1	-
PC2	Pressure	32	31-33	Vapour flow rate	1812	1712-1912	1	12
TC_1	Temperature	33	28-38	Cooling duty	-1.92	-3/-1	1	20

As before, the disturbances seen at flash inlet are available from the steady state simulation. Control of level, temperature and pressure is excellent. No input saturation occurs. Trends of interest are the amounts of benzene in the vapour stream and methane in the liquid stream. They follow the increase or decrease in plant throughput almost proportionally.

17.2.5 Plantwide Control of the HDA plant

In a first alternative the toluene may be set on feed control, giving a direct measure of the achievable production. Hydrogen is added such to keep constant hydrogen/toluene ratio at reactor inlet. This solution implies a composition analyser, which should not arise problems. For this controller we have the following characteristics:

- Process variable range: 4.9 ... 5.1
- Manipulated variable range: 100 ... 300 kmol/h
- Controller gain: 1 %/%
- Integration time: 20 min.

Steady-state analysis have shown that one cannot set simultaneously the ratio hydrogen/toluene and the purge flow rate, because of material balance inconsistency. For this reasons the proposed control structure let free the output.

Alternatively (Luyben, 1999), the make-up of toluene can be done in the recycle of toluene, whose flow rate can be set constant for a given production. The flow rate of fresh hydrogen can be controlled with the pressure on the gas recycle line. The purge flow can be manipulated to keep constant the amount of methane purged from the plant.

The above structures can be assembled in the control structure of the whole plant. The flowsheet has been already illustrated in Fig. 13.36. The closed-loop response of some key variables is displayed in Figure 13.37 for a nominal throughput in toluene of 125 kmol/h with increase/decrease variation of 25 kmol/h (20%) respectively. It may be seen that the plant reacts smoothly at these large variations. Note that at higher production the product purity decreases only very slightly from 0.9986 to 0.9984, but the production of Heavies is practically doubled from 3 to 6 kmol/h, mainly because more toluene lost. The same is valid for benzene lost in purge. Therefore, if the environmental regulations are regarded, the control of these two columns should be improved.

17.3 CONTROL OF IMPURITIES IN A COMPLEX PLANT

The management of impurities is an important issue both in Process Design and Operation. A key point is the interaction between these two aspects. Strict environmental regulations forbid the dump of harmful materials in the environment. Therefore waste minimisation, aiming to zero effluents, is a fundamental feature of sustainable process design. The increased number of recycles in integrated plants, makes the control and the operation much more difficult.

The inventory of impurities is a plantwide control problem, because it involves both the reaction and separation subsystems through recycles. Ideally, the inventory of each component should be traced from the source to its final destination. Recent systematic studies on the dynamics and control of the recycle systems have been started, as described in the Chapter 13. Luyben and Tyreus (1998) proposed a ten steps plantwide control design procedure (section 13.7). The step 7 consists of '*Checking component balances*: identify how chemical components enter, leave, and are generated or consumed in the process. At this stage it is necessary to find the specific mechanism or control loop to guarantee that there will be no uncontrollable build-up of any chemical component within the process'.

The present case study will show how to solve quantitatively this problem. It will be demonstrated that in the case of large complex plants the inventory of the main components and of impurities cannot be managed separately, because they are coupled through recycles. The interactions can hinder or help the solution of the problem, depending on the competition between positive and negative feedback effects. The implementation of a control structure based on the viewpoint of stand-alone units can lead to conflicts. Hence, a systemic approach based on a quantitative evaluation of the recycle effects is needed (Dimian et al., 2000, 2001).

17.3.1 Methodology

The methodology presented below is suitable to handle complicated material balance problems. Moreover, this approach enables to develop design alternatives that are not visible at the process synthesis stage. The procedure (Figure 17.15) can be summarised in the following steps:

1. Problem definition. Firstly the key components are identified. These are products, sub-products and intermediates, as well as impurities with significant effect on product quality and operation. Then the impurities are traced by means of 'tables' containing sources, sinks, exit streams, transit units and process streams. Formation and depletion of impurities must be supported by a consistent stoichiometry. Then an operating window is defined in terms of production rate, operation parameters and technological constraints. In principle, this step may identify a number of flowsheet alternatives, but supplementary alternatives may arise during the application of the procedure.

2. Calibration of a steady state Plant-Simulation-Model. This activity might be the most time consuming. For an existing plant, it can be combined with data reconciliation, although this can be applied with reasonable accuracy only for the main components.

The tuning of the stoichiometry, as well as the identification of parameters in the thermodynamic models could be done in a systematic manner by applying a V-lifecycle modelling (Chapter 2).

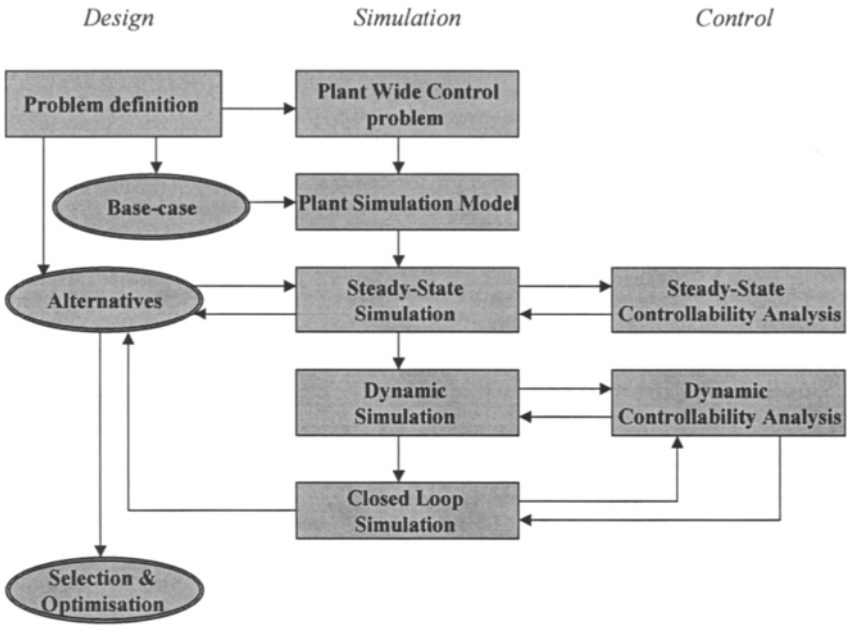

Figure 17.15 Methodology for the control of impurities in a complex plant

3. Plantwide control problem.

a. *Control objectives.* The strategic plantwide control objective is the minimisation of the total process waste. Potential toxic material must be converted in benign material, or to be stored and sent to post-treatment. Key impurities are considered those that are object of analytical control procedures, both in reactants and products, as well as internal process streams.

b. *Process constraints.* These are maximum tolerable amounts or/and concentrations of impurities in products and process effluent streams (purges, vents, and bleeds), as well as in internal streams or inventory of selected units. In addition, we have to consider maximum tolerable losses of reactants and products in effluent streams. These constraints are defined by environmental regulations, product quality and equipment protection.

c. *Controlled variables (outputs).* Type and location of the measurements is based on process engineering judgement. These are typically quality requirements of intermediate reactants, and concentration of key impurities on selected internal process streams.

d. *Manipulated variables (inputs).* These are available degrees of freedom left after considering the inventory control of the main components. They may include manipulated variables left for quality control of selected separation units, as well as

streams belonging to the input/output structure of the process, as make-up, purge or bleed streams.
e. *Disturbances.* These may be flow rates and concentrations of key impurities produced by the process, or introduced with the inflow of reactants. Disturbances must be defined in term of amplitude and frequency range. Setpoint changes, due to optimisation or/to design modifications, as re-routing of some streams, have also to be considered.
f. *Scaling of variables and disturbances.* Proper scaling is necessary for a meaningful computation of controllability indices (see Chapter 12).

4. Steady state controllability analysis. A simple and efficient plantwide control structure can be built with multi-SISO PID controllers. This step enables to evaluate the control structures of decentralised (integral) feedback control. The main actions are:
Determine steady-state gains for plant and disturbances.
Evaluate the feasibility of input/output combinations by single value decomposition (SVD) analysis.
Estimate feasible pairing by relative gain array (RGA) and Niederlinski index.

5. Dynamic flowsheeting. The detail of modelling depends on the dynamics of units involved in the plantwide control problem. However, the availability of suitable dynamic models for the wide variety of unit operations involved in practice is questionable. The simplification of the steady-state Plant Simulation Model to a tractable dynamic model, but still able to represent the relevant dynamics of the actual problem, is a practical alternative. In this case detailed models are necessary for the key units, where impurities are generated and eliminated, as kinetic models for reactors and dynamic models for some distillation columns. For other units, steady-state models are sufficient.

6. Dynamic controllability analysis. Based on the non-linear plant model, a linear dynamic model is derived, either as a set of transfer functions (identification method), or as a state-space description (matrices A, B, C. D). The last alternative is offered in some advanced packages, as Aspen Dynamics^{TM}, but the applicability to very large problems should be verified. Then a standard controllability analysis versus frequency can be performed. The main steps are:

- Compute RGA and RGA-number. Check the pairing suggested by the steady-state analysis over the frequency range where control is needed. Evaluate the effect of interactions.
- Check input constraints by means of closed loop disturbances gain (CLDG). Modify the design if necessary.
- Estimate controllability performances of the selected structures by performance relative gain array (PRGA) and relative disturbances gain (RDG).

Repeat the procedure for each alternative decentralised control structure.
For details about different controllability measures see the Chapter 12 from this book, or the Chapter 10 of the book of Skogestad and Postlethwaite (1996).

7. Closed loop simulation. Here the first task consists of implementing and tuning the controllers. The use of prescribed local control structures, or setting perfect control for fast loops simplifies this task and preserves the plantwide character of the analysis. Here

the plantwide control structures identified by the controllability analysis are tested by full non-linear simulation. Evidently, this step is time-consuming and should be applied only to the most promising design alternatives only.

8. Design alternatives. For each flowsheet alternative identified at the point 1 the procedure should be repeated and alternatives ranked. Supplementary alternatives may arise during the analysis by design evolution. The generation of a base-case is recommended, against which the other alternatives can be evaluated. Design modifications may concern the (re)sizing of unit operations, and alternative flowsheet (recycle) structures.
Some alternatives can be rejected during the steps 4-6 when controllability analysis indicates clearly inferior dynamic behaviour. However, some design improvements can be suggested by the controllability measures, as described at the points 4 and 6. Essentially, they should ensure: 1) The effect of interactions should not prevent the implementation of a decentralised control system (RGA and RGA number), 2) The magnitude of inputs must be effective in controlling the outputs at steady-state (SVD and CLDG analysis).

9. Design actions. The results of such study are:
- Identification of the best flowsheet alternative and suggestions for plantwide control strategy.
- Design and sizing modifications of units, as for example the replacement of obsolete internals of distillation columns by material with better performance.

17.3.2 Process description

A *balanced* VCM process produces only vinyl-cloride by combining three reaction steps: direct ethylene chlorination to 1,2-dichloroethane (DCE), cracking of DCE to VCM, and recovery of HCl by oxychlorination with ethylene. The global stoichiometry may be described by the simplified scheme:

Chlorination: $C_2H_4 + Cl_2 \rightarrow 1,2-C_2H_4Cl_2\ (DCE) + impurities$ (1)

Cracking: $DCE \rightarrow C_2H_3Cl\ (VCM) + HCl + impurities$ (2)

Oxychlorination: $C_2H_4 + 2\,HCl + 1/2\,O_2 \rightarrow DCE + H_2O + impurities$ (3)

The above steps are conducted in three different reactors. Differences of individual VCM licensers are mainly due to the reaction systems. The reactors determine the amount of impurities, and consequently the purification equipment and energy requirements. Details about technology may be found in Ullmann (vol. A6, 1986). Proper handling of impurities is a crucial for sustainability of a VCM process. This problem is a complex combination of chemistry, thermodynamics, design and control, whose solution has a generic value for large-scale complex processes.

17.3.2.1 Base-case flowsheet

Figure 17.16 presents a simplified flowsheet, which concentrates the essential features of an industrial process, but does not reproduce a particular technology. The chlorination of ethylene to DCE takes place in a gas-liquid type reactor (R1), working at near atmospheric pressure and 353 K, using $FeCl_3$ as catalyst. After purification, the thermal cracking of DCE takes place in a tubular reactor (R2) at high temperature (500 to 600 K) and pressure (0.5 to 1.5 MPa). The by-product HCl is recovered as DCE by oxyclorination of ethylene in a fluid bed type (R3). Note that the flowsheet may consider the processing of an external DCE stream. Thus, the amount of ethylene and chlorine is 'balanced' to consume the entire HCl produced in the cracking section.

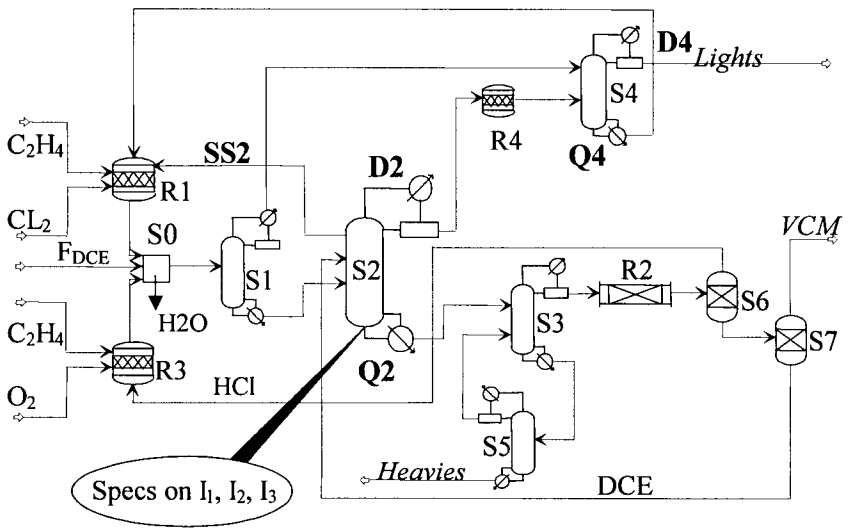

Figure 17.16 Base case flowsheet of a balanced VCM process

Despite a good selectivity, the amount of impurities in a VCM process is considerable due to the large scale. As an order of magnitude the waste production is of 25 kg/tonne lights and heavies.

The removal of impurities in a VCM process is known to be difficult. These may accumulate in the recycle loops and cause unstable operation. Among the large number of impurities, three are of particular importance: (I_1) chloroprene (nbp 332.5 K), (I_2) trichloroethylene (nbp 359.9 K), and (I_3) tetrachloromethane (nbp 349.8). Both I_1 and I_2 are 'bad' for operation, being non-saturated components. The first can easy polymerise above 8% and plugs the equipment. The second favours coke formation in the cracking reactor. Contrary, I_3 is a 'good' impurity, having a catalytic action in the cracking reactor by reducing the temperature and improving the selectivity. In some patents it is introduced deliberately.

The source of chloroprene (I_1) is the cracking section, trichloroethylene (I_2) appears mainly in the oxychlorination, while tetrachloromethane (I_3) is produced both in chlorination and oxy-chlorination, but may be present as impurity in the initial feed.

These impurities must be removed selectively from DCE (nbp 356.8 K) sent to cracking. Both I_1 and I_2 must be kept low, while I_3 must be kept close to an optimal value. This is the incentive of the plantwide control problem.

Crude DCE produced in the reactors R1 and R3 are sent to S0, a black-box unit that simulates the washing/drying operation. A first amount of dissolved gases and very light impurities is removed in the unit S1, and sent further to the distillation column S4, which is the exit of light impurities.

After pre-treatment, the crude DCE is sent to purification in the distillation column S2, the key unit of the separation system. This column receives DCE from three reactor systems, and is the place where three large recycle loops cross. The top distillate of S2 should remove the light impurities mentioned above. The purification from heavies is continued in the distillation columns S3 and S5.

The separation of impurities in S2 is affected by volatility constraints. At 350 K, the top temperature, the volatility of I_1, I_2, and I_3 relative to DCE is of about 1.9, 0.94 and 1.6. Therefore, the top distillate of S2 can remove easily I_1 and I_3, but not I_2. Note also that the top distillate of S2 cannot contain more than 8% I_1.

To prevent the accumulation of I_2, a side stream drawn from S2 is sent to the reactor R1, where chlorination to heavies takes place. Because of constraint on I_1, the top distillate of S2 carries with a significant amount of DCE, which has to be recovered and recycled by the column S4. By recycling the bottom of S4 to the reactor R1, some amounts of impurities I_1 and I_2 are converted in heavies. This operation helps to reduce the accumulation of undesired impurities, particularly of I_2, but affects the operation of the reactor R1.

Therefore, there is rational to introduce a specialised reactor for the conversion of non-saturated impurities in heavies by liquid-phase chlorination. This new reactor, designated by R4, placed between S2 and S4, gives the opportunity for flowsheet alternatives as described in the next section.

Note that all the heavy impurities, produced by the process or by converting lights to heavies, are removed by the distillation columns S3 and S5. They work in tandem in order to limit the losses in DCE. Unlike the distillation of light impurities, there is no heavy impurity that constraints the purification of DCE.

Note that S2 is a large distillation column, with about 50 theoretical stages, operating at high reflux. The separation in S3 is easy, and requires only few stages, Note that S4 and S5 are small units, but of particular importance, because of their function: S4 is the only exit of light impurities (Lights), while S5 is the only exit of the heavy impurities (Heavies).

After thermal cracking the reaction mixture is quenched and cooled (non-presented). The recovery of HCl, and the separation of VCM from un-reacted DCE takes place in the units S6 and S7, respectively.

17.3.2.2 Alternatives flowsheets

Chemical conversion of impurities in R4 makes possible alternative recycle structures by keeping the same equipment, but changing the stream connections. The recycle of impurities to R1 may cancel. Figure 17.17 shows three supplementary alternatives to the base-case.

In *alternative A*, the bottom of S4 is sent directly to the column S5. The removal loop of lights S2-R4-S4-S5-S2 crosses the removal loop of heavies S2-S3-S5-S2 in the

column S5. This modification diminished heavies both in R1 and S2. Because of higher throughput the design of S5 requires revision.

In *alternative B*, the bottom of S4 returns directly to S2. The loop for removal lights is shorter, but a larger amount of heavies increases the danger of fouling of the column S2.

In *alternative C*, the bottom of S4 goes directly to the finishing column S3, which is now subject to more fouling. Moreover, a fault of S4 will affect immediately the cracking section.

From the three alternatives, *A* is technologically the safest, but implies the revamp of S5. Alternative *B* is simpler, but needs to review the internals of S2, which is an expensive column. The alternative *C* is the simplest, but less safe in operation. It may be expected that each alternative will have distinct controllability properties. The final selection must take into account this important feature, as well as the cost of modifications.

Summing up, the tracing mechanism of key impurities is as follows:

- I_1: generated in R2, converted to heavies in R1 and R4, concentrated in S2 to leave by S4 in Lights.
- I_2: generated in R3, converted to heavies in R1 and R4, concentrated in S2, leaves by the path S2-S3-S5 in Heavies.
- I_3: appears in R1, and R3, leaves the process by the path S2-S4 in Lights.

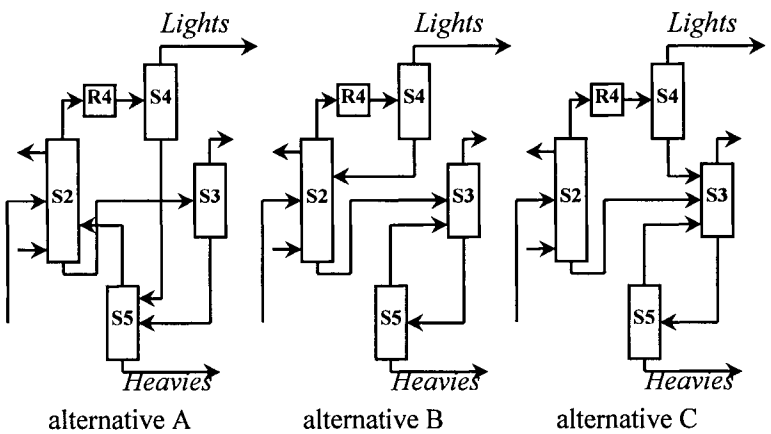

Figure 17.17 Flowsheet alternatives

17.3.3 Plant Simulation Model

A steady-state *Plant Simulation Model* of an existing plant helped to calibrate the base-case model on a representative operating point. Some details of an industrial process were skipped, but the omission of these details does influence neither the plantwide material balance nor the process dynamics. The units S0, S6 and S7 may be considered black-boxes. Contrary, S1 to S5 are rigorous distillation columns, modelled as sieve trays. In steady-state all the reactors are described by stoichiometric approach, but kinetic models are used for R1 and R4 in dynamic simulation.

Note that the reaction network has been formulated such to use a minimum of representative components, but to respect the atomic balance. This approach is necessary because yield reactors can misrepresent the process. Details enabling a full simulation are given in Dimian et al. (2001).

17.3.4 Plantwide control problem

The quality of the intermediate DCE must fulfil strict purity specifications. Low impurity levels imply high energetic consumption, but higher impurity amounts are not desired for operation. The intermediate DCE is conditioned mainly in the distillation column S2. In the bottom product the concentration of the two 'bad impurities' I_1 and I_2 must not exceed an upper limit, of 100 and 600 ppm, respectively, while the concentration of the good impurity I_3 must be kept around optimal value of 2000 ppm. Because these impurities are implied in all three reaction systems through recycles that cross in the separation system, their inventory is a plantwide control problem. The problem is constraint by technological and environmental constraints, as mentioned.

The advanced removal of I_1 and I_2 must find a compromise with optimal concentration of I_3 in the bottom product of column S2. These contradictory requirements cannot be fulfilled by any stand-alone design of S2. The control of impurities becomes possible only by exploiting the positive feedback effects of the recycle loops balanced by the negative feedback effects of chemical conversion and exit streams.

Hence, the plantwide control objective is the quality of DCE sent to the cracking section, for which three specifications are required: These are the *outputs* of the plantwide control problem. We assume that they are available by direct concentration measurements, as by IR spectroscopy or on-line chromatography.

An analysis of the degrees of freedom indicates as a first choice manipulated variables belonging to the column S2, used for quality control: D2- distillate flowrate, SS2 - side stream flowrate, and Q2 - reboiler duty. We may also consider manipulated variables belonging to the column S4, adjacent and connected with S2 by a recycle, but dynamically much faster. Thus, supplementary outputs are: D4-distillate flow rate, and Q4-reboiler duty. Hence, the *inputs* are the variables D2, SS2, Q2, D4 and Q4.

The scaling for outputs has considered a maximum error of (100-nominal value) for I_1, (600-nominal value) for I_2, and 500 for I_3. The inputs have been scaled with 25% of nominal values.

A major disturbance of the material balance simulated here by a step variation in the external feed (F_{DCE}), a disturbance of 75 kmol/h. The plant throughput is of 1000 kmol/h equivalent DCE, while the load of the column S2 is of about 2000 kmol/h. A second significant disturbance is X_{I3}, the fraction of impurity I_3 introduced by the external DCE feed. A molar fraction of 0.012 has been considered, about 20% from the I_3 inventory. The most probable range of frequencies for disturbance rejection is 0.1-1 rad/h for throughput, and 0.1-10 rad/h for impurities.

17.3.5 Steady state controllability analysis

Because of different recycle structures, the base-case and the alternatives *A*, *B* and *C* will have slightly different nominal operating points. Table 17.14 shows the scaled static gains for the base-case. The reboiler duty (Q2) has the highest influence on the all

outputs, particularly on I_1. The distillate D2 affects more I_3, but D4 and Q4 give even higher gains. I_2 is more sensitive to SS2. The system is sensitive to disturbances, particularly to DCE flow rate (F_{DCE}). The examination of the static gains indicates some coupling possibilities, as Q2-I_1, SS2-I_2, and D2-I_3 or D4-I_3, but also the existence of strong interactions (high negative values).

Table 17.14 Scaled static gain matrix of the base-case

	D2	SS2	Q2	D4	Q4	F_{DCE}	X_{I3}
I_1	-0.076	-0.184	-4.325	-0.154	-0.041	3.303	0.096
I_2	-0.140	-0.302	-2.298	-0.215	-0.061	2.061	0.157
I_3	0.737	0.156	-0.908	-2.136	-0.727	2.237	1.853

D_2 will affect all the impurities, but preferentially I_3 in the base-case and the alternatives *A* and *B*, while in the alternative *C* the effect is more important on I_2. Similarly, the static gains of other manipulated variables can be examined. However, a one-by-one investigation is not able to quantify the effect of interactions. Therefore it is necessary to perform an RGA analysis.

17.3.5.1 RGA analysis

Table 17.15 presents the RGA diagonal elements for the three most promising combinations. All diagonal control structures are feasible at steady-state, but with different pattern of interactions. Niederlinski index **NI** was used to assess the stability of pairing. This index is positive in all the control structures, but results are not reported here. The loops Q2-I_1 and SS2-I_2 are more interactive than the loop controlling I_3 with either D2, D4 or Q4. The use of D4 offers the best de-coupling. Note that the RGA elements of the loops with I_1 and I_2 are always larger than one, while the RGA elements of the loops with I_3 are in some cases less than one. We recall that RGA element larger than one means that the open loop gain exceeds the closed loop gain, so the interactions work in an opposite direction. It can be concluded that the effect of Q2 and SS2 on the control of I_1 and I_2 are reduced by the other loop controlling I_3.

Thus, the effect of interactions on the control of I_3 depends both on the recycle structure and the manipulated variable. Distillate rate D2 gives more interactions compared with the case where the manipulated variable belongs only to S4 (either D4 or Q4). The use of manipulated variables from different units should not be a surprise when these are, dynamically speaking, close enough, as it is the case with S2 and S4. In the base-case and alternative *B* the effect of the S4 variables on I_3 is enhanced by closing the other loops, while in alternatives *A* and *C* this effect is hindered.

However, at this point there is not a clear distinction between the base-case and alternatives, although we expected a difference because of the very different units involved in recycles. A dynamic controllability analysis is needed.

Table 17.15 RGA diagonal elements

I_1, I_2, I_3	Base-case	alt A	alt B	alt C
Q2, SS2, D2	1.47, 2.01, 1.34	1.58, 1.27, 1.10	1.37, 1.27, 0.89	1.63, 0.96, 0.83
Q2, SS2, D4	1.43, 1.35, 0.96	1.51, 1.38, 1.13	1.43, 1.29, 0.92	1.61, 1.43, 1.06
Q2, SS2, Q4	1.43, 1.36, 0.97	1.65, 1.48, 1.25	1.43, 1.30, 0.93	1.74, 1.57, 1.19

17.3.5.2 Dynamic simulation

The dynamic simulation model has been adapted to meet the constraints of a large scale problem and of the equation solving mode of Aspen Dynamics. The final model contained more than 6000 equations. Since the change in material balance (inventory) takes place at long time scales, some substantial simplifications of the local control of units can be considered. Finally, the plantwide control problem is reduced to analyse a 3x7 system, where three outputs (concentration of impurities I_1, I_2, and I_3) should be controlled with three among five inputs (D2, SS2, Q2, D4, and Q4), in the presence of two disturbances (F_{DCE}, X_{I3}). Because of decentralised control, at most three SISO controllers should be physically implemented.

17.3.5.3 Step responses for the Base-Case

The responses to perturbations for the base-case are illustrates by the Figure 17.18. Increasing the distillate flow rate D2 of column S2 diminishes the impurities I_1 and I_2, and increases I_3 (Figure 17.18a). More distillate from D2 to the reactor R4 reduces the conversion of impurities in Heavies. A higher load of column S4 makes distillate more light-impurity I_1. The other two impurities I_2 and I_3 are recycled to reactor R1. Here I_2 is transformed into heavies, further removed through S5, but I_3 will accumulate. Initially, the accumulation of I_3 is fast, taking approximately 1½ hour. Because at higher concentration more I_3 distillates through the path S2-S4, its accumulation slows down to zero. Steady state is reached for I_1 and I_2 after 10 hours, while I_3 needs six time more. Note that the largest steady state effect is for I_3, followed by I_2 and I_1. Because of a faster response, a controller would affect mainly I_1 and I_3, but only slightly I_2. This first insight suggests that the steady state and the dynamic behaviour would be different.

Increasing the side stream flow rate SS_2, stimulates the accumulation of I_3 but diminishes both I_1 and I_2. The strongest effect is on I_2. By increasing the recycle flow through R1, more impurities I_1 and I_2 are transformed into heavies, and their inventories decreases (negative feedback). Note that at shorter time, a faster accumulation of I_3 (positive feedback) takes place, compensated later by the exit through the column S4 (negative feedback). The dynamics is fast for I_1 and I_3, and slow for I_2, which in turn gives the largest steady-state response.

The reboiler duty Q2 has a strong and fast effect on all impurities (Figure 17.18b). The curves show two competing effects, stripping-out and accumulation through recycles. The first is faster at very short time, but is balanced by the second at longer times. The most important effect is on the impurity I_1, both dynamically and at steady-state.

The column S4, the exit point of light impurities, has an essential role on the plantwide dynamics. The positive feedback effect of recycles can be better exploited to compensate the loss in the good impurity I_3. This time the effect is much stronger and opposite at steady state: triple steady-state gain, but manipulated variable smaller by an order of magnitude. The distillation rate D4 can produce a snow-ball effect on the impurity I_3. This phenomenon might happen if the maximum magnitude of D4 is set too low to restrict the losses in DCE. Hence, D4 is a good candidate as a plantwide manipulated variable, but the design of the column S4 must be adapted to work is synergy with column S2.

Summing up, the dynamic simulation shows that the dynamic response at shorter times is qualitatively different from the steady-state behaviour. Because of higher initial

dynamic gains, the control of loops for I_1 and I_3 will dominate the control of I_2, even when the steady-state gain of the last would be much larger. The time scale of the plantwide dynamics is two order-of-magnitude slower than of local control loops. The open loop response shows the behaviour of a stable system, although a strong steady-state non-linear effect (snow-ball) can occur if the exit rates of impurities (streams Lights or Heavies) are pushed to very low bounds.

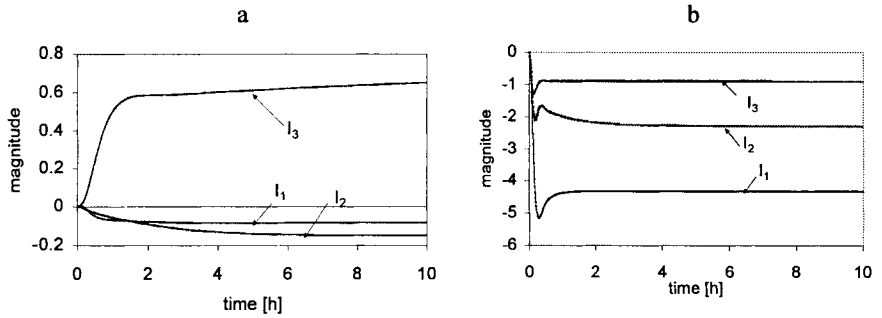

Figure 17.18 Open loop dynamic responses in the base case

17.3.5.4 Step responses for Alternatives

It should be remembered that the alternative flowsheets have been obtained by re-routing the bottom product of the column S4 after suppressing the recycle to R1. Different recycle paths are created. As before, the response of I_3 with D2 or D4 is of greatest interest. Because the dynamic simulation shows similar profiles for the alternatives *A* and *B* with the base-case, they are not presented. However, they are different in the alternative *C* (Figure 17.19a). Remember that in the first two alternatives the bottom product from S4 is sent to the column S2, either via S5 or directly, while in the third case there is not such loop. If D2 rises suddenly, in the beginning there is a fast accumulation of I_3, because the amount leaving the system through S4 is still small. After reaching a higher concentration, the impurity becomes more volatile and leaves easier the plant. As a result, the negative feedback effect increases. The compensation of two effects takes a relatively long time. Because the negative feedback is not longer delayed, the shape of the time profiles and the steady-state values in the alternative *C* are different compared with other alternatives.

Figure 17.19b presents a direct comparison of all alternatives with respect of impurity I_1. It may be seen that the effect depends on the recycle structure: deflation for the base-case and inflation in alternatives *A* and *C*, while in the alternative *B* the steady state effect is almost negligible. The explanation can be found in the negative feedback effect of reactor R1, where I_1 is destroyed in heavies. In alternatives, by suppressing the back flow from S4 to R1, the converted I_1 diminishes and the accumulation becomes positive. The effect is maximum in alternative *C* and minimum in the alternative *B*, corresponding to differences in the path of the recycle loops.

Again, the short time and long time dynamics are quite different. This phenomenon can be explained by the fact that the removal of impurities through the column S4 can

reach a quasi steady-state value only after a sufficient accumulation (positive or negative) takes place.

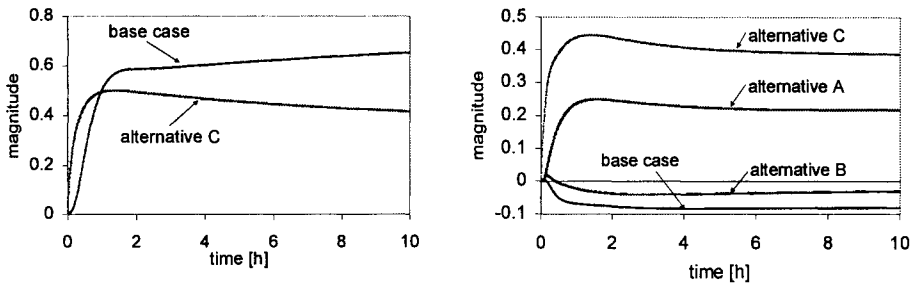

Figure 17.19 Open loop dynamic responses in the three alternatives

17.3.6 Dynamic controllability analysis

A scaled linearised state-space description around the nominal operating point of the dynamic model has been generated. The matrices *A*, *B*, *C*, and *D* have been exported in MATLAB®, where a controllability analysis as function of frequency has been performed. Alternatively, transfer functions have been generated. The results are similar.

The steady-state analysis indicated good sensitivity of the controlled variables to inputs and the possibility to reject disturbances with a diagonal multi-SISO control structures, as for example Q2-I_1, SS2-I_2, D2-I_3 (see also Table 4). Although there are some differences in the open loop behaviour of flowsheet alternatives as compared to the base-case, these do not justify a net preference. On the other hand, the steady state RGA analysis predicted that a control structure using D2 to control I_3 should be more affected by interactions as by manipulating D4 or Q4, but the differences cannot be evaluated only by the inspection of numerical values. Because a steady-state analysis cannot predict how the real disturbances would be handled by the control system, a deeper controllability analysis is necessary in the frequency domain. The battery of indices has been tried in each case, as described by Groenendijk et al.(2000). Here we give only representative results.

17.3.6.1 RGA-number

RGA-number, defined as $\|RGA - I\|_{sum}$, gives a quantitative measure of the interactions in a diagonal decentralised control structure. The lower RGA-number the more preferred is the control structure. A value close to zero means quasi-independent SISO controllers. Note that a good controllability can be obtained up to the frequency where the RGA number does not exceed 1. Consequently, graphical representations versus frequency enable to evaluate the robustness of control faced to a certain frequency range of disturbances.

Figure 17.20a shows the evaluation of three control structures in the base-case: (1) Q2-I_1, SS2-I_2, D2-I_3, (2) Q2-I_1, SS_2-I_2, D_4-I_3, and (3) Q_2-I_1, SS_2-I_2, Q_4-I_3. All show quasi-constant low values at lower frequencies, up to 0.5 rad/h, in agreement with the steady-state analysis. Rapidly increased RGA-number at higher frequencies indicates a

degradation of controllability, because of negative off-diagonal RGA elements. Note that the structures using manipulations from the column S4, namely D4 and Q4, are somewhat less affected. Consequently, the control of all three impurities might be difficult for disturbances above 0.5 rad/h.

If the loop SS_2-I_2 is removed, the situation improves considerably. Indeed, the steady-state analysis suggested that best pairing is Q2-I_1 and D4-I_3. Figure 17.20b presents RGA number for the base-case and alternatives with these combinations, when the control becomes a simple 2x2 structure. In the first place, the plot indicates that base-case and alternative *B* are practically unaffected by interactions at low frequencies. They behave much better compared to alternatives *A* and *C*. The mentioned pairing is feasible for the base-case and the flowsheets A and C up to 10 rad/h, while in alternative *B* the upper bound is somewhat lower. This frequency range is realistic from plantwide point of view. Hence, the above control structures seem to have good properties. This fact has been verified by closed loop simulation.

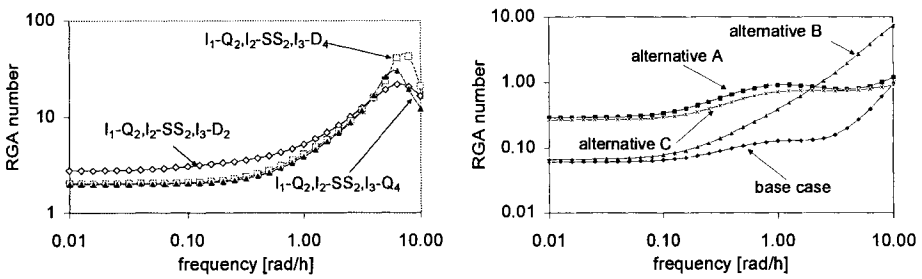

Figure 17.20 RGA number. a) control alternatives in the base-case b) structure I1-Q2 and I3-D4 in all alternatives

17.3.6.2 Closed loop performance

After evaluating feasible pairing, we can estimate their performance by using Closed Loop Disturbances Gain (CLDG) index. To keep the control error between acceptable bounds, the closed loop disturbance gain should be smaller than the loop transfer function $(1+g_{ii}(s)k_i(s))$, for each disturbance, where $g_{ii}(s)$ is the open loop input-output transfer function and $k_i(s)$ is the controller model.

Figure 17.21a shows the closed loop disturbance gain and loop transfer function for the control of I_3 with D2 for X_{I3} as disturbance. The loop transfer function with a proportional controller of gain 1 is insufficient to overcome the CLDG element at lower frequencies. To keep I_3 between bounds, the loop transfer function should be larger, but the effect cannot be achieved by increasing the scaled controller gain, constrained at maximum 1. The situation is worse in the other alternatives. This analysis has been confirmed by closed loop simulation. The situation can improve if D4 is used instead D2.

RGA analysis has shown that leaving I_2 uncontrolled would improve the rejection properties of the remaining controllers. When the interactions between the controllers are taken into account, only two controllers, Q_2-I_1 and D_4-I_3, are sufficient to keep I_2 between bounds, because the disturbances affect the outputs in the same direction. In

this case the reboiler duty and the side draw also affect the impurities I_1 and I_2 in the same direction. So both controllers are supporting each other in rejecting the disturbance. Because the power of Q2 is much larger than SS2, the controller Q2-I_1 is dominating, and the controller SS2-I_2 is not needed.

Closed loop simulations with only the controller Q2-I_1 implemented show that the effect of the disturbance F_{DCE} on I_2 is reduced by 80% (Figure 17.21b). I_2 is below its maximum and further reduction is not needed. Still, a controller would be required only if I_2 must be kept on setpoint, but this operation would create more problems that it solves. Hence, leaving I_2 free, but having the guarantee of a bounded variation, is a rational compromise that preserves the robustness of the control system. Hence, the plantwide control objective can be achieved with only two control loops, Q2-I_1 and D4-I_3. As we have demonstrated, over a practical range of frequency these are almost de-coupled.

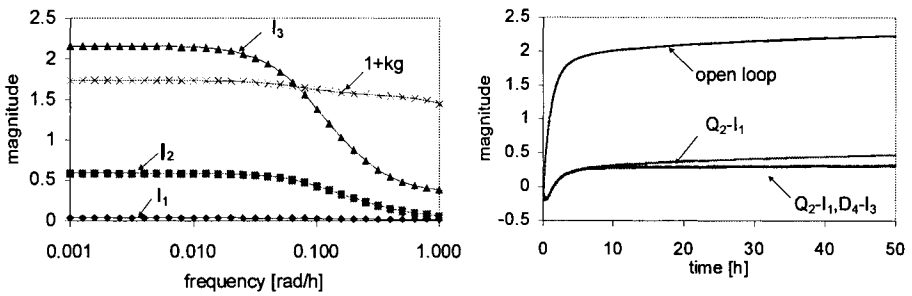

Figure 17.21 Closed Loop Performance Gain a) controllers I_1-Q2, I_2- SS2 and I_3-D2 b) I_1-Q2; I_2-SS2 and I_3-D4

17.3.6.3 Closed loop simulation

Firstly, the implementation of three PI controllers has been tried. Figure 17.22a shows the results obtained in attempting to control the good impurity I_3 with the structure Q2-I_1, SS2-I_2 and D2-I_3. The attempt failed, the system cannot be stabilised because of heavy interactions. As shown, the impurity I_3 accumulates and exceeds its bound. The input magnitude of D2 is indeed too small to control I_3, as was indicated by the analysis of the closed loop performance. Changing D2-I_3 with D4-I_3 does not change fundamentally the situation. Thus, the simultaneous control of the three impurities is not possible. This result was not predictable from the steady-state analysis, but it has been foreseen by the dynamic controllability analysis. Thus, it was decided to let the loop SS2-I_2 on manual.

Figure 17.22b shows the result obtained by implementing the controllers Q2-I_1 and D4-I_3, where only the P component has been considered, with the scaled gains from the CLDG plot. The impurities I_1 and I_3 can be kept between bounds. The interactions enable to keep equally the impurity I_2 between bounds, such as its control is not needed. Hence, the use of only two PI controllers to control three impurities is possible, because it takes profit from the co-operative effect of interactions. Note that using manipulated variables from different units is not a current practice. However, the principle of

proximity is preserved, because the columns S2 and S4 are dynamically adjacent. Moreover, the dynamics of the impurities is dominated by the effect of recycles.

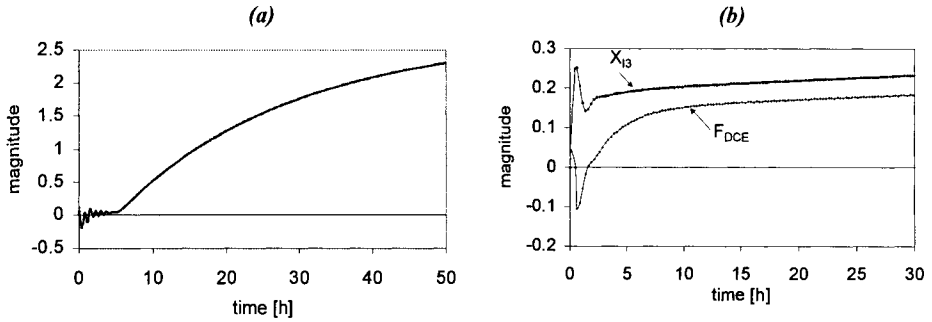

Figure 17.22 Closed loop simulation. a) controllers I_1-Q2, I_2- SS2 and I_3-D2 for feed disturbance b) I_2-SS2 and I_3-D4 for both feed and concentration disturbances

17.3.6.4 Selection of the best alternative

The plantwide controllability analysis enables a rational decision regarding the optimal management of the inventory of impurities in the case of a complex plant. The case study of VCM plant has shown that the most significant improvement came from the chemical conversion of impurities that diminishes the positive feedback of recycles. This alternative was the *base-case* examined in this study. The other flowsheet alternatives were obtained by re-routing the recycles. Controllability study and close loop simulations has shown that the *base-case* and the *alternative B* have the best dynamic properties. Remember that the last consists in re-routing the bottom of the exit column of impurities, not to the reactor R1 but to the purification column S2. This modification has a definite advantage: let R1 working cleaner. Thus, the *alternative B* is preferred. Moreover, it offers the shortest path of impurities, and consequently a faster dynamics, together with protection against the failure of other units. The revamp consists only in re-piping, and optionally in replacing the internals in the lower part of the column S2 with fouling-resistant trays or packing.

Another interesting design measure that becomes necessary after such study is the insertion of a reservoir to damp disturbances higher than 10 rad/h. In like manner, the choice of measuring devices and of sampling rate should be made in agreement with the above plantwide dynamics.

17.3.6.5 Conclusions

If the inventory of main components can be handled by local control loops, the inventory of impurities has essentially a plantwide character. The rates of generation, mainly in chemical reactors, and of depletion (exit streams and chemical conversion), as well as the accumulation (liquid phase reactors, distillation columns and reservoirs) can be balanced by the effect of recycles in order to achieve an acceptable level. Because

several units with large holdup may be involved, as liquid-phase reactors and distillation columns, this problem can be solved only by a systems approach.

Interactions through recycles can be exploited to create plantwide control structures that are not possible when a stand-alone approach is adopted. In this case, acceptable control of three key impurities can be achieved with only two control loops.

Chemical conversion of impurities is an efficient way to counteract the accumulation of impurities by a positive feedback effect of recycles. Re-routing the connection of separation units can generate flowsheet alternatives with different controllability properties.

In this case study, the steady-state controllability analysis was not able to make a clear distinction, but the frequency analysis showed that two alternatives offered a better rejection of disturbances. The analysis, based on steady-state and dynamic controllability measures, requires only a limited closed loop non-linear simulation.

This investigation can be applied preferably in revamping projects, where the information about the material balance can be exploited by tuning a rigorous plant simulation model. The approach is recommended also for designing new plants, but a detailed description of the chemical reaction network producing impurities is needed.

17.4 REFERENCES

Bildea, C. S., S. Cruz, Dimian, A. C., Iedema, P., 2002, Design of tubular reactors in recycle systems, Proceedings ESCAPE-12, Elsevier, 439-444

Dimian, A. C, Process Integration course, 1996, University of Amsterdam

Dimian A. C., A. J., Groenendijk, P. Iedema, 1996, System analysis in handling impurities, ESCAPE 6, Computers & Chem. Engng., vol. 20 Suppl., p. s805-810

Dimian A. C., A. J., Groenendijk, P., Iedema, 2001, Recycle interaction effects on the control of impurities in a complex plant, Ind. Eng. Chem. Res., p. 5784-5794

Douglas, J. M., Conceptual Design of Chemical Processes, 1988, McGraw-Hill

Groenendijk, A. J., A. C., Dimian, P. Iedema, 2000, Systems approach for evaluating dynamics and plantwide control of complex plants, AIChEJ, vol. 46, p. 119-132

Luyben, W. L., B. D., Tyreus, M. L., Luyben, 1998, Plantwide Process Control, McGraw-Hill

Ullmann's Encyclopedia of Industrial Chemistry, VCH Publ., Weinheim, vol. A6, 1986, 263.

This Page Intentionally Left Blank

APPENDICES

This Page Intentionally Left Blank

APPENDIX A:
ESTIMATION OF BASIC EQUIPMENT COST

1. Purchased Cost of Equipment (PCE)

The correlations given below are based on data from Coulson & Richardson (1993) updated from mid 1992 to mid 2002 by considering an annual inflation rate of 3% (multiplication factor 1.3439) and an exchange rate 1 £ = 1.831 €.

1.1 Pressure vessels.

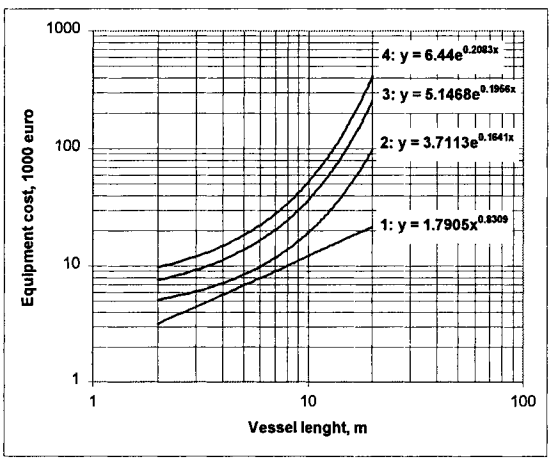

Figure A1 Horizontal pressure vessels. Diameters (m): 1 - 0.5; 2 - 1; 3 - 2.0; 4 - 3.0

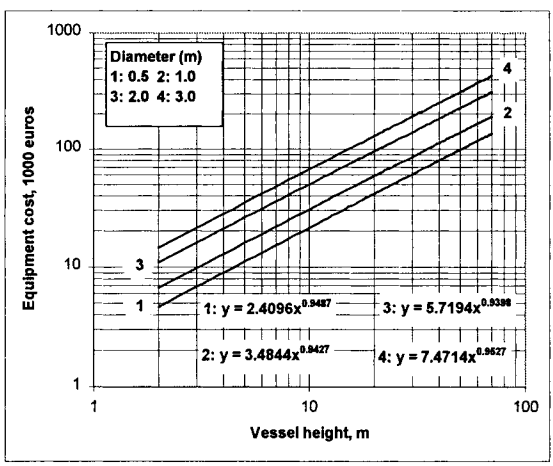

Figure A2 Vertical pressure vessels. Diameters (m): 1 - 0.5; 2 - 1; 3 - 2.0; 4 - 3.0

Table A1 Correction factors for pressure vessels

Material	F_m	Pressure	F_p
Carbon steel (CS)	1	1-5 bar	1
Stainless steel (SS)	2	5-10	1.1
Monel	3.4	20	1.2
SS clad	1.5	40	1.6
Monel clad	2.1	60	2.2

1.2 Heat exchangers (shell-and-tubes)

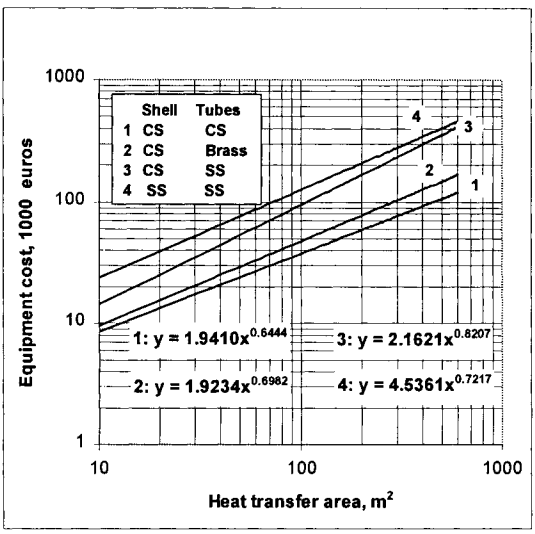

Figure A3 Shell & tubes heat exchangers 1-CS/CS; 2-CS/brass; 3-CS/SS; 4 -SS/SS

1.3 Internals of distillation columns.

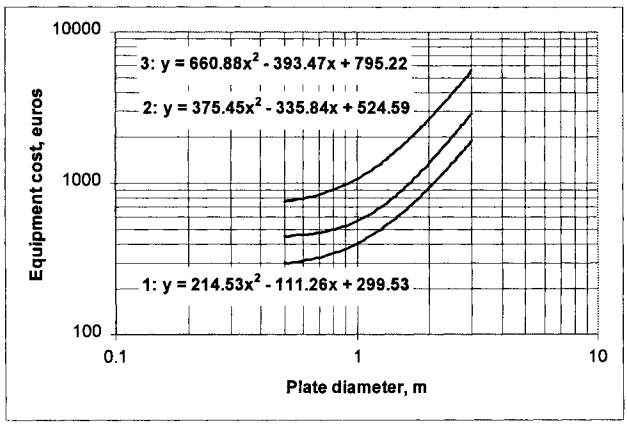

Figure A4 Cost of trays: 1-sieves, 2-valves, 3-bubble cap. Multiply by 1.7 for SS.

Table A2 Column packing cost

	Cost €/m^3		
Packing size (mm)	25	38	50
Saddles, ceramic	1770	1300	1230
Pall rings, plastic	1380	840	520
Pall rings, stainless steel	3130	1820	1750

1.4 Other major equipment items

The cost of other equipment items may be estimated by using the relation $PCE = CS^n$ with the constants C and S as given in Table A3.

Table A3 Cost of equipment, mid 2002 (adapted from Coulson & Richardson, 1993)

Equipment	Size unit, S	Size range	Constant C, €	Index n	Comment
Agitators	Power,	5-75			
Propeller	kW		2600	0.5	complete
Turbine			8200	0.5	unit
Boilers	Steam,				
1-10 bar	kg/h	<50000	30	0.8	oil, gas fired
10-60 bar			50	0.8	
Conveyers	Length, m				
Belt 0.5 m		2-40	2500	0.75	
Belt 1 m			3800	0.75	
Compressors	Power,				electric
Centrifugal	kW	20-500	1300	0.8	max. press
Reciprocating			1800	0.8	50 bar
Centrifuge	Diameter,				
Horizontal	m	0.5-1.0	75000	1.3	
Vertical			75000	1.0	
Crushers	Flow				
Cone	t/h	20-200	5000	0.85	
Pulverisers	kg/h		4400	0.35	
Dryers	Area, m^2				
Rotary		5-30	15000	0.45	carbon steel
Pan		2-10	10000	0.35	
Evaporators	Area, m^2	10-1000			
Vertical tube			15000	0.45	carbon steel
Falling film			28000	0.35	
Filters	Area, m^2				
Plate and frame		5-30	6000	0.60	carbon steel
Vacuum drum		1-10	23000	0.60	
Furnaces	Duty, kW				
Cylindrical box		10^3-10^4	190	0.77	carbon steel
		10^3-10^5	290	0.77	SS=2.5 CS
Reactors	Capacity,				
Jacketed	m^3	3-30	20000	0.40	carbon steel
Agitated			26000	0.45	glass lined

Table A3 - continuation

Tanks	Capacity,				atmospheric
Vertical	m^3	1-50	3200	0.60	pressure
Horizontal		10-100	3800	0.60	carbon steel
Storage	Capacity,				
Floating roof	m^3	50-8000	3800	0.55	SS = 2.5CS
Cone roof		50-8000	3100	0.55	

2. Cost equations

Alternatives equations for the purchased and installed cost of equipment are given below. These have been adapted from Douglas (1988), which in turn originate from the data of Guthrie (1969)[1]. The capacity data are expressed in metric units. The values are more suited for US market. The M&S factor for mid 2002 was 1095.

2.1 Pressure vessels, column and reactors

Purchased Cost ($) = (M&S/280) $(957.9\ D^{1.066}\ H^{0.82}\ F_c)$ (A1)

Installed Cost ($) = (M&S/280) $(957.9\ D^{1.066}\ H^{0.82})(2.18+F_c)$ (A2)

with both D (diameter) and H (height) expressed in meter. The factor $F_c=F_m\ F_p$ takes into account material F_m and pressure F_p. The last can be correlated by the expression:

$$F_p = 1 + 0.0074(P-3.48) + 0.00023(P-3.48)^2 \quad \text{(A3)}$$

with P in bar. The material factor can be determined from the Table A4.

Table A4 Material factors for pressure vessels

Shell material	Carbon steel	Stainless steel	Monel	Titanium
F_m clad	1.00	2.25	3.89	4.25
F_m solid	1.00	3.67	6.34	7.89

2.1 Trays

Installed Cost ($) = (M&S/280) $97.2\ D^{1.55}\ H\ F_c$

For standard 24 in. tray spacing the overall correction factor is $F_c=F_t+F_m$. Tray factor F_t is 0 for sieve trays, 1.8 for bubble cap, and about 3 for more complicated trays. Material factor F_m is 1.0 for carbon steel, 1.7 for stainless steel, but much higher for high alloys.

[1] Guthrie, K. M., Chem. Eng. 76(6), March 24 (1969)

2.1 Heat exchangers (shell-and-tubes)

Purchased Cost ($) = (M&S/280)(474.7 $A^{0.65}$ F_c) (A4)

Installed Cost ($) = (M&S/280)(474.7 $A^{0.65}$)(2.29+F_c) (A5)

The heat exchange area A is in m^2, and $20 < A < 500$ m^2/shell. $F_c = F_m (F_d + F_p)$ where F_m, F_d and F_p are correction factors for material, design type and design pressure given in the Tables A5 and A6.

Table A5 Material factors for shell & tubes heat exchangers

Shell/ Tubes	CS/ CS	CS/ Brass	CS/ Monel	CS/ SS	SS/ SS	Monel/ Monel	CS/ Titanium
F_m	1.0	1.30	2.15	2.81	3.75	4/25	8.95

Table A6 Correction factors for shell & tubes heat exchangers

Design type	F_d	Design pressure, bar	F_p
Kettle reboiler	1.35	<10	0.0
Floating head	1.00	20	0.10
U-tube	0.85	30	0.25
Fixed-tube sheet	0.80	60	0.52
		75	0.55

2.4 Furnaces

A-frame construction with multiple tube banks, field erected.

Purchased cost ($) = (M&S/280)(15668$Q^{0.85}$ F_c) (A6)

Installed cost ($) = (M&S/280)(15668$Q^{0.85}$)(1.27+$F_c$) (A7)

Q is the duty expressed in MW, with 20<Q<300. The correction factor $F_c = F_d + F_m + F_p$ is given in Table A7.

Table A7 Correction factors for furnace cost

Design type	F_d	Radiant tube material	F_m	Design pressure, bar	F_p
Process heater	1.0	Carbon steel	0	< 40	0
Pyrolysis	1.1	Chrome/Molibden	0.35	100	0.15
Reformer (no catalyst)	1.35	Stainless	0.75	150	0.30
				200	0.60

2.5 Gas Compressors

Centrifugal machine, motor drive, base plate and coupling.

Purchased cost ($) = (M&S/280)(664.1$P^{0.82}$ F_c) (A8)

P is the brake power in kW, with 25<P<750 kW. The correction factor F_c is given in Table A8.

Table A8 Correction factor for compressors

Design type	F_c
Centrifugal, motor	1.00
Reciprocating, steam	1.07
Centrifugal, turbine	1.15
Reciprocating, motor	1.29
Reciprocating, gas engine	1.82

Turbo Blowers

Purchased cost ($) = (M&S/280) CQ^m (A9)

The capacity Q is expressed in m^3/s. Constant C and exponent m depend on the maximum discharge pressure drop as follows:

Discharge pressure drop, bar	0.2	0.6	2
Constant C	2282	7271	4821
Exponent m	0.529	0.598	0.493
Q range, m^3/s	0.05-5	0.5-15	1-7.5

APPENDIX B:
COST OF UTILITIES

Table B1shows indicative values for the cost of some major utilities for The Netherlands (2001), comparatively with data for USA as given in Peters & Timmerhaus (1991). No attempt was made to account for the effect of inflation since the price of energy does not follow necessarily the general trend of consumer prices.

Table B1 Cost of utilities

Utility	NL (2001)	USA (1991)
Process water	0.15 €/ m³	0.13 $/m³
Natural gas	0.2 €/m³ 4 €/GJ	0.28 $/m³
Electricity	0.130 €/kWh public 0.066 €/kWh industry	0.06 $/kWh public 0.02-0.065 $/kWh industry
Fuel Oil	230 €/ton 4 €/GJ	179.6-253.6 $/t
Cooling water (tower)	0.025-0.05 €/m³	0.016-0.068 $/ m³
Chilled water (10 °C)	0.15-0.30 €/m³	0.2 $/m³
Demineralised water	1.0-1.5 €/m³	0.5-0.9 $/m³
Steam		
• From fired boilers	14-19 €/ton	10-12 $/t HP
• With power generation	9- 13 €/ton	5-10 $/t LP
Compressed air (9 bar)	0.01 €/m³	0.007$/ m³
Refrigeration	12-15 €/GJ	2 $/ton-day (ammonia) (1ton-day =0.303 GJ)
Biodegradation	20-30 €/t	100-200 $/t organics
Landfill	62 €/t	27.5 $ /t

The oil & gas market has a strong influence on the price of utilities. A consistent method for estimating the cost of utilities can be developed based on thermo-chemical calculations and typical efficiency of industrial processes, as power plants, boilers, turbines, refrigeration cycles, etc. Each utility can be related to its equivalent fuel value, as indicated by the Table B2 (Douglas, 1988). Once the cost of fuel known, the price of other utilities can be easily determined. Note that the prices in Table B2 are only for illustration purposes.

A common unit in energy production is BFOE (barrel fuel oil equivalent) based on a low heating value (LHV) of 6.05E6 Btu or 6.38GJ (1Btu=1.055 kJ). Note that 1barrel is 42 gallon or 1.5898E-1m³. For estimations it may be considered that 1200 Btu LHV is necessary per lb steam, as well as an investment of $80 lb/hr steam. For heating fuel

[1] Gary, J., Handwerk, G., Petroleum Refining, third edition, Marcel Dekker, 1994

oils can be used, as No. 1 fuel (35 ∘API or 850 kg/m³) similar to kerosene, or No.2 fuel (30 ∘API or 876 kg/m³) comparable to diesel.[2]

Table B2 Cost ratios of utilities

	Factor	Price
Fuel (oil or gas)	1.0	4.00 $ /10⁶ Btu or 4 $/GJ
Steam		
600 psig at 750 F	1.30	5.29 $/1000 lb or 11.66 $/ton
Saturated steam		
600 psig	1.13	4.52 $/1000 lb or 9.96 $/ton
250 psig	0.93	
150 psig	0.85	
50 psig	0.70	
Electricity	1.0	0.04 $/kWh
Cooling water	0.75	0.03 $/1000 gal or 0.008/m³

[2] Gary, J., Handwerk, G., Petroleum Refining, third edition, Marcel Dekker, 1994

APPENDIX C:
MATERIALS OF CONSTRUCTION

Here we discuss only some basic aspects regarding the preliminary selection of materials with respect to equipment design and costing evaluation. More information can be found in engineering handbooks, as Perry (1997), Coulson & Richardson (1993) and Ullmann's Encyclopedia (1992). The following criteria should be kept in view:

1. Resistance to process conditions, as corrosion, erosion, stress variation, as well as extreme temperatures.
2. Processibility of material in the form of parts used in equipment manufactures, as sheets, piping, profiles, including welding properties.
3. Contamination properties regarding the interaction between material and fluid and its consequence on both process and mechanical behaviour of the equipment.
4. The cost of materials and of processing.

The materials of construction can be classified as follows:

1. Ferrous metals and alloys, as cast iron, low-alloy steels, stainless steel and higher alloy steel.
2. Nonferrous metals and alloys, as nickel and nickel alloys, copper and alloys, titanium, zirconium, etc.
3. Inorganic non-metallic, as glass and glassed steel, porcelain and stone.
4. Plastic and thermoplastic material, as PVC, PE, rubber and thermosetting plastics.

Here we refer only to the first two categories that dominate process equipment manufacture, more particularly to ferrous metals and alloys.

Resistance to fluid corrosion is by far the most important aspect. This topic is discussed in detail in the mentioned references, where extensive corrosion tables are given. From this point of view process fluids can be classified as follows:

1. Hydrocarbon mixtures, usually non-aggressive for carbon and low-alloy steel, but aggressive for plastics.
2. Non-oxidising and reducing media
   a. Acid solutions excluding hydrochloric, phosphoric, sulphuric.
   b. Neutral solutions, as non-oxidising salts, chlorides, sulphates.
   c. Ammonium hydroxide and amines.
3. Oxidising media
   a. Acid solutions, e.g. nitric acid,
   b. Neutral or alkaline solutions, e.g. persulfates, peroxides, chromates,
   c. Pitting media, as acid ferric chloride solutions.
4. Neutral waters
   a. Fresh water supplies, slow moving or turbulent.
   b. Seawater, low moving or turbulent.
5. Gases
   a. Steam, dry or wet.
   b. High-temperature (furnace) gases with oxidising effect.
   c. Hydrogen-rich gases with pitting effect.
   d. Halogens and halide acids.

Besides fluid corrosion a particular attention has to be given to extreme temperature conditions in which the equipment should work or ensure safety operation. Temperatures higher than 600 °C require special high-temperature steels. The same is valid for cryogenic conditions, where material still should have good toughness at low temperatures. The mechanical strength of steels degrades significantly with increasing temperature, particularly near to the creep limit.

When wall thickness is calculated, care should be given to correct estimation of the tensile strength (stress) at the design temperature. This aspect is important when selecting high-alloy and special steels that are much more expensive than carbon steel and mild alloy (see Table 2). Note that the thermal conductivity of stainless steels is considerably lower than of carbon steel, implying much higher heat transfer resistance. For example, thermal conductivity of carbon steel is about 50 W/m K, but only 10-15 W/m K for stainless steels.

Commonly metallic materials of constructions are discussed briefly below. Specific information about properties and applications can be found in quality standards practiced in each country, as for example SAE, AISI, ASTM (USA), BS (UK), DIN (Germany), NF (France), UNI (Italy), NEN (The Netherlands), etc.

A. Iron and carbon steel

Low carbon steel (CS) is the most used and cheapest engineering material. It is suitable for hydrocarbon and organic solvents, except chlorinated solvents. Concentrated sulphuric acid and caustic alkalies can be stored occasionally in CS. High silicon irons can be used for storing acids. Surface treatment (quenching, tempering, nitriding, age hardening) can be used to improve the resistance to corrosion resistance or higher temperature. Coating with protected sheets of more resistant materials can be also applied, leading to important cost reduction.

B. Stainless steels

A wide range is available in a great variety of compositions that can be tailored for specific application. According to their microstructure the stainless steels can be classified in three main categories:

1. Ferric steels, with 13-20% Cr, < 0.1% C, but no nickel
2. Austenitic steels, with 18-29% Cr, > 7% Ni
3. Martensitic, with 10-12%Cr, 0.2-0.4%C, and up to 2% Ni.

The class of austenitic stainless steels is by far the most used. Adding nickel improves considerably the resistance to corrosion, which can enhanced further by adding molibden. Both ferric and austenitic alloys cannot be hardenable by heat treatment. Among different types of stainless steels the most used in process industries are of austentic types. The main are briefly described.

1. Type 18Cr/8Ni SS type (304 in USA, 801B in UK, and by X5CrNi18 9 in Germany) is the most used in process industry. It is suitable for most of the applications except furnace gases, static see water, and pitting media. It has a fair to good resistance to acids solutions. The low carbon variant 304L is recommended for thicker welded parts. The version 321 stabilised with titanium is more suitable for higher temperatures.
2. Type 18Cr/8Ni/2Mo (316 in USA, 845B in UK, X5 Cr NiMo 18 12) where molibden has been added to improve the resistance to reducing media, and dilute

acid solutions, is almost an universal steel. However, mechanical processing is more difficult. For welding thick parts the low carbon version 316L is more suitable.

Table 1 shows some typical values for the stress that may be considered in mechanical design calculation as function of temperature. It can be seen that a safety factor of about is taken into account at higher temperatures compared with the nominal tensile strength. Although the corrosion resistance of standard steels 304 and 316 types is good, their thermal resistance above 600 °C is not satisfactory. Heat-resistant steels for furnaces and cracking units are discussed in Ullmann (1992).

C. Nickel alloys

Three classic nickel alloys are the most known in process industry. Monel, a nickel-copper alloy in the ratio 2:1, is after stainless steel the most popular. It stands better than stainless steel against ferric chloride, acid solutions, alkalies, reducing media and see water. Inconel (76%Ni, 7% Fe, 15% Cr) can be used for high temperature applications and furnace gases (sulphur free). Hastelloy alloys are high resistant to strong mineral acids, as HCl, and strong oxidising media. However, all these materials are more expensive than the stainless steel, so their use should be restricted to strictly necessary.

Table C1 Typical design stress (adapted after Coulson & Richardson, 1993)

Material	Tensile strength (N/mm^2)	Design stress at temperature °C in N/mm^2				
		100	200	300	400	500
Carbon steel	360	125	105	85	70	
Low alloys steel	550	240	240	235	220	170
Stainless steel series 340 (18Cr/8Ni)	510	145	115	105	100	90
Stainless steel series 316 (18Cr/8Ni/2Mo)	520	150	120	110	105	95

Table 2 gives a price scale with reference to carbon steel. The price of steel is very variable depending on country, process, shape, etc. Example of mean prices on the period 1997-2001 recorded by the inspection of several Internet sites are: 250/350 €/tonne for hot rolled sheets, 350/500 €/tone for cold rolled sheets, 400 €/tonne for coiled plates. A reasonable composite steel price for process industries purposes would be about 400 €/tonne.

Table C2 Relative cost of material of construction

Carbon steel	1
Low alloy steels (Cr-Mo)	2
Austentic steel type 304 (18/8 CrNi)	2 - 6
Austentic type 316	2.5 - 8
Copper	5.7
Monel	25
Titanium	26

Appendix D:
Saturated Steam Properties

		Specific volume		Enthalpy			Entropy		
T	P	V_l	V_v	H_l	ΔH_v	H_v	S_l	ΔS_v	S_v
°C	kPa	m^3/kg	m^3/kg	kJ/kg	kJ/kg	kJ/kg	kJ/kg.K	kJ/kg.K	kJ/kg.K
0	0.6106	0.000999	206.42	- 0.017	2501.3	2501.3	-0.0031	9.1572	9.1541
5	0.8724	0.001000	147.09	20.432	2490.2	2510.6	0.07178	8.9528	9.0246
10	1.2287	0.001000	106.3	41.105	2478.8	2520.0	0.14592	8.7545	8.9005
15	1.7071	0.001001	77.846	61.946	2467.2	2529.2	0.21916	8.5624	8.7815
20	2.3414	0.001002	57.726	82.909	2455.5	2538.4	0.29143	8.3761	8.6676
25	3.1728	0.001003	43.313	103.96	2443.5	2547.5	0.36265	8.1957	8.5583
30	4.2505	0.001004	32.862	125.06	2431.5	2556.6	0.43278	8.0208	8.4536
35	5.6330	0.001006	25.196	146.18	2419.4	2565.6	0.50180	7.8513	8.3532
40	7.3890	0.001008	19.511	167.32	2407.2	2574.5	0.56971	7.6871	8.2568
50	12.355	0.001012	12.028	209.56	2382.7	2592.2	0.70220	7.3733	8.0755
60	19.946	0.001017	7.6696	251.71	2358.0	2609.7	0.83041	7.0779	7.9083
70	31.196	0.001023	5.0418	293.76	2333.1	2626.9	0.95460	6.7991	7.7537
80	47.404	0.001029	3.4067	335.73	2308.0	2643.7	1.07510	6.5354	7.6105
90	70.169	0.001036	2.3600	377.66	2282.5	2660.2	1.19220	6.2853	7.4774
100	101.33	0.001044	1.6722	419.61	2256.5	2676.1	1.3062	6.0473	7.3535
110	143.38	0.001052	1.2095	461.65	2230.0	2691.6	1.4175	5.8201	7.2376
120	198.70	0.001061	0.8912	503.85	2202.7	2706.5	1.5263	5.6026	7.1289
130	270.34	0.001070	0.6680	546.26	2174.5	2720.7	1.6328	5.3937	7.026.S
140	361.64	0.001080	0.5084	588.93	2145.2	2734.2	1.7373	5.1924	6.9297
150	476.30	0.001091	0.3924	631.92	2114.8	2746.8	1.8399	4.9979	6.8378
160	618.38	0.001102	0.3068	675.25	2083.2	2758.4	1.9408	4.8093	6.7501
170	792.32	0.001114	0.2426	718.96	2050.0	2769.0	2.0401	4.626	6.6661
180	1002.9	0.001127	0.1939	763.07	2015.4	2778.4	2.1379	4.4474	6.5853
190	1255.2	0.001141	0.1564	807.60	1979.0	2786.6	2.2343	4.2729	6.5072
200	1554.7	0.001156	0.1273	852.59	1940.8	2793.3	2.3295	4.1018	6.4312
210	1907.3	0.001172	0.1044	898.05	1900.5	2798.6	2.4235	3.9337	6.3572
220	2319.1	0.001189	0.0861	944.05	1858.2	2802.2	2.5166	3.768	6.2845
230	2796.6	0.001208	0.0715	990.63	1813.4	2804.0	2.6088	3.6041	6.2129
240	3346.6	0.001228	0.0597	1037.9	1766.0	2803.9	2.7005	3.4415	6.1420
250	3976.2	0.001251	0.0501	1086.0	1715.7	2801.6	2.7918	3.2795	6.0714
260	4692.8	0.001275	0.0421	1135.0	1662.1	2797.1	2.8831	3.1175	6.0006
270	5504.3	0.001302	0.0356	1185.1	1604.8	2789.9	2.9745	2.9546	5.9291
280	6418.7	0.001332	0.0301	1236.6	1543.3	2779.8	3.0665	2.7899	5.8565
290	7444.6	0.001366	0.0255	1289.6	1476.8	2766.4	3.1595	2.6224	5.7819
300	8591.0	0.001404	0.0216	1344.7	1404.6	2749.3	3.2538	2.4507	5.7045
310	9867.7	0.001447	0.0183	1402.0	1325.6	2727.6	3.3499	2.2732	5.6232
320	11286	0.001499	0.0155	1462.0	1238.4	2700.4	3.4484	2.0879	5.5362
330	12858	0.001560	0.0130	1525.4	1140.7	2666.1	3.55	1.8913	5.4413
340	14599	0.001637	0.0108	1593.7	1028.6	2622.2	3.6572	1.6775	5.3347
350	16527	0.001740	0.0088	1669.8	894.27	2564.0	3.7744	1.4351	5.2094
360	18668	0.001895	0.0069	1760.9	720.17	2481.1	3.9133	1.1374	5.0507
370	21052	0.002219	0.0049	1895.5	438.99	2334.5	4.1202	0.6826	4.8028
374	22090	0.003155	0.0031	2099.3	0	2099.3	4.4298	0	4.4298

ANNEXE E - VAPOUR PRESSURE OF SOME HYDROCARBONS

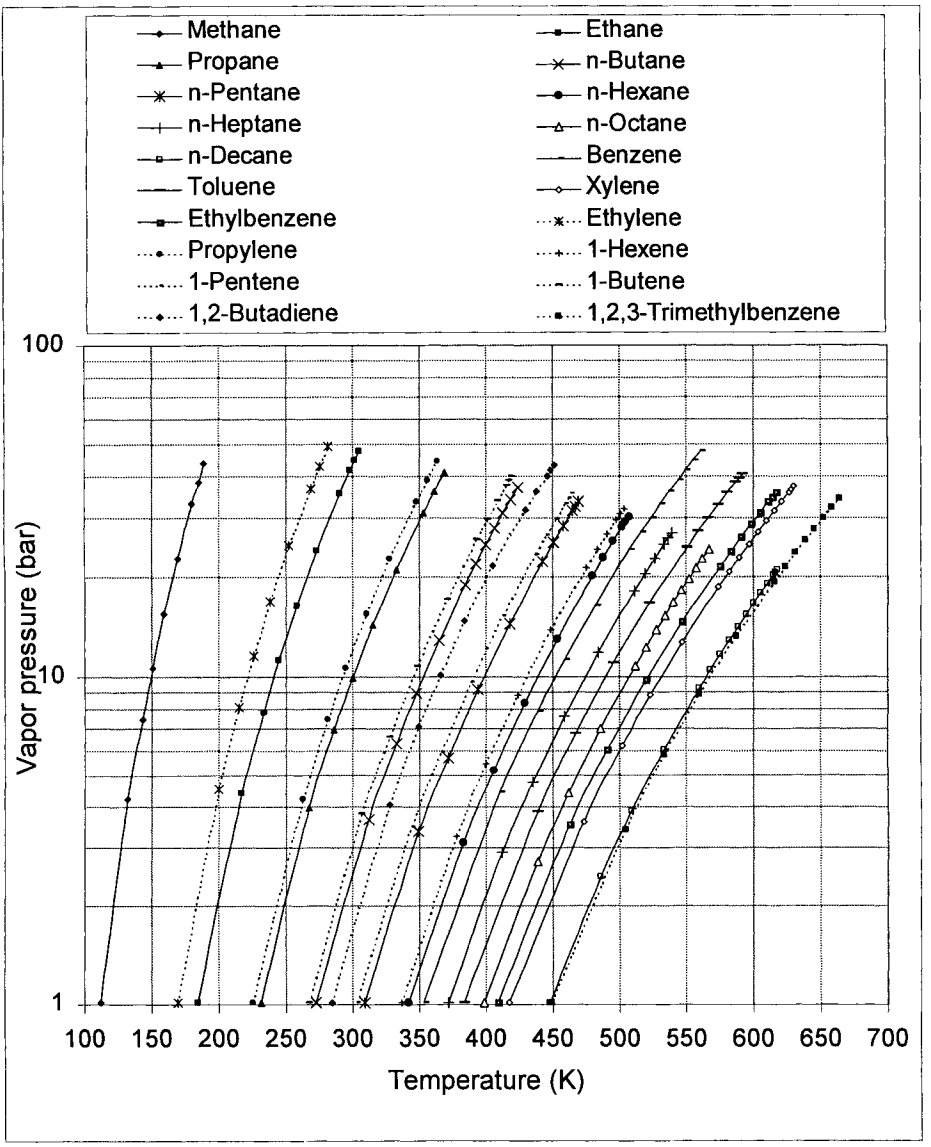

APPENDIX F - VAPOUR PRESSURE OF SOME ORGANIC COMPONENTS

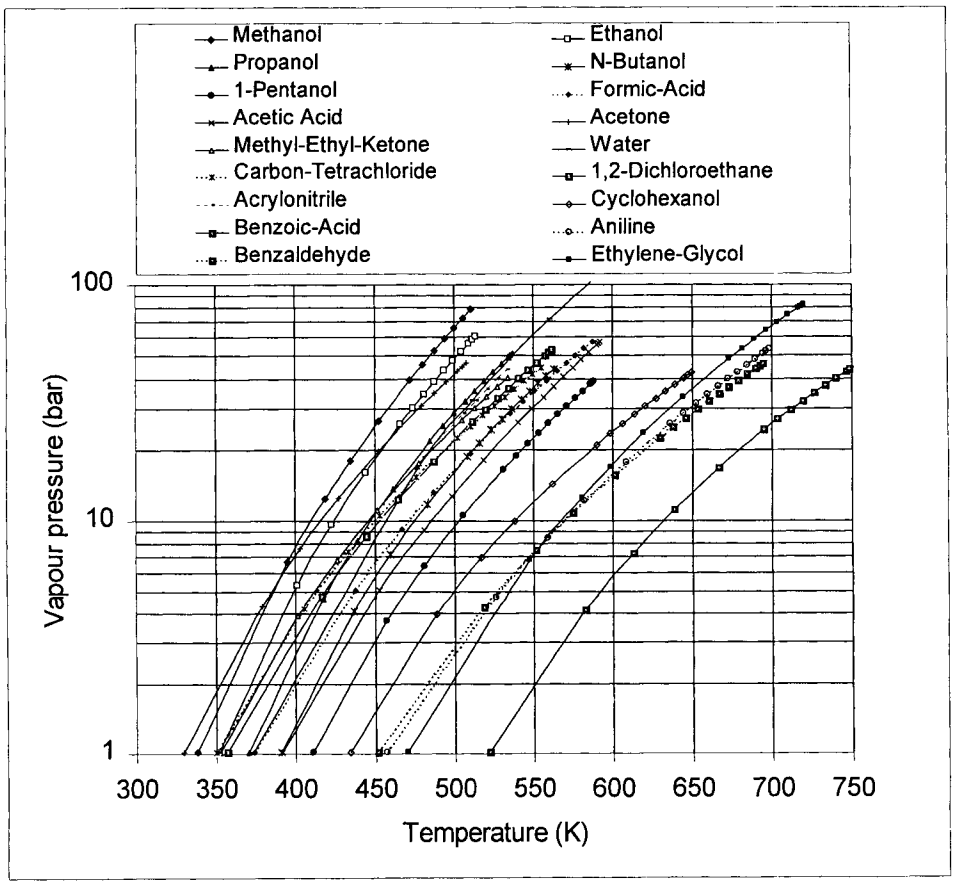

Appendix G:
Conversion factors to SI Units

To convert from unit	To SI unit	Multiply by
Length		
in	m	2.5400×10^{-2}
ft	m	0.3048
Mass		
lb	kg	0.45359
Force		
lbf	N	4.4482
kgf	N	9.81
Temperature		
°C	K	°C+273.15
°F	K	(°F+459.67)/1.8
°R	K	°R/1.8
Pressure		
in. of water (60 °F)	Pa	2.4884×10^{2}
atm	Pa	1.0133×10^{5}
psi	Pa	6.8948×10^{3}
torr (mmHg, 0 °C)	Pa	1.3332×10^{3}
Volume		
ft^3	m^3	2.8317×10^{-2}
in^3	m^3	1.6387×10^{-3}
gal	m^3	3.7854×10^{-3}
bbl (42 gal)	m^3	0.15899
Density		
lb/in^3	kg/m^3	2.7680×10^{4}
lb/ft^3	kg/m^3	16.018
Energy		
Btu	J	1.0544×10^{3}
Btu/lb	J/kg	2.3244×10^{3}
Btu/lb/°F	J/kg/K	4.1840×10^{3}
kcal	J	4180
Power		
HP (550 ft.lbf/s)	W	7.457×10^{2}
Btu/hr	W	0.2931
kcal/h	W	1.1622
ton of refrigeration	kW	3.517
Heat transfer coefficient		
$Btu/h/ft^2/°F$	$W/m^2/s$	5.6783
$kcal/h/m^2/°C$	$W/m^2/K$	1.162
Pressure drop		
psi/ft	kPa/m	2.2621×10^{1}

This Page Intentionally Left Blank

INDEX

A

Adiabatic temperature change, 324
Air-cooled heat exchangers, 635
Alkylation processes, 293
Alpha function in EOS, 141
Alternatives of design, 9
Ammonia/water phase equilibrium, 216
Annuity, 579
Appropriate Placement, 394, 428, 442
Attainable Region, 341
Azeotropic distillation, 289
- heterogeneous, 373
- ethanol dehydration, 376
- homogeneous, 359
- boundary crossing, 365
- entrainer selection, 359, 364
- feasibility, 361
- three-column alternatives, 366
- two-column sequence, 367

Azeotropic mixtures
- classification, 354
- right-triangle diagrams, 354
- ternary diagrams, 350

B

Balanced composite curves, 395
Bandwidth in MIMO systems, 487
Basic flowsheet structures, 543
Batch reactor, 76
Battery limit, 583
Boundary Value method, 383
BWR EOS, 164

C

Capacity ratio method, 585
Capital-cost law, 407
Capital recovery factor, 580
Capitalised costs, 601
Carnot cycle, 436
Cascade diagram, 402
Cash flow, 574
Chemical Engineering Plant cost, 588
Chemical Process Industries, 2
Closed Loop Disturbance Gain, 491
Co-generation, 438
Column Profiles, 448
Combined processes, 291
Combined separation processes, 378
Compact heat exchangers, 636
Complementary sensitivity function, 474
Complex columns, 283
Composite Curves, 393, 397
Compound interests, 578
Compressors selection, 253, 636
Computed Aided Process Engineering, 34
Computer Aided Design, 51
Computer Aided Operation, 51
Computer simulation
- applications, 35
- approach, 41
- definition, 34
- historical view, 40
- main software, 56
- software selection, 55

Conceptual Process Design, 7, 13
Condition number, 487, 497
Control of distillation columns, 510
Control of impurities, 520
- analysis, 659
- methodology, 662

Control of reactants in recycles, 518
Control structures in recycle systems, 509
Control systems
- performance, 476
- stability, 475, 484

Controllability analysis
- chemical reactor, 479
- distillation column, 494
- MIMO systems, 483
- SISO systems, 472

Controllability measures, 486
Controllability
- heat-integrated reactors, 533
- heat-integrated columns, 454

Controllers in flowsheeting, 79
Convexity, 342
Correction factor for LMTD, 632
Cost indexes, 587
Cost of recycles, 253
Costs of a project, 573
Critical parameters, 139
Continuous Stirred Tank Reactor, 311
Cubic Equations of State, 141, 164
Cumulative cash flow, 576

D

DAE systems, 119
Damköhler-number (plant), 524
Data extraction in Pinch Analysis, 406
Data regression, 202
Databases for physical properties, 77
Decentralized control, 489
Degrees of freedom analysis, 81-89
Degrees of freedom
- flowsheet, 89
- unfeasible specifications, 90
Departure functions, 171, 176
Depreciation, accounting methods, 589
Depreciation of equipment, 580, 590
Design and controllability, 503
Design decisions, 8, 18, 242
Design of equipment
- chemical reactors, 606
- distillation columns, 612
- extraction equipment, 623
Detailed factorial method, 584
Direct sequence, 280
Discounted Cash Flow Rate of Return, 600
Distillation
- batch distillation, 73
- inside-out algorithm, 72
- interlinked columns, 73
- refining columns, 73
- shortcut design, 380, 612
Distillation boundary, 352
Distillation Curves Map, 353
Distillation pinch, 381
Distillation regions, 349
Disturbance Condition Number, 489
Dividing-wall column, 458
Dynamic controllability analysis, 493
Dynamic effects
- energy recycle, 533
- material recycle, 522
Dynamic flowsheeting, 114, 117, 493, 651
Dynamic modelling
- distillation, 125
- flash, 121
- model formulation, 115
Dynamic simulation
- controllers, 131
- distillation, 128
- flash, 123
- stirred tank reactor, 115, 129
- tubular reactor, 130

E

Economic evaluation, 602
Economic Potential, 246, 252, 294, 573
Effects of recycles on dynamics, 505
Efficiency of trays, 619
Engineering method, 8
Enhanced distillation, 289
Enthalpy/entropy departure functions, 174
Enthalpy/entropy computation, 153
Environmental protection, measures 24
Environmental protection, 6, 22
Equations of state
- cubic, 140, 164
- polar fluids, 168
- virial, 140, 163
Ethanol dehydration, entrainer
- hydrocarbon, 373
- tetrahydrofurane, 367
- glycol, 289
Excess Gibbs energy
- activity coefficients, 191
- modelling, 181, 192
Extractive distillation, 289, 363

F

Feed control
- one limiting reactant, 513
- two limiting reactants, 518
Feed Effluent Heat Exchanger design, 533
Feed policy of reactants, 513
Feed purification, 240
Feedback control, 473
Feedback effects, 507
Fenske-Underwood-Gilliland (FUG), 380, 612
Financial computations, 581
Fixed capital breakdown, 583
Flooding point, 619
Flowsheeting
- analysis tools, 106
- calculation sequence, 96
- convergence, 103
- definition, 34
- in-line programming, 80
- methodology, 41, 44
- optimisation of a gas plant, 109
- optimisation, 107
- results, 105
- software architecture, 46
- thermodynamic options, 77
Flowsheeting, steady state, 59, 87, 642

Free energy functions, 146
Frequency response characteristics, 474
Fugacity
- computation, 157
- definition, 155
- mixtures, 161, 162
- pure components, 159

G

Gas-Liquid Equilibrium, 212
Gas Separation Manager, 267
Gas Separation system, 264
Gas turbine, 439
Gibbs-Duhem equation, 137, 150, 203
Gibbs free energy minimisation, 75
Gibbs free energy, 146
Grand Exergy Composite, 443
Graphical User Interface (GUI), 41-49
Grid diagram, 394

H

HDA process
- description, 60, 231, 640
- dynamic simulation, 651
- energy integration, 232, 641
- infeasible specifications, 93
- liquid separation section, 285, 649
- material balance, 243
- optimisation, 231, 643
- plantwide control, 512, 546, 651
- steady state simulation, 642
- subsystems, 258

Heat engines, 436
Heat exchangers, design of, 625
Heat Exchangers Network, 392
Heat integrated columns, 453
Heat integrated PFR, 533
Heat integration
- chemical reactors, 459
- distillation, 443
- heat & power, 436
- topological analysis, 414
- Total Site profiles, 460

Heat integration, controllability issues, 454
Heat pumps, placement, 440
Heat pumps driven distillation, 450
Heat transfer coefficients, 629
Heat transfer fluids, 625
Heat transfer in mixed vessels, 610
Heat Exchanger Network design
- evolution, 427
- general approach, 415
- optimisation, 425
- reduction of units, 422
- stream splitting, 419

Henry constant, 212
Heterogeneous reactions, 319
Heuristics
- liquid separations, 278
- vapour & gas separations, 268
- zeotropic mixtures, 282

Hierarchical Approach
- data & requirements, 236
- input/output-analysis, 238
- number of plants, 239
- outline, 234
- reactor design issues, 251
- recycle structure, 248
- separation system, 255

Hydraulic design of columns, 619
Hydrogen Pinch, 429

I

Ideal solution, 182
Immiscibility and azeotropy, 223
Immiscible systems, 220
Independent reactions, 301
Index problem, 119
Indirect sequence, 280
Inflation, 582
Input constraints, 478
Input/Output controllability analysis, 492
Input/Output structure, 240
Inputs for perfect control, 489
Integrated Process Design, 3, 15
- trends, 19
- systematic methods, 17

Integrated systems, 52-57
Integration of control and design, 533, 543
Integration of simulation tools, 50
Interaction parameters, 185, 187
Internal Site Battery Limits (ISBL), 586
Internet simulation, 55
Inventory, 503
Inverse response, 477

K

K-values
- asymmetric definition, 213
- EOS approach, 183, 219

- ideal, 182
- liquid activity approach, 189
- real, 184
Kremser's method, 617

L

L-L extraction, 291
Laws of thermodynamics, 142
Least-square regression, 204
Lee-Kesler method, 164
Lewis & Randall rule, 182, 214
Life Cycle Analysis, 28
Life cycle modelling, 11-15
Liquid activity models, 195-199
Liquid Separation Manager, 273
Liquid Separation system, 271
List processing method, 281
LNG/LPG plant, 101
Local models, 120
Loop transfer function, 474

M

Management of impurities, 659
Marshall & Swift cost index, 587
Mass Exchange Network, 430
Material balance with recycles, 249
Mathematical Programming, 392
Maximum-likelihood regression, 205
McCabe-Thiele method, 613
Membrane separation, 624
Methanol process, 41
Minimum energy of separation, 443
Minimum Energy Requirements (MER), 392
Minimum reflux, 381
Minimum singular value, 487
Mixed Integer Linear Programming (MILP), 427
Mixed Integer Non linear Programming (MINLP), 427
Mixing rules, 185
Mixing, power of, 609
Modelling liquid activity, 194
Multiple steady states, 326
Multiple steady states in control
- adiabatic reactor in recycles, 530
- plantwide control, 520
- second-order reaction, 528

N

Net Present Value (NPV), 599
Network of thermodynamic properties, 151
Niederlinski index, 490

O

Onion diagram, Process Integration, 15
Operating costs, 573, 591
Optimisation of conversion, 295
Optimisation, 107
Optimisation, HDA process example, 644
Overall heat transfer coefficients, 630
Overall material balance, 243

P

Packing characteristics, 622
Padé approximation, 478
Parametric sensitivity, 326
Payback time, 597
Peneloux correction, 167
Peng-Robinson EOS, 141, 166
Performance Relative Gain Array, 491
Petlyuk column, 458
Phase diagrams, 139
Phase envelope, 188
Phase equilibrium
- calculation from fugacity, 160
- condition, 148
PID controller, 131
Pinch Design method, 413
Pinch Point Analysis, 392, 395
Pinch Point principle, 393, 403
Plant Design project, 564
Plant Simulation Model, 38, 57
Plantwide control
- HDA process, 651
- integration with flowsheet synthesis, 537
- VCM process, 667
Plantwide control of impurities, 658
Plate heat exchangers, 636
Plug Flow Reactor, 312
Plus/Minus principle, 395, 428
Preferred separation, 382
Preliminary cost estimation, 572
Pressure-swing distillation, 290
Pressure drop calculation, 631
Principle of corresponding states, 142
Problem Table algorithm, 400
Process Design creative aspects, 7

Process Design project, 558
Process Flow Diagram, 43
Process Integration concept, 13, 392, 430
Process Integration teaching
- course, 561
- project, 563
Process Intensification, 9,
Process Simulation Diagram, 43, 44
Process Simulation, 13
Process Synthesis Hierarchical Appr., 230
Process Systems Engineering, 11
Profit formation, 574
Profitability analysis, 595
Profitability measures, 599
Property charts, 175
Propylene-oxide methylation, 515
Propylene purification, heat pump, 452
Pump selection, 638
Purchased Cost of Equipment, 585
PVT behaviour, 138

R

Rackett method, 167
Rankine cycle, 437
Raoult-Dalton law, 183
Rate of Return on Investment , 596
Reaction kinetics, 304
Reaction rate, 302
Reaction systems
- Attainable Region, 341
- optimisation methods, 347
Reactive Distillation, 292
Reactor-Separator-Recycle systems, 522
Reactor-separator system, 507
Reactor control in recycle systems, 526
Reactor design
- gas/liquid-reactors 322
- heat transfer, 330
- kinetic approach, 311
- non-ideal models, 318
- optimum temperature profile, 322
- performance, 313
- shortcut methods, 313
- solid catalysed reactions, 319
- stability, 326
Reactor selection, benzene alkylation, 335
Reactor simulation
- equilibrium reactor, 75, 84
- kinetic model, 76
Reactors, ideal models, 75
Redlich-Kwong EOS, 141
Refrigeration cycles, 442
Relative Gain Array (RGA), 488, 491
RGA number, 490
Removal of lights & heavies, 272
Residual property, 172
Residue Curves Map, 348
Right-Half-Plane (RHP) zeros, 477
Road map of the book, 3

S

Salt distillation, 290
Selection of reactors, 331
Selectivity, 305
Self regulation, 521
Sensitivity analysis, 602
Sensitivity function, 474
Separation methods,
- gas mixtures, 265
- liquid mixtures, 274
Separation regions, 355
Separation sequence
- alternatives, 280
- optimisation, 286
Separation system synthesis, 259-262
Sequential-Modular flowsheeting, 96
Shell and tube heat exchangers, 633
Shifted temperature scale, 400
Simulation of complex plants, 33, 38
Singular Value Decomposition (SVD), 486
SISO controllers, 131
Sizing of separation columns, 618
Smoker method, 615
Snowball effect, 509
Soave-Redlich-Kwong EOS, 141, 166
Software architecture
- Equation-Oriented, 49
- open software, 54
- Sequential-Modular, 47
Space velocity, 313
Split sequencing
- gas separations, 267
- liquid separations, 276
Steam turbines, 438
Stirred Tank Reactor, 311
Stirred tank reactors, 608
Stoichiometry, 300
Stream report, 105
Stream segmentation, 405
Successive Quadratic Programming, 108
Supercritical extraction, 292
Supertargeting, 393, 406

Sustainable Development, 3, 6, 27
Synthesis of reaction systems, 340
Systems Approach
- analysis, 4, 8, 11
- synthesis, 3, 8, 15
Systems Engineering, 2, 11

T

Tearing of recycle loops, 99
TEMA standards, 633
Temperature driving force, 632
Thermal coupling, 447
Thermally coupled columns, 457
Thermodynamic consistency, 203
Thermodynamic separation efficiency, 445
Thermodynamic models, comparison, 209
Thermodynamic options, 77
Threshold problems, 409
Time value of money, 578
Total Capital Investment, 574
Total Site targets, 461
Transhipment problem, 426
Typical investments, 587

U

UNIFAC, prediction accuracy of, 201
Unit Operations in simulation, 69-76
Utilities
- multiple levels, 412
- placement, 409
- variable temperature, 412

V

Van de Vusse reaction, 343
Van der Waals EOS, 165
Vapour-Liquid Equilibrium, 182
Vapour compression cycle, 441
Vapour Recovery system, 264
VCM process, case study, 662
Vessels, mechanical design of, 611

W

Waste minimisation, 430
Water Pinch, 429, 431
Working capital, 584